Nagar Yuwak Shikshan Sanstha's

Yeshwantrao Chavan College of Engineering

(An Autonomous Institution affiliated to Rashtrasant Tukadoji Maharaj Nagpur University)

Hingna Road, Wanadongri, Nagpur - 441 110

NAAC Accredited with 'A++' Grade

Ph.: 07104-242919, 242623, 242588

Summary of 3.4.4

Number of books and chapters in edited volumes / books published per teacher during the year

Year	**2022**
Number	209
No. of Teachers	328
No. of books and chapters in edited volumes per Teachers	0.637

Supporting Documents

1. Published Books
2. Papers in book chapters
3. Papers in Conference Proceding

Dr. U. P. Waghe

(Principal)

Y. C. COLLEGE OF ENGINEERING AN AUTONOMOUS INSTITUTION SEAL NAGPUR

Published Books

Earthquake Geotechnics pp 139–152 | Cite as

Filter Paper Calibration Using Osmotic Coefficients to Measure Total Soil Suction

P. B. Pande, S. R. Khandeshwar & S. P. Bajad

Conference paper | First Online: 04 January 2022

Part of the Lecture Notes in Civil Engineering book series (LNCE,volume 187)

Abstract

Suction is the pivotal parameter in arena of unsaturated soil. Filter paper method is the ea and cost-effective method for quantifying suction in which the calibration of filter paper i indispensable. The calibration curve with respect to total suction is impractical for measur suctions a smaller than 1000 kPa. Thus, the distinct calibration curves are needed for measuring matric suction. Filter paper procedure is suitable up to the development of calibration curve in concern with total suction but difficult pertaining to development of r suction calibration curve. Normally the pressure plate and pressure membrane were prefe for developing calibration curves, nevertheless these methods are having some limitation such as time consuming, skill and unavailability of equipment. The objective of this paper sidestep those limitations by adopting the prescribed procedure of establishing both curv required for measuring total as well as matric suction from filter paper technique. In this p the calibration equation for quantifying total suction was recognized from the wetting calibration curve achieved for Whatman No. 42 filter papers and matched with calibration equations developed by several other researchers. The total suction calibration equation v so selected that percentage error between obtained and selected must be less than 5%. T the drying calibration curve developed by the same researcher for the same filter paper w used for matric suction assessment of clayey soil used in this study. The procedure is

International Conference on Advances in Civil Engineering
↳ ACE 2020: **Recent Advancements in Civil Engineering** pp 223–230 | Cite as

Artificial Neural Network (ANN) Models for Prediction of Steel Fibre-Reinforced Concrete Strength

A. M. Shende, K. P. Yadav & A. M. Pande

Conference paper | First Online: 15 December 2021

Part of the Lecture Notes in Civil Engineering book series (LNCE,volume 172)

Abstract

The objective of the present research paper is to develop artificial neural network simulation and analyse the most important π-term from five independent pi terms (aspect ratio, aggregate–cement ratio, water–cement ratio, percentage of fibre and control strength) for prediction of SFRC strength. The output of this network can be evaluated by comparing it with experimental strength and the predicted ANN simulation strength. The study becomes more fruitful when the most influencing π-term is calculated for the prediction of SFRC strength.

Keywords

ANN model **5 independent π terms** **Predicted SFRC strength**

International Conference Advances in Civil Engineering (ACE 2020)
5-7 November 2020, Visvesvaraya National Institute of Technology, Nagpur (India)

Artificial Neural Network (ANN) Models for Prediction of Steel Fibre Reinforced Concrete Strength.

Dr.A.M.Shende[1, a], Dr.K.P.Yadav[2,b] Dr.A.M.Pande [3,c]

[1] principal,priyadarshini.J.L.College of Engineering,Nagpur ,Maharastra,India

[2]Vice chancellor, sangam University,Bhilwara,Rajasthan,India

[3]Director R &D ,Y.C.C.E,Nagpur,India

[a]abhaymshende3@gmail.com, [b]drkpyadav732@gmail.com, [c]anantpande.ycce@gmail.com

Abstract. The object of the present research paper is to develop Artificial Neural Network Simulation and analyse most important π-term from five independent pi terms. (Aspect ratio, aggregate-cement ratio, water-cement ratio, percentage of fibre and control strength)) For prediction of SFRC strength. The output of this network can be evaluated by comparing it with experimental strength and the predicted ANN simulation strength. The study becomes more fruitful when most influencing π-term is calculated for the prediction of SFRC strength.

Kew words: ANN model; 5 independent π Terms: predicted SFRC strength

1. Introduction

To arrive at mathematical model, the process started with development of some preliminary mathematical relations and then arriving at some single generalized equations. Mathematical models are developed to predict the strength of SFRC for different grade of concrete, for different Aspect ratio and different percentage of steel [5-8] [9-13].

Shende .A.M et.al [7-10] studied the investigation for 1) Grade of concreteM20, M30 and M40 2) Aspect Ratio 50, 60 and 67 3) Percentage of steel fibres 0%, 1%, 2% and 3%.The mathematical modeling to calculate predicted compressive strength, flexural strength and split tensile strength of SFRC are studied by shende [4]in 2013.In this paper an attempt is made to extend the work by developing artificial neural network model by using five independent π terms that is control strength ,percentage of steel fibre, Aspect ratio, water cement ratio and Aggregate cement ratio for the prediction of steel fibre reinforced concrete compressive strength ,flexural And split tensile strength.

1.1 Artificial Neural Network Simulation is developed to predict strength of SFRC by using Control Strength, percentage of fibers, Aspect ratio, water cement ration and Aggregate cement ration. The Experimental data-based modeling has been achieved through mathematical models for the five independent pi terms. In such complex phenomenon involving non-linear systems it is also planned to develop artificial neural network (ANN). The output of this network can be evaluated by comparing it with observed data. For development of ANN, the designer has to recognize the inherent pie terms that are predicted SFRC strength. Same ANN Simulation model can predict compressive strength, flexural strength and split tensile strength.

International Conference Advances in Civil Engineering (ACE 2020)
5-7 November 2020, Visvesvaraya National Institute of Technology, Nagpur (India)

Artificial Neural Network (ANN) Models for Prediction of Steel Fibre Reinforced Concrete Strength.

Dr.A.M.Shende[1,a], Dr.K.P.Yadav[2,b] Dr.A.M.Pande [3,c]

[1] principal,priyadarshini.J.L.College of Engineering,Nagpur ,Maharastra,India

[2]Vice chancellor, sangam University,Bhilwara,Rajasthan,India

[3]Director R &D ,Y.C.C.E,Nagpur,India

[a]abhaymshende3@gmail.com, [b]drkpyadav732@gmail.com, [c]anantpande.ycce@gmail.com

Abstract. The object of the present research paper is to develop Artificial Neural Network Simulation and analyse most important π-term from five independent pi terms. (Aspect ratio, aggregate-cement ratio, water-cement ratio, percentage of fibre and control strength)) For prediction of SFRC strength. The output of this network can be evaluated by comparing it with experimental strength and the predicted ANN simulation strength. The study becomes more fruitful when most influencing π-term is calculated for the prediction of SFRC strength.

Kew words: ANN model; 5 independent π Terms: predicted SFRC strength

1. Introduction

To arrive at mathematical model, the process started with development of some preliminary mathematical relations and then arriving at some single generalized equations. Mathematical models are developed to predict the strength of SFRC for different grade of concrete, for different Aspect ratio and different percentage of steel [5-8] [9-13].

Shende .A.M et.al [7-10] studied the investigation for 1) Grade of concreteM20, M30 and M40 2) Aspect Ratio 50, 60 and 67 3) Percentage of steel fibres 0%, 1%, 2% and 3%.The mathematical modeling to calculate predicted compressive strength, flexural strength and split tensile strength of SFRC are studied by shende [4]in 2013.In this paper an attempt is made to extend the work by developing artificial neural network model by using five independent π terms that is control strength ,percentage of steel fibre, Aspect ratio, water cement ratio and Aggregate cement ratio for the prediction of steel fibre reinforced concrete compressive strength ,flexural And split tensile strength.

1.1 Artificial Neural Network Simulation is developed to predict strength of SFRC by using Control Strength, percentage of fibers, Aspect ratio, water cement ration and Aggregate cement ration. The Experimental data-based modeling has been achieved through mathematical models for the five independent pi terms. In such complex phenomenon involving non-linear systems it is also planned to develop artificial neural network (ANN). The output of this network can be evaluated by comparing it with observed data. For development of ANN, the designer has to recognize the inherent pie terms that are predicted SFRC strength. Same ANN Simulation model can predict compressive strength, flexural strength and split tensile strength.

1.2 Artificial Neural Network Simulation [1]

An artificial neural network (ANN) consists of three layers i.e. the input layer, the hidden layer and the output layer. Its nodes represent neurons of the brain.The specific mapping performed depends upon the architecture and synaptic weight values between the neurons of ANN network. An artificial neural network is highly distributed representation and transformation that works in parallel. The control is distributed by highly interconnected. It is utmost important to compare the data generated through, experimentally observed data and ANN data to validate the phenomenon.

2. Procedure for Artificial Neural Network Phenomenon

The observed data from the experimentation is separated into two parts viz. input data or the data of independent pi terms and the output data or the data of dependent pi terms. The input data and output data are imported to the program respectively. Through principle component analysis the normalized data is uncorrelated. This is achieved by using "prestd" function. The input and output data is then categorized in three categories viz. testing, validation and training. The common practice is to select initial 75% training, last 75% data for validation and middle overlapping 50% data for testing. This is achieved by developing a proper code.

1. The data is then stored in structures for training, testing and validation.
2. Looking at the pattern of the data feed forward back propagation type neural network is chosen.
3. This network is then trained using the training data. The computational errors in the actual and target data are computed and then the network is simulated.
4. The uncorrelated output data is again transformed on to the original form by using "poststd" function.
5. After simulating the ANN, it is found that experimentally observed values are very close and in good agreement with the ANN predicted values.

Figure 1shows simple multilayer feed forward network for ANN and figure 2 shows the flow diagram of ANN simulation.

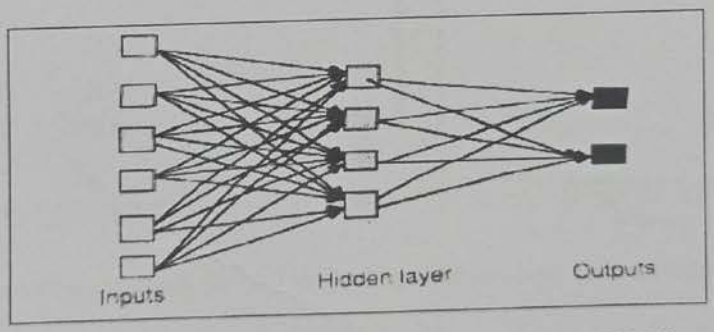

Fig.1 Simple multilayer feed forward network (ANN) [3]

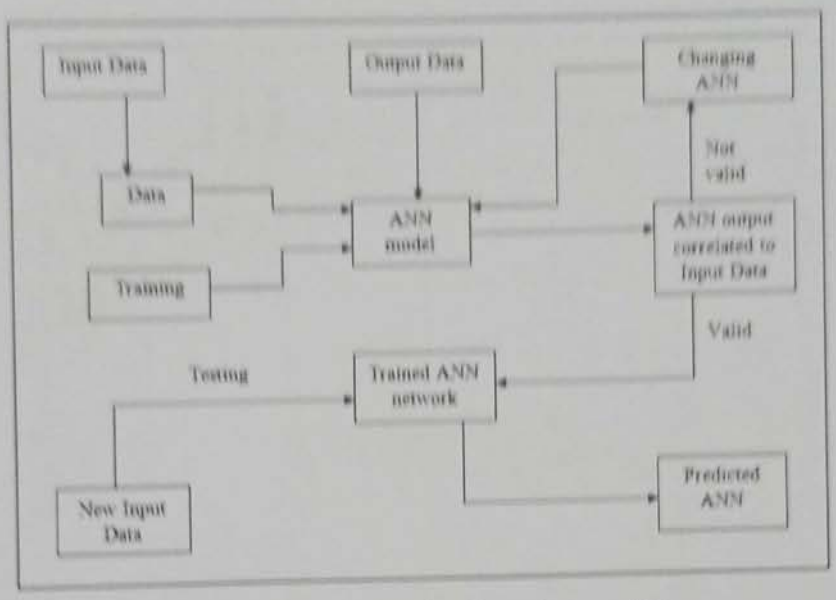

Fig. 2 ANN Simulation flow diagram [3]

Table 1 shows comparison of the values of dependent pi terms computed by experimentation, and ANN and. The values of R squared error in ANN, number of iterations, values of the regression coefficients for dependent pi terms and the plots of the actual data and target data for the dependent pi terms are shown in Figures for all response/ dependent variables.

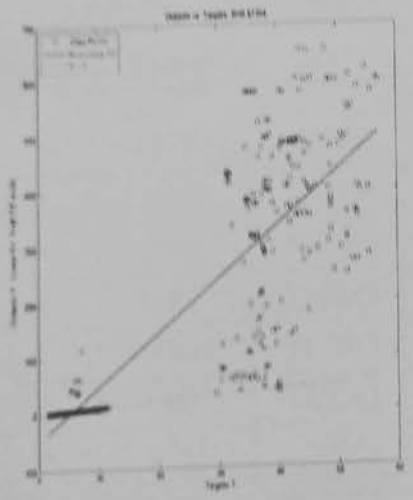

Fig. 3 Target vs output graph (R^2=0.7569)

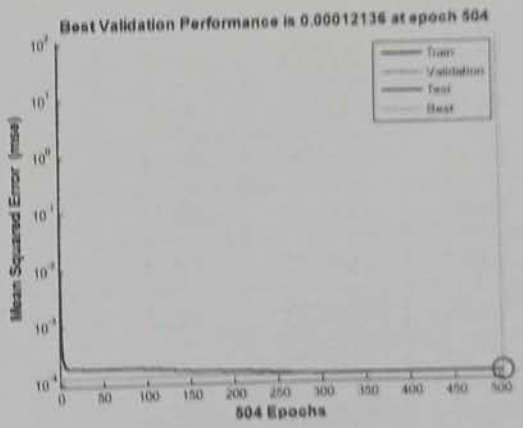

Fig. 4 Shows best validation performance (a)

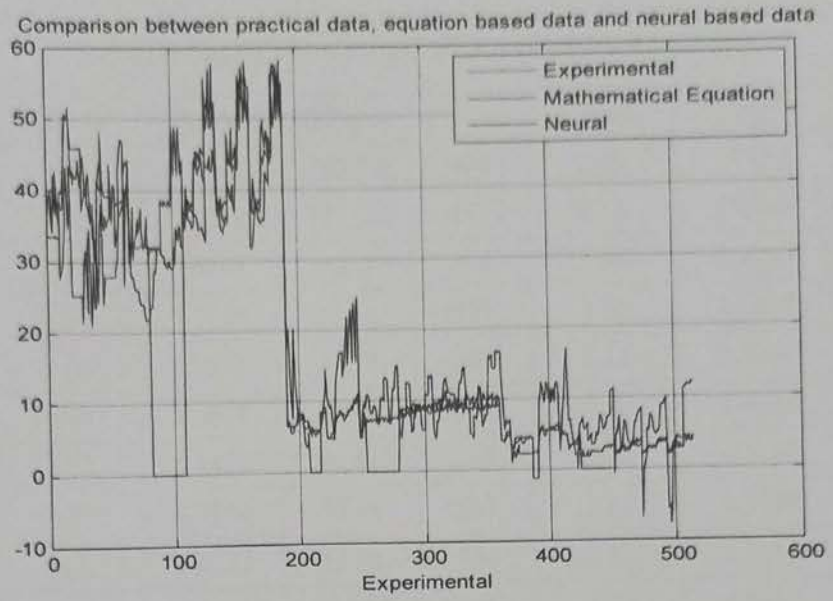

Fig. 5 Comparisons between experimental data and ANN predicted strength

Table 1 Performance analysis of ANN and Comparison of Experimental and predicted strength (out of 511 reading first 30 are reported here) [4]

Sr No	Expem	ANN	% Error	Sr No	Expem	ANN	% Error
1	35.9	38.5987	7.52	16	50.64	43.2541	14.59
2	39.06	39.2254	0.42	17	50.3	34.9614	30.49
3	39.74	39.1644	1.45	18	50.99	38.7512	24.00
4	39.6	37.3213	5.75	19	51.74	43.2541	16.40
5	35.3	34.3013	2.83	20	42.07	25.3025	39.86
6	42	38.9383	7.29	21	42.81	25.3025	40.90
7	36.83	37.3213	1.33	22	40.88	25.3025	38.11
8	42.74	39.2254	8.22	23	42.22	25.3025	40.07
9	37.21	38.5987	3.73	24	41.73	25.3025	39.37
10	34.9	34.3013	1.72	25	43.11	25.3025	41.31
11	38.43	27.745	27.80	26	44.44	25.3025	43.06
12	37.4	28.8231	22.93	27	40.58	25.3025	37.65
13	37.5	30.2178	19.42	28	43.11	25.3025	41.31
14	45.47	34.9614	23.11	29	42	21.6538	48.44
15	47.54	38.7512	18.49	30	45	29.5809	34.26

Table 2 Performance analysis of ANN and Comparison of Experimental and predicted strength (out of 511 reading Last 30 are reported here) [4]

Sr No	Expem	ANN	% Error	Sr No	Expem	ANN	% Error
480	2.94	7.5136	155.56	496	2.48	-7.951	420.63
481	2.87	7.3098	154.70	497	2.15	-5.080	336.30
482	2.77	7.0995	156.30	498	3.68	3.3104	10.04
483	3.04	5.1728	70.16	499	3.11	3.0076	3.29
484	2.69	4.8827	81.51	500	3.33	2.7036	18.81
485	2.55	4.5849	79.80	501	3.4	4.4983	32.30
486	3.82	5.1421	34.61	502	2.97	4.3142	45.26
487	3.82	5.3294	39.51	503	3.14	4.1259	31.40
488	4.1	5.4323	32.50	504	3.18	4.2223	32.78
489	3.96	8.6742	119.05	505	2.83	4.0866	44.40
490	3.54	8.874	150.68	506	3.04	3.9522	30.01
491	3.54	8.9836	153.77	507	4.25	11.1336	161.97
492	3.54	9.3628	164.49	508	4.39	11.2961	157.31
493	3.96	9.6801	144.45	509	4.25	11.5593	171.98
494	2.55	-5.885	330.81	510	4.1	11.7152	185.74
495	2.26	-5.163	328.48	511	4.39	11.8019	168.84

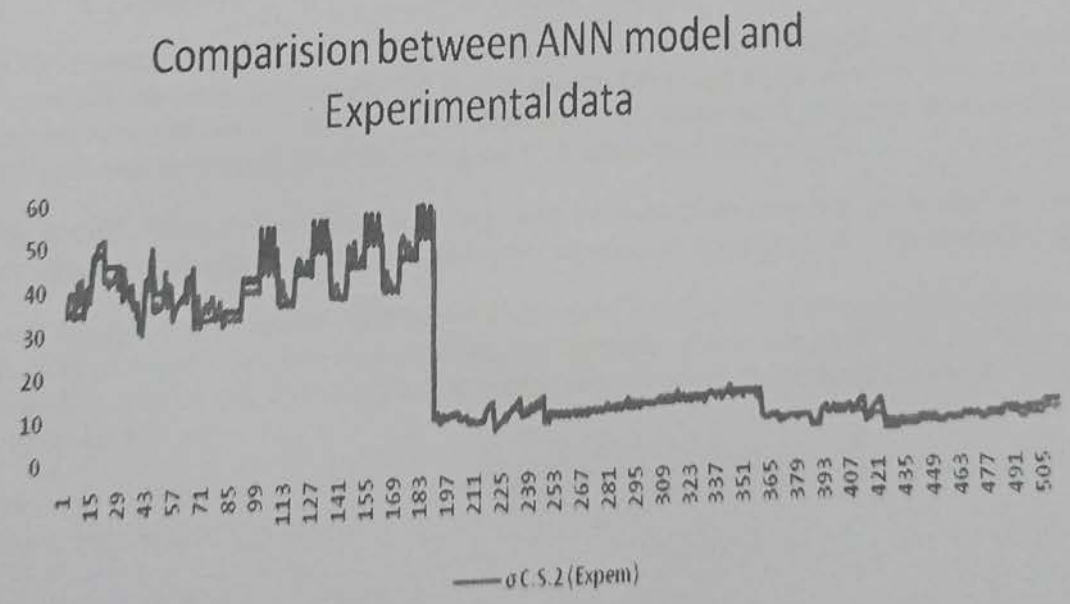

Fig. 6 Graphical comparison between ANN Model and Experimental data-based model for prediction of SFRC strength

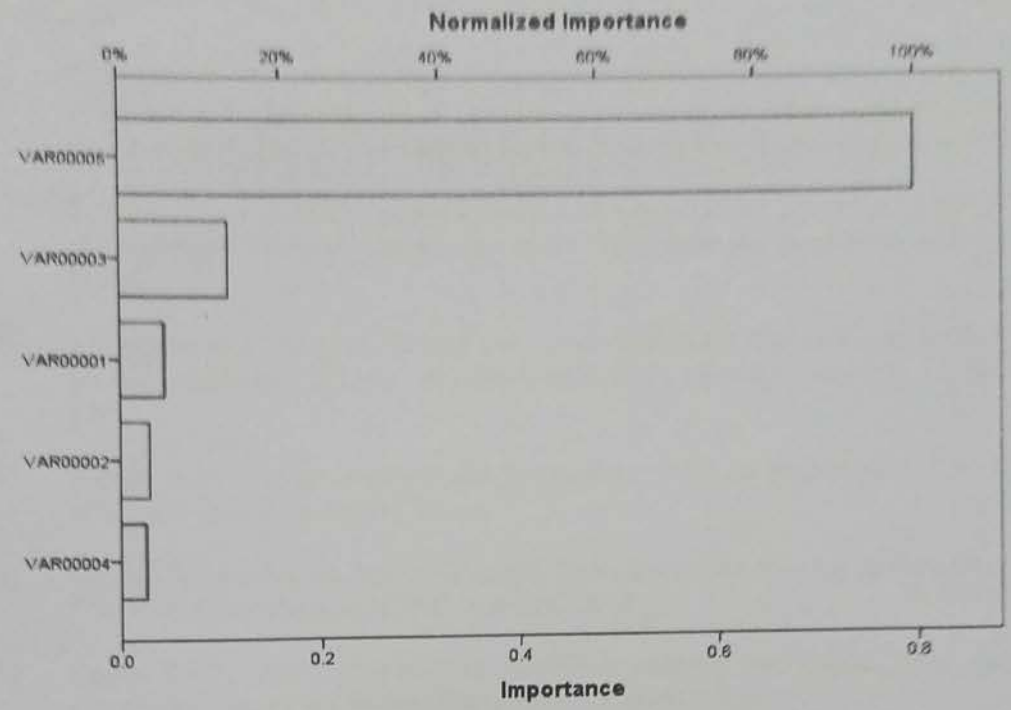

Fig. 7 Shows the importance of π terms in ascending order

It can be seen that the highest change takes place in strength, because of the π term π5(control strength) whereas the least change takes place due to π4.(Aspect Ratio) Thus, π5 related to control strength Variables is most important π term .

3 Conclusions

ANN Simulation model developed for prediction of SFRC strength, using strength of controlled concrete, percentage of fibres, aspect ratio, aggregate cement ratio and water cement ratio can very well be used in prediction of compressive strength, flexural strength and split tensile strength of SFRC using the five parameters listed above.

The significance of this model can very well be seen from the data presented in column experimental strength and the predicted ANN simulation strength in table no1and table No 2.

From fig no 6 it is clear that ANN simulation model developed for prediction of compressive strength, Flexural strength and split tensile strength when compared with experimental strength it is observed that predicted strengths and observed experimental strength are close to each other

Figure No 7 shows the importance of independent π terms .Control strength π5 is the most influencing terms in this model.

References

[1] P. Modak & Mrs. S. D. Moghe, "Design & Development of a Human Powered Machine for the Manufacture of Lime-Fly-ash-Sand-Bricks" Human Power Vol. 13, pp 3-8, 1998, Journal of International Human Powered Vehicle Association, U.S.A.

[2] R. Bapat, "Experimental Optimization of a Manually Driven Flywheel Motor" M.E. (By Research) Thesis of Nagpur University 1989, under the supervision of Dr. J. P. Modak.

[3] S.D.Moghe & J.P.Modak, "Design and Development of a Human Powered Machine for the Manufacture of Lime - Fly-ash-Sand Bricks", Human Power, Vol. 13, pp 3-8, 1998

[4] Shende A.M. The investigation and comparative study on properties of steel fibre reinforced concrete members, Thesis

[5] Clifford N. MacDonald, Julian Trangsrud, 2004, Steel Fibre Reinforced Concrete Pre-Cast Pipe, Proceedings of ICFRC, Vol I, pp 19-28.

[6] Coutts R.S.P., 2005, A review of Australian research into natural fibre cement composites Cement & Concrete Composites. 27, pp 518-526.

[7] Shende A.M. & Pande A.M., 2011, 'Experimental study and prediction of Tensile Strength for Steel Fiber Reinforced Concrete', International Journal of Civil and Structural Engineering", Vol.1, No 4, pp 910-917

[8] Haroon S.A., Nur Yazdani & Kamal Tawfiq, 2004, Properties of Fibre Reinforced Concrete for Florida Applications, Proceedings of ICFRC, Vol I, pp 135-144.

[9] Jagannathan, 2010, Flexural Strength Characteristics of Hybrid Fibre Reinforced Cementitious Matrix, Proceeding of International conference on Innovation, Vol I, pp 347-353.

[10] Shende A.M. & Pande A.M., 2011, 'Mathematical Model to Calculate Predicted Compressive Strength and Its Comparison with Observed Strength', International Journal of Multidisciplinary Research and Advances in Engg. (IJMRAE), Application, Vol. 3, No. IV, pp 145-156

[11] Sashidhar C., Rao H. S. & Ramana N.V., 2004, Strength Characteristics of Fiber-Reinforced Concrete with Metakaolin, Proceedings of ICFRC, Vol I, pp 247-256.

[12] Shende A.M. & Pande A.M., 2011, 'Comparative study on Steel fibre reinforced cum control concrete under flexural and deflection', International Journal of Applied Engineering Research", Vol. 1, No 4, pp 942-950

Head
Department of Civil Engineering
Y. C. College of Engineering
NAGPUR-441 110

Materials Today: Proceedings xxx (xxxx) xxx

Contents lists available at ScienceDirect

Materials Today: Proceedings

journal homepage: www.elsevier.com/locate/matpr

Development of self-compacting concrete blended with sugarcane bagasse ash

Monali Wagh [a,*], U.P. Waghe [b]

[a] Research Scholar & Assistant Professor ,Department of Civil Engineering, Yeshwantrao Chavan College of Engineering, Nagpur, India
[b] Professor, Department of Civil Engineering, Yeshwantrao Chavan College of Engineering, Nagpur, India

ARTICLE INFO

Article history:
Available online xxxx

Keywords:
Self-compacting concrete
Sustainability
Segregation
Strength Properties

ABSTRACT

Self-compacting concrete (SCC) can be flows in crowded reinforcement without segregation and it flows under its own weight without vibration. Sugarcane Bagasse ash (SCBA) (agricultural waste) is present in massive amounts in India. The use of SCBA in SCC is described in this paper as a feasible solution to environmental concerns. The usage of bagasse ash is important for sustainable development since it decreases carbon emissions and structural costs. The goal of this study is to discover and compare the fresh and strength properties of SCC made using SCBA as replacement of cement in 0, 10, 15 and 20%. The fresh characteristics of SCC are marginally lowered when the proportion of SCBA increases due to partial cement replacement, but they remain within the EFNARC range. It has been discovered that using it in SCC improves its strength properties.

Selection and peer-review under responsibility of the scientific committee of the International Conference on Latest Developments in Materials & Manufacturing.

1. Introduction

Sugar cane is one of the most widely farmed crops in the world, with a total production of over 1500 million tonnes in over 110 nations [1]. Every year, India produces around 10 million tonnes of SCBA and 300 million tonnes of sugarcane [2]. The sugar processing industry produces SCBA as a by-product. Many researchers proposed that bagasse ash is pozzolanic in nature and it improves the properties of concrete [3]. SCBA's pozzolanic reactivity is fundamental to the reported results [4]. SCBA contains amorphous silica, which produces pozzolanic action [5]. As a result, scientists have looked at the utilization of SCBA as a pozzolanic supplementary cementitious materials in order to limit CO_2 emissions into the environment [6,7]. Adding up to 15% SCBA reduced porosity and sorptivity while increasing strength and durability properties [8].

SCC is a rising concrete with new properties like filling, passing through congested reinforcement, and resistance to segregation. A higher binder concentration (400–600 kg/m^3), a low water- powder ratio, a smaller coarse aggregate quantity, and a superplasticizer admixture are all required for SCC mixtures [9]. Add a viscosity modifying admixture (VMA) to the SCC mixture to accomplish the viscosity property [10]. In SCC, the addition of alternate cement-based materials saves material costs while improving self-compaction. SCC research has recently focused on the incorporation of extra cementitious materials with the goal of alleviating solid waste disposal issues. When agricultural by-products like SCBA are employed in concrete manufacturing, significant energy and cost reductions is attainable [10]. For achieving self-consolidation is to substantially surge the volume of fine materials such as SCBA without raising the pricing [11]. Because SCBA has a larger percentage of amorphous silica, it is an outstanding pozzolanic material and may be utilised as an advantages cementitious material [12]. The strength properties of specimens formed from a combination of 30% SCBA and 30% BFS in place of OPC was equivalent to that of the control.

In SCC, significantly enhanced sulphate resistance, particularly in mixtures with the greatest SCBA ratio [13]. Ingredients for a particular SCC including bagasse ash are 35.63 percent less expensive than those for a control concrete [11]. GGBFS, SCBA, and fly ash have enhanced the strength, and durability because of silica rich content [13]. With the accumulation of SCBA to SCC, the resistance to sulphate assault is reduced [14]. SCC slump flow improves with more bagasse ash, and filling and passing ability improves [15]. Low permeability, decreased ion penetration, and strong resistance to heat assault were seen in concrete replaced with SCBA, resulting

* Corresponding author.
E-mail address: wagh.monali4@gmail.com (M. Wagh).

https://doi.org/10.1016/j.matpr.2021.12.459

Selection and peer-review under responsibility of the scientific committee of the International Conference on Latest Developments in Materials & Manufacturing.

proved durability [16]. When cement is substituted in the concrete with 10% SCBA and 10% micro silica by weight proportion, the concrete has the best tolerance to sulphate and chloride attack [17]. With the accumulation of SCBA in concrete, decreases weight loss by sulfuric acid attack [18].

The goal of this study is to use SCBA as an advantageous cementitious material in the formation of SCC that is environmentally friendly. An exploratory approach is used to examine the fresh and strength characteristics of the proposed SCC. This research would add to a growing body of information about the use of agricultural wastes in the production of environmentally friendly concrete.

2. Materials Used:

2.1. Cement (OPC)

The OPC cement of grade 43 was used to make self-compacting concrete. The cement conformed through IS 8112–2013. For all concrete mixtures, Ultra Tech cement was utilised to cast cubes, beams and cylinders.

2.2. Aggregate

The fine and coarse aggregate used in the studies conformed to IS 383 provisions. The fine aggregate was sieved using a 4.75 mm sieve, while the coarse aggregates were 10 mm and 20 mm in size. The specific gravity of fine aggregate, 10 mm and 20 mm coarse aggregate are 2.68, 2.86 and 2.90 respectively.

2.3. Sugarcane bagasse ash (SCBA)

The SCBA utilised in this investigation was collected from sugarcane industry Devhala district, Tumsar, India. Chemical composition of sugarcane bagasse ash by X-ray fluorescence (XRF) was investigated and shown in Table. 1. At IBM Nagpur, XRF tests were performed. Furthermore, the findings of the X-ray fluorescence study on SCBA reveal that this material has a high silica content of 54.93 percent SiO_2, followed by Al_2O_3 37.14%, TiO_2 2.53% and Fe_2O_3 1.15%. The colour of SCBA is grey (Fig. 1). The specific gravity of sugarcane bagasse ash is 1.9. SCBA is irregular in shape, as demonstrated by SEM examination. (Fig. 2). Fig. 3 shows the result of EDS analysis for SCBA. From EDS analysis, it is observed that the silica content is higher than other elements (see Figs. 4-9).

2.4. Superplasticizer

Visco-Flux 5507 was used as superplasticizer in SCC. The relative density is 1.11 at 27 °C with pH is greater than 6. This product confirmed with ASTMC-494 Type A and F and IS 9103–1999.

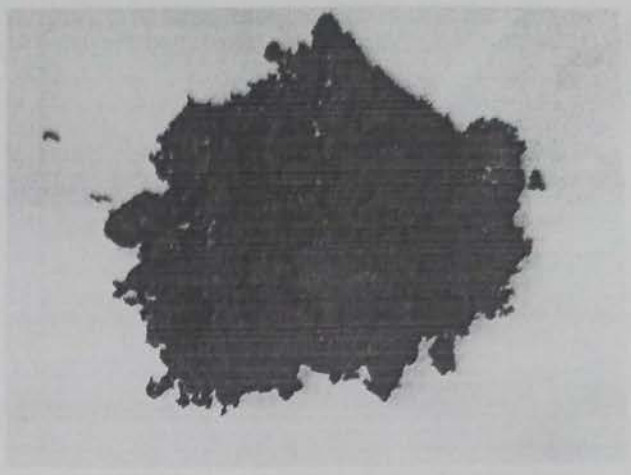

Fig. 1. Photos of SCBA sample utilised in this research.

Fig. 2. Scanning electron micrographs for SCBA.

2.5. Viscosity modifying admixture (VMA)

AC-Gel-Build was used as VMA in SCC. The relative density is 1.0 with pH value in between 5 and 8. This product confirmed with IS 9103–1999.

3. Experimental Programme:

Table 2 shows mix proportioning data of the SCBA integrated self-compacting concrete along with their specified designation. The SCC mixes contains 0%, 10%, 15% and 20% of SCBA as a supplementary to the cement designated as SCCB0, SCCB10, SCCB15 and SCCB20 respectively. For this study, total 4 trial mixes are produced by incorporating various percentage of SCBA. Total 9 cube

Table 1
Chemical compositions of cement and SCBA using X-ray fluorescence.

Materials	Chemical composition (%)								
	Na_2O	MgO	Al_2O_3	SiO_2	SO_3	K_2O	P_2O_5	SrO	BaO
Bagasse Ash	0.18	0.19	37.14	54.93	0.15	0.15	0.11	0.02	0.02
Cement	0.7	1.92	4.29	22.93	0.35	0.9	–	–	–
	CeO_2	TiO_2	Cr_2O_3	Fe_2O_3	MnO_2	CaO	Cl	ZrO_2	Bi_2O_3
	0.05	2.53	0.03	1.15	0.02	1.3	0.02	0.04	0.03
	–	–	–	2.89	–	66.2	–	–	–

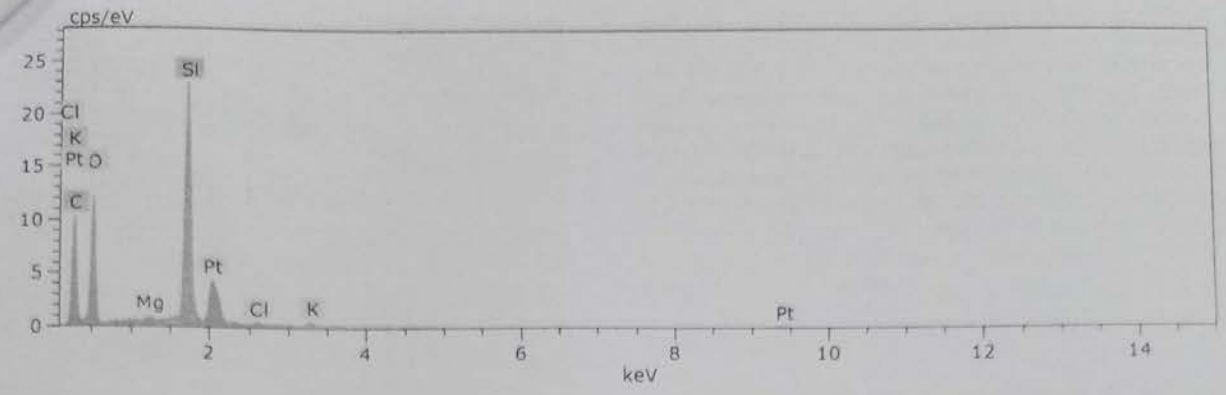

Fig. 3. Energy Dispersive X-ray Spectroscopy for SCBA.

Fig. 4. The photo shows Slump Flow test.

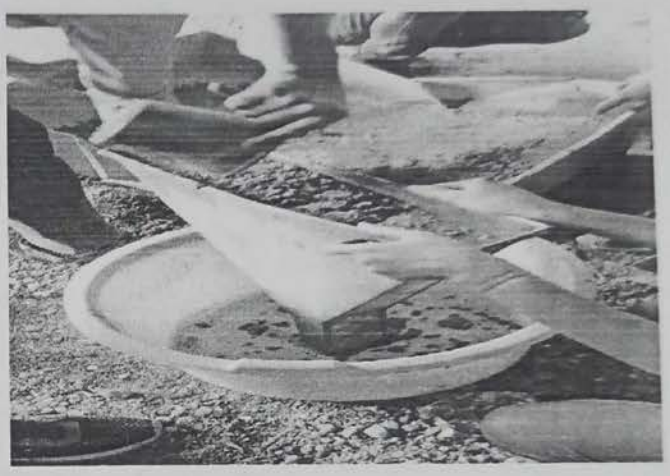

Fig. 6. The photo shows V-Funnel test.

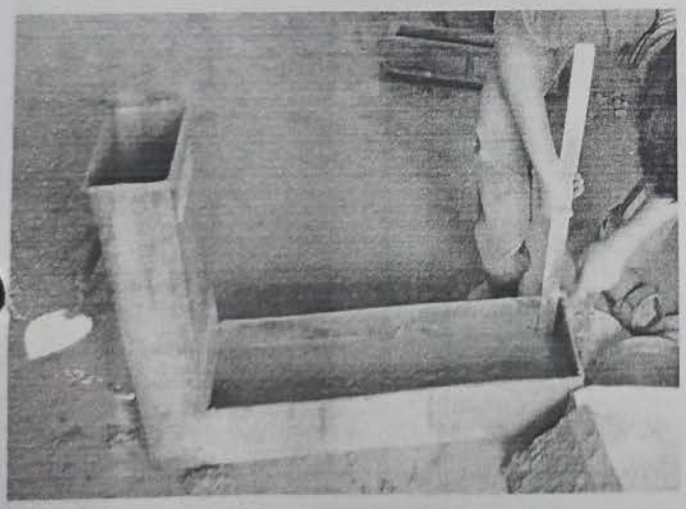

Fig. 5. The photo shows L-Box test.

Fig. 7. The photo Cube, Beam and Cylinder prepared.

of size 150mmx150mmx150mm and 9 beams of size 100 mm x100mm x500mm are prepared for each mix proportion. Viscoflux 5507, a high range water lowering concrete additive, was employed to create excellent workability and flowability. The amount of superplasticizer was used constant as 1.2% by weight of the binder ingredient. The VMA dosage of 0.3% by total weight of the binder ingredient is incorporated in the work. Slump-flow, V-funnel test, T500 slump and L-box test were all assessed in the fresh test. Compressive strength (CS) and the flexural strength (FS) was all tested at various ages in the hardened condition. Table 3.

4. Result and Discussion:

4.1. Slump flow test

Values of slump were measured on all SCC mixtures and completely fell within the limits of 650 mm to 800 mm for slump flow

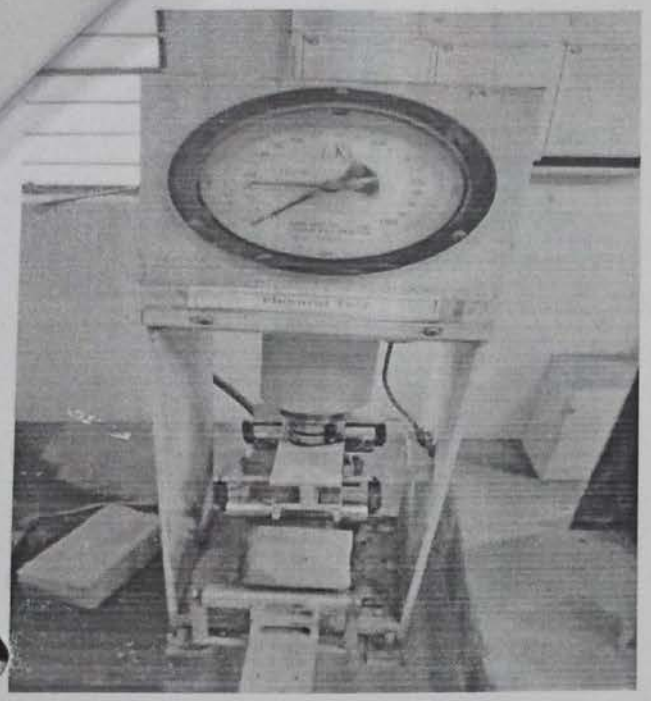

Fig. 8. The photo shows Flexural strength test.

Fig. 9. The photo shows Compressive strength test.

(see Fig. 10), which are adequate for several situations and suggested by EFNARC. When compared to the control sample (SCCB0), which had the most slump and slump flow, substituting SCBA in mixes leads to lower flowability [9]. In a newly developed SCC, the larger the quantity of supplementary cementitious materials, the slump flow shows the lower value than the control sample. In comparison to the control group, the slump flow values of fresh SCC mixtures containing 10%, 15%, and 20% SCBA was reduced from 693 mm to 689 mm, 671 mm, 667 mm respectively. The above finding was in line with earlier observations [10] and it might be due to various of factors.

4.2. T 500 slump flow test

The average diameter of slump flow of the SCC mixes was in between 650 and 700 mm which indicating reasonable flowability. The easiest method for determining the flowability of SCC is T-500 slump flow testing. According to EFNARC recommendations (EFNARC, 2002), the time necessary for the SCC combinations to spread 50 cm ranged from 2 to 5 s [9]. The slump flow time surges with the amount of SCBA in self-compacting concrete. The slump flow time increases with the use of SCBA in SCC because of high surface area. Maximum slump flow time is recorded for SCCB20.

4.3. V-Funnel Test

The EFNARC specified that V-funnel flow times should be between the time period of 6 to 12 s [9]. The V-funnel timings in mixes SCCB0, SCCB10, SCCB15 and SCCB20 were all within the required range. Because the particles soaked water, the flow time rose as the amount of SCBA grew, resulting in extraordinarily viscous mixtures [10]. As shown in Fig. 11, the V funnel timing were recorded in between 7 and 11 sec. When SCBA were replaced with OPC, the flow duration of fresh concrete was consistently increased, as shown in Fig. 11. The flow time recorded is largest for SCCB20 which is 36% superior than the control mix.

4.4. L-Box test

The L-Box test determines the capability to pass through densely congested reinforcing by its own weight. The higher values of H_2/H_1 ratio shows the higher passing capability, and vice versa. Fig. 11 shows that, with the addition of SCBA in SCC resulted in the lower values of H_2/H_1 ratio as compare to the control SCC mix. The values of H_2/H_1 ratio were in the range of 0.86 to 0.91 as shown in Fig. 11.

4.5. Compressive strength (CS)

The CS was performed for the all mixes of SCC at of 7 days, 14 days and 28 days. The CS for the control mix of SCC were 35.04, 42.89 and 48.81 N/mm^2 at 7, 14 and 28 days respectively. The CS of the SCC made with the use of SCBA as a partial substitution to the cement, were comparable to the control mix. The CS of control mix of SCC at 7, 14 and 28 days were 35.04, 42.89 and 48.81Mpa respectively. The SCC blended with SCBA performed

Table 2
Mix Proportion of developed SCC.

No.	Type	Mix I.D.	Cement %	SCBA %	Aggregates(kg/m^3)		Fly Ash(kg/m^3)	Superplasticizer (%)
					Coarse	Fine		
1	Single	SCCB0	100	0	796.6	928.38	110	1.2
2	Binary	SCCB10	90	10	796.7	888.06	110	1.2
3	Binary	SCCB15	85	15	796.7	874.61	110	1.2
4	Binary	SCCB20	80	20	796.8	861.17	110	1.2

Properties of developed SCC.

Sr. No.	Type	Mix I.D.	Slump flow Dia. in (mm)	T-500 in (sec)	V-funnel Time (sec)	L box Test (H_2/H_1)
1	Single	SCCB00	693	3.6	7.56	0.91
2	Binary	SCCB10	689	3.91	9.01	0.89
3	Binary	SCCB15	671	4.1	9.54	0.87
4	Binary	SCCB20	667	4.3	10.3	0.86

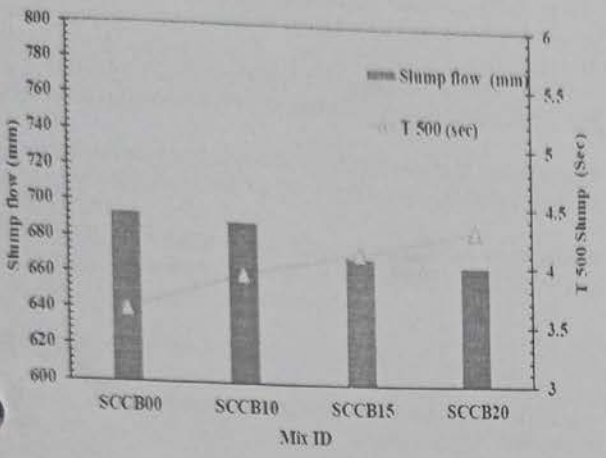

Fig. 10. Slump Flow and T-500 Slump Time of newly prepared SCC with respect control mix.

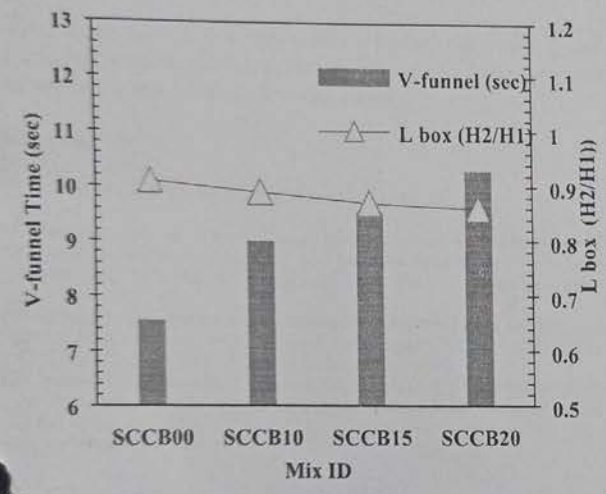

Fig. 11. V-funnel Time & L-Box (H2/H1) of newly prepared SCC with respect control mix.

3.8%, 1.26% greater strength for SCCB10 and SCCB15 respectively as equated to control mix at 7 days. The strength of SCBA blended SCC were comparable or even superior than that of control mix of SCC. For SCCB10, the strength of SCC was 5.02% greater than that of SCCB0 at 28 days as shown in Fig. 12. When compared to a control mix, SCC combined with 10% bagasse ash increases CS, split tensile strength, and FS by 8.5, 35, and 33% respectively [14]. Improved the strength properties as well as impact resistance if SCC containing 5% of bagasse ash [15]. The CS of SCC with 20% SCBA as replacement of cement was nearer to control mix [20].

4.6. Flexural strength (FS)

Fig. 13 exhibited the FS of all developed SCC mixes blended with SCBA. The FS of SCCB0 were 3.92, 4.80, and 5.93 MPa at 7 days,

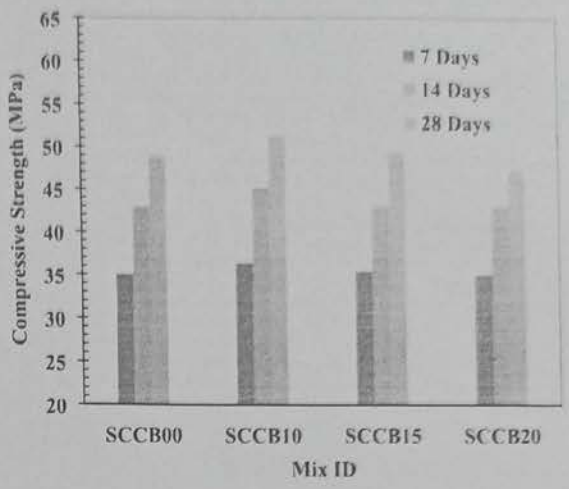

Fig. 12. CS of developed SCC blended with SCBA at 7, 14 and 28 days.

14 days and 28 days respectively. The FS of developed SCC with 10% substitution of cement with SCBA were 10.46% greater than that of control mix. The maximum strength occurred for SCCB10 mixes. At the age of 7 days, the FS of SCC blended with 10% and 15% SCBA were 11.22% and 5.44% superior than that of SCCB0. At 28 days, the FS of SCC blended with 10% and 15% SCBA were 10.46% and 3.43% higher than that of SCCB0. Furthermore, when the SCBA replacing level grew, the strength of the mixture improved, indicating that the pozzolanic hydration of SCBA progressed with time [9].

Further increase of SCBA up to 20% in SCC, reduces the FS little bit. The optimum percentage of SCBA in SCC was observed to be 15% as a replacement by cement. Boukendakdji et al. observed that the pattern of strength variation induced by slag substitution was comparable in SCC with 10% to 15% slag substitution [21].

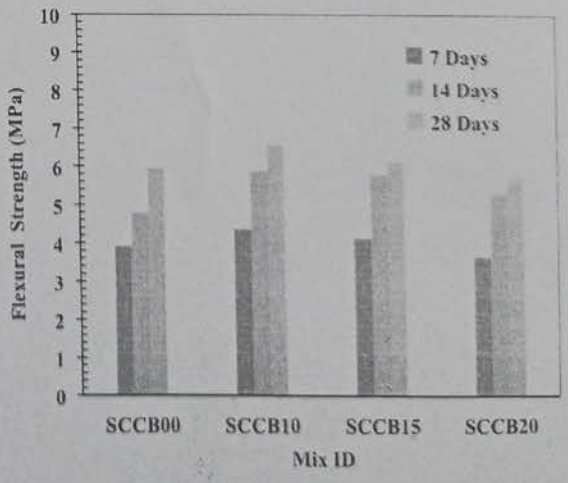

Fig. 13. FS of developed SCC blended with SCBA at 7, 14 and 28 days.

...usion:

1. In the development of SCC, the use of SCBA as a cement substitute may be advantageous.
2. Fresh properties of SCC are slightly reduced as percentage of bagasse ash as partial substitution of cement increases, but are within the range of EFNARC.
3. Slump flow and L-box results are marginally reduced when SCBA is used as a substitution of the cement in developed SCC.
4. V-funnel time and T-500 slump increases with the increase of SCBA as a substitution of the cement in developed self-compacting concrete but within the range of EFNARC.
5. Optimum percentage of SCBA as a substitution of cement in SCC is 15%.
6. The compressive strength (CS) of developed SCC blended with SCBA were 5.02% greater for SCCB10 and comparable to control mix for SCCB15 at 28 days.
7. The flexural strength of SCC blended with SCBA were 10.46% and 3.43% enhanced for SCCB10 and SCCB15 respectively at 28 days as compare to control mix.

CRediT authorship contribution statement

Monali Wagh: Conceptualization, Data curation, Writing – ...iew & editing. **U.P. Waghe:** Methodology, Validation, Investigation.

Declaration of Competing Interest

The authors declare that they have no known competing financial interests or personal relationships that could have appeared to influence the work reported in this paper.

References

[1] J. A. Patel and D. B. Raijiwala, "Use of Sugar Cane Bagasse Ash as Partial," vol. 15, no. 5, 2015.

[2] S. Dhengare *et al.*, "Utilization of Sugarcane Bagasse Ash As a Supplementary Cementitious Material in Concrete and Mortar-a Review," *Int. J. Civ. Eng. Technol.*, vol. 0976, no. 4, pp. 94–106, 2015, [Online]. Available: www.jifactor.com.

[3] N. Chusilp, C. Jaturapitakkul, K. Kiattikomol, Utilization of bagasse ash as a pozzolanic material in concrete, Constr. Build. Mater. 23 (11) (2009) 3352–3358, https://doi.org/10.1016/j.conbuildmat.2009.06.030.

[4] J.T. Kolawole, A.J. Babafemi, E. Fanijo, S. Chandra Paul, R. Combrinck, State-of-the-art review on the use of sugarcane bagasse ash in cementitious materials, Cem. Concr. Compos. 118 (2021) 103975, https://doi.org/10.1016/j.cemconcomp.2021.103975.

[5] S.A. Khawaja, U. Javed, T. Zafar, M. Riaz, M.S. Zafar, M.K. Khan, Eco-friendly incorporation of sugarcane bagasse ash as partial replacement of sand in foam concrete, Clean. Eng. Technol. 4 (2021) 100164, https://doi.org/10.1016/j.clet.2021.100164.

[6] E.M.R. Fairbairn, B.B. Americano, G.C. Cordeiro, T.P. Paula, R.D. Toledo Filho, M. M. Silvoso, Cement replacement by sugar cane bagasse ash: CO2 emissions reduction and potential for carbon credits, J. Environ. Manage. 91 (9) (2010) 1864–1871, https://doi.org/10.1016/j.jenvman.2010.04.010.

[7] J.P. Moretti, S. Nunes, A. Sales, Self-compacting concrete incorporating sugarcane bagasse ash, Constr. Build. Mater. 172 (2018) 635–649, https://doi.org/10.1016/j.conbuildmat.2018.04.024.

[8] J.d.S. Andrade Neto, M.J.S. de França, N.S.d. Amorim Júnior, D.V. Ribeiro, Effects of adding sugarcane bagasse ash on the properties and durability of concrete, Constr. Build. Mater. 266 (2021) 120959, https://doi.org/10.1016/j.conbuildmat.2020.120959.

[9] D.H. Le, Y.N. Sheen, M.N.T. Lam, Fresh and hardened properties of self-compacting concrete with sugarcane bagasse ash–slag blended cement, Constr. Build. Mater. 185 (2018) 138–147, https://doi.org/10.1016/j.conbuildmat.2018.07.029.

[10] G. Sua-lam, N. Makul, Use of increasing amounts of bagasse ash waste to produce self-compacting concrete by adding limestone powder waste, J. Clean. Prod. 57 (2013) 308–319, https://doi.org/10.1016/j.jclepro.2013.06.010.

[11] T. Akram, S.A. Memon, H. Obaid, Production of low cost self compacting concrete using bagasse ash, Constr. Build. Mater. 23 (2) (2009) 703–712, https://doi.org/10.1016/j.conbuildmat.2008.02.012.

[12] W. Ahmad, A. Ahmad, K.A. Ostrowski, F. Aslam, P. Joyklad, P. Zajdel, "Sustainable approach of using sugarcane bagasse ash in cement-based composites: A systematic review", *Case Stud. Constr. Mater.* 15 (2021) e00698, https://doi.org/10.1016/j.cscm.2021.e00698.

[13] A.S. Suprakash, S. Karthiyaini, M. Shanmugasundaram, Future and scope for development of calcium and silica rich supplementary blends on properties of self-compacting concrete - A comparative review, J. Mater. Res. Technol. 15 (2021) 5662–5681, https://doi.org/10.1016/j.jmrt.2021.11.046.

[14] A. Khatun, K. Singh, R. Sharma, Utilization of bagasse ash as a partial replacement of cement in self compacting concrete, Int. J. Civ. Eng. Technol. 9 (7) (2018) 1078–1088.

[15] S.A. Zareei, F. Ameri, N. Bahrami, Microstructure, strength, and durability of eco-friendly concretes containing sugarcane bagasse ash, Constr. Build. Mater. 184 (2018) 258–268, https://doi.org/10.1016/j.conbuildmat.2018.06.220.

[16] B. Yogitha, M. Karthikeyan, M.G. Muni Reddy, Progress of sugarcane bagasse ash applications in production of Eco-Friendly concrete - Review, Mater. Today Proc. 33 (xxxx) (2020) 695–699, https://doi.org/10.1016/j.matpr.2020.06.191.

[17] M.I. Khan, M.A.A. Sayyed, M.M.A. Ali, Examination of cement concrete containing micro silica and sugarcane bagasse ash subjected to sulphate and chloride attack, Mater. Today Proc. 39 (xxxx) (2020) 558–562, https://doi.org/10.1016/j.matpr.2020.08.468.

[18] P. Chindaprasirt, P. Sujumnongtokul, P. Posi, ScienceDirect Durability and Mechanical Properties of Pavement Concrete Containing Bagasse Ash, Mater. Today Proc. 17 (2019) 1612–1626, https://doi.org/10.1016/j.matpr.2019.06.191.

[19] P. Dinakar, Design of self-compacting concrete with fly ash, Mag. Concr. Res. 64 (5) (2012) 401–409, https://doi.org/10.1680/macr.10.00107.

[20] A.G. Abdel-Rahman, Mechanical Properties of Self Compacting Concrete, ERJ. Eng. Res. J. 25 (2) (2002) 1–11, https://doi.org/10.21608/erjm.2002.70617.

[21] O. Boukendakdji, S. Kenai, E.H. Kadri, F. Rouis, Effect of slag on the rheology of fresh self-compacted concrete, Constr. Build. Mater. 23 (7) (2009) 2593–2598, https://doi.org/10.1016/j.conbuildmat.2008.02.024.

Materials Today: Proceedings
Volume 61, Part 3, 2022, Pages 1109-1114

Effect of addition of glass fibre on sugar cane bagasse ash under compressive loading

Harshal R. Nikhade [a], B. Ram Rathan Lal [b]

https://doi.org/10.1016/j.matpr.2021.11.063

Abstract

This research defines the result of studies on a Sugar cane bagasse ash (SCBA) material through laboratory experiment. The material prepared with mix ratio (0.2 % to 1.0 %), Blast furnace slag as mix ratio proportion (10%), glass fibre as reinforcing materials, cement (10%,15% and 20%) and water (50%,60%) for mix in to homogeneous slurry were added to material. The consequence of mix ratio percentages on density, compressive strength are studied. It was observed that the density of materials with inclusion of glass fibre ranging between 1101 kg/m^3 to 1326 kg/m^3. The compressive strength of material increases as percentages of cement increase from 10 to 20%. The compressive strength of materials influenced considerably by mix ratio 0.2 % to 1.0 %. The stress–strain outline was observed to be nonlinear for every mix ratio percentage and curing duration.

Previous Next

Keywords

Bagasse ash; Cement; Blast furnace slag; Density; Compressive strength

Special issue articles Recommended articles

Cited by (0)

Materials Today: Proceedings xxx (xxxx) xxx

Contents lists available at ScienceDirect

Materials Today: Proceedings

journal homepage: www.elsevier.com/locate/matpr

Utilization of phosphogypsum and rice husk to develop sustainable bricks

Sanjay P. Raut [a], Uday Singh Patil [b,*], Mangesh V. Madurwar [c]

[a] Department of Civil Engineering, Yeshwantrao Chavan College of Engineering, Nagpur 441110, India
[b] Department of Civil Engineering, Yeshwantrao Chavan College of Engineering, Nagpur 441110, India
[c] Department of Civil Engineering, Visvesvaraya National Institute of Technology, Nagpur 440010, India

ARTICLE INFO

Article history:
Received 24 September 2021
Received in revised form 28 January 2022
Accepted 6 February 2022
Available online xxxx

Keywords:
Sustainable bricks
Rice husk ash
Phosphogypsum

ABSTRACT

Rapid industrialization and advancement in technology have led to the creation of bulk loads of waste material. Subsequently, the management of these waste materials has been a topic of major concern due to their complex treatment processes. As a result, utilizing these wastes with new ideas has presented viable solutions to global concerns in recent years. One of them is the utilization of waste materials in manufacturing sustainable brick. In the present study, phosphogypsum (PG), rice husk ash (RHA), and cement are used in different proportions [PG-65% to 82.5%, RHA-2.5% to 15%, cement-15% to 20%] to develop sustainable bricks. The developed sustainable bricks were tested as per the Indian and ASTM Standards. Findings revealed that the compressive strength and water absorption value of composition 'H' [PG(77.5%). RHA(7.5%). CEMENT(15%)] meet the requirement of IS 3495:1992. The designed sustainable brick of composition 'H' is shown to have a higher specific heat capacity than commercially available fly ash bricks (FAB) and burnt clay bricks (BCB); hence the developed sustainable brick (composition H) is found to be thermally insulated. Present research can be used by various resource persons who are active in developing sustainable construction materials or bricks from industrial wastes.

Selection and peer-review under responsibility of the scientific committee of the Sustainable Materials and Practices for Built Environment.

1. Introduction

Bricks contain the majority of the embodied energy in a unit of a wall. They are the fundamental building unit of any structure. The interest in developing bricks from diverse industrial or agricultural wastes has increased because population expansion outpaces available housing. The production of building materials has an irreversible impact on the environment. The construction industry's growth is reliant on finite natural resources, thus forcing manufacturers to seek alternative solutions. Due to the increased demand for construction materials, several academics or researchers are attempting to turn industrial wastes into sustainable construction materials. Recycling and reusing these wastes in developing sustainable construction materials may help to reduce reliance on natural resources, conserve non-renewable resources, improve population health and security, and reduce waste disposal costs. The most efficient use of waste materials in the creation of sustainable bricks is a great approach to solve the problem of waste storage while also cutting the cost of construction materials. Globally, different waste materials are produced in industries viz. chemical solvents, paints, agricultural wastes, paper products, industrial by-products, metals, construction wastes, and radioactive wastes. A variety of these wastes has been used for manufacturing sustainable materials like agro-industrial wastes [1], granulated blast-furnace slag, waste paper pulp, waste steel slag, rice husk ash, expanded polystyrene [2], etc. Some of them have become prime waste materials for brick production, and others are still undergoing research works. In this study, statistics about phosphogypsum (PG) and rice husk ash (RHA) have been described to get a general idea of the potentiality of these waste materials. The PG comes from phosphoric acid factories' filtration process [3,4]. Approximately 4–6 Tonnes [5] of PG is generated per ton of P_2O_5 recovered. If PG is dumped in an open area, it could endanger the ecosystem. The handling and control of PG is also a critical challenge in plants owing to their massive volumes, as well as the likelihood of dust, and heavy metals emissions. [6] There are 11 phosphoric acid pro-

* Corresponding author at: Department of Civil Engineering, Yeshwantrao Chavan College of Engineering, Nagpur 441110, India
E-mail address: patil.udaysingh4@gmail.com (U.S. Patil).

https://doi.org/10.1016/j.matpr.2022.02.122
2214-7853/
Selection and peer-review under responsibility of the scientific committee of the Sustainable Materials and Practices for Built Environment.

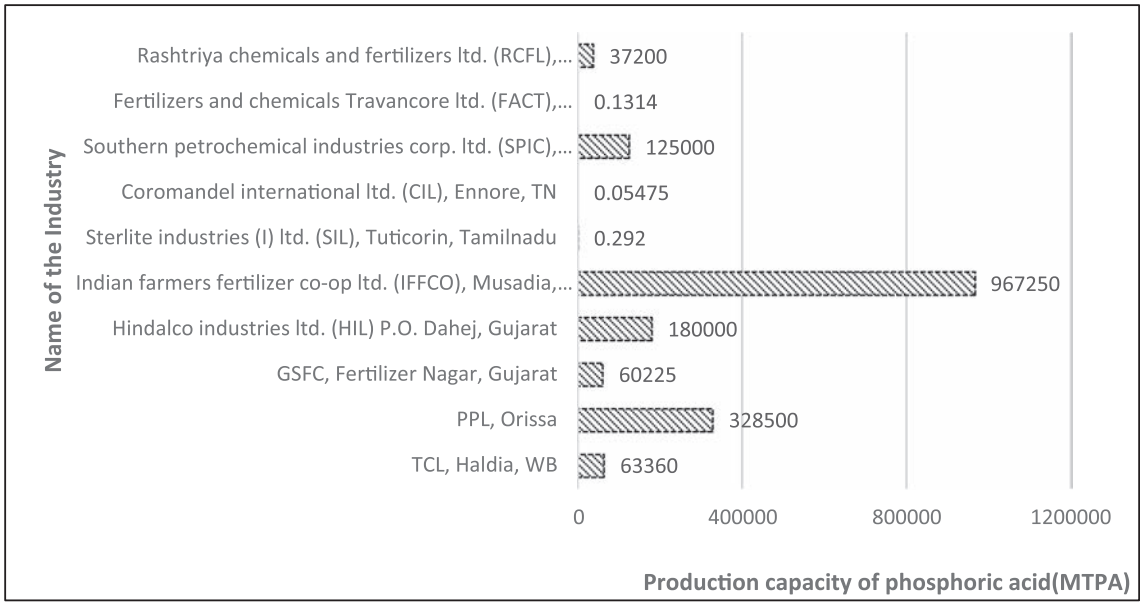

Fig. 1. Details about phosphoric acid manufacturing in India [6].

duction units in India, which are spread over 7 states as shown in Fig. 1. PG is currently stored, and some of it is exported to other businesses for usage as a raw material in cement manufacturing, for alkali soil additives, and reconditioning. The Hazardous Waste Rules [7], exempted PG from the Schedule-I hazardous waste category and mandated that PG from phosphoric acid fertilizer plants be managed according to the CPCB guidelines. PG production in the country is estimated to be over 11 million tonnes per year (based on the assumption that 5 tonnes of PG are produced for every tonne of phosphoric acid). Fig. 1 depicts the country's phosphoric acid production scenario by industry [6].

RHA is a rice milling waste product [8]. It is formed from burned rice paddy husks. Non-crystalline amorphous RHA is created by burning rice husks at temperatures between 500 and 800 °C. RHA contains 90% amorphous silica [9]. Because of its high surface area and high silica concentration, it has good pozzolanic activity. India produces roughly 24 million tonnes of rice husk each year [10]. It is used as fuel in boilers and to generate electricity in the industrial sector. Rice husk has a high ash percentage, ranging from 15 to 20% when compared to other forms of biomass utilized for gasification [11]. RHA is mostly made up of silica. With such a high silica content in the ash, extracting silica from it becomes cost-effective, which has a large market and reduces the need for ash disposal. Rice husk is used for a variety of purposes, including as a fuel in brick kilns, furnaces [12], for parboiling (Rice mills), as a cleaning agent in the machine sector, and in the manufacture of construction materials. Although rice husk has a variety of well-known uses, only a small fraction of it is actually used; the rest is thrown away or used as cattle feed. Because there is so much rice husk produced, the issues associated with its exploitation must be addressed not only in terms of quality but also in terms of quantity. However, efficient brick production is the most promising and profitable use of this ash. Thus, the objective of this study is to develop sustainable bricks using wastes viz. PG, and RHA along with cement as a binding material. Numerous compositions have been explored and tested as per various standards to produce brick with enhanced properties.

2. Material and methodology

2.1. Material

In this study, the PG is procured from Samudrapur Dist. Wardha (Fig. 2). RHA is procured from Ellora Industries, Tumsar, Dist. Bhandara (Fig. 3). Ordinary Portland Cement of grade 43, is employed as a binder for the development of sustainable bricks. The chemical composition was determined by the XRF (Xray-Fluorescence) test at the Indian Bureau of Mines, Nagpur.

2.2. Development of sustainable bricks

To prepare sustainable bricks possible proportions of raw materials were made as shown in Table 1. After that, the raw materials were hand-mixed until they were homogeneous [13]. (Fig. 4) The

Fig. 2. Production of PG from the fertilizer industry.

Fig. 3. Rice Husk Ash.

Table 1
Proportioning of raw materials for sustainable bricks.

Composition name	Phosphogypsum (%)	Cement (%)	Rice husk ash (%)
A	65	20	15
B	70	17	13
C	80	19	1.0
D	80	15	5.0
E	80	17	3.0
F	72.5	15	12.5
G	75	15	10
H	77.5	15	7.5
I	80	15	5.0
J	82.5	15	2.5

Fig. 4. Brick casting work.

mixture is then molded at various proportions in a mould of size 190 × 75 × 100 mm. After that, the developed bricks are dried in the open air for 15 to 20 days as shown in Fig. 5. The dried bricks are subsequently put through a series of testing in compliance with various standards (Table 2).

The initial five compositions namely A to E and the bricks developed using 0–50% PG was not effective as the bricks produced resulted in poor structural formation and also developed shrinkage cracks resulting in a strength low enough to be broken by hand. Hence, it was not possible to carry out tests on them. The next five compositions i.e F to J had constant cement content with increasing PG and decreasing RHA content. The resulting bricks were firm and strong. Therefore, the study is conducted on these five compositions to develop a sustainable brick.

Fig. 5. Manufactured bricks kept for sun drying.

Table 2
Various tests performed on sustainable bricks.

Sr. No.	Tests Performed	IS Codes/References
1	Density and Dimension Test	IS 1077.1992 [14]
2	Compressive Strength Test	IS 3495 Part I.1992 [15]
3	Water Absorption Test	IS 3495 Part II.1992 [15]
4	Voidage Test	IS 3495 Part II.1992 [15]
5	Efflorescence Test	IS 3495 Part III.1992 [15]
6	Specific Heat Capacity	–
7	Shear Bond Test	Source - [16]
8	Flexure Bond Test	ASTM C1072 [17]

3. Results and discussion

3.1. Chemical characterization of PG and RHA

Table 3 shows the findings of the XRF study of PG and RHA. According to the results, the principal ingredients in the PG sample are CaO, F, P_2O_5, SO_3, and SiO_2. The specific gravity of PG is found to range from 2.3 to 2.6, and a maximum dry bulk density varies between 1470 kg/m^3 to 1670 kg/m^3. PG sample is found to have a pH of 2.9, indicating their acidic nature. The major oxides that are found in the RHA samples are iron oxide, silicon dioxide, and aluminium oxide. The specific gravity of RHA is found to be 2.13 and the density of 2216.5 kg/m^3. The specific gravity of cement used is found to be 3.15 and its density is 1440 kg/m^3. From the

Table 3
Chemical composition of phosphogypsum and rice husk ash elements (%).

Chemical composition	Phosphogypsum (PG)%	Rice Husk Ash (RHA)%
Na_2O	0.11	0.12
MgO	0.02	0.44
Al_2O_3	0.13	0.46
SiO_2	1.74	88.32
P_2O_5	1.04	–
SO_3	52.94	–
CaO	38.87	0.67
TiO_2	0.05	–
Fe_2O_3	0.16	0.67
SrO	0.04	–
Y_2O_3	0.008	–
F	0.32	–
K_2O	–	2.91
L.O.I	3.97	5.81

sieve analysis of PG and RHA samples, the majority of particles were found to be retained on a 0.075 mm sieve i.e (31% and 80% respectively).

3.2. Test on sustainable bricks

The results are tabulated for the five compositions namely F, G, H, I, and J, and a comparative study amongst them with commercially available common burnt clay bricks (BCB) and fly ash bricks (FAB) was carried out for each test.

3.2.1. Dimension test

The size of bricks was kept similar to the conventional BCB and FAB bricks (Table 4). The dimensions of bricks are found to slightly differ from standard modular dimension size with a fluctuation margin of ±5 mm.

3.2.2. Density test

As can be seen from Fig. 6, The density of the bricks is observed to increase as the quantity of PG increases, but the RHA decreases. The lowest density was obtained as 1282.05 Kg/m^3 and a maximum of 1695 Kg/m^3 was observed. The density of BCB is around 1700 Kg/m^3. Thus, in comparison, it can be inferred that the PG-RHA bricks are light-weighted and hence have a lower density than BCB and FAB. This suggests that using the RHA and PG in the right amounts can significantly reduce the unit weight of bricks.

3.2.3. Water absorption test

From Fig. 7, It is observed that as the content of PG increases, the water absorption capacity decreases. However, water absorption values of PG and RHA incorporated bricks were higher than BCB and FAB bricks. But, from the obtained results, it is evident that all the composition has a water absorption capacity of less than 20% which agrees with the Indian standard [11]. The water absorption capacity of bricks I and J also satisfied the Chinese standards (JC/T422-2007) [18] wherein the top limit is given as 18%.

3.2.4. Voidage test

The volume of voids in brick should be minimum. Therefore, composition 'H' filters out to be better than any other composition in achieving the voidage criteria (Fig. 8). The fine texture of RHA and PG provides improved particle packing density due to the filler effect, as a result, the void percentage between particles decreases.

3.2.5. Efflorescence test

The bricks were tested in accordance with IS 3495. Part 3 [15]. Fig. 9, It is observed that there was no perceptible deposit of efflorescence after the conduction of the test on any of the tested sample compositions. Therefore, the liability of efflorescence is nil.

3.2.6. Specific heat capacity test

The specific heat of brick is calculated by using a temperature gun (Fig. 11) to measure the average temperatures on all surfaces of the brick before and after an hour in the oven. The specific heat

Table 4
Result of dimension test.

Composition	Length (mm)	Width (mm)	Height (mm)
BCB	195	100	70
FAB	195	100	70
F	195	100	70
G	195	100	70
H	195	100	70
I	195	100	70
J	195	100	70

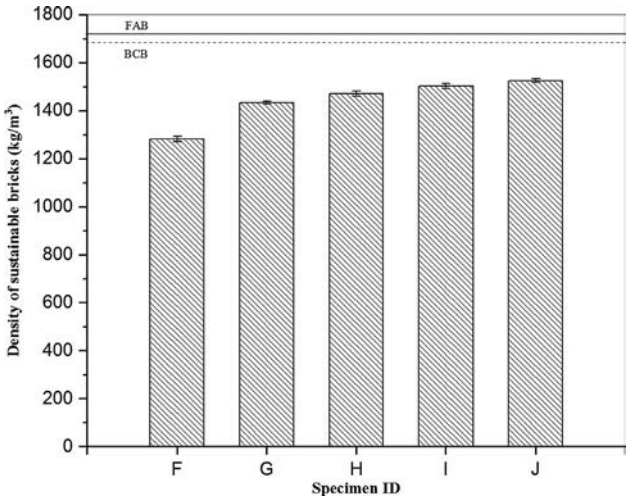

Fig. 6. Density of specimens.

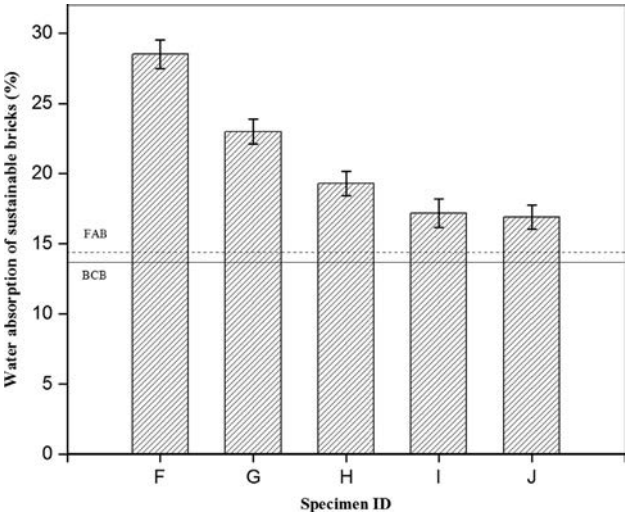

Fig. 7. Water absorption values of specimens.

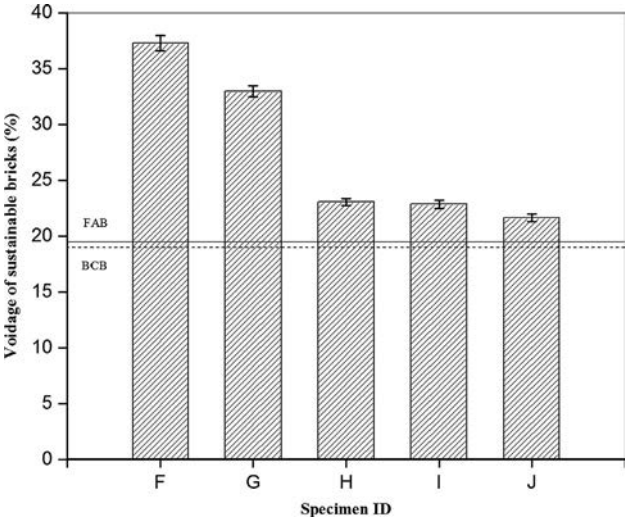

Fig. 8. Voidage test.

Fig. 9. Efflorescence test.

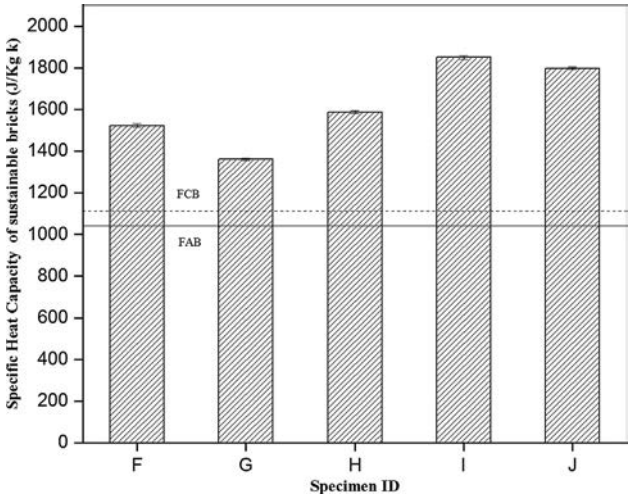

Fig. 10. Specific heat capacity test.

capacity is computed using the energy consumed (q) per brick to generate this temperature difference (t) by the known mass (m) of brick, as shown in Table 5. From Table 5 and Fig. 10, it is evident that PG incorporated bricks require more amount of heat than a common BCB to have their temperature increased by one degree Celsius. Therefore, all sample compositions are more effective in temperature control than BCB.

3.2.7. Compressive strength

Fig. 12 shows the results obtained as an average of measurements taken on three specimens of various compositions. It can be seen that as the percentage of PG increases, the brick's compressive strength increases. i.e up to 77.5%, thereafter slightly decreases but the change observed is very small. Similar results were reported in the past study [19] i.e PG incorporated clay brick showed an increase in strength up to 75%, after which a decrease in strength was observed. Sample composition 'H' clearly has the highest failure load and has a compressive strength of 3.7 N/mm^2 which is more than 3.5 N/mm^2 prescribed by Indian Standard for common brick [14] (see Fig. 13).

3.2.8. Load compression curve

From Fig. 14, it is evident that the line for composition H shows lesser compression as compared to other compositions as the load gradually increases. Also, the area under the curve for composition H is more compared to other compositions. Thus it can be inferred that the energy absorption capacity for bricks made with H composition is higher when compared with the other compositions.

3.2.9. Shear bond strength test

The experimental setup for determining shear bond strength is shown in Fig. 15. This strength is related to the mortar/brick bond. It usually falls in the range of 0.10 to 0.30 Mpa. Fig. 16, The test carried out on sample compositions indicates that sample 'H' has the highest shear strength i.e 0.125 Mpa when compared with other compositions and conventional BCB bricks.

Fig. 11. Measurement of temperature by temperature gun.

3.2.10. Flexure bond strength test

Fig. 17 shows the experimental setup of the flexural bond strength test. Masonry performs well in compression but not so well in tension. Its flexure bond strength is thus determined and it depends on the mortar/brick bond. From Fig. 18, It can be seen that the flexure strength of sample 'H' is 0.09 Mpa whereas sample 'J' has the lowest strength.

Table 5
Result of specific heat capacity test.

Composition	Before avg temp. (k)	After avg temp. (k)	Change in temperature Δt (k)	Mass	Specific heat capacity (J/Kg k)
BCB	7375	10378.83	3003.83	0.236	1143.18
FAB	7376	10590.74	3214.74	0.236	1065.42
F	7374	10355.76	2981.76	0.178	1522.80
G	7374.2	10360.87	2986.67	0.199	1360.88
H	7376	10437.22	3061.22	0.167	1587.60
I	7375	10442.10	3067.10	0.143	1850.54
J	7374	10370.48	2996.48	0.150	1797.84

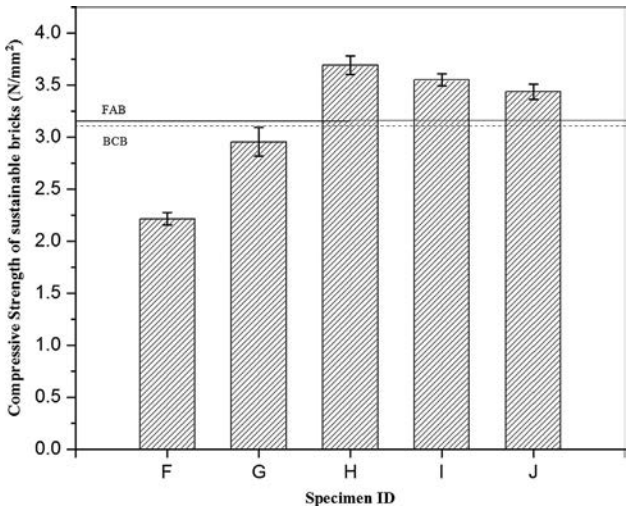

Fig. 12. Compressive strength test.

Fig. 13. Test setup for compressive strength.

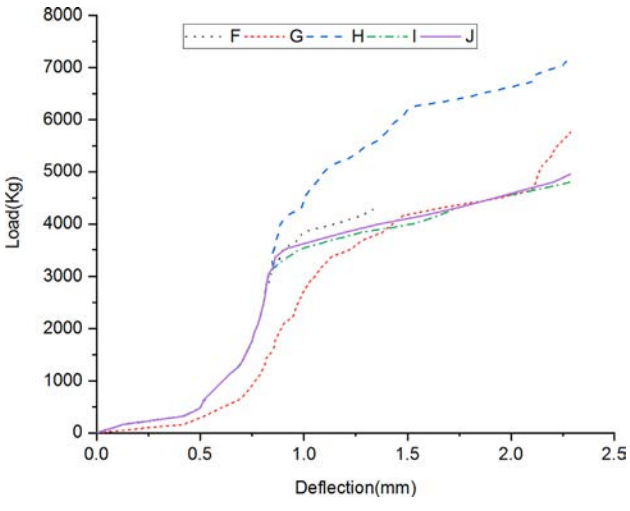

Fig. 14. Combined load-deformation curve of all bricks.

Fig. 15. Test setup for shear bond strength.

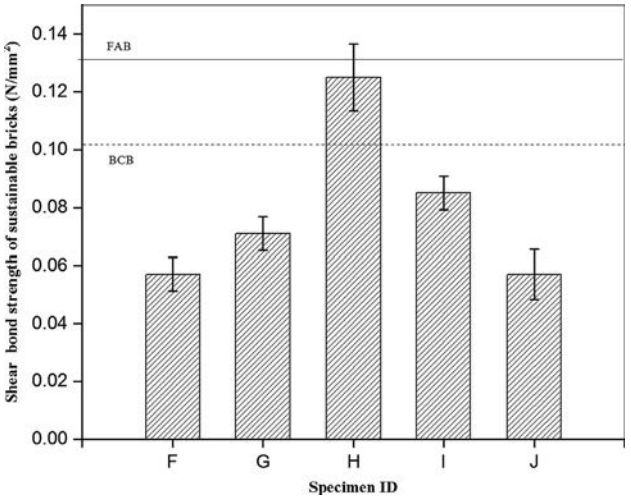

Fig. 16. shear bond strength of specimens.

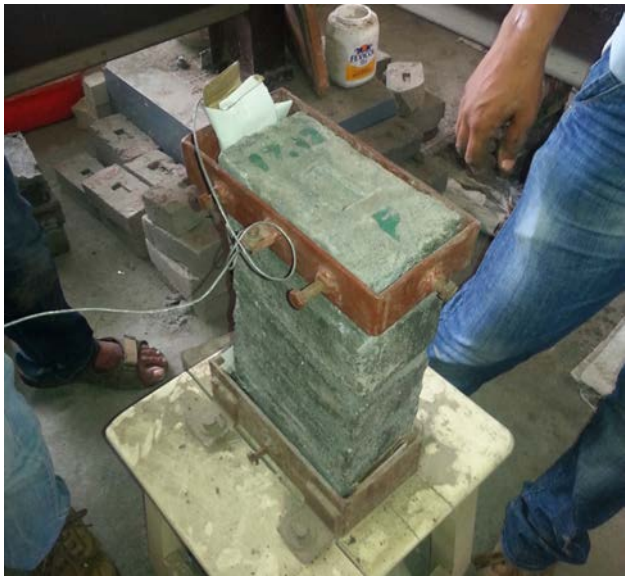

Fig. 17. Test setup for flexure bond strength.

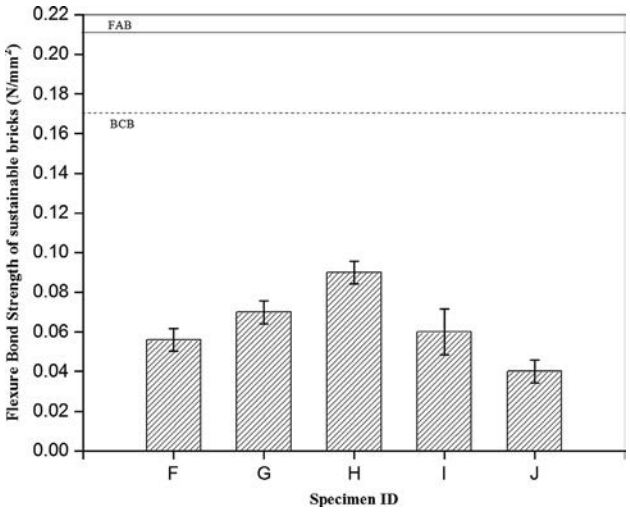

Fig. 18. Flexure bond strength test.

4. Conclusion

the following conclusions can be drawn from this exhaustive study.

1. The brick composition 'H' has better brick properties than other compositions. It has a compressive strength of 3.7 N/mm^2, water absorption of 19.3%, voidage of 23.07%, flexure bond strength of 0.09 N/mm^2, and shear bond strength of 0.125 N/mm^2.
2. The developed sustainable bricks exhibit better thermal insulation than commercially available BCB and FAB.
3. The optimum percentages of PG in the brick increases the mechanical strength of bricks.
4. The value of water absorption of bricks decreases with a percentage increase of PG.
5. As the RHA percentage increases, the water absorption of brick increases, and the compressive strength of brick reduces. Thus the optimum range of RHA is suggested.
6. The results also show that the PG-RHA bricks with proper composition have higher strength compared to conventional BCB and FAB.

As a result, it can be stated that the use of PG and RHA in the brick manufacturing process can be made environmentally friendly if it is done properly and in the right optimum proportion. Bricks created from these wastes might be considered a better alternative to traditional BCB and FAB. This characteristic can be used to turn waste into wealth.

CRediT authorship contribution statement

Sanjay P. Raut: Conceptualization, Methodology, Formal analysis. **Uday Singh Patil:** Methodology, Writing - original draft, Writing - review & editing. **Mangesh V. Madurwar:** Conceptualization, Methodology, Formal analysis.

Declaration of Competing Interest

The authors declare that they have no known competing financial interests or personal relationships that could have appeared to influence the work reported in this paper.

References

[1] V.D. Katare, M.V. Madurwar, S. Raut, Agro-Industrial Waste as a Cementitious Binder for Sustainable Concrete: An Overview, Sustainable Waste Management: Policies and Case Studies, 2020, pp. 683-702.
[2] V.V. Sakhare, S.P. Raut1, S.A. Mandavgane, R.V. Ralegaonkar, Development of sustainable retrofitting material for energy conservation of existing buildings, Int. J. Civil Eng., 13(4A) (2015) 411-418.
[3] T.P. Mashifana, Chemical treatment of phosphogypsum and its potential application for building and construction, Procedia Manuf. 35 (2019) 641–648.
[4] R. Pérez-López, A.M. Álvarez-Valero, J.M. Nieto, Changes in mobility of toxic elements during the production of phosphoric acid in the fertilizer industry of Huelva (SW Spain) and environmentalimpact of phosphogypsum wastes, J. Hazard. Mater. 148 (3) (2007) 745–750.
[5] A.M. Rashad, Phosphogypsum as a construction material, J. Cleaner Prod. 166 (2017) 732–743.
[6] M. o. E. F. &. C. C. CPCB, Guidelines for Management, Handling, Utilisation and Disposal of Phosphogypsum Generated from Phosphoric Acid Plants, Delhi, India: Central Pollution Control Board, 2014-15.
[7] M. o. E. a. Forest, The Hazardous Wastes (Management, Handling And Transboundary Movement) Rules, 2008, Ministry of Environment and Forest, New Delhi, India, 2008.
[8] SK.S. Hossain, L. Mathur, P.K. Roy, Rice husk/rice husk ash as an alternative source of silica in ceramics: a review, J. Asian Ceram. Soc. 6 (4) (2018) 299–313.
[9] B. Singh, in: Waste and Supplementary Cementitious Materials in Concrete, Woodhead Publishing, 2018, pp. 417–460, https://doi.org/10.1016/B978-0-08-102156-9.00013-4.
[10] P.N. Babaso, H. Sharanagouda, Rice Husk and Its Applications: Review, Int. J. Curr. Microbiol. Appl. Sci. 6 (10) (2017) 1144–1156.
[11] A. Nuamah, A. Malmgren, G. Riley, E. Lester, in: Comprehensive Renewable Energy, Elsevier, 2012, pp. 55–73, https://doi.org/10.1016/B978-0-08-087872-0.00506-0.
[12] B. Mistry, Properties and Industrial Applications of Rice Husk, Int. J. Eng. Sci. Computing 6 (10) (2016) 2677–2679.
[13] Patil Udaysingh, Raut Sanjay Padmakar, Ralegaonkar Rahul V, Madurwar Mangesh V, Sustainable building materials using textile effluent treatment plant sludge: a review, Green Materials, 2021, pp. 1-15, 10.1680/jgrma.21.00027.
[14] IS 1077:1992, Common Burnt Clay Building Bricks- Specification, India: Bureau Of Indian Standards, 1992.
[15] IS 3495 (Parts 1 to 4): 1992 Methods of Tests of Burnt Clay, India: Bureau of Indian Standards.
[16] G. Sarangapani, B.V. Venkatarama Reddy, K.S. Jagadish, Brick-Mortar Bond and Masonry Compressive Strength, J. Mater. Civ. Eng. 17 (2) (2005) 229–237.
[17] ASTM C1072, - Standard Test Methods for Measurement of Masonry Flexural Bond Strength,2019 Edition, December 1, 2019.
[18] Non-fired rubbish gangue brick. JC/T422-2007. Bureau of Building Materials Industry of China, Beijing, 2007 [in Chinese with English abstract].
[19] J. Zhou, H. Gao, Z. Shu, Y. Wang, C. Yan, Utilization of waste phosphogypsum to prepare non-fired bricks by a novel Hydration-Recrystallization process, Constr. Build. Mater. 34 (2012) 114–119.

Materials Today: Proceedings xxx (xxxx) xxx

Contents lists available at ScienceDirect

Materials Today: Proceedings

journal homepage: www.elsevier.com/locate/matpr

Use of industrial waste burnt residue to develop sustainable brick

S.S. Meshram [a,*], S.P. Raut [b], M.V. Madurwar [c]

[a] Department of Civil Engineering, YCCE, Nagpur 44110, India
[b] Department of Civil Engineering, YCCE, Nagpur 441110, India
[c] Department of Civil Engineering, VNIT, Nagpur 440012, India

ARTICLE INFO

Article history:
Available online xxxx

Keywords:
Cupola slag
Fly ash
Cement
Sustainable brick
Burnt-residue

ABSTRACT

An increase in environmental concern has occurred from the accumulation of mismanaged industrial burned residue, particularly in developing countries. Recycling these wastes as a sustainable building material seems to be a potential solution not only to the pollution problem, but also to the cost of green building design. In order to develop sustainable construction materials, industrial and incinerated left-over materials are being used. The goal of this research is to find out more about the probability of replacing natural soil in brick production with burned industrial waste, such as Cupola Slag and fly ash. This study is based on various mix proportions for making bricks keeping constant cement by 10 %. Brick mixture was prepared with cupola slag and fly ash for various proportions. From the five distinct mixes with variable CS from 80% to 60%, the M1 mix with 80 % CS, 10% FA, 10% Cement had the highest compressive strength 4.5 N/mm^2. Compressive strength for burnt clay bricks is 3.5 N/mm^2 which is less than cupola slag bricks, while the brick mix M5 (60 CS: 30 FA: 10 cement) had the lowest water absorption and density 6.53 % and 1350.57 kg/m^3. This study reveals that used of cupola slag and fly ah in combination gives satisfactory results to be used in making sustainable bricks. This study also reflects the use of burnt residue to developed sustainable building blocks.

Selection and peer-review under responsibility of the scientific committee of the Sustainable Materials and Practices for Built Environment.

1. Introduction

As a result of urbanization, a large quantity of solid waste was produced, and disposal of this waste became a big issue. Dumping and land-filling of solid waste causes environmental deterioration such as ground water contamination due to leaching, soil pollution, and human health concerns. In recent years, solid waste utilization has grown in potential to recycle valuable materials while reducing solid waste volume, other pollutants, and disposal costs. Brick is a widely utilized building material all over the world. Brick plays an essential part in the construction sector due to its exceptional qualities like as low cost, high strength, and long durability [1]. Because of the high demand for building materials, particularly in the previous decade as a result of rising population, there is a gap in demand–supply management of these resources. As a result, experts are working to create and develop sustainable alternative building material options to suit the ever-increasing demand. Lightweight construction materials low-cost and environmentally friendly are becoming increasingly popular in the construction sector has demanded research on ways to do so while still following the standards material criteria. [2]. Approximately 960 million tonnes of solid waste are created per annum in India as waste material of industrial, mining, and mining operations [3]. Various industrial and agricultural wastes are now being used to create building blocks that provide a long-term answer for the construction sector [4]. Cupola slag is a waste product produced by the cast iron industry when molten steel is alienated from impurities in cupola furnaces [5]. During the cast iron production process in cupola furnaces, roughly 57 percent of the waste is produced. Industry produces between 50 and 3000 tonnes of C.I [6]. In concrete, cupola slag has been used as a partial cement substitute [7]. Cupola slag was also employed in concrete to evaluate its behavior as a partial replacement for both coarse and fine aggregate combinations [8]. For increasing various thermo-mechanical properties, several types of bricks such as burnt clay bricks, fly ash bricks, stone masonry, refractory bricks, solid sand lime bricks, blocks, and thermos acoustic bricks can be employed [9]. Different waste materials were used to make sustainable bricks, including co-fired blended ash, spent mushrooms compost, electric arc furnace

* Corresponding author.
E-mail address: sangitameshram3@gmail.com (S.S. Meshram).

https://doi.org/10.1016/j.matpr.2022.02.336

Selection and peer-review under responsibility of the scientific committee of the Sustainable Materials and Practices for Built Environment.

dust, recycle paper mills waste, ground granulated blast furnace Slag, Sugarcane Bagasse ash, waste glass sludge, waste tyre rubber, construction waste, and residues made from recycled paper. The use of waste glass sludge improved the thermal performance of bricks [10].

Several studies have employed cupola slag as a substitute for cement, fine and coarse aggregate in concrete, pavement, and mortar. Furthermore, there is no research on cupola slag utilized in bricks. This can be put to good use in the manufacture of building blocks. Using this cupola slag as a raw material for making sustainable building materials will not only address the issue of environmental pollution, but it will also improve construction efficiency makes the construction materials sustainable and cost-effective. Cupola slag (CS) was used as the principal raw material in this investigation, along with fly ash as an industrial waste and a consistent cement percentage. Cupola slag and fly ash were physically and chemically characterised in order to determine their suitability as a raw material for developing sustainable building blocks. The physico-mechanical properties of the developed bricks were tested. This research focuses on the efficient use of cupola slag to generate cost-effective, long-lasting, and high-performance building blocks, providing another option for industrial waste management and pollution prevention.

2. Materials And Test Methods

2.1. Raw materials and preparation of brick specimen

Cupola slag and fly Ash (FA) was utilized as an industrial waste in this paper. As a binding material, cement was used. Though the cement percentage was kept constant, variable proportions of fly ash and cupola slag were utilized to provide a wide range of results. Fly ash is a finely distributed residue formed by the burning of pulverized coal that is conveyed away from the combustion chamber by exhaust gases. Coal-fired power plants and steam plants produce fly ash. Coal is commonly pulverized and mixed with air in a boiler's combustion chamber, where it quickly burns, producing molten mineral residue and the heat. Fly ash was gathered from the thermal power plant in Khaperkheda, Nagpur, Maharashtra as shown in Fig. 1. Cupola slag is a type of industrial waste that comes from the steel industry Neco Heavy Engineering and casting limited, MIDC Hingna, Nagpur, Maharashtra. This can only be used for land filling purposes. Cupola slag is a thick substance with a lot of iron filling shown in Fig. 2 (a). Before employing slag in bricks, it must be sieved. It was sieved using a 1.18 mm IS sieve as per Fig. 2 (b). As a binding material, OPC grade 53 cement was used. It was utilized in all proportions with a minimum percentage and a constant proportion.

Fig 1. Fly ash dumped at Thermal Power plant.

The quantity of raw materials necessary was first determined using various combinations of cupola slag, fly ash, and cement, as well as the dimensions of the mould (190 × 90 × 90 mm) and densities of all raw materials. Cupola slag was dry mixed with fly ash and cement in the quantities listed in Table 1. The water was then added into the dry mixture by hand mixing, and blending was resumed until a homogenous consistency was reached. A frog with dimensions of 140 × 60 × 10 mm was cast using the same dimensioned hardwood piece as the brick. Bricks (Fig. 3) were made with the proper moulds. The bricks are next dried for seven days in the sun in a rain-protected shed.

2.2. Test methodology

The chemical constituents of raw materials were analyzed out using X-ray fluorescence (XRF). Using an XRF spectrometer, the elemental composition of cupola slag was examined (Indian bureau of Mines, Nagpur). IS 2386 (Part III):1963 was used to calculate the specific gravity of raw materials [12]. The cupola's particle size distribution was also examined. Block densities are calculated according to IS 2185 (Part 1): 2005 [13]. IS 3495 (Part 1): 1992 was used to conduct compressive strength tests on cupola slag brick specimens (Fig. 3) [14]. All generated bricks were exposed to compressive load at a constant rate of 14 N/mm^2 per minute until failure happened. The weight of bricks soaked in water for 24 h and oven dried brick specimens were used to determine water absorption for bricks. A total of 100 brick specimens were made of various concentrations.

3. Results and discussion

3.1. Properties of raw materials

3.1.1. Chemical composition

The chemical composition of cupola slag and fly ash is shown in Table 2. Cupola slag has substantial amounts of silica and alumina, making it ideal for brick production. The cupola slag also contained trace levels of calcium oxide, magnesium oxide, and iron oxides. The presence of a large amount of silica in the cupola slag improves the binding properties of the brick specimen. Fly ash also has a higher concentration of silica. Cupola slag has more calcium oxide than fly ash, which may contribute to pozzolanic activity. The majority of the chemical composition is made up of SiO_2 and CaO. When Al_2O_3 and MgO were present, more cementitious hydration products were produced. The presence of large quantities of silicon, calcium, and aluminium oxides in the cupola slag indicates that the material has a high reactivity potential. If the content of silica (SiO_2) is greater than 25 %, Sum of Silica (SiO_2), Alumina (Al_2O_3) and iron oxide (Fe_2O_3) is greater than or nearly Equal to 70% and Sulphur (SO_3) is less than 5%, the material can be utilized as a supplementary cementitious material. Cupola slag also has a larger percentage of lime, which aids in the improvement of binding properties.

3.1.2. Specific gravity and unit weight

CS and FA had specific gravities of 2.917 and 1.87, respectively. The water absorption of CS and FA was 0.37 percent and 11 percent, respectively, with CS having much lower water absorption than FA. CS and FA had a density of 1477. 71 kg/m^3 and 1310 kg/m^3 could help reduce the weight of a single brick, resulting in a

Fig. 2. (a) Cupola Slag before sieving (b) Cupola Slag after sieving.

Table 1
Mix proportions of raw materials for bricks.

Mix	No of Specimen	Cupola Slag (%)	Fly Ash (%)	Cement (%)
M1	20	80	10	10
M2	20	75	15	10
M3	20	70	20	10
M4	20	65	25	10
M5	20	60	30	10

Fig. 3. Brick Specimen.

Table 2
Chemical Properties of the raw materials.

Chemical composition	Cupola Slag (CS)	Fly ash (FA) [11]
Lime, CaO (%)	24.27	1.49
Silica, SiO_2	36.86	58.69
Alumina, AL_2O_3	7.5	25.1
Iron oxide, Fe_2O_3	21.79	5.8
Magnesia, MgO	1.22	2.22
Sulphur trioxide, SO_3	0.11	0.12
Sodium Oxide, Na_2O	0.15	0.59
Potassium oxide, K_2O	0.9	4.04
Titanium Oxide, Tio_2	0.97	–
Pentium Oxide, P_2O_5	0.23	–
Sodium Oxide, NaO	0.15	–
Strontium Oxide, SrO	0.03	–
Barium Oxide, BaO	0.04	–
Magnesium dioxide, MnO_2	1.76	–
Chromium trioxide, CrO3	0.11	–
Zirconium dioxide, ZrO2	0.3	–
Tin oxide, SnO2	0.02	–
Free Cl	–	1.28

lighter, more cost-effective construction. The physical parameters of cement are also shown in Table 3.

3.1.3. Particle size distribution

Fig. 4 depicts the particle size distribution of cupola slag. It was discovered that 95% of the cupola slag particles were classified as sand (Table 4). This suggests that the slag particles from the cupola can be used to make bricks. Only 5% of the particles were classified as silt. There are no particles in the gravel and clay categories, as shown in the table. Fig. 5 indicated the particle size distribution for fly ash. It was discovered that 96% of the fly ash particles were classified as sand.

3.2. Mechanical properties

3.2.1. Density

Hollow (open and closed cavity) concrete blocks bearing units must have a minimum block density of 1500 kg/m^3 according to IS 2185 (Part 1):2005. After 28 days, minimum compressive strengths of 3.5, 5.5, 7.0, 8.5, 10.0, 12.5 and 15.0 N/mm^2 are required. As the percentage of CS in the mix increases, the density of the bricks dropped (Fig. 6). When the amount of CS increased from 80 % to 60 %, the dry density reduced by 20%, from 1670.45 kg/m^3 to 1350.57 kg/m^3, as indicated in Table 5. Because of the lower density of fly ash and cupola slag in the brick mix, this trend in density was noticed. This came in handy for making lightweight bricks. As a result, lighter bricks were more cost-effective, economical, and convenient to carry. For all mix proportions, the density of cupola slag bricks is comparable to commercially available fly ash bricks and burnt clay bricks shown in Table 8.

3.2.2. Water absorption

Water absorption has a substantial impact on the quality and strength of bricks. Fig. 7 shows that after introducing cupola slag into the brick mix, water absorption drops from 11.7 to 6.53 % as the proportion of cupola slag lowers according to Table 6. As long as water absorption is less than 15%, as indicated by IS 1077:1992,

Table 3
Physical Properties of the cement, fly ash and cupola slag.

S.N	Tests Performed	Test Results		
		Cement	Fly Ash	Cupola Slag
1	Specific Gravity	3.15	1.87	2.917
2	Density	1440 kg/m^3	1310 kg/m^3	1477.71 kg/m^3
3	Standard Consistency	32 %	–	–
4	Fineness	5 %	15.03	–
5	Water Absorption	–	11 %	0.37 %
6	Initial Setting Time	75 min	–	–
7	Final Setting time	130 min	–	–

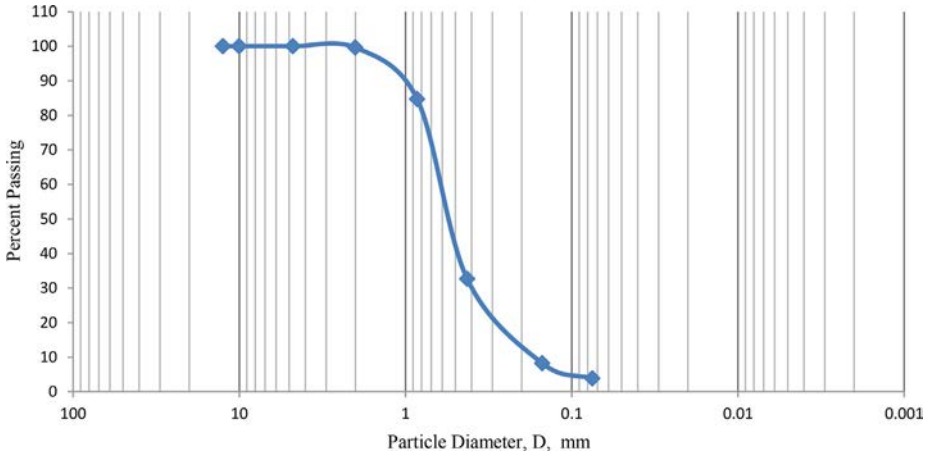

Fig. 4. Particle size distribution for Cupola Slag.

Table 4
Cupola Slag Particle size distribution.

Percentage Distribution	Size Specifications (in mm)	Cupola Slag	Fly ash
Clay	<0.002	0	0
Silt	0.002–0.075	5	4
Sand	0.075–2	95	96
Gravel	>2	0	0

higher brick classes can be utilised, and values less than 20% can be used for brick classes up to 12.5. The addition of CS can thus aid in the production of more durable, cost-effective, and environmentally friendly masonry bricks. Water absorption values of cupola slag bricks for all the mix proportion are less as compared to commercially available fly ash bricks and burnt clay bricks (Table 8).

3.2.3. Compressive strength

Compressive strength is the main characteristic since it indicates the brick's strength and quality. Fig. 8 indicates the results for all of the bricks that were tested. Table 7 shows that the compressive strength of M1 to M5 mixes drops from 4.5 N/mm^2 to 3.6 N/mm^2, a reduction of 12.5 % (Fig. 9). The M1 percentage mix (80 CS: 10 FA: 10 cement) yielded the highest strength. This is because of the chemical makeup of the basic components. Higher compressive strength of bricks mixes with cupola slag due to lower CaO content in the chemical composition. The minimum compres-

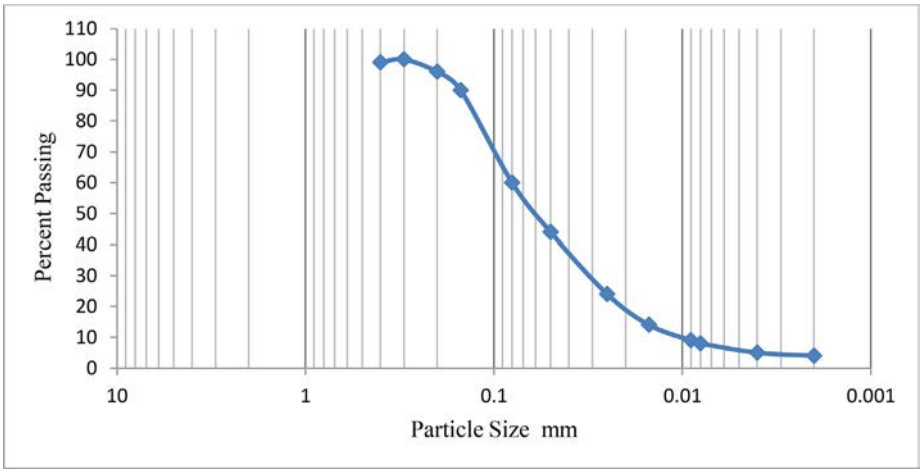

Fig. 5. Particle size distribution for Fly Ash.

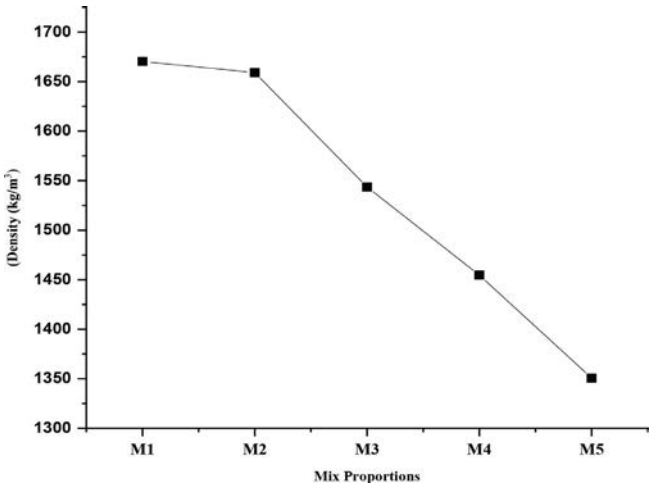

Fig. 6. Density for brick specimens.

Table 5
Density for brick specimens.

Mix Proportion	Density (kg/m^3)
M1	1670.45
M2	1659.1
M3	1543.56
M4	1454.64
M5	1350.57

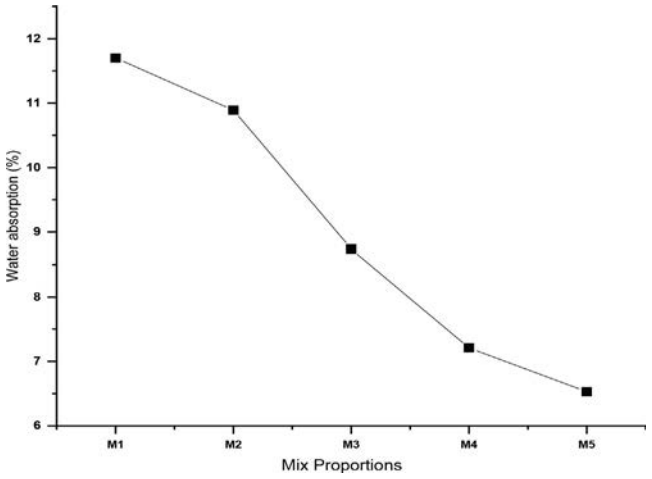

Fig. 7. Effect of CS on water absorption.

Table 6
Water Absorption for brick specimens.

Mix Proportion	Water Absorption (%)
M1	11.7
M2	10.89
M3	8.74
M4	7.21
M5	6.53

sive strength requirements are 3.5 N/mm^2 according to Indian standard code 1077:1992 [15]. All cupola slag brick specimens passed the IS criteria for compressive strength. It also complies with the I Class brick 4 N/mm^2 criteria. As a result, created blocks

Fig. 8. Compression Test on brick Specimen.

Table 7
Compressive strength of brick specimens incorporating CS.

Mix Proportion	Compressive Strength (N/mm^2)
M1	4.5
M2	4.2
M3	4
M4	3.7
M5	3.6

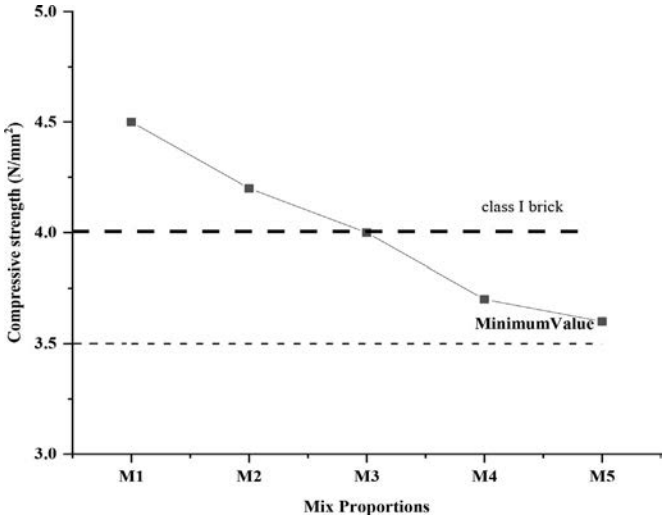

Fig. 9. Compressive strength of brick specimens incorporating CS.

can be employed in environmentally friendly building. Fly ash bricks have a minimum compressive strength of 5.4 N/mm^2, while burnt clay ricks have a minimum compressive strength of 3.5 N/mm^2. When compared to regular burnt clay bricks, cupola slag has higher compressive strengths in all proportions, and when compared to commercially available fly ash bricks, the maximum value is about 4.5 N/mm^2 as per Table 8.

3.2.4. Thermal conductivity

Thermal comfort of human being is based on the amount of heat conduction through the building components, which can be

Table 8
Comparison between Cupola slag bricks, burnt clay bricks, fly ash bricks.

Types of Bricks	Density(kg/m^3)	Compressive Strength (N/mm^2)	Water Absorption(%)	Thermal Conductivity (W/mK)
Burnt Clay Bricks	1650	3.5	27.11	1.24
Fly ash bricks	1700	5.8	18.43	1.1
Cupola Slag bricks	1670.45	4.5	11.7	0.8

reduced by means of thermal protection in building external walls and roofs. The proper use of thermally insulated sustainable construction material in building reduces the cooling/heating load. For good thermally efficient building blocks the requirement is low thermal conductivity. Thermal conductivity is estimated for best combination of brick mix. Thermal conductivity for M1 mix is 0.8 W/mK as per Table 8 which is less than fly ash brick and burnt clay bricks.

4. Conclusion

Dumping on land and disposing of cupola slag results in contamination of the soil, which has a direct influence on the ecosystem. As a result, its productive usage in the construction of bricks provides an alternative remedy for such issues to some extent. Cupola slag as a by-product of the cast iron industry was combined with fly ash as an industrial waste in the construction of bricks with a constant cement ratio. The presence of silica and alumina in the cupola slag indicates that it could be used to make sustainable building blocks. From the five distinct mixes with variable CS from 80% to 60%, the M1 mix with 80 percent CS, 10% FA, 10% Cement had the highest compressive strength 4.5 N/mm^2. Compressive strength for burnt clay bricks is 3.5 N/mm^2 which is less than cupola slag bricks, while the brick mix M5 (60 CS: 30 FA: 10 cement) had the lowest water absorption and density 6.53 percent and 1350.57 kg/m^3 when compared with fly ash bricks and burnt clay bricks it has higher water absorption and density as 18.43 % and 27.11 %, 1700 kg/m^3 and 1650 kg/m^3. Thermal conductivity for M1 mix is 0.8 W/mK which is less than fly ash brick and burnt clay bricks as 1.1 and 1.24. The water absorption value for all of the mixes was determined to be less than 20%, indicating that they meet the specifications. As a result, cupola slag can be used to create long-lasting construction blocks. Cupola slag is a discarded product from the iron industry which can be utilised to make bricks, as well as reducing its disposal and land filling issues, which helps to reduce land pollution. Based on the findings of the tests, it is suggested that CS will be utilised in the production of large-scale building bricks to improve the physico-mechanical properties of bricks, thereby contributing to cost-effective, ecologically friendly, and sustainable building construction.

CRediT authorship contribution statement

S.S. Meshram: Conceptualization, Methodology, Formal analysis. **S.P. Raut:** Methodology, Writing – review & editing. **M.V. Madurwar:** Visualization, Investigation.

Declaration of Competing Interest

The authors declare that they have no known competing financial interests or personal relationships that could have appeared to influence the work reported in this paper.

References

[1] Z. Zhang, Y.C. Wong, A. Arulrajah, S. Horpibulsuk, Review of studies on bricks using alternative materials and approaches, Constr. Build. Mater. 188 (2018) 1101–1118.
[2] S.P. Raut, R.V. Ralegaonkar, S.A. Mandavgane, Development of sustainable construction material using industrial and agricultural solid waste: A review of waste-create bricks, Constr. Build. Mater. 25 (10) (2011) 4037–4042.
[3] C. Bories, M.-E. Borredon, E. Vedrenne, G. Vilarem, Development of eco-friendly porous fired clay bricks using pore-forming agents: A review, J. Environ. Manage. 143 (2014) 186–196.
[4] A. Pappu, M. Saxena, S.R. Asolekar, Solid wastes generation in India and their recycling potential in building materials, J. Building Environ. 42 (6) (2007) 2311–2320.
[5] R. Balaraman, S. Anne Ligoria, Utilization of Cupola Slag in Concrete as Fine and Coarse Aggregate, Int. J. Civil Eng. Technol. (IJCIET) 6 (8) (2015) 06–14.
[6] Vishwash K. Mistry, B.R. Patel, D.J. Varia, Suitability of Concrete Using Cupola Slag as Replacement of Coarse Aggregate, Int. J. Scientific Eng. Res. 7 (2) (2016).
[7] J.O. Afolayan, S.A. Alabi, Investigation on the Potentials of Cupola Furnace Slag in Concrete, Int. J. Integrated Eng. 5 (2013) 59–62.
[8] R. Balaraman, Dr. N.S. Elangovan. "Behaviour of Cupola Slag in Concrete as Partial Replacement with a Combination of Fine and Coarse Aggregates". (2018).
[9] D.S. Vijayan, A. Mohan, J. Revathy, D. Parthiban, R. Varatharajan, Evaluation of the impact of thermal performance on various building bricks and blocks: A review, Environ. Technol. Innovation 23 (2021), https://doi.org/10.1016/j.eti.2021.101577 101577.
[10] S.M.S. Kazmi, M.J. Munir, Y.-F. Wu, A. Hanif, I. Patnaikuni, Thermal performance evaluation of eco-friendly bricks incorporating waste glass sludge, J. Cleaner Prod. 172 (2018) 1867–1880.
[11] T. Bilir, O. Gencel, Ilker Bekir Topcu, Properties of mortars with fly ash as fine aggregate, Constr. Build. Mater. 93 (2015) 782–789.
[12] IS 2386 (Part III):1963 – Methods of tests for aggregate of concrete.
[13] IS 2185(Part 1): 2005 – Concrete Masonry Units- Specification.
[14] IS 3495 (Part 1): 1992 – Methods of tests of Burnt Clay Building bricks.
[15] IS 1077:1992 - Common Burnt Clay Building Bricks - Specification

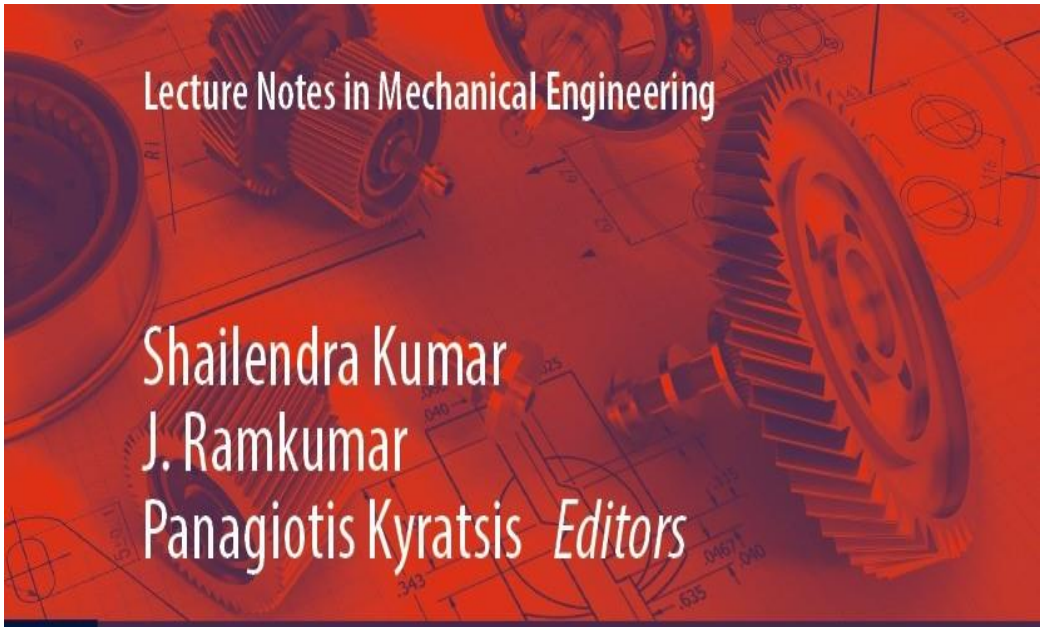

Lecture Notes in Mechanical Engineering

Shailendra Kumar
J. Ramkumar
Panagiotis Kyratsis *Editors*

Recent Advances in Manufacturing Modelling and Optimization

Select Proceedings of RAM 2021

Springer

Recent Advances in Manufacturing Modelling and Optimization pp 623–638Cite as

Electrically Operated Hygiene Bin to Simplify the Initial Stage of Diaper Composting

- Dipti N. Kashyap,
- Rounak Choudhury,
- Pranav Thete,
- Savita Baviskar &
- Pravesh Khatwani

- Conference paper
- First Online: 22 April 2022

Part of the Lecture Notes in Mechanical Engineering book series (LNME)

Abstract

The proposed study is to make a compact electrically operated hygiene bin to reduce the waste generated by the sanitary products like diapers contributing to land pollution. The bin is capable of extracting the biodegradable inner cellulose from the inner layer which is usually made up of polymers. As the disposed diaper takes long time to degrade and thus contributing to land pollution. The proposed machine can tear off the inner layer of diaper and exposes the inner trapped cellulose which will make the composting easy and is applicable for all kinds of sanitary products. This will give new ideas for the generation of biogas and manure. This will result in the reduction of the unwanted generated sanitary waste which could take several years to get degraded if disposed in landfills and can contribute adversely if incinerated that is contributing to the air pollution. Thus, this model could contribute to sustainable development.

Keywords

- **Diaper**
- **Sanitary waste**
- **Composting**
- **Biogas**
- **Manure**
- **Sustainable development**
- **Land pollution**
- **Air pollution**

References

1. Zulfikar Z, Aditama W, Nasrullah (2019) Decomposition process of disposable baby diapers in organic waste with Takakura Method. Int J Sci Healthcare Res 4(1). ISSN: 2455-7587

Google Scholar

2. Ferronato N, Pinedo MLN, Torretta V (2020) Assessment of used diapers composting in Bolivia. MDPI Sustain 12:5055.https://doi.org/10.3390/su12125055
3. Colon J, Ruggieri L, Sanchez A, Gonzalez A, Puig I (2010) Possibilities of composting disposable diaper with municipal solid waste. Res Gate Waste Manage Res 29(3):249–259. https://doi.org/10.1177/0734242X10364684

CrossRef Google Scholar

4. Itsubo N, Wada M, Imai S, Myoga A, Makino N, Shoatake K (2020) Life cycle assessment of the closed-loop recycling of used disposable diaper. MDPI; Resources 9:34. https://doi.org/10.3390/resources9030034
5. Kosemund K, Schlatter H, Ochsenhrit JL, Krause EL, Marsman DS, Erasala GN (2008) Safety evaluation of super absorbent Baby Diaper. Elsevier. https://doi.org/10.1016/j.yrtph.2008.10.005

CrossRef Google Scholar

6. Gerba CP, Huber MS, Naranjo J, Rose JB, Bradford S (1994) Occurrence of enteric pathogens in composted domestic solid waste containing disposable diapers. Sci Direct, Waste Manage Res 13(4):315–324

Google Scholar

7. Rycke AD, Lentz R, Franke M, Prinsen WA (1998) Diapers recycled as compost. integrated soil and sediment research: a basis for proper protection. Soil Environ 1. Springer, Dordrecht, pp 713–723. https://doi.org/10.1007/978-94-011-2008-1_154
8. Khoo SC, Phang XY, Ng CM, Lim KL, Lam SS, Ma NL (2018) Recent technologies for treatment and recycling of used disposable baby diapers. Sci Direct Process Safety Environ Protect 123(2019):116–129

Google Scholar

9. Anderson GF (1991) Recycling the components of used single use human waste collecting and/or absorbing products. United States Patent, Patent number: 4,990,244

Google Scholar

10. Cina Y (1994) Process of recycling of disposable diapers and the machine components thereof. United States Patent, Patent number: 5,322,225

Google Scholar

11. Bartlett BL, Woodenville W (1994) Disposable diaper recycling process. United States Patent, Patent number: 5,292,075

Google Scholar

12. Wilske B, Bai M, Lindenstruth B, Bach M, Rezaie Z, Frede H-G, Breuer L (2013) Biodegradability of poly-acrylate super absorbent in agricultural soil. Springer, Berlin. https://doi.org/10.1007/s11356-013-2103-1

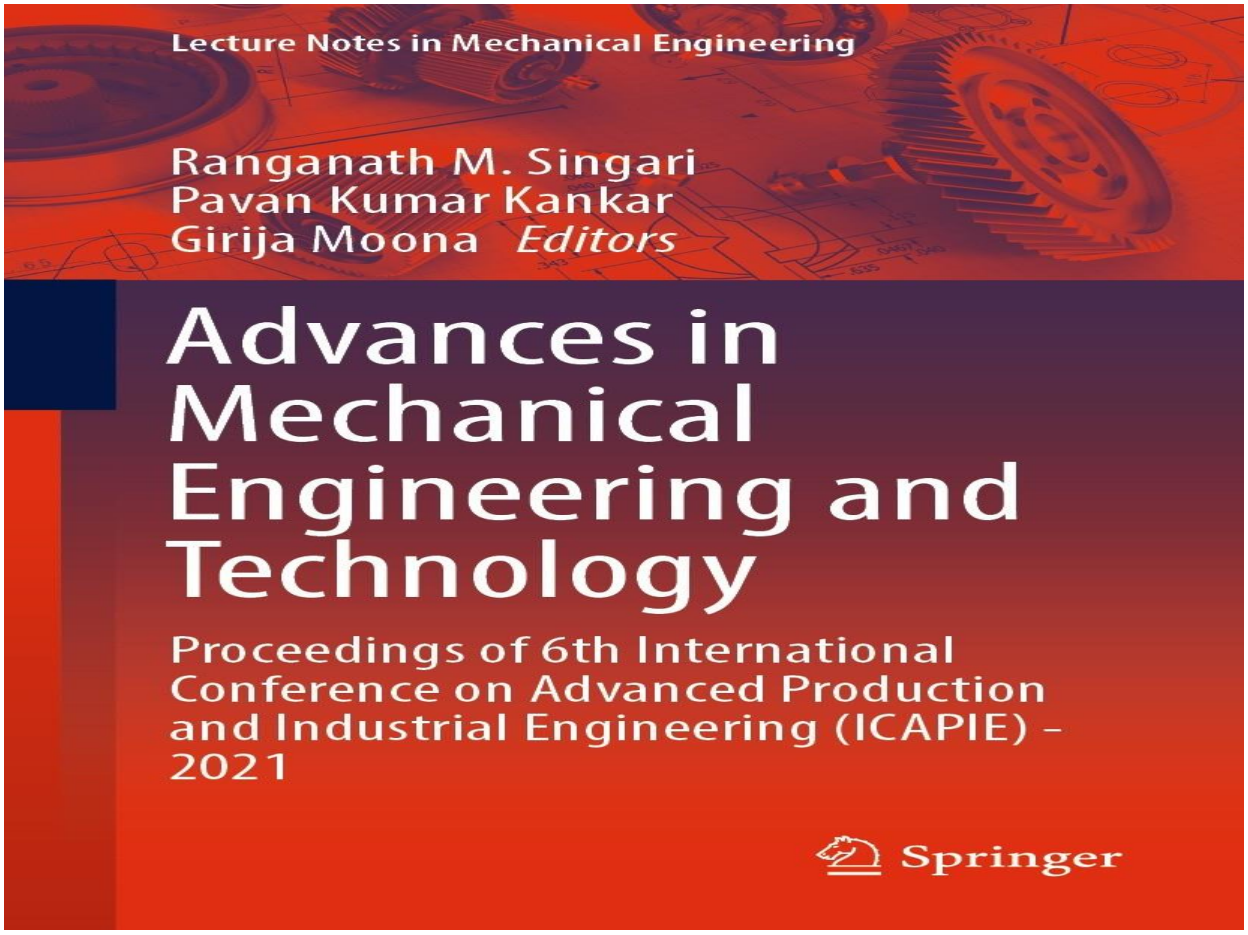

Advances in Mechanical Engineering and Technology pp 127–139Cite as

1. Home
2. Advances in Mechanical Engineering and Technology
3. Conference paper

Design and Performance of Plate-Fin Heat Exchanger: A Brief Review

- Vivek M. Korde,
- Gauri S. Gotmare,
- Priya K. Kachhwah &
- Divyanshu Lokhande

- Conference paper
- First Online: 23 March 2022
- **640** Accesses

Part of the Lecture Notes in Mechanical Engineering book series (LNME)

Abstract

Enhancement of heat transmission properties and pressure loss efficiency with light size and moderate cost in, widely used, compact heat exchangers is an ever-demanding and ongoing

research in the field of heat exchanger applications. This study reviews the numerical and experimental investigations in which different active and passive methods such as using various types of fin geometries, porous fins, fins with grooves or vortex generators, and nanofluids are discussed meticulously to enhance the thermohydraulic effectiveness of plate-fin heat exchangers (PFHE). Some important friction factor and j factor correlations are also discussed. Overall, this review will guide the innovative plate-fin heat exchanger (PFHE) design for a specific purpose.

Keywords

- **Plate fin**
- **Augmentation**
- **Pressure loss**
- **Fins**
- **Compact**

Abbreviations

Re_H:
Reynolds number based on height

f:
Friction factor

Ac:
Minimum free flow area, m^2

Da:
Darcy number, K/H2

L:
Length of porous fin, m

H:
Height of channel, m

A_0:
Total heat transfer surface area of porous fin, m^2

j^*:
Modified j factor

s:
Flow maldistribution parameters

h:
Velocity ratio

j:
Colburn factor

CFD:
Computational fluid Dynamics

Re:
Reynolds number

h:
Fin height, m

s:
Fin spacing, mm

A:
Wave amplitude, mm

L:
Fin wavelength, m

VG:
Vortex generator

CFU:
Common flow up

EG:
Ethylene glycol

Nu:
Nussult number

JF_i***:***
Thermal Hydraulic performance Factor

Φ ***:***
Nanoparticles weight fraction

Pr:
Prandtl number

μμw ***:***
Wall fluid viscosity

μμm ***:***
Average fluid viscosity

l:
Lance length of fin, m

t:
Thickness, m

s:
Fin spacing, m

H:
Height of fin, m

HTE:
Heat transfer enhancement

PPF:
Plain plate fin

JF:
Thermal hydraulic performance factor

R:
Humped radii

εNTU ***:***
Effective number of transfer units

s1:
Non-louvered inlet and exit

s2:
Redirection length of fin

Kc:
Total heat transfer coefficient of cold fluid

CFD:
Common flow down

IRW:
Inline row winglet

SRW:
Staggered rows of winglets

PFHE:
Plate-fin heat exchanger

WFP:
Wavy plate fins

E:
Friction power per unit surface area, w/m^2

E***** ***:***
Core Volume Goodness Index

*****aha***** ***:***
Friction power

*****a ***:***
Overall surface efficiency

h_a***:***
Coefficient of heat transfer at air side ,$wm^2\ ^0c$

F_p***:***
Fin pitch, mm

D_e***:***
Hydraulic diameter

F_h***:***
Fin height, m

t:
Thickness of fin, m

h:
Coefficient of heat transfer , $wm^2\ ^0c$

ΔP ***:***
Pressure drop

***** ***:***
Crease angle

***** ***:***
Crease cycles

References

1. Kang HJW, Li HZ, Li RC, Xin WQ (1994) Tao experimental study on heat transfer and pressure drop characteristics of four types of plate fin-and-tube heat exchanger surfaces. J Thermal Sci 3

   Google Scholar

2. Kim SY, Paek JW, Kang BH (2000) Flow and heat transfer correlations for porous fin in a plate-fin heat exchanger thermal/flow control research center. Korea Institute of Science and Technology, Seoul, Korea, pp 130–650

   Google Scholar

3. Wen J, Li Y, Zhou A, Zhang K (2005) An experimental and numerical investigation of flow patterns in the entrance of plate-fin heat exchanger. Department of Refrigeration and Cryogenics Engineering, School of Energy and Power Engineering, Xi'an Jiaotong University, Xi'an, p 710049

   Google Scholar

4. Sheik Ismail L, Ranganayakulu C (2008) Heat transfer and flow friction correlations for compact wavy plate fin heat exchangers aeronautical. Development Agency, Bangalore, p 560 017

   Google Scholar

5. De Schampheleire S, De Kerpel K, Ameel B, Huisseune H, De Paepe M (2016) Thermal analysis of a commercial plate fin heat exchanger with non-uniform inlet flow conditions. Heat and Combustion Mechanics, Ghent University, Ghent, Belgium, Department of Flow

   Google Scholar

6. Anupam Sinha K, Raman A, Chattopadhyay H, Biswas G (2011) Effects of different orientations of winglet arrays on the performance of plate-fin heat exchangers. Central Mechanical Engineering Research Institute (CSIR). Durgapur, India, p 713209

   Google Scholar

7. Jeong CH, Kim HR, Ha MY, Son SW, Lee JS, Kim PY (2013) Numerical investigation of thermal enhancement of plate-fin type heat exchanger with Creases and holes in construction machinery. Appl Thermal Eng S1359–4311(13)00678–9

Google Scholar

8. Aliabadi MK, Hormozi F, Rad EH (2013) New correlations for wavy plate-fin heat exchangers: different working fluids. Int J Numer Methods Heat Fluid Flow 24(5):1086–1108. Emerald Group Publishing Limited 0961–5539

Google Scholar

9. Junqi D, Yi Z, Gengtian L, Weiwu X (2013) Experimental study of wavy fin aluminum plate fin heat exchanger. Experimental Heat Transfer 26:384–396. 2013 Copyright © Taylor & Francis Group, LLC ISSN: 0891–6152 print/1521–0480

Google Scholar

10. Khoshvaght-Aliabadi M, Hormozi F, Zamzamian A (2013) Role of channel shape on the performance of plate-fin heat exchangers: Experimental assessment. School of Chemical, Petroleum, and Gas Engineering, Semnan University, Semnan, Iran, pp 35131–19111

Google Scholar

11. Khoshvaght-Aliabadi M (2015) Thermal performance of plate-fin heat exchanger using passive techniques: vortex-generator and Nanofluid. Heat Mass Transfer. Springer, Berlin. https://doi.org/10.1007/s00231-015-1603-6
12. Du J, Qian Z-Q, Dai Z-Y (2015) Experimental study and numerical simulation of flow and heat transfer performance on an offset plate-fin heat exchanger. Springer, Berlin. https://doi.org/10.1007/s00231-015-1695
13. .Kuchhadiyaa BB, Rathod PP (2016) Experimental investigation of thermal behaviour of cross-flow plate-fin heat exchanger with offset strip fin. In: 3rd international conference on innovations in automation and mechatronics engineering, ICIAME

Google Scholar

14. Praveen kumara BM, Kaushik ND, Ajith P (2016) A study on the heat transfer enhancement of fin with grooves by natural convection 5(8). an ISO 3297: 2007

Google Scholar

15. Khoshvaght-Aliabadi M, Jafari A, Sartipzadeh O, Salami M (2016) Thermal–hydraulic performance of wavy plate-fin heat exchanger using passive techniques: perforations, winglets, and Nanofluids. Int Commun Heat Mass Transfer 78:231–240

Google Scholar

16. Mete Ozturk M, Dogan B, Erbay B (2017) Thermo-hydraulic performance assessment of a compact heat exchanger by varying plate fins. In: 6th international conference on renewable energy research and application

Google Scholar

17. Juan D, Hai-Tao Z (2017) Numerical simulation of a plate-fin heat exchanger with offset fins using porous media approach. Springer, GmbH Germany Heat Mass Transfer. https://doi.org/10.1007/s00231-017-2168-3
18. Zhang X, Wangb Y, Li M, Wang S, Li X (2017) Improved flow and heat transfer characteristics for heat exchanger by using a new humped wavy fin. Appl Therm Eng 124:510–520

CrossRef Google Scholar

19. Javaherdeh K, Vaisi A, Moosavi R, Esmaeilpour M (2017) Experimental and numerical investigations on louvered fin-and-tube heat exchanger with variable geometrical parameters. J Thermal Sci Eng Appl. https://doi.org/10.1115/1.4035449
20. Samadifar M, Toghraie D (2018) Numerical simulation of heat transfer enhancement in a plate-fin heat exchanger using a new type of vortex generators. Appl Therm Eng S1359–4311(17):36306–36308

Google Scholar

21. Yang H, Wen J, Wang S, Li Y (2018) Effect of fin types and prandtl number on performance of plate-fin heat exchanger: experimental and numerical assessment. Appl Therm Eng S1359–4311(18):30778–30786

Google Scholar

22. Xiaoxiang L, Anlin W, Fumin L (2019) Research and structural optimization of heat dissipation performance plate-fin heat exchanger. In: 2019 2nd world Conference on mechanical engineering and intelligent manufacturing

Google Scholar

23. Morteza K-A, Mortazavi S (2019) Combined effects of holes and winglets on chevron plate-fins to enhance the performance of a plate-fin heat exchanger working with Nanofluid. J Thermal Energy Gener Transp Storage Conversion. https://doi.org/10.1080/08916152.2019.1569176
24. Ma'arof MIN, Chala GT, Husain H, Mohamed MS (2019) Influence of fins designs, geometries and conditions on the performance of a plate-fin heat exchanger-experimental perspective. J Mech Eng Sci 13(1):4368–4379. ISSN: 2289–4659; e-ISSN: 2231–8380

Google Scholar

25. Haoa J-H, Chena Q, Rena J-X, Zhanga M-Q, Aic J (2019) An experimental study on the offset-strip fin geometry optimization of a plate-fin heat exchanger based on the heat current model. Appl Thermal Eng 154:111–119

Google Scholar

26. Gong J, Onishi J, He A, Kametani Y, Hasegawa Y, Shikazono N (2020) Heat transfer enhancement and pressure loss in a plate-fin heat exchanger with V-shaped oblique wavy surface. Int J Heat Mass Transfer 161:120263

Google Scholar

27. Ozturk MM (2020) Effect of fin type on performance of compact heat exchangers with mini-channel. Heat Transfer Eng https://doi.org/10.1080/01457632.2020.1860522
28. Dodiya K, Bhatt N, Lai F (2020) Louvered fin compact heat exchanger—a comprehensive review. Int J Ambient Energy https://doi.org/10.1080/01430750.2020.1839549
29. Abu-Khader MM (2012) Plate heat exchangers: recent advances. Renew Sustain Energy Rev 16(4):1883–1891. https://doi.org/10.1016/j.rser.2012.01.009
30. Guo K (2015) Optimization of Plate/Plate-Fin Heat Exchanger Design, A thesis submitted to The University of Manchester for the degree of Doctor of Philosophy, Centre for Process Integration, School of Chemical Engineering and Analytical Science

Google Scholar

31. Xue Y, Ge Z, Du ID X, Yang L (2018) On the heat transfer enhancement of plate fin heat exchanger. Energies

Google Scholar

Download references

Author information

Authors and Affiliations

1. **Department of Mechanical Engineering, Yeshwantrao Chavan College of Engineering, Nagpur, 441110, India**
Vivek M. Korde, Gauri S. Gotmare, Priya K. Kachhwah & Divyanshu Lokhande

Editor information

Editors and Affiliations

1. **Department of Design, Department of Mechanical Engineering, Delhi Technological University, New Delhi, India**

Prof. Ranganath M. Singari
2. **Department of Mechanical Engineering, Indian Institute of Technology Indore, Indore, Madhya Pradesh, India**
Dr. Pavan Kumar Kankar
3. **Physico-Mechanical Metrology, CSIR - National Physical Laboratory, New Delhi, India**
Dr. Girija Moona

Rights and permissions

Copyright information

About this paper

Cite this paper

Korde, V.M., Gotmare, G.S., Kachhwah, P.K., Lokhande, D. (2022). Design and Performance of Plate-Fin Heat Exchanger: A Brief Review. In: Singari, R.M., Kankar, P.K., Moona, G. (eds) Advances in Mechanical Engineering and Technology. Lecture Notes in Mechanical Engineering. Springer, Singapore. https://doi.org/10.1007/978-981-16-9613-8_12

Download citation

- DOIhttps://doi.org/10.1007/978-981-16-9613-8_12
- Published23 March 2022
- Publisher NameSpringer, Singapore
- Print ISBN978-981-16-9612-1
- Online ISBN978-981-16-9613-8
- eBook PackagesEngineeringEngineering (R0)

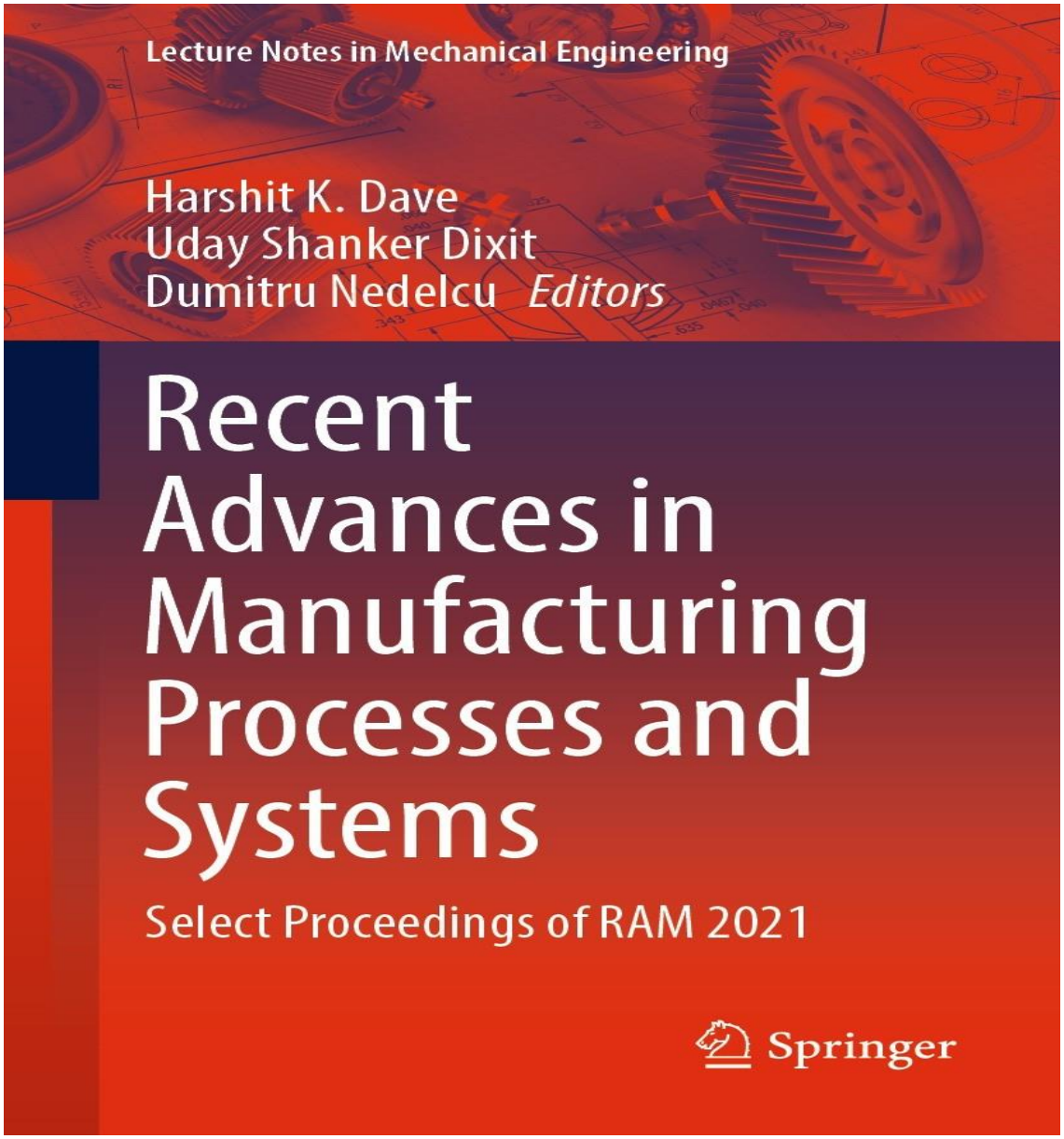

Recent Advances in Manufacturing Processes and Systems pp 437–443Cite as

Evaluating Torsional Properties of FDM Components for Various Layer Heights

- Prasad A. Hatwalne &
- S. B. Thakare

- Conference paper
- First Online: 03 March 2022

Circuit is open

Part of the Lecture Notes in Mechanical Engineering book series (LNME)

Abstract

In the below presented work, the steps are taken to evaluate torsional strength of parts developed using fused deposition modelling (FDM). For this test, samples were 3D printed using ABS material and then investigated to understand the influence of layer height on the torsional strength of components. The parts were fabricated and tested as per ASTM standards with varying the layer height of 0.14 mm, 0.16 mm and 0.22 mm. Further, the parts were applied with acetone bath treatment and its effect on torsion strength is also investigated. The obtained values of torsional properties were compared with the injection moulded parts from literature. The results show that torsional properties of components manufactured by FDM are significantly influenced by variation in layer height. Comparatively, injection moulded parts were found to have better torsional properties.

Keywords

- **Fused deposition modelling (FDM)**
- **Injection moulding**
- **Torsional strength**

References

1. Dey A, Yodo N (2019) A systematic survey of FDM process parameter optimization and their influence on part characteristics. J Manuf Mater Process 3(3):64–70

Google Scholar

2. Rajpurohit SR, Dave H (2018) Effect of process parameters on tensile strength of FDM printed parts. Rapid Prototyping J 24(8):1317–1324

CrossRef Google Scholar

3. Alafaghani A, Qattawi A, Alrawi B, Guzman A (2017) Experimental optimization of fused deposition modelling processing parameters: a design-for-manufacturing approach. Procedia Manuf 10:791–803

CrossRef Google Scholar

4. Garg A, Bhattacharya A, Batish A (2017) Chemical vapor treatment of ABS parts built by FDM: Analysis of surface finish and mechanical strength. Int J Addit Manuf technology 89:2175–2191

CrossRef Google Scholar

5. Shubham P, Sikidar A, Chand T (2016) The influence of layer thickness on mechanical properties of the 3D printed ABS polymer by fused deposition modeling. Key Eng Mater 706:63–67

CrossRef Google Scholar

6. Gerg A, Bhattacharya A, Batish A (2016) On surface finish and dimensional accuracy of FDM parts after cold vapor treatment. Mater Manuf Process 31(4):522–529

CrossRef Google Scholar

7. Rauta S, Jattib VKS, Khedkar NK, Singh TP (2014) Investigation of the effect of built orientation on mechanical properties and total cost of FDM parts. In: Procedia materials science, 3rd international conference on material processing andmaterial charecterisation vol 6, pp 1625–1630

Google Scholar

8. Nancharaiah T, Raju DR, Raju VR (2010) An experimental investigation on surface quality and dimensionalaccuracy of FDM components. Int J Emerg Technol 1(2):106–111

Google Scholar

9. Gebisa AW, Lemu HG (2019) Influence of 3D printing process parameters on tensile property of ULTEM 9085. In: Procedia manufacturing, 14th global congress on manufacturing and management, vol 30, pp 331–338

Google Scholar

10. Vălean C, Marșavina L, Mărghita M, Linul E, Razavi J, Berto F (2020) Effect of manufacturing parameters on tensile properties of FDM printed specimens. In: Procedia

structural integrity, MedFract1 the 1st mediterranean conference on fracture and structural integrity, vol 26, pp 313–320

Google Scholar

11. Afrose MF, Masood SH, Iovenitti P, Nikza M, Sbarski I (2016) Effects of part build orientations on fatigue behaviour of FDM-processed PLA material. Prog Addit Manuf 1:21–28

CrossRef Google Scholar

12. Balderrama-Armendariz CO etal (2018) Torsion analysis of the anisotropic behavior of FDM technology. Int J Adv Manuf Technol 96:307–317

Google Scholar

Download references

Author information

Authors and Affiliations

1. **Department of Mechanical Engineering, YCCE Nagpur, Nagpur, India**
Prasad A. Hatwalne
2. **Department of Mechanical Engineering, PRMIT&R, Badnera, India**
S. B. Thakare

Editor information

Editors and Affiliations

1. **Department of Mechanical Engineering, S. V. National Institute of Technology, Surat, Gujarat, India**
Dr. Harshit K. Dave
2. **Department of Mechanical Engineering, Indian Institute of Technology Guwahati, Guwahati, Assam, India**
Dr. Uday Shanker Dixit
3. **Gheorghe Asachi Technical University of lasi, Iasi, Romania**
Prof. Dumitru Nedelcu

Rights and permissions

Copyright information

About this paper

Cite this paper

Hatwalne, P.A., Thakare, S.B. (2022). Evaluating Torsional Properties of FDM Components for Various Layer Heights. In: Dave, H.K., Dixit, U.S., Nedelcu, D. (eds) Recent Advances in Manufacturing Processes and Systems. Lecture Notes in Mechanical Engineering. Springer, Singapore. https://doi.org/10.1007/978-981-16-7787-8_34

Download citation

- .RIS
- .ENW
- .BIB

- DOIhttps://doi.org/10.1007/978-981-16-7787-8_34
- Published03 March 2022
- Publisher NameSpringer, Singapore
- Print ISBN978-981-16-7786-1
- Online ISBN978-981-16-7787-8
- eBook PackagesEngineeringEngineering (R0)

Volume 62, Part 2, 2022, Pages 1115-1121

Optimization of green sand process for quality improvement in castings by using combination of Taguchi Techniques-GRA-PCA

Author links open overlay panel S.S. Chaudhari, S.N. Aloni
Show more

https://doi.org/10.1016/j.matpr.2022.04.322Get rights and content

Abstract

The castings produced by a sand casting process have multiple quality features. The quality of a casting always depends upon proper controlling of enormous parameters involved in the process as well as proper combination among these parameters, while some of the defects are found persisting and difficult to avoid. Controlling the process to avoid the rejections of cast components due to the presence of such persisting defects mainly depends on the right understanding of the parameters associated with it. In the work presented in this paper, the primary focus is on the optimization of essential parameters of the green sand process to minimize the occurrences of these persisting defects in gray iron automotive components through experimental investigation using

effective approach. The study applies the Taguchi‟s „Design of Experiments‟ approach in combination with grey relational analysis (GRA) and principal component analysis (PCA) for determining the optimal level of parameters to minimize the defects Shrinkage porosity (SP), blowholes (BH), sand inclusion (SI), scabbing (SC) and low hardness (LH), which are persisting in the foundry industry producing cylinder heads and other castings required in the automotive, factory situated in central India. Optimal levels of parameters were determined by the single grey relational grade (GRG) obtained from GRA for overall improvement in multi-quality characteristics. PCA is used to determine the corresponding weighting values of each performance. The outcomes of this study assure that the approach used in this work, is useful to foundry industries to minimize the persisting casting defects.

Introduction

The green sand process for casting production is the most famous casting process and is widely used in small, medium and large-scale foundry industries for manufacturing grey iron (GI) castings. Among the several possible defects in castings produced by a green sand casting process, some of the casting defects are persisting and more challenging to avoid. Monore [1] stated that, Porosity is one of the most persistent casting defects and common complaint of casting users, the final reliability of a casting and mechanical properties of the casting is greatly influenced by the presence of such defects. Krause [2], reported that gray cast iron is most favorable among all the cast irons mainly, because of its capacity to be cast into intricate shapes at a comparatively lower production cost. Alagarsamy [3], tried to illustrate the systematic approach for the correct identification of casting defects to reduce rejections, particularly, ambiguous casting defects such as porosity and inclusions. He also exemplifies the mechanism of defect formation. In the actual case study described, shrinkage and a porosity defect in spheroidal graphite cast iron is correctly identified through defect mapping and analysis and is resolved by controlling key process factors. Rehman, et. al. [4], discussed the factors that measure the performance of green manufacturing (GM) in India, and find out the status of understanding and execution of GM in India.

Saikaya et.al. (2015) [5] applied an effective approach for optimizing the multi-response output such as vibration signals, cutting force, and surface roughness in the milling process. The effect of process parameter such as depth of cut, feed rate, cutting speed, and number of inserts on multi-response outputs was investigated and parameters were simultaneously optimized by using Taguchi-based gray relational analysis. Kaushik and Singhal (2018) [6] analyzed the effect of three process parameters; load, sliding distance and wt. % of SiC on the multi-quality characteristics of metal matrix composites by using the hybrid Taguchi-Grey relational Analysis (GRA) -Weight method.. Zerti et. al. (2018) [7], optimized the machining parameters. Grey relational analysis "GRA" based on Taguchi design was proposed in his study for simultaneous improvement of surface quality and productivity. Confirmation experiments proved the powerful improvement of experimental results and effectiveness of the multi-optimization technique applied.P.D. Kamble (2017) [8], in this paper Taguchi philosophy is used for design of experiment. The response factor surface roughness is evaluated experimentally for turning process. The cutting speed, feed rate, nose radius, depth of cut are used as controllable factors. Signal to noise ratio of surface roughness is tabulated by Smaller-the-better Taguchi quality characteristic Experimentation is conducted by orthogonal array L27. From the review of the above significant studies on multi-objective optimization of respective manufacturing process, it is revealed that in most of the above studies a combination of Taguchi method with grey relational analysis (GRA) and principal component analysis (PCA) for determining the optimal level of parameters found very powerful to deal with multi-objective optimization problem.

Section snippets

Experimental design

The Taguchi approach to parameter design is a powerful technique among optimization techniques that can be effectively, applied to foundry industries, Bendell A et.al.(2019) [9]. Taguchi-based GRA is a statistical method to analyze the complex multi-response systems. It was proposed by Deng, in 1982, to measure the degree of approximation among the sequences with the help of gray

relational grade (GRG) to explore the relationship between responses and input parameters [10], [11].

Taguchi based grey relational analysis (GRA) coupled with principal component analysis (PCA)

Grey system theory provides an effective solution for optimization of the multiple performance characteristics. Grey relational analyses based on this theory provide relation between process parameters and multi-responses. GRA uses a grey relational grade to evaluate the multiple performance characteristics. As a result, optimization of multiple performance characteristics can be converted into optimization of a single grey relational grade as shown in Table 5. The stepwise procedure of GRA

Result and discussion

The observations made from the analysis of the results obtained are mentioned below.

- 1.
  The optimal combination for multi-performance obtained from combination of proposed methods that is, Taguchi-GRA-PCA is set with levels as, A1, B2, C2, D2, E2, F2, G2, H2, J1, K2, L1, M2, N3, O1, P1,Q3,R2,S3,T1.
- 2.
  Based on the analysis of variance, the process parameters that significantly affects the multi-performance characteristics is carbon equivalent (CE), pouring temperature, steel scrap, green compression

Declaration of Competing Interest

The authors declare that they have no known competing financial interests or personal relationships that could have appeared to influence the work reported in this paper.

Acknowledgements

The author acknowledges the guidance and support by foundry industry personnel‟s for conduction of experiments and recording of outcomes required for subsequent study in this work.

I, Dr. Sharad S. Chaudhari is a Mechanical Engineer. I am working as a Associate Professor in Yeshwantrao Chavan College of Engineering (YCCE), Wanadongri, Nagpur-441110, India. I received my MTech in Production Engineering and PhD from Nagpur University. My area of specialization is Production Engineering and Manufacturing Science. He is having more than 22 years of experience in teaching. Currently, his focus areas for research are foundry issues and modernisation, industrial safety and risk

References (20)

- Monroe R. Porosity in Castings.AFS Transactions, American Foundry Society, Schaumburg, IL USA,...
- Krause DE.Gray Iron-A Unique Engineering Material. Gray, Ductile, and Malleable Iron Castings-Current Capabilities,...
- Alagarsamy A.Casting defect analysis procedure and A case history.Keith Mills Symposium on Ductile Iron...
- M.A.A. Rehman *et al.*

  Research instrument design for performance measures of green manufacturing practices in India – a pilot study
  Int. J. Environment and Waste Management.
  (2015)
- M. Sarıkaya *et al.*

  Modeling and multi-response optimization of milling characteristics based on Taguchi and gray relational analysis
  J Engineering Manufacture
  (2015)
- N. Kaushik *et al.*

  Wear conduct of aluminum matrix composites: A parametric strategy using Taguchi based GRA integrated with weight method‟
  Cognet Enginnering
  (2018)
- O. Zerti *et al.*

Simultaneous improvement of surface quality and productivity using grey relational analysis based Taguchi design for turning couple (AISI D3 steel/ mixed ceramic tool (Al2O3 + TiC))
Inter. J. Industrial Eng. Computations
(2018)

- P.D. Kamble, “Taguchi Approach for Experimental Investigation to Minimize Surface Roughness for Turning EN 24 Steel”,...
- A. Bendell *et al.*

(eds.). Taguchi methods: applications in world industry
(1989)

- J.I. Deng

Control problems of grey systems
Systems Control Lett
(1982)
There are more references available in the full text version of this article.

Cited by (2)

- Metal encapsulation of waste foundry sand stabilized with alkali-activated binder: Batch and column leaching tests
2023, Journal of Environmental Management

Show abstract

- Elastic-viscoplastic constitutive equations of K439B superalloy and thermal stress simulation during casting process
2023, China Foundry

I, Dr. Sharad S. Chaudhari is a Mechanical Engineer. I am working as a Associate Professor in Yeshwantrao Chavan College of Engineering (YCCE), Wanadongri, Nagpur-441110, India. I received my MTech in Production Engineering and PhD from Nagpur University. My area of specialization is Production Engineering and Manufacturing Science. He is having more than 22 years of experience in teaching. Currently, his focus areas for research are foundry issues and modernisation, industrial safety and risk management, minimum quantity lubrication. He has many publications in journals of national and international repute.My research work is published in reputed international Journals and also presented in Institutes of National repute, IIT's and NIT's and Autonomous Institutes.

View full text

Volume 57, Part 1, 2022, Pages 316-320

Experimental investigation of different electrical configurations and topologies for Photovoltaic system

Author links open overlay panel
Rajkumar B. Chadge [a], Neeraj Sunheriya [a], Jayant P. Giri [a], Naveen Shrivastava [b]
Show more

https://doi.org/10.1016/j.matpr.2022.03.097Get rights and content

Abstract

The recent solar technology offers clean, economic andenvironment friendly energy applications to society. Photovoltaic (PV) modules are directly converted the incident solar radiations into electrical energy. These modules are connected in different electrical configurations and topologies. These configurations and topologies are decided as per the power requirement. The selection of variety of electrical configurationsand type of topologies arecritical for performance of the PV system. This research paper aims to Experimental investigationthe different PV array configurations (Series Parallel and Total cross Tied) with two different topologies (4SX5P and 5SX4P) in non-shading and partially shaded condition. It is observed that impedance of solar panel and input resistance playing important role in achieving maximum power output of PV system. The 4Sx5P topology shows the maximum power of 12 W is

observed at 8 am for uniform condition and 11.7 W is at 9:30 a.m. for partial shaded. Similarly 18.57 W at 9:15 a.m. for uniform condition and 15.26 W at 10:45 a.m. are observed for partial shaded condition of 5Sx4P topology. The power generated in both topologies is almost following the same pattern. From above graph it is clear that approximately 9–13% power variation was observed in uniform and partial shading condition for both the topologies.

Introduction

Energy is the most important factor for the economic as well as social and technological development of both developing and developed countries [1]. Mostly we are depending on different non renewable energy sources for satisfying our daily energy demand. In non-renewable energy sources fossil fuel are playing crucial role for managing these demands. But scarcity of fossil fuel, continuous price hike and environmental concern are the major bottle neck for usingthese for a long time. Detail literature review shows that lot of work was already carried out for minimizing the adverse effect of fossil fuels but these efforts are not enough as per different published reports on global disturbance. In recent year's renewable energy sources like solar energy, wind energy, bio gas and fuel cell technology are showing potential for bridging the gap of future energy demands with environmental concern. These energy sources having their own challenges and at the same time also providing different opportunities. Zero carbon emission, easy availability and environment friendlyare the important characteristics which attract lot of research on renewable energy sources.

Recently it is observed that solar technology is one of the most promising areas for future energy demand. Solar energy can be used in a direct or indirect way for producing the energy. In indirect utilization of solar energies like wind energy, hydro energy, ocean energy etc. observe that solar energy having secondary effect on production. Photoelectric and photo thermal are the direct conversion of energy from solar radiation. Photoelectric conversion direct directly converts the incident radiation into electrical energy while the photo thermal conversion directly convert the incident radiation into thermal energy. On grid, off grid and hybrid solar power plant are works on the principle of photoelectric conversion.

Solar water heater, solar cooker are working on the principle of solar photo thermal conversion.

The maximum achievable efficiency of polycrystalline silicon solar cells is 20–30%, which will further reduced by 5% due to the conventional series or parallel configurations. The present paper suggested the arrangement of some new configurations and their performance under non shaded and partially shaded conditions.

This paper based on the experimental investigation of photoelectric conversion. This conversion works on the principle of photoelectric effect. The silicon semiconductor materials are used for absorbing the incident radiations in Photoelectric effect. When these materials are exposed to light, the photons of light are absorbed by the semiconductor crystal which causes number of free electrons in the crystal. This resulted production of electricity. It is observed that when the radiations are incident on the silicon cell, some of the radiations are reflected, some are transmitted through the materials and remaining is absorbed by the material. These losses reduce the efficiency of the system. These silicon cells are arranged in different combination of solar panel or solar modules. These solar panels are electrically connected in different combination of topologies and configurations. These combinations are decided on the basis of project requirement and the applications. This selection played important role for enhancing the performance of the solar system.

Section snippets

Literature review

Solar panel is an array of number of PV cell. Cellsdirectly transform the sun’s photons into electricity. These PV cells are available in different electrical and physical characteristics. Bansal et al. checked the detailed performance and done the degradation analysis on different type of PV power plants with different topologies. They found that HIT appears to be the most promising technology followed by pc-Si and a-Si technology for all conditions [2]. Jaiswal et al. presented an effectual

Experimental setup

The experimentation was carried out to determine an optimum PVarray configuration under different operating conditions. PV array configurations have been tested (SP and TCT) in two different topologies (4SX5P and 5SX4P). The tests have been carried out at the outdoor location of YCCE (latitude: 21.1110625), college campus Wanadongari, Nagpur.

The aluminum frame is fabricated with the PV solar modules dimensions. 20 poly-crystalline PV modules (60 W) were fitted in the frame. These modules are

Variation of power and time

All experiments are carried out from morning 6 a.m. to evening 6p.m. under actual atmospheric condition of the stated site. The fix load of 20 W was applied for all topologies.

Conclusions

Following are mentioned the conclusions of the investigations done on Solar PV Array by varying parameters.

This research work carried out SP and TCT array configuration with two different topologies (4SX5P and 5SX4P) in uniform and partially shaded condition. However all configurations can be taken at the same time to get better results. The impedance of solar panel and input resistance playing important role in achieving maximum power output of PV system. As soon as resistance increases the

Declaration of Competing Interest

The authors declare that they have no known competing financial interests or personal relationships that could have appeared to influence the work reported in this paper.

References (9)

- N. Bansal *et al.*

  Comparative investigation of performance evaluation, degradation causes, impact and corrective measures for ground mount and rooftop solar PV plants – a review

Sust. Energy Technol. Assess.
(2021)
- S. Pujan Jaiswal *et al.*

  Opportunities and challenges of PV technology in power system
  Mater. Today: Proc. DOI
  (2021)
- D. Kumar *et al.*

  A simplifiedsimulation model of silicon photovoltaic modules for performance evaluation at DifferentOperating conditions
  Optik
  (2020)
- Engin Karatepe *et al.*

  Development of a suitable model for characterizing photovoltaic arrays with shaded solar cells
  Solar Energy
  (2007)

There are more references available in the full text version of this article.

Cited by (2)

- The Effects of Non-Uniformly-Aged Photovoltaic Array on Mismatch Power Loss: A Practical Investigation towards Novel Hybrid Array Configurations
  2023, Sustainability (Switzerland)
- Optical Developments in Concentrator Photovoltaic Systems—A Review
  2023, Sustainability (Switzerland)

View full text

Available online at www.sciencedirect.com

ScienceDirect

materialstoday: PROCEEDINGS

[Name of the proceedings]

Comparative analysis of different lattice topologies for cellular structure optimization in additive manufacturing

Chetan Mahatme[1a] Jayant Giri[a] Rajkumar Chadge[a] Ashish Bhagat[b]

[1a]*Assistant Professor,Yeshwantrao Chavan College of Engineering, Nagpur,441110,India*
[a]*Associate Professor,Yeshwantrao Chavan College of Engineering, Nagpur,441110,India*
[a]*Assistant Professor,Yeshwantrao Chavan College of Engineering, Nagpur,441110,India*
[b]*Research Consultant, Jawaharlal Nehru Medical College, DMIMS, Sawangi(M), Wardha,442001,India*

Abstract

Cellular structures are prominent over solid structures in Additive manufacturing because of their inherent features like reduced weight, more strength, and porosity. A cylindrical component was designed and then different lattice topologies like grid, vin tile and hexagon were used to create the internal cellular structure. A comparative analysis was then carried out on these cellular structures based on different unit cell sizes, variable strut thickness, coefficient of volume reduction (VRC) and surface area coefficient (SAC). The effect of these parameters on mechanical properties was studied and correlated. These different cellular structures were then fabricated using PLA (Polylactic acid) material on a Makerbot Replicator + 3-D printer. These cellular structures were then simulated through FEA by providing loading and boundary conditions and the results were then evaluated and validated with experimentation work. The yielded results shown lowest stress and smallest of the deformation for vin tile lattice structure as compared to grid and hexagon lattice cellular structures. Physical experimentation results also validated the simulation outputs. This study was not limited to only creation of different cellular structures but it also compared how the structures behave mechanically through unit cell parameters like VRC and SAC. The cellular structures were tested virtually using FEA and physical experimentation was carried out on the 3-d printed samples. The results obtained through both the tests confirmed that vin tile cellular structure bears less stress and lowest deformation as compared to grid and hexagon cellular structures when subjected to same compressive loading conditions.

Keywords: Additive manufacturing (AM); Cellular structure; Finite element analysis (FEA); Structural optimization;

1. Introduction

Cellular structures are mostly seen in nature and are derived for designing various engineering applications. These structures have properties like they are lightweight in nature and use less material than solid structures. Structurally optimized and well adapted to their surroundings are the key features of these structures [1]. While designing these cellular structures the nature focused on reducing down the weight while using energy efficient ways to create them. The cellular structures available in nature are honeycombs, bone, wood, foam, etc.

Cellular structure are commonly used in industry and are prepared through manufacturing techniques like foaming, sintering, casting and vapor deposition method (VDM) [2]. These methods are conventional ones and are mostly suitable for creating simple cellular structures. The complex cellular structures can be prepared nowadays using modern manufacturing techniques like Additive Manufacturing (AM). It provides the means to create these complex geometries with variable density [3-7]. As in AM the base material is in powder or droplets of liquid form, it drastically reduces the material use and ultimately reduces the cost [8,9]. AM can be done through various techniques. [3-5,10-

* Chetan Mahatme. Tel.: +91-8983760646
E-mail address: chetanmahatme@gmail.com, 9829@ycce.in

15]. AM materials include glass, metals, sand, polymers, etc [3-5,14,15]. The layering resolution is also reaching to microns(<10μ). Advanced composite structures with complex geometries can also be manufactured now by using combination of AM materials i.e. polymer and powder simultaneously with complex topology [17,18].

Medical field application of cellular structures includes creation of scaffolds, implants for teeth and bone and engineered tissues [18-23]. Use of cellular structures for manufacturing bone implants consider various factors like pore size, internal connectivity of pores, volume reduction coefficient and permeability of the structure [24]. Various cellular structures were investigated in several studies for their mechanical performance. In biomedical field, Li X et. al. analyzed Ti6Al4V implant for compressive load with honeycomb lattice structure[25]. Hu LL and Yu TX studied cellular structure under low velocity impacts using hexagonal lattice structures [26], Sullivan et al. investigated open-celled foams using tetrakaidecahedron lattice for Young's modulus, tensile strength and poisons ratio [27]. Babaee et al. investigated rhombic dodecahedron lattice structure for mechanical properties [28]. Jan Wieding et. al. evaluated open-porous scaffolds under various loading conditions [29], G. Campoli et.al. evaluated the finite element models for prediction of properties of cellular bio-materials created through AM techniques (SLM & SEBM) [30], Elastic, compressive and shear strength were corelated with relative density of the 3-d structure by Wallach JC and Gibson LJ [31], variable density cellular structures and its optimization was proposed for AM by Zhang P. et.al. [32], octahedral lattice structure was tested for various mechanical properties by Hedayati et al. [33]. Kalayu M. A. et.al. mechanically investigated the performance of various cellular structures [34]. Mahatme C. et.al. investigated the mechanical properties for vin tile lattice structure [35]. Giri, J. et.al. investigated effect of process parameters in FDM process [36]. The work here has the objective of creating cellular structures by incorporating different lattice topologies and then analyzing those structures under compressive loads for comparison. The solid component used as a basis for creating different cellular structures is a cylindrical part of 50mm diameter and 40mm height. The behavior of cellular structures having different lattice topology with different unit cell sizes was observed under compressive load. For analyzing and simulating the component under compressive load, method of Finite Element Analysis was used. The cellular structures were then 3d printed and tested physically to validate the results obtained through FEA method.

The work done here dealt with the comparative analysis of cellular structures created with different lattice topologies and different unit cell sizes and their structural performance under compressive loading conditions. The study is not limited to the structural performance under compressive loading but also considered key parameters like reduction of volume and overall surface area and their effect on the overall performance of the cellular structure. The cellular structures were also optimized through the optimization toolbox in Autodesk Netfabb and compared with the non-optimized structures. Finally, for evaluation of optimized as well as non-optimized cellular structures, they were tested experimentally as well as through FEA method.

2. Methodology

The procedure that was followed during this comparative study and the material used is explained in this section.

2.1 Cell structure

Cellular structures with different lattice topologies were created virtually and physically. The FEA analysis and physical compressive tests were performed on these cellular structures. Autodesk Netfabb software was used for designing the cellular structure as well as for FEA analysis. Figure 1 shows the solid cylindrical component used for creating the different cellular structures.

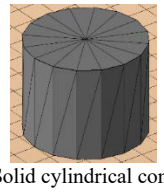

Fig. 1 Solid cylindrical component

2.2 Unit cell and different lattice topologies

For the purpose of comparative analysis, the Grid, Vin tile and hexagon lattice topologies were used. A dedicated 3d-printing software, Autodesk Netfabb was used for creating the cellular structures using these lattice topologies. A

Solid cylindrical component (Figure 1) was transformed into different cellular structures by inserting a lattice cell structure inside it (Figure 3). Combination of different lattice topologies with different unit cell sizes that were used for creating different cellular structures for comparison (Table 1). An example is shown in Figure 3, where the grid lattice cell structure was incorporated in a cylindrical component. Cellular structures created were then exported as .stl (standard tessellation language) files for structural optimization, FEA analysis and fabrication purpose.

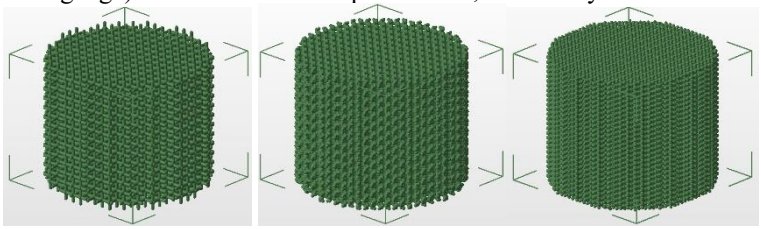

(a) (b) (c)

Fig. 2 Lattice cell structures a) Grid b) Vin tile c) Hexagon

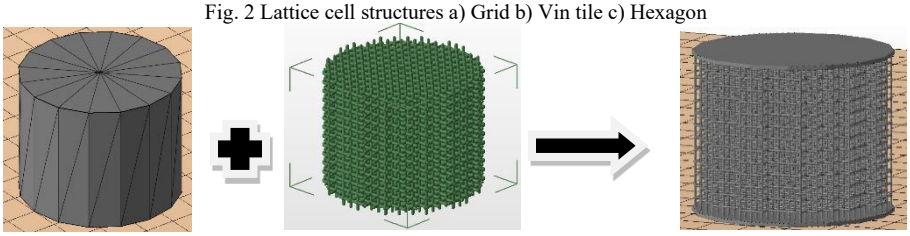

Fig. 3 Process of cellular structure design (Example: Grid lattice topology)

2.3 Parameters considered

The comparative analysis of cellular structures having different lattice topologies was mainly based on structural behaviour under compressive loading conditions. The other important parameters which were considered for evaluation of the different lattice structures were SAC and VRC. SAC stands for surface area coefficient and VRC stands for volume reduction coefficient. Both these parameters were equally important while comparing the cellular structures. Increase in SAC denotes the increase in porosity of the cellular structure while increase in VRC denotes the weight reduction in cellular structure. While comparing these cellular structures mechanically based on strength to weight ratio and porousness these parameters had to be considered.

2.4 Fabrication of samples

The samples were fabricated using PLA (polylactic acid) material. The PLA material properties are given in the Table 2 and 3. The 1kg PLA filament spool was procured from Makerbot and was used for 3d printing the samples. Table 1 shows the combinations of geometrical variations that was used for creating the samples. The CAD file of solid component shown in Figure 1 was converted into STL file and cellular structures were created using different lattice topologies shown in Table 1. The cellular structures were then checked for errors in Netfabb. Inbuilt repair scripts available in Netfabb was used to reduce down the triangulation errors of these cellular structures. These repaired cellular structures were then 3d printed on Makerbot replicator+. The thickness of layer as 0.1mm and infill density as 10% was kept common for all these cellular structures while printing. Forty-five cellular structures were created using Netfabb using the combination as shown in Table 1 and thirteen of them were fabricated based on minimum displacement criteria. Physical compressive tests were performed on these samples as shown in Figure 5. The layer resolution for 3d printer was 0.1 mm. The shrinkage and distortion were minutely visible when the virtual cellular structure was compared with the actual physical fabricated sample. Kechagias et al. [28] related this deformation to the minimum layer thickness selected while printing the samples. The shrinkage in fabricated samples was because of cooling effect to which the samples were subjected when they cooled down to room temperature.

Table 1. Lattice topologies and Unit cell size combinations

Lattice topologies	Size: Unit cell (mm)	Strut Thickness (mm)	Thickness (Threshold in mm)
Grid, Vin tile and Hexagon	3 x 3 x 3 to 7 x 7 x 7	0.5, 1.0, 1.5	0.5

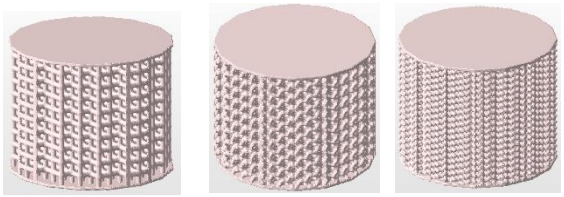

(a) (b) (c)

Fig. 4 Cellular structure (a) Grid (b) Vin Tile (c) Hexagon

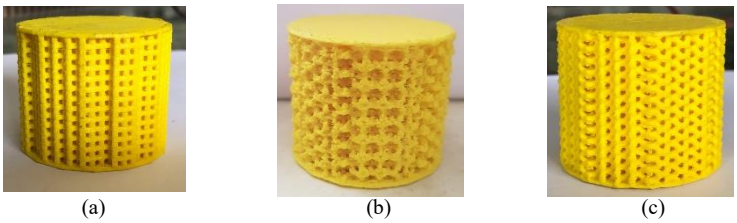

(a) (b) (c)

Fig. 5 Printed samples (a) Grid (b) Vin Tile (c) Hexagon

Table 2. PLA material properties

Melting point (M.P.)	Heat Deflection Temperature (HDT)	Solubility (water)	Density	Shrink Rate
151 to 162 °C (300 to 320 °F)	126 °F (52 °C)	0 mg/ml	1.24 g/cm−3	0.37-0.41% (0.0037-0.0041 in/in)
Young's Modulus (MPa)	Tensile strength (MPa)	Flexural Strength	Impact Strength (Un-notched) IZOD (J/m)	Poisson's ratio(μ)
2.50e+03	50	80 MPa	96.1	0.36

2.5 FEA Analysis

The Finite Element Analysis was used to computationally simulate the physical conditions on the cellular structures. Simulation of physical conditions and theoretical analysis of structures behaviour was done through this technique. Same loading conditions were provided to all the samples and then their performance was compared. FEA analysis was done on Autodesk Netfabb. The loading was given to the sample as a pressure on top surface and a restraint was provided at the bottom surface as fixed. The restraint at the bottom was used as a boundary condition and to restrict the motion of bottom surface in all possible directions. For analysis, Table 2 PLA material properties were used. The mechanical performance of different cellular structures given in Table 1 was then compared on the basis of lattice and skin deformation and Maximum Von Mises Stress.

2.6 Physical Testing

The fabricated samples were then physically tested under same compressive loading conditions and FEA simulation results were compared for validation. Compressive testing was done on the universal testing machine of make FIE UTES-HGFL-60-C having maximum capacity of 600kN. The samples were placed between the platens of UTM as shown in Figure 6. Position and orientation of the sample was same as in FEA simulation work. Gradual loading was then applied to the sample and the displacement and load were recorded through UTM display.. For the compressive test $\boldsymbol{v}$ was considered even in all directions.

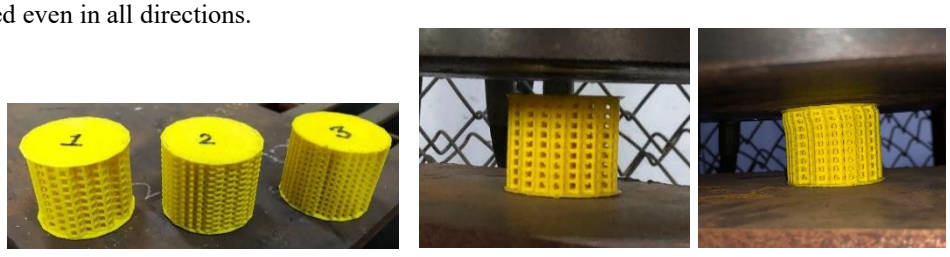

(a) (b)

(c) (d)

Fig. 6 UTM test setup (a) before starting the test, (b) Grid: during and after test (c) Vin tile: during and after test (d) Hexagon: during and after test

2.7 Optimization process

Cellular structures have inherent advantage of weight reduction and efficient structural optimization. Most of the work was done across the globe by various researchers in this field. The primary focus was to find optimized unit cell configuration so as to meet intended functional requirements [37-41]. Bendsoe and Kikuchi proposed a mathematically driven approach for topology optimization. The main focus was optimum material use with main focus on performance [42]. In Evolutionary Structural Optimization (ESO) method the material was gradually removed from the design space [43]. Ning et al worked on an analytical approach to determine the Johnson-Cook constants for structural optimization of cellular structures [44].

In this study Autodesk Netfabb software lattice optimization utility was used for structural optimization. The process flow followed was like this: 1. Defining unit cell and its parameters like strut thickness (max. min. and threshold). 2. Mesh generation and smoothness method. 3. Load and boundary conditions for FEA analysis. Autodesk Netfabb integrated ADS Nastran V12.1 (FEA solver) was used for performing the simulation. The lattice and skin was set for optimization in the solver. Maximum Optimization time and iteration were set to 10 minutes and 5 iterations. 1mm was set as target maximum displacement. MiniOpt optimization algorithm was used and kernels were kept as it is. Hence KernelOpt was omitted for optimization.

3. Results and discussion

3.1. Results: FEA

Stress and displacement variation are shown in Figure 7 for the cellular structures. Because of the variation in lattice structure stress variation is there. Variable thickness of the cells also contributed to the stress variation. The Grid cellular structure with 3 x 3 x 3 mm unit cell size with 1.5 mm cell thickness showed deformation of 0.656188 mm while in Vin tile cellular structure 3 x 3 x 3 mm unit cell size with 1.5 mm cell thickness showed deformation of 0.185991mm. For Hexagon cellular structure with 3 x 3 x 3 mm unit cell size with 1.5 mm cell thickness showed deformation of 0.17612 mm This shows that the 3 x 3 x 3 mm unit cell size with 1.5 mm cell thickness proved to be more efficient in terms of minimum deformation and maximum stress bearing capacity. The supremacy of this structure was also confirmed by the obtained VRC and SAC values (Table 3). High VRC and SAC values for this sample indicated the high material reduction and more porous nature.

Table 3. FEA results

Lattice Topology	Size: Unit Cell (mm)	Strut Thickness (mm)	SAC	VRC	Structure : Non-optimized			
					Von Mises Stress (MPa)		Deformation(mm)	
					Lattice	Skin	Lattice	Skin
Grid Cellular Lattice Structure	3 x 3 x 3	0.5	4.853	0.125	4.9369E+08	3.82E+07	5.995809	6.044762
	3 x 3 x 3	1.0	7.153	0.312	1.2004E+08	6.72E+06	1.485588	1.500261
	3 x 3 x 3	1.5	7.446	0.56	5.1329E+07	2.76E+06	0.656188	0.663963
	4 x 4 x 4	0.5	2.975	0.088	8.7919E+08	1.36E+08	10.7309	10.90733
	4 x 4 x 4	1.0	4.482	0.191	2.6424E+08	3.29E+07	2.7043	2.758883
	4 x 4 x 4	1.5	5.394	0.347	1.1886E+08	1.12E+07	1.187052	1.210815
	5 x 5 x 5	0.5	2.038	0.072	1.5801E+06	1.22E+08	20.958	22.359
	5 x 5 x 5	1.0	3.013	0.133	4.5555E+08	3.72E+07	5.2314	5.607207
	5 x 5 x 5	1.5	3.717	0.226	2.6.8963e6	1.69E+07	2.272848	2.422262

	6 x 6 x 6	0.5	1.758	0.067	2.7898E+09	4.29E+08	29.63401	32.050041
	6 x 6 x 6	1.0	2.544	0.114	1.0554E+09	1.56E+08	7.461509	8.545643
	6 x 6 x 6	1.5	3.149	0.187	4.8673E+08	6.00E+07	3.248033	3.685827
	7 x 7 x 7	0.5	1.518	0.062	4.3406E+09	7.73E+08	45.2033	61.445499
	7 x 7 x 7	1.0	2.125	0.097	1.6102E+09	2.11E+08	12.04606	17.32139
	7 x 7 x 7	1.5	2.618	0.151	7.3835E+08	8.62E+07	5.10969	7.146599
Vin tile Cellular Lattice Structure	3 x 3 x 3	0.5	10.299	0.267	8.8455E+08	5.70E+07	5.8538	5.872522
	3 x 3 x 3	1.0	35.468	1.415	1.0996E+08	4.54E+06	0.591069	0.592816
	3 x 3 x 3	1.5	98.145	4.912	3.7768E+07	2.22E+06	0.185991	0.186702
	4 x 4 x 4	0.5	6.794	0.174	2.1196E+09	9.62E+07	16.692	16.8064
	4 x 4 x 4	1.0	11.984	0.592	2.3998E+08	2.07E+07	1.457536	1.467781
	4 x 4 x 4	1.5	36.844	2.01	8.2585E+07	2.07E+06	0.422477	0.427619
	5 x 5 x 5	0.5	4.827	0.128	3.7239E+09	1.42E+08	38.0387	38.4265
	5 x 5 x 5	1.0	6.962	0.356	4.8152E+08	4.65E+07	3.191447	3.271274
	5 x 5 x 5	1.5	16.163	0.999	1.5141E+08	1.18E+07	0.867472	0.902106
	6 x 6 x 6	0.5	3.718	0.105	5.8762E+09	1.81E+08	75.1479	75.659843
	6 x 6 x 6	1.0	5.484	0.26	7.3625E+08	5.74E+07	5.795874	5.817815
	6 x 6 x 6	1.5	8.192	0.575	2.3090E+08	2.24E+07	1.508669	1.521126
	7 x 7 x 7	0.5	3.008	0.091	1.0984E+10	3.00E+08	133.67	135.16
	7 x 7 x 7	1.0	4.531	0.21	1.0935E+09	8.01E+07	10.37549	10.56457
	7 x 7 x 7	1.5	5.342	0.395	3.4922E+08	4.19E+07	2.666243	2.723572
Hexagon Cellular Lattice Structure	3 x 3 x 3	0.5	12.772	0.327	7.9354E+08	4.98E+07	5.277265	5.299514
	3 x 3 x 3	1.0	46.714	1.831	8.1885E+07	2.16E+06	0.540505	0.544873
	3 x 3 x 3	1.5	128.37	6.352	2.7591E+07	1.93E+06	0.17612	0.178449
	4 x 4 x 4	0.5	8.186	0.205	1.7863E+09	9.21E+07	14.99835	15.11241
	4 x 4 x 4	1.0	15.153	0.738	1.9906E+08	1.76E+07	1.34431	1.354767
	4 x 4 x 4	1.5	46.627	2.569	6.2832E+07	1.72E+06	0.401619	0.405083
	5 x 5 x 5	0.5	5.857	0.149	3.1701E+09	1.35E+08	34.12756	34.5807
	5 x 5 x 5	1.0	8.452	0.437	3.8060E+08	3.51E+07	2.780602	2.795874
	5 x 5 x 5	1.5	20.834	1.283	1.0968E+08	7.43E+06	0.751503	0.757614
	6 x 6 x 6	0.5	4.488	0.12	5.0248E+09	2.00E+08	67.475	68.312
	6 x 6 x 6	1.0	6.7	0.323	6.2378E+08	4.41E+07	5.226516	5.276895
	6 x 6 x 6	1.5	10435	0.736	1.8105E+08	1.18E+07	1.298878	1.3071
	7 x 7 x 7	0.5	3.485	0.1	8.8876E+09	2.56E+08	122.08	123.62
	7 x 7 x 7	1.0	5.313	0.247	9.7769E+08	7.00E+07	9.223155	9.137981
	7 x 7 x 7	1.5	6.243	0.48	2.8942E+08	3.07E+07	2.205045	2.223026

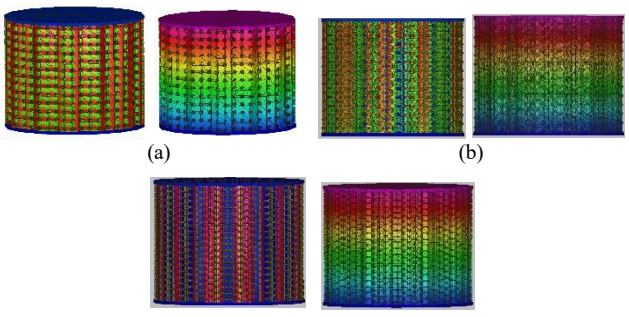

Fig. 7 Stress and displacement in unit cell (a) Grid 3 x 3 x 3-1.5 (b) Vin tiles 3 x 3 x 3-1.5 (c) Hexagon 4 x 4 x 4-1.5

3.2. Structural optimization results

Figure 8 shows the simulation results for the Optimized cellular structure. In grid lattice structure, maximum Von Mises Stress was 2.5% less and maximum displacement 37.5% less than that of non-optimized cellular structure. Similar reductions were also observed in vin tile and hexagon lattice structures. These reductions in optimized cellular structures were because of stiffening of struts and strengthening of load bearing sections of the structures. The comparative results are as depicted in Table 4.

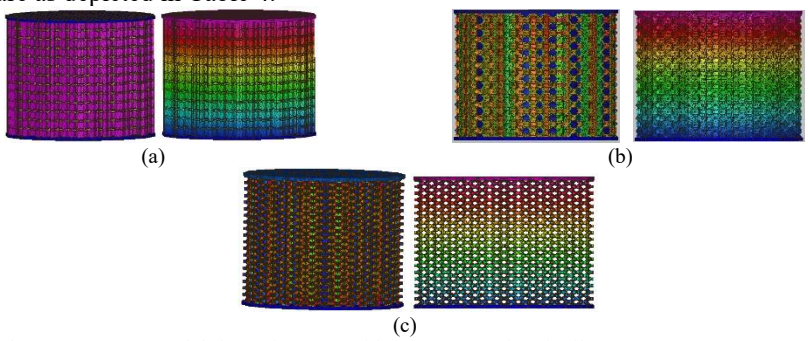

Fig. 8 Optimized structure (stress and deformation) (a) Grid 3 x 3 x 3-1.5 (b) Vin tiles 3 x 3 x 3-1.5 (c) Hexagon 4 x 4 x 4-1.5

3.3 Mechanical properties: comparison

As can be seen from Table 4, Optimized cellular structures have less Von mises stress and smaller deformation as compared to non-optimized ones because of variable density internal structure. The results obtained in simulation study have pointed out that the optimized cellular structures are stiffer than the non-optimized cellular structures when the unit cell parameters are kept constant.

Table 4. Mechanical properties

	Grid 3 x 3 x 3-1.5		Vin tile 3 x 3 x 3-1.5		Hexagon 4 x 4 x 4-1.5	
	Stress (max.) (MPa)	deformation (max.) (mm)	Stress (max.) (MPa)	deformation (max.) (mm)	Stress (max.) (MPa)	deformation (max.) (mm)
Optimized	50.04	0.41	32.64	0.102	58.36	0.212
Non-optimized	51.32	0.656	37.76	0.185	62.83	0.401

4. Conclusions

In this study, we have designed various cellular structures using unit cell of grid, vin tile and hexagon lattice topology. The cellular structures were then structurally optimized and compared. For comparison purpose physical tests were performed on samples. FEA analysis was done and optimization methods were used for optimizing the structures. Cellular structures were formed using solid cylindrical part and evaluation was done under compressive loading conditions for stress and displacement. While optimizing the structures, strut thickness, volume reduction coefficient, surface area coefficient was taken into account. Optimization utility in Autodesk Netfabb software was used for FEA simulation and structural optimization. For validation of the simulation results, physical compression tests were also carried out on different samples on UTM. FEA simulation results and the physical compression test results were compared and they were in close agreement with each other.

It is seen from the result that the vin tile cellular structure with 3 x 3 x 3mm unit cell size with 1.5 mm strut thickness had smallest of the deformation and lowest of the stress as compared to grid and hexagon lattice cell structures. Grid cellular structure with 3 x 3 x 3mm unit cell size with 1.5 mm strut thickness and Hexagon 4 x 4 x 4mm unit cell size with 1.5 mm strut thickness also showed promising results with less than 1mm deformation but the von mises stress within those structures were far more than vin tile cellular structure. While comparing the structures on the basis of VRC and SAC with less than 1mm deformation, vin tile cellular structure was once again superior to grid and hexagon structure. The study hence done a comparative evaluation of the grid, vin tile and hexagon cellular structures and their effectiveness when used for superior mechanical performance intended under compressive loading conditions.

References

[1] Wester T (2002) Nature teaching structures. Int J Sp Struct 17: 135–147. https://doi.org/10.1260/026635102320321789

[2] Banhart, J., 2001, "Manufacture, Characterisation and Application of Cellular Metals and Metal Foams," Prog. Mater. Sci., 46(6), pp. 559–632.

[3] Gibson, I., Rosen, D. W., and Stucker, B., 2010, Additive Manufacturing Technologies, Springer, New York.

[4] Kruth, J.-P., Leu, M., and Nakagawa, T., 1998, "Progress in Additive Manufacturing and Rapid Prototyping," CIRP Ann. Manuf. Technol., 47(2),pp. 525–540.

[5] Wohlers, T., 2011, Wohlers Report 2011: Additive Manufacturing and 3D Printing, State ofthe lndustry, Wohlers Associates, Ft. Collins, CO.

[6] Scott, J., Gupta, N., Weber, C. L., Newsome, S., Wohlers, T., and Caffrey, T., 2012, Additive Manufacturing: Status and Opportunities, Science and Technology Policy Institute, Washington, DC, pp. 1–29.

[7] Conley, J., and Marcus, H., 1997, "Rapid Prototyping and Solid Free Form Fabrication," ASME J. Manuf. Sci. Eng., 119(4B), pp. 811–816.

[8] Beyer, C., "Additive Manufacturing—Implications of a Breakthrough Technology," ASME J. Manuf. Sci. Eng. (to be published).

[9] Haapala, K. R., Zhao, F., Camelio, J., Sutherland, J. W., Skerlos, S. J., Dornfeld, D. A., Jawahir, I., Clarens, A. F., and Rickli, J. L., 2013, "A Review of Engineering Research in Sustainable Manufacturing," ASME J. Manuf. Sci.Eng., 135(4), p. 041013.

[10] Gu, D., Meiners, W., Wissenbach, K., and Poprawe, R., 2012, "Laser Additive Manufacturing of Metallic Components: Materials, Processes and Mechanisms," Int. Mater. Rev., 57(3), pp. 133–164.

[11] Murr, L. E., Gaytan, S. M., Ramirez, D. A., Martinez, E., Hernandez, J., Amato, K. N., Shindo, P. W., Medina, F. R., and Wicker, R. B., 2012, "Metal Fabrication by Additive Manufacturing Using Laser and Electron Beam Melting Technologies," J. Mater. Sci. Technol., 28(1), pp. 1–14.

[12] Bartolo, P. J., 2011, Stereolithography: Materials, Processes and Applications, Springer, New York.

[13] Edwards, P., O'Conner, A., and Ramulu, M., 2013, "Electron Beam Additive Manufacturing of Titanium Components: Properties and Performance," ASME J. Manuf. Sci. Eng., 135(6), p. 061016.

[14] Schultz, B., and Rohatgi, P., 2014, "Laser Engineered Net Shaping Process for 316L/15% Nickel Coated Titanium Carbide Metal Matrix Composite," ASME J. Manuf. Sci. Eng., 136(5), p. 051007.

[15] Luo, J., Pan, H., and Kinzel, E., "Additive Manufacturing of Glass," ASME J. Manuf. Sci. Eng. (to be published).

[16] Dimas, L. S., Bratzel, G. H., Eylon, I., and Buehler, M. J., 2013, "Tough Composites Inspired by Mineralized Natural Materials: Computation, 3D Printing, and Testing," Adv. Funct. Mater., 23(36), pp. 4629–4638.

[17] Li, Y., Kaynia, N., Rudykh, S., and Boyce, M. C., 2013, "Wrinkling of Interfacial Layers in Stratified Composites," Adv. Eng. Mater., 15(10), pp. 921–926.

[18] Ali D, Sen S (2017) Finite element analysis ofmechanical behavior, permeability and fluid induced wall shear stress of high porosity scaffolds with gyroid and lattice-based architectures. J Mech Behav Biomed Mater 75:262–270. https://doi.org/10.1016/j.jmbbm.2017.07.035

[19] Karageorgiou V, Kaplan D (2005) Porosity of3D biomaterial scaffolds and osteogenesis. Biomaterials 26:5474–5491. https://doi.org/10.1016/j.biomaterials.2005.02.002

[20] Yan C, Hao L, Hussein A et al (2015) Microstructure and mechanical properties of aluminium alloy cellular lattice structures manufactured by direct metal laser sintering. Mater Sci Eng A 628:238–246. https://doi.org/10.1016/j.msea.2015.01.063

[21] Jetté B, Brailovski V, Dumas M, Simoneau C, Terriault P (2018) Femoral stem incorporating a diamond cubic lattice structure: design, manufacture and testing. J Mech Behav BiomedMater 77:58–72. https://doi.org/10.1016/j.jmbbm.2017.08.034

[22] Kang H, Lin CY, Hollister SJ (2010) Topology optimization of three dimensional tissue engineering scaffold architectures for prescribed bulk modulus and diffusivity. Struct Multidiscip Optim 42: 633–644. https://doi.org/10.1007/s00158-010-0508-8

[23] Higuchi A, Ling QD, Hsu ST, Umezawa A (2012) Biomimetic cell culture proteins as extracellular matrices for stem cell differentiation. Chem Rev 112:4507–4540. https://doi.org/10.1021/cr3000169

[24] Hollister S (2006) Porous scaffold design for tissue engineering. Nat Mater 5:590. https://doi.org/10.1038/nmat1683

[25] Li X, Wang C, Zhang W, Li Y (2010) Fabrication and compressive properties of Ti6Al4V implant with honeycomb-like structure for biomedical applications. Rapid Prototyp J 16:44–49.

https://doi.org/10.1108/13552541011011703
[26] Hu LL, Yu TX (2013) Mechanical behavior of hexagonal honeycombs under low-velocity impact – theory and simulations. Int J Solids Struct 50:3152–3165. https://doi.org/10.1016/J.IJSOLSTR. 2013.05.017
[27] Sullivan RM, Ghosn LJ, Lerch BA (2008) A general tetrakaidecahedron model for open-celled foams. Int J Solids Struct 45:1754–1765. https://doi.org/10.1016/J.IJSOLSTR.2007. 10.028
[28] Babaee S, Jahromi BH, Ajdari A et al (2012) Mechanical properties of open-cell rhombic dodecahedron cellular structures. Acta Mater 60:2873–2885. https://doi.org/10.1016/J.ACTAMAT.2012.01.052
[29] Wieding J, Wolf A, Bader R (2014) Numerical optimization of open-porous bone scaffold structures to match the elastic properties of human cortical bone. J Mech Behav Biomed Mater 37:56–68.https://doi.org/10.1016/j.jmbbm.2014.05.002
[30] Campoli G, Borleffs MS, Amin Yavari S et al (2013) Mechanical properties of open-cell metallic biomaterials manufactured using additive manufacturing. Mater Des 49:957–965. https://doi.org/10.1016/j.matdes.2013.01.071
[31] Wallach JC, Gibson LJ (2001) Mechanical behavior of a three- dimensional truss material. Int J Solids Struct 38:7181–7196. https://doi.org/10.1016/S0020-7683(00)00400-5
[32] Zhang P, Toman J, Yu Y et al (2014) Efficient design-optimization of variable-density hexagonal cellular structure by additive manufacturing: theory and validation. J Manuf Sci Eng 137: 021004. https://doi.org/10.1115/1.4028724
[33] Zadpoor AA, Hedayati R (2016) Analytical relationships for prediction of the mechanical properties of additively manufactured porous biomaterials. J Biomed Mater Res - Part A 104:3164– 3174. https://doi.org/10.1002/jbm.a.35855
[34] Kalayu Mekonen Abate, Aamer Nazir,Yun-Peng Yeh, Jia-En Chen & Jeng-Ywan Jeng (2019) Design, optimization, and validation of mechanical properties of different cellular structures for biomedical application The International Journal of Advanced Manufacturing Technology https://doi.org/10.1007/s00170-019-04671-5
[35] Mahatme, C., Giri, J., Chadge, R., Sonwane, S. (2021) Compression deformation analysis of cellular lattice structure for structural optimization in additive manufacturing, Materials Today: Proceedings, 2021, 47, pp. 4214–4220, https://doi.org/10.1016/j.matpr.2021.04.463
[36] Giri, J., Chiwande, A., Gupta, Y., Mahatme, C., Giri, P.(2021), Effect of process parameters on mechanical properties of 3d printed samples using FDM process, Materials Today: Proceedings, 2021, 47, pp. 5856–5861, https://doi.org/10.1016/j.matpr.2021.04.283
[37] Sigmund O, Maute K (2013) Topology optimization approaches: a comparative review. Struct Multidiscip Optim 48:1031–1055. https://doi.org/10.1007/s00158-013-0978-6
[38] Wang Y, Zhang L, Daynes S et al (2018) Design of graded lattice structure with optimized mesostructures for additive manufacturing. Mater Des 142:114–123. https://doi.org/10.1016/j.matdes. 2018.01.011
[39] Huang X, Xie YM (2008) Optimal design of periodic structures using evolutionary topology optimization. Struct Multidiscip Optim 36:597–606. https://doi.org/10.1007/s00158-007-0196-1
[40] Huang X, Xie YM (2010) A further review of ESO type methods for topology optimization. Struct Multidiscip Optim 41:671–683. https://doi.org/10.1007/s00158-010-0487-9
[41] Torquato S, Hyun S, Donev A (2003) Optimal design ofmanufacturable three-dimensional composites with multifunctional charac- teristics. J Appl Phys 94:5748–5755. https://doi.org/10.1063/1. 1611631
[42] Bendsoe MP, Kikuchi N (1988) Generating optimal topologies in structural design using a homogenization method. Comput Methods Appl Mech Eng 71:197–224
[43] Xie YM, StevenGP (1996) Evolutionary structural optimization for dynamic problems. Comput Struct 58:1067–1073. https://doi.org/ 10.1016/0045-7949(95)00235-9
[44] Ning J, Liang SY (2018) Model-driven determination of Johnson- cook material constants using temperature and force measurements.Int J Adv ManufTechnol 97:1053–1060

Materials Today: Proceedings xxx (xxxx) xxx

Contents lists available at ScienceDirect

Materials Today: Proceedings

journal homepage: www.elsevier.com/locate/matpr

Spot welding analysis of dissimilar joint by finite element analysis

Chetan Tembhurkar [a,c,*], Sachin Ambade [b], Ravinder Kataria [a], Aditya Tikle [c]

[a] School of Mechanical Engineering, Lovely Professional University, Phagwara 144001, India
[b] Mechanical Engineering Department, Yeshawantrao Chavan College of Engineering, Nagpur 441110, India
[c] Mechanical Engineering Department, Priyadarshini College of Engineering, Nagpur 440016, India

ARTICLE INFO

Article history:
Received 12 August 2021
Received in revised form 16 September 2021
Accepted 23 September 2021
Available online xxxx

Keywords:
316L ASS
430 FSS
Spot welding
ANSYS

ABSTRACT

Spot welded dissimilar lap joint of austenitic and ferritic stainless steel were performed to reveal the ultimate strength of the joint. The failure analysis at the spot weld is structural and the lap joint is subjected to tensile load. The stress distribution of the applied load corresponds to the tensile load of the specimen based on the observed fracture mechanism. It was found that the ultimate strength from the experimental is 9 percent greater than the Von Mises stress. Experimental data from the tensile test using universal test machine as well as finite element analysis using ANSYS are used to validate the results.

Selection and peer-review under responsibility of the scientific committee of the 2nd International Conference on Functional Material, Manufacturing and Performances

1. Introduction

Spot welding is widely used in automotive sheet metal joining and it is the main joining technique in the automotive industry [1,2] . In modern automobiles, stainless steels such as austenitic and ferritic stainless steels are used in chassis, bodywork and catalytic converters [3]. Therefore, the analysis of welding force under various welding conditions is very important for the vehicle design [4]. The variables considered in industry to practice the analysis of the spot weld for design purpose are welding parameters, sheet thickness and weld nugget size. Due to its complexity, it is difficult to analyze the stresses developed in the joint. The sensitivity analysis technique is used to determine the mechanical properties such as material hardness [5]. The various types of welding processes used to weld dissimilar metals are tungsten inert gas welding, friction stir welding etc [6–7]. Ahmet Hasanbasog lu and Ramazan Kacar [8] found that higher the maximum welding current, the higher the tensile strength of the welding material due to the size of the nugget. M. Alenius et.al [9] found that the breaking load in the cross-tensile specimens was about 72–78% more than that of the lap shear test, and that the combination failed in both the tests. The strength and thickness of the stainless steel depend upon the lap shear strength of the dissimilar metal joints. M. Pouranvari and S. P. H. Marashi [10] studied the mechanical properties (hardness values) of spot welds. This significantly affects the fracture behavior and fracture pattern of spot welds. The critical Fusion Zone (FZ) required to ensure Potential Failure (PF) mode during tensile testing of RSW stainless steels increases or decreases in dissimilar spot welds and low carbon galvanized steel. This may be due to the low weld hardness of FZ stainless-steel. Danial Kianersi, et.al [11] investigated the tensile and shear strength of the welded material by increasing the weld nugget size and increasing the welding current to 8 kA, but further increasing the welding current to 9 kA had a negative effect. The minimum and maximum tensile and shear forces as well as the maximum loads of 2450 N and 8070 N are indicated for welding currents of 4 kA and 8 kA. A.B. Verma,et,al [12] found that the welding current is an important controlling factor affecting the tensile shear strength of the weld samples in resistance spot welding. As the welding current increases, the size of weld nugget also increases. This improves the tensile strength of the weld.Anand Prakash Singh,et.al [13] conducted hardness testing and the Rockwell hardness number for stainless steel grade 202 and grade 316 comes out to be 23–25 HRC and 82–83 HRB respectively and optimum value of hardness of the joint comes out to be 22–24 HRC on current value 12kA after which it started decreasing. It can be concluded that greater the welding current, greater the welding heat input and hence higher the probability of failure. Hence, the high welding current reduces the hardness. In this paper, the spot-welded dissimilar joint is used to predict the ultimate strength and maximum deformation from the universal testing machine and it is compared with the von

* Corresponding author.
E-mail address: chetantembhurkar@gmail.com (C. Tembhurkar).

https://doi.org/10.1016/j.matpr.2021.09.410
2214-7853/
Selection and peer-review under responsibility of the scientific committee of the 2nd International Conference on Functional Material, Manufacturing and Performances

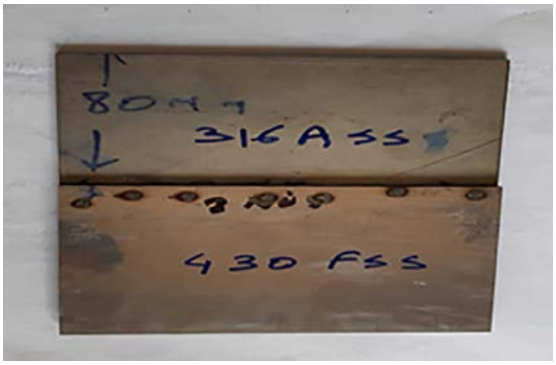

Fig. 1. 316L ASS and 430 FSS Dissimilar spot-welded plates.

Fig. 2. Tensile test specimen according to ASTM E8 standard.

mises stress and maximum deflection of finite element analysis under static loading conditions. This analysis is used to predict the stresses developed in the weld prior to welding [14].

2. Experimental work

In Fig. 1, the two plates of 100 mm length, 75 mm width and 3 mm thickness of 430 FSS and 316L ASS were spot welded. The ten spots of 10 mm diameter were spotted at the lap joint of the two plates. The length of overlap between the two plates is 10 mm during welding. The plates were cut by electrical discharge machine to obtain tensile test specimens in accordance with ASTM E8 standard [15–16] as shown in Fig. 2. The chemical composition calculated with optical emission spectroscopy (OES) with weight percentage for 316L ASS and 430 FSS is presented in table 1.

Table 1. The chemical composition (wt %) of 430 FSS and 316L ASSTable 2.Table 3.

The welding parameters are determined during welding, the welding current is 8kA, squeeze time (cycle) is two welds, and weld cooling condition is atmosphere. Fig. 3 shows the spot-welding machine used for welding.

Table 3
Impact test.

Sample	Impact energy (Joules)
316L ASS BM	54
430 FSS BM	28
316L ASS and 430 FSS	3.33

Fig. 3. Spot Welding machine.

3. Results and discussion

3.1. Experimental test results

3.1.1. Tensile test results

The ultimate stress, yield stress, maximum displacement and percentage elongation were evaluated by means of Universal testing machine. The maximum load applied at the load rate of 30 KN/min and strain rate of 15 mm/min. The ultimate tensile stress and

Table 1
The chemical composition (wt %) of 430 FSS and 316L ASS.

Sample	C	Si	Mn	P	Cr	Mo	Ni	Fe
316L ASS	0.0264	0.345	1.088	0.036	16.384	2.006	9.757	Bal.
430 FSS	0.0403	0.411	0.378	0.017	16.392	0.001	0.190	Bal.

Table 2
Stress evaluation of spot weld by Universal Testing Machine.

Sample	Ultimate Tensile stress (MPa)	Yield stress (MPa)	Max Displacement (mm)	Elongation (%)
316L ASS	562	359	13.2	52
430 FSS	432	317	10.3	25
316L ASS and 430 FSS	563.563	415.385	15.7	14.207

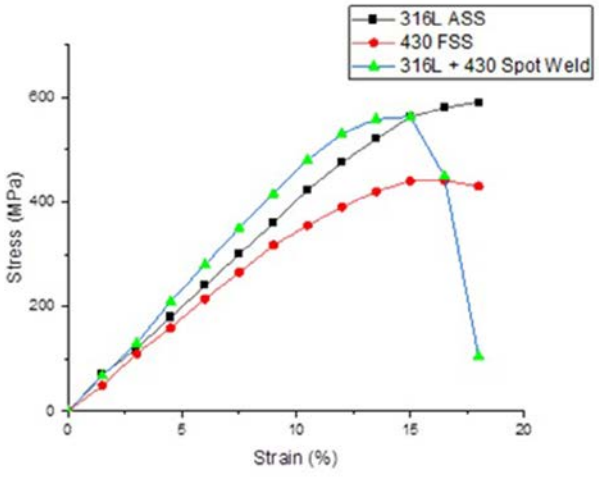

Fig. 4. a) Stress Strain curve b) Fractured specimen of dissimilar spot weld.

maximum displacement of the spot weld joint obtained from universal testing machine is shown in table 2. The stress strain curve and fracture specimen are shown in Fig. 4a) and Fig. 4b) respectively. The ultimate stress of the spot weld is greater than the base metal this indicates that the strength is more prominent in lap shear mode [17].

3.1.2. Impact test results

The impact energy was evaluated by means of Charpy impact test having sample size 55 × 10 × 3 mm^3 and the results have been shown in table 3. The resultant toughness obtained from spot weld is avg.3.33 J which is due to the welding current which affects the toughness of the spot weld, as the welding current increases it will increase the bonding area [18].

3.2. ANSYS results

3.2.1. Creation of model by ANSYS

The finite element model (FEM) is created by using two plates 316L ASS and 430 FSS by using ANSYS R18.2 workbench [19]. The spot-welded plates of dimension as per ASTM E8 standard (length (L)-150 mm, gauge length (G) – 45 mm, Width (W) – 12.5 mm, Width of Grip Section (C) – 20 mm, Length of grip section (B)- 55 mm, Radius of fillet- 12.5^0 , thickness of plate (T) – 3 mm) which is created in design modeler of ANSYS. The element type used is SOLID 183 which is used for metals such as stainless steel [19]. The tensile specimen in ANSYS is shown in Fig. 5.

3.2.2. Meshing of dissimilar spot-welded plates

The meshing is created by using hexahedral mesh size of 0.8 mm and having 44,715 number of nodes and 8520 number of

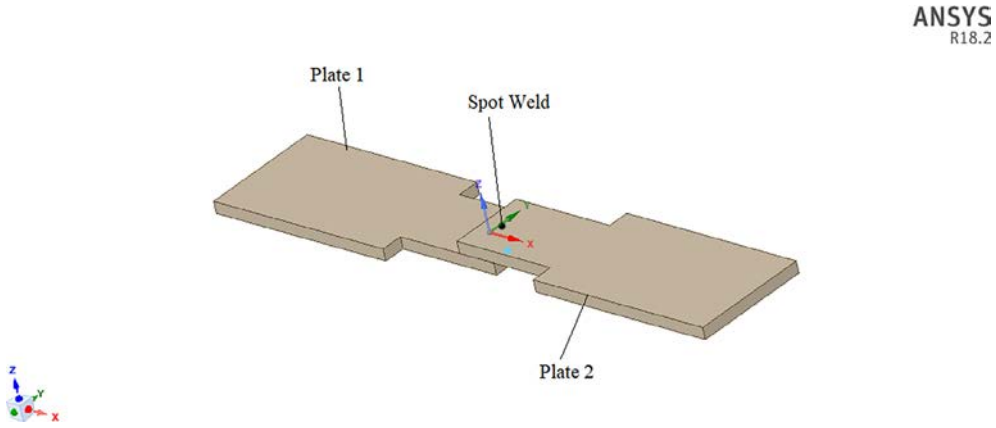

Fig. 5. Modelling.

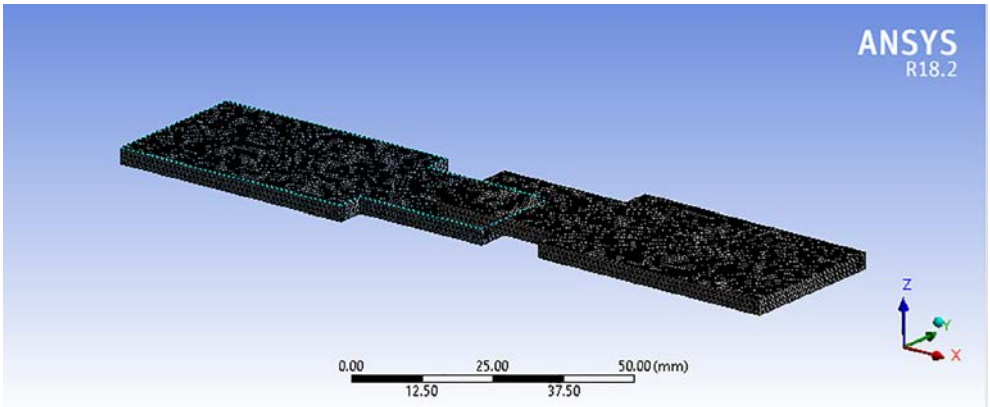

Fig. 6. Meshing.

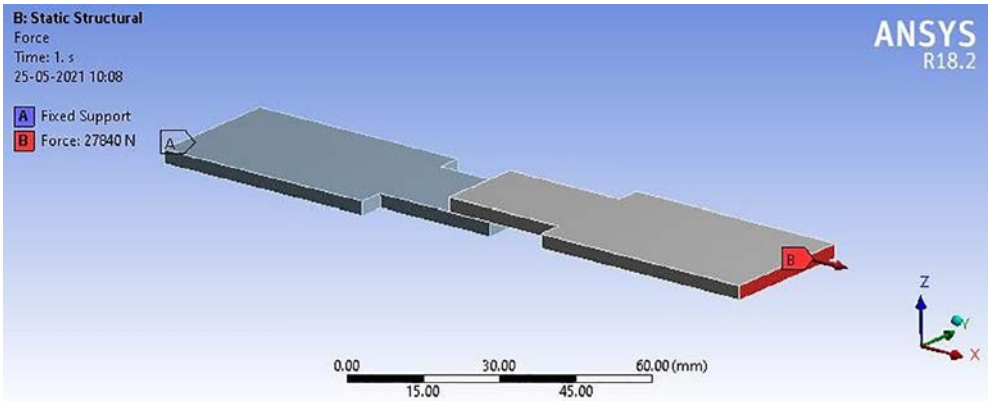

Fig. 7. Boundary conditions.

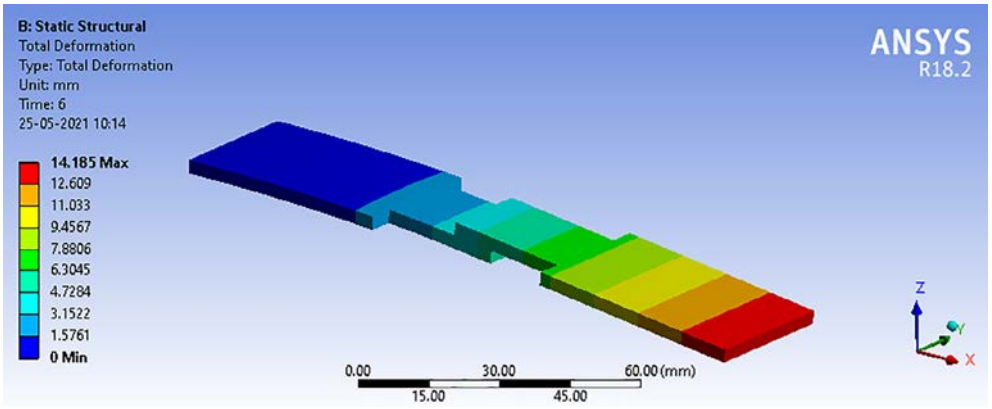

Fig. 8. Deformation in spot welded plates.

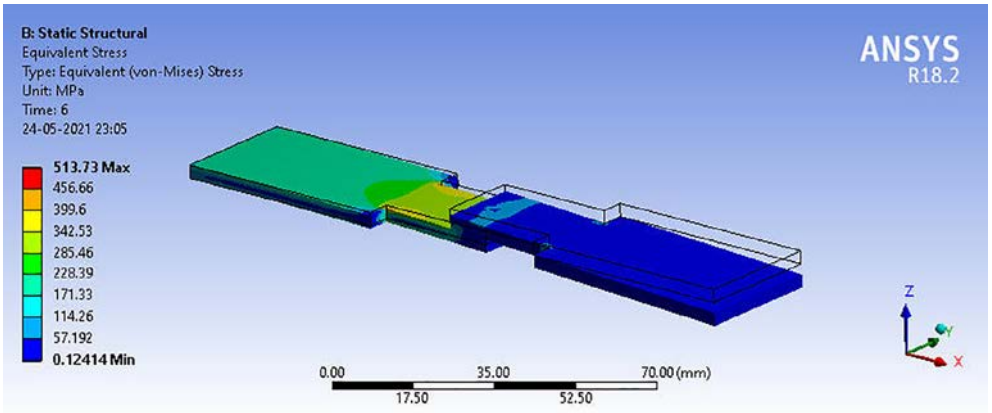

Fig. 9. Von mises stress.

elements having element quality 0.9856. As the number of mesh size is less it increases the accuracy of the results [20]. The meshing of dissimilar weld joints is shown in Fig. 6

3.2.3. Boundary conditions

The boundary conditions applied is necessary to solve equilibrium equation at each element such that continuity is achieved at each node to obtain the stress [21]. The boundary conditions were applied at one end of the dissimilar spot weld joint assuming one side of the joint is fixed (as point B). The material properties are assumed to be isotropic. The boundary conditions applied between the two plates is shown in Fig. 7.

3.2.4. Displacement in plates

The finite element analysis can be used for finding the maximum displacement with the load acting on it [22].The displacement between the two plates were calculated and it was found that maximum displacement between the spot-welded plates were 14.185 mm. The maximum displacement calculated by ANSYS R18.2 is shown in Fig. 8.

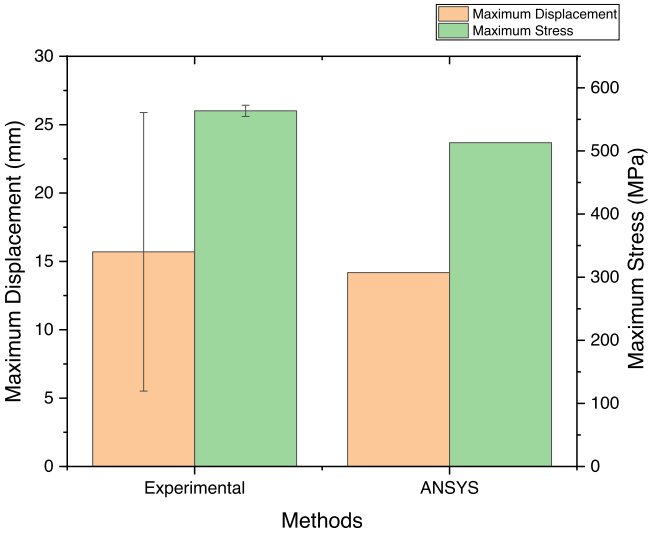

Fig. 10. Error graph with experimental and ANSYS results.

3.2.5. Von Mises stresses

The Von Mises stresses were calculated at the spot weld joint and it was found that the maximum Von Mises stress were found to be 513.73 MPa. The Von Mises stress are in counterpart with ultimate tensile stress (563.563 MPa) and it is less than the yield strength of the joint (415.385 MPa) therefore the spot weld joint can sustain the load applied on it [23].The Von Mises stress calculated by ANSYS R18.2 is shown in Fig. 9.

The error in percentage graph comparing experimental with ANSYS results is shown in Fig. 10.

4. Conclusions

- The maximum displacement obtained with experimental was 15.7 mm and from ANSYS 18.2 the maximum deformation obtained is 14.185 mm.
- The ultimate tensile stress from experimental was 563.563 MPa whereas from ANSYS R18.2 the Von Mises stress is 513.13 MPa.
- The structural analysis results of spot weld joints with experimental (avg.9.57 % error in percentage) are in counterpart with ANSYS results.

CRediT authorship contribution statement

Chetan Tembhurkar: Conceptualization, Methodology, Writing – original draft, Writing – review & editing. **Sachin Ambade:** Software, Validation. **Ravinder Kataria:** Supervision. **Aditya Tikle:** .

Declaration of Competing Interest

The authors declare that they have no known competing financial interests or personal relationships that could have appeared to influence the work reported in this paper.

All authors declare that the work is original and not published elsewhere and there is no conflict of interest between the authors.

References

[1] H.L. Lin, T. Chou, C.P. Chou, Modelling and optimization of the resistance spot welding process via a Taguchi-neural approach in the automobile industry, Proc. Inst. Mech. Eng. Part D J. Automob. Eng. 222 (8) (2008) 1385–1393, https://doi.org/10.1243/09544070JAUTO270.

[2] H. Eisazadeh, M. Hamedi, A. Halvaee, New parametric study of nugget size in resistance spot welding process using finite element method, Materials & Design 31 (1) (2010) 149–157.

[3] P. Snelgrove "Stainless steel automotive and transport developments", International Stainless Steel Forum 2016 1 5 www.worldstainless.org.

[4] J. Yu, J. Shim, S. Rhee, Characteristics of resistance spot welding for 1GPa grade twin induced plasticity steel, Mater. Trans. 53 (11) (2012) 2011–2018, https://doi.org/10.2320/matertrans.M2012167.

[5] S.N. Waghmare, S.D. Shelare, C.K. Tembhurkar, S.B. Jawlekar, Development of a model for the number of bends during stirrup making process, Advances in Metrology and Measurement of Engineering Surfaces (2020) 69–78, https://doi.org/10.1007/978-981-15-5151- 2_7.

[6] S. Ambade, A. P. Patil, C. K. Tembhurkar, and D. B. Meshram, "Effect of filler and autogenous welding on microstructure, mechanical and corrosion properties of low nickel Cr-Mn ASS," Advances in Materials and Processing Technologies, pp. 1–16, 2021.

[7] Y. Sharma Vasudev H",A Short Note on the Friction Stir Welding of the Aluminum Alloys S. Singh C. Prakash S. Ramakrishna G. Krolczyk Advances in Materials Processing Lecture Notes in Mechanical Engineering 2020 Springer Singapore 10.1007/978-981-15-4748-5_12.

[8] A. Hasanbaşoğlu, R. Kaçar, Resistance spot weldability of dissimilar materials (AISI 316L-DIN EN 10130–99 steels), Mater. Des. 28 (6) (2007) 1794–1800, https://doi.org/10.1016/j.matdes.2006.05.013.

[9] M. Alenius, P. Pohjanne, M. Somervuori, and H. Hänninen, "Exploring the mechanical properties of spot welded dissimilar joints for stainless and galvanized steels," Weld. J. (Miami, Fla), vol. 85, no. 12, 2006.

[10] M. Pouranvari, S.P.H. Marashi, Critical review of automotive steels spot welding: Process, structure and properties, Sci. Technol. Weld. Join. 18 (5) (2013) 361–403, https://doi.org/10.1179/1362171813Y.0000000120.

[11] D. Kianersi, A. Mostafaei, A.A. Amadeh, Resistance spot welding joints of AISI 316L austenitic stainless steel sheets : Phase transformations, mechanical properties and microstructure characterizations, J. Mater. (2014), https://doi.org/10.1016/j.matdes.2014.04.075.

[12] A. B. Verma, S. U. Ghunage, and B. B. Ahuja, "Resistance Welding of Austenitic Stainless Steels (AISI 304 with AISI 316)," 5th International & 26th ALL India Manufacturing Technology,Design and Research Conference (AIMTDR-2014) IIT Guwahati,Assam,India. December 12th-14th, 2014.

[13] Anand Prakash Singh,Dharamvir Mangal, "Study and assessment of mechanical properties of resistance spot weld of two dissimilar metals (AISI)," International Journal of Engineering Sciences & research technology" vol.no.6,no.10,2017, pp.297–302.

[14] G.I. Mahiskar, R.B. Chadge, S.P. Ambade, A.P. Patil, Thermo-mechanical Analysis of Multi-pass Bead-on-Plate Welding, Procedia Materials Science 5 (2014) 2522–2531.

[15] C. Tembhurkar, R. Kataria, S. Ambade, J. Verma, A. Sharma, S. Sarkar, Effect of Fillers and Autogenous Welding on Dissimilar Welded 316L Austenitic and 430 Ferritic Stainless Steels, J. Mater. Eng. Perform. 30 (2) (2021) 1444–1453, https://doi.org/10.1007/s11665-020-05395-4.

[16] S. Ambade, C. Tembhurkar, A. P. Patil, P. Pantawane, and R. P. Singh, "Shielded metal arc welding of AISI 409M ferritic stainless steel: study on mechanical, intergranular corrosion properties and microstructure analysis," World Journal of Engineering, vol. ahead-of-print, no. ahead-of-print, Aug. 2021.

[17] J. Wang, Y. Xia, Q. Zhou, and J. Zhang, "Simulation of Spot Weld Pullout by Modeling Failure Around Nugget," SAE Technical Paper Series, Apr. 2006.

[18] M. Alizadeh-Sh, S.P.H. Marashi, M. Pouranvari, Resistance spot welding of AISI 430 ferritic stainless steel: Phase transformations and mechanical properties, Materials & Design 1980–2015 (56) (Apr. 2014) 258–263.

[19] C. Tembhurkar, R. Kataria, S. Ambade, J. Verma, Transient analysis of gta-welded austenitic and ferriticstainless steel, Lect. Notes Mech. Eng. (2020) 59–65, https://doi.org/10.1007/978-981-15-4748-5_6.

[20] N.A. Nazri, M.S.M. Sani, Finite element normal mode analysis of resistance welding jointed of dissimilar plate hat structure, IOP Conference Series: Materials Science and Engineering 257 (Oct. 2017) 012059.

[21] C.K. Tembhurkar, S.D. Shelare, Air Engine Piston : A Finite Element Approach, LAP LAMBERT Academic Publishing, Germany, December 2018.

[22] S.D. Shelare, K.R. Aglawe, P.B. Khope, Computer aided modeling and finite element analysis of 3-D printed drone, Materials Today: Proceedings (2021).

[23] S. Waghmare, N. Mungle, C. Tembhurkar, S. Shelare, N. Pathare, Design and analysis of power screwfor manhole cover lifter, Int. J. Recent Technol. Eng. 8 (2) (2019) 2782–2786, https://doi.org/10.35940/ijrte.B2628.078219.

Volume 62, Part 2, 2022, Pages 981-986

Performance evaluation of CNC turning process for tool tip temperature and tool wear by Taguchi method

Author links open overlay panelPrashant D. Kamble [a], Atul C. Waghmare [b], Ramesh D. Askhedkar [c], Shilpa B. Sahare [a], Manoj Patil [d], Sunil V. Prayagi [a]

https://doi.org/10.1016/j.matpr.2022.04.147Get rights and content

Abstract

The performance of the CNC turning process is experimentally evaluated in this paper. The independent variables are feed rate, depth of cut, nose radius, tool type, and environmental condition. Three different levels of predictors are selected. The dependent variables are TTT (tool tip temperature) and TW (tool wear). The machine is run at 1337 RPM. The chatter in the spindle is included as an uncontrollable variable (Noise Factor) with three different values. The number of observations is calculated by Taguchi Method. The experimentation is conducted on CNC Spinner Lathe Machine. The responses are measured by a Non-contact laser gun and Canny Method in MATLAB software. The analysis is performed by Taguchi philosophy and ANOVA. The best setting for responses is identified by the main effect plot. The prediction of the output parameters at optimum levels is done by additive model.

Minimum Tool Tip Temperature (50.545 °C) is achieved when Environmental condition is at high level (minimum quantity lubrication), Nose Radius is at low level (0.4 mm), Feed rate is at low level (0.15 mm/rev), Depth of cut is at low level (0.5 mm) and tool type is at high level (CVD Coated insert). Minimum Tool Wear (0.0401 mm) is achieved when Environmental condition is at high level (minimum quantity lubrication), Nose Radius is at high level (1.2 mm), Feed rate is at high level (0.35 mm/rev), Depth of cut is at low level (0.5 mm) and tool type is at high level (CVD Coated insert).

Introduction

Nowadays, it is very important to satisfy the end-users (Customers) as much as product quality is considered. Quality is nothing but the measure of performance of product after selling to the customer. And productivity is very crucial to the manufactures, when profit is considered. Both quality and productivity are contradictive in nature. Hence it becomes necessary to identify the best setting of factors related process/product that will satisfy both quality and productivity. Multi-objective optimization is a tool which helps to achieve this.

In machining process, especially in turning, milling and drilling, condition of cutting tool decides the quality of surface finish and MRR (Material removal rate). TTT and TW decide the condition of cutting tool. If the tool is not damaged (wear), the predefined value of quality characteristics can be achieved. But if the machining is done with damaged cutting tool, even if the optimal setting is used, the quality of finished products get degraded. Hence, in this paper, the tool tip temperature and tool wear are considered for performance evaluation of Turing process. AISI 4340 is used as workpeice material and coated (PVD & CVD) as well as uncoated inserts are used as cutting tool. Shilpa B. Sahare *et al.* [1], this paper described the use of Taguchi philosophy to optimize milling process for the workpeice AI2024. A comparative study is done for different type of lubrications though experimentation. A flow rate was the key factor for performance evaluation of lubrication. A regression model is generated for prediction of responses. P.P. Shirpurkar *et al.* [2], surface finish and machine tool vibration are output factors in this research study. Taguchi method is used to find the better values of responses. In design of experiment, Taguchi L_{16} orthogonal array is used. Analysis of variance is used for the data analysis. Anwarul Haque *et al.* [3], this paper investigated the optimal setting of wire EDM process parameters. The factors used are Ton, Toff, Wp, Wf. The workpiece is HCHCr. The orthogonal array L-9 is used. GRA (Grey relational Analysis) is implemented to MOO (multiple objective optimization). Analysis is done in Minitab 15 software. The experimental result revealed that the Wire EDM process is improved by the optimum setting of input parameters. P.D Kamble *et al.* [4], researcher used GRA and TM (Taguchi method) to optimize the turning process. The aim was to reduce the values of SR (Surface Roughness) and TW (Tool Wear) at a time. Basic turning factors are considered for experimentation. The effect on Surface Roughness and Tool Wear is tested for different Environmental Conditions like dry, wet and MQL. Machine tool is CNC Spinner Lathe machine. Workpeice used is AISI 4340 steel. The multi-optimization is carried out by Grey Relational Analysis. L_{27} Orthogonal Array (OA) is used for number of experimentation. ANOVA and response table are used for data analysis. P.D. Kamble [5], in this paper Taguchi philosophy is used for design of experiment. The response factor surface roughness is evaluated experimentally for turning process. The cutting speed, feed rate, nose radius, depth of cut are used as controllable factors. Signal to noise ratio of surface roughness is tabulated by Smaller-the-better Taguchi quality characteristic. No replication or repetition of output parameter is done, only one value for one setting is considered. Experimentation is conducted by orthogonal array L27. Main effect plot is generated in MINITAB software and

optimal setting is predicted. K. Rajkumar *et al* [7], this paper explained the performance of machining process by using different tool inserts like cBN and PCD inserts. Composite material, especially aluminium based composite is used for its vast applications in transportation, aerospace, automobiles and defence. The performance of turning process is evaluated with PCD and cBN inserts. These tools have lesser tool wear attainment. Shilpa Sahare *et al* [8], in this paper researchers used Taguchi Method to obtain the better values of responses. L_9 orthogonal array was adopted for experimentation. To match the latest scenario of manufacturing system, MQL (minimum quantity lubrication) was used. ANN technique along with Taguchi to find the regression model. Ahilan, C *et al* [9], this paper focused on optimization of multiple output factors of turning process. GRA (grey relational analysis) was jointly used with Taguchi method. S45C Carbon Steel was used as workpiece material. It is concluded that "Process parameters can be improved by Taguchi method". Jasper, S *et al* [10], this paper discussed the optimization of multiple output factors of turning process. PCA (Principal component analysis) was combined with Taguchi method. A mathematical model was made for two factors. Harun Akkuş *et al* [11], this paper described the Taguchi philosophy in optimizing the process for turning AISI 1040 steel. L_{16} (Taguchi Orthogonal array) is used for experimentation. ANOVA and S/N are implemented to select the optimized factor. Tzeng Chorng-Jyh *et al* [12], in this work, optimization of multi parameter optimization was done by GRA (Grey Relational Analysis) with Taguchi Method. L_9 (Taguchi Orthogonal Array) experimentation was conducted. It is revealed that "Depth of cut is the most significant factor to get better roughness". Sahoo *et al* [13], researchers investigated that Taguchi method is good for minimizing the number of experimentations. Further it is stated that depth of cut is the significant parameter for optimizing the MRR. S. Madhavi *et al* [14], this work focused on process optimization by Taguchi Method. It is stated that this method was suitable to obtain best values of surface finish with more hardness. Ahmet Hasçalık *et al* [15], in this study, optimization of turning Ti-6Al-4V material was done by Taguchi approach. Life of tool and roughness of material's surface were optimized at a time.

Section snippets

Experimentation

The experimentation is conducted on CNC lathe machine. The workpiece is AISI 4340 steel bat. The length of bar is 8 cm and diameter is 5 cm. In the workplace (industry), the equipment's used in Hydraulic system such as split bush are manufactured by this material. Further, it is used to manufacture gear shaft, landing gears, propellers etc. It is the alloy of high tensile steel. It has good wear resistance and high strength. Table 1 shows the chemical composition of workpiece.

Before the

Data analysis

Data analysis by Taguchi method is performed as follows.

- (a)
  Selection of S/N ratio equation.

Depending upon the nature of response, the equation is selected. The smaller values of TTT and TW are preferable, hence Lower-the-Better S/N ratio is selected.��=-10log1�∑�2

- (b)
  Calculation of S/N ratio. TTT and TW with S/N ratio is enumerated in Table 2.

- (c)
  Computation of Response Table for mean S/N ratio for every level of TTT and TW.

- (d)
  Prediction of optimal setting.

Result

Minimum TTT (50.545 °C) is achieved when FR (mm/rev) is 0.15, DOC (mm) is 0.5 with CVD Coated insert of 0.4 mm NR under minimum quantity lubrication and minimum Tool Wear (0.0401 mm) is achieved when FR (mm/rev) is 0.35, DOC is 0.5 mm with CVD Coated insert of 1.2 mm NR under minimum quantity lubrication.

Low feed rate is preferable for achieving low temperature at tool tip with CVD Coated insert. Low Depth of cut is advised for machining of AISI 4340 steel to achieve low temperature at tool. It

Conclusion

Taguchi Technique is applied effectively to find best output. The decision made are mentioned bellows:

- 1.
  Taguchi technique is fruitfully utilized to enhance TTT and TW

- 2.
  Quality characteristic Tool tip temperature is optimized to 50.545 °C

- 3.
  Quality characteristic Tool wear is optimized to 0.0401 mm.

- 4.
  Table 4 shows the best setting for TTT and TW.

- 5.
  The optimal setting for TTT is CE = MQL, NR (mm) = 0.4, FR (mm/rev) = 0.15, DOC (mm) = 0.5 and TT = Coated (CVD) insert.

- 6.
  The optimal setting for TW is CE = MQL,

Declaration of Competing Interest

The authors declare that they have no known competing financial interests or personal relationships that could have appeared to influence the work reported in this paper.

References (15)

- K. Rajkumar *et al.*

  Machining characteristics evaluation of aluminium composites based on cBN and PCD inserts
  Mater. Today: Proc.
  (2018)
- C.-J. Tzeng *et al.*

  Optimization of turning operations with multiple performance characteristics using the Taguchi method and Grey relational analysis
  J. Mater. Process. Technol.
  (2009)
- S. Krishna Madhavi *et al.*

  Evaluation of optimum turning process of process parameters using DOE and PCA Taguchi method
  Mater. Today: Proc.
  (2017)
- Shilpa B. Sahare *et al.*

  Experimental investigation of end milling operation on Al2024
  Mater. Today: Proc.
  (2017)
- P.P. Shirpurkar *et al.*

  Optimization of CNC Turning Process Parameters for Prediction of Surface Roughness by Taguchi Orthogonal Array
  Int. J. Eng. Res. Technol.
  (2014)
- Anwarul Haque *et al.*

  Multiple Optimization of Wire EDM Machining Parameters Using Grey Based Taguchi Method for Material HCHCR
  Int. J. Modern Eng. Res.
  (2014)
- P.D. Kamble *et al.*

  Application of hybrid Taguchi-Grey relational analysis (HTGRA) multi-optimization technique to minimize surface roughness and tool wear in turning AISI4340 steel
  J. Phys. Conf. Ser.
  (2021)

There are more references available in the full text version of this article.

Cited by (0)

View full text

2022 International Conference on Emerging Trends in Engineering and Medical Sciences (ICETEMS) | 978-1-6654-6112-2/22/$31.00 ©2022 IEEE | DOI: 10.1109/ICETEMS56252.2022.10093365

Brain Tumor Segmentation and Model Optimization for 3-D Printing

Chetan Mahatme
Department of Mechanical Engineering
Yeshwantrao Chavan College of Engineering
Nagpur, India
chetanmahatme@gmail.com
https://orcid.org/0000-0001-5602-2450

Jayant Giri
Department of Mechanical Engineering
Yeshwantrao Chavan College of Engineering
Nagpur, India
jayantpgiri@gmail.com
https://orcid.org/0000-0001-9072-0607

Rajkumar Chadge
Department of Mechanical Engineering
Yeshwantrao Chavan College of Engineering
Nagpur, India
rbchadge@rediffmail.com
https://orcid.org/0000-0003-4438-2613

Punit Fulzele
Dept. of Pedodontics
Jawaharlal Nehru Medical College,
Datta Meghe Institute of Medical Sciences,
Sawangi (M), Wardha, India
punitr007@gmail.com

***Abstract*— Medical image acquisition is generally done through Magnetic Resonance Imaging (MRI) or computerized tomography (CT) scan which is a non-intrusive technique. For identifying the Tumor in the brain, a segmentation process is used which involves using image processing algorithms on MRI scans. While many approaches have been used for brain tumor segmentation, the manual segmentation process is tedious and has inherent problems associated with it. This paper proposes an implementation of 3-D slicer segmentation of the brain tumor model along with STL model optimization using Autodesk Netfabb. This will provide an effective way of reducing the STL errors in the segmented 3-D models. These optimized models can then be 3-D printed which will provide accurate information on tumor shape and size to the medical professionals. The process of STL model optimization shows very promising results on the MRI dataset used in this case study and it achieves the creation of error-free STL models for 3-D printing. Additionally, this work demonstrates the effective use of the 3-D slicer along with Autodesk NetFabb, to considerably reduce the STL errors which were generated in the conventional process of manual segmentation. The manual segmentation process was tedious and required force smoothening of 3-D slicer models obtained after segmentation leading to faulty 3-D model printing.**

Keywords*— *medical image segmentation, 3-D printing, optimization, STL error

I. INTRODUCTION

Early detection of a brain tumor is important for exploring and improving the treatment possibilities. The process of tumor diagnosis generally falls into two categories. The first one is anatomy-related computed tomography (CT) and MRI (magnetic resonance imaging) and the other is PET and SPECT. The output of MRI scans creates different contrast levels of the tissue which provides various details of a structure. The brain tumor diagnosis modalities include weighted (T1 & T2), gadolinium contrast enhancement (T1-Gd), and fluid-attenuated inversion recovery (FLAIR). Tumors in comparison to normal tissues look dark using T1, and bright using T2. The brain tissue pressured by the tumor also looks bright using T2 [1]. Most of the time, T1 separated normal tissues from the tumor. T2 generally separates the edema region, the edges of the tumor are identified using T1-Gd, and FLAIR is utilized for separating the edema region and the CSF. The tissues can be separately identified based on their contrast in different modalities. The various challenges involved in the segmentation of brain tumors are varying tumor sizes, location, shape, and non-homogenous tissue intensities [2]. Present techniques involve manual segmentation of the tumor through image processing tools. Manual segmentation of the edges of the tumor is a tedious task. In addition to the segmentation process, validation of the accuracy of the results is currently much limited. Nowadays 3-D printing is an emerging technology through which we can create physical objects layer-by-layer. The use of this technology has been widely embraced in the medical imaging domain, prosthetics, and implants. These 3-D printed models help to improve the understanding of the human brain anatomy and other important organs.

The 3-D prints of the human brain are found to help understand the structure of the brain and position of the tumor for pre-surgical simulation [3]. 3-D printing was not popular before for analyzing brain tumors. The creation of patient-specific 3-D printed brain tumor models was first done in a pediatric patient and successfully showed the use of 3-D printing in the creation of anatomical parts [4]. A detailed review on the use of 3-D printing for simulating cranial neurosurgery using 3-D printed models in pre-operative simulation and training for the neurosurgeons was successfully performed [5]. A computerized image processing software for preoperative surgical planning using MRI images was developed for analyzing brain tumors [4]. An extensive review was also undertaken on informative techniques for visualization in 3-D from MRI data [6]. A Pineal gland tumor 3-D model using CT and MRI images was created for a 4-month-old male patient and was used in neuro-endoscopic training and simulation [7]. Due to the complexity of internals in the brain, the use of rapid prototyping technology for neurosurgery simulation is still vastly unexplored. In preoperative planning of brain surgeries, the safest approach is which causes minimum brain tissue damage [8, 9]. Since its introduction, medical imaging techniques, mostly MRI have been used by neurosurgeons for planning brain surgeries. Due to the contrast difference, these images can show a clear visual distinction between the healthy and tumor tissue [10, 11].

These days, virtual reality simulation of surgical procedures was emulated by surgeons. Current advances in virtual surgical simulation using MRI for brain surgery using haptic devices have largely improved the outcomes of neurosurgery which facilitated the surgeons to virtually simulate the surgery by using a computer and select the optimal procedure while carrying out the actual surgery [12]. Though such advancements are there, the major drawback of these techniques is that the perception of depth information on a 2-D screen is quite difficult, and also these simulations do not permit realistic interaction with the physical anatomy, which 3-D printed models can only offer.

In a recent study, interactive virtual simulation (IVS) which is a virtual reality pre-surgical simulation combined with 3-D printed models showed how 3-D printing can be used for preoperative planning and rehearsal for deep brain tumors [13]. The main advantages of using this approach for pre-surgical planning include more understanding of complex anatomy which helped in the complicated procedure of bone dissection which is necessary to create canals in the base of the skull without damaging the surrounding tissue. Novel approaches to neurological 3-D printing are more related to developing methods to create 3-D brain models with details of cerebral blood circulation. Though advancements are there in virtual surgical simulation for preoperative planning, it is not sufficient in providing the total real experience of surgeries or planning a surgical path with real instruments. These limitations are large because of the requirement of computer skills and hardware for its widespread application.

Now, the first application of 3-D printing in neurosurgical planning combinedly used standard CT and MR angiography data for 3-D printing (SLA) cerebrovascular models of patients diagnosed with cerebral aneurysms and cerebral arteriovenous malformations (AVM) [14]. These vasculature models were solid structures and were complete replicas of the original. They showed the lumen structure which is highlighted by contrast in CTA or blood flow in MRA. Further, SLA 3-D printed models of cerebral aneurysms with parent and surrounding vessels were created from 3-D CT scans and 3-D rotational angiography data [15]. With the help of this data, small vessels were fabricated with a resolution of 0.4 mm. But, as these models were made up of solid resin material, they were unsuitable for evaluating neck geometry, simulating clipping, and practicing dissection procedures. Hence, though these models were having higher resolution, they were not helpful in presurgical planning. Later studies demonstrated the first 3-D printed hollow models of cerebral aneurysms which could be practically used for preoperative planning and surgical training [16]. In another approach, a hollow, capable elastic cerebral 3-D printed model was fabricated for surgical simulation, which demonstrated an aneurysm and the parent artery using an FDM-based 3D printer [17].

In recent studies, different algorithms are used for medical image segmentation [18]. The segmentation to 3-D print workflow with different segmentation packages is also analyzed for an in-hospital scenario [19]. A detailed review of 3-D printing parameters, slicing, supports and post-processing techniques were also done [20]. The effect of different process parameters like infill density and layer thickness was also assessed for the accuracy of 3-D printed parts [21]. The voxel mapping decoupling fast calculation algorithm was also developed for region recognition in STL which involved the use of interference ratio for estimating the complexity of the 3-D model [22].

In all these approaches the 3-D printed model of the anatomical part was created directly from the STL model obtained from the segmentation software using MRI/CT data. In some cases, the segmented models were smoothened with third-party software but that resulted in losing out the important shape and size characteristics of the anatomical part in consideration. In some cases, the surface of the printed part is smoothened by using external processes. In both cases, the 3-D printed anatomical part was not accurately replicated. Taking this into consideration, this study aims at reducing or eliminate these errors in STL models by providing a simple process of STL model optimization. The methodology followed for obtaining the desired results is explained in further sections.

II. METHODOLOGY

The process followed in this research work for carrying out the optimization of 3-D models obtained through the process of medical image segmentation involves the work-flow as shown in fig. 1. The different stages for generating STL models are Acquisition of Medical Image, Segmentation using image processing tools, creation of ROI, and 3-D Model generation. Medical Image Datasets are mainly CT or MRI. For dental applications, orthopedics, etc., CT scan images are preferred, whereas MRI images can be acquired by not exposing the patients to harmful radiation. For medical imaging of soft tissue such as tendons, ligaments, and the brain, MRI is preferred. The MRI images available in the respective dataset are used here for the creation of STL models using open-source software called 3-D slicer.

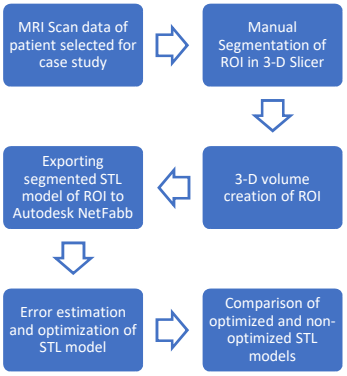

Fig. 1. Workflow followed in the research work

A. Case study

The case study involves a patient already diagnosed with a brain tumor. The MRI scan data of this patient is in the form of 2-D images which are used for diagnosing the patient's medical condition. The MRI scan data involves a NiFTi or .nii file which includes the stacks of many 2-D images. The region of interest (ROI) i.e., brain tumor is then extracted from these 2-D images and combined layer-by-layer to form a 3-D volumetric surface model.

B. Dataset

The MRI datasets (Brain Tumor Segmentation BraTS) are obtained from the challenge for biomedical image analysis called "Medical Segmentation Decathlon" [23], in which different teams compete with their algorithms on different tasks as well as modalities. These datasets were available under personal and non-profitable use licenses. The dataset

has 750 multi-parameter-based magnetic resonance images (mp-MRI) from either glioblastoma or lower-grade glioma-diagnosed patients.

C. Selection of Dataset

The MRI dataset is selected based on the tumor position in the brain. The specifications of the dataset selected are given in Table I. The selection of this dataset is done because of the challenge of locating these complex and heterogeneously-located targets [18].

TABLE I. MEDICAL IMAGE DATASET SPECIFICATIONS

Anatomy	*Neuroimaging file format*	*File Name*	*Modality*	*Protocol*	*Target*
Brain	(NiFTi)	BRATS_221.nii	mp-MRI	FLAIR, T1w, T1 \w Gd, T2w	Edema, enhancing and non-enhancing tumor

III. RESULTS

The MRI dataset of the patient selected for the case study is first imported into the 3-D slicer. The image segmentation process is then carried out manually for separating the ROI. The main segmentation effect used for separating the ROI was the Threshold.

A. Output from the 3-D slicer

The manual segmentation is processed on MRI data in a 3-D Slicer by using slices of images in 3 views namely axial, coronal and sagittal, concurrently, as shown in Fig. 2. After carrying out the manual segmentation of ROI from the MRI, the 3-D model of the brain tumor obtained is shown in Fig. 3. The segmentation settings used are listed in Table II. These extracted tumors are then exported as STL models to Autodesk NetFabb for further processing.

TABLE II. MANUAL SEGMENTATION SETTINGS

Effect	*Editable Intensity Range*	*Segmentation Planes*	*Surface Smoothing*
Threshold	883.79 to 2132.65	Axial, Coronal, and Sagittal	No

B. Optimization in NetFabb

The 3-D brain tumor model obtained through a 3-D slicer is then imported into Autodesk Netfabb software. The STL model is then analyzed for errors. The errors present in the STL model are listed in Table III. Fig. 4 below also shows the visual representation of the errors present in the 3-D model. The STL model is then optimized with the help of custom Lua scripting created in the Autodesk Netfabb software. The Lua script has multiple repair tasks which involved stitching triangles, closing trivial holes, fixing flipped triangles, removing degenerated faces, etc. By repairing the errors in the STL mesh, the mesh becomes continuous. This continuous mesh is then suitable for 3-D printing and the shape of the 3-D model of a brain tumor will be accurately printed with any 3-D printer.

TABLE III. STL ERROR ESTIMATIONS

Model	*Mesh*	*Open Border Edges*	*Surface Holes*	*Inverted Orientations of triangles*
Segmented Brain Tumor	Open	56	17	200

C. Comparative analysis of STL models

The 3-D models obtained directly through a 3-D slicer without any optimization and the 3-D model obtained through Autodesk Netfabb are compared. The comparison data is shown in Table IV. The STL model shown in Fig. 5 (b) shows the mesh comparison and surface deviation from the actual model as 0mm i.e. it shows that the surface contours are accurately preserved during the STL optimization process.

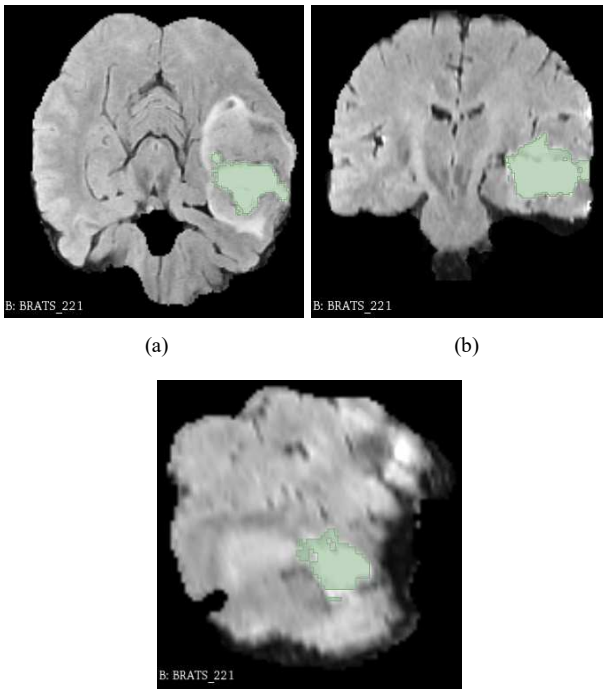

(a) (b)

(c)

Fig. 2. Segmentation of MRI data in 3-D Slicer (a) Axial (b) Coronal (c) Sagittal

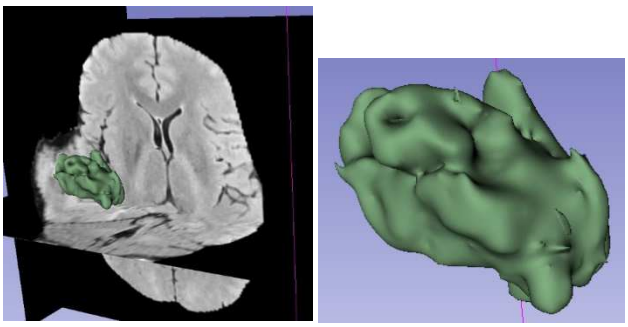

(a) (b)

Fig. 3. 3-D model of ROI segmented from MRI data (a) 3-D model (with MRI image in the backdrop) and (b) 3-D model (individual)

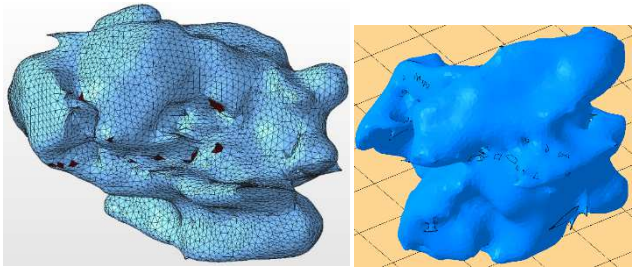

(a) (b)

Fig. 4. STL errors in the 3-D model imported from 3-D slicer (a) Meshed model with highlighted errors (b) CAD model with errors

TABLE IV. ERROR OPTIMIZATION RESULTS

Model	*Mesh*	*Open Border Edges*	*Surface Holes*	*Inverted Orientations of triangles*
Segmented Brain Tumor	Closed	0	0	0

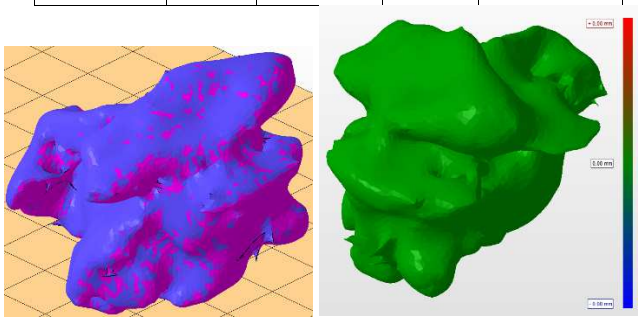

(a) (b)

Fig. 5. Mesh comparison of the non-optimized and optimized model (a) Mesh overlapped (b) Surface deviation after mesh optimization

IV. CONCLUSION

Medical image segmentation is a very difficult task when done manually and the resulting 3-D models have inherent problems. These problems include non-conforming surface geometries to the actual anatomical part. These errors in 3-D models obtained through segmentation arise due to voids and misplaced voxels while surface creation from segmented images. The comparative analysis of 3-D models created using the segmentation process in the 3-D slicer and optimized models produced in Autodesk NetFabb provide a way of analyzing the effect of errors and deviation in the model shape and size. In this way, the efficient, optimized, true-to-shape 3-D can be created and further can be used for 3-D printing. For further work in this area, machine learning techniques, specifically deep learning, with the help of python tools like PyTorch and PyVista can be used to produce error-free STL models directly through the 3-D slicer with an integrated python environment. These accurate models when 3-D printed can then be utilized by medical professionals for pre-operative planning, training, simulation, and patient awareness and can effectively reduce the hazards during the surgery.

ACKNOWLEDGMENT

The work has not received any funding from external agencies.

REFERENCES

[1] Bauer S, Wiest R, Nolte L et al (2013). A survey of MRI-based medical image analysis for brain tumor studies. Phys Med Biol, 13, 97-129.

[2] Wang Z (2018). Automatic brain tumor segmentation by deep convolutional networks and graph cuts. Comput Sci, 2018,Corpus ID: 13995863

[3] Mullar A, Krishna KG, Uhl E "The Applications of Rapid Prototyping techniques in cranial reconstruction and preoperative planning in neurosurgery", J craniofacial surgery – 2003, pg no 899 – 914.

[4] Ivan Lau, Andrew squwlch, Yung wan, "Patient specific 3D printed model in delineating brain glioma and surrounding structure in a pediatric patient", published in wolten kluwer – 2017.

[5] Vakharia VN, Vakharia NN, Hill CS " Review of 3D printing on cranial neurosurgery simulation training", World neuro surgery – 2016, pg no 188 – 198.

[6] Kikins R, Gleoson PL, Moriatry TM, "Computer Assisted Interactive 3D planning for neurosurgical procedures", neurosurgery – 1996.

[7] Michael kuhlmann, James Drake, "Development of 3D patient specific brain model with a pineal region tumor and hydrocephalus for neuroendoscopic simulation and training," published in RCSI - 2013, volume – 6, number – 1, pg no 68 – 71.

[8] B.S. Spottiswoode et al., Preoperative three-dimensional model creation of magnetic resonance brain images as a tool to assist neurosurgical planning. Stereotact. Funct. Neurosurg. 91(3), 162–169 (2013)

[9] J. Kettenbach et al., Computer-based imaging and interventional MRI: applications for neurosurgery. Comput. Med. Imaging Graph. 23(5), 245–258 (1999)

[10] J. Hirsch et al., An integrated functional magnetic resonance imaging procedure for preoperativemapping of cortical aread associated with tactile, motor, language, and visual functions. Neurosurgery 47(3), 711–722 (2000)

[11] J. Geerts et al., Functional magnetic resonance imaging for preoperative localisation of eloquent brain areas relative to brain tumours: clinical implementation in a regional hospital. JBR-BTR Organe Société R. Belge Radiol. SRBR Orgaan Van K. Belg. Ver. Voor Radiol. KBVR 90(4), 258–263 (Jan. 2007)

[12] G.M. Lemole, P.P. Banerjee, C. Luciano, S. Neckrysh, F.T. Charbel, Virtual reality in neurosurgical education. Neurosurgery 61(1), 142–149 (2007)

[13] M. Oishi, M. Fukuda, N. Yajima, and K. Yoshida, Interactive presurgical simulation applying advanced 3D imaging and modeling techniques for skull base and deep tumors: Clinical article, J. Of, (2013)

[14] P.S. D'Urso et al., Stereolithographic (SL) biomodelling in craniofacial surgery. Br. J. Plast. Surg. 51(7), 522–530 (Oct. 1998)

[15] G.Wurm, B. Tomancok, P. Pogady, K. Holl, J. Trenkler, Cerebrovascular stereolithographic biomodeling for aneurysm surgery. Technical note. J Neurosurg 100(1), 139–145 (2004)

[16] T. Kimura et al., Simulation of and training for cerebral aneurysm clipping with 3-dimensional models. Neurosurgery 65(4), 719– 726 (2009)

[17] T. Mashiko et al., Development of three-dimensional hollow elastic model for cerebral aneurysm clipping simulation enabling rapid and low cost prototyping. World Neurosurg 83(3), 351– 361 (2015)

[18] Fogarasi, M., Coburn, J.C. & Ripley, B. Algorithms used in medical image segmentation for 3D printing and how to understand and quantify their performance. 3D Print Med 8, 18 (2022). https://doi.org/10.1186/s41205-022-00145-9

[19] Wijnen N, Brouwers L, Jebbink EG, Heyligers JM, Bemelman M. Comparison of segmentation software packages for in-hospital 3D print workflow. Journal of Medical Imaging. 2021;8(3): 034004

[20] Piedra-Cascón W, Krishnamurthy VR, Att W, Revilla-León M. 3D printing parameters, supporting structures, slicing, and post-processing procedures of vat-polymerization additive manufacturing technologies: A narrative review. J Dent. 2021;109: 103630.

[21] Jayant Giri, Anagha Chiwande, Yash Gupta, Chetan Mahatme, Pallavi Giri, Effect of process parameters on mechanical properties of 3d printed samples using FDM process, Materials Today: Proceedings, Volume 47, Part 17, 2021, Pages 5856-5861, ISSN 2214-7853, https://doi.org/10.1016/j.matpr.2021.04.283.

[22] Bo, Q., Hongri, F. & Jianrui, Z. Fast calculation algorithm for region recognition and model interference ratio in the STL model based on voxel mapping decoupling. Int J Adv Manuf Technol 119, 1553–1578 (2022). https://doi.org/10.1007/s00170-021-08116-w

[23] Michela Antonelli, Annika Reinke, Spyridon Bakas et al., The Medical Segmentation Decathlon, arXiv:2106.05735, https://doi.org/10.48550/arXiv.2106.05735

2022 International Conference on Emerging Trends in Engineering and Medical Sciences (ICETEMS) | 978-1-6654-6112-2/22/$31.00 ©2022 IEEE | DOI: 10.1109/ICETEMS56252.2022.10093565

Experimental analysis of twin blade contra-rotating wind turbine

Neeraj Sunheriya
Department of Mechanical Engineering
Yeshwantrao Chavan College of Engineering
Nagpur, India
neeraj.sunheriya@gmail.com

Rajkumar B. Chadge
Department of Mechanical Engineering
Yeshwantrao Chavan College of Engineering
Nagpur, India
rbchadge@rediffmail.com

Jayant P Giri
Department of Mechanical Engineering
Yeshwantrao Chavan College of Engineering
Nagpur, India
jayantpgiri@gmail.com

Sachin G Mahakalkar
Department of Mechanical Engineering
Rajiv Gandhi College of Engineering & Research
Nagpur, India
sachu_gm@yahoo.com

Pratik Lande
Department of Mechanical Engineering
Yeshwantrao Chavan College of Engineering
Nagpur, India
pratklande@gmail.com

Ashuosh Bagde
Jawaharlal Nehru Medical College,
Datta Meghe Institute of Medical Sciences,, Sawangi (M), Wardha., India
bagde.ashu@gmail.com

***Abstract*—Responding to current energy demand scenario, there will be a more demand in coming years. The energy requirements of developed and developing country continuously increasing, that will increase the exploration of renewable energy sources, needs more efficient system to meet requirement. The wind energy is one of the area to satisfy current scenario. To meet it, it is important issue to concentrate on small wind energy industry apart from commercial systems. Another critical aspect of wind energy usage is the efficiency with which usable energy is converted into producing power. Enhance technologies such as twin blade contra rotating rotors, generators, gears and lube oils, aero foil shapes and profile, smart pitch control rotors etc. will minimizes the total cost and increase total output power. The purpose of this work is, therefore, to support the effectiveness of employing Twin-blade contra-rotating system to enhance performance of twin blade contra-rotating wind turbine system. With this idea, the contra-rotating system works more efficient and produced more power in a unit turbine area. To support this approach, a research model was developed and tested under a variety of operating conditions. To verify turbine system a test were carried out in wind tunnel. Result are presented for cases of different wind speeds, Reynolds number and different angle of attack for blades. The result exhibit a significant increase in wind energy conversion efficiency in case of twin blade contra-rotating system and good response to low wind speed compared to single rotor system of same type.**

Keywords— wind turbine, contra rotating rotor, wind tunnel, betz limits, angle of attack, NREL S809 aerofoil profile.

I. INTRODUCTION

The wind power business is the world's fastest expanding electric power industry [1]. Global installed capacity now exceeds 32000MW, with a predicted annual growth rate of 10,000MW over the next five years. The quick development of technology used to materialise wind turbines equipment used to produce electric power from the wind may be ascribed to the remarkable expansion of this business. For economic reasons, the majority of wind turbine technology research has concentrated on huge wind turbines (60-80m tower and 70-100m blade span). Despite a declining global economy, India's power demand increased in 2012. Electricity scarcity is prevalent, and more than 40% of the population lacks access to modern energy services. Between 2005 and 2030, India's power demand is expected to more than treble. The Central Electricity Authority forecasted the demand for 350-360 GW of total generating capacity by 2022 in the newly announced NEP (2012).

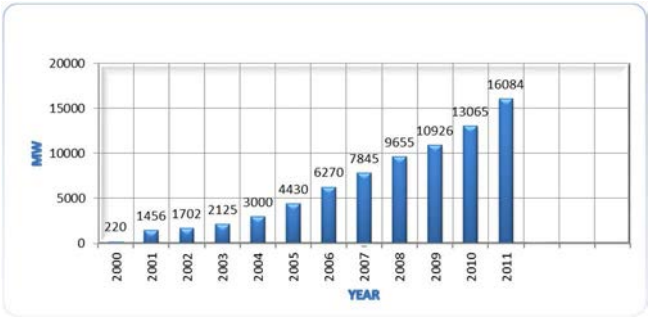

Fig. 1. India's cumulative wind installation growth rate per year in MW

A. Objectives and scope

The objective of this work was to study the effect of blade angles on the power generated by wind turbine. For this purpose, a wind tunnel was fabricated to perform experiment. A laboratory base small contra rotating wind turbine system with NREL S809 aero foil shaped blade profile was manufactured. Apart from blade angle, the effects of other parameters like wind velocity, Reynolds number and distance between blade rotors also studied. To reach this goal, the following sections completed:-

- Reviewed the literature related to design and fabrication of wind tunnel, contra rotating turbine, aerofoil blade profile, other research papers related to design and fabrication of small wind turbine and various assumptions and working conditions, papers related to NREL aerofoil blades data.
- On the basis of literature reviewed, wind tunnel and NREL S809 aerofoil blade profile selected for this work and decided the parameters which has to consider for this work.
- Fabricated the laboratory based horizontal axis twin blade contra rotating wind turbine system and wind tunnel according to design considerations. Series of experiment on fabricated wind turbine setup was done by varying turbine parameters such as blade angle, distance between rotor blades, wind velocity and Reynolds Number and studied it effects on wind turbine power output.

II. LITERATURE REVIEW

The literature review was mainly carried out to know various developments related to wind turbine technology from last one to two decades. This gives better understanding regarding the concept of wind turbine analysis and recent trend related to turbine technology. On the basis of literature review, it is comes in focus that from last many years, The research work related to wind turbine is concentrating on to improve the performance of wind turbine by different design approach or by varying design geometry of blade profile. Many articles from journal and conference were studied which included latest developments related to wind technology. Some of the articles related to this research work are discussed here.

Extensive literature is presented by many of the authors about the design of wind turbines [8]. Eggleston, David M. and Forrest S. Stoddard (1987) [2] made a design of wind turbine. It provided information related to aerodynamic test on blade. Somers. D.(July 1987)[3] discussed the NREL S809 aerofoil blade profile performance in wind tunnel under different operating condition to evaluate stresses and forces developed on boundary surface of aerofoil section of blades. Selig, Michael S. and Bryan D. McGranahan (2004) [4], investigated the data related to wind tunnel test for six aerofoil blade profile on small rotor size is given and evaluate various parameters. Experiment was conducted in wind tunnel in laminar steady flow field for various profiles and performance is studied. John Larson(February 2008) [5] gives information of test to find effect of chord length and taper of blade of blade performance. By varying chord length and taperness of blade measure power produced by generator and by analyzing the result, proposed the statement regarding research work. Dr. James Dann's (2010) [9], worked on the building of a test wind tunnel to do a experiment on 1:18 scale down car models to find lift and drag for acting on scale models of cars. In this work, performed various experiments on car models to find aerodynamic drag forces acting on car and propose a best aerodynamic car model which offer minimum resistant to wind velocity. Riadh W. Y. Habash, VoicuGroza, Yeu Yang, Charles Blouin, Pierre Guillemette (2010) [14], A series of experiment on small contra rotating wind converter to predict the performance of turbine and effect on power of turbine. Fabrication of the metallic exhaust 3 blade rotor was done and performed tunnel experiment on it and proposed result on smoke test to predict the flow visualization over the blade. A full examination of wind turbine blade design loads is provided, detailing gravitational, aerodynamic, gyroscopic, centrifugal, and operating circumstances. Rajeevalochanam et al. (2020) [1] modified the contra rotating blade for the application of turbo fan engine. They compared the performance of contra rotating and co rotating turbines. They found that according to flow estimates, performance is increased by 2%. Hosotani et al. (2019) [16] have performed a Study on high pressure design of contra-rotating small hydro-turbines. They found that the maximum efficiency of front rotor is 67% with at 4^0 deflection angle.

By the literature review, it is observed that very limited work is carried out on the analysis of contra rotating turbine. The works mainly focus on profile of blade, design of blade.In view of above, It is propose to carry out the experimental analysis of contra rotating wind turbine to investigate the effects of blade angle, wind velocity, Reynolds Number and distance between rotors on the power output of wind turbine.

III. EXPERIMENTATION

A. Experimental Approach

Designing of turbine blade is very important issue. Turbine performance directly depends on blade design because blade is part which comes in contact with wind and extract energy from it. So if blade design is not correct then plant efficiency goes down. Wind turbine blades are shaped to generate the maximum power from the wind. The blade design process starts with a "best guess" compromise between aerodynamic and structural efficiency. There are various aerofoil shapes are available, but NACA series and NREL series are frequently employed due to their good performance. It is decided to choose aerofoil profile from NREL series for our research work. National Research Energy Laboratory (NREL) formerly the Solar Research Energy Institute (SREI) is a Colorado based research organization which is doing a research work related to aerofoil shape of blade for space work. It developed series of aerofoil shape for various purposes. The S809 aerofoil shape profile is selected because it is from the family of big turbine recommended profile.

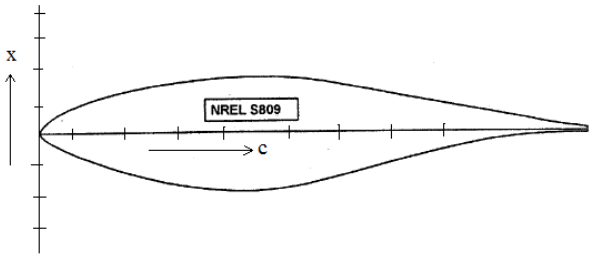

Fig. 2. Shape of S809 aerofoil profile.[10]

The NREL S809 aerofoil profile was used to manufacture blade of HAWT of overall diameter 190 mm with radius of blade 80mm and hub diameter 20m. Wood (tike wood) is used to manufacture a blade profile with wooden hub with 3 mm diameter as shown in fig. 2. Its specification and shape is shown below.

Table I. Design specification of S809 aerofoil profile[10]

Design specification of S809 aerofoil profile	
Camber	0.0095C
Maximum thickness	0.2099C
Lead Edge Radius	0.0123C
Trailing Edge Angle(^{0}c)	3.68
Where C is chord length	

Table II Details of chord length and chord thickness for different section

Blade section	Chord length (mm)	Chord thickness (mm)
Section 1	42.66	8.95
Section 2	21.33	4.48
Section 3	14.22	2.99
Section 4	10.67	2.23
Section 5	8.53	1.89

Several consideration needs be taken in to account to properly design the blade with required properties. The main design considerations based on literature survey are listed below.

Maximum wind speed is 10 m/s

Lift co-efficient is 0.7 for optimum design

Tip speed ratio is 5

Number of blade is 3

Blade Length(R) is 80 mm
Hub Height is 20 mm

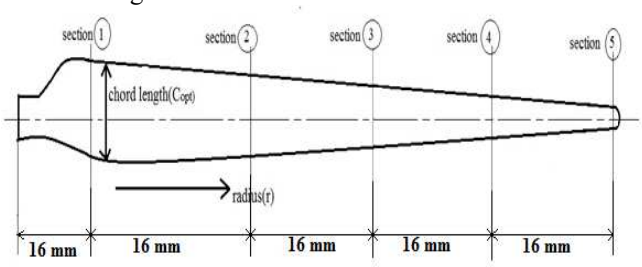

Fig. 3. Different section of turbine blade NREL S809

Fig. 4. Manufactured wooden NREL S809 aerofoil blade

Wind tunnel is a convergent-throat-divergent like section which is used to perform in-house test facility for various machine prototypes or models. Wind tunnel had a facility to simulate wind tunnel in-house condition with actual working condition of prototype and perform various research work on it related to study and find effect of all this on the machine. Wind tunnel test is a good research tool to perform various research which required high cost and time consuming to perform on site in actual working condition. Wind tunnel testing are very effective tool in the fields of aerospace, automobile aerodynamics design, wind turbine research work etc. Various components of wind tunnel with overall dimension discuss below.

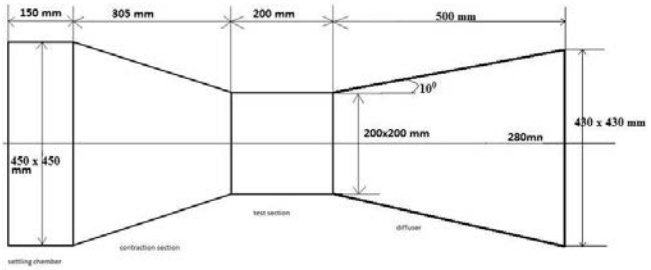

Fig. 5. Wind tunnel with overall dimensions

The initial stage in wind tunnel design is to specify the size, form, and intended air velocity of the test chamber.

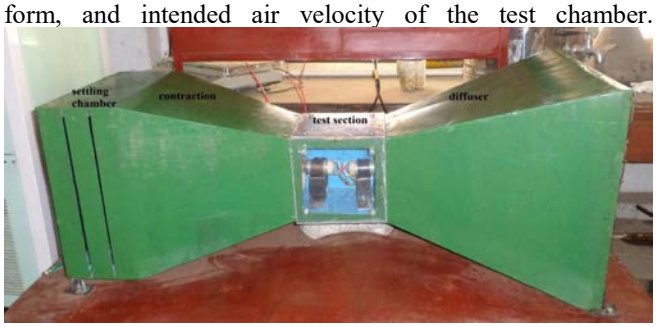

Fig.6. Inner view of test section with in-house blades and generators.

Test section is a place where object to be placed and various test performed on it. In this scenario, a square test chamber with a 200mm side and an air velocity of 10 m/s was utilised. The length of the test chamber must be between 0.5 and 3 times its side length. As a result, in this investigation, the length of the test chamber was fixed to one time the side of the test section. Inside test section two stand are fabricated to keep generator set at their place firmly and turbine blades are place on shaft of each generator set in opposite direction as shown in figure 6.

The objective of this work is to study the effects of blade angle, wind velocity, Reynolds number and distance between rotor blades on the power produced by wind turbine. To achieve this goal, an experimental test setup is required. So for this purpose an experimental test setup was fabricated to carry out this work. The test setup consists of wind tunnel with equipments and a model of contra rotating wind turbine system with NREL S809 blade profile as shown in figure below. In fabricated wind tunnel we can get 10 m/sec maximum possible wind velocity.

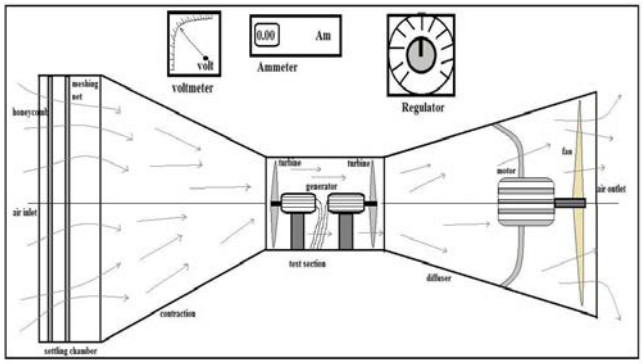

Fig. 7. Systematic diagram of wind tunnel test setup

B. Analytical Approach

Wind energy is widely and freely available on the earch which is actually the kinetic energy between the passages of air flow. The electrical energy generation is possible from wind energy with the help of electro mechanical conversion devices like wind mills or wind turbines. When air is in motion, its kinetic energy may be calculated as

$$E_K = \frac{1}{2}mu^2 \quad (1)$$

Where mass of the air denoted by m and average wind speed at specific time is denoted by u. so the derivative of wind energy with respect to time is generally denoted as wind power and may be expressed as

$$P_W = \frac{dE_K}{dt} = \frac{1}{2}mu^2 \quad (2)$$

The mass flow rate of is also one of the important driving factor while checking the performance of a wind turbine which can be calculated as

$$m = \rho Au \quad (3)$$

Where

ρ = air density and

A= swept area of blades, from the equation 2 and 3 the available power in wind Pw can be calculated as

$$P_W = \frac{1}{2}\rho Au^3 \quad (4)$$

IV. Results and Discussions

A series of experiment performed inside fabricated wind tunnel related to twin blade contra rotating wind turbine. In

this research work, the main aim is to find effect of variation in performance deciding parameters and study the effect of it. To achieve this goal, we decided to focus on wind velocity, Reynolds number, Distance between blades and blade angle (angle of attack). After a series of experiments the various results obtained from this study is discuss below with the observation table for experimental and analytical approaches.

Table III. Observation table for experimental readings of Power for change in wind velocity in wind tunnel

Velocity m/sec	Front blade power (watt)			Back blade power (watt)			Total power (watt)
	volt	Current	Power watt	Volt	Current	Power watt	
10	23.5	0.08	1.88	11	0.04	0.44	2.32
9	22	0.06	1.32	10	0.04	0.4	1.72
8	18.5	0.05	0.925	8.3	0.03	0.249	1.174
7	14	0.04	0.56	4	0.02	0.08	0.64
6	12	0.03	0.36	0	0	0	0.36
5	8	0.02	0.16	0	0	0	0.16
4	4	0.00	0	0	0	0	0

The figure 8 shows relation between turbine power and wind velocity. It shows power of front rotor, power of back rotor and total power. As velocity increase power of turbine also increase, 5 m/s is a cut in velocity for front rotor and 6.5 m/s is a cut in velocity for back rotor of turbine.

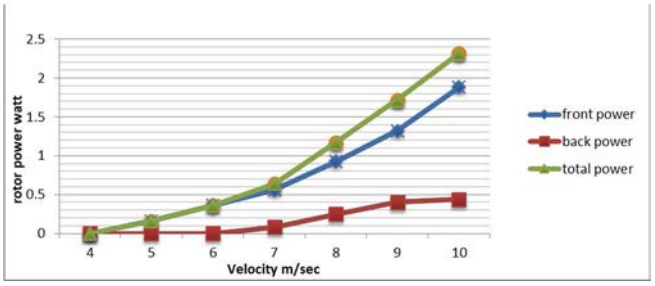

Fig. 8. Graph of effect of change in wind velocity on output power of wind turbine.

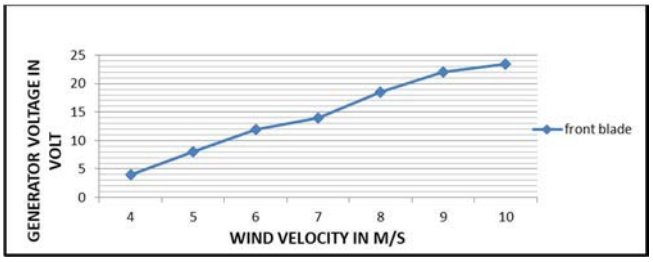

Fig. 9. Graph showing relation between generator voltage and wind velocity for front blade

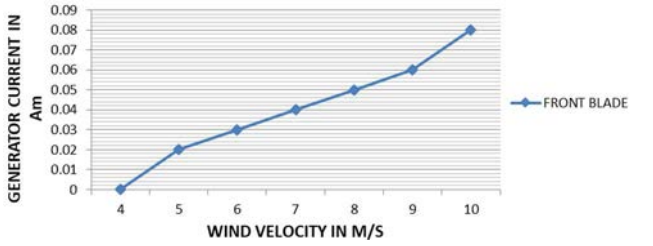

Fig. 10. Graph showing relation between generator current and wind velocity for front blade

Figure 9 is the graph plotted for generator power verses wind velocity. It shows effect of velocity on voltage of generator, as the velocity increase voltage also increase. But at higher velocity more voltage generated as compare to lower velocity.

The graph plotted between generator current and wind velocity for front blade. It is observed from graph, the current rapidly increase with velocity at low velocity value as compare to high wind velocity value. As shown in graph, generator voltage for back blade is plotted against wind velocity. It is observed that up to 6 m/s velocity there is no voltage generation in back blade.

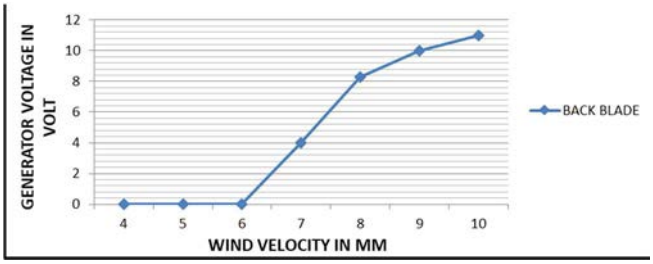

Fig. 11. Graph showing relation between generator voltage and wind velocity for back blade

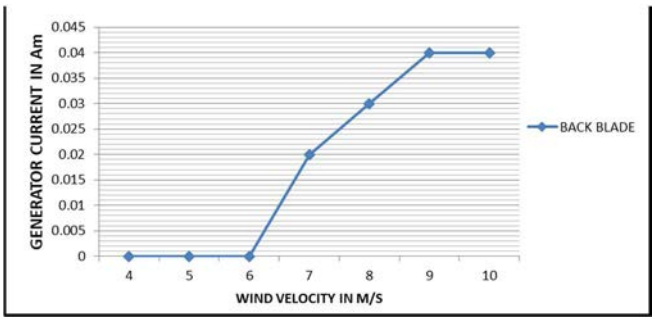

Fig. 12. Graph showing relation between generator current and wind velocity for back blade

As shown in graph, generator current for back blade is plotted against wind velocity. It is observed that up to 6 m/s velocity there is no current generation in back blade. After 6 m/s current increase with increase in velocity up to 9 m/s and after it value is steady.

Table IV. Experimental and analytical readings for rotor output power

velocity m/s	analytical readings(watts)		experimental readings(watts)	
	front power	back power	front power	back power
10	17.77	10.15	1.88	0.44
9	12.95	8.29	1.32	0.4
8	9.09	4.48	0.93	0.25
7	6.09	1.62	0.56	0.08
6	3.84	0.81	0.36	0
5	2.22	0.48	0.16	0
4	1.14	0.35	0	0

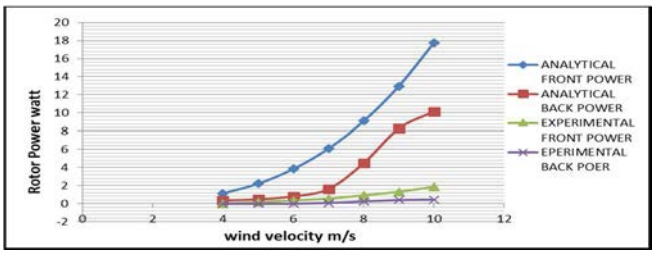

Fig. 13. Comparison of experimental power and analytical power

The figure 13 shows data related to analytical and experimental results. As observed, the power generated in

case of analytical analysis is more compared to experimental data. In actual case, only 1.2% of wind power is converted into electric power.

Table V. Experimental and analytical readings for front rotor output power

velocity m/s	analytical front power (watt)	experimental front power (watt)
10	17.77	1.88
9	12.95	1.32
8	9.09	0.925
7	6.09	0.56
6	3.84	0.36
5	2.22	0.16
4	1.14	0

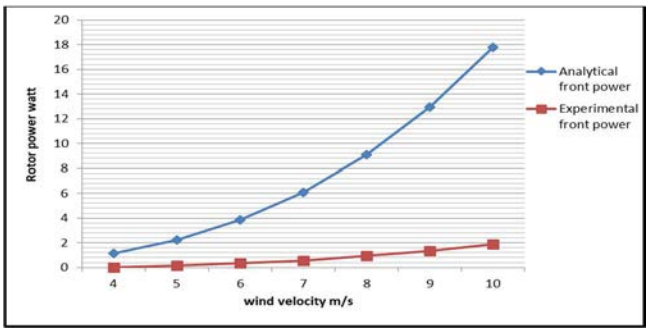

Fig. 14. Graph for analytical and experimental calculated power for front rotor

The above graph shows relation between analytical power and experimental power for front turbine generated by DC generator for different wind velocity. The graph shows that in case of actual working condition, less power is generated by turbine compared to analytical power .

Table VI. Experimental and analytical readings for back rotor output power

velocity m/s	Analytical back power (watt)	experimental back power (watt)
10	10.15	0.44
9	8.29	0.4
8	4.48	0.249
7	1.62	0.08
6	0.81	0
5	0.48	0
4	0.35	0

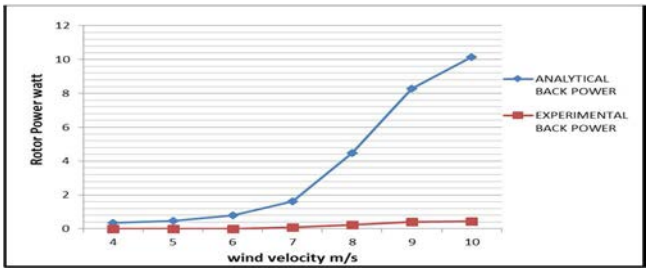

Fig. 15. Graph for analytical and experimental calculated power for back rotor

The figure 15 shows relation between analytical power and experimental power for back turbine generated by DC generator for different wind velocity. The graph shows that in case of actual working condition, less power is generated by turbine compared to analytical power .

V. Conclusions

Twin blade contra rotating wind turbine system was studied. Based on experimental results, it was concluded that:

- The contra rotating wind turbine produced 25% more power compared to single rotor from the same wind stream.
- By varying the blade angles it was observed that, it affects the rotational speed of rotor. The blade angles 4^0 and 6^0 are the angles at which the contra rotating turbine with NREL S809 blade profile produced more power compared to other angle. It was also observed that blade angles from 4^0-10^0 was the range up to which turbine produced more power compared to angles greater than 10^0.
- By varying the distance between rotors, it was observed that there was no specific trend is observed. The 25 mm rotor distance is a distance at which maximum power is generated.

References

[1] Prathapanayaka Rajeevalochanam, S.N. Agnimitra Sunkara, Seepana Venkata Ramana Murthy, R. Senthil Kumaran, Design of a two spool contra-rotating turbine for a turbo-fan engine, Propulsion and Power Research, Volume 9, Issue 3, 2020, Pages 225-239, ISSN 2212-540X, https://doi.org/10.1016/j.jppr.2020.08.001.

[2] "NREL Airfoil Families for HAWTs", J. L. TangIer, D. M. Somers, NREl/I'P-442-7109 • UC Category: 1211 • DE95000267,2010.

[3] "Performance of a Contra-Rotating Small Wind Energy Converter", Riadh W. Y. Habash1, Voicu Groza1, Yeu Yang2, Charles Blouin2, Pierre Guillemette3, 1 School of Information Technology and Engineering, University of Ottawa, Ottawa, Ontario, Canada, 2 TRIAS Innovations, Canada

[4] "The Effect of Cord Length and Taper on Wind Turbine Blade Design",John Larson, AME 40463, February 2008.

[5] "Wind Turbine Design – With Emphasis on DarrieusConcept",book, Ion Paraschivoiu, Presses internationals Polytechnique publication, December 2009.

[6] http://navier.stanford.edu/bradshaw/tunnel/index.html, This is Bradshaw and Mehta's (or Mehta and Bradshaw's) website, which contains various articles related to wind turbine manufacturing and important issues related to wind turbine technologies.

[7] Mehta RD, Bradshaw P (1979). Design rules for small low speed wind tunnels. Aeronaut J: 443-449.

[8] "Wind Turbine Engineering Design", Eggleston, David M. and Forrest S. Stoddard, Van Nostrand Reinhold, New York, 1987.

[9] Somers. D., "Design and Experimental Results for the S809 Airfoil," Airfoils, Inc., State College, Pennsylvania, 1987.

[10] Selig, Michael S. and Bryan D. McGranahan "Wind Tunnel Aerodynamic Test of Six Airfoils for Use on Small Wind Turbines", National Renewable Energy Laboratory.Subcon-tractorReport,October2004. http://www.nrel.gov/docs/fy05osti/34515.pdf.

[11] "Aerodynamics of Wind Turbines book",Martin O. L. Hansen,Earthscan, Londan, 2008, page no.27-40.

[12] "Influence of the Number of Blades on the Mechanical Power Curve of Wind Turbines", M.Predescu,A.Bejinariu,O.Mitroi,A.Nedelcu, International Conference on Renewable Energies and Power Quality (ICREPQ'09), 2009.

[13] " Building and Testing a Wind Tunnel",Dr. James Dann's, Applied science research class, spring 2010.

[14] "India Wind Energy Outlook 2012", Global Wind Energy Council, World Institute of Sustainable Energy and Indian Wind Turbine Manufacturing Association, 'Wind Power India 2012' - an "Wind Turbine Blade Design", Review,Peter J. Schubel and Richard J. Crossley, Energies, 5, 3425-3449; doi:10.3390/en5093425,2012.

[15] Md. Arifuzzaman, Mohammad Mashud, IOSR Journal of Engineering (IOSRJEN), Volume 2, Issue 10 (October 2012), PP 83-92.

international wind energy conference & exhibition, Chennai, November 28-30, 2012.

[16] Takuji Hosotani, Toru Shigemitsu, Yuki Kawaguchi and Tomofumi Ikebuchi, “Study on high pressure design of contra-rotating small Hydroturbine” 2019, IOP Conf. Ser.: Earth Environ. Sci. 240 042013

Breaking The Chain Of Transmission Of Covid-19 By Social Distancing

Shubhada Gade[1], Alma Lakra[2], Gangaram Bhadarge[3] and Ujwalla Gawande[4]

ECS Transactions, Volume 107, Number 1

Citation Shubhada Gade *et al* 2022 *ECS Trans.* **107** 20283

DOI 10.1149/10701.20283ecst

[1] Jawaharlal Nehru Medical College,

[2] Datta Meghe Medical College

[3] Datta Meghe Institute of Medical Sciences

[4] Yeshwantrao Chavan College of Engineering

Abstract

While the virus's intermediate point of origin and spread to humans is unknown, it has been shown that it is capable of rapid human-to-human transmission. The virus was primarily transmitted from person to person by physical interaction. Coughing, sneezing, and laughing cause droplets. Fever, chills, cough, sore throat, breathing difficulties, myalgia or fatigue, nausea, vomiting, and diarrhoea are common signs of COVID-19 infection. Cardiovascular damage, respiratory failure, acute respiratory distress syndrome, and even death may occur in severe

situations. AIM: Breaking the chain of transmission of COVID-19 by Social Distancing MATERIAL AND METHOD: A primary research study has been done using an online questionnaire created using Google form. An observation study design has been used. The respondents were sent a survey of three questions including consent forms to participants in survey, using mail ID's and social media platforms. The material required for the review was taken from the databases of PubMed, Web of science, the from the website of World Health Organization, International diabetes federation and the patients data of SMHRC and DMMC Wanadongari Nagpur.

Sustainable Communication Networks and Application pp 709–717

Competitive Analysis of Web Development Frameworks

Priyanka Jaiswal & Sumit Heliwal

Conference paper | First Online: 17 January 2022

Part of the Lecture Notes on Data Engineering and Communications Technologies book series (LNDECT,volume 93)

Abstract

In day-to-day working, when we are dealing with collecting and managing information for business, designing of interface plays a very important role. For designing an interface, different web designing frameworks are required. This review paper is based on discussion and comparison of different frameworks which are currently used in the industry and are in demand in the industry. It will help one to choose between the different frameworks and get an idea about their uses and where to use them. Anyone can understand and can choose between different frameworks. It will help newbies to get started and make choices about the framework. This review paper focuses on the pros and cons and their requirements for deployment. This paper is also focused on the time requirement, access, what they provide, where they are used, when to use, and how to choose upon it. It also includes the starting requirements and what goals user can achieve using different frameworks. It also includes the basic structure of a Web application or the basic requirements of a web application to start. The comparative study broadly consist of Bootstrap,

Django, and .NetBootstrap, Django, Net and other web development framework.

Keywords

Web development **Bootstrap** **Django** **.net** **Python** **C#** **HTML** **CSS**

References

1. S. Al Perumal, M. Tabassum, N.M. Norwawi, G. Al Narayana Samy, S.A. Perumal, Development of an efficient timetable system using angular JS and bootstrap 3. in *2018 8th IEEE International Conference on Control System, Computing and Engineering (ICCSCE)*, (2018), pp. 70–75. https://doi.org/10.1109/ICCSCE.2018.8685002

2. J. Wang, B. Zhang, J. Guo, H. Wang, The design of instant messaging system based on web. in *2017 8th IEEE International Conference on Software Engineering and Service Science (ICSESS)*, (2017) pp. 288–291. https://doi.org/10.1109/ICSESS.2017.8342916

3. V.S. Pawar, P. Jaiswal, Use of web services for integrating geospatial system with other systems. CHEMIK 99–105 (2020). Retrieved from http://www.chemikinternational.com/index.php/chemik/article/view/39

4. Q. Yu, W. Yang, The analysis and design of system of experimental consumables based on django and QR code. https://doi.org/10.1109/IICSPI48186.2019.9095914

5. O. Krejcar, M. Macecek, Development of bar code scanner application for windows mobile devices using a symbol mobility developer kit for .NET compact framework. https://doi.org/10.1109/ICMEE.2010.5558524

6. Z. Jin, J. Wang, S. Zhang, Design and implementation of WA face recognition system based on small wechat program. https://doi.org/10.1109/CSEI47661.2019.8938841

7. K. Kungcharoen, P. Palangsantikul, W. Premchaiswadi, Development of object detection software for a mobile robot using an aforce. Net Framework. https://doi.org/10.1109/ICTKE.2012.6152407

8. Hammad-ul-Hasnain, Building mobile application with .NET compact framework. https://doi.org/10.1109/SCONEST.2005.4382871

9. W. Wiphusitphunpol, T. Lertrusdachakul, Fetch performance comparison of object relational mapper in .NET platform. https://doi.org/10.1109/ECTICon.2017.8096264

10. W. Jiang, M. Zhang, B. Zhou, Y. Jiang, Y. Zhang, Responsive web design mode and application. in *2014 IEEE Workshop on Advanced Research and Technology in Industry Applications* (WARTIA) (Ottawa, ON, 2014), pp. 1303–1306.https://doi.org/10.1109/WARTIA.2014.6976522

11. S.S. Gaikwa, P. Adkar, A review paper on bootstrap framework. Iconic Res. Eng. J. **2**(10) (2019)

12. N. Li, B. Zhang, The design and implementation of responsive web page based on HTML5 and CSS3. in *2019 International Conference on Machine Learning, Big Data and Business Intelligence* (MLBDBI), Taiyuan, China (2019), pp. 373–376. https://doi.org/10.1109/MLBDBI48998.2019.00084

13. S. Syafiq, M. Daud, H. Hasan, A. Zairi, S. Imri, E. Akmar, N. Rahim, Comparison of web development using framework over library

14. R. Bastola, P. Campus, Developing domain ontology for issuing certificate of citizenship of Nepal. J. Inf. Technol. **2**(02), 73–90 (2020)

Author information

Authors and Affiliations

Department of IT, Yeshwantrao Chavan College of Engineering (YCCE), Nagpur, India

Priyanka Jaiswal & Sumit Heliwal

Editor information

Editors and Affiliations

Department of Electrical and Electronics Engineering, Shree Venkateshwara Hi-Tech Engineering, Erode, Tamil Nadu, India

Dr. P. Karrupusamy

Department of Automatics and Applied Software, Aurel Vlaicu University of Arad, Arad, Romania

Dr. Valentina Emilia Balas

Department of Computer Science, Kennesaw State University, Kennesaw, GA, USA

Dr. Yong Shi

Rights and permissions

Reprints and Permissions

Copyright information

About this paper

Cite this paper

Jaiswal, P., Heliwal, S. (2022). Competitive Analysis of Web Development Frameworks. In: Karrupusamy, P., Balas, V.E., Shi, Y. (eds) Sustainable Communication Networks and Application. Lecture Notes on Data Engineering and Communications Technologies, vol 93. Springer, Singapore. https://doi.org/10.1007/978-981-16-6605-6_53

.RIS .ENW .BIB

DOI	Published	Publisher Name
https://doi.org/10.1007/978-981-16-6605-6_53	17 January 2022	Springer, Singapore

Print ISBN	Online ISBN	eBook Packages
978-981-16-6604-9	978-981-16-6605-6	Engineering Engineering (R0)

Efficient Approach for Attendance Management using Local Binary Pattern

Publisher: IEEE

Ujwalla Gawande ; Amisha Chikate ; Piya Kaware ; Sharwari Dhakhale **All Authors**

Abstract: In an academic institution, attendance management is a tedious task. Automatic real-time attendance management system is needed. We propose an efficient, novel, and intel... **View more**

Metadata

Abstract:
In an academic institution, attendance management is a tedious task. Automatic real-time attendance management system is needed. We propose an efficient, novel, and intelligent attendance management system using Local Binary Patterns (LBP). It first detects the face of a student and enrolls the attendance automatically. Second, the subject teacher can export attendance in real-time. The proposed method overcomes existing face detection limitations, such as pose variation, illumination variation, and occlusion. Experimental results show significant performance improvement as compared to the existing attendance management system.

Published in: 2022 2nd International Conference on Intelligent Technologies (CONIT)

Date of Conference: 24-26 June 2022

INSPEC Accession Number: 21992349

Date Added to IEEE *Xplore*: 18 August 2022

DOI: 10.1109/CONIT55038.2022.9848248

ISBN Information:

Publisher: IEEE

Conference Location: Hubli, India

Contents

I. Introduction

Maintaining regular class attendance while engaging in other academic activities is a tedious task for students. Due to the COVID-19 pandemic, face masks are mandatory to reduce the virus spread probability. In the conventional approach, proxy attendance is the biggest issue as students acknowledge absent students. Teacher finds it tedious to identify students whenever student faces are occluded with a face mask. Currently, there is a need for real-time attendance management that can detect the student face even if student face is occluded with the face mask and register student attendance as per the respective subject time and date scheduled automatically. Again, in case student-relevant face is not available at a specific time, then student attendance should be marked as absent.

Sign in to Continue Reading

Authors

Figures

References

Keywords

Metrics

References

References is not available for this document.

References

References is not available for this document.

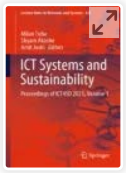

ICT Systems and Sustainability pp 113–121

Efficient Attendance Management System Based on Face Recognition

Ujwalla Gawande, Pratyush Joshi, Sumedh Ghatwai, Shreyas Nemade, Soham Balkothe & Nishant Shrikhande

Conference paper | First Online: 04 January 2022

Part of the Lecture Notes in Networks and Systems book series (LNNS,volume 321)

Abstract

Every education institution nowadays is concerned about student attendance and performance. In the current academic system, consistent class attendance of students plays a significant role in their performance, assessment, and quality monitoring. The traditional approach of taking attendance in several institutions is by calling the names of students one after the other or each student manually signs on the papers. In existing approaches, taking and tracking student's attendance manually, losing attendance sheets, dishonesty of students, and high error scales are open challenges face by the faculties. It is a complex process, requires time, and causes manual paperwork. We proposed an efficient and robust approach for an attendance monitoring system using the face of a human. The proposed algorithm first detects and recognizes the student's faces from videos or images. Second, mark the attendance using a neural network model and texture features. Experiments were conducted on the commercially available datasets. The proposed approach is compared with the

traditional attendance marking system in terms of time and accuracy. Our approach resolves the state-of-the-art approach challenges and saves time to monitor the students.

Keywords

Face recognition **Automated student attendance system**

OpenCV **Neural network**

References

1. Epstein & Sheldon (2002) Present and accounted for: improving student attendance through family. J Edu Res 95(5):308–318

2. Ready D (2010) Socioeconomic disadvantage, school atte, early cognitive development: the differential effects of school exposure. Soc Edu 83(4):271–286

3. Bruner C, Discher A, Chang H (2011) Chronic elementary absenteeism: a problem hidden in plain sight. Attendance Works and Child & Family Policy Center

4. Kambi BIL, Chunsheng G (2017) Enhancing face identification using LBP and K-nearest neighbors. J Imag 3(37):1–12

5. Jain SK, Joshi U, Sharma BK (2011) Attendance management system. Masters Project Report, Rajasthan Technical University, Kota

6. Bhalla V, Singla T, Gahlot A, Gupta V (2013) Bluetooth based attendance management system. Int J Innov Eng (IJIET) 3(1):227–233

7. Bah SM, Ming F (2020) An improved face recognition algorithm and its application in attendance management system. Array 5:1–7

8. Joardar S, Chatterjee A, Rakshit A (2015) A real-time palm dorsa subcutaneous vein pattern recognition system using collaborative representation-based classification. IEEE Trans Instrum Meas 64(4):959–966

9. Jain K, Ross A, Nandakumar K (2011) Introduction to biometrics. Springer, pp 1–208

10. Jain K, Flynn P, Ross AA (2010) Handbook of biometrics. Springer, New York

11. Schroff, Kalenichenko D, Philbin J (2015) FaceNet: a unified embedding for face recognition and clustering. In: 2015 IEEE on CVPR, Boston, MA, pp 815–823

12. Kanti J, Papola A (2014) Smart attendance using face recognition. Int J Adv Res Comput Commun Eng 3(6):7321–7324

13. Mohamed K, Raghu C (2012) Fingerprint attendance system for classroom needs. In: India conference, annual IEEE, pp 433–438

14. Lim T, Sim S, Mansor M (2009) RFID based attendance system. In: 2009 IEEE symposium on industrial electronics and applications, ISIEA, vol 2, pp 778–782

15. Kadry S, Smaili K (2007) A design and implementation of a wireless iris recognition attendance management system. Info Tech Control 36(3):323–329

16. Viola & Jones (2004) Robust real-time face detection. IJCV 57(2):137–154

17. Jin H, Liu Q, Lu H, Tong X (2004) Face detection using improved LBP under Bayesian framework. In: Proceedings of international conference on image and graphics, pp 306–309

18. Reddy AM, Krishna V, Sumalatha L (2018) Face recognition based on cross diagonal complete motif matrix. Int J Image Grap Sig Proc 3:59–66

19. Hoang A, Sriprasertsuk P, Kameyama W (2013) Fish detection by LBP cascade classifier with optimized processing pipeline. IPSJ SIG Techn Rep 82(9):1–20

Author information

Authors and Affiliations

Department of Information Technology, Yeshwantrao Chavan College of Engineering, Nagpur, Maharashtra, 441110, India

Ujwalla Gawande, Pratyush Joshi, Sumedh Ghatwai, Shreyas Nemade, Soham Balkothe & Nishant Shrikhande

Editor information

Editors and Affiliations

Singidunum University, Belgrade, Serbia

Dr. Milan Tuba

ITM University, Gwalior, Madhya Pradesh, India

Dr. Shyam Akashe

Global Knowledge Research Foundation, Ahmedabad, Gujarat, India

Dr. Amit Joshi

Rights and permissions

Copyright information

About this paper

Cite this paper

Gawande, U., Joshi, P., Ghatwai, S., Nemade, S., Balkothe, S., Shrikhande, N. (2022). Efficient Attendance Management System Based on Face Recognition. In: Tuba, M., Akashe, S., Joshi, A. (eds) ICT Systems and Sustainability. Lecture Notes in Networks and Systems, vol 321. Springer, Singapore. https://doi.org/10.1007/978-981-16-5987-4_12

.RIS .ENW .BIB

DOI	Published	Publisher Name
https://doi.org/10.1007/978-981-16-5987-4_12	04 January 2022	Springer, Singapore

Print ISBN	Online ISBN	eBook Packages
978-981-16-5986-7	978-981-16-5987-4	Intelligent Technologies and Robotics Intelligent Technologies and

Robotics (R0)

Impact of COVID-19 on Mental Health

Riya Deshmukh[1], Ragini Patil[1], Dr. Ujwal Gajbe[2], Ujwalla Gawande[3] and Swati Maldhure[4]

ECS Transactions, Volume 107, Number 1

Citation Riya Deshmukh *et al* 2022 *ECS Trans.* **107** 17699

DOI 10.1149/10701.17699ecst

[1] Datta Meghe Medical College,

[2] Datta Meghe Medical College

[3] Yeshwantrao Chavan College of Engineering

[4] n/a

Abstract

The new COVID, later dubbed coronavirus, is an incurable disease that can be transmitted to humans. It originally appeared in late December 2019 in the Chinese city of Wuhan, where it documented cases of pneumonia of unclear etiology. After its rise, it marked as an episode that caused real concern for the general public by the WHO, and in the middle of January 2020, the WHO declared a global pandemic due to a dramatic increase in global diseases affecting many nations. More than 108 million cases had been validated.

worldwide as of February 14, 2021, with 5.99 million cases reported in the Eastern Mediterranean region. As a result of this global emergency, segregation and detention measures were being taken by international and governmental organizations to prevent the spread of the disease. Additional measures include airline suspension, large assembly congestion, and compulsory use of face masks in many countries, community evacuation, telephone work, child education, and home-based care. Conclusion: There is a need to build the mindfulness among the different media stages about mental difficulties during pandemics and feature the significance of looking for help and taking part in actual work for the administration of emotional well-being messes. Moreover, an increment in mindfulness among the medical care experts in recognizing and focusing on the high-hazard gatherings of the populace who are in danger in creating psychological well-being issues is crucially significant.

Login

Access through your institution

IOPscience login

ECS member access

Find out more about journal subscriptions at your site.

Purchase from

Article Galaxy
CCC RightFind

Purchase this article from our trusted document delivery partners.

Make a recommendation

To gain access to this content, please complete the Recommendation Form and we will follow up with your librarian or Institution on your behalf.

For corporate researchers we can also follow up directly with your R&D manager, or the information management contact at your company. Institutional subscribers have access to the current volume, plus a 10-year back file (where available).

You may also like

JOURNAL ARTICLES

Meta-analytic evidence for a robust and positive association between individuals' pro-environmental behaviors and their subjective wellbeing

A Study to Assess the Impact of Mindfulness Meditation on Perceived Stress Levels and Subjective Well-Being Among Housewives

The Relationship between Mindfulness and Safety Performance of Building Repair and Maintenance: An Empirical Study in Australia

Entrepreneurial Mindfulness Based on Artificial Intelligence

From the Editor: The Presents of Presence

Manipulating attention via mindfulness induction improves P300-based brain–computer interface performance

IOT Based Patient Health Monitoring System Using ThingSpeak

Publisher: IEEE

Bhushan Bawankar ; Bhushan Manjre ; Vaibhav P Uplanchiwar **All Authors**

Abstract: Sensors technology in the Wireless mode is the central dogma of research and automation in today's health-care systems. Heart patients are on huge risk of instant death t... **View more**

Metadata

Abstract:
Sensors technology in the Wireless mode is the central dogma of research and automation in today's health-care systems. Heart patients are on huge risk of instant death today because of lack of medical assistance in the next moment of cardiac arrest like situations. Here, we proposed system which is especially for conveying live track record of the old age patients to their doctors and relatives. At last we have proposed a novel approach for constant monitoring of the sensitive patients to prevent their sudden death rate using wireless sensor technology and here the Internet will of course be the medium of communication. The proposed system will monitor the health of patients by using a temperature and heartbeat sensor. The Arduino-uno is connected to both sensors. Using internet, our goal is to create a system that can be used to monitor a patient's body at any time. The purpose of our system is to measure some biological parameters of the ill person like body temperature, heart rate, blood pressure and other parameters using sensors and the data collected by the sensors will be sent to IOT Cloud platform with the help of WIFI-Module. Hence with the health data of the patient stored on the cloud, the doctors and the relatives can keep track of their patient's health on their smartphones. Also, the Wi-Fi module's (ESP8266) power consumption can be lowered as much as possible. As a result, our designed system has a low level of complexity, low power consumption, and is very portable for patient monitoring.

Published in: 2022 International Conference on Emerging Trends in Engineering and Medical Sciences (ICETEMS)

Date of Conference: 18-19 November 2022

INSPEC Accession Number: 22932608

Date Added to IEEE *Xplore*: 11 April 2023

DOI: 10.1109/ICETEMS56252.2022.10093488

ISBN Information:

Publisher: IEEE

Conference Location: Nagpur, India

References

References is not available for this document.

Contents

Sign In or Purchase to Read Full Text

Authors

Figures

References

Keywords

Metrics

More Like This

Data Collection in Studies on Internet of Things (IoT), Wireless Sensor Networks (WSNs), and Sensor Cloud (SC): Similarities and Differences
IEEE Access
Published: 2022

Side-Channel Resistant 2048-Bit RSA Implementation for Wireless Sensor Networks and Internet of Things
IEEE Access
Published: 2023

Loading [MathJax]/extensions/MathZoom.js

Show More

References

References is not available for this document.

Mental Health During COVID-19 Pandemic

Ankita Kapse[1], Ragini Patil[2], Dr. Ujwal Gajbe[3], Ujwalla Gawande[4] and Jeeteesha Meshram[5]

ECS Transactions, Volume 107, Number 1

Citation Ankita Kapse *et al* 2022 *ECS Trans.* **107** 17643

DOI 10.1149/10701.17643ecst

[1] Jawaharlal Nehru Medical College,

[2] Datta Meghe Medical College,

[3] Datta Meghe Medical College

[4] Yeshwantrao Chavan College of Engineering

[5] n/a

Abstract

The outburst of coronavirus in December 2019 from Wuhan, China led to the global COVID-19 pandemic. COVID-19 was declared as a pandemic by the WHO at the beginning of 2020. This resulted in lockdowns in many countries as a preventive measure. Due to the lockdowns, people were forced to stay at home, which increased the feeling of loneliness, anxiety, depression, or suicidal thoughts. Mental health is the least discussed topic but most important. With the

outbreak of the highly infectious virus, public fear, anxiety, stress due to lethality, and uncertainty also follows. This review article is aimed to explore the impact of the COVID-19 pandemic on the mental health of individuals and groups of individuals. A twenty percent increase in mental illnesses was reported in a survey by the Indian Psychiatric Society since the coronavirus outbreak in India. In China, a study showed 16.5% moderate to severe depressive symptoms, 28.8% moderate to severe anxiety symptoms, and 8.1% moderate to severe stress due to COVID-19. Different countries all over the world showed similar statistics. Conclusion: The COVID-19 pandemic has probably been the greatest pandemic in modernized human history. To prevent the transmission of coronavirus, the lockdown was imposed, which forced everyone to stay at home. The isolation had an adverse effect on the mental health of individuals.

Login

Access through your institution

IOPscience login

ECS member access

Find out more about journal subscriptions at your site.

Purchase from

Article Galaxy
CCC RightFind

Purchase this article from our trusted document delivery partners.

Make a recommendation

To gain access to this content, please complete the Recommendation Form and we will follow up with your librarian or Institution on your behalf.

For corporate researchers we can also follow up directly with your R&D manager, or the information management contact at your company. Institutional subscribers have access to the current volume, plus a 10-year back file (where available).

You may also like

JOURNAL ARTICLES

Community lockdowns in social networks hardly mitigate epidemic spreading

$PM_{2.5}$ exposures increased for the majority of Indians and a third of the global population during COVID-19 lockdowns: a residential biomass burning and environmental justice perspective

Symbolic dynamics to enhance diagnostic ability of portable oximetry from the Phone Oximeter in the detection of paediatric sleep apnoea

The comparisons between thermography and ultrasonography with physical examination for wrist joint assessment in juvenile idiopathic arthritis

Profile of eicosanoids in breath condensate in asthma and COPD

Saving the world from your couch: the heterogeneous medium-run benefits of COVID-19 lockdowns on air pollution

Available online at www.sciencedirect.com

ScienceDirect

Procedia Computer Science 218 (2023) 2438–2447

Procedia Computer Science

www.elsevier.com/locate/procedia

International Conference on Machine Learning and Data Engineering

Real-Time Deep Learning Approach for Pedestrian Detection and Suspicious Activity Recognition

Ujwalla Gawande[a], Kamal Hajari[b], Yogesh Golhar[c]

[a] *IT Department, Yeshwantrao Chavan College of Engineering, Nagpur, Maharashtra, India-441110*
[c] *CSE Department, St. Vincent Palloti College of Engineering, Nagpur, Maharashtra, India-441108*

Abstract

Pedestrian detection, tracking, and suspicious activity recognition have grown increasingly significant in computer vision applications in recent years as security threats have increased. Continuous monitoring of private and public areas in high-density areas is very difficult, so active video surveillance that can track pedestrian behavior in real time is required. This paper presents an innovative and robust deep learning system as well as a unique pedestrian data set that includes student behavior like as test cheating, laboratory equipment theft, student disputes, and danger situations in institutions. It is the first of its kind to provide pedestrians with a unified and stable ID annotation. Again, presented a comparative analysis of results achieved by the recent deep learning approach to pedestrian detection, tracking, and suspicious activity recognition methods on a recent benchmark dataset. Finally, paper concluded with investigation new research directions in vision-based surveillance for practitioners and research scholars.

Keywords: Pedestrian detection; Video Surveillance; Tracking; Suspicious activity.

1. Introduction

Video surveillance is now installed everywhere to track and monitor pedestrians or criminals in streets, airports, banks, prisms, laboratories, shopping centers, etc. [1]. The surveillance system is based on a closed-circuit television (CCTV) system. Recently, Pan-Tilt-Zoom (PTZ) cameras have many advantages over traditional CCTV cameras. The main advantage of a PTZ camera is that it allows users to view more content than a fixed camera. The featuresof the PTZ camera include: 1) The user can pan left and right and tilt up and down to obtain a complete 180° view,whether it is left or right or up and down. If installed and positioned correctly, advanced PTZ cameras can provide a complete 360° field of view. Therefore, a single pan/tilt camera can replace two or even three fixed-view cameras,which is very suitable and can almost eliminate most of the blind spots on cameras with deviated fixed-view angles.A PTZ camera is programmed to rotate automatically in multiple directions at a different view of an area.Researchers main focus is

10.1016/j.procs.2023.01.219

to develop a video surveillance system that can assess pedestrian methods in real time [2]. The challenge of identifying pedestrians in crowded environments becomes extremely challenging in real-time when low-resolution images, motion blur, contrast illumination, scale or size of pedestrian changes, and entirely orpartially obscured outlines are present. Fig.1 describes the proposed approach motivation. Pedestrian publicuniversity dataset such as INRIA [2], Caltech [1], MS COCO [3], KITTI [5], and ETH [4] datasets, pedestrian casesare typically modest. Due to restrictions such as 1) cloudy presentation, 2) confused and imprecise boundary, 3) duplicated pedestrian occurrences, 4) tiny and big dimension occurrences with distinctive properties, etc., localizing these small instances in the presence of illumination change and occlusion is a vital operation. The advanced research onpedestrians" analysis conducted on publicly available benchmark datasets.

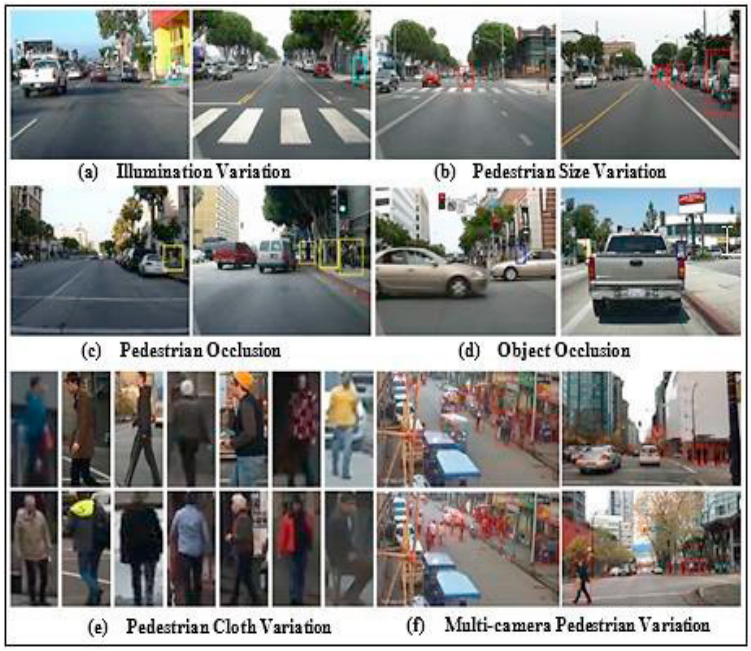

Fig.1. (a) Issues and challenges of ETH [2] and Caltech [3] datasets. (a) pedestrian significant change in the visual as the illumination changes. (b) pedestrian scale or size changes in images changed significantly. (c) pedestrian occlusion affects the detection and tracking results. (d) pedestrian occlusion with other road objects effects detection accuracy. (e) pedestrian cloth variation affects the detection algorithm accuracy. (f) Multi-camera captured direction represents a different visual appearance.

These datasets have several limitations, including: 1) a limited variety of pedestrian instances captured in a supervised pattern. 2) The size of the dataset is small and contains the least scenarios. 3) limited environment such as urban road and city only. No student behavior dataset is available. A robust and novel deep learning model and student academic environment dataset. During each sequence of frames in the video, human experts annotated the behavior of student pedestrians. It provides data in three categories. 1) Using bounding boxes to locate pedestrians. 2) fully labelled; 3) unique IDs are used as a class category for annotated pedestrians. The proposed contributions are as follows:

1. To solve existing state-of-the-art database concerns such as size and illumination variance in pedestrian images, It presents the unique enhanced Mask R-CNN deep learning architecture.
2. Student's normal and suspicious activities are recorded in the proposed dataset.
3. Within the framework of the proposed pedestrian dataset for academic settings along with comprehensive review of previous work and compare existing techniques.

The remaining research paper is categorized as follows: the most significant contribution of the new pedestrian dataset, as well as concerns and challenges in the academic context discuss in section 2. A deep learning architecture is described in section 3. The outcomes of the empirical examination are discussed in section 4. Finally, in the Section 5 the research paper ended with conclusion and research direction.

2. Related Work

This section describes the most relevant and recent pedestrian datasets. In addition, it discusses the advanced deep learning approaches to pedestrian detection, tracking, and suspicious activity recognition, along with its limitation.

2.1. State-of-the-art Pedestrian Dataset

Currently pedestrian datasets used by researchers for pedestrian detection, tracking, and suspicious activity recognition. First, the Caltech dataset contains 2,300 unique pedestrians and 350,000 annotated bounding boxes to represent these pedestrians. This dataset was created on the city road and using the camera mounted on the vehicle [3]. Second, the MIT dataset is the well-known pedestrian dataset, which consists of high-quality pedestrian sample images. It contains 709 unique pedestrians. Whether in front view or back view, the range of pose images taken on city streets [4] is relatively limited. Third, Daimler, this dataset captures people walking on the street through cameras installed on vehicles in an urban environment during the day. The data set includes pedestrian tracking attributes, annotated labelled bounding boxes, ground truth images, and floating disparity map files.

The training set contains 15560 pedestrian images and 6744 annotated pedestrian images. The test set contains 21,790 pedestrian images and 56,492 annotated images [5]. The ATCI dataset is a pedestrian database acquired by a normal car"s rear-view camera, and it"s used to test pedestrian recognition in parking lots, urban environments city streets, and private as well as public lanes. The data set contains 250 video clips, each of 76 minutes, and 200,000 marked pedestrian bounding boxes, captured in day-light scenes, with contrasting weather scenarios [6]. The ETH dataset is used to observe the traffic scene from the inside of the vehicle. The behavior of pedestrians is recorded and placed over vehicles. In an urban setting, the dataset can be used for pedestrian recognition and tracking via mobile platforms. Road cars and pedestrians, are included in the dataset [7]. The TUD-Brussels dataset was created usinga mobile platform in an urban environment.

Crowded urban street behavior was recorded vehicle embedded cameras. It can be used in car safety scenarios in urban environments [8]. One of the most abstract pedestrian detection data sets is the INRIA dataset. It incorporates human behavior, as well as a mobile camera and complex background scenes, with various variations in posture, appearance, dress, background, lighting, contrast, etc. [9]. The PASCAL Visual Object Classes (VOC) 2017 and 2007 collection contains static objects in an urban setting with various viewpoints and positions. This dataset was created with the goal of recognizing visual object classes in real-world scenarios. Animals, trees, road signs, vehicles, and people are among the 20 different categories in this collection [10]. The Common Object in Context was constructed using the MS COCO 2018 dataset [11]. (COCO). The 2018 dataset wasrecently utilized to recognize distinct things in the context while focusing on stimulus object detection.

The annotations include different examples of things connected to 80 different object categories and 91 different human segmentation categories. For pedestrian instances, there are key point annotations and five picture labels per sample image. (1) real-scene object detection with segmentation mask, (2) panoptic semantic segmentation, (3) pedestrian keypoint detection and evaluation, and (4) Dense Pose estimation in a congested scene is among the COCO 2018 dataset challenges [12].

For street picture segmentation, the Mapillary Vistas Research dataset is employed [13]. Pedestrians and other non-living categories are solved using panoramic segmentation, which successfully merges the concepts of semantic and instance segmentation. A comparison of pedestrian databases and their video surveillance purposes is shown inTable 1. In addition, we've included proposed dataset, which will be introduced in the next section. The connection is made based on the dataset's use, size, environment, label, and annotation.

2.1. Proposed Deep learning architecture and Academic Environment Pedestrian Dataset

In this section, the proposed framework from a different perspective, as captured by a high-qualityDSLR camera. The proposed video acquisition framework records the video at 30f/s along with 384x2160 resolution. The size of the dataset is 100GB. The student behavior frames shown in Fig.2. The orientation of the camera is in the range of 45^{o} to 90^{o}. Yeshwantrao Chavan College of Engineering (YCCE), Nagpur student academic activity behavior recorded in the proposed dataset. The student age is between 22-27, including both male and female. Out of which, 65% are male

and 35% are female. The academic environment dataset consists of different behaviors such as lab student activities, exam hall, classroom, student cheating behavior, dispute, and stealing a mobile phone and lab electronic devices [34].

Table 1. Comparison of benchmark pedestrian dataset the pedestrian detection, tracking.

Dataset	Dataset size	Annotation	Environment	Year	Ref.	Issues and Challenges
Caltech	250000 frames	2300 unique pedestrian	City street	2012	[3]	Only urban roads are captured.
MIT	709 unique pedestrians	No annotated pedestrian	Day light scenario	2000, 2005	[4]	Missing annotation not allow userto verify different techniques.
Daimler	15,560 unique pedestrians	Ground truth withbounding boxes.	City street	2016	[5]	Only urban roads are captured.
GM-ATCI	Video clips:250	Annotated pedestrian bounding boxes: 200K	Day and complex weather and lighting	2015	[6]	Only urban roads are captured. Side view of road not captured.
ETH	Videos	Annotated cars and pedestrians	City street	2010	[7]	Small size dataset. Limited scenarios cover.
TUD Brussels	1092 frames	Pedestrian Annotation	City street	2009	[8]	Only urban roads are captured.
INRIA	498 images	Manual Annotations	City street	2005	[9]	Only urban roads are captured.
PASCAL VOC 2012	11,530 images, 20 objects classes	ROI Annotated 27,450	City street	2012	[10]	Only urban roads are captured.
MS COCO 2017	328,124 images	Segmented people object	City street	2017	[11]	Only urban roads are captured.
MS COCO 2015	328,124 images	Segmented people object	City street	2015	[12]	Only urban roads are captured.
Mapillary Vistas dataset 2017	152 obj. , 25300 img.	Instance segmentation	City street	2017	[13]	Only urban roads are captured. Side view of road not captured.

At the frame level, domain experts annotate the pedestrian video sequence. The labelling stage contains three phases: 1) human identification. 2) tracking, and 3) detection of suspicious activities. First, Mask R-CNN [12] method was used to determine the location of the pedestrian in the frame, followed by manual validation and correction of the data. Next, a deep sort [14] model was used for extracting tracking information. At last, with these two basic operations, get a rectangle bounding box around pedestrians that defines the ROI foreach human. The last stage of the updating process is performed manually, with human expert knowledge in the academic environment. Height, age, enclosing box, unique Id, feet, frame, body size, hairstyle, hair color, head attachments, clothing, mustache stubble activities, and accessories are all given for each human instance in the frame mostly on the label.

Fig.2: An example of the designed database. Lab fight between two girls – 1st Row. The scenario of snatching the phone is depicted in the 2nd row. A scenario of a student threatening is depicted in the 3rd row. The 4th row describes thesame critical situation. The 5th row depicts a situation in which students steal lab material. The sixth row depicts exam cheating scenario in examination hall.

3. Recent Deep Learning Architecture

The current deep learning-based pedestrian detection, tracking, and suspicious activity recognition systems are not as accurate and fast as human vision [2]. Pedestrian detection, tracking, and activity recognition are now separated into two categories: CNN and deep learning. V. Jones [3] approach used in pedestrian detection for face recognition. Again, HOG [5] and DPM [4] conventional approaches are used for pedestrian detection. These procedures are computationally intensive and time-consuming, and they necessitate the participation of humans. CNN-based deep learning techniques have grown in prominence as a result of their accuracy in pedestrian identification [7,8]. R-CNN [9] is the first deep learning model for object detection. Multiple stage convolutional network such Mask R-CNN [9], R-CNN family other variant as (Fast and Faster R-CNN model) [9][10][11][12]. Other, CNN models having single stages such as You Only Look Once (YOLO) [14] and SSD [15] are examples of deep learning approaches.As a result, real-time pedestrian detection is now unsuitable. As a result, Redmon et al. [15] introduced the YOLO net, that is an object regression architecture, to increase detection speed and accuracy. The proposed improved YOLOv5 method effectively detects small and constant pedestrians.

2.1. YOLOv5 Deep Learning Architecture

The YOLOv5 detector has only one stage. The YOLOv5 architecture contains three sections. 1) A solid foundation. 2) The output, and 3) the neck. The input picture features are extracted first by the backbone portion. For scale invariant feature extraction, CNN and max-pooling backbone networks are used [29]. The feature map development process is divided into four tiers in the backbone network. Each layer generates a feature map with the following dimensions: 152x152 pixels, 76x76 pixel resolution, 38x38 pixel resolution, and 19x19 pixel resolution. The neck network integrates feature maps of several levels to capture additional contextual information and prevent information loss. For multi-scale features, a recursive neural network is created, and pixel grouping backbone networks are employed for feature engineering. In a top-down method, semantic features are provided via a feature pyramid network. The bottom-up approach uses a pixel aggregation network for object localization. In the neck network, it can see three feature fusion components of different scales with sizes of 76x76x255, 38x38x255, and 19x19x255, where 255 is the network's image intensity range. The CSP network aims to improve inference speed. In the neck, the CSP network replaces the leftover units with CBL modules. The SPP module combines the benefits of the largest pooling with the flexibility of varying kernel sizes. The feature map in the input is mostly compressed. It compresses the extracted feature, resulting in a considerable reduction in feature extraction time. Again, it compresses features and removes the most important ones. Following that, it went through the intricacies of the upgraded YOLOv5 architecture.

2.1. Improved Mask R-CNN Deep Learning Architecture

To detect pedestrians on several scales, by leveraging scale-independent convolutional feature construction, the suggested Improved Mask R-CNN addresses the existing approach difficulties. Fig.3 depicts the basic concept of scale-independent feature map generation. A unique Improved R-CNN framework based on the Faster R-CNN pipeline [12] has been proposed as a result of the aforesaid proposal. The proposed Improved R-CNN is a unified architecture that combines a scale-independent feature map with a two-stage backbone network.

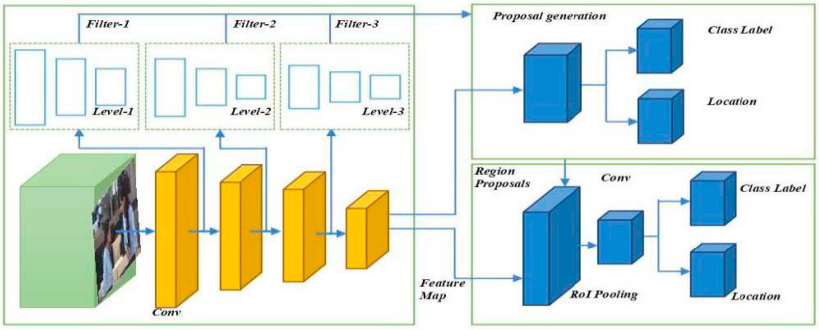

Fig.3. Depicts the basic concept of scale independent feature map generation.

The Improved R-CNN, as illustrated in Fig.4, takes input image and runs it through the common convolutional layers to obtain its whole local features. The scale-independent feature map and multiple backbone structure, that is useful for the present input about certain scales, may always help to increase the decisive outcomes. As a result, improved R-CNN can outperform traditional R-CNN detection across a large number of input scales. Improved R-CNN is also particularly efficient and effective of training and testing time because it combines convolutional characteristics for the input image. The traditional Mask R-CNN uses a binary convolution mask for every candidate region.

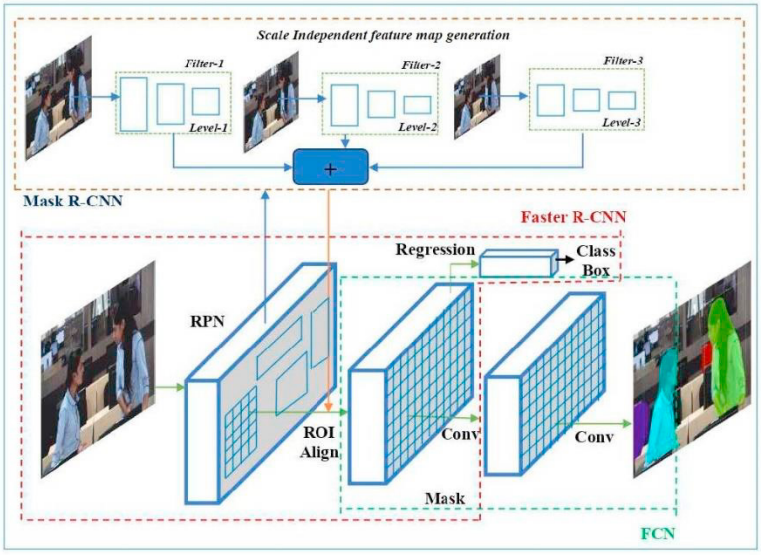

Fig.4. Improved Mask R-CNN Architecture.

A normalized framework is used to train the Scale invariant modified Mask R-CNN on the Microsoft COCO pedestrian dataset. Its testing section consisted of two primary steps: proposal region construction and pedestrian classification. The RoIs generated by the proposed region generation process might not even contain the requested object. The Region of Interest are categorized as an object or the background in the classification step. The traditional R-CNN network is very expensive for the original image to the network, notwithstanding its remarkable outcomes in

general of object detection accuracy. The RoIs must be generated using the proposal region generation technique, which takes time. Since the exponential function for the items is unavailable, the tiniest objects are not categorized efficiently. Mask R-CNNs in a practical utility for pedestrian monitoring are limited due to these two flaws. In the traditional Mask R-CNN, the human examples, which differ in scale, are not recognized adequately. As a result, this problem must be addressed by creating scale-independent extracted features for the various scales of human instances. To construct the probability value, the multi resolution images were mixed with various sizes of anchor box. This score is then combined with the feature map created previously in the process. Because of the scale-independent feature map, the region proposal accuracy improves. The steps in creating a scale-independent map for object detection discuss in brief as follows:

Algorithm: Features extraction algorithm for generation Scale-independent Object detection

Input: *MultiScaleFeature*, scale invariant mask, *MultiScaleImage,* multi-scale image,
Output: *scaleFeatureMatrix*, the scale-independent matrix
Read all the image at multiple scale.
for *scalefeatureMatrix*f_i ← 1 to *K* do
  Multi-scale image convolution process
  for *MultiScalFj* ← 1 to *T* do
    Multi-scaled invariant mask generated and convolved
    CScoreConv (MultiScaleImage, MultiScaleFeature)
    if *CScoreConv = null* then
      exit out of iteration
    else
      CuScore ← *CuScore* + *CuScore*
    end
  end
  scaleFeatureMatrix ← *CuScore*
end

To identify the varied scale pedestrian efficiently, scale-independent local features are combined with other convolution layers. Following that, the RoI align procedure is used to align each region's suggestions. Other Mask R-CNN processes are used in subsequent processing. The Mask R-CNN architecture for pedestrian detection has been discussed. Finally, the bounding box and segmented mask are used to represent all of the discovered and finally, results are represented using class annotation for each object in the scene.

4. Result and Discussion

In this section, the results of three tasks performed using methods regarded to be cutting-edge technology as pedestrian detection, tracking, and suspicious activity recognition. It also presents the results acquired using such strategies in the academic environment database, it also presents baseline findings usingthe same technique in a well-known dataset. Pedestrian Detection is the first step. Both the R-FCN [15] and RetinaNet [16], Mask R-CNN [17] deep learning frameworks excelled in the PASCAL VOC [17] problems,particularly in pedestrian identification.

4.1 Performance evaluation on the state-of-the-art Pedestrian Detection

The R-FCN [15] and RetinaNet [16], Mask R-CNN [17] computational intelligence system provides the benchmark performance for pedestrian detection given that both performed very well in the PASCAL VOC [17] challenges, particularly in the pedestrian detection issues. It compared the predicted dataset performance of the two methods with the results seen in the PASCAL VOC 2007 and 2012 datasets. On top of the ResNet, RetinaNet leverages the Feature Pyramid Network (FPN) as its support system. Variations in position are encoded using a particular convolutional layer by R-FCN [15]. Instead of a completely linked layer, it makes use of ROI max pooling. Again, try Mask R-CNN on the suggested dataset. The dataset is divided into three categories: training (60%) and testing (20%) for real-time queries. The experimental findings for the proposed and current methodologies are presented in Table 2. AP_{IoU}=0:5

represents the Average Precision (AP) at the Intersection of Union (IoU) values of the common evaluation measure with the value set to 0.5.

Table 2. Comparative analysis of proposed method and existing method on Proposed dataset And PASCAL VOC 2007

Methodology	**Backbone Structure**	**PASCAL VOC Dataset**	**Proposed Dataset**
R-FCN CNN Net [15]	ResNet-101 Network	84.43 ± 1.85	59.29 ± 1.31
RetinaNet CNN Net [16]	ResNet-50 Network	86.44 ± 1.03	63.10 ± 1.64
Proposed Mask R-CNN	ResNet-101 Network	87.41 ± 1.02	65.10 ± 1.44

4.2 Performance evaluation on the state-of-the-art human Tracking in Surveillance System

The Tracktor CV [2] and V-IOU [18] techniques give the state-of-the-art, for two reasons: 1) best performer in the MOT challenge; and 2) open source pre-builded framework. The two phases of the TracktorCV approach are as follows: 1) a regression component that uses the output of the detector stage to modify the bounding box's current location; and 2) a detecting component that keeps the set of frames for the subsequent frames. For both methodologies, it is seen that there is a positive association between failures that are connected to crowds and two worrying instances: 1) scenarios where trajectories intersect individuals at every second due to dense pedestrian congestion; and 2) when crucial deformations of the person silhouettes occur. The proposed database comprises of more intricate pictures with dense backdrops, including several situations with organization. It provides an overview of the findings in Table 3.

Table 3. Performance comparison of the two cutting-edge tracking methods using the suggested dataset and MOT datasets.

Methodology	Backbone	MOTA Measure	MOTP Measure	F1-Measure
TracktorCv [2]	MOT-17	65.20 ± 9.60	62.30 ± 11.00	89.60 ± 2.80
	Proposed dataset	56.00 ± 3.70	55.90 ± 2.60	87.40 ± 2.00
V-IOU [18]	MOT-17	52.50 ± 8.80	57.50 ± 9.50	86.50 ± 1.90
	Proposed dataset	47.90 ± 5.10	51.10 ± 5.80	83.30 ± 8.40
Proposed Mask R-CNN	MOT-17	67.50 ± 9.80	59.50 ± 10.50	89.50 ± 2.87
	Proposed dataset	70.90 ± 6.12	57.10 ± 15.80	83.10 ± 18.39

4.3 Performance evaluation on the state-of-the-art Pedestrian Suspicious Activity Recognition

In surveillance videos, abnormal activities are detected by varying object behaviors in scenes with varying appearances, scales, lighting conditions, and occluded trajectories. In a crowd area, detecting individual pedestrians is an important process. The aforementioned techniques are not suitable in these circumstances. The use of motion has been the focus of other recent investigation groups [20][21]. The extraction of local spatiotemporal cuboids from optical flow or gradient patterns has also been attempted [23]. Challa S.K. et al. [24] presented a multi-branch CNN-BiLSTM model for human activity recognition using wearable sensor data. An activity recognition algorithm based on CNN filters is used in this approach. Next, Jain R. et al. [25] proposed a deep ensemble learning approach for lower extremity activities recognition using wearable sensors. Semwal V. B. and colleagues [26] proposed an improved method for the selection of features for the recognition of human walking activities using bio-geography optimization. An ensemble learning approach was used by Semwal et al. [27] in order to create an optimized hybrid deep learning model for recognizing human walking activities. Other handcrafted features were considered by another author. An invariant gait recognition-based person identification method was presented by Semwal et al. [28]. According to Bijalwan et al. [29], multi-sensor based biomechanical gait analysis can be carried out using wearable sensors combined with vision. Semwal et al. [30] presented a pattern identification of different human joints for different human walking styles using an inertial measurement unit (IMU) sensor. Dua N. et al. [31] proposed a multi-input CNN-GRU based human activity recognition using wearable sensors. Bijalwan V. et al. [32] proposed a heterogeneous Computing Model for Post-injury Walking Pattern restoration and Postural Stability Re-habilitation Exercise Recognition". Again, although the above methods have proved their effectiveness in experiments, most of them only cover the detection of abnormal activities in local or global areas. As shown in Table 4, joint deliberation of motion

flows pattern, varying size of objects, and interactions between adjacent objects can be used to represent pedestrian activities in a high-density scene and enhance the performance of unusual activity detection.

Table 4. Comparative analysis of frame level Suspicious activity recognition using Equal Error Rate (EER).

Methodology/Technique	Pedestrian 1 (%)	Pedestrian 2 (%)	Average (%)
Social Force Map [22]	36.5%	35.0%	35.7%
MDT-spatial [23]	32%	38%	34%
Multibranch CNN-BiLSTM model [24]	44%	26%	32%
Lower extremity activities recognition [25]	45%	27%	35%
Optimized feature selection [26]	46%	29%	38%
Hybrid deep learning model [27]	48%	25%	34%
Pose Invariant Gait [28]	45.2%	29%	33%
Multi-sensor Gait [29]	45%	31.2%	39%
Human joints using IMU [30]	41%	27%	35%
Multi-input CNN-GRU [31]	38%	37%	37%
Heterogeneous Computing Model [32]	47%	31%	40%

5. Conclusion

In this paper, the academic environment database is proposed, which comprises video sequences of pedestrians in indoor academic environments that are annotated at the frame level. The pedestrian database contains the behavior of students in the institution. This is the first of its kind dataset that provides a unified and stable pedestrian ID annotation, making it suitable for pedestrian detection, tracking, and behaviour detection. It also proposed a scale-invariant Mask R-CNN model for robust and efficient pedestrian detection. Again, the proposed framework is also useful in suspicious activity recognition on recent benchmark databases. This well-organized comparison helps to identify problems and challenges in this domain. In the future, more experimentation is required for pose estimation and pedestrian trajectory identification and detection.

References

[1] Ahmed M., Jahangir M., Afzal H. (2015) “Using Crowd-source based features from social media and Conventional features to predict the movies popularity”, *IEEE International Conference on Smart Cities, Social Community and Sustained Community*, China, pp. 273–278.

[2] Bergmann P., Meinhardt T., Taixe L. (2019) “Tracking without bells and whistles”, *IEEE International Conference ICCV*, Seoul, Korea, pp. 1-16.

[3] Dollar P., Wojek C., Schiele B., and Perona P. (2012) “Pedestrian Detection: An Evaluation of the State of the Art”, *IEEE Transactions on Pattern Analysis and Machine Intelligence (TPAMI)*, **34 (4)**: 743-761.

[4] Samsi S., Weiss M., Bestor D., Li D., Jones M., Reuther A., Edelman D., Arcand W. and Byun C. (2021) “The MIT Supercloud Dataset”, *International Cornell Journal of Distributed, Parallel, and Cluster Computing*, **2108 (02037)**: 1-10.

[5] Silberstein S., Levi D., Kogan V. and Gazit R. (2014) “Vision-based pedestrian detection for rear-view cameras”, *IEEE Intelligent Vehicles Symposium*, pp. 853-860, Dearborn, MI, USA.

[6] Alom M. and Taha T. (2017) “Robust multi-view pedestrian tracking using neural networks”, *IEEE National Conference on Aerospace and Electronics*, pp. 17-22, Dayton, OH, USA.

[7] Zhang X., Park S., Beeler T., Bradley D., Tang S., Hilliges O. (2020) “ETH Gaze: A Large-Scale Dataset for Gaze Estimation Under Extreme Head Pose and Gaze Variation” *European Conference on Computer Vision (ECCV),* Springer. Lecture Notes in Computer Science, pp. 1-10.

[8] Wojek C., Walk S., Schiele B., (2009) “Multiresolution model for Object Detection”, *IEEE Computer Vision and Pattern Recognition (CVPR)*, June 20-25, 2009, Miami, Florida, USA.

[9] Nguyen T., Soo K., (2013). “Fast Pedestrian Detection Using Histogram of Oriented Gradients and Principal Components Analysis”. *International Journal of Contents*, **2013 (1)**: 1-20.

[10] Everingham, M., Van L., Williams, C. (2010) “The Pascal Visual Object Classes (VOC) Challenge”, *International Journal of Computer Vision*, Springer, **88 (1)**: 303–338.

[11] Lin T. (2014), “Microsoft COCO: Common Objects in Context. ECCV 2014”, *Lecture Notes in Computer Science, Springer*, **8693 (1)**: 740-755.

[12] Nicolai W., Bewley A., Dietrich P. (2017) "Simple online and real-time tracking with a deep association metric", *IEEE International Conference on Image Processing (ICIP)*, pp. 3645–3649.

[13] Jifeng D., Yi L., Kaiming H., Sun J., (2016) "R-FCN: Object detection via region-based fully convolutional networks", *IEEE Computer Vision and Pattern Recognition (CVPR)*, pp. 1-11.

[14] Everingham, M., Eslami, S., V. G., Williams C., Winn J. (2015) "The PASCAL VOC Challenge: A Retrospective", *International Journal of Computer Vision (IJCV), Springer*, **11 (1)**: 98-136.

[15] Kaiming H., Georgia G., Dollar P. and Girshick R. (2020) "Mask R-CNN, *IEEE Transactions on Pattern Analysis and Machine Intelligence (TPAMI)*, **42 (2)**: pp. 386-397.

[16] Viola P. and Jones M. (2001) "Rapid object detection using a boosted cascade of simple features," *IEEE Computer Vision and Pattern Recognition (CVPR)*, USA, pp. I-I.

[17] Felzenszwalb P., Girshick R., McAllester D. and Ramanan D. (2010) "Object detection with discriminatively trained part- based models", *IEEE Transactions on Pattern Analysis and Machine Intelligence (TPAMI)*, **32 (9)**: 1627–1645.

[18] Dalal N. and Triggs B. (2005) "Histograms of oriented gradients for human detection", *IEEE Computer Vision and Pattern Recognition (CVPR)*, San Diego, CA, USA, pp. 886–893.

[19] Muhammad N., Hussain M., Muhammad G., Bebis G., (2011), "Copy-move forgery detection using dyadic wavelet transform," *International Conference on Computer Graphics*, Singapore, pp. 103–108.

[20] Muhammad G., Hossain M., Kumar N., (2021) "EEG-based pathology detection for home health monitoring", *IEEE Journal on Selected Areas in Community*, **39 (2)**: 603–610.

[21] Muhammad G., Alhamid M., and Long X., (2019) "Computing and processing on the edge: Smart pathology detection for connected healthcare", *IEEE Network*, **33 (1)**: 44–49.

[22] Girshick R., Donahue J., Darrell T., and Malik J., (2014), "Rich feature hierarchies for accurate object detection and semantic segmentation" *IEEE Computer Vision and Pattern Recognition (CVPR),* Columbus, OH, USA, pp. 580–587.

[23] He K., Zhang X., Ren S., and Sun J., (2015) "Spatial pyramid pooling in deep convolutional networks for visual recognition", *IEEE Transactions on Pattern Analysis and Machine Intelligence (TPAMI),* **37 (9)**: 1904–1916.

[24] Girshick R., (2015) "Fast R-CNN", *IEEE International Conference on Computer Vision*, Santiago, Chile, pp. 1440–1448.

[25] Ren S., He K., Girshick R. and Sun J., (2016) "Faster R-CNN: Towards real-time object detection with region proposal networks", *IEEE Transactions on Pattern Analysis and Machine Intelligence (TPAMI),* **39 (6)**: 1137–1149.

[26] He K., Gkioxari G., Dollar P., and Girshick R., (2017) "Mask R-CNN" *IEEE Computer Vision and Pattern Recognition (CVPR)*, Venice, Italy, pp. 2980–2988.

[27] Liu W., Anguelov D., Erhan D., Szegedy C., Reed S., (2016) "SSD: Single shot multi-box detector" *European Conference on Computer Vision (ECCV)*, Cham, Springer, pp. 21–37.

[28] Redmon J., Girshick R. and Farhadi A., (2016) "You only look once: unified, real-time object detection", *IEEE Computer Vision and Pattern Recognition (CVPR)*, Las Vegas, NV, USA, pp. 779–788.

[29] Senst T. and Sikora T, (2018) "Extending IOU based multi-object tracking by visual information", *IEEE International Conference on Advanced Video and Signal Based Surveillance*, Auckland, New Zealand, pp. 1-7.

[30] Barnardin K. and Stiefelhagen R. (2008) "Evaluating Multiple Object Tracking Performance: The CLEAR MOT Metrics", EURASIP *Journal on Image and Video Processing*, Springer, **1 (1)**: 246-309.

[31] Kratz L. and Nishino K. (2012) "Tracking Pedestrians Using Local Spatio-Temporal Motion Patterns in Extremely Crowded Scenes" *IEEE Transactions on Pattern Analysis and Machine Intelligence (TPAMI)*, **34 (5)**: 987-1002.

[32] Wang S. and Miao Z. (2010) "Anomaly Detection in Crowd Scene", *IEEE International Conference on Signal Processing*, pp. 1220-1223, Oct. 24-28, Beijing, China.

[33] Wang S., Miao Z. (2010) "Anomaly Detection in Crowd Scene Using Historical Information", *IEEE Intelligence Signal Processing and Communication System*, pp. 1-4.

A fixed point theorem for extended B-metric space satisfying rational type contractive condition

Cite as: AIP Conference Proceedings **2435**, 020047 (2022); https://doi.org/10.1063/5.0083599
Published Online: 18 March 2022

Anushree A. Aserkar and M. P. Gandhi

A Fixed Point Theorem for Extended B-Metric Space Satisfying Rational Type Contractive Condition

Anushree A. Aserkar[a] and M. P. Gandhi[b]

Department of Mathematics & Humanities, Yeshwantrao Chavan College of Engineering, Nagpur, India.

[a]*Corresponding Author: aserkar_aaa@rediffmail.com*
[b]*Electronic mail: manjusha_g2@rediffmail.com*

Abstract. For a complete extended b-metric space with continuous mapping satisfying the rational type contractive condition, a distinctive common fixed point theorem is established. Our outcome is the extension of several results available in the literature, from metric space to extended b-metric space. In specific, Dass and Gupta[Indian J. Pure Appl. Math. 6, 1455–1458 (1975)], Jaggi[Indian J. Pure Appl. Math. 8, 223–230 (1977)], Alqahtani et.al.[J. Inequal. Appl. Paper No. 220, 11 pp (2019)] and even the well-known Banach contraction mapping theory are extracted. A proper example is also given in sustenance of it.

INTRODUCTION

In fixed point theory, the Banach contraction theorem is a fundamental and remarkable result. It has huge applications in almost all areas of mathematical sciences for example to prove the existence of solutions of ordinary and partial differential equations, integral equations, system of linear equations, closed orbit of dynamical systems. It has been expanded and generalized in various directions and spaces over the years. Rational type expressions were considered in the contraction condition in the results of Dass and Gupta[2] and Jaggi[3].

Jaggi[3] defined the main result for complete metric space.

1.1-Theorem[3]-Let (X,d) be a complete metric space and $\mathrm{I}: X \to X$ be a continuous mapping. If there exists $\delta, \rho \in [0,1)$ with $\delta + \rho < 1$ such that

$$d(\mathrm{I}a, \mathrm{I}b) \le \delta \cdot \frac{d(a,\mathrm{I}a)\,d(b,\mathrm{I}b)}{d(a,b)} + \rho \cdot d(a,b)$$ for all distinct $a, b \in X$, then I has a unique fixed point in X.

Dass and Gupta [2] have presented the result in complete metric space.

1.2-Theorem [2]- Let (X,d) be a complete metric space and $\mathrm{I}: X \to X$ be a continuous mapping. If there exists $\delta, \rho \in [0,1)$ with $\delta + \rho < 1$ such that

$$d(\mathrm{I}a, \mathrm{I}b) \le \delta \cdot d(b,\mathrm{I}b)\frac{\{1 + d(a,\mathrm{I}a)\}}{1 + d(a,b)} + \rho \cdot d(a,b)$$ for all distinct $a, b \in X$, then I has a unique fixed point in X. Moreover, the sequence $\{\mathrm{I}^n x\}$ converges to a unique fixed point u for all $a \in X$.

One of important extension of metric spaces is b-metric space. This concept was introduced by Bakhtin[4] in 1989 and Czerwik[5,6] in 1993.

Later the notion of extended b-metric space was introduced by Kamran et.al. [7] which is an extension of b-metric space.

Proceedings of the Third International Conference on Frontiers in Industrial and Applied Mathematics 2020
AIP Conf. Proc. 2435, 020047-1–020047-10; https://doi.org/10.1063/5.0083599
Published by AIP Publishing. 978-0-7354-4177-4/$30.00

1.3-Extended b-metric space [7]: Let X be a non-empty set and $\Omega : X \times X \to [1,\infty)$. A function $d_\Omega : X \times X \to [0,\infty)$ is called an extended b-metric space, if for all $a,b,c \in X$, it satisfies

(1) $d_\Omega(a,b) = 0$ if and only if $a = b$;

(2) $d_\Omega(a,b) = d_\Omega(b,a)$

(3) $d_\Omega(a,c) \le \Omega(a,c)\{d_\Omega(a,b) + d_\Omega(b,c)\}$.

The pair (X, d_Ω) is called an extended b-metric space.

It is obvious that an extended b-metric space is a metric space $\Omega(a,b) = s \ge 1$ where s is a real number and it is a metric space if $\Omega(a,b) = 1$.

Alqahtani et. Al.[1] in 2019, have extended and generalized the results of Dass and Gupta [2] and Jaggi [3] for extended b-metric space.

1.4-Theorem [1]- Let (X, d_Ω) be an extended *b*-metric space and $\mathrm{I} : X \to X$ a continuous mapping such that, for all distinct $a,b \in X$

$d_\Omega(\mathrm{I}a, \mathrm{I}b) \le \lambda M(a,b)$ where $\lambda \in [0,1)$ and

$$M(a,b) = \max\left\{ d_\Omega(a,\mathrm{I}a)\frac{[1+d_\Omega(b,\mathrm{I}b)]}{1+d_\Omega(a,b)}, d_\Omega(b,Tb)\frac{[1+d\Omega(a,\mathrm{I}a)]}{1+d_\Omega(a,b)}, \frac{d_\Omega(b,\mathrm{I}b)\,d_\Omega(a,\mathrm{I}a)}{d_\Omega(a,b)}, d_\Omega(a,b) \right\}$$ Also

for each $a_0 \in X$, $\lim_{m,n\to\infty} \Omega(a_n, a_m) < \frac{1}{\lambda}$, where $a_n = \mathrm{I}^n a_0$, $n \in N$.

Then I has a unique fixed point u. Also for each $a \in X$, we have $\mathrm{I}^n a \to u$

PRELIMINARIES

2.1-Definition[7]: Let (X, d_Ω) be an extended *b*-metric space.

A sequence $\{a_n\}$ in X converges to $a \in X$, if for every $\varepsilon > 0$ there exists $n(\varepsilon) \in N$ such that $d_\Omega(a_n, a) < \varepsilon$, for all $n \ge n(\varepsilon)$. In this case, we write $\lim_{n\to\infty} a_n = a$.

A sequence $\{a_n\}$ in X is said to be Cauchy if for every $\varepsilon > 0$ there exists $n(\varepsilon) \in N$ such that $d_\Omega(a_m, a_n) < \varepsilon$, for all $m,n \ge n(\varepsilon)$.

An extended *b*-metric space (X, d_Ω) is complete if every Cauchy sequence in X is convergent.

Notice that the extended b-metric does not need to be continuous.

MAIN RESULT

Our result is for complete extended b-metric space with continuous mapping satisfying rational type contractive condition. It extends the results of Dass and Gupta [2] and Jaggi [3] and generalizes the results of Alqahtani et. al.[1].

3.1-THEOREM:

Let (X, d_Ω) be a complete extended *b*-metric space and $\mathrm{I} : X \to X$ a continuous mapping such that, for all distinct $a,b \in X$

$$d_\Omega(Ia, Ib) \le \lambda N(a,b) \qquad \ldots(3.1.1)$$

where $\lambda \in [0,1)$ and

$$N(a,b) = \max\left\{ \begin{array}{l} d_\Omega(a,\mathrm{I}a)\dfrac{\left[1+d_\Omega(b,\mathrm{I}b)\right]}{1+d_\Omega(a,b)}, d_\Omega(b,\mathrm{I}b)\dfrac{\left[1+d_\Omega(a,\mathrm{I}a)\right]}{1+d_\Omega(a,b)}, \dfrac{d_\Omega(b,\mathrm{I}b)\,d_\Omega(a,\mathrm{I}a)}{d_\Omega(a,b)}, \\ d_\Omega(a,\mathrm{I}b)\dfrac{\left[1+d_\Omega(b,\mathrm{I}a)\right]}{\left[d_\Omega(a,\mathrm{I}b)+d_\Omega(b,\mathrm{I}a)\right]}, d_\Omega(b,\mathrm{I}a)\dfrac{\left[1+d_\Omega(a,\mathrm{I}b)\right]}{\left[d_\Omega(a,\mathrm{I}b)+d_\Omega(b,\mathrm{I}a)\right]}, \\ \dfrac{d_\Omega(a,\mathrm{I}b)\,d_\Omega(b,\mathrm{I}a)}{1+d_\Omega(a,b)}, \dfrac{d_\Omega(a,\mathrm{I}a)\,d_\Omega(a,\mathrm{I}b)+d_\Omega(b,\mathrm{I}b)\,d_\Omega(b,\mathrm{I}a)}{\left[d_\Omega(a,\mathrm{I}b)+d_\Omega(b,\mathrm{I}a)\right]}, d_\Omega(a,b) \end{array} \right\}$$

Also for each $a_0 \in X$, $\lim_{m,n\to\infty} \Omega(a_n,a_m) < \dfrac{1}{\lambda}$, where $a_n = \mathrm{I}^n a_0$, $n \in N$.

Then I has a unique fixed point u. Also for each $a \in X$, we have $\mathrm{I}^n a \to u$.

Proof: Let $a_0 \in X$ and define the iterative sequence $\{a_n\}$ by $a_n = \mathrm{I}^n a_0$ (equivalently $a_{n+1} = \mathrm{I}a_n$) where I^n stands for the map obtained by n-time composition of I with I.

If for some $a_{n_0} = a_{n_0+1} = \mathrm{I}a_{n_0}$ for some $n_0 \in N$, then $u = a_{n_0}$ forms a unique fixed point for I. So, we assume that $a_n = a_{n+1}$ for all $n \in N$.

Putting $a = a_{n-1}, b = a_n$ in (3.1.1), we get

$d_\Omega(\mathrm{I}a_{n-1}, \mathrm{I}a_n) \le \lambda N(a_{n-1}, a_n)$

i.e. $d_\Omega(a_n, a_{n+1}) \le \lambda N(a_{n-1}, a_n)$ …(3.1.2)

where $N(a_{n-1},a_n) = \max\left\{ \begin{array}{l} d_\Omega(a_{n-1},\mathrm{I}a_{n-1})\dfrac{\left[1+d_\Omega(a_n,\mathrm{I}a_n)\right]}{1+d_\Omega(a_{n-1},a_n)}, d_\Omega(a_n,\mathrm{I}a_n)\dfrac{\left[1+d_\Omega(a_{n-1},\mathrm{I}a_{n-1})\right]}{1+d_\Omega(a_{n-1},a_n)}, \\ \dfrac{d_\Omega(a_n,\mathrm{I}a_n)\,d_\Omega(a_{n-1},\mathrm{I}a_{n-1})}{d_\Omega(a_{n-1},a_n)}, d_\Omega(a_{n-1},\mathrm{I}a_n)\dfrac{\left[1+d_\Omega(a_n,\mathrm{I}a_{n-1})\right]}{\left[d_\Omega(a_{n-1},\mathrm{I}a_n)+d_\Omega(a_n,\mathrm{I}a_{n-1})\right]}, \\ d_\Omega(a_n,\mathrm{I}a_{n-1})\dfrac{\left[1+d_\Omega(a_{n-1},\mathrm{I}a_n)\right]}{\left[d_\Omega(a_{n-1},\mathrm{I}a_n)+d_\Omega(a_n,\mathrm{I}a_{n-1})\right]}, \dfrac{d_\Omega(a_{n-1},\mathrm{I}a_n)\,d_\Omega(a_n,\mathrm{I}a_{n-1})}{1+d_\Omega(a_{n-1},a_n)}, \\ \dfrac{d_\Omega(a_{n-1},\mathrm{I}a_{n-1})\,d_\Omega(a_{n-1},\mathrm{I}a_n)+d_\Omega(a_n,\mathrm{I}a_n)\,d_\Omega(a_n,\mathrm{I}a_{n-1})}{\left[d_\Omega(a_{n-1},\mathrm{I}a_n)+d_\Omega(a_n,\mathrm{I}a_{n-1})\right]}, d_\Omega(a_{n-1},a_n) \end{array} \right\}$

$$= \max\left\{ \begin{array}{l} d_\Omega(a_{n-1},a_n)\dfrac{\left[1+d_\Omega(a_n,a_{n+1})\right]}{1+d_\Omega(a_{n-1},a_n)}, d_\Omega(a_n,a_{n+1})\dfrac{\left[1+d_\Omega(a_{n-1},a_n)\right]}{1+d_\Omega(a_{n-1},a_n)}, \\ \dfrac{d_\Omega(a_n,a_{n+1})\,d_\Omega(a_{n-1},a_n)}{d_\Omega(a_{n-1},a_n)}, d_\Omega(a_{n-1},a_{n+1})\dfrac{\left[1+d_\Omega(a_n,a_n)\right]}{\left[d_\Omega(a_{n-1},a_{n+1})+d_\Omega(a_n,a_n)\right]}, \\ d_\Omega(a_n,a_n)\dfrac{\left[1+d_\Omega(a_{n-1},a_{n+1})\right]}{\left[d_\Omega(a_{n-1},a_{n+1})+d_\Omega(a_n,a_n)\right]}, \dfrac{d_\Omega(a_{n-1},a_{n+1})\,d_\Omega(a_n,a_n)}{1+d_\Omega(a_{n-1},a_n)}, \\ \dfrac{d_\Omega(a_{n-1},a_n)\,d_\Omega(a_{n-1},a_{n+1})+d_\Omega(a_n,a_{n+1})\,d_\Omega(a_n,a_n)}{\left[d_\Omega(a_{n-1},a_{n+1})+d_\Omega(a_n,a_n)\right]}, d_\Omega(a_{n-1},a_n) \end{array} \right\}$$

$$= \max\left\{ d_\Omega\left(a_{n-1}, a_n\right) \frac{\left[1 + d_\Omega\left(a_n, a_{n+1}\right)\right]}{1 + d_\Omega\left(a_{n-1}, a_n\right)}, d_\Omega\left(a_n, a_{n+1}\right), 1, d_\Omega\left(a_{n-1}, a_n\right) \right\}$$

Case-I: If

$$N\left(a_{n-1}, a_n\right) = \max\left\{ d_\Omega\left(a_{n-1}, a_n\right) \frac{\left[1 + d_\Omega\left(a_n, a_{n+1}\right)\right]}{1 + d_\Omega\left(a_{n-1}, a_n\right)}, d_\Omega\left(a_n, a_{n+1}\right), 1, d_\Omega\left(a_{n-1}, a_n\right) \right\} = d_\Omega\left(a_n, a_{n+1}\right)$$

Then from (3.1.2), we get $d_\Omega\left(a_n, a_{n+1}\right) \le k d_\Omega\left(a_n, a_{n+1}\right)$ which is a contradiction.

Case-II: If

$$N\left(a_{n-1}, a_n\right) = \max\left\{ d_\Omega\left(a_{n-1}, a_n\right) \frac{\left[1 + d_\Omega\left(a_n, a_{n+1}\right)\right]}{1 + d_\Omega\left(a_{n-1}, a_n\right)}, d_\Omega\left(a_n, a_{n+1}\right), 1, d_\Omega\left(a_{n-1}, a_n\right) \right\} = d_\Omega\left(a_{n-1}, a_n\right)$$

Then from (3.1.2), we get $d_\Omega\left(a_n, a_{n+1}\right) \le \lambda d_\Omega\left(a_{n-1}, a_n\right)$ ….(3.1.3)

Case-III: If

$$N\left(a_{n-1}, a_n\right) = \max\left\{ d_\Omega\left(a_{n-1}, a_n\right) \frac{\left[1 + d_\Omega\left(a_n, a_{n+1}\right)\right]}{1 + d_\Omega\left(a_{n-1}, a_n\right)}, d_\Omega\left(a_n, a_{n+1}\right), 1, d_\Omega\left(a_{n-1}, a_n\right) \right\}$$

$$= d_\Omega\left(a_{n-1}, a_n\right) \frac{\left[1 + d_\Omega\left(a_n, a_{n+1}\right)\right]}{1 + d_\Omega\left(a_{n-1}, a_n\right)}$$

Now, Case-III-(A) if $\max\left\{ d_\Omega\left(a_n, a_{n+1}\right), d_\Omega\left(a_{n-1}, a_n\right) \right\} = d_\Omega\left(a_n, a_{n+1}\right)$

i.e. $d_\Omega\left(a_{n-1}, a_n\right) \le d_\Omega\left(a_n, a_{n+1}\right)$ ….(3.1.4)

$$d_\Omega\left(a_n, a_{n+1}\right) \le d_\Omega\left(a_{n-1}, a_n\right) \frac{\left[1 + d_\Omega\left(a_n, a_{n+1}\right)\right]}{1 + d_\Omega\left(a_{n-1}, a_n\right)}$$

$$\therefore d_\Omega\left(a_n, a_{n+1}\right)\left\{1 + d_\Omega\left(a_{n-1}, a_n\right)\right\} \le d_\Omega\left(a_{n-1}, a_n\right)\left[1 + d_\Omega\left(a_n, a_{n+1}\right)\right]$$

$$\Rightarrow d_\Omega\left(a_n, a_{n+1}\right) + d_\Omega\left(a_n, a_{n+1}\right) d_\Omega\left(a_{n-1}, a_n\right) \le d_\Omega\left(a_{n-1}, a_n\right) + d_\Omega\left(a_{n-1}, a_n\right) d_\Omega\left(a_n, a_{n+1}\right)$$

$\Rightarrow d_\Omega\left(a_n, a_{n+1}\right) \le d_\Omega\left(a_{n-1}, a_n\right)$ which is a contradiction from (3.1.4).

Now, Case-III-(B) if $\max\left\{ d_\Omega\left(a_n, a_{n+1}\right), d_\Omega\left(a_n, a_n\right) \right\} = d_\Omega\left(a_n, a_n\right)$

i.e. $d_\Omega\left(a_n, a_{n+1}\right) \le d_\Omega\left(a_{n-1}, a_n\right)$ ….(3.1.5)

i.e. $d_\Omega\left(a_{n-1}, a_n\right) \le d_\Omega\left(a_{n-1}, a_n\right) \frac{\left[1 + d_\Omega\left(a_n, a_{n+1}\right)\right]}{1 + d_\Omega\left(a_{n-1}, a_n\right)}$

$\Rightarrow 1 + d_\Omega\left(a_{n-1}, a_n\right) \le 1 + d_\Omega\left(a_n, a_{n+1}\right) \Rightarrow d_\Omega\left(a_{n-1}, a_n\right) \le d_\Omega\left(a_n, a_{n+1}\right)$ which is a contradiction from (3.1.5)

Thus Case-III does not hold.

Case-IV: $N\left(a_{n-1}, a_n\right) = \max\left\{ d_\Omega\left(a_{n-1}, a_n\right) \frac{\left[1 + d_\Omega\left(a_n, a_{n+1}\right)\right]}{1 + d_\Omega\left(a_{n-1}, a_n\right)}, d_\Omega\left(a_n, a_{n+1}\right), 1, d_\Omega\left(a_{n-1}, a_n\right) \right\} = 1$

Then from (3.1.2), we get $d_\Omega\left(a_n, a_{n+1}\right) \le \lambda < 1$ which is always not true.

Hence Case-II holds. So, from (3.1.3)

$d_\Omega\left(a_n, a_{n+1}\right) \le \lambda d_\Omega\left(a_{n-1}, a_n\right)$

.

.

$d_\Omega\left(a_n, a_{n+1}\right) \le \lambda^n d_\Omega\left(a_0, a_1\right) \qquad \because \lambda \in [0,1)$

$\lim_{n\to\infty} d_\Omega\left(a_n, a_{n+1}\right) \le \lim_{n\to\infty} \lambda^n d_\Omega\left(a_0, a_1\right) = 0$ ….(3.1.6)

By the definition of extended b-metric space (3), $d_\Omega\left(a,c\right) \le \theta\left(a,c\right)\left\{d_\Omega\left(a,b\right) + d_\Omega\left(b,c\right)\right\}$

Using the above triangle inequality, $n \ge 1, p \ge 1$

$$\begin{aligned}
d_\Omega\left(a_n, a_{n+p}\right) &\le \Omega\left(a_n, a_{n+p}\right)\left\{d_\Omega\left(a_n, a_{n+1}\right) + d_\Omega\left(a_{n+1}, a_{n+p}\right)\right\} \\
&\le \Omega\left(a_n, a_{n+p}\right) d_\Omega\left(a_n, a_{n+1}\right) + \Omega\left(a_n, a_{n+p}\right)\Omega\left(a_{n+1}, a_{n+p}\right)\left\{d_\Omega\left(a_{n+1}, a_{n+2}\right) + d_\Omega\left(a_{n+2}, a_{n+p}\right)\right\} \\
&\le \Omega\left(a_n, a_{n+p}\right) d_\Omega\left(a_n, a_{n+1}\right) + \Omega\left(a_n, a_{n+p}\right)\Omega\left(a_{n+1}, a_{n+p}\right) d_\Omega\left(a_{n+1}, a_{n+2}\right) + \ldots\ldots \\
&\qquad + \Omega\left(a_n, a_{n+p}\right)\Omega\left(a_{n+1}, a_{n+p}\right)\ldots\Omega\left(a_{n+p-1}, a_{n+p}\right) d_\Omega\left(a_{n+p-1}, a_{n+p}\right) \\
&\le \Omega\left(a_n, a_{n+p}\right)\lambda^n d_\Omega\left(a_0, a_1\right) + \Omega\left(a_n, a_{n+p}\right)\Omega\left(a_{n+1}, a_{n+p}\right)\lambda^{n+1} d_\Omega\left(a_0, a_1\right) + \ldots\ldots \\
&\qquad + \Omega\left(a_n, a_{n+p}\right)\Omega\left(a_{n+1}, a_{n+p}\right)\ldots\Omega\left(a_{n+p-1}, a_{n+p}\right)\lambda^{n+p-1} d_\Omega\left(a_0, a_1\right) \\
&= d_\Omega\left(a_0, a_1\right)\lambda^n \sum_{i=0}^{p-1} \lambda^i \prod_{j=0}^{i} \Omega\left(a_{n+j}, a_{n+p}\right).
\end{aligned}$$

Now, $\sum_{i=0}^{p-1} \lambda^i \prod_{j=0}^{i} \Omega\left(a_{n+j}, a_{n+p}\right) \le \sum_{i=0}^{p-1} \lambda^i \times \prod_{j=0}^{i} \Omega\left(a_{n+j}, a_{n+p}\right)$.

Using ratio test, we observe that the series $\sum_{i=0}^{p-1} \lambda^i \times \prod_{j=0}^{i} \Omega\left(a_{n+j}, a_{n+p}\right)$ converges to some $\mu \in \left(0, \infty\right)$.

From ratio test, $\lim_{i\to\infty} \frac{a_{i+1}}{a_i} = \lim_{i\to\infty} \lambda\Omega\left(a_i, a_{i+p}\right) < 1$.

Thus we get $\mu = \sum_{i=0}^{\infty} \lambda^i \times \prod_{j=0}^{i} \Omega\left(a_{n+j}, a_{n+p}\right)$ with $\mu_n = \sum_{i=0}^{n} \lambda^i \times \prod_{j=0}^{i} \Omega\left(a_{n+j}, a_{n+p}\right)$

Consequently, we observe that, $d_\Omega\left(x_n, x_{n+p}\right) \le \lambda^n d_\Omega\left(a_0, a_1\right)\left(\mu_{n+p-1} - \mu_{n-1}\right)$ …(3.1.7)

Taking $n \to \infty$ in (3.1.7), we get $\left\{a_n\right\}$ is a cauchy sequence in extended b-metric space.

As $\left(X, d_\Omega\right)$ is a complete extended b-metric space, we conclude that there exists $u \in X$ such that $a_n \to u$ as $n \to \infty$.

From to the continuity of I, we get

$\mathrm{I}u = \mathrm{I}\lim_{n\to\infty} a_n = \lim_{n\to\infty} \mathrm{I}a_n = \lim_{n\to\infty} a_{n+1} = u$.

Unique: let if possible there are two fixed points say $u \ne v$ such that $\mathrm{I}u = u \ne v = \mathrm{I}v$,

Putting $x = u, y = v$ in (3.1.1), we get

$d_\Omega\left(\mathrm{I}u, \mathrm{I}v\right) \le \lambda N\left(u, v\right)$ …(3.1.8)

where $\lambda \in [0,1)$ and

$$N(u,v)=\max\left\{\begin{array}{l} d_\Omega(u,\mathrm{I}u)\dfrac{\left[1+d_\Omega(v,\mathrm{I}v)\right]}{1+d_\Omega(u,v)}, d_\Omega(v,\mathrm{I}v)\dfrac{\left[1+d_\Omega(u,\mathrm{I}u)\right]}{1+d_\Omega(u,v)}, \dfrac{d_\Omega(v,\mathrm{I}v)d_\Omega(u,\mathrm{I}u)}{d_\Omega(u,v)}, \\ d_\Omega(u,\mathrm{I}v)\dfrac{\left[1+d_\Omega(v,\mathrm{I}u)\right]}{\left[d_\Omega(u,\mathrm{I}v)+d_\Omega(v,\mathrm{I}u)\right]}, d_\Omega(v,\mathrm{I}u)\dfrac{\left[1+d_\Omega(u,\mathrm{I}v)\right]}{\left[d_\Omega(u,\mathrm{I}v)+d_\Omega(v,\mathrm{I}u)\right]}, \\ \dfrac{d_\Omega(u,\mathrm{I}v)d_\Omega(v,\mathrm{I}u)}{1+d_\Omega(u,v)}, \dfrac{d_\Omega(u,\mathrm{I}u)d_\Omega(u,\mathrm{I}v)+d_\Omega(v,\mathrm{I}v)d_\Omega(v,\mathrm{I}u)}{\left[d_\Omega(u,\mathrm{I}v)+d_\Omega(v,\mathrm{I}u)\right]}, d_\Omega(u,v) \end{array}\right\}$$

$$=\max\left\{0,0,0,d_\Omega(u,v),\frac{\left[d_\Omega(u,\mathrm{I}v)\right]^2}{1+d_\Omega(u,v)},0,d_\Omega(u,v)\right\}=d_\Omega(u,v)$$

$\therefore d_\Omega(u,v)\le\lambda d_\Omega(u,v)$ $\quad\because \lambda<1$

$\Rightarrow d_\Omega(u,v)=0\Rightarrow u=v$. Thus the fixed point is unique.

In the following we have simplified the condition by omitting the continuity of the mapping.

3.2-THEOREM

Let (X,d_Ω) be a complete extended b-metric space and $\mathrm{I}:X\to X$ is mapping such that

$d_\Omega(\mathrm{I}a,\mathrm{I}b)\le\lambda N(a,b)$ …(3.1.9)

for all distinct $a,b\in X$,where $\lambda\in[0,1)$ and

$$N(a,b)=\max\left\{\begin{array}{l} d_\Omega(a,\mathrm{I}a)\dfrac{\left[1+d_\Omega(b,\mathrm{I}b)\right]}{1+d_\Omega(a,b)}, d_\Omega(b,\mathrm{I}b)\dfrac{\left[1+d_\Omega(a,\mathrm{I}a)\right]}{1+d_\Omega(a,b)}, \dfrac{d_\Omega(b,\mathrm{I}b)d_\Omega(a,\mathrm{I}a)}{d_\Omega(a,b)}, \\ d_\Omega(a,\mathrm{I}b)\dfrac{\left[1+d_\Omega(b,\mathrm{I}a)\right]}{\left[d_\Omega(a,\mathrm{I}b)+d_\Omega(b,\mathrm{I}a)\right]}, d_\Omega(b,\mathrm{I}a)\dfrac{\left[1+d_\Omega(a,\mathrm{I}b)\right]}{\left[d_\Omega(a,\mathrm{I}b)+d_\Omega(b,\mathrm{I}a)\right]}, \\ \dfrac{d_\Omega(a,\mathrm{I}b)d_\Omega(b,\mathrm{I}a)}{1+d_\Omega(a,b)}, \dfrac{d_\Omega(a,\mathrm{I}a)d_\Omega(a,\mathrm{I}b)+d_\Omega(b,\mathrm{I}b)d_\Omega(b,\mathrm{I}a)}{\left[d_\Omega(a,\mathrm{I}b)+d_\Omega(b,\mathrm{I}a)\right]}, d_\Omega(a,b) \end{array}\right\}$$

Also for each $a_0\in X$, $\lim_{m,n\to\infty}\Omega(a_n,a_m)<\dfrac{1}{\lambda}$, where $a_n=\mathrm{I}^n a_0$, $n\in N$.

Then I has a unique fixed point u. Also for each $a\in X$, we have $\mathrm{I}^n a\to u$.

Proof: Proceeding in the same way as in theorem-3.1.1, we get that $\{a_n\}$ is a Cauchy sequence.

As stated X is a complete extended b-metric space, there exists $u\in X$, such that $a_n=\mathrm{I}^n a_0$ converges to u , that is $\lim_{n\to\infty}d_\Omega(a_n,u)=0$ ….(3.1.10)

By the definition of extended b-metric space (3), $d_\Omega(a,c)\le\Omega(a,c)\{d_\Omega(a,b)+d_\Omega(b,c)\}$

$d_\Omega(u,\mathrm{I}u)\le\Omega(u,\mathrm{I}u)\{d_\Omega(u,\mathrm{I}a_n)+d_\Omega(\mathrm{I}a_n,\mathrm{I}u)\}$ From (3.1.9), we get

$\le\Omega(u,\mathrm{I}u)\{d_\Omega(u,\mathrm{I}a_n)+\lambda N(a_n,u)\}$ …(3.1.11)

$$N(a_n,u)=\max\left\{\begin{array}{l} d_\Omega(a_n,\mathrm{I}a_n)\dfrac{\left[1+d_\Omega(u,\mathrm{I}u)\right]}{1+d_\Omega(a_n,u)},d_\Omega(u,\mathrm{I}u)\dfrac{\left[1+d_\Omega(a_n,\mathrm{I}a_n)\right]}{1+d_\Omega(a_n,u)},\dfrac{d_\Omega(u,\mathrm{I}u)d_\Omega(a_n,\mathrm{I}a_n)}{d_\Omega(a_n,u)},\\ d_\Omega(a_n,\mathrm{I}u)\dfrac{\left[1+d_\Omega(u,\mathrm{I}a_n)\right]}{\left[d_\Omega(a_n,\mathrm{I}u)+d_\Omega(u,\mathrm{I}a_n)\right]},d_\Omega(u,\mathrm{I}a_n)\dfrac{\left[1+d_\Omega(a_n,\mathrm{I}u)\right]}{\left[d_\Omega(a_n,\mathrm{I}u)+d_\Omega(u,\mathrm{I}a_n)\right]},\\ \dfrac{d_\Omega(a_n,\mathrm{I}u)d_\Omega(u,\mathrm{I}a_n)}{1+d_\Omega(a_n,u)},\dfrac{d_\Omega(a_n,\mathrm{I}a_n)d_\Omega(a_n,\mathrm{I}u)+d_\Omega(u,\mathrm{I}u)d_\Omega(u,\mathrm{I}a_n)}{\left[d_\Omega(a_n,\mathrm{I}u)+d_\Omega(u,\mathrm{I}a_n)\right]},d_\Omega(a_n,u) \end{array}\right\}$$

$$=\max\left\{\begin{array}{l} d_\Omega(a_n,a_{n+1})\dfrac{\left[1+d_\Omega(u,\mathrm{I}u)\right]}{1+d_\Omega(a_n,u)},d_\Omega(u,\mathrm{I}u)\dfrac{\left[1+d_\Omega(a_n,a_{n+1})\right]}{1+d_\Omega(a_n,u)},\dfrac{d_\Omega(u,\mathrm{I}u)d_\Omega(a_n,a_{n+1})}{d_\Omega(a_n,u)},\\ d_\Omega(a_n,\mathrm{I}u)\dfrac{\left[1+d_\Omega(u,a_{n+1})\right]}{\left[d_\Omega(a_n,\mathrm{I}u)+d_\Omega(u,a_{n+1})\right]},d_\Omega(u,a_{n+1})\dfrac{\left[1+d_\Omega(a_n,\mathrm{I}u)\right]}{\left[d_\Omega(a_n,\mathrm{I}u)+d_\Omega(u,a_{n+1})\right]},\\ \dfrac{d_\Omega(a_n,\mathrm{I}u)d_\Omega(u,a_{n+1})}{1+d_\Omega(a_n,u)},\dfrac{d_\Omega(a_n,a_{n+1})d_\Omega(a_n,\mathrm{I}u)+d_\Omega(u,\mathrm{I}u)d_\Omega(u,a_{n+1})}{\left[d_\Omega(a_n,\mathrm{I}u)+d_\Omega(u,a_{n+1})\right]},d_\Omega(a_n,u) \end{array}\right\}$$

Taking $\lim_{n\to\infty}$ and considering (3.1.6), (3.1.10), we get

$d_\Omega(u,\mathrm{I}u)\le\Omega(u,\mathrm{I}u)\lambda d_\Omega(u,\mathrm{I}u)\qquad\because\Omega(u,Tu)\lambda\ne 0$

$\Rightarrow d_\Omega(u,\mathrm{I}u)=0\Rightarrow \mathrm{I}u=u$.

Again the unique fixed point may be proved following the same steps as in theorem-3.1.1

3.3-COROLLARY

Let (X,d_Ω) be a complete extended *b*-metric space and $\mathrm{I}:X\to X$ a continuous mapping such that, for all distinct $a,b\in X$

$$d_\Omega(\mathrm{I}a,\mathrm{I}b)\le\alpha_1 d_\Omega(a,\mathrm{I}a)\frac{\left[1+d_\Omega(b,\mathrm{I}b)\right]}{1+d_\Omega(a,b)}+\alpha_2 d_\Omega(b,\mathrm{I}b)\frac{\left[1+d_\Omega(a,\mathrm{I}a)\right]}{1+d_\Omega(a,b)}+\alpha_3\frac{d_\Omega(b,\mathrm{I}b)d_\Omega(a,\mathrm{I}a)}{d_\Omega(a,b)}$$
$$+\alpha_4 d_\Omega(a,\mathrm{I}b)\frac{\left[1+d_\Omega(b,\mathrm{I}a)\right]}{\left[d_\Omega(a,\mathrm{I}b)+d_\Omega(b,\mathrm{I}a)\right]}+\alpha_5 d_\Omega(b,\mathrm{I}a)\frac{\left[1+d_\Omega(a,\mathrm{I}b)\right]}{\left[d_\Omega(a,\mathrm{I}b)+d_\Omega(b,\mathrm{I}a)\right]}$$
$$+\alpha_6\frac{d_\Omega(a,\mathrm{I}b)d_\Omega(b,\mathrm{I}a)}{1+d_\Omega(a,b)}+\alpha_7\frac{d_\Omega(a,\mathrm{I}a)d_\Omega(a,\mathrm{I}b)+d_\Omega(b,\mathrm{I}b)d_\Omega(b,\mathrm{I}a)}{\left[d_\Omega(a,\mathrm{I}b)+d_\Omega(b,\mathrm{I}a)\right]}+\alpha_8 d_\Omega(a,b)$$

where $\alpha_i\in[0,1),i=1,2,3,4,5,6,7,8$ with $\sum_{i=1}^{8}\alpha_i\le 1$ also for each $a_0\in X$, $\lim_{m,n\to\infty}\Omega(a_n,a_m)<\dfrac{1}{\sum_{i=1}^{8}\alpha_i}$, where $a_n=\mathrm{I}^n a_0$, $n\in N$. Then I has a unique fixed point u. Also for each $a\in X$, we have $\mathrm{I}^n a\to u$..

Proof: The result is easily obtained from Theorem-3.1 by taking $\lambda=\sum_{i=1}^{8}\alpha_i<1$..

3.4-REMARK

1- Corollary-3.3 is an extension of Jaggi[3] to extended b-metric space if we consider $\alpha_3 + \alpha_8 < 1$ and $\alpha_1 = \alpha_2 = \alpha_4 = \alpha_5 = \alpha_6 = \alpha_7 = 0$.

2- Corollary-3.3 is an extension of Dass and Gupta [2] to extended b-metric space if we consider $\alpha_2 + \alpha_8 < 1$ and $\alpha_1 = \alpha_3 = \alpha_4 = \alpha_5 = \alpha_6 = \alpha_7 = 0$.

3.5-EXAMPLE

Let $X = \left\{\frac{1}{2}, \frac{1}{4}, \frac{1}{8}\right\}$, $\Omega : X \times X \to [1, \infty)$ such that $\Omega(a,b) = a + b + 1$

$d_\Omega : X \times X \to [0, \infty)$ such that $d_\Omega\left(\frac{1}{2}, \frac{1}{4}\right) = d_\Omega\left(\frac{1}{4}, \frac{1}{2}\right) = 1$, $d_\Omega\left(\frac{1}{2}, \frac{1}{8}\right) = d_\Omega\left(\frac{1}{8}, \frac{1}{2}\right) = 2$,

$d_\Omega\left(\frac{1}{4}, \frac{1}{8}\right) = d_\Omega\left(\frac{1}{8}, \frac{1}{4}\right) = 3$, $d_\Omega\left(\frac{1}{2}, \frac{1}{2}\right) = d_\Omega\left(\frac{1}{4}, \frac{1}{4}\right) = d_\Omega\left(\frac{1}{8}, \frac{1}{8}\right) = 0$,

$\lambda = \frac{7}{12}$ and $\mathrm{I} : X \to X$ is defined as $\mathrm{I}\left(\frac{1}{2}\right) = \mathrm{I}\left(\frac{1}{4}\right) = \frac{1}{4}$, $\mathrm{I}\left(\frac{1}{8}\right) = \frac{1}{2}$.

We may well prove that $\mathrm{I}^n a \to \frac{1}{4}$, as $n \to \infty$ for all $a \in X$.

$\lim_{m,n \to \infty} \Omega\left(\mathrm{I}^m x, \mathrm{I}^n x\right) = \frac{1}{4} + \frac{1}{4} + 1 = \frac{3}{2} < \frac{1}{\lambda} = \frac{12}{7}$.

$\Omega\left(\frac{1}{2}, \frac{1}{4}\right) = \frac{1}{2} + \frac{1}{4} + 1 = \frac{7}{4}$, $\Omega\left(\frac{1}{2}, \frac{1}{8}\right) = \frac{1}{2} + \frac{1}{8} + 1 = \frac{13}{4}$, $\Omega\left(\frac{1}{8}, \frac{1}{4}\right) = \frac{1}{8} + \frac{1}{4} + 1 = \frac{11}{8}$.

$1 = d_\Omega\left(\frac{1}{2}, \frac{1}{4}\right) \le \Omega\left(\frac{1}{2}, \frac{1}{4}\right)\left\{d_\Omega\left(\frac{1}{2}, \frac{1}{8}\right) + d_\Omega\left(\frac{1}{8}, \frac{1}{4}\right)\right\} = \frac{7}{4}(2+3) = \frac{35}{4}$,

$2 = d_\Omega\left(\frac{1}{2}, \frac{1}{8}\right) \le \Omega\left(\frac{1}{2}, \frac{1}{8}\right)\left\{d_\Omega\left(\frac{1}{2}, \frac{1}{4}\right) + d_\Omega\left(\frac{1}{4}, \frac{1}{8}\right)\right\} = \frac{13}{8}(1+3) = \frac{13}{2}$,

$3 = d_\Omega\left(\frac{1}{4}, \frac{1}{8}\right) \le \Omega\left(\frac{1}{4}, \frac{1}{8}\right)\left\{d_\Omega\left(\frac{1}{4}, \frac{1}{2}\right) + d_\Omega\left(\frac{1}{2}, \frac{1}{8}\right)\right\} = \frac{11}{8}(1+2) = \frac{33}{8}$,

Hence it is proved that d_Ω is an extended b-metric space.

Case-I: If $a = \frac{1}{2}, b = \frac{1}{4}$,

$LHS = d_\Omega\left(\mathrm{I}\frac{1}{2}, \mathrm{I}\frac{1}{4}\right) = 0$,

$$RHS = \lambda N\left(\frac{1}{2},\frac{1}{4}\right) = \frac{7}{12}\max\left\{\begin{array}{l} d_\Omega\left(\frac{1}{2},\mathrm{I}\frac{1}{2}\right)\frac{\left[1+d_\Omega\left(\frac{1}{4},\mathrm{I}\frac{1}{4}\right)\right]}{1+d_\Omega\left(\frac{1}{2},\frac{1}{4}\right)}, d_\Omega\left(\frac{1}{4},\mathrm{I}\frac{1}{4}\right)\frac{\left[1+d_\Omega\left(\frac{1}{2},\mathrm{I}\frac{1}{2}\right)\right]}{1+d_\Omega\left(\frac{1}{2},\frac{1}{4}\right)}, \frac{d_\Omega\left(\frac{1}{4},\mathrm{I}\frac{1}{4}\right)d_\Omega\left(\frac{1}{2},\mathrm{I}\frac{1}{2}\right)}{d_\Omega\left(\frac{1}{2},\frac{1}{4}\right)} \\ d_\Omega\left(\frac{1}{2},\mathrm{I}\frac{1}{4}\right)\frac{\left[1+d_\Omega\left(\frac{1}{4},\mathrm{I}\frac{1}{2}\right)\right]}{\left[d_\Omega\left(\frac{1}{2},\mathrm{I}\frac{1}{4}\right)+d_\Omega\left(\frac{1}{4},\mathrm{I}\frac{1}{2}\right)\right]}, d_\Omega\left(\frac{1}{4},\mathrm{I}\frac{1}{2}\right)\frac{\left[1+d_\Omega\left(\frac{1}{2},\mathrm{I}\frac{1}{4}\right)\right]}{\left[d_\Omega\left(\frac{1}{2},\mathrm{I}\frac{1}{4}\right)+d_\Omega\left(\frac{1}{4},\mathrm{I}\frac{1}{2}\right)\right]} \\ \frac{d_\Omega\left(\frac{1}{2},\mathrm{I}\frac{1}{4}\right)d_\Omega\left(\frac{1}{4},\mathrm{I}\frac{1}{2}\right)}{1+d_\Omega\left(\frac{1}{2},\frac{1}{4}\right)}, \frac{d_\Omega\left(\frac{1}{2},\mathrm{I}\frac{1}{2}\right)d_\Omega\left(\frac{1}{2},\mathrm{I}\frac{1}{4}\right)+d_\Omega\left(\frac{1}{4},\mathrm{I}\frac{1}{4}\right)d_\Omega\left(\frac{1}{4},\mathrm{I}\frac{1}{2}\right)}{\left[d_\Omega\left(\frac{1}{2},\mathrm{I}\frac{1}{4}\right)+d_\Omega\left(\frac{1}{4},\mathrm{I}\frac{1}{2}\right)\right]}, d_\Omega\left(\frac{1}{2},\frac{1}{4}\right) \end{array}\right\}$$

$$= \frac{7}{12}\max\left\{\frac{1}{2},0,0,\frac{1}{2},0,0,1,1\right\} = \frac{7}{12}$$

$\therefore LHS \le RHS$

Case-II: If $a = \frac{1}{2}, b = \frac{1}{8}$,

$$LHS = d_\Omega\left(\mathrm{I}\frac{1}{2},\mathrm{I}\frac{1}{8}\right) = 1,$$

$$RHS = \lambda N\left(\frac{1}{2},\frac{1}{8}\right) = \frac{7}{12}\max\left\{\begin{array}{l} d_\Omega\left(\frac{1}{2},\mathrm{I}\frac{1}{2}\right)\frac{\left[1+d_\Omega\left(\frac{1}{8},\mathrm{I}\frac{1}{8}\right)\right]}{1+d_\Omega\left(\frac{1}{2},\frac{1}{8}\right)}, d_\Omega\left(\frac{1}{8},\mathrm{I}\frac{1}{8}\right)\frac{\left[1+d_\Omega\left(\frac{1}{2},\mathrm{I}\frac{1}{2}\right)\right]}{1+d_\Omega\left(\frac{1}{2},\frac{1}{8}\right)}, \\ \frac{d_\Omega\left(\frac{1}{8},\mathrm{I}\frac{1}{8}\right)d_\Omega\left(\frac{1}{2},\mathrm{I}\frac{1}{2}\right)}{d_\Omega\left(\frac{1}{2},\frac{1}{8}\right)}, d_\Omega\left(\frac{1}{2},\mathrm{I}\frac{1}{8}\right)\frac{\left[1+d_\Omega\left(\frac{1}{8},\mathrm{I}\frac{1}{2}\right)\right]}{\left[d_\Omega\left(\frac{1}{2},\mathrm{I}\frac{1}{8}\right)+d_\Omega\left(\frac{1}{8},\mathrm{I}\frac{1}{2}\right)\right]}, \\ d_\Omega\left(\frac{1}{8},\mathrm{I}\frac{1}{2}\right)\frac{\left[1+d_\Omega\left(\frac{1}{2},\mathrm{I}\frac{1}{8}\right)\right]}{\left[d_\Omega\left(\frac{1}{2},\mathrm{I}\frac{1}{8}\right)+d_\Omega\left(\frac{1}{8},\mathrm{I}\frac{1}{2}\right)\right]}, \frac{d_\Omega\left(\frac{1}{2},\mathrm{I}\frac{1}{8}\right)d_\Omega\left(\frac{1}{8},\mathrm{I}\frac{1}{2}\right)}{1+d_\Omega\left(\frac{1}{2},\frac{1}{8}\right)}, \\ \frac{d_\Omega\left(\frac{1}{2},\mathrm{I}\frac{1}{2}\right)d_\Omega\left(\frac{1}{2},\mathrm{I}\frac{1}{8}\right)+d_\Omega\left(\frac{1}{8},\mathrm{I}\frac{1}{8}\right)d_\Omega\left(\frac{1}{8},\mathrm{I}\frac{1}{2}\right)}{\left[d_\Omega\left(\frac{1}{2},\mathrm{I}\frac{1}{8}\right)+d_\Omega\left(\frac{1}{8},\mathrm{I}\frac{1}{2}\right)\right]}, d_\Omega\left(\frac{1}{2},\frac{1}{8}\right) \end{array}\right\}$$

$$= \frac{7}{12}\max\left\{3,\frac{4}{3},1,0,1,0,2,2\right\} = \frac{7}{6}$$

$\therefore LHS \le RHS$

Case-III: If $a = \frac{1}{4}, b = \frac{1}{8}$,

$$LHS = d_\Omega\left(\mathrm{I}\frac{1}{4}, \mathrm{I}\frac{1}{8}\right) = 1,$$

$$RHS = \lambda N\left(\frac{1}{4}, \frac{1}{8}\right) = \frac{7}{12}\max\left\{\begin{array}{l} d_\Omega\left(\frac{1}{4}, \mathrm{I}\frac{1}{4}\right)\frac{\left[1+d_\Omega\left(\frac{1}{8}, \mathrm{I}\frac{1}{8}\right)\right]}{1+d_\Omega\left(\frac{1}{4}, \frac{1}{8}\right)}, d_\Omega\left(\frac{1}{8}, \mathrm{I}\frac{1}{8}\right)\frac{\left[1+d_\Omega\left(\frac{1}{4}, \mathrm{I}\frac{1}{4}\right)\right]}{1+d_\Omega\left(\frac{1}{4}, \frac{1}{8}\right)}, \\ \frac{d_\Omega\left(\frac{1}{8}, \mathrm{I}\frac{1}{8}\right)d_\Omega\left(\frac{1}{4}, \mathrm{I}\frac{1}{4}\right)}{d_\Omega\left(\frac{1}{4}, \frac{1}{8}\right)}, d_\Omega\left(\frac{1}{4}, T\frac{1}{8}\right)\frac{\left[1+d_\Omega\left(\frac{1}{8}, T\frac{1}{4}\right)\right]}{\left[d_\Omega\left(\frac{1}{4}, T\frac{1}{8}\right)+d_\Omega\left(\frac{1}{8}, T\frac{1}{4}\right)\right]}, \\ d_\Omega\left(\frac{1}{8}, \mathrm{I}\frac{1}{4}\right)\frac{\left[1+d_\Omega\left(\frac{1}{4}, \mathrm{I}\frac{1}{8}\right)\right]}{\left[d_\Omega\left(\frac{1}{4}, \mathrm{I}\frac{1}{8}\right)+d_\Omega\left(\frac{1}{8}, \mathrm{I}\frac{1}{4}\right)\right]}, \frac{d_\Omega\left(\frac{1}{4}, \mathrm{I}\frac{1}{8}\right)d_\Omega\left(\frac{1}{8}, \mathrm{I}\frac{1}{4}\right)}{1+d_\Omega\left(\frac{1}{4}, \frac{1}{8}\right)}, \\ \frac{d_\Omega\left(\frac{1}{4}, \mathrm{I}\frac{1}{4}\right)d_\Omega\left(\frac{1}{4}, \mathrm{I}\frac{1}{8}\right)+d_\Omega\left(\frac{1}{8}, \mathrm{I}\frac{1}{8}\right)d_\Omega\left(\frac{1}{8}, \mathrm{I}\frac{1}{4}\right)}{\left[d_\Omega\left(\frac{1}{4}, \mathrm{I}\frac{1}{8}\right)+d_\Omega\left(\frac{1}{8}, \mathrm{I}\frac{1}{4}\right)\right]}, d_\Omega\left(\frac{1}{4}, \frac{1}{8}\right) \end{array}\right\}$$

$$= \frac{7}{12}\max\left\{0, \frac{1}{2}, 0, 1, 2, \frac{3}{4}, 3, 3\right\} = \frac{7}{4}$$

$\therefore LHS \leq RHS$

Thus all the conditions of theorem-3.2 are satisfied. Hence the fixed point is $a = \frac{1}{4}$.

CONCLUSION

A unique common fixed point theorem has been established in extended b-metric space satisfying rational type contractive condition, which extends and generalizes earlier results available in the literature.

REFERENCES

1. B. Alqahtani; A. Fulga, E. Karapınar and V. Rakoˇcevi´c, “Contractions with rational inequalities in the extended b-metric space,” J. Inequal. Appl. Paper No. 220, 11 pages (2019).
2. B. K. Dass, S. Gupta, “An extension of Banach contraction principle through rational expressions,” Indian J. Pure Appl. Math. **6**, 1455–1458 (1975).
3. D.S. Jaggi, “Some unique fixed point theorems,” Indian J. Pure Appl. Math. **8**, 223–230 (1977).
4. I.A. Bakhtin, “The contraction principle in quasimetric spaces,” Funct. Anal. **30**, 26-37(1989).
5. S. Czerwik, “Contraction mappings in b-metric spaces,” Acta Math. Inform., Univ. Ostrav., **1**, 5-11 (1993).
6. S. Czerwik, “Nonlinear set-valued contraction mappings in b-metric spaces,” Atti Semin. Mat. Fis. Univ. Modena **46**(2), 263-276 (1998).
7. T. Kamran, M. Samreen, O.U. Ain, “A generalization of b-metric space and some fixed point theorems,” Mathematics **5**, 19 (2017).

Proceedings of the International Conference on Automation, Computing and Renewable Systems (ICACRS 2022)
IEEE Xplore Part Number: CFP22CB5-ART: ISBN: 978-1-6654-6084-2

Design and Security Analysis of Isoidentity based Isobeta Cryptosystem

Nilesh Bhosale
Department of Applied Mathematics, Yeshwantrao Chavan College of Engineering,
Nagpur, M.S., India 441110
nileshbhosale897@gmail.com

Rupesh Pohane
Department of Mathematics, Suryodaya College of Engineering and Technology,
Nagpur, M.S., India
rupeshpohane@gmail.com

Siddhant Meshram
Computer Science Department at New York University, Room 305, 251 Mercer Street, New York, NY 10012
sidmeshram97@gmail.com

Akshaykumar Meshram*
Department of Applied Mathematics, Yeshwantrao Chavan College of Engineering,
Nagpur, M.S., India 441110
akshaykjmeshram@gmail.com

Malabika Adak
Department of Applied Mathematics, Yeshwantrao Chavan College of Engineering,
Nagpur, M.S., India 441110
malabikaadak@yahoo.co.in

K. T. V. Reddy
Faculty of Engineering and Technology, Datta Meghe Institute of Medical Sciences (Deemed to be University), Sawangi (Meghe),
Wardha, M. S., India 442004
ktvreddy.feat@dmimsu.edu.in

*Corresponding Author

2022 International Conference on Automation, Computing and Renewable Systems (ICACRS) | 978-1-6654-6084-2/22/$31.00 ©2022 IEEE | DOI: 10.1109/ICACRS55517.2022.10029185

Abstract*— Digital data protection frameworks inclusive of cryptographic mechanisms and signature crypto mechanisms are essential for stable data communication in open network systems. An extensive open-key folder is not necessary for $\mathcal{ID}$-based crypto mechanisms like $\mathcal{ID}$ -based crypto mechanisms, the $\mathcal{ID}$ -basedsignature mechanisms, else $\mathcal{ID}$ -basedkey circulation mechanisms are between the enhanced an opposing for create stable and protected digital data communication for enormous-scale open network systems recommended by Shamir. This article suggests an isoidentity based isobeta crypto mechanism build on the generalized isodiscrete isologarithm isoproblem and isointeger isofactorization isoproblem that is one of the initial implementations of Shamir's for security norms. Also, we examine the security adverse a conjuration of certain clients in the suggested mechanism, and demonstrate the probability of establishing a higher secure mechanism.

Keywords*— Cryptography, Isomathematics of first-kind ($\mathcal{IFK}$) , Isobeta cryptographic mechanism, Isodiscrete isologarithm isoproblem ($\mathcal{IDLP}$) , Generalized Isodiscrete isologarithm isoproblem ($\mathcal{GIDLP}$) , and Isointeger isofactorization isoproblem ($\mathcal{IIFP}$).

I. INTRODUCTION

For stable and protected data transmission, essentials to be collective close session key among two clients. Close session key circulation will be a significant issue as the number of clients is expanding in the open network system. The model for the open key circulation system ($\mathcal{OKCS}$) presented by Diffie and Hellman in 1976 [1]. In the $\mathcal{OKCS}$, every client require to choose a close key and numerate an analogous openkey and save in open directory. The collective closes sessionkey will be mutual among binary clients; can be numerate by some one client, created on his/her individual close key and the other client's open key. The $\mathcal{OKCS}$ runs an aesthetic approach to simplify the key circulation issue, the primary thinking is the validation of the open keys utilized in the cryptographic mechanisms. The framework of an identity is presented by Shamir [2] in 1984. In an identity mechanism, every client requires to identify himself/herself from key authentication isocenter ($\mathcal{KAC}$) prior to connecting the open network system. The $\mathcal{KAC}$ will approve and give his/her close key if client's identity is recognized. Thus, a client requires individual "identity" of his/her connection client and the openkey of the $\mathcal{KAC}$, at one time with his/her closekey, to interconnect with other clients. Hence no open folder compulsory in this mechanism. After all, Shamir did not succeed to build an identity-based cryptosystem, however succeed just to build an identity-based signature mechanism. Thereafter many scholar suggested several classes of $\mathcal{ID}$-based cryptographic mechanism. An identity-based key transmission mechanism is presented by Okamoto [3] in 1988 and extensive their mechanism for client recognition presented by Ohta [4]. The above-mentioned mechanism utilized the RSA openkey crypto mechanism having security is built on the computational difficulty of factoring product of two huge primes. An $\mathcal{ID}$- based crypto mechanism build on the discrete logarithm problem presented by Tsujii and Itoh [5] along with discrete exponent which utilized the ElGamal openkey crypto mechanism.

A non-interactive $\mathcal{ID}$ -Based open-key circulation mechanism presented by Maurer and Yacobi [6] in 1991 in which no additional authentication by certificates as the open keys are oneself authenticated. The amended variant of this mechanism presented in [7]. With multi purposes like an identification mechanism, $\mathcal{ID}$-Based signature mechanism, and a conference key circulation mechanism required strong computational efficiency as the computational difficulty of the mechanism is heavy. Factoring and discrete logarithm based open key crypto mechanism presented by L. Harn [8]. A modified $\mathcal{ID}$ -Based encryption mechanism of integer factorization problem, which is incapable as plaintext is converted bit-by-bit and henceforth the output of converted plaintext turns into protracted. A mechanism that can transfer the entire crypto mechanism build on discrete logarithm the $\mathcal{ID}$-based mechanism presented by Wei Bin lee and Kuan Chieh Liao [9] in 2004. An $\mathcal{ID}$-based crypto mechanism and modified $\mathcal{ID}$ -based crypto mechanism build on double generalized discrete logarithm problem presented by C. Meshram [10-12]. Lightweight crypto mechanisms for end-to-end encryption process in IoT field presented by Chatterjee, Chakraborty and Mandal [13] in 2019.

In 2020, crypto mechanisms build on quadratic-exponentiation-randomized and partial discrete logarithm

problem presented in [14]. Key exchange protocol build on isoring isopolynomials coefficient presented in [15]. Lately, Key exchange protocol and isocrypto mechanism build on Santilli's isomathematics presented in [16-18]. Improvements in the cloud safety with crypto mechanisms, deep learning and block-chain presented by Hari Krishnan Andi [19] in 2021.

In 2022, isokey interchange protocol, beta and IsoQER cryptosystem build on isonumber presented in [20-22].

In light of the perception that new crypto mechanism generally encounter security difficulties and privacy concerns and numerous crypto frameworks build on integer factorization & discrete logarithm have been implemented. Isokey creation segment with low computational complexity for transformation procedure is main role in our crypto mechanism such as no correction in initial Shamir mechanism. Thus propose crypto mechanism have identical protection as the initial one and preserves entire advantages of the $\mathcal{ID}$-based mechanism.

In this study, we suggested unique $\mathcal{ID}$ -beta cryptosystem called isoidentity based isobeta cryptosystem ($\mathcal{IIBC}$). The safety of suggested isobeta cryptosystem on isomathematics, generalized isodiscrete isologarithm problem with individual discrete exponent and isointeger isofactorization. Our system does not need any shared initial communications in all data transmission and every assumption excepting the complexity of the generalized isodiscrete isologarithm problem. Therefore the suggested system is a tangible model of an $\mathcal{ID}$-based cryptosystem that fulfills Shamir's primal idea [2].

II. Relevant Mathematical Definitions

In this section, we resolve rapidly relevant mathematical definitions utilizes to design $\mathcal{IIBC}$ over isofields.

A. Mathematical definition of $\mathcal{IFK}$

Isonumbers $\hat{\xi} = \xi\hat{\mathfrak{T}}$ is an element in the rings $\hat{\mathcal{F}} = \hat{\mathcal{F}}(\hat{\xi}, +, \hat{\times})$ where $\xi \in \mathcal{F}, \hat{\mathfrak{T}} = 1/\hat{\mathfrak{J}}$ is a well behaved, invertible and Hermitean quantity external from the original field $\hat{\mathfrak{T}} = 1/\hat{\mathfrak{J}} \notin \mathcal{F}$ and $\xi\hat{\mathfrak{T}}$ is the multiplication in $\mathcal{F}$ equipped with the isoaddition $\hat{\xi} + \hat{r} = (\xi + r)\hat{\mathfrak{T}}$ with traditional additive unit $0 = 0\hat{\mathfrak{T}} = 0, \hat{\xi} + 0 = \hat{\xi} + 0 = \hat{\xi}$, $\forall \hat{\xi} \in \hat{\mathcal{F}}$ and the isomultiplication $\hat{\xi} \hat{\times} \hat{r} = \hat{\xi}\hat{\mathfrak{J}}\hat{r} = \xi\hat{\mathfrak{T}}\hat{\mathfrak{J}}r\hat{\mathfrak{T}} = (\xi r)\hat{\mathfrak{T}}$ with $\hat{\mathfrak{T}} = 1/\hat{\mathfrak{J}}$ is the correct left and right novel unit ($\hat{\mathfrak{T}} \hat{\times} \hat{\xi} = \hat{\xi} \hat{\times} \hat{\mathfrak{T}} = \hat{\xi}$, $\forall \hat{\xi} \in \hat{\mathcal{F}}$) called isounit satisfy

$\hat{\xi}^{\hat{\mathfrak{T}}} = \xi\hat{\mathfrak{T}}$, $\hat{\xi}^{-\hat{\mathfrak{T}}} = \xi^{-1}\hat{\mathfrak{T}}$,

$\hat{\xi}^{\hat{\mathfrak{T}}} \hat{\times} \hat{\xi}^{-\hat{\mathfrak{T}}} = \hat{\xi}^{\hat{0}} = \hat{\mathfrak{T}} = \hat{\mathfrak{J}}^{-1} \neq 1$,

$\hat{\xi}^{\hat{r}} = \xi^{r}\hat{\mathfrak{T}}$, $\hat{\xi}^{-\hat{r}} = \xi^{-r}\hat{\mathfrak{T}}$,

$\hat{\xi}^{\hat{r}} \hat{\times} \hat{\xi}^{-\hat{r}} = \hat{\xi}^{\hat{0}} = \hat{\mathfrak{T}} = \hat{\mathfrak{J}}^{-1} \neq 1$,

$\hat{\xi}^{\frac{\ell}{r}} = \xi^{\frac{\ell}{r}}\hat{\mathfrak{T}}$, $\hat{\xi}^{-\frac{\hat{\ell}}{r}} = \xi^{-\frac{\ell}{r}}\hat{\mathfrak{T}}$,

$\hat{\xi}^{\ell/r} \hat{\times} \hat{\xi}^{-\hat{\ell}/r} = \hat{\xi}^{\hat{0}} = \hat{\mathfrak{T}} = \hat{\mathfrak{J}}^{-1} \neq 1$,

$\hat{\xi} \hat{\times} \hat{\mathfrak{T}} = \hat{\xi}\hat{\mathfrak{J}}\hat{\mathfrak{T}} = \hat{\xi}$,

$\hat{\xi} \hat{\times} \hat{r} = \xi\hat{\mathfrak{T}}\hat{\mathfrak{J}}r\hat{\mathfrak{T}} = \xi r\hat{\mathfrak{T}} = \xi\hat{r}$,

$\hat{\xi} \hat{\times} \hat{r}^{-\hat{2}} = \xi\hat{\mathfrak{T}}\hat{\mathfrak{J}}r^{-2}\hat{\mathfrak{T}} = \xi/r^{2}\hat{\mathfrak{T}}$

where $\hat{\mathfrak{T}}$ is named as isounit, $\hat{\mathfrak{J}}$ is named as isoinverse of $\hat{\mathfrak{T}}$; $\hat{\xi}^{-\hat{r}}$ is named as isoinverse of $\hat{\xi}^{r}$; $(\hat{\xi}^{\hat{r}}, \hat{\times})$.

B. Mathematical definition of $\mathcal{GIDLP}$

Let $\hat{\mathcal{G}}$ be cyclic isogroup of order $\hat{e}$ such that isonumber $\hat{s} \equiv \hat{g}\hat{t}$ for isonumber $\hat{t} \in [0, \hat{e} - 1]$ then $\hat{g}$ primitiveisoroot of the isogroup is knowing $\mathcal{GIDLP}$.

C. Mathematical definition of $\mathcal{IIFP}$

To numerate isoprime isonumbers $\hat{\mathbb{N}} = \widehat{z_1} * \widehat{z_2} * \widehat{z_3} \cdots \widehat{z_e}$, an decomposition for positive isointeger $\hat{\mathbb{N}}$ is knowing $\mathcal{IIFP}$.

III. Introduction of the $\mathcal{IIBC}$

Establishment for the isocenter and every customer:

Step 1: Every customer creates a $\hat{n}$ −dimensional isobinary isovector for his/her $\mathcal{ID}$ and records with the isocenter. The isocenter stocks it in open/public folder. We indicate customer $\hat{\jmath}$'s $\mathcal{ID}$ by $\mathcal{ID}_{\hat{\jmath}} = (\hat{y}_{\hat{\jmath}1}, \hat{y}_{\hat{\jmath}2}, \hat{y}_{\hat{\jmath}3}, \hat{y}_{\hat{\jmath}4}, \dots\dots\dots, \hat{y}_{\hat{\jmath}\hat{n}})$, $\hat{y}_{\hat{\jmath}\hat{\imath}} \in \{0,1\}$, $(1 \leq \hat{\imath} \leq \hat{n})$. (1)

Step 2: The isocenter creates binary isoprime isonumbers $\hat{\mathcal{P}}$ and $\hat{\mathcal{Q}}$, numerate $\hat{\mathbb{N}} = \hat{\mathcal{P}} * \hat{\mathcal{Q}}$. (2)

Thus, the isocenter elect an irrational isonumber $\hat{d}$, $1 \leq \hat{d} \leq \varphi(\hat{\mathbb{N}})$ satisfy $\gcd(\hat{d}, \varphi(\hat{\mathbb{N}})) = 1$ for iso-Euler function $\varphi(\hat{\mathbb{N}}) = (\hat{\mathcal{P}} - 1)(\hat{\mathcal{Q}} - 1)$ of $\hat{\mathbb{N}}$. Then isocenter circulates $(\hat{d}, \hat{\mathbb{N}})$ as the openkey.

Every customer can numerate the customer $\hat{\jmath}'s$ extended $\mathcal{ID}$ as $\mathcal{EID}_{\hat{\jmath}}$;

$\mathcal{EID}_{\hat{\jmath}} = (\mathcal{ID}_{\hat{\jmath}})^{\hat{d}} (\mathrm{mod}\hat{\mathbb{N}}) = (\hat{\xi}_{\hat{\jmath}1}, \hat{\xi}_{\hat{\jmath}2}, \hat{\xi}_{\hat{\jmath}3}, \hat{\xi}_{\hat{\jmath}4}, \dots\dots\dots, \hat{\xi}_{\hat{\jmath}\hat{k}})$,
$\hat{\xi}_{\hat{\jmath}\hat{\imath}} \in \{0,1\}, (1 \leq \hat{\imath} \leq \hat{k})$ (3)

Where $\hat{k} = |\hat{\mathbb{N}}|$ is a bits of $\hat{\mathbb{N}}$

Step 3: isocenter's conceal data: The isocenter elects an irrationa huge isoprime $\hat{\mathcal{P}}$ and $\hat{\mathcal{Q}}$, numerates $\hat{\mathbb{N}} = \hat{\mathcal{P}}\hat{\mathcal{Q}}$ and createss $\hat{n}$ −dimensional isovector $\vec{\hat{x}}$ over $\hat{\mathcal{Z}}^{*}_{\varphi(\hat{\mathbb{N}})}$ such that

$\vec{\hat{x}} = (\hat{x}_1, \hat{x}_2, \hat{x}_3, \dots, \hat{x}_{\hat{n}})$, (4)

$1 \leq \hat{x}_{\hat{\jmath}} \leq \varphi(\hat{\mathbb{N}})(1 \leq \hat{\jmath} \leq \hat{n})$,

$\hat{x}\hat{u} \neq \hat{x}\hat{v}(\mathrm{mod}\varphi(\hat{\mathbb{N}})), \hat{u} \neq \hat{v}$ (5)

for $\hat{n}$-dimensional binary isovector $\hat{u}$ and $\hat{v}$ and stock it as the isocenter s conceal data. To prevent the inadvertent chance of certain customers, closedkeys take care by equation (5). The isocenter elects a super collective isosequences consistent to $\hat{x}$ as $\hat{x}'_{\hat{\jmath}}(1 \leq \hat{\jmath} \leq \hat{n})$ that $\sum_{1 \leq \hat{\jmath} \leq \hat{n}} \hat{x}'_{\hat{\jmath}} < \varphi(\hat{\mathbb{N}})$ (6)

to creates the vector $\vec{\hat{x}}$ is to utilize the Merkle and Hellmans crypto mechanisms [10].

Step 4: Numerates $\hat{n}$-dimensional vector $\vec{\hat{x}}$ as

$\hat{x}_{\hat{\jmath}} = \hat{x}'_{\hat{\jmath}}\hat{r}\left(\mathrm{mod}\varphi(\hat{\mathbb{N}})\right)(1 \leq \hat{\jmath} \leq n)$ (7)

for an exclusive isointeger $\hat{r}$ satisfy $\gcd(\hat{r}, \varphi(\hat{\mathbb{N}})) = 1$, where $\vec{\hat{x}} = (\hat{x}_1, \hat{x}_2, \hat{x}_3, \dots, \hat{x}_n)$. (8)

Step 5: Elect an exclusive isointeger $\hat{c}, (1 \leq \hat{c} \leq \varphi(\hat{\mathbb{N}}))$ satisfy $\hat{d}\hat{c} \equiv 1(\mathrm{mod}\varphi(\hat{\mathbb{N}}))$ (9)

Step 6: Isocenter public data: Numerates $\hat{n}$-dimensional isovector $\hat{\hbar}$ by elects a random isointeger $\hat{\alpha}$ of $\hat{\mathcal{Z}}^{*}_{\hat{\mathbb{N}}}$ as

$\hat{\hbar} = (\hat{\hbar}_1, \hat{\hbar}_2, \hat{\hbar}_3, \dots\dots, \hat{\hbar}_n)$, (10)

$\hat{\hbar}_{\hat{\jmath}} = \hat{\alpha}^{\hat{x}_{\hat{\jmath}}} \mathrm{mod}\hat{\mathbb{N}}\ (1 \leq \hat{\jmath} \leq n)$, (11)

The isocenter notifies all entity $(\hat{\mathbb{N}}, \hat{d}, \hat{\hbar})$ as open data.

Step 7: Every customer closedkey: customers $\hat{\jmath}'$s closedkey $\hat{\mathcal{S}}_{\hat{\jmath}}$ is numerate by inner isoproduct of $\hat{x}$ and $\mathcal{EJD}_{\hat{\jmath}}$ as

$$\hat{\mathcal{S}}_{\hat{\jmath}} = \hat{x}\mathcal{EJD}_{\hat{\jmath}} \,(\mathrm{mod}\varphi(\hat{\mathbb{N}})) = \textstyle\sum_{1\le\hat{\imath}\le n}\, \hat{x}_{\hat{\imath}}\hat{\xi}_{\hat{\jmath}\hat{\imath}}\mathrm{mod}(\varphi(\hat{\mathbb{N}})) \quad (12)$$

IV. SCHEME INITIALIZATION FACTORS

A. Isocenter *conceal data:*

For $\hat{n}-$dimensional isovector $\hat{x}$ and isointeger $\hat{c}$, the *isocenter* stock $(\hat{x}, \hat{c})$ as secrete data.

B. Isocenter *Public data:*

For $\hat{n}-$dimensional isovector $\hat{\hbar}$, huge isoprime isonumber $\hat{\mathbb{N}}$ and arbitrary isointeger $\hat{d}$, the isocenter stock $(\hat{\hbar}, \hat{\mathbb{N}}, \hat{d})$ as a public data.

C. Customer i's secretes keys: $\left(\hat{\mathcal{S}}_{\hat{\jmath}}\right)$

D.Customer i's public data: $\mathcal{JD}_i$ *is a* $\hat{n}$ *-dimensional isovector*

V. PROCEDURE OF THE ISOBETA CRYPTOSYSTEM

To sends data $\mathcal{D}$ to customer-1 then customer-2 follows following procedure;

A. Encryption process:

Customer-2, numerates $\hat{\zeta}_1$ from corresponding public data $\hat{\hbar}$ and by creates $\mathcal{EJD}_1$ from $\mathcal{JD}_1$;

$$\hat{\zeta}_1 = \prod_{1\le\hat{\jmath}\le n} \hat{\hbar}_{\hat{\jmath}}^{\hat{\xi}_{1\hat{\jmath}}}(\mathrm{mod}\hat{\mathbb{N}})$$
$$= \prod_{1\le\hat{\jmath}\le n} \left(\hat{\alpha}^{\hat{x}_{\hat{\jmath}}}\right)^{\hat{\xi}_{1\hat{\jmath}}(\mathrm{mod}\hat{\mathbb{N}})}$$
$$= \hat{\alpha}^{\Sigma_{1\le\hat{\jmath}\le n}\hat{x}_{\hat{\jmath}}\hat{\xi}_{1\hat{\jmath}}\mathrm{mod}\left(\varphi(\hat{\mathbb{N}})\right)}(\mathrm{mod}\hat{\mathbb{N}})$$
$$= \hat{\alpha}^{\hat{\mathcal{S}}_1}(\mathrm{mod}\hat{\mathbb{N}}) \quad (13)$$

Suppose $\mathcal{D}(1 \le \mathcal{D} \le \hat{\mathbb{N}} - 1)$ be a data

To communicated data $\mathcal{D}(1 \le \mathcal{D} \le \hat{\mathbb{N}} - 1)$, Customer-2 utilized $\hat{\zeta}_1$ and elect an arbitrary isointeger $\hat{d}$ satisfy gcd $(\hat{d}, \varphi(\hat{\mathbb{N}})) = 1$ to numerate ciphertext $\hat{\mathcal{C}} = \left(\mathcal{D}\hat{\alpha}^{\hat{\mathcal{S}}_1}\right)^{\hat{d}}(\mathrm{mod}\hat{\mathbb{N}})$. (14)

B. Decryption process:

Customer-1 does the following procedure to retrieve the data $\mathcal{D}$ from the ciphertext $\hat{\mathcal{C}}$;

Customer-1 refers the ciphertext $\hat{\mathcal{C}}$ to customer-2 through an unsecured channel. After receiving ciphertext from Customer-1, He/She numerate

$$\hat{\xi}_2 = \hat{\alpha}^{\varphi(\mathbb{N})-\hat{\mathcal{S}}_1}(\mathrm{mod}\mathbb{N}) = \hat{\alpha}^{-\hat{\mathcal{S}}_1}(\mathrm{mod}\mathbb{N}) \quad (15)$$

$$\left(\hat{\xi}_2\right)^{\hat{d}}(\mathrm{mod}\mathbb{N}) = \left(\hat{\alpha}^{-\hat{\mathcal{S}}_1}\right)^{\hat{d}}\mathrm{mod}\mathbb{N} \quad (16)$$

Utilizing his/her closedkey $\hat{\mathcal{S}}_1$ retrieved customer-2's the data $\mathcal{D}$ by eqn.(15) and (16) to numerate

$$\left(\left(\hat{\xi}_2\right)^{\hat{d}} * \hat{\mathcal{C}}\right)^{\hat{c}}\left(\mathrm{mod}\hat{\mathbb{N}}\right) = \left(\hat{\alpha}^{-\hat{\mathcal{S}}_1\hat{d}}\mathcal{D}^{\hat{d}}\hat{\alpha}^{\hat{\mathcal{S}}_1\hat{d}}\right)^{\hat{c}}\left(\mathrm{mod}\hat{\mathbb{N}}\right)$$
$$= \mathcal{D}^{\hat{d}\hat{c}}(\mathrm{mod}\hat{\mathbb{N}}) = \mathcal{D}(\mathrm{mod}\hat{\mathbb{N}})$$

VI. SECURITY ANALYSIS

The safety of suggested $\mathcal{JIBC}$ design on the index problem in the isomultiplicative isocyclic isogroup $\hat{\mathcal{Z}}_{\hat{\mathbb{N}}}^*$, for isounber $\hat{\mathbb{N}} = \hat{\mathcal{P}} * \hat{\mathcal{Q}}$ and $\varphi(\hat{\mathbb{N}})$ isoEuler function of $\hat{\mathbb{N}}$.

Theorem-1: A $\hat{n}-$dimensional isovector $\hat{x}'$ over $\hat{\mathcal{Z}}_{\hat{\mathbb{N}}}^*$ can determine by $(\hat{n}+1)$ customers' $\hat{\jmath}, (1 \le \hat{\jmath} \le \hat{n}+1)$ which is identical to the genuine isocenter's safe data.

Proof: The under-mentioned system of isolinear congruence's for $(\hat{n}+1)$ customers' $\hat{\jmath}, (1 \le \hat{\jmath} \le \hat{n}+1)$ conspire;

$$\begin{bmatrix} \mathcal{EJD}_1 \\ \mathcal{EJD}_2 \\ \mathcal{EJD}_3 \\ \vdots \\ \mathcal{EJD}_{\hat{n}+1} \end{bmatrix}\begin{bmatrix} \hat{x}_1 \\ \hat{x}_2 \\ \hat{x}_3 \\ \vdots \\ \hat{x}_{\hat{n}} \end{bmatrix} = \begin{bmatrix} \hat{\mathcal{S}}_1 \\ \hat{\mathcal{S}}_2 \\ \hat{\mathcal{S}}_3 \\ \vdots \\ \hat{\mathcal{S}}_{\hat{n}+1} \end{bmatrix}(\mathrm{mod}\varphi(\hat{\mathbb{N}})) \quad (17)$$

There exists an $(\hat{n}+1)$-dimensional isovector $\hat{\mathcal{P}}$ on the isointeger isoring for every $\mathcal{EJD}_{\hat{\jmath}}$ is an $\hat{n}$-dimensional binary isovector satisfy $\sum_{1\le\hat{\jmath}\le\hat{n}+1}\hat{\mathcal{P}}_{\hat{\jmath}}\mathcal{EJD}_{\hat{\jmath}} = 0$

We have, $\sum_{1\le\hat{\jmath}\le\hat{n}+1}\, \hat{\mathcal{P}}_{\hat{\jmath}}\hat{\mathcal{S}}_{\hat{\jmath}} = 0(\mathrm{mod}\varphi(\hat{\mathbb{N}}))$ (18)

$\sum_{1\le\hat{\jmath}\le\hat{n}+1}\, \hat{\mathcal{P}}_{\hat{\jmath}}\hat{\mathcal{S}}_{\hat{\jmath}} = \hat{\mathcal{H}}\varphi(\hat{\mathbb{N}})$ (19)

and consequently $\sum_{1\le\hat{\jmath}\le\hat{n}+1}\, \hat{\mathcal{P}}_{\hat{\jmath}}\hat{\mathcal{S}}_{\hat{\jmath}} = \hat{\mathcal{H}}\varphi(\hat{\mathbb{N}})$ (20)

Thus $(\hat{n}+1)$ customers ensure an isointeger isomultiple of $\varphi(\hat{\mathbb{N}})$, and compute the isofactorization of $\hat{\mathbb{N}}$ is $\hat{\mathcal{H}} \ne 0$. Therefore, the isocenter's safe data can be determine by $(\hat{n}+1)$ customers conspiracy.

Theorem-2: the isocenter's secret data $\hat{x}$ determine by $(\hat{n}+2)$ customers' $\hat{\jmath}, (1 \le \hat{\jmath} \le \hat{n}+2)$ with exalted probability.

Proof: The under-mentioned system of isolinear congruence's for $(\hat{n}+1)$ customers $\hat{\jmath}, (1 \le \hat{\jmath} \le \hat{n}+1)$ conspire;

$$\begin{bmatrix} \mathcal{EJD}_1 \\ \mathcal{EJD}_2 \\ \mathcal{EJD}_3 \\ \vdots \\ \mathcal{EJD}_{\hat{n}+1} \end{bmatrix}\begin{bmatrix} \hat{x}_1 \\ \hat{x}_2 \\ \hat{x}_3 \\ \vdots \\ \hat{x}_{\hat{n}} \end{bmatrix} = \begin{bmatrix} \hat{\mathcal{S}}_1 \\ \hat{\mathcal{S}}_2 \\ \hat{\mathcal{S}}_3 \\ \vdots \\ \hat{\mathcal{S}}_{\hat{n}+1} \end{bmatrix}(\mathrm{mod}\varphi(\hat{\mathbb{N}})) \quad (21)$$

$$= \hat{\mathcal{L}}\hat{x}(\mathrm{mod}\varphi(\hat{\mathbb{N}})) \quad (22)$$

There exist positive isointegers $\hat{\mathcal{P}}_{\hat{\jmath}}(1 \le \hat{\jmath} \le \hat{n}+1)$ satisfy

$$\begin{bmatrix} \mathcal{EJD}_1 \\ \mathcal{EJD}_2 \\ \mathcal{EJD}_3 \\ \vdots \\ \mathcal{EJD}_{\hat{n}+1} \end{bmatrix}\begin{bmatrix} \hat{x}_1 \\ \hat{x}_2 \\ \hat{x}_3 \\ \vdots \\ \hat{x}_{\hat{n}+1} \end{bmatrix} = \begin{bmatrix} \hat{\mathcal{S}}_1 \\ \hat{\mathcal{S}}_2 \\ \hat{\mathcal{S}}_3 \\ \vdots \\ \hat{\mathcal{S}}_{\hat{n}+1} \end{bmatrix} - \begin{bmatrix} \hat{\mathcal{P}}_1 \\ \hat{\mathcal{P}}_2 \\ \hat{\mathcal{P}}_3 \\ \vdots \\ \hat{\mathcal{P}}_{\hat{n}+1} \end{bmatrix}\varphi(\hat{\mathbb{N}}) \quad (23)$$

for the isomatrix $\hat{\mathcal{L}}$ consist of $\hat{n}$ linearly independent column isovectors over the isointeger isoring.

Thus equation (23) implies:

$$\begin{bmatrix} \mathcal{EJD}_1 \\ \mathcal{EJD}_2 \\ \mathcal{EJD}_3 \\ \vdots \\ \mathcal{EJD}_{\hat{n}+1} \end{bmatrix}\begin{bmatrix} \hat{x}_1 \\ \hat{x}_2 \\ \hat{x}_3 \\ \vdots \\ \hat{x}_{\hat{n}} \\ -1 \end{bmatrix} = -\begin{bmatrix} \hat{\mathcal{P}}_1 \\ \hat{\mathcal{P}}_2 \\ \hat{\mathcal{P}}_3 \\ \vdots \\ \hat{\mathcal{P}}_{\hat{n}+1} \end{bmatrix}\varphi(\hat{\mathbb{N}}) \quad (24)$$

$$= \hat{\mathcal{L}}'\hat{x}' \quad (25)$$

We get $\hat{x}' \ne (\mathrm{mod}\varphi(\hat{\mathbb{N}}))$ for nonsingular isomatrix $\hat{\mathcal{L}}'$ over the isointeger isoring along with Indefeasible probability if the isomatrix $\hat{\mathcal{L}}$ in eqn. (22) consist of $\hat{n}$ isolinearly independent isocolumn isovectors over the isointeger isoring.

On the contrary, we get under-mentioned eqn. of isoinear congruence's:

$$\hat{\mathcal{L}}'\hat{x}' = 0(\mathrm{mod}\varphi(\hat{\mathbb{N}})) \quad (26)$$

Above outcome invalidate for nonsingular isomatrix $\hat{\mathcal{L}}'$ $\left(\hat{x}' = (\mathrm{mod}\varphi(\hat{\mathbb{N}}))\right)$ over $\hat{\mathcal{Z}}_{\hat{\mathbb{N}}}^*$. $\mathrm{Det}\left(\hat{\mathcal{L}}'\right)$ is isodivisible by

$\varphi(\hat{\mathbb{N}})$ for singular isomatrix $\hat{\mathcal{L}}'$ $\left(\det \hat{\mathcal{L}}' = 0(\mathrm{mod}\varphi(\hat{\mathbb{N}}))\right)$ over $\hat{\mathcal{Z}}_{\hat{\mathbb{N}}}^{*}$ with exalted probability. If isomatrix $\hat{\mathcal{L}}''$ represent as above by the other $(\hat{n}+1)$ customers among $(\hat{n}+2)$ conspire and $\det\left(\hat{\mathcal{L}}''\right)$ is isodivisible by $\varphi(\hat{\mathbb{N}})$ with exalted probability satisfy $GCD\left(det\,\hat{\mathcal{L}}', det\,\hat{\mathcal{L}}''\right) = \hat{d}\varphi(\hat{\mathbb{N}})$ for a small positive isointeger $\hat{d}$. Thus we can numerate $\varphi(\hat{\mathbb{N}})$ capably and determine the isocenter's safe data is exactly the equal as Attack (Theorem1).

To improvement of security of the crypto mechanisms, the isocenter segmentation a 512-dimensional binary isovector $\hat{\mathcal{A}}$ into 256 segments, each two bits, satisfy

$$\hat{\mathcal{A}} = (\hat{a}_1, \hat{a}_2, \hat{a}_3, \dots\dots \hat{a}_{511}, \hat{a}_{512}) = (\mathrm{seg}_1, \mathrm{seg}_2, \mathrm{seg}_3, \dots\dots \mathrm{seg}_{511}, \mathrm{seg}_{512})$$

Numerates $\hat{h}(\hat{\jmath}; \hat{\imath}\hat{n}) = \hat{\alpha}^{\mathrm{a}(\hat{\jmath};\hat{\imath}\hat{n})}(\mathrm{mod}\hat{\mathbb{N}})$ for every $\mathrm{seg}_{\hat{\jmath}}$ $(1 \le \hat{\jmath} \le 256; \hat{\imath}, \hat{n} \in \{0,1\})$ and circulates to all customers. Also, the isocenter numerates every customer's closed isokey as follows;

$\hat{\mathcal{S}}_{\hat{n}} = \sum_{1\le\hat{\jmath}\le 256} \hat{x}\left(\hat{\jmath}; \mathrm{seg}_{\hat{n}\hat{\jmath}}\right)(\mathrm{mod}\varphi(\hat{\mathbb{N}}))$ and circulates to all customers over an extremely protected channel. This is precisely the identical as in the prime crypto mechanisms. In the prime crypto mechanisms, isocenter's safe data is compute by 512 customers conspiracy, whereas in our crypto mechanisms it is compute by 1024 customers conspiracy. Also, the running cost for encryption isokey creation in our crypto mechanisms is half of the prime crypto mechanisms. The isocenter's open data in the crypto mechanisms is about twice than the prime crypto mechanisms. Additionally generalizations, every $\mathcal{EID}_{\hat{\jmath}}$ is segmentation into 128-segments each four bits are feasible.

Now, we explore the presentation of proposed mechanism insofar as isonumber of isokeys, computational complexity and communication costs. The interval run to execute isomodular computation require per bit size of $\hat{\mathrm{I}} = |\hat{\mathrm{I}}|$ as below;

1. isoexponentiation= $\mathcal{T}_{\_exp}$
2. isomultiplication= $\mathcal{T}_{\_mul}$
3. isosquare computation= $\mathcal{T}_{\_squ}$
4. isoinverse computation= $\mathcal{T}_{\_inv}$
5. isohash function= $\mathcal{T}_{\_hash}$

Proposed isoidentity based isobeta crypto mechanism	
The isonumber of isokeys	Secretes key =4
	Public key =4
Isocomputational complexity	Encryption : $\mathcal{T}_{\_exp}+2\mathcal{T}_{\_mul}+\mathcal{T}_{\_hash}$
	Decryption : $\mathcal{T}_{\_exp}+\mathcal{T}_{\_mul}$
Isocommunication cost	Encipher : $2n$
	Deciphertion: $2n$

VII. Conclusion

In this study, the suggested crypto mechanism fulfills Shamir's prime theories in a rigorous sense. This variant of crypto mechanisms absolutely delivers novel crypto mechanisms with a more and advanced level of security created on formulation of $\mathcal{IFK}$ $\mathcal{GIDLP}$, and $\mathcal{IIFP}$.The offered crypto mechanisms also involves minimal processes in encryption and decryption algorithms and consequently makes it is much effective. The present crypto mechanism delivers the extraordinary outcome from the safety point of view, as we aspect the issue of simplifying $\mathcal{GIDLP}$ and $\mathcal{IIFP}$ together in the isomultiplicative isogroup of finite isofields as matched to the other crypto mechanism. One should break $\mathcal{GIDLP}$ and $\mathcal{IIFP}$ together to break our crypto mechanisms as we aspect the trouble of simplifying the classical $\mathcal{GIDLP}$ in the shared isogroups.

Acknowledgment

The authors would like to thank anonymous reviewers for their careful and helpful comments.

References

[1] W. Diffie and M.E. Hellman, "New direction in Cryptography", IEEE Trans.Inform.Theory, vol. 22, pp 644-654,1976.

[2] Shamir, "Identity-based cryptosystem and signature scheme," Advances in Cryptology: Proceedings of Crypto'(Lecture Notes in Computer Science 196). Berlin, West Germany: Springer-Verlag, vol. 84, pp. 47-53, 1985.

[3] E. Okamoto, "Key Distribution Systems Based on Identification Information," In Advances in Cryptology, Crypto 1987, pp. 194-202. LNCS Vol. 293/1988.

[4] K. Koyama, and O. Kazuo, "Identity-based Conference Key Distribution Systems" CRYPTO (1987).

[5] S. Tsujii, and T. Itoh, "An ID-based cryptosystem based on the discrete logarithm problem" IEEE Jounral on selected areas in communications, vol. 7, pp. 467-473, 1989.

[6] U. M. Maurer, Y. Yacobi, "Non-interactive public key cryptography" Cryptology—Eurocrypt'91, New York: Springer, pp. 498–507.1991.

[7] U. M. Maurer, Y. Yacobi, "A non-interactive public-key distribution system" Des. Codes Cryptogr. , vol. 9(3), pp.305–316, 1996.

[8] L. Harn, "Public key cryptosystem design based on factoring and discrete logarithm" IEEE Pro. Comput. Digit. Tech, vol.141, no.3, pp.193-195,1994.

[9] W-B Lee and Kuan-Chieh Liao, "Constructing identity-based cryptosystems for discrete logarithm based cryptosystems" Journal of Network and Computer Applications, vol. 27, pp. 191–199, 2004.

[10] C. Meshram, "Modified ID-Based Public key Cryptosystem using Double Discrete Logarithm Problem" International Journal of Advanced Computer Science and Applications,Vol. 1, No.6, pp.30-34, 2010

[11] C. Meshram, "A Cryptosystem based on Double Generalized Discrete Logarithm Problem" Int. J. Contemp. Math. Sciences, Vol. 6, no. 6, 285 -297,2011.

[12] C. Meshram and S. A. Meshram, "An identity based beta cryptosystem," 2011 7th International Conference on Information Assurance and Security (IAS), pp. 298-303, 2011. doi: 10.1109/ISIAS.2011.6122836.

[13] R. Chatterjee, R. Chakraborty, and J. K. Mondal. "Design of Lightweight Cryptographic Model for End-to-End Encryption in IoT Domain." IRO Journal on Sustainable Wireless Systems, Vol. 1, no. 4, pp. 215-224, 2019. doi: 10.36548/jsws.2019.4.002.

[14] C. Meshram, M. S. Obaidat and A. Meshram, "New efficient QERPKC based on partial discrete logarithm problem," 2020 International Conference on Computer, Information and Telecommunication Systems (CITS), Hangzhou, China, 2020, pp. 1-5, doi: 10.1109/CITS49457.2020.9232533.

[15] A. Meshram, C. Meshram, S. D. Bagde and R. R. Meshram., "RIPIC based key exchange protocol," Advances in Mathematics: Scientific Journal, 9(12) (2020) 11169–11177. doi:10.37418/amsj.9.12.97

[16] M. S. Dani, A. Meshram, C. Meshram, and N. M. Wazalwar., "An efficient key exchange scheme using santilli'sisofields second-kind for secure communication," Advances in Mathematics: Scientific Journal, Vol. 10, No. 2, pp. 1131–1139, 2021. doi: 10.37418/amsj.10.2.39

[17] M. S. Dani, A. Meshram and C. Meshram., "Santilli'sisofields firstkind based key exchange protocol," Journal of Physics: Conference Series, 1913 (1), 012095, 2021. doi:10.1088/1742-6596/1913/1/012095

[18] A. B. Thatere, A. Meshram, C. Meshram, N. M. Wazalwar, "SIFK based Isobeta Cryptosystem," International Journal of Engineering Trends and Technology, Vol. 69.7, pp. 76-79, 2021. doi: 10.14445/22315381/IJETT-V69I7P211

[19] H. K. Andi, "Estimating the Role of Blockchain, Deep Learning and Cryptography algorithms in Cloud Security." Journal of Trends in Computer Science and Smart Technology, vol. 3, no. 4, pp. 305-313, 2021. doi:10.36548/jtcsst.2021.4.006.

[20] M. S. Dani, A. Meshram, R. Pohane, and R. R. Meshram, "Isonumber based Iso-Key Interchange Protocol for Network Communication," International Journal of Computer Science and Network Security, Vol. 22 No. 2 pp. 209-213, 2022. http://paper.ijcsns.org/07_book/202202/20220227.pdf

[21] A. Meshram, R. Pohane and R. Thakre, "Developing a framework of beta cryptosystem based on Santilli's isofields second-kind," 2022 International Conference for Advancement in Technology (ICONAT), 2022, pp. 1-4, doi: 10.1109/ICONAT53423.2022.9726000.

[22] N. Bhosale, A. Meshram, R. Pohane, M. Adak, D. Bawane and K. T. V. Reddy, "Design of IsoQER Cryptosystem using IPDLP," IEEE International Conference on Emerging Trends in Engineering and Medical Sciences (ICETEMS), 18-19 November 2022 (accepted).

Design of IsoQER Cryptosystem using IPDLP

2022 International Conference on Emerging Trends in Engineering and Medical Sciences (ICETEMS) | 978-1-6654-6112-2/22/$31.00 ©2022 IEEE | DOI: 10.1109/ICETEMS56252.2022.10093351

Nilesh Bhosale
Department of Applied Mathematics, Yeshwantrao Chavan College of Engineering,
Nagpur, M.S., India 441110
nileshbhosale897@gmail.com

Akshaykumar Meshram*
Department of Applied Mathematics, Yeshwantrao Chavan College of Engineering,
Nagpur, M.S., India 441110
akshaykjmeshram@gmail.com
*Corresponding Author

Rupesh Pohane
Department of Mathematics, Suryodaya College of Engineering and Technology,
Nagpur, M.S., India 441204
rupeshpohane@gmail.com

Malabika Adak
Department of Applied Mathematics, Yeshwantrao Chavan College of Engineering,
Nagpur, M.S., India 441110
malabikaadak@yahoo.co.in

Dnyaneshwar Bawane
Department of Applied Mathematics, Yeshwantrao Chavan College of Engineering,
Nagpur, M.S., India 441110
dnyanesh02@gmail.com

K. T. V. Reddy
Faculty of Engineering and Technology, Datta Meghe Institute of Medical Sciences (Deemed to be University), Sawangi (Meghe),
Wardha, M. S., India 442004
ktvreddy.feat@dmimsu.edu.in

***Abstract*—The suggested IsoQuadratic Exponentiation Randomized isocryptosystem design is the unique approach for public key encipher algorithm using IsoPartial Discrete Logarithm Problem and preservation of the recommended IsoQuadratic Exponentiation Randomized isocryptosystem be established against hardness of IsoPartial Discrete Logarithm Problem. Therewith, we demonstrated the possibility of an additional secured algorithm. The offered unique IsoQuadratic Exponentiation Randomized isocryptosystem is suitable for low bandwidth transmission, low storage and low numeration in cyberspace.**

Keywords—Isomathematics, IsoQuadratic Exponentiation Randomized, IsoPartial Discrete Logarithm Problem, Security Analysis.

I. INTRODUCTION

The cyber mechanism acquire innovatory development in every single lifestyle. Thus, digital information storage, its transmission and the consequence are the most important phases in it. Instinctively, safety of the digital information is an entirely interest in this issue. Cryptosystem is a mechanism of secure digital information and transmission with codes in order that at most individuals for that the digital information is expected can interpret and transmit it. A Primary aim of public/open key cryptosystem ($\mathcal{OKC}$) is to permit two individual to interchange classified digital information, even if they have not ever connected and can interconnect only via open network that is being observed by an antagonist. Cryptosystem is specify during the time that procedure as far as protocols and techniques that be mandatory for protected transmission in the existence of interloper. The pair, Open key ($\mathcal{OK}$) and secrete/close key ($\mathcal{CK}$) is an important set in cryptosystem. In closed key cryptosystem, a closed key essential known by the sender and the receiver to have the enciphering and the deciphering digital information. Hence, the closed key encipher is essential to share the key. As it happens, it is hard to manage such secure cryptosystem.

By resolving the hardness of open key cryptosystem follow in remarkable increase in the number of researcher engaged in the field of cryptosystem in renowned article "New Direction in Cryptography" suggested by Diffie and Hellman in 1976 [1]. Numerous $\mathcal{OK}$ encipher constructions particular numeral hypothetical cryptosystem acceptances are established on discrete logarithm ($\mathcal{DL}$) or factoring an humongous composite integer recommended in [2-3].

The inestimable word difficulty for groups and semigroups based public-key cryptosystems recommended by Wagner et al. in 1984 [4]. Wagner's design created neither on word problem, besides alternative, normally simple, assumption problem pointed out by Birget et al. in 2005 [5]. In addition, Birget et al. recommended a new $\mathcal{OKC}$ and that is established on finitely presented groups with hard word problem. The safety based on given mechanism depend on as long as most proportion over the cryptographic hypotheses. As a consequence of the particular presumptions as it may be break successfully, at that point the cryptosystem won't be safe any longer [6].

The framework for ID-based cryptographic structures (ID_b_CS) developed by Shamir in [7]. From that point forward, an opinion of exploration has been dedicated for creating different types of ID_b_CS. Okamoto et al. in [8] offered a thought for ID_b key delivery structures in 1988. These structures utilize the variation of RSA $\mathcal{OKC}$ for activities in to such an extent that n is a result of two huge primes, ideally, the safety of these structures depends on the calculation distress of determine the factoring of this huge composite digit n.

By using the ElGamal $\mathcal{OK}$ cryptographic structure with $\mathcal{DL}$ developed ID_b_CS by Tsujii and Itoh in [9]. The primary key distribution mechanism generated on paired individual presumption, that one incompetent, as it was exceptionally hard to take module primes, u and v recommended by K.S. McCurley in [10]. For maintain acceptable competence, a cryptosystem structures that depended on two distinct cryptographic presumptions: Factoring (FAC) and $\mathcal{DL}$ suggested by Harn et al. in [11]. Subsequently, various $\mathcal{OKC}$ were recommended in [12-14], a substantial segment of which build upon on combining pair of problems such $\mathcal{DL}$, Elliptic Curve $\mathcal{DL}$, FAC. For cyberspace, the safety and safety development mentioned by Obaidat and Boudriga in [15]. Modified $\mathcal{OK}$ cryptosystem constructed on discrete logarithm problem suggested by Meshram [16-19]. Dihedral and

Suzuki-2 group based $\mathcal{OKC}$ presented by Meshram et al. [20-23] in which the necessary to elect some arbitrary integer either by the individual or by the reliable authority.

Recently, in 2020, a new $\mathcal{PDLP}$ based $\mathcal{OKC}$ mechanism offered in [24] and isomathematics based key interchange mechanism recommended in [25]. In 2021, key interchange mechanism construct on santilli's isofields first and second kind suggested in [26-27], isobeta cryptosystem mechanism construct on santilli's isofields first-kind presented in [28] and comprehensive chaotic-maps based off-line electronic cash mechanism offered in [29]. In 2022, isobeta cryptosystem mechanism construct on santilli's isofields second-kind offered in [30] and isokey interchange framework based on Isonumber suggested in [31].

In this script, we design IsoQuadratic Exponentiation Randomized ($\mathcal{IsoQER}$)isocryptosystem mechanism build on IsoPartial Discrete Logarithm Problem ($\mathcal{IPDLP}$) that increases the comprehensive safety and requirements a small isonumber of in both of the encipher and deciphertion procedures. Thusly, the offered cryptosystem structure is increasingly pragmatic for practical utility.

The design toward remainder of this script is organized as per the following: In Section II, we instantly present the required isomathematical hypothesis applied in the script. In the section III, the framework for $\mathcal{IsoQER}$ cryptosystem is presented. In Sections IV, consistency of the suggested mechanism is analysed. In Sections V, we validated offered $\mathcal{IsoQER}$ isocryptosystem mechanism by established supporting example. In Sections VI, we investigate the efficiency of the recommended mechanism. In Sections VII, efficiency implementation of suggested $\mathcal{IsoQER}$ isocryptosystem mechanism. Eventually, we wind up the script in Section VIII.

II. Background and Material

The safety of the presented $\mathcal{IsoQER}$ isocryptosystem mechanism is the complexity of the $\mathcal{IPDLP}$ in the isogroup where the signature is established. We quickly survey the definitions from [32-34].

A. Isomathematical Postulate

A generalisation of computation in traditional mathematics is known as isomathematics. We can show that three multiplied by four is equal to sixty (for $\hat{\zeta} = 5$) by taking advantage of isomathematics.

Computation in traditional mathematics:

In traditional mathematics, computation with respect to additive unity "0" and multiplicative unity "1" for real number λ and μ define as;

$$\lambda + 0 = \lambda,\ \lambda - 0 = \lambda, \lambda^0 = 1, \lambda \times 1 = 1 \times \lambda = \lambda,$$
$$\lambda \div 1 = \lambda, 1 \div \lambda = \frac{1}{\lambda}, \lambda \times \mu = \lambda\mu, \lambda \div \mu = \frac{\lambda}{\mu} \text{ etc.}$$

Computation in isomathematics:

In isomathematics, Isosum $\hat{+}$, isominus $\hat{-}$, isoproduct $\hat{\times}$ and isodivision $\hat{\div}$ computations for isozero $\hat{\mathcal{K}}$ and $\hat{\zeta}$ called inverse of isounit $\hat{\eta} \neq 1$ such that $\hat{\zeta}\hat{\eta} = 1$ define as;

$$\lambda \hat{+} \mu = \lambda + \hat{\mathcal{K}} + \mu, \lambda \hat{-} \mu = \lambda - \hat{\mathcal{K}} - \mu,$$
$$\lambda \hat{\times} \mu = \lambda\hat{\zeta}\mu, \text{ and } \lambda \hat{\div} \mu = \left(\frac{\lambda}{\mu}\right)\hat{\eta}.$$

B. $\mathcal{IPDLP}$

For isoproduct $\hat{n} = \hat{u} * \hat{v}$ is a secure isoprime isomodulus of two enormous isoprime isonumbers $\hat{u} = 2\hat{u}' + 1$ and $\hat{v} = 2\hat{v}' + 1$ where $\hat{u}'$ and $\hat{v}'$ as well isoprime isonumbers. $\hat{\chi}(\hat{\ell})$ represent the arrangements of scure isoprime isonumbers for length $\hat{\ell}$.

Now define $\hat{\xi}(\hat{n}) = 2\hat{u}'\hat{v}'$, $ord(\hat{G}) = \frac{\hat{\xi}(\hat{n}^2)}{2} = \hat{v}\hat{v}'\hat{u}\hat{u}' = \frac{\hat{n}\hat{\xi}(\hat{n})}{2}$ for isocyclic isogroup of quadratic residues modulo $\hat{n}^2$ by $\hat{G} = \mathbb{QR}_{\hat{n}^2}$. Then maximal order of an isofactor in this isogroup represent by $\frac{\hat{n}\hat{\xi}(\hat{n})}{2}$ and $\hat{\gamma} = (1 + \hat{r}\hat{n})$ is for each isofactor of order $\hat{n}$.

Definition ($\mathcal{IPDLP}$): For feasibility, $\hat{r} = 1$ such that $\hat{g}^{\hat{\xi}(\hat{n})} mod \hat{n}^2 = (1 + \hat{n})\ mod\ \hat{n}^2$ with isofactor of maximal order $\hat{g}$ in $\hat{G}$.

We modify $\mathcal{PDLP}$ [35] *into* $\mathcal{IPDLP}$ to compute $\hat{w}\ (mod\ \hat{n})$ for given $\hat{g}$ and $\hat{k} = \hat{g}^{\hat{w}} mod\ \hat{n}^2$ (for few $\hat{w} \in [1, ord\ (\hat{G})]$

Postulate **(** $\mathcal{IPDLP}$ *over* $\hat{\mathcal{Z}}^*_{\hat{n}^2}$ **):** To each and every probabilistic polynomial time (PPT) algorithm $\hat{\mathcal{A}}$ effectively exists a negligible function $negl()$ for sufficient enormous $\hat{\ell}$ such that

$$\Pr\Big[\hat{\mathcal{A}}(\hat{n}, \hat{g}, \hat{k}) = \hat{w}\ (mod\ \hat{n}) \mid \hat{v}, \hat{u} \leftarrow \mathcal{SP}\left(\frac{\hat{\ell}}{2}\right); \hat{n} = \hat{u}\hat{v}; \hat{g} \leftarrow \hat{G}; \hat{w} \leftarrow [1, ord\ (G)]; \hat{k} \leftarrow \hat{g}^{\hat{w}} (mod\ \hat{n}^2)\Big] = \text{negl}(\hat{\ell})$$

III. Suggested $\mathcal{IsoQER}$ Cryptosytem using $\mathcal{IPDLP}$

The $\mathcal{IsoQER}$ cryptosystem mechanism is represent as below:

The safety of suggested $\mathcal{IsoQER}$ cryptosystem mechanism is based on the indelicacy of the $\mathcal{IPDLP}$.

A. Key Creation Procedure:

Every element ought to carry $\mathcal{IsoQER}$ $\mathcal{OK}$ and a congruous $\mathcal{CK}$.

Following procedure follow by individual- $\mathcal{M}$*:*

a. Take arbitrarily pair of enormous different isoprimes $\hat{u}$ and $\hat{v}$ having identical size.

b. Determine $\hat{n}^2 = \hat{u}^2 * \hat{v}^2$ and Isoeuler-phi function $\varphi(\hat{n}^2) = (\hat{u}^2 - 1)(\hat{v}^2 - 1)$.

c. Take a arbitrarily isointeger $\hat{s}, 1 < \hat{s} < \varphi(\hat{n}^2)$, such that $gcd(\hat{s}, \varphi(\hat{n}^2)) = 1$.

d. Take a arbitrarily isointeger $\hat{w},\ 2 \leq \hat{w} < \varphi(\hat{n}^2) - 1$.

e. For an isoelement in the isomultiplicative isogroup $\hat{z} \in \hat{\mathcal{Z}}^*_{\hat{n}^2}$, determine $\hat{z}^{\hat{w}}\ mod(\hat{n}^2)$.

f. Eventually, determine the distinctive isointeger $\hat{t}, 1 < \hat{t} < \varphi(\hat{n}^2)$; such that $\hat{s}\hat{t} = 1 mod\ (\varphi(\hat{n}^2))$ applying the extended Euclidean algorithm.

Individual- $\mathcal{M}$'s $\mathcal{OK}$ is $(\hat{n}, \hat{s}, \hat{z}, \hat{z}^{\hat{w}})$, and the conformable $\mathcal{CK}$ is $(\hat{t}, \hat{w})$.

B. Encipher Procedure:

Following procedure follow by individual- $\mathcal{N}$ to encrypts an information $\hat{\mathfrak{T}}$ for individual- $\mathcal{M}$*:*

a. The information $\hat{\mathfrak{T}} \in [1, \mathrm{n} - 1]$.

b. Take a arbitrarily isointeger $\hat{r}$

c. Determine $\hat{d} = \hat{z}^{\hat{r}} mod(\hat{n}^2)$, and determine $\hat{e} = \hat{\mathfrak{T}}.\left(\hat{z}^{\hat{w}}\right)^{\hat{r}} mod(\hat{n}^2)$.

d. Determine the concordant, $\hat{\alpha} = \hat{\beta}^{\hat{s}} mod(\hat{n}^2)$.

e. Eventually, determine $\hat{\mu} = \hat{e}^{\hat{s}} mod(\hat{n}^2)$.

Thus, $\hat{c} = (\hat{\alpha}, \hat{\mu})$ is the resultant isocipher-text.

C. Decryption Procedure:

Initially, individual- $\mathcal{M}$ determine $\hat{\alpha}^{\varphi(\hat{n})-\hat{w}} mod(\hat{n}^2)$ that equal to $\hat{\alpha}^{-\hat{w}} mod(\hat{n}^2)$ for decrypt, and afterwards the plaintext is retrieve by determine $\left(\hat{\alpha}^{-\hat{w}} * \hat{\mu}\right)^{\hat{t}} mod(\hat{n}^2) = \hat{\mathfrak{T}}$ *[7].*

IV. Consistency of the Proposed Mechanism:

During encipher procedure;

$$\hat{\alpha} = \hat{\beta}^{\hat{s}} mod(\hat{n}^2) = \left(\hat{z}^{\hat{r}}\right)^{\hat{s}} mod(\hat{n}^2)$$

$$\hat{\mu} = \hat{e}^{\hat{s}} mod(\hat{n}^2) = (m.\left(\hat{z}^{\hat{w}\hat{r}}\right))^{\hat{s}} mod(\hat{n}^2)$$

The decryption mechanism determine;

$$\hat{\alpha}^{\varphi(\hat{n})-\hat{w}} mod(\hat{n}^2) = \hat{\alpha}^{-\hat{w}} mod(\hat{n}^2)$$

$$\left(\hat{\alpha}^{-\hat{w}} * \hat{\mu}\right)^{\hat{t}} mod(\hat{n}^2) = \left(\hat{z}^{-\hat{w}\hat{r}\hat{s}}.\hat{\mathfrak{T}}^{\hat{s}}.\hat{z}^{\hat{w}\hat{r}}\right)^{\hat{t}} mod(\hat{n}^2)$$

$$= \hat{\mathfrak{T}}^{\hat{s}d} mod(\hat{n}^2) = \hat{\mathfrak{T}}\, mod(\hat{n}^2).$$

V. Example

For simplicity, assume pair of isoprime $\hat{u}' = 11$ and $\hat{v}' = 29$ such that $\hat{n} = \hat{u} * \hat{v} = 23 * 59$

A. Key Creation Procedure:

Following procedure follow by individual- $\mathcal{M}$*:*

a. Take arbitrarily pair of enormous different isoprimes $\hat{u}$ and $\hat{v}$ having identical size.

b. Determine $\hat{n}^2 = \hat{u}^2 * \hat{v}^2 = 23^2 * 59^2 = 529 * 3481 = 1841449$ and Isoeuler-phi function $\varphi(\hat{n}^2) = (\hat{u}^2 - 1)(\hat{v}^2 - 1) = (529 - 1)(3481 - 1) = 528 * 3480 = 1837440$.

c. Take a arbitrarily isointeger $\hat{s} = 7, 1 < \hat{s} < \varphi(\hat{n}^2)$, such that $gcd\left(\hat{s}, \varphi(\hat{n}^2)\right) = gcd(7, 1837440) = 1$

d. Take a arbitrarily isointeger $\hat{w} = 3,\ 2 \leq \hat{w} < \varphi(\hat{n}^2) - 1 = 2 \leq (\hat{w} = 3) < 1837440 - 1$.

e. For an isoelement in the isomultiplicative isogroup $\hat{z} \in \hat{\mathcal{Z}}^*_{\hat{n}^2}$, determine $\hat{z}^{\hat{w}}\ mod(\hat{n}^2) = 1675^3\ mod(1841449) = 44027$ for any element $\hat{z} = 1675$, of the isomultiplicative isogroup $\hat{\mathcal{Z}}^*_{\hat{n}^2}$

f. Eventually, determine the particular isointeger $\hat{t} = 524983, 1 < \hat{t} < \varphi(\hat{n}^2)$; such that $\hat{s}\hat{t} = 1 mod\ (1837440)$ applying the extended Euclidean algorithm.

Individual- $\mathcal{M}$'s $\mathcal{OK}$ is $\left(\hat{n}^2, \hat{s}, \hat{z}, \hat{z}^{\hat{w}}\right) = (1841449, 7, 1675, 4699421875)$, and the conformable $\mathcal{CK}$ is $(\hat{t}, \hat{w}) = (524983, 3)$.

B. Encipher Procedure:

Following procedure follow by individual- $\mathcal{N}$ to encrypts an information $\hat{\mathfrak{T}}$ for individual- $\mathcal{M}$*:*

a. The information $\hat{\mathfrak{T}} = [1, \hat{n}^2 - 1] = [1, 1841448]$.

b. Take a arbitrarily isointeger $\hat{r} = 5$.

c. Determine

$$\hat{d} = \hat{z}^{\hat{r}} mod(\hat{n}^2) = 1675^5 mod(1841449) = 694404,$$

and determine

$$\hat{e} = \hat{\mathfrak{T}}.\left(\hat{z}^{\hat{w}}\right)^{\hat{r}} mod(\hat{n}^2).\left(\hat{z}^{\hat{w}}\right)^{\hat{r}} mod(\hat{n}^2)$$

$$= 63 * (1675^3)^5 mod(1841449)$$

$$= 63 * 25125\ mod(1841449)$$

$$= 1582875\ mod(1841449) = 1582875$$

d. Determine the concordant, $\hat{\alpha} = \hat{\beta}^{\hat{s}} mod(\hat{n}^2) = \left(\hat{z}^{\hat{r}}\right)^{\hat{s}} mod(\hat{n}^2) = (1675)^{\hat{s}\hat{r}} mod(1841449) = 1769949$.

e. Eventually, determine $\hat{\mu} = \hat{e}^{\hat{s}} mod(\hat{n}^2) = (\hat{\mathfrak{T}}.\left(\hat{z}^{\hat{w}\hat{r}}\right))^{\hat{s}} mod(\hat{n}^2) = (1582875)^7 mod(1841449) = 1417409$.

Thus,
$\hat{c} = (\hat{\alpha}, \hat{\mu}) = (1769949, 1417409)$ is the resultant isocipher-text.

C. Decryption Process:

Initially, individual- $\mathcal{M}$ determine $\hat{\alpha}^{\varphi(\hat{n})-\hat{w}} mod(\hat{n}^2)$ that equal to $\hat{\alpha}^{-\hat{w}} mod(\hat{n}^2)$ for decrypt, and afterwards the plaintext is retrieve by determine $\left(\hat{\alpha}^{-\hat{w}} * \hat{\mu}\right)^{\hat{t}} mod(\hat{n}^2) = (1769949^{-3} * 1417409)^{524983} mod(1841449) = 63 = \hat{\mathfrak{T}}$.

VI. Security Analysis

Randomization enhance the conservation of the mechanism. $\mathcal{IsOQER}$ isocryptosystem mechanism is a randomized encipher mechanism, in which, the arbitrarily isointeger $\hat{r}$ take by the individual- $\mathcal{N}$. Four isomodular exponentiations steps needs in encipher procedure. A benefit of the $\mathcal{IsOQER}$ isocryptosystem mechanism which is based on the $\mathcal{IPDLP}$, the isomultiplicative isogroup $\hat{\mathcal{Z}}^*_{\hat{n}^2}$ in no way on a mandatory basis to be a cyclic isogroup, and evenhandedness, it is not mandatory that the isofactor $\hat{z}$, an generator of the group. The needlessness of determine a generator of the isogroup outstretches the technique to incorporate un-cyclic isogroups, moreover preventing the take a look at for the group being un-cyclic or cyclic.
As of the antagonist approaching when the isofactor $\hat{z}$ is not a generator of the isogroup, as determine to the power of the exponent $\hat{w}$; the value is not distinctive, that creates the problem more durable to resolve than $\mathcal{IPDLP}$. Because $\mathcal{IPDLP}$ involves that, the element utilized could be generator of a cyclic isogroup. Moreover, determine a generator would conditioned the length of the compound isointeger $\hat{n}$ that needed to be massive to extend the safety. Remember the exponentiations mandatory for the isocipher may be spiteful towards choosing $\hat{r}$ to possess small overacting weights. The isociphered is twofold as prolonged because the congruous plaintext.

Now, We will demonstration that suggested $\mathcal{IsOQER}$ isocryptosystem mechanism is experientially secured by thinking about subsequent three standard attacks.

A. Isodirect attack:

Antagonist aspirate to devise every $\mathcal{CK}$ make using of all information available from the mechanism.

For this state, antagonist essentials to take care of isointeger factorization problem and $\mathcal{IPDLP}$. The extremely

perfect possibility to determine the isomodulus $\hat{n}^2 = \hat{u}^2 * \hat{v}^2$, is by make using of the isonumber isofield sifter strategy [36]. However, this mechanism is at most dependent on the dimension of isomodulus $\hat{n}^2$ and that is computing insolvable to isofactor an isointeger of length bit-1024 and overhead. Ensuing, overcome the security of offered mechanism, we should take enormous isoprimes to preserve a tactical range among attacks make using of unprecedented reason isofactorization mechanism [37]. We are able to attain and match a identical safety level for $\mathcal{IPDLP}$ by taking the isomodulus $\hat{n}^2 = \hat{u}^2 * \hat{v}^2$ with $\frac{\hat{u}-1}{2}$ and $\frac{\hat{v}-1}{2}$ in that order are isoproduct of paired bit -512 enormous isoprimes.

B. Isofactoring attack:

Let us assume that time antagonist constructively break the isointeger factorization, thus antagonist be recognizable with the $(\hat{t}, \hat{w})$. By this data, antagonist determine $\hat{c} = \left(\hat{z}^{\hat{r}\hat{s}} mod(\hat{n}^2), \hat{e}^{\hat{s}} mod(\hat{n}^2)\right)$ and retrieve the genuine information $\hat{\mathfrak{T}}$, one has to eliminate with the term $\hat{z}^{\hat{r}}$ of C and this probably should be possible on the off chance that one identifies the $\mathcal{CK}$ $(\hat{t}, \hat{w})$. But the $\mathcal{IPDLP}$ remains hard to simplify, therefore the antagonist would unsuccessful.

C. $\mathcal{IPDLP}$ attack:

Let us assume that time antagonist constructively break the $\mathcal{IPDLP}$ and accordingly accomplish the close isointeger $\hat{r}$. Antagonist then gets that $\hat{\alpha}^{\varphi(\hat{n})-\hat{w}} mod\left(\hat{n}^2\right) = \hat{\alpha}^{-\hat{w}} mod(\hat{n}^2)$ and $\left(\hat{\alpha}^{-\hat{w}}\right)^{\hat{s}} mod(\hat{n}^2)$

Hence, the antagonist tries to retrieve the genuine information $\hat{\mathfrak{T}}$ from the equation;

$$\hat{c} = \left(\hat{z}^{\hat{r}\hat{s}} mod(\hat{n}^2), \hat{e}^{\hat{s}} mod(\hat{n}^2)\right) = \left(\hat{e}^{\hat{s}} \hat{z}^{\hat{r}\hat{s}} mod(\hat{n}^2)\right)$$

At the moment, the exponent $\hat{s}$ is open, one has to eliminate with the term $\hat{z}^{\hat{r}}$ of $\hat{c}$ and determine $\hat{e}^{\hat{s}}$. Regrettably, to reaffirm of genuine information, antagonist necessity has the confidential $\hat{r}$ in hand, on the other hand this is impracticable in the meantime the isointeger factorization is hard to break.

VII. Efficiency Performance

In this part, we investigate the exhibition of suggested mechanism as far as isonumber of isokeys, communication costs and computational complexity.

The accompanying symbols are utilized to investigate the exhibition of the mechanism.

The time run to perform isomodular performance require with bit size of $\hat{\ell} = |\hat{\ell}|$ as follows;

1. isoexponentiation= $exp\_\mathcal{T}$
2. isomultiplication= $mul\_\mathcal{T}$
3. isosquare computation= $squ\_\mathcal{T}$
4. isoinverse computation= $inv\_\mathcal{T}$
5. isohash function= $hash\_\mathcal{T}$

Herewith, we neglect the period execution isomodular isosubtraction or isoaddition enumeration and we suppose that the possibility of the bit being take as 0 or 1 is 0.5

The executions of suggested $\mathcal{IsoQER}$ cryptosystem mechanism is brief as in Table.

For encipher, the individual- $\mathcal{N}$ carry through $810 mul\_\mathcal{T} + hash\_\mathcal{T}$ time complexity. For decipherment, the individual- $\mathcal{M}$ carry through $572\ mul\_\mathcal{T}$ time complexity make using of the conversion $exp\_\mathcal{T} = 240 mul\_\mathcal{T}$ [38].

Eventually, $4|n|$ is the size of components of the mechanism or communication costs.

TABLE I. Comparison between Meshram et al [24] mechanism and our suggested mechanism

$\mathcal{QER}$ mechanism	Meshram et al mechanism [24]	our suggested mechanism
The number of keys	$\mathcal{CK}$ =4	$\mathcal{CK}$ =4
	$\mathcal{OK}$ =4	$\mathcal{OK}$ =4
Computational complexity	Encipher $2exp\_\mathcal{T}$+2 $mul\_\mathcal{T}$ + $hash\_\mathcal{T}$	Encipher $exp\_\mathcal{T}$+$mul\_\mathcal{T}$+ $hash\_\mathcal{T}$
	Deciphertion: $2exp\_\mathcal{T}$+$2mul\_\mathcal{T}$	Deciphertion: $exp\_\mathcal{T}$+$mul\_\mathcal{T}$
Communication cost	Encipher: $2n$	Encipher : n
	Deciphertion: $2n$	Deciphertion:n

VIII. Conclusion

Established on the complexity of the $\mathcal{IPDLP}$ in the isogroup, we suggested a unique $\mathcal{IsoQER}$ isocryptosystem mechanism in this script. To grant the possibility of enormous block sizes which improve the safety level on the insolence of both the IF and $\mathcal{PDLP}$ improve the security. The encipher promoter is chosen to be co-isoprime to the expand isoeuler-phi function that get additional safety as compare to the traditional case. The suggested procedure is indistinguishable to these used in n along the enlargement to include negative isointegers. Eventually, the suggested mechanism delivers the exceptional outcome from the safety frame of reference, define in consequence we face the difficult of simplifying $\mathcal{IPDLP}$ over the isomultiplicative isogroup of finite isofields as related to the other crypto mechanism.

Acknowledgment

The authors would like to thank anonymous reviewers for their careful and helpful comments.

References

[1] W. Diffie and M E Hellman, "New directions in cryptography," IEEE Transactions on Information Theory, vol. 22, pp. 644-654, 1976.

[2] T. EIGamal, "A Public-Key Cryptosystem and a Signature Scheme Based on Discrete Logarithms Advances in Cryptology," Proc. of CRYPTO, vol. 84, pp. 10-18, 1985.

[3] R. L. Rivest, A. Shamir, and L. Adleman, "A Method for Obtaining Digital Signatures and Public-Key Cryptosystems," Communications of the ACM, vol. 21, pp. 120-126, 1978.

[4] N.R. Wagner, M.R. Magyarik, "A public-key cryptosystem based on the word problem", In G.R. Blakley and D.Chaum (Eds): CRYPTO'84, LNCS 196, Springer- Verlag, pp. 19-36, 1985.

[5] J. Birget,, S.S. Magliveras and M. Sramka, "On public-key cryptosystems based on combinatorial group theory", Cryptology ePrint Archive: Report 2005/070, 2005.

[6] A. Shamir, "Identity-based cryptosystem and signature scheme," Advances in Cryptology: Proceedings of CRYPTO, vol. 84, pp. 47-53, 1985.

[7] E. Okarnoto and K. Tanaka, "Key distribution system based on identification information," IEEE Jou. Selecr. Areas Commun., vol. 7, pp.481-485, 1989.

[8] S. Tsujii and T. Itoh, “An ID-based cryptosystem based on the discrete logarithm problem,” IEEE Jounral on selected areas in communications, vol. 7, pp. 467-473, 1989.
[9] K. S. McCurley, "A Key Distribution System Equivalent to Factoring," Journal of cryptology, vol. 1,pp. 95-105, 1988.
[10] L. Harn and S. Yang, "ID-Based Cryptographic Schemes for User Identification, Digital Signature, and Key Distribution," IEEE Journal on Selected Areas in Communications, vol. 11, pp. 757-760, 1993.
[11] Z. Shao, "Signature Schemes Based on Factoring and Discrete Logarithms," IEE Proceedings-Computers and Digital Techniques, vol. 145,(1998), pp. 33-36.
[12] R. Guo, Q. Wen, Z. Jin, and H. Zhang, "Pairing Based Elliptic Curve Encryption Scheme with Hybrid Problems in Smart House," Fourth International Conference on Intelligent Control and Information Processing (ICICIP), pp. 64-68, 2013.
[13] D. Poulakis, "A Public Key Encryption Scheme Based on Factoring and Discrete Logarithm," Journal of Discrete Mathematical Sciences and Cryptography, vol. 12, pp. 745-752, 2009.
[14] P. Goswami, M. M. Singh, and B. Bhuyan, "A New Public Key Scheme Based on Integer Factorization and Discrete Logarithm," Palestine Journal of Mathematics, vol. 6(2), pp. 580-584, 2017.
[15] M. Obaidat and N. Boudriga, “Security of e-Systems and Computer Networks,” Cambridge University Press, ISBN 9780511536700, 2007.
[16] C. Meshram and S.S. Agrawal, “Enhancing the security of A Public key cryptosystem based on DLP $\gamma \equiv \alpha^{a}\beta^{b} \pmod p$”, International Journal of Research and Reviews in Computer Science 1 (4), pp.67-70, 2010.
[17] C. Meshram, “A Cryptosystem based on Double Generalized Discrete Logarithm Problem”, International Journal of Contemporary Mathematical Sciences, 6(6), pp. 285-297, 2011.
[18] C. Meshram and S. A. Meshram, “PKC Scheme Based on DDLP”, International Journal of Information & Network Security, 2 (2), pp. 154-159, 2013.
[19] C. Meshram, “The Beta Cryptosystem”, Bulletin of Electrical Engineering and Informatics, 4 (2), pp. 155-159, 2015.
[20] A. Meshram, C. Meshram, N. W. Khobragade, “Public Key Cryptographic Technique Based on Suzuki 2-Group,” International Journal of Advanced Research in Computer Science, vol. 08 (03), pp. 300-305, 2017.
[21] A. Meshram, C. Meshram, N. W. Khobragade, “An IND-CCA2 secure Public Key Cryptographic Protocol using Suzuki 2-Group,” Indian Journal of Science and Technology, vol. 10 (12), pp. 01-08, 2017.
[22] A. Meshram, C. Meshram, N. W. Khobragade, “An IND-CPA secure PKC Technique based on Dihedral Group,” Indian Journal of Computer Science and Engineering, vol. 08 (02), pp. 88-94, 2017.
[23] A. Meshram, C. Meshram, N. W. Khobragade, “An IND-CCA2 secure PKC Protocol using Dihedral Group,” 7th International Conference on Resent Engineering & Technology, Hyderabad, pp. 106-112,7th April 2017.
[24] C. Meshram, M. S. Obaidat and A. Meshram, “New efficient QERPKC based on partial discrete logarithm problem”, International Conference on Computer, Information and Telecommunication Systems (CITS), Hangzhou, China, (2020), 1-5, doi: 10.1109/CITS49457.2020.9232533.
[25] A. Meshram, C. Meshram, S. D. Bagde and R. R. Meshram, “RIPIC based key exchange protocol”, Advances in Mathematics: Scientific Journal, vol. 9 (12), pp. 11169–11177, 2020. doi.org/10.37418/amsj.9.12.97
[26] M. S. Dani, A. Meshram, and C. Meshram, “Santilli’s isofields first-kind based key exchange protocol” Journal of Physics: Conference Series, 1913, 012095, 2021. doi:10.1088/1742-6596/1913/1/012095.
[27] M. S. Dani, A. Meshram, C. Meshram, and N. M. Wazalwar, “An efficient key exchange scheme using santilli’s isofields second-kind for secure communication”, Advances in Mathematics: Scientific Journal, vol. 10 (2), pp. 1131–1139, 2021.
[28] A. B. Thatere, A. Meshram, C. Meshram, and N. M. Wazalwar, “SIFK based Isobeta Cryptosystem”, International Journal of Engineering Trends and Technology, vol. 69 (7), pp. 76-79, 2021. doi: 10.14445/22315381/IJETT-V69I7P211.
[29] C. Meshram, M. S. Obaidat, K. -F. Hsiao, A. L. Imoize and A. Meshram, "An Effective Fair Off-Line Electronic Cash Protocol using Extended Chaotic Maps with Anonymity Revoking Trustee," 2021 International Conference on Communications, Computing, Cybersecurity, and Informatics (CCCI), 2021, pp. 1-5, doi: 10.1109/CCCI52664.2021.9583217.
[30] A. Meshram, R. Pohane and R. Thakre, "Developing a framework of beta cryptosystem based on Santilli's isofields second-kind," 2022 International Conference for Advancement in Technology (ICONAT), 2022, pp. 1-4, doi: 10.1109/ICONAT53423.2022.9726000.
[31] M. S. Dani, A. Meshram, R. Pohane, and R. Meshram, “Isonumber based Iso-Key Interchange Protocol for Network Communication”, International Journal of Computer Science and Network Security, vol. 22 (2), pp. 209-213, 2022.
[32] C. X. Jiang, “Foundations of Santillis Isonumber Theory with Applications", ISBN 1-57485-056-3, Hadronic Press, 2002.
[33] Paillier P. Public key cryptosystem based on discrete logarithm residues. In Eurocrypt’ 99, Lecture Notes in Computer Science, Springer, Berlin., 1592, pp. 223-238, 1999.
[34] Das A, Adhikari A. An efficient IND-CCA2 secure Paillier-based cryptosystem. Information Processing Letters., vol. 112, pp. 885–888, 2012.
[35] A. K. Lenstra and M.S. Manasse, “Factoring by electronic mail” Advances in CrvDtolorv - EUROCRYPT ’89 Chrineer Berlin, pp. 355-371, 1990.
[36] J. Gordon, “Strong RSA keys,” Electron. Letter, 20, vol. 12, pp. 514-516, 1984.
[37] Waters B., Efficient identity-based encryption without random oracles, Advances in Cryptology-CRYPTO 2005, Lecture Notes in Computer Science. Berlin: Springer-Verlag, vol. 3494, pp. 114-127, 2005.
[38] N. Koblizt, A. Menezes, and S. Vanstone, “The state of elliptic curve cryptography”, Design, Codes Cryptography, vol. 19, pp. 173-193, 2000.

An Efficient Digital Short Signature Scheme using CCM for HC-IoT Environments

2022 International Conference on Communications, Computing, Cybersecurity, and Informatics (CCCI) | 978-1-6654-8617-0/22/$31.00 ©2022 IEEE | DOI: 10.1109/CCCI55352.2022.9926688

Chandrashekhar Meshram
Department of Post Graduation Studies and Research in Mathematics Jayawanti Haksar Government Post Graduation College, Betul, M.P., India 460001
cs_meshram@rediffmail.com

Ismail Bahkali
Department of Information Science, King Abdulaziz University, Jeddah 21589, Saudi Arabia
ibahkali@kau.edu.sa

Mohammad S. Obaidat
Life Fellow of IEEE and Fellow of SCS Chair & Professor, Computer Science Department, and Director of Cybersecurity Center, University of Texas-Permian Basin, Odessa, TX 79762, USA, with KASIT, The University of Jordan, Amman, Jordan, and University of Science and Technology Beijing, Beijing, China
msobaidat@gmail.com,
m.s.obaidat@ieee.org

Akshaykumar Meshram
Department of Applied Mathematics, Yeshwantrao Chavan College of Engineering, Nagpur, M.S., India.
akshaykjmeshram@gmail.com

Agbotiname Lucky Imoize*
Department of Electrical and Electronics Engineering, Faculty of Engineering, University of Lagos, Akoka, Lagos 100213, Nigeria. Department of Electrical Engineering and Information Technology, Institute of Digital Communication, Ruhr University, 44801 Bochum, Germany
aimoize@unilag.edu.ng

Kuei-Fang Hsiao
Senior Member of IEEE
Computer Science Department University of Texas-Permian Basin, Odessa, TX 79762, USA,
kfhsiao@gmail.com

***Abstract*—With billions of life-improving applications proliferating the global space, the Human-Centered Internet of Things (HC-IoT) grips excellent promise. The Internet will comprise more than 50 billion linked things, comprising mobile devices, GPS devices, sensors, actuators, and all the smart things that can be imagined. The HC-IoT comprises many smart gadgets to distribute identified information via online platforms. The goal is to encrypt messages between the sender and receiver during data exchange with the right instruction to challenge any human malicious attack. Different signature-based schemes have been proposed to ensure secure communication of critical user information. Smart gadgets claim lightweight characteristics, posing remarkable strengths and safety. The core challenge with signature-based techniques is the incurred computational cost owing to the enormous resources required for signature and verification procedures. The current paper projects an efficient Digital Short Signature (DSS) Scheme that uses Conformal Chaotic Maps (CCM) for protected communication in HC-IoT-based smart devices. The security of the projected scheme is thoroughly connected to a CCM in the random oracle model (ROM). The proposed DSS- CCM scheme offers more security assurance than the existing signature systems. The presented scheme would find practical applications in smart cards and emerging wireless security systems.**

Keywords—Human-Centered Internet of Things (HC-IoT), Digital Short Signature (DSS), Conformable Chaotic Maps (CCM), Confidentiality, Provable security.

I. INTRODUCTION

This is the period of the Internet of Things (IoTs), wherein numerous categories of computers are linked to the Internet. Such systems include manufacturing devices, energy meters, household appliances, mining sensors, industry tools, agricultural equipment, environmental monitoring equipment, healthcare monitoring instruments, surveillance systems, smart cities, and grids. These systems comprise M2M (Machine-to-Machine) frameworks, and through the advantages of IoT enabling tools, the control or monitoring of numerous types of frameworks at the fingertips is very simple. IoT-enabled computers can share and exchange information for cloud loading over a public network. IoT is a powerful tool that applies to several domains, demonstrating its importance and significant benefits. The concept of the "Internet of Things (IoT)" was coined, and IoT apps came into being from the development of simple, intelligent gadgets to human-oriented gadgets [1], where incredible development in IoTs has been recorded.

IoT systems were generally embraced for use in several fields, such as smart automation and human-centric architectural designs. Recently, researchers have adopted various methodologies and IoT experiments that enable systems in an extensive series of applications [2]. Several systems have been introduced using the notion of the Internet of Things to analyze real-world problems [3]. This development drives IoT-based research to find new ways to harness the immense strength of the Internet of Things. Integrating various medical systems with IoT has given a new direction to provide on-demand healthcare services to people, i.e., patients more specifically. IoT devices and different resources communicate in the healthcare information management system to provide better healthcare services [4].

IoT devices are not limited to edge computing but are connected to edge nodes. Edge nodes track and analyze data generated by IoT devices and subsequent responses to devices, users or data centers, respectively. Here, vast quantities of messages are exchanged so that a viable security scheme is protected for such messages, namely certificateless multi-message and multi-receiver signcryption (CLMMSC), and utilizing the ECC [5] becomes the best choice. In addition, a proxy signature [6] can be adopted using a certificate without pairing to secure data exchange in industrial IoT. Additionally, quality of service (QoS) optimization in vehicle communication is becoming a challenge because of vehicle mobility. Therefore, new security algorithms are required for the future generation of IoT systems and multimedia transmission in a vehicle-to-vehicle. So, new security algorithms are required [7].

978-1-6654-8617-0/22/$31.00 ©2022 IEEE

In the existing literature, different protection schemes have been identified. The devices allow protection in IoT environments. Due to different standards and varying communication protocols, traditional security mechanisms cannot be applied directly to the IoT environment. The systematic analysis of IoT-related security issues is presented in early works [8-14]. The security challenges are choosing the right cryptographic algorithms, encryption techniques, secure communication and sensor data, etc.

The capability of an IoT device is insufficient to be used at low ends with limited resources such as computing resources, power, etc. For IoT security, we need a roadmap to adapt cognitive and systemic methods toward addressing device heterogeneity and resolving escalating security issues such as identity, privacy, trust, and access control. The research on cryptographic technologies [15] addressed the pros and cons of encryption algorithms when sharing data for IoT applications such as smart homes, vehicles, and health, over untrusted networks.

Currently, information is exchanged between devices in the human-centered IoT over public communication channels. As a result, malicious practices are aimed at stealing or altering user data. The key obstacle, as a result, is to preserve confidentiality and privacy during transmission. Therefore, we need a robust and efficient security apparatus for seamless information flow. IoT devices are resource-constrained, and substantial computation resources are required. Ibrahim et al. [16] demonstrated a new variant of symmetric conformable fractional derivatives and generalizations of complex variables. Similarly, Goufo [17] analyzed an autonomous multi-dimensional chaotic framework with multi-wing attractors based on fractal-fractional derivatives with the fractional order. The standard DSA, such as RSA [18], ElGamal [19], and ECDSA [20], are not suitable for use. We need an easy and lightweight signature protection structure for HC-IoT. A chaotic map-based digital signature scheme is more effective and computationally less expensive, which is proposed in the current study.

Here, we use chaotic maps to propose a digital signature scheme for human-centered IoT security. Chaotic maps are utilized in [21] to propose the security technique for ID-based digital signatures. The security of the scheme pledge support is based on the expectations of the chaotic map's inflexibility (Diffie-Hellman) and complexity (DL). In [22], data integrity protection for Wireless Sensor Networks (WSN) utilizing bilinear pairing for the ID-based mutual signature approach was presented. A designated verifier verifies the mutual signature from the cluster, precisely WSN. The authors employ the popular aggregate signature and ID-based cryptography structures to maximize bandwidth usage by ensuring data integrity. The security analysis is presented on the CDH assumption in ROM.

Pairing for the group signature method is likewise being implemented progressively in Industrial IoT [23] to protect incident statements (in the publish/contribute stage), i.e., the exchange of messages between IoT nodes. It can be avoided using a group signature mechanism, certificate management, node breach decoupling, and exciting resource application. To this end, it adopts the bilinear pairings and ID-based cryptosystem. The issue with this method is the key revoke, which is with the publisher exiting the group. The authors used the technique in [24] to address the key issue of revocation, but due to associated costs, there is no promise to achieve an optimal solution. Nonetheless, testing the bilinear maps used in pairing-based signature schemes takes time. Moreover, these signature techniques are not as effective as DSA-based signature techniques in terms of computational efficiency. As a result, the storage efficiency of signatures obtained by pairing comes at the expense of the alarming computational complexity.

Our contribution: This paper describes a digital short signature technique for smart gadgets in HC-IoT contexts that is both efficient and secure. The key benefit of this approach over the DSA procedure is a one-fourth processing time savings in the verification process and the frequency of signatures. The method is demonstrated with clear step-by-step, and exceptional principles for providing notional proof based on the probability theory. An efficient proof of security exists for unforgeability underneath adaptive chosen attacks in ROM, i.e., the projected scheme offers superior safety assurances than the other existing signature techniques. The presented technique does not use pairings, which makes implementation more flexible and improves efficiency. It is dependent on the relatively new and experimental hardness conventions accompanying cryptography using pairing.

Road map of the article: This article is arranged as follows. The definitions and terminologies for the current scheme are described in Section II. The new DSS-CCM scheme, which is based on the conformable calculus to simplify the Chebyshev polynomial, is introduced in Section III. Section IV explains the security examination under provably security in the ROM and utilizes a reductionist security proof against forgery under the adaptive chosen message attacks (EUF-CMA) in the ROM. Lastly, Section V gives the conclusions.

II. Background and Material

This section focuses on Chebyshev polynomial and conformable Chebyshev chaotic maps, and their usage in the projected scheme.

A. Chebyshev chaotic polynomials

The operatory of Chebyshev sequential polynomials (CSP) is investigated (see [25]). In version x, CSP $\Upsilon_{\eta}(x)$ is a η -degree polynomial. Let $x \in [-1, 1]$ represent the arrangement and η be an integer. In general, CSP reported the following:

$$\Upsilon_{\eta}(x) = cos(\eta \times cos^{-1}(x)), \Upsilon_0(x) = 1, \Upsilon_1(x) = x,$$

$$\Upsilon_{\eta}(x) = 2x\Upsilon_{\eta-1}(x) - \Upsilon_{\eta-2}(x);\ \eta \geq 2$$

Under this circumstance, the functional $cos^{-1}(\tau)$ and $\cos(\tau)$ are denoted as $cos^{-1}: [-1, 1] \rightarrow [0, \pi]$ and $\cos: R \rightarrow [-1, 1]$.

CSP [25-31] has two main characteristics: chaotic and semi-group.

(1) The chaotic characteristics: The CSP map is represented as $\Upsilon_{\eta}: [-1, 1] \rightarrow [-1, 1]$ with degree $\eta > 1$, is a chaotic map associated with the functional (invariant density) $f^*(x) = \frac{1}{(\pi\sqrt{1-x^2})}$.

(2) The possessions of a "semi-group" meet the following criteria:

$\Upsilon_a(\Upsilon_c(x)) = \cos(a\cos^{-1}(\cos(c\cos^{-1}(x)))) = \cos(ac\cos^{-1}(x)) = \Upsilon_{ca}(x) = \Upsilon_c(\Upsilon_a(x))$,
where $x \in [-1, 1]$ and a and c are positive integers.

Two analyses of Chebyshev polynomials take into account handling in polynomial time:

(1) The discrete log (DL) is tasked with creating an integer w such that $\Upsilon_a(x) = y$ is true given two items x and y

(2) Because of three elements τ, $\Upsilon_a(x)$, and $\Upsilon_c(x)$ the Diffie-Hellman problem (DHP) is to measure $\Upsilon_{ac}(x)$.

B. Conformable Chaotic Maps (CCM)

The conformable calculus (CC) was earlier called conformable fractional calculus [32]. Generally, the concept of chaos theory has been widely applied in several works of literature [33]-[50]. Nonetheless, it is definitely of the recognized entities upon which the properties of fractional calculus (derivatives of non-integer power) are formulated. CC is fundamentally concerned with the steps that follow:

Suppose $\nu \in [0, 1]$ is an arbitrary fractional value. If and only if δ^0 is the self-operator and δ^1 is the typical difference operational, then an operator $\delta^\nu$is conformably differential. Specifically, if and only if for differentiable utility $\vartheta = \vartheta(x)$, then $\delta^\nu$is conformable,

$$\delta^0 \vartheta(x) = \vartheta(x), \qquad \delta^1\vartheta(x) = \vartheta'(x).$$

Anderson et al. [32] have proposed a unique formulation of CC derived from control theory to denote the performance of a proportional-differentiation controller that conforms to the error function. The instruction is organized as follows.

Definition 2.1 Assume that $\nu \in [0, 1]$, then:

$$\delta^\nu\vartheta(x) = \pi_1(\nu, x)\vartheta(x) + \pi_0(\nu, x)\vartheta'(x),$$

where the functions π_1 and π_0 attain the boundaries

$$\lim_{\alpha \to 0} \pi_1(\nu, x) = 1, \qquad \lim_{\alpha \to 1} \pi_1(\nu, x) = 0,$$

$$\lim_{\alpha \to 0} \pi_0(\nu, x) = 0, \quad \lim_{\alpha \to 1} \pi_0(\nu, x) = 1.$$

To attain the overhead description, we shall deliberate $\pi_1(\nu, x) = (1-\nu)x^\nu$ and $\pi_0(\nu, x) = \nu x^{1-\nu}$, or $\pi_1(\nu, x) = \frac{(1-\nu)}{\Gamma(1+\nu)}$ and $\pi_0(\nu, x) = \frac{\nu}{\Gamma(1+\nu)}$ where $\delta^\nu\vartheta(x)$ is named the conformable differential operator for the function $\vartheta(x)$. As a result, the fractional tuning connections between the function ϑ and its derivative are π_1, π_0.

Using the concept of CC to describe the polynomial $\Upsilon_n(x)$, we arrive at the following:

Since $\Upsilon'_\eta(x) = 2\eta\,\Upsilon_{\eta-1}(x)$, then (1):

$$\Upsilon^\nu_\eta(x) := \delta^\nu\Upsilon_\eta(x) = \pi_1(\nu, x)\Upsilon_\eta(x) + \pi_0(\nu, x)\Upsilon'_\eta(x) \quad (1)$$

Equation (1) can be replaced by (2)

$$\Upsilon^\nu_\eta(x) = \pi_1(\nu, x)\Upsilon_\eta(x) + 2\eta\,\pi_0(\nu, x) * \omega(x)\Upsilon_{\eta-1}(x) \quad (2)$$

where $\omega(x) = 1 + 2x + (4x^2 - 1) + \cdots + (n-1)$ - times. Eq. (2) is called the Conformable Chebyshev polynomials (CCP). Formulary recurrent can be seen in the following result:

Proposition 2.1. The CCP [48] satisfies the frequent relatives defined by (3)

$$\Upsilon^\nu_\eta(x) = [2x\,\pi_1(\alpha, x) + 2\eta\,\pi_0(\nu, x) * \omega(x)]\ \Upsilon_{\eta-1}(x) - \pi_1(\nu, x)\Upsilon_{\eta-2}(x) \quad (3)$$

Proposition 2.2. The semi-group characteristics clamps for CCP situated on the interval (-∞,∞) [48] i.e.

$$\Upsilon^\nu_k\left(\Upsilon^\nu_\eta(x)\right) = \Upsilon^\nu_\eta\left(\Upsilon^\nu_k(x)\right) = \Upsilon^\nu_{k\eta}(x) \quad (4)$$

III. The Proposed DSS Scheme for HC-IoT Environments

This section demonstrates the new DSS scheme using CCM for the HC-IoT framework. The proposed scheme consists of the following phases:

Setup: Let q and p be big primes with $p|(q-1)$. Also, let $G_{g,q} = \{g^0, g^1, \ldots g^{p-1}\} \subseteq Z^*_q$ with order q, where g is an originator with p order. Let H_2 and H_1 be one-way hash functions where:

$H_2 : \{0,1\}^* \to Z^*_q$ and $H_1 : \{0,1\}^* \times Z^*_q \to \{0,1\}^{m_p/2}$

The bit length of $p\ by\ |p| = m_p$ and that of $q\ by\ |q| = m_q$ is indicated here. The notation $b \overset{R}{\leftarrow} S$ means that b is chosen from a S set at arbitrary uniformly. We shall now explain the DSS scheme in a complete sense.

Key generation (**Gen**):

1. Select a random $d \in_R Z^*_p$ as the secret key.
2. The analogous public key is given by $\kappa \leftarrow \Upsilon^\nu_d(g)(mod\ p)$, where $\nu \in [0, 1]$ is a fractional (arbitrary) number.

Signing (Sign): The involvements are the κ public key and a message $M \in \{0,1\}^*$ and the private key d.

1. First, select a random $number\ r \in_R Z^*_p$.
2. Calculate $y \leftarrow H_2(M), l \leftarrow y.\Upsilon^\nu_r(g)(mod\ p), W \leftarrow H_1(M, l)$ and $U \leftarrow (r - Wd)(mod\ p)$.
3. The signature on the $\mathfrak{M}$ message is $\sigma = (W, U)$.

Verification (**Ver**)**:** The involvements are the public key κ, the message $\mathfrak{M}$, and the signature $\sigma \leftarrow (W, U)$.

1. Calculate $y \leftarrow H_2(M), l' \leftarrow yY^\nu_W(\kappa)\Upsilon^\nu_U(g)(mod\ p)$ and $W' \leftarrow H_1(\mathfrak{M}, l')$.
2. If $W = W'$, **Ver** returns true; otherwise, it returns false.

Reliability of the projected DSS Algorithm: Since $U \leftarrow (r - Wd)(mod\ p)$ and $l \leftarrow y.\Upsilon^\nu_r(g)(mod\ p)$, $r \leftarrow (U + Wd)(mod\ p)$ imply $\Upsilon^\nu_W(\kappa)\Upsilon^\nu_U(g)(mod\ p) \leftarrow \Upsilon^\nu_r(g)(mod\ p)$ and $l' \leftarrow yY^\nu_W(\kappa)\Upsilon^\nu_U(g)(mod\ p) \leftarrow y.\Upsilon^\nu_r(g)(mod\ p) = l$. So $W' \leftarrow H_1(M, l') = H_1(M, l) = W$. Hence, the signature $\sigma \leftarrow (W, U)$ created by the signing algorithm **Sign** is permanently valid.

IV. Security Examination

Our security model works upon three consecutive levels to ensure the safety of the system. Analysis of the sample of the security for proposed digital signature techniques is done in the first phase. The random oracle and the "provable security" are monitored at the second level, with the presupposition about the complexity of CCM in the milieus of Human-centered Internet and Things. A near-reductionist technique is offered at the end to conclude that our DSS scheme is competent enough to safeguard and obstruct the forgery present in the setup of chosen attacks in ROM supposing CCM, which are hard under HC-IoT environments.

Theorem 4.1. Let $G_{g,q}$ be a (t', ε')- CCM group, then the DSS scheme is $(t, \zeta_{H_1}, \zeta_{H_2}, \zeta_{sig}, \varepsilon)$ −secure against EUF-CMA in the ROM, where

$$t' \approx 3\left(\frac{t}{2} + \mathcal{C}_e\left(\frac{(\zeta_{H_2}+2\zeta_U)}{2}\right)\right) and$$

$$\varepsilon' \approx \left(\varepsilon - \frac{1}{2^{m_p/2}} - \frac{(\zeta_U + \zeta_{H_1})\zeta_U}{2^{m_q}}\right)^3 \left(\frac{(\zeta_{H_1}+2)}{16\zeta_{H_1}}\right) + \left(\frac{\varepsilon}{2} - \frac{1}{2^{(m_p/2+1)}} - \frac{(\zeta_U + \zeta_{H_1})\zeta_U}{2^{(m_q+1)}}\right)$$

Here $\mathcal{C}_e$ denotes the expense of calculation of an extended exponentiation in $G_{g,q}$ group.

Proof: The security of the DSS scheme is verified by taking advantage of the ROM. Suppose we get a EUF-CMA invader $\mathcal{U}$ where $(t, \zeta_{H_1}, \zeta_{H_2}, \zeta_{sig}, \epsilon)$ −splits the DSS scheme. That is, A is a PPT program that is given an extended public sequence of random bits and can ask the random oracles H_1, H_2, S a polynomial number of questions.

As a "simulator", we want to construct a process Υ, receipts (q, p, g, κ) as input. Υ makes an effort to use $\mathcal{U}$ to figure out the CCM, i.e., $\Upsilon_\kappa(g)$ as a computer programme. Process Υ simulates one or two DSS schemes and turns to invader A. Process Υ replies to hash inquiries $H_2$and H_1 by A, signature S inquiries, and strives to run A's probable fakes (M, σ) into a CCM, i.e., $\Upsilon_\kappa^\nu(g)(mod\ p)$ result. Process Υ launches the first simulation by furnishing (q, p, g, κ) and an extended sequence of arbitrary bits for A. Then, Υ counters as surveys to A's inquiries:

Answering H_1*-oracle inquiries*: If A subjects a random oracle inquiry (M_i, γ_i) in which $1 \le i \le \zeta_{H_1}$, Υ searches the H_1^L (inquiry-reply list) in which entries comprise $((M_i, \gamma_i)W_i)$ tuples to gain the conforming answer. If tuple$((M_i, \gamma_i), W_i)$ is in H_1^L, Υ responses with W_i. Then Υ uniformly and arbitrary creates W_i from $\mathcal{Z}_p^*$, replies with it, and augments tuple$((M_i, \gamma_i), W_i)$ to H_1^L.

Answering H_2 *-oracle inquiries*: If $\mathcal{U}$ focuses on an arbitrary oracle inquiry (M_i) where $1 \le i \le \zeta_{H_2}$, Υ examining the H_2^L (H_2 -list) for items consisting of $((M_i), \gamma_i, t_i)$ Tuples to obtain the appropriate response. If the H_2^L comprises a $((M_i), \gamma_i, t_i)$ tuple then Υ retorts with γ_i.

If (M_i) is the latest query, Υ will search for the H_1^L. If H_2^L comprises some $((M_i, \gamma_i)W_i)$ tuples, Υ decides on one γ_i, create t_i from $\mathcal{Z}_p^*$ uniformly arbitrary, works out $\gamma_i \leftarrow \gamma_i \Upsilon_{t_i}^\nu(g)(mod\ p)$ and retorts with γ_i. Υ joins H_2^L with $((M_i), \gamma_i, t_i)$.

If no $((M_i, \gamma_i)W_i)$ occurs in H_1^L, then Υ uniformly creates t_i at random from $\mathcal{Z}_p^*$, computes $\gamma_i = \Upsilon_{t_i}^\nu(g)(mod\ p)$ and replies with γ_i. Υ joins the $H_2^L$with $((M_i), \gamma_i, 0)$.

Answering S-oracle inquiries: If $\mathcal{U}$ focuses on an enquiry for signature (M_i) in which $1 \le i \le \zeta_U$, Υ looks up for the S^L (list of inquiries–answer) in which entries comprise (M_i, W_i, U_i) to gain the exact answer. If there is (M_i, W_i, U_i) arises in S^L then Υ replies with(W_i, U_i).

In the circumstance that (M_i) is the latest inquiry for signature, Υ searches for the H_2^L for the first time. If H_2^L comprises a $((M_i), \gamma_i, t_i)$ tuple, Υ decides on γ_i. Otherwise, Υ uniformly constructs t_i at random from $\mathcal{Z}_p^*$, figures out $\gamma_i \leftarrow \Upsilon_{t_i}^\nu(g)(mod\ p)$, and includes the tuple$((M_i), \gamma_i, 0)$to the H_2^L.

Then Υ unvaryingly opts for U_i, W_i' from $\mathcal{Z}_p^*$ at random and computes $\gamma_i \leftarrow \gamma_i \Upsilon_{W_i'}^\nu(\kappa)\Upsilon_{U_i}^\nu(g)(mod\ p)$. Υ retorts with (M_i, W_i', U_i), upgrades (M_i, W_i', U_i), to S-list, and upgrades the tuple(M_i, W_i', γ_i) to H_1^L. In the case of $((M_i, \gamma_i)W_i)$ is in the H_1-list with $W_i \ne W_i'$, the simulation will be terminated and revived (this regrettable episode is at most $\frac{(\zeta_{H_1}+\zeta_{H_2})}{2^{m_p/2}}$ probability). So, it is observed here that the oracles-based simulation produces atypical outputs compared to real attacks.

We speculate invader $\mathcal{U}$ persists in a new permissible message and signature tuple (M, W, U) with probability ϵ. If $\mathcal{U}$ has not looked for $H_2(M)$ or $H_1(M, \gamma)$, the probability is $Pr\{H_1(M, H_2(M)\Upsilon_U^\nu(g)\Upsilon_W^\nu(\kappa)) \leftarrow W\} < \frac{\nu}{2^{m_p/2}} \le \frac{1}{2^{m_p/2}}$ since both $H_2(M)$ and $H_1(M, \gamma)$ are chosen randomly. Therefore, with the probability $\left(\varepsilon - \frac{1}{2^{m_p/2}} - \frac{\zeta_U(\zeta_U+\zeta_{H_1})}{2^{m_q}}\right)$ that the invader $\mathcal{U}$ ensues a fresh signature (M, W, U) such that $H_1(M, H_2(M)\Upsilon_U^\nu(g)\Upsilon_W^\nu(\kappa)(mod\ p)) \leftarrow W$ and $H_2(\mathfrak{M}) \in H_2^L$, $H_1(M, \gamma) \in H_1^L$.

The H_2^L comprises two kinds of entries. If $H_2(\mathfrak{M}) = \gamma\Upsilon_t^\nu(g)(mod\ p)$, then $H_2(M)\Upsilon_U^\nu(g)\Upsilon_W^\nu(\kappa)(mod\ p) = \gamma$ denotes $\Upsilon_1^\nu(\Upsilon_U^\nu(g))\Upsilon_W^\nu(\kappa)(mod\ p) = 1$, and $d \leftarrow (-t - U)/W$. With the belief that the numeral of H_1-inquiry $(\mathfrak{M}, \gamma)$ with $H_2(M) = \gamma\Upsilon_t^\nu(g)$is $\mathcal{V}_{p_{H_1}}$. Hence the probability of resolving the CCM is $\mathcal{V}$ in the first simulation.

We suppose that Υ acquires the message and signature pair (M_j, W_j, U_j) in the first simulation, with $W_j \leftarrow H_1(M_j, \gamma_j)$ and $H_2(M_j) \ne \gamma_j\Upsilon_{t_j}^\nu(g)$. Process Υ will commence the second simulation with the $(1 - \mathcal{V})$ probability if the similar $(q, p, g, \kappa)$is furnished. Υ grants the invader $\mathcal{U}$ the similar random bits arrangement, analogous random replies to signature and hash function inquiries identical to the first simulation before $\mathcal{U}$ requests for $H_1(M_j, \gamma_j)$.

In this argument, various sequences of random bits, different estimates, and signatures for random functions are offered by Υ. The only variance is that if H_2-inquiry (M_j) is demanded after this argument, Υ retorts with the estimate similar to the first simulation. At this point, we make the most of the "Forking lemma" in [33]. Our anticipation that produces signature (M_j, W_j, U_j) this time round such that $H_2(M_i) \ne \gamma_i\Upsilon_{t_i}^\nu(g)(mod\ p)$ and $H_2(M_i)\Upsilon_{U_i}^\nu(g)\Upsilon_{W_i}^\nu(\kappa)(mod\ p)$ or the signature(M_j, W'_j, U'_j) with $W'_j \ne W_j$.

Thus, now the "Splitting lemma" [34] is working to quantify the probability at which $\mathcal{U}$ would work as projected. Let U represent a set of probable random functions estimates and random bits series that bring invader $\mathcal{U}$ up to the argumentation where $\mathcal{U}$ appeals for $H_1(M_j, \gamma_j)$ and let V represent a set of probable random functions estimates and random bits series after that. By extrapolation, the probability that $\mathcal{U}$ produces a forgery by providing a sequence of random bits and $(d||\kappa)$ estimates are ϵ for any omnipresence $d \in U, \kappa \in V$. Using "Splitting lemma", an "agreeable" subset happens $\Omega \in U$ such that:

(i) $Pr\{d \in \Omega\} \ge \epsilon/2$.

(ii) The probability that A dispensed the random bits and random estimates arrangements $(\mathcal{b}||\kappa)$ in which $\mathcal{b} \in \Omega;\ \kappa \in V$, create a forgery is at least $\varepsilon/2$.

In the first simulation, the arrangements of random bit and function estimates given to the argumentation are expected to be $\mathscr{b}$. As a result, in the case of any $\kappa \in V$, the probability that A, provided $(\mathscr{b}||v)$, generates a fake in the second simulation is $(\varepsilon/2)^2$. Fake signature probability $(M_i, W_i, \mho_i)$ with $H_2(M_i) = \wr_i \Upsilon_{t_i}^{v}(g)(mod\ \mathfrak{p})$ and $H_2(M_i)\Upsilon_{\mho_i}^{v}(g)\Upsilon_{W_i}^{v}(\kappa)(mod\ \mathfrak{p}) = \wr_i$ is δ. Forged signature probability $(M_j, W'_j, \mho'_j)$ with $W'_j \neq W_j$ is $(1-\gamma)/((1-\gamma)\zeta_{H_1} = 1/\zeta_{H_1}$.

As far as the second simulation is considered, the probability of Υ solving the CCM will be:

$$\left(\frac{\varepsilon}{2} - \frac{1}{2^{(m_{\mathfrak{p}}/2+1)}} - \frac{(\zeta_{\mho} + \zeta_{H_1})\zeta_{\mho}}{2^{(m_q+1)}}\right)^2 \left(\frac{\gamma\zeta_{H_1}+1}{\zeta_{H_1}}\right)\left(\varepsilon - \frac{1}{2^{(m_{\mathfrak{p}}/2)}} - \frac{(\zeta_{\mho} + \zeta_{H_1})\zeta_{\mho}}{2^{(m_q)}}\right)$$

$$\approx \left(\varepsilon - \frac{1}{2^{m_{\mathfrak{p}}/2}} - \frac{(\zeta_{\mho} + \zeta_{H_1})\zeta_{\mho}}{2^{m_q}}\right)^3 \left(\frac{\gamma\zeta_{H_1}+1}{4\zeta_{H_1}}\right)$$

In a nutshell, we detect that process Υ at least solves the CCM with probability (nearly):

$$(1-\gamma)\left(\varepsilon - \frac{1}{2^{m_{\mathfrak{p}}/2}} - \frac{(\zeta_{\mho} + \zeta_{H_1})\zeta_{\mho}}{2^{m_q}}\right)^3 \left(\frac{\gamma\zeta_{H_1}+1}{4\zeta_{H_1}}\right) + \gamma\left(\varepsilon - \frac{1}{2^{(m_{\mathfrak{p}}/2)}} - \frac{(\zeta_{\mho} + \zeta_{H_1})\zeta_{\mho}}{2^{(m_q)}}\right)$$

In one simulation, the calculation stage is $(t + (2\zeta_{\mho} + \zeta_{H_2})\mathcal{C}_e)$. The concluding stage in the calculation is:

$$(1-\gamma)2\left(t + (2\zeta_{\mho} + \zeta_{H_2})\mathcal{C}_e\right) + \gamma\left(t + (2\zeta_{\mho} + \zeta_{H_2})\mathcal{C}_e\right) = \left(t + (2\zeta_{\mho} + \zeta_{H_2})\mathcal{C}_e\right)(2-\delta).$$

The probability γ approximation is as follows: Only one H_1-inquiry and one H_2-inquiry is tolerable for each $\mathfrak{M}$ appeal; similar to the slightly weaker SO-CMA security system, i.e., the invader A appeals $(M, \wr)$for both H_1-inquiry and one H_2-inquiry. Process Υ retorts concurrently with $H_1(M, \wr) = W$, and $H_2(M) = \wr\, \Upsilon_t^{v}(g)(mod\ \mathfrak{p})$. In this case, $\gamma = 1$. We are assured of compelling reductionist proof for safety.

Each H_1-query $(M, \wr)$ is subsequently the H_2-query (M) is in contradiction to this optimistic estimate. Consequently, we find suitable security reductionist proof identical to the Schnorr signature system when $\gamma = 0$. We are eclectically letting $\gamma = 1/2$ since the set of random bits and function estimates invader $\mathcal{A}$offers are random. As a result:

$$t' \approx 3\left(\frac{t}{2} + \mathcal{C}_e\left(\frac{(\zeta_{H_2}+2\zeta_{\mho})}{2}\right)\right) \text{ and}$$

$$\varepsilon' \approx \left(\varepsilon - \frac{1}{2^{m_{\mathfrak{p}}/2}} - \frac{(\zeta_{\mho} + \zeta_{H_1})\zeta_{\mho}}{2^{m_q}}\right)^3 \left(\frac{(\zeta_{H_1}+2)}{16\zeta_{H_1}}\right) + \left(\frac{\varepsilon}{2} - \frac{1}{2^{(m_{\mathfrak{p}}/2+1)}} - \frac{(\zeta_{\mho} + \zeta_{H_1})\zeta_{\mho}}{2^{(m_q+1)}}\right)$$

It should be observed that the efficacy of the reductionist technique is subjected to H_1-query command and H_2-inquiry for the indistinguishable message that invader A is asking for. Thus, we have a reason to presume that this reductionist proof is comprehensive, lying amidst loose and tight ([35]).

The security of hash functions is as follows: To get a digital signature, we set $\mathfrak{p}$ to 160 bits. By birthday attacks, it is simple to reclaim M and M′messages such that $H_1(M, \wr) = H_1(M', \wr)$ and the hash estimate of H_1 is 80 bits. If the invader requisites a signature on M, the signature of the signer would be centered on a random number $\wr'$rather than $\wr$. Even though we are in doubt about the possibility of the outcome, other $\mathfrak{M}'$ message with $H_1(M, \wr) = H_1(M', \wr')$, we are in no doubt that finding $\mathfrak{M}'$ with $H_2(M') = H_2(M)$ is unachievable for the reason that the hash estimate of H_2 is at least 1024 bits.

Meanwhile, no mechanism will be able to recuperate $\mho, W$ from the multivariate congruence $H_1(M, H_2(M)\Upsilon_{\mho}^{v}(g)\Upsilon_{W}^{v}(\kappa)(mod\ \mathfrak{p})$ or find $\wr, \mho$ from $H_2(M)\Upsilon_{\mho}^{v}(g)\Upsilon_{H_1(M,\wr)}^{v}(\kappa)(mod\ \mathfrak{p}) = \wr$. The probability is high because the ROM assumes that hash functions are perfect.

$$\Pr_{\wr \in Z_q}\{H_1(M, \wr) = W | \forall M \in \{0,1\}^*, \forall\, W \in 2^{m_{\mathfrak{p}}/2}\} = \frac{1}{2^{m_{\mathfrak{p}}/2}}.$$

V. Conclusion

The security of sensitive information/data is essential in HC-IoT platforms to protect against forgery attacks. The digital short signature scheme is a tested option for confirming the proprietorship and legitimacy of interacting parties in asymmetric key cryptography. This article uses Conformal Chaotic Maps (CCM) for protected communication in the HC-IoT environment to demonstrate an efficient, provably secure method for digital signatures. Underneath the EUF-CMA at ROM, the projected DSS-CCM scheme is existentially unforgeable. Overall, key findings revealed that it is more difficult to crack the projected DSS-CCM scheme than the conventional DSA, based on a discrete logarithm. Future work would investigate the implementation of the projected DSS-CCM scheme in a realistic HC-IoT environment.

References

[1] J. Chin, V. Callaghan, and S. B. Allouch, "The Internet-of-Things: Reflections on the past, present and future from a user-centered and smart environment perspective", *Journal of Ambient Intelligence and Smart Environments*, vol. 1, pp. 45–69, 2019. DOI. 10.3233/AIS-180506.

[2] M. Dachyar, T. Y. M. Zagloel, and L. R. Saragih, "Knowledge growth and development: internet of things (IoT) research, 2006–2018", *Heliyon,* vol. 5, no. 8, pp. e02264, 2019.

[3] P. P. Ray, "A survey on Internet of Things architectures", *Journal of King Saud University – Computer and Information Sciences,* vol. 30, no. 3, pp. 291-319, 2018.

[4] S. Zeadally, and O. Bello, "Harnessing the power of Internet of Things based connectivity to improve healthcare", *Internet of Things,* vol. 100074, pp. 1-14, 2019. https://doi.org/10.1016/j.iot.2019.100074

[5] C. Peng, J. Chen, M. S. Obaidat, P. Vijayakumar, and D. He, "Efficient and Provably Secure Multi-receiver Signcryption Scheme for Multicast Communication in Edge Computing", *IEEE Internet of Things Journal,* 2019, DOI. 10.1109/JIOT.2019.2949708.

[6] G. K. Verma, B. B. Singh, N. Kumar, M. S. Obaidat, D. He, and H. Singh, "An Efficient and provable certificate-based proxy signature scheme for IIoT environment", *Information Sciences,* vol. 518, pp. 142-156, 2020.

[7] A. H. Sodhro, M. S. Obaidat, Q. H. Abbasi, P. Pace, S. Pirbhulal, G. Fortino, M. A. Imran, and M. Qaraqe, "Quality of Service Optimization in an IoT-Driven Intelligent Transportation System" *IEEE Wireless Communications*, vol. 26, pp. 10-17, 2020.

[8] H. Suo, J. Wan, C. Zou and J. Liu, "Security in the Internet of Things: A Review", *In 2012 Int. Conf. on Computer Science and Electronics Engineering,* Hangzhou, pp. 648-651, 2012.

[9] M. A. Iqbal, O. G. Olaleye and M. A. Bayoumi, "A Review on Internet of Things (IoT): Security and Privacy Requirements and the Solution Approaches", *Global Journal of Computer Science and*

Technology: E Network, Web & Security, vol. 16, no. 7, ver. 1.0, 2016.

[10] X. Liu, M. Zhao, S. Li, F. Zhang and W. Trappe, "A Security Framework for the Internet of Things in the Future Internet Architecture", *Future Internet*, vol. 9, no. 3, pp. 27, 2017.

[11] A. R. Sfar, E. Natalizio, Y. Challal and Z. Chtourou, "A Roadmap for Security Challenges in Internet of Things", *Digital Communications and Networks*, vol. 4, no. 2, pp. 118-137, 2018.

[12] C. Maple, "Security and privacy in the internet of things", *Journal of Cyber Policy*, vol. 2, no. 2, pp. 155-184, 2017.

[13] M. M. Noor and W. H. Hassan, "Current research on Internet of Things (IoT) security: A survey", *Computer Networks*, vol. 148, pp. 283-294, 2019.

[14] J. Porras, J. Khakurel, A. Knutas and J. P¨ank¨al¨ainen, "Security Challenges and Solutions in the Internet of Things", *Journal of NBICT*, vol. 1, pp. 177-206, 2018.

[15] S. Zeadally, A. K. Das, N. Sklavos, "Cryptographic technologies and protocol standards for Internet of Things", *Internet of Things,* 100075, 2019.

[16] R. W. Ibrahim, R. M. Elobaid, S. J. Obaiys, "Symmetric Conformable Fractional Derivative of Complex Variables", *Mathematics,* vol. 8, no. 363, 2020, doi:10.3390/math8030363

[17] E. F. Doungmo Goufo, "Fractal and fractional dynamics for a 3D autonomous and two-wing smooth chaotic system", Alexandria Engineering Journal, pp. 1-8, 2020, https://doi.org/10.1016/j.aej.2020.03.011

[18] R. Rivest, A. Shamir and L. Adleman, "A Method for Obtaining Digital Signatures and Public-Key Cryptosystems", *Communications of the ACM,* vol. 21, no. 2, pp. 120–126, 1978.

[19] T. ElGamal, "A Public-Key Cryptosystem and a Signature Scheme Based on Discrete Logarithms", *IEEE Transactions on Information Theory*, vol. 31, no. 4, pp. 469–472, 1985.

[20] D. Johnson, A. Menezes and S. Vanstone, "The elliptic curve digital signature algorithm (ECDSA)", *International journal of information security*, vol. 1, no. 1, pp. 36-63, 2001.

[21] S. K. Hafizul Islam, "Identity-based encryption and digital signature schemes using extended chaotic maps", *IACR Cryptology*, *ePrint Archive*, vol. 275, 2014.

[22] L. Shen, J. Ma, X. Liu, F. Wei and M. Miao, "A Secure and Efficient ID-Based Aggregate Signature Scheme for Wireless Sensor Networks", *IEEE Internet of Things Journal,* vol. 4, no. 2, pp. 546-554, 2017.

[23] C. Esposito, A. Castiglione, F. Palmieri and A. D. Santis, "Integrity for an Event Notification Within the Industrial Internet of Things by Using Group Signatures", *IEEE Transactions on Industrial Informatics,* vol. 14, no. 8, pp. 3669-3678, 2018.

[24] G. Ateniese, D. Song and G. Tsudik, "Quasi-efficient revocation of group signatures", *Proc. of the 6th Financial Cryptography Conference, Lecture Notes on Computer Science,* vol. 2357, pp. 88–98, 2016.

[25] J. C. Mason and D. C. Handscomb, "Chebyshev polynomials", *Chapman & Hall/CRC,* Boca Raton, 2003.

[26] P. Bergamo, P. D'Arco, A. Santis and L. Kocarev, "Security of public key cryptosystems based on Chebyshev polynomials", *IEEE Trans Circuits Syst* I, vol. 52, no. 7, pp. 1382–1393, 2005.

[27] S. Han and E. Chang, "Chaotic map based key agreement with/out clock synchronization", *Choas Soliton and Fractals*, vol. 39, no. 3, pp. 1283–1289, 2009.

[28] L. Zhang, "Cryptanalysis of the public key encryption based on multiple chaotic systems", *Chaos Solitons and Fractals*, vol. 37, no. 3, pp. 669–674, 2008.

[29] F. Chen, X. Liao, K. W. Wong, Q. Han and Y. Li, "Period distribution analysis of some linear maps", *Commun Nonlinear Sci. Numer. Simul,* vol. 17, pp. 3848–3856, 2012.

[30] C. Meshram, C. C. Lee, S. G. Meshram and C. T. Li, C.T, "An efficient ID-based cryptographic transformation model for extended chaotic-map-based cryptosystem", *Soft Computing*, vol. 23, no. 16, pp. 6937-6946, 2019.

[31] C. Meshram, C. T. Li and S. G. Meshram, "An efficient online/offline ID-based short signature procedure using extended chaotic maps", *Soft Computing*, vol. 23, no. 3, pp. 747-753, 2019.

[32] D. R. Anderson, E. Camrud, D. J. Ulness, "On the nature of the conformable derivative and its applications to physics", *arXiv preprint arXiv:1810.02005,* 2018.

[33] Z. Shao, "A provably secure short signature scheme based on discrete logarithms", *Information Sciences*, vol. 177, no. 23, pp. 5432-5440, 2007.

[34] M. Bellare and P. Rogaway, "Random oracles are practical: a paradigm for designing efficient protocol", *Proc. of the 1st ACM Conference on Computer and Communication Security,* ACM Press, New York, pp. 62–73, 1993.

[35] E. J. Goh and S. Jarecki, "A signature scheme as secure as the Diffie–Hellman problem", *Proc. of Eurocrypto'03, LNCS*, Springer-Verlag, Berlin, vol. 2656, pp. 401–415, 2003.

[36] H. Cui, R. H. Deng, J. K. Liu, X. Yi and Y. Li, "Server-Aided Attribute-Based Signature With Revocation for Resource-Constrained Industrial-Internet-of-Things Devices", *IEEE Transactions on Industrial Informatics,* vol. 14, no. 8, pp. 3724-3732, 2018.

[37] G. Zhang, Y. Liao, Y. Fan, Y. Liang, "Security Analysis of an Identity-Based Signature from Factorization Problem", *IEEE Access,* vol. 8, pp. 23277–23283, 2020.

[38] C. Meshram and M. S. Obaidat, "An Efficient Provably Secure IBS Technique using Integer Factorization Problem", *Lecture Notes in Networks and Systems,* Springer (IC4S 2019), vol. 121, pp. 427-439, 2020.

[39] M. A. Mughal, X. Luo, A. Ullah, S. Ullah and Z. Mahmood, "A Lightweight Digital Signature Based Security Scheme for Human-Centered Internet of Things", *IEEE Access,* vol. 6, pp. 31630-31643, 2018.

[40] A. M. Benasser and A. Samsudin, "A new Identity Based Encryption (IBE) scheme using extended Chebyshev polynomial over finite fields Zp", *Physics Letters A,* vol. 374, no. 46, pp. 4670-4674, 2010.

[41] M. H. Ibrahim, S. Kumari, A. K. Das, M. Wazid and V. Odelu, "Secure anonymous mutual authentication for star two-tier wireless body area networks", *Computer methods and programs in biomedicine*, vol. 135, pp. 37-50, 2016.

[42] O. Mir, T. van der Weide and C. C. Lee, "A Secure User Anonymity and Authentication Scheme Using AVISPA for Telecare Medical Information Systems", *J. Med. Syst.,* vol. 39, no. 89, pp. 1-16, 2015, DOI 10.1007/s10916-015-0265-8

[43] C-C. Lee, C-T. Li, S-T. Chiu and Y-M. Lai, "A new three-party-authenticated key agreement scheme based on chaotic maps without password table", *Nonlinear Dynamics,* vol. 79, no. 4, pp. 2485-2495, 2014a.

[44] C-C. Lee, D-C. Lou, C-T. Li and C-W. Hsu, "An extended chaotic-maps-based protocol with key agreement for multiserver environments", *Nonlinear Dynamics,* vol. 76, no. 1, pp. 853-866, 2014b.

[45] C-C. Lee, C-T. Li, C-W. Hsu, "A three-party password-based authenticated key exchange protocol with client anonymity using extended chaotic maps", *Nonlinear Dynamics,* vol. 73, no. 1-2, pp. 125-132, 2013b.

[46] C-C. Lee and C-W. Hsu, "A secure biometric-based remote client authentication with key agreement scheme using extended chaotic maps", *Nonlinear Dynamics,* vol. 71. no. 1-2, pp. 201-211, 2013.

[47] C-C. Lee, C-L. Chen, C-Y. Wu, S-Y. Huang, "An extended chaotic maps-based key agreement protocol with client anonymity", *Nonlinear Dynamics,* vol. 69, no. 1-2, pp. 79-87, 2012.

[48] C. Meshram, A. L. Imoize, A. Aljaedi, A. R. Alharbi, S. S. Jamal, S.K. Barve, "A Provably Secure IBE Transformation Model for PKC Using Conformable Chebyshev Chaotic Maps Under Human-Centered IoT Environments", *Sensors*, vol. 21, no. 21, pp. 7227, 2021.

[49] C. Meshram, A. L. Imoize, S. S. Jamal, P. Tambare, A. R. Alharbi, and I. Hussain, "An Efficient Three-Factor Authenticated Key Agreement Technique Using FCM Under HC-IoT Architectures," *Computers, Materials & Continua*, vol. 72, no. 1. pp. 1373–1389, 2022, doi: 10.32604/cmc.2022.024996.

[50] C. Meshram, A. L. Imoize, S. S. Jamal, A. Aljaedi, and A. R. Alharbi, "SBOOSP for Massive Devices in 5G WSNs Using Conformable Chaotic Maps," *Computers, Materials & Continua*, vol. 71, no. 3. pp. 4591–4608, 2022, doi: 10.32604/cmc.2022.022642.

Applied Analysis, Computation and Mathematical Modelling in Engineering, pp 271–281

Numerical Solution of Laplace and Poisson Equations for Regular and Irregular Domain Using Five-Point Formula

Malabika Adak

Conference paper | First Online: 30 June 2022

Part of the Lecture Notes in Electrical Engineering book series (LNEE,volume 897)

Abstract

In many areas of science and engineering, to determine the steady-state temperature, potential distribution, electricity, gravitation, Laplace and Poisson elliptic partial differential equation is required to solve. It is difficult to obtain an analytical solution of most of the partial differential equations that arise in mathematical models of physical phenomena. So, five-point finite difference method (FDM) is used to solve the two-dimensional Laplace and Poisson equations on regular (square) and irregular (triangular) region. To solve partial differential equation, specific boundary conditions

ECS Transactions

Review Article on Guillain Barre Syndrome

Akshat Pratap Singh[1], Sonali Rode[2], Minal Kalambe[3], Pratibha Dawande[1] and Nitin Wange[4]

ECS Transactions, Volume 107, Number 1

Citation Akshat Pratap Singh *et al* 2022 *ECS Trans.* **107** 18531

Abstract

Guillain-Barré syndrome (GBS) is an autoimmune disease caused by a viral or viral infection and can be reduced. The most common HIV virus is Campylobacter June, which is a major cause of bacterial gastroenteritis worldwide. Immune-mediated immune responses may play a role in the development of GBS by interacting with brain tissue. Because the infected organism contains homologous epitopes, it initiates molecular and cell immune responses that interact with the ganglioside surface areas of the peripheral nerve (cell imitation). The immune response to epitopes in the upper layer of Schwann cells acts as a target for acute inflammatory demyelinating neuropathy (85%) caused by a reaction to epitopes found in the Schwann-cell surface or myelin. A strong axonal variation of GBS is caused by a reaction to epitopes found in the axonal membrane (15 percent of cases). Although caring for these people may be difficult, complete predictions are good. The basis of treatment is to provide the best

2022 International Conference for Advancement in Technology (ICONAT)
Goa, India. Jan 21-22, 2022

Developing a framework of beta cryptosystem based on Santilli's isofields second-kind

Akshaykumar Meshram*
Department of Applied Mathematics, Yeshwantrao Chavan College of Engineering,
Nagpur, M.S., India 441110
akshaykjmeshram@gmail.com
*Corresponding Author

Rupesh Pohane
Department of Applied Mathematics, Suryodaya College of Engineering and Technology,
Nagpur, M.S., India 440027
rupeshpohane@gmail.com

Roshan Thakre
Department of Mathematics, Dharampeth M.P.Deo Memorial Science College,
Nagpur, M.S., India 440033
rthakre57@gmail.com

***Abstract*— Society initiated use of several gadgets for various purposes with the expansion in high-tech mechanisms, smart devices etc. So, there is enormous interest of data safety in cyberspace. The present endeavor takes the unique framework to create beta cryptosystem ($\mathcal{bc}$) built on santilli's isofields second-kind ($\mathcal{sisk}$), its safety is located in generalized isodiscrete-logarithm-problem ($\mathcal{gidlp}$) , isointeger-factorization-problem ($\mathcal{iifp}$) and $\mathcal{sisk}$ in the isoproduct isogroup of isofinite $\mathcal{sisk}$. To break the proposed framework of $\mathcal{bc}$ is to search isonumber from $\mathcal{sisk}$ and numerate both discrete $\mathcal{gidlp}$ and $\mathcal{iifp}$ side by side in the isoproduct isogroup of isofinite $\mathcal{sisk}$ in order to fetch genuine plaintext against the available cipertext and therefore present framework is feasible to succeed a greater level of safety.**

***Keywords*— public key cryptosystem ($\mathcal{pkc}$), $\mathcal{gidlp}$, $\mathcal{iifp}$ and $\mathcal{sisk}$.**

I. INTRODUCTION

In 1976, Diffie-Hellman recommended framework of key establishment mechanism for safe transmission between two subscribers, each subscriber requires two keys, namely, public key for encrypt the data in the form of ciphertext and secret key for decrypt ciphertext to retrieve original data [1]. The Diffie-Hellman key establishment mechanism is an important aspect in securing cyberspace. Henceforth, various $\mathcal{pkc}$ mechanisms were recommended and built on hard mathematical constructions that safety is reliant on the unfeasible factoring of enormous digit [2], insolubility of computing the square root modulo of enormous composite digit [3]. An effective $\mathcal{pkc}$ framework built on $\mathcal{dlp}$ that is complexity of prime field or elliptic curve described over a finite field recommended by ElGamal [4]. If mathematical construction for $\mathcal{dlp}$ and $\mathcal{ifp}$ are determined then entire $\mathcal{pkc}$ built on $\mathcal{dlp}$ and $\mathcal{ifp}$ are not authentic. Thus, $\mathcal{pkc}$ built on particular mathematical construction have safety concerns, consequently scholars have recommended $\mathcal{pkc}$ framework built on multiple hard mathematical constructions. Numerous $\mathcal{pkc}$ framework built on jointly $\mathcal{dlp}$ and $\mathcal{ifp}$ [5-12]. In 2017, Meshram et al. recommended few $\mathcal{pkc}$ frameworks built on mathematical construction based on $suzuki-2$ and $dihedral\ group$ [13-15]. A new perspective of $\mathcal{pkc}$ frameworks built on $partial\ \mathcal{dlp}$ recommended in [16]. In 2020, Meshram et al. recommended key exchange frameworks built on Santilli's isomathematics [17]. Futhermore, in 2021, Dani et al. recommended key exchange frameworks built on $\mathcal{si}$ first-kind and $\mathcal{sisk}$ [18-19], Thatere et al. recommended $iso\ \mathcal{bc}$ framework built on $\mathcal{si}$ first-kind [20] and Meshram et al. offered extended chaotic maps based off-line electronic cash protocol [21].

Unfortunately, $\mathcal{pkc}$ frameworks built on $\mathcal{dlp}$ and $\mathcal{ifp}$ have safety concerns as per our observation. Thus, we have recommended a novel $\mathcal{bc}$ built on $\mathcal{sisk}$, $\mathcal{gidlp}$ and $\mathcal{iifp}$ along its guaranteed safety, furthermore, we validated that it is enormously effective to be implemented in the cyberspace.

Accordingly, this article is separated into five parts. Mathematical background is explained in $part-II$ followed by $part-III$ which describes the $\mathcal{bc}$ framework. In $part-IV$, we have given subsidiary example for validation of recommended $\mathcal{bc}$ followed by $part-V$ which gives detailed safety analysis and efficiency performance. The last $part-VI$ delivers the Conclusion.

II. RESPECTIVE MATHEMATICAL MATERIAL

In this part, we will shortly present the respective mathematical material used to create $\mathcal{bc}$ built on $\mathcal{sisk}$, along with $\mathcal{gidlp}$ and $\mathcal{iifp}$ over isofields.

A. Mathematical construction of $\mathcal{sisk}$

If the isounit $\hat{\mathbb{I}}$ belong to the original field $\mathbb{F}$ and inverted isounit $\hat{\mathbb{I}}$ satisfy $\hat{\mathbb{I}}\hat{\mathbb{I}}=1$ such that $1\neq\hat{\mathbb{I}}=\frac{1}{\hat{\mathbb{I}}}\in\mathbb{F}$ then the product describe as $m\hat{\times}n=m\hat{\mathbb{I}}n\in\hat{\mathbb{F}}$ for each $m,n\in\mathbb{F}$ not raised to $\hat{m}=m\hat{\mathbb{I}}$ satisfy every theorem of a field is known as isoproduct in $\mathcal{sisk}$ [22].

B. Mathematical construction of $\mathcal{gidlp}$

The problem is to search an isonumber $\hat{a}\in[0,r-1]$ satisfy $\hat{b}\equiv\hat{g}\hat{a}$ for cyclic isogroup $\hat{G}$ of order $\hat{r}$, a primitive isoroot $\hat{g}$ of the isogroup isonumber $\hat{b}$ is known as $\mathcal{gidlp}$.

C. Mathematical construction of $\mathcal{iifp}$

The problem is to compute decomposition for positive isointeger $\hat{N}$ into isoprime isonumbers $\hat{N}=\widehat{p_1}*\widehat{p_2}*\widehat{p_3}\cdots\widehat{p_r}$ is known as $\mathcal{iifp}$.

III. PROPOSED THE RECOMMENDED FRAMEWORK

In this part, we have developed a framework of $\mathcal{bc}$ by utilizing $\mathcal{sisk}$ over isofield. The framework is inclusive of three procedures:

2022 International Conference for Advancement in Technology (ICONAT) | 978-1-6654-2577-3/22/$31.00 ©2022 IEEE | DOI: 10.1109/ICONAT53423.2022.9726000

Procedure-A: Key Design Mechanism:

Runs under below mentioned mechanism by subscriber-I for key design

i. Elect dual $\widehat{\mathcal{K}}$ and $\hat{\mathcal{L}}$, an extensive isoprime isonumbers with identical size.
ii. Compute isonumbers $\widehat{\mathcal{N}} = \widehat{\mathcal{K}} * \hat{\mathcal{L}}$ satisfy the isoeulerphi operate $\varphi(\widehat{\mathcal{N}}) = (\widehat{\mathcal{K}} - 1)(\hat{\mathcal{L}} - 1)$.
iii. Elect a random isonumbers $\hat{s}$ belong to $[1, \varphi(\widehat{\mathcal{N}})]$ satisfy greatest common divisor of $\hat{s}$ and $\varphi(\widehat{\mathcal{N}})$ is unity.
iv. Elect a random isonumbers $\hat{t} \in [2, \varphi(\widehat{\mathcal{N}}) - 1]$ and certain random isonumbers $\widehat{u}$ of the isoproduct isogroup $\widehat{\mathbb{Z}}^*_{\widehat{\mathcal{N}}}$ for computing $\widehat{v}_1 = \widehat{u}^{\hat{t}} (mod\ \widehat{\mathcal{N}})$.
v. Utilizing extended Euclidean mechanism to compute $\hat{s}\hat{q} \equiv 1 (mod\ \widehat{\mathcal{N}})$ for unique isonumbers $\hat{q} \in [1, \varphi(\widehat{\mathcal{N}})]$.

Hence, $(\widehat{\mathcal{N}}, \hat{s}, \widehat{u}^{\hat{t}})$ is an asymmetric isokey for corresponding isoprivate isokey $(\hat{q}, \hat{t}, \widehat{u})$

Procedure-B: Encryption Mechanism

Runs under below mentioned mechanism by subscriber-II for encrypt the data $\widehat{\mathcal{M}}(\hat{Q})$ to subscriber-I:

i. By utilizing asymmetric isokey $(\widehat{\mathcal{N}}, \hat{s}, \widehat{u}^{\hat{t}})$, an original data as $\hat{Q}$ satisfy $1 \le \hat{Q} \le \widehat{\mathcal{N}} - 1$, hashed and assume that the resultant in the form of $\widehat{\mathcal{M}}(\hat{Q})$.
ii. The ciphertext $\widehat{\mathfrak{C}}$ represents as $\left(\widehat{\mathcal{M}}(\hat{Q})\widehat{u}^{\hat{t}}\right)^{\hat{s}} (mod\ \widehat{\mathcal{N}})$

Procedure-C: Decryption Mechanism

Runs under below mentioned mechanism by subscriber-I to recover the original data $\widehat{\mathcal{M}}(\hat{Q})$ against the ciphertext $\widehat{\mathfrak{C}}$

i. Compute $\widehat{v}_2 = \widehat{u}^{\varphi(\widehat{\mathcal{N}})-\hat{t}} (mod\ \widehat{\mathcal{N}}) = \widehat{u}^{-\hat{t}} (mod\ \widehat{\mathcal{N}})$
ii. Then compute $\widehat{v}_3 = (\widehat{v}_2)^{\hat{s}} (mod\ \widehat{\mathcal{N}})$
iii. Compute $\left((\widehat{v}_2)^{\hat{s}} * \widehat{\mathfrak{C}}\right)^{\hat{q}} (mod\ \widehat{\mathcal{N}})$ to recover the original data $\widehat{\mathcal{M}}(\hat{Q})$

IV. SUBSIDIARY EXAMPLE FOR VALIDATION OF RECOMMENDED FRAMEWORK:

In this part, we have tested a subsidiary example for validation of recommended $\mathcal{bc}$ framework:

Procedure-A: Key Design Mechanism:

Runs under below mentioned mechanism by subscriber-I for key design

i. For given isonumbers $\widehat{\mathcal{N}}$, compute the isoeulerphi operate $\varphi(\widehat{\mathcal{N}}) = (\widehat{\mathcal{K}} - 1)(\hat{\mathcal{L}} - 1)$.
ii. Elect a random isonumbers $\hat{s} = 11 \in [1, \varphi(\widehat{\mathcal{N}})]$ satisfy $gcd(11,1176) = 1$.
iii. Elect a random isonumbers $\hat{t} = 19 \in [2, \varphi(\widehat{\mathcal{N}}) - 1]$ and certain random isonumbers $\widehat{u} = 10$ of the isoproduct isogroup $\widehat{\mathbb{Z}}^*_{\widehat{\mathcal{N}}}$ for computing $\widehat{v}_1 = \widehat{u}^{\hat{t}} (mod\ \widehat{\mathcal{N}}) = 10^{19} (mod\ 1247)$.
iv. Utilizing extended Euclidean mechanism to compute $11\hat{q} \equiv 1\ (mod\ 1247)$ for unique isonumbers $\hat{q} = 107 \in [1, \varphi(\widehat{\mathcal{N}})]$.

Hence, $(\widehat{\mathcal{N}}, \hat{s}, \widehat{u}^{\hat{t}})$ is an asymmetric isokey for corresponding isoprivate isokey $(\hat{q}, \hat{t}, \widehat{u})$

Procedure-B: Encryption Mechanism

Runs under below mentioned mechanism by subscriber-II for encrypt the data $\widehat{\mathcal{M}}(\hat{Q})$ to subscriber-I:

i. By utilizing asymmetric isokey $(\widehat{\mathcal{N}}, \hat{s}, \widehat{u}^{\hat{t}})$, an original data as $\hat{Q}$ satisfy $1 \le \hat{Q} \le \widehat{\mathcal{N}} - 1$, hashed and assume that the resultant in the form of $\widehat{\mathcal{M}}(\hat{Q}) = 1122$.
ii. The ciphertext $\widehat{\mathfrak{C}}$ represents as $\left(\widehat{\mathcal{M}}(\hat{Q})\widehat{u}^{\hat{t}}\right)^{\hat{s}} (mod\ \widehat{\mathcal{N}}) = 791$

Procedure-C: Decryption Mechanism

Runs under below mentioned mechanism by subscriber-I to recover the original data $\widehat{\mathcal{M}}(\hat{Q})$ against the ciphertext $\widehat{\mathfrak{C}}$

i. Compute $\widehat{v}_2 = \widehat{u}^{\varphi(\widehat{\mathcal{N}})-\hat{t}} (mod\ \widehat{\mathcal{N}}) = \widehat{u}^{-\hat{t}} (mod\ \widehat{\mathcal{N}}) = 917$.
ii. Then compute $\widehat{v}_3 = (\widehat{v}_2)^{\hat{s}} (mod\ \widehat{\mathcal{N}}) = 483$
iii. Compute $\left((\widehat{v}_2)^{\hat{s}} * \widehat{\mathfrak{C}}\right)^{\hat{q}} (mod\ \widehat{\mathcal{N}}) = 1122$ to recover the original data $\widehat{\mathcal{M}}(\hat{Q})$

V. SAFETY ANALYSIS AND EFFICIENCY PERFORMANCE

In this part, we have analyzed the safety and efficiency performance of recommended $\mathcal{bc}$ framework in following sub-part;

A. Consistency:

By showing below mentioned theorem to validate my recommended cryptosystem.

Theorem: If isokey design mechanism and encryped mechanism run efficiently then decrypted mechanism of encryption data in decrypted mechanism is appropriate.

Proof: If all encrypted data is correct then ciphertext $\widehat{\mathfrak{C}} = \left(\widehat{\mathcal{M}}(\hat{Q})\widehat{u}^{\hat{t}}\right)^{\hat{s}} (mod\ \widehat{\mathcal{N}})$ in encryption mechanism and $\widehat{v}_2 = \widehat{u}^{\varphi(\widehat{\mathcal{N}})-\hat{t}} (mod\ \widehat{\mathcal{N}}) = \widehat{u}^{-\hat{t}} (mod\ \widehat{\mathcal{N}})$ in decryption mechanism,

And $(\widehat{v}_2)^{\hat{s}} (mod\ \widehat{\mathcal{N}}) = \left(\widehat{u}^{-\hat{t}}\right)^{\hat{s}} (mod\ \widehat{\mathcal{N}})$, $\left((\widehat{v}_2)^{\hat{s}} * \widehat{\mathfrak{C}}\right)^{\hat{q}} (mod\ \widehat{\mathcal{N}}) = \left(\widehat{u}^{-\hat{t}\hat{s}} \left(\widehat{\mathcal{M}}(\hat{Q})\right)^{\hat{s}} \widehat{u}^{\hat{t}\hat{s}}\right)^{\hat{q}} (mod\ \widehat{\mathcal{N}}) = \left(\widehat{\mathcal{M}}(\hat{Q})\right)^{\hat{s}\hat{q}} (mod\ \widehat{\mathcal{N}}) = \widehat{\mathcal{M}}(\hat{Q}) (mod\ \widehat{\mathcal{N}})$

B. Safety Analysis:

- The recommended framework of $\mathcal{bc}$ is safe against below mentioned offensives, if attacker is unable to search $\hat{\mathbb{I}}$, an isounit of $\mathcal{bc}$
- It show that the $\mathcal{bc}$ framework is safe against under mentioned common offensives, if attacker is able to

search $\hat{\mathbb{I}}$.

- *Isodirect offensive*: By using the isonumber isofield sieve mechanism that is built on the size of isomodulus $\widehat{\mathcal{N}}$, attacker has to compute iifp and gidlp. Elect dual $\widehat{\mathcal{K}}$ and $\hat{\mathcal{L}}$ with $\frac{\widehat{\mathcal{K}}-1}{2}$ and $\frac{\hat{\mathcal{L}}-1}{2}$, an extensive isoprime isonumbers with identical size (of size 512-bit each) such that isomodulus $\widehat{\mathcal{N}} = \widehat{\mathcal{K}} * \hat{\mathcal{L}}$ to increase the safety of recommended $\mathcal{bc}$ framework.

- *Isofactoring offensive*: Assume that attacker have the confidential isonumbers $(\hat{u}, \hat{t})$ and recover the original data by exclude $\hat{u}^{\hat{t}}$ from ciphertex $\widehat{\mathfrak{C}}$. On the other hand gidlp still difficult to compute and therefore attacker would fail.

-*Isodiscrete logarithm offensive*: Assume that attacker recover the original data from ciphertex $\widehat{\mathfrak{C}}$ by computing gidlp and able to search confidential isonumbers $\hat{t}$ as attacker will aware to $\hat{v}_2$ and $(\hat{v}_2)^{\hat{s}}(mod\ \widehat{\mathcal{N}}) = (\hat{u}^{-\hat{t}})^{\hat{s}}(mod\ \widehat{\mathcal{N}})$. Regrettably, to recover the original data, attacker need have the confidential isonumbers $\hat{p}$ but this is infeasible as iifp is difficult to compute.

C. Efficiency performance:

For investigation and execution of the recommended $\mathcal{bc}$ framework in terms of transmission costs, isonumber of isokeys, and numerical intricacy. $\hat{\tau}_{-isoexp}$, $\hat{\tau}_{-isopro}$, $\hat{\tau}_{-isosq}$,$\hat{\tau}_{-isosq\_rt}$, $\hat{\tau}_{\_isoinv}$ and $\hat{\tau}_{-isohash}$ is the duration taken for performing isomodular isoexponentiation, isoproduct, isosquare, isosquare-root, isoinverse and isohash map computation respectively.

TABLE I. JUXTAPOSITION BETWEEN RECOMMENDED $\mathcal{bc}$ FRAMEWORK AND SIMILAR SUGGESTED $\mathcal{bc}$ FRAMEWORK IN [30]

$\mathcal{bc}$ framework	Thatere et al[30]	our recommended framework
asymmetric isokey	3	3
isoprivate isokey	3	3
numerical intricacy	encryption: $2\hat{\tau}_{exp} + \hat{\tau}_{mul} + \hat{\tau}_{hash}$ decryption: $3\hat{\tau}_{exp} + \hat{\tau}_{mul}$	encryption: $\hat{\tau}_{exp} + \hat{\tau}_{mul} + \hat{\tau}_{hash}$ decryption: $2\hat{\tau}_{exp} + \hat{\tau}_{mul}$
communication cost	encryption: $2n$ decryption: n	encryption: n decryption: n

VI. CONCLUSION

In this article, we have recommended new $\mathcal{bc}$ framework built on $\mathcal{sisk}$, gidlp and iifp in the isoproduct isogroup of isofinite isofields $\mathcal{sisk}$. If attacker is capable to compute mentioned offensive together then developed $\mathcal{bc}$ framework is broken and this is enormously unfeasible to happen. The offered $\mathcal{bc}$ framework remains safe as another problem is difficult to compute at the best in more timeframe. If the attacker anyhow achieves to search confidential isonumbers to one of the primary hard problem. Moreover, recommended $\mathcal{bc}$ framework is safe against the isodirect offensive, the isofactoring offensive and the isodiscrete logarithm offensive.

REFERENCES

[1] W. Diffie, M. Hellman, "New Directions in Cryptography", IEEE Transactions On Information Theory, vol.22, no.6, pp. 644-654, 1976.

[2] R. L. Rivest, A. Shamir, L. Adleman., "A Method to Obtain Digital Signature and Public key Crytosystem" Commun. ACM, vol 21, pp 121-126, 1978.

[3] M. Rabin, "Digitalized Signatures and Public Key Functions as Intractable as Factorization", 1st Edition, Massachusetts Institute of Technology, Laboratory for Computer Science, Ft. Belvoir Defense Technical Information Center, pp 18, 1979.

[4] T. ElGamal, "A public Key Cryptosystem and a Signature Scheme based on Discrete Logarithms", IEEE Transactions on Information Theory, Vol 31, pp 469-472, 1985.

[5] E.S. Ismail and M.S.N. Hijazi, "A New Cryptosystem Based on Factoring and Discrete Logarithm Problems" Journal of Mathematics and Statistics, vol.7 (3), pp. 165-168, 2011.

[6] C. Meshram and S. Meshram "PKC Scheme Based on DDLP" International Journal of Information & Network Security (IJINS), Vol.2 (2), April 2013, pp. 154-159.

[7] C. Meshram and S. Meshram "A Public Key Cryptosystem based on IFP and DLP" International Journal of Advanced Research in Computer Science, vol.2 (5), 2011 pp. 616-619.

[8] C. Meshram, "A Cryptosystem based on Double Generalized Discrete Logarithm Problem" International Journal of Contemporary Mathematical Sciences, Vol. 6(6), 2011, pp. 285 – 297.

[9] C. Meshram and S. Agrawal, "Enhancing the security of A Public key cryptosystem based on DLP γ≡ αaβb (mod p)" International Journal of Research and Reviews in Computer Science Vol.1 (4), pp.67-70, 2010.

[10] C. Meshram and S. Agrawal, "A New Design of Public Key Encryption Scheme Based on Double Discrete Logarithm Problem" Proceedings of International Conference on Challenges and Application of Mathematics in Science and Technology (CAMIST). January 11-13, 2010, pp. 495- 502.

[11] C. Meshram, "New PKC Technique based on DDLP in Metacyclic Group"- Proceedings of National Conference on Establishing Kinship between Mathematical Science and Society (NCKMS). October 30-31, 2009, pp. 141-147.

[12] G. C. Sheng "Multiplicative Learning with Errors and Cryptosystems" International Journal of Information & Network Security, Vol.3 (2), pp. 92-97, 2014.

[13] A. Meshram, C. Meshram and N. W. Khobragade, "An IND-CPA secure PKC technique based on dihedral group", Indian Journal of Computer Science and Engineering (IJCSE), vol. 8(2), pp.88-94, 2017.

[14] A. Meshram, C. Meshram and N. W. Khobragade, "An IND-CCA2 secure public key cryptographic protocol using suzuki 2-group", Indian Journal of Science and Technology, vol. 10(12), pp.01-08, 2017. doi: 10.17485/ijst/2017/v10i12/111588

[15] A. Meshram, C. Meshram and N. W. Khobragade, "Public key cryptographic technique based on suzuki 2-group", International Journal of Advanced Research in Computer Science, vol. 8 (03), pp.300-305, 2017.

[16] C. Meshram, M. S. Obaidat and A. Meshram, "New efficient QERPKC based on partial discrete logarithm problem", International Conference on Computer, Information and Telecommunication Systems (CITS), Hangzhou, China, (2020), 1-5, doi: 10.1109/CITS49457.2020.9232533.

[17] A. Meshram, C. Meshram, S. D. Bagde and R. R. Meshram, "RIPIC based key exchange protocol", Advances in Mathematics: Scientific Journal, vol. 9 (12), pp. 11169–11177, 2020. doi.org/10.37418/amsj.9.12.97

[18] M. S. Dani, A. Meshram, and C. Meshram, "Santilli's isofields first-kind based key exchange protocol" Journal of Physics: Conference Series, 1913, 012095, 2021. doi:10.1088/1742-6596/1913/1/012095.

[19] M. S. Dani, A. Meshram, C. Meshram, and N. M. Wazalwar, "An efficient key exchange scheme using santilli's isofields second-kind for secure communication", Advances in Mathematics: Scientific Journal, vol. 10 (2), pp. 1131–1139, 2021.

[20] A. B. Thatere, A. Meshram, C. Meshram, and N. M. Wazalwar, "SIFK based Isobeta Cryptosystem", International Journal of Engineering Trends and Technology, vol. 69 (7), pp. 76-79, 2021. doi: 10.14445/22315381/IJETT-V69I7P211.

[21] C. Meshram, M. S. Obaidat, K. -F. Hsiao, A. L. Imoize and A. Meshram, "An Effective Fair Off-Line Electronic Cash Protocol using Extended Chaotic Maps with Anonymity Revoking Trustee," 2021 International Conference on Communications, Computing, Cybersecurity, and Informatics (CCCI), 2021, pp. 1-5, doi: 10.1109/CCCI52664.2021.9583217.

[22] C. X. Jiang, "Foundations of Santillis Isonumber Theory with Applications", ISBN 1-57485-056-3, Hadronic Press, 2002.

2022 International Conference on Emerging Trends in Engineering and Medical Sciences (ICETEMS) | 978-1-6654-6112-2/22/$31.00 ©2022 IEEE | DOI: 10.1109/ICETEMS56252.2022.10093529

Effect of graphene on electrochemical performance of carbon nanofibers synthesized by electrospinning

D. V. Jamkar
Department of Applied Physics
YCCE
Nagpur, India
jamkardipti13@gmail.com

H. V. Ganvir
Department of Applied Physics
YCCE,
Nagpur, India
hrwasnik@gmail.com

R. Mahajan,
Pharmacy Department,
Nagpur College of Pharmacy
Nagpur, India
renukamahajan@ncpngp.com

S. B. Kondawar
Department of Physics
RTMNU
Nagpur India,
sbkondawar@yahoo.co.in

P. Kumar,
Faculty of Engineering & Technology,
DMIMSU,
Sawangi, India ,
pavank.feat@dmimsu.edu

***Abstract*-Carbon nanofibers (CNFs) of polyacrylonitrile (PAN)/N,N-dimethyl formamide (DMF) solution were synthesized by electrospinning method proceeded by stabilisation and carbonization in a tubular furnace of quartz. The electrochemical behaviour of the prepared sample was improved by employing Graphene nanosheets and porous graphene/carbon nanofibers (G/CNFs) via electrospinning technique were prepared. Further prepared samples were examined by UV–VIS spectroscopy and scanning electron microscopy (SEM) . These studies reveal nanoscale fibres of CNFs and G/CNFs with varying diameters from 300-600 nm with substantial porosity. The electrochemical performance of as prepared(pure) and Graphene embedded samples were studied at various scan rates using cyclic voltammetry. Pure CNFs exhibit a deformed rectangular CV curve with sharp redox peaks, whereas G/CNFs have a roughly rectangle-profile without redox peaks analogous to double-layer capacitor. Galvanostatic charge - discharged technique was employed for the measurement of specific capacitance. Samples CNFs and G/CNFs reflect improved electrochemical performance that may be corelated to the interlaying graphene nanosheets, which improves the internal electrical conductivity of G/CNFs.**

Keywords- PAN nanofibers, Carbon nanofibers, Electrospinning, Graphene/ carbon nanofibers Electrochemical performance.

I Introduction

In recent years, among the various nanostructured carbon compounds, graphene and carbon nanofibers (CNFs) have attained an increasing amount of interest for their use in supercapacitors. Among the 2D materials, graphene is the most recent discovery and is composed of a single layer of carbon atoms **[1-3]**, and is characterised by its unusual band structure with its quasi-particles similar to massless, chiral fermions.

Graphene has outstanding mechanical capabilities and a massive specific surface area (up to 3100 m^2/gm for a single graphene nanosheet), making it a promising material for a variety of applications with exceptional thermal and electrical conductivity and is simple to fabricate and functionalize **[4-10]**.

Massive volumes of slough graphene nanosheets from natural graphite were created inexpensively and without chemical oxidation, till date. As a novel class of carbon nanomaterials. These graphene nanosheets having a thickness of 3-5 nm and few monolayers exhibit amazing physical properties with good chemical properties**[11]**for Energy conversion and storage via electrochemistry. The porous electrodes of high-specific-capacitance supercapacitors, which are primarily based on the arrangement of graphene thin sheet into an aqueous electrolyte, have been infused with many graphene-based nanomaterials. **[12]**

The distinctive surface carbon orbital stacking patterns, CNFs have more functionalized surface area than CNTs. Recent research indicates that CNFs can enhance the kinetics of electron transport, reduce electrode surface fouling, and increase electrocatalytic activity in electrochemical investigations.**[13]**

Electrospinning is a low-cost, scalable, nonmanufacturing technique for creating nanofibers of polymers, composite, polymer-derived carbon materials, metals, metal oxides, ceramics, and other materials. It also offers a variety of methods for producing low-cost, porous, nanofibrous electrodes that might be utilised in supercapacitors and rechargeable batteries. CNFs, which are produced by carbonising manufactured electro-spun polymer nanofibers, display exceptional electrical and thermal conductivities as well as excellent connectivity for electrical and thermal current transmission, attracting the attention of material scientists and engineers worldwide. **[11]**

The chemical and physical characteristics of the electrode material employed in supercapacitors are crucial to the performance of many carbon-based storage devices. **[13-15]**As the electrode materials have a significant impact on

978-1-6654-6112-2/22/$31.00 ©2022 IEEE

the electrochemical performance of energy storage devices, it is critical to develop materials with high capacitance and power density in order to satisfy the needs of industry. Electrode electrochemical performance is affected by characteristics such as surface area, pore diameter, surface functions that facilitate a fast oxidation-reduction process, and electrical conductivity.

Electrodes made from carbonaceous materials are now under development because to their great chemical stability, low toxicity, low cost, and simplicity of manufacture. [16,17] Electrospun carbon nanofibers are an excellent option for electrode materials due to their high surface area and porosity. However, current applications of carbon nanofibers in supercapacitors have restricted their energy and power density. Aiming to improve the carbon nanofibers' electrochemical performance, modifications are made to the material. Nonwoven carbon webs were produced by Kim et al. by electrospinning**[**18].

Extended activation time during carbonization was demonstrated to be beneficial in the production of porous structural fibres. Fibre surface area increased, leading to improved capacitance. Similarly, carbon nanofibers with a porous structure may be generated by adding poly-methyl-hydro siloxane (PMHS) to the PAN precursor chemical mixture[19]. We built supercapacitor electrodes using continuous graphene-embeaded CNFs (G/CNFs).

The objective of this research was to emphasise electrospun CNFs' continuity and electrical conductivity and graphene's huge specific surface area along with strong electrical conductivity for storage of electrical energy. Electrospinning a solution made of polyacrylonitrile (PAN) and N,N-dimethylformamide (DMF) containing oxidised graphene nanosheets, then stabilising and finally carbonising the resulting porousG-CNFs was used to make them. Characterization and comparison with pure electrospun CNFs were performed on the electrochemical characteristics and chemical geometryof the innovative G/CNFs based electrodes.

II. Experimental Techniques

A. Synthesis Materials

Poly-acrylonitrile (PAN, Mw = 150,000) powder and N,N-dimethylformamide(DMF, 99%) were purchased from SigmaAldrichChemical Co. XG Sciences, Inc.(Lansing, MI,USA) provided highly graphitic graphene nanosheets that were as-grown.The average thickness of the oxidised graphene nanosheets was 6-8 nm, and they included oxygen at a weight percent of 1 wt%. No additional purification or alterations were made to any of the compounds before their use.

B. Synthesis of G/CNF films

Electrospinning yielded graphene-embeaded polyaniline (G/PAN) nanofibers, which were then employed as a starting material in the fabrication of graphene carbon nanotubes (G/CNFs). For the purpose of electrospinning G/PAN nanofibers, the following solution was prepared: grapheme nanosheets and PAN in DMF. PAN powder dissolved in DMF to form an 8wt% solution, and then oxidised graphene nanosheets (0.2 wt%) in DMF were added and stirred for 1hr at 60°C.For the electrospinning procedure the ready-to-use solution was poured into a syringe that had a stainless-steel spinneret attached to it, and it was then connected to a source of positive high-voltage DC power. The nanofibers were collected using a laboratory-made, 33-cm-diameter metal disc that was grounded electrically.

By providing a positive dc voltage of 18 kV across a gap of 22 cm across the spinneret and the grounded nanofiber collector, a strong DC electric field of 75-80 kV /m was produced. A digital flow controller, was employed to keep the electrospinning solution flowing at a steady 0.6 ml/hr.

After going through electrospinning, the synthesized G/PAN fiber films that were generated were scraped off the aluminium foil that was on the rotating discand then dried at 80 °Cin an oven for 10hr before undergoing stabilisation. In a tubular furnace of quartz, the as-prepared G/PAN nanofiber films were stabilised and carbonised.

For oxidative stabilisation of PAN, the G/PAN nanofiber films that had been electrospun were first heated at a rate of 1 degree Celsius per minute and then maintained at a temperature of 250 degrees Celsius for one hour in air. The film was then carbonised while the temperature was raised from 200°C to 800 °C in a nitrogen environment at a rate of 5 °C per minute and annealed at for 30 minutes at 800 °C. After that, the furnace was cooled by lowering the temperature 400 degrees Celsius in nitrogen, and the temperature kept constant at that level for one hour by injecting air. This step was essential for the activation of the carbonised G/PAN nanofibers.**[20,21].**

For the comparative study, pure CNF films were also synthesised utilising an 8 wt% PAN/DMF solution and the aforementioned processing conditions.

C. Sample Characterization

Both the CNF and G/CNF sample's surface morphology were studied by means of a scanning electron microscope (Carl Zeiss EVO18). UV-Visible spectroscopy was used to investigate the chemical composition of porous G/CNFs.

D. Electrochemical measurement

The electrochemical efficiency of three-electrode cells was studied. The specimen was mounted on a support that also functioned as the instrument's working electrode. In the three-electrode testing, a platinum foil served as the counter electrode and SCE electrode served as the reference electrode (0.242 V vs. SHE). Nitrogen was removed from a 0.5 M Na_2SO_4 electrolyte. The electrolyte was 0.5 M Na_2SO_4, which is a very dilute solution. Each sample's mass was calculated before the electrochemical tests were performed.

III. Results and discussions

A. Morphology and structural characterization

Typical scanning electron images of CNFs and G/CNFs are shown in Fig. 1. (a) and Fig. 1.(b) respectively. These CNFs had a diameter varying from 300 to 600 nm and a very smooth surface, and they were created by carbonising the precursor as-electrospun PAN nanofibers at 800ºC.

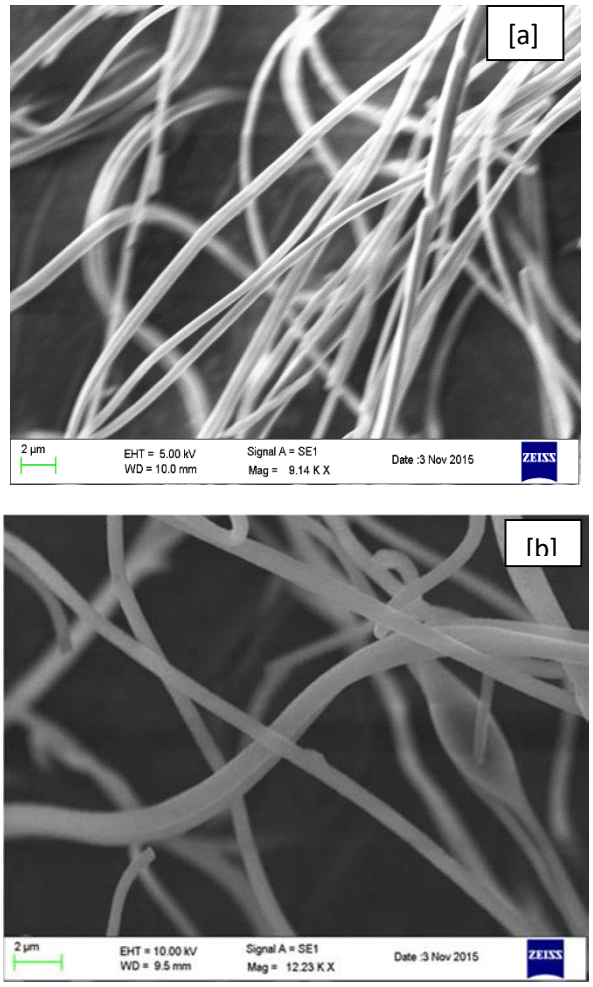

Fig. 1. (a): SEM image of CNFs; and (b) SEM image of G/CNFs.

Fig. 1. (b) illustrates how graphene inclusion causes some CNFs to have graphene sheets deposit on them. Due to their high electrical conductivity and large surface area, graphene nanosheets may allow for thinner electrodes and a reduction in the need for conductive fillers. **[11]**

UV-Visible spectra of CNFs and spectra of G/CNFs are shown in Fig 2.(a) and 2.(b) respectively.

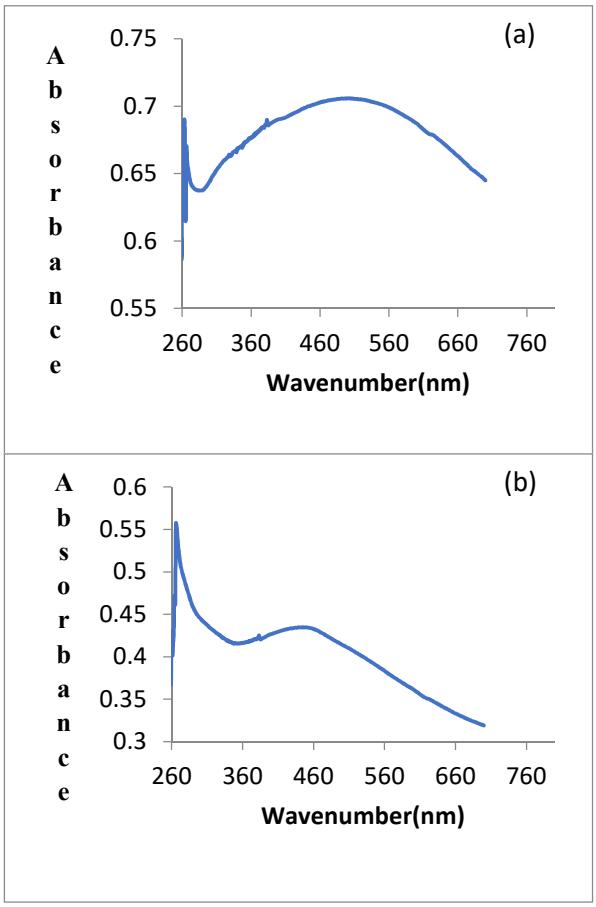

Fig. 2. (a): UV Spectra of CNFs; and (b) UV Spectra of G/CNFs.

For CNFs peak is observed at 505 nm and for G/CNFs peak is observed at 445 nm. It shows that by the addition of graphene in CNFs peak is shifted toward blue shift.

B. Electrochemical characterization:

Cyclic Voltammetric measurements were conducted for pure CNFs and G/CNFs to examine their electrochemical performance as supercapacitor electrodes in a 6 M KOH aqueous solution. Common CV graphs for electrodes of the CNF and G/CNF examined at 5–100 mV/s scan rates are shown in Fig 3. The CV curves of G/CNF electrodes have a roughly rectangular profile, analogous to that of a perfect double-layer capacitor, and there are no obvious redox peaks. To evaluate the electrochemical behaviour, at varying current densities, the GCD performance of electrodes made of CNF and G/CNF were investigated. The mean specific capacitance (SpC) of all the porous electrodes was computed by using:

$$C=\frac{I}{M}\times\frac{\Delta t}{\Delta V}$$

where I denotes steady charge/discharge current in amperes, t indicates discharge period in seconds, V signifies potential difference in volts, and M accounts for the combined mass of CNFs at the two electrodes during the discharge process (g).

Fig. 3 shows the CV curves of carbon nanofibers and graphene carbon nanofibers samples at various scan speeds ranging from 5 to 100 mV/s. As can be seen in Fig. 3(a) and (b), the carbon nanofibers take on a rectangular shape when the scan rate is between 5 and 100 mV/s.The optimum electrode materials may rapidly and uniformly produce a double layer in the linked topography between the electrode and the electrolyte. If the voltage scanning direction is reversed, the current can quickly return to its steady state. For this reason, the cyclic voltammetry curve for the perfect electrode material is nearly rectangular. At a scan rate of 5–100 mVs^{-1}, the integral area of a graphene carbon cyclic voltammetry curve is observed.

Pure CNFs and G/CNFs were evaluated using galvanostatic charge-discharge (GCD) measurement.For high-performance and useful EDLCs, the ability to keep a high capacitance during fast the processes is charge/discharge is a must. Using discharge curves, Equation (1) may be used to determine the electrode material's specific capacitance (Cs).

$$C_s = \frac{i\Delta t}{m(Vf-Vi)} \qquad (1)$$

Where, indicates the discharge current,, m defines the active material's mass in the electrode, Δt denotes the time required for a full discharge, V_f and V_i denotes respectively the potential limits of a full discharge. [22, 23]

Fig. 4 shows GCD profiles of CNFs and G/CNFs at current densities between 0.6A/g and 1.4 A/g. According to the CV curves, the shape of the charge/discharge curves looks like a triangle. This shows that the electric double-layer capacitance is working. At different current densities, Table 1 shows the specific capacitance CNFs and G/CNFs that have been calculated and found to be:

Table 1: Specific Capacitance of CNFs and G/CNFs at different current densities

Current Density	SpC (Fg^{-1}) of CNFs	SpC (Fg^{-1})) of G/CNFs
0.6	205.72	608.58
0.8	182.86	360
1.0	121.67	316.67
1.2	116.10	250
1.4	109.67	233.33

When the SpC of CNFs and G/CNFs at various current densities is analysed in Table 1, it is discovered that G/ CNFs have larger capacitance than CNFs. G/CNFs have a greater supercapacitance because of the additive impact that graphene and carbon nanofibers have on one another. Graphene may be linked together or shaped into beads in order to produce carbon nanofibers, resulting in a 3D porous network with a larger surface area of graphene. **[21].**

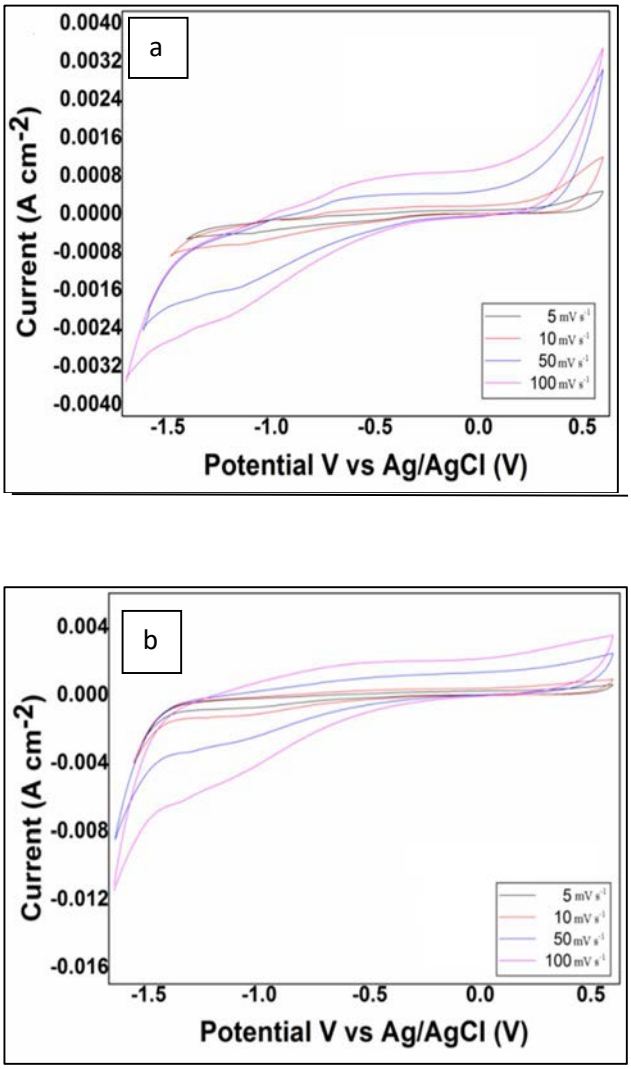

Fig. 3. (a) CV Curve of CNFs; and (b) CV Curve of G/CNFs.

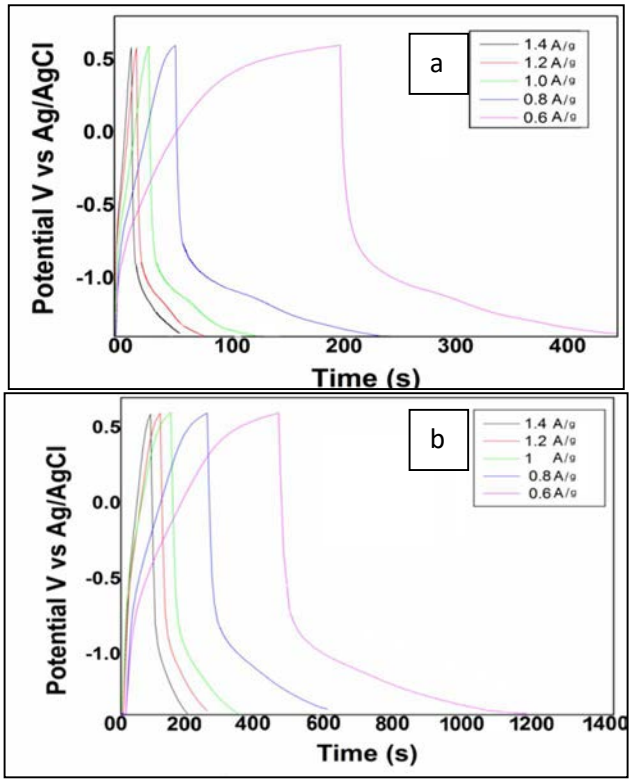

Fig. 4. (a) GCD of CNFs; and (b) GCD of G/CNFs.

IV. Conclusion

In this study prepared and structural with electrochemical characterization of a porous G/CNFs-based electrode material for high-performance batteries and supercapacitor is presented. The porous G/CNFs were effectively generated throughout the procedure through the process of electrospinning a chemical mixture of PAN in DMF that has been dispersed with oxidised graphene nanosheets, and then carbonising the material in a furnace. The graphene nanosheets implanted in carbonised PAN nanofibers had good connectivity, which enhanced the specific surface area along with the electrical conductivity of the G/CNFs that were produced therefore.

References

1. M.I.Katsnelsona, K. S. Novoselov , “Graphene: New bridge between condensed matter physics and quantum electrodynamics”, in Solid State Communications, 2007,144, pp. 3–13.
2. J.C.Meyer, A.K. Geim, M.I.Katsnelsond, K.S. Novoselov,D. Obergfelle, S. Rothe,C. Girita, A.Zettl , “On the roughness of single- and bi-layer graphene membranes”, in Solid State Communications, 2007,143, pp.101–109.
3. P. Blake,R. Yang,S.V. Morozov, F.Schedina,L. A.Ponomarenko, A.A.Zhukov, R.R. Nair, I.V Grigorieva, K.S.Novoselov, A.K. Geim , “Influence of metal contacts and charge inhomogeneity on transport properties of graphene near the neutrality point”, in Solid State Communications ,2009, 149 ,p. 1068–1071.
4. N.M.R. Peres, F.Guinea, A.H.C.Neto, “Electronic properties of two-dimensional carbon”,in Annals of Physics ,2006,321,pp. 1559–1567.
5. K. I. Bolotin,K.J.Sikes,Z. Jianga, M. Klima, Fudenberg. G , Hone. J , Kim. P. ,H. Stormer, “Ultrahigh electron mobility in suspended graphene”, in Solid State Communications ,2008 ,146 ,pp.351–355.
6. I.Calizo, S. Ghosh, W. Z.Bao, F.Miao,C.N.Lau, A.A.Balandin, “Raman nanometrology of graphene: Temperature and substrate effects”, in Solid State Communications , 2009,149, pp. 1132–1135.
7. J. R. Potts, D.R. Dreyer,S.Park, C. W. Bielawski. R. S. Ruoff, “Graphene-based polymer Nanocomposites”, in Polymer ,2011,52, pp. 5-25.
8. A.H.C Neto,V.N.Kotov, J. Nilsson, V.M.Pereira, N.M.R .Peres, B. Uchoa, “Adatoms in graphene”,in Solid State Communications,2009, 149, pp. 1094–1100.
9. S.I. Abdullah ,M.N.M.Ansari, “.Mechanical properties of graphene oxide (GO)/epoxy composites”,in HBRC Journal ,2015,11, pp.151–156.
10. Z. J.Li., B.C .Yang, S.R. Zhang, C.M. Zhao, “Graphene oxide with improved electrical conductivity for supercapacitorelectrodes”,in Applied Surface Science, 2012,258 , pp. 3726–3731.
11. Z.Zhou, W. Xiang-Fa,”Graphene-beaded carbon nanofibers for use in supercapacitor electrodes: Synthesis and electrochemical characterization”, in Journal of Power Sources, 2013, 222,pp.410-416.
12. P.Muthirulan ,R.Velmurugan, “Direct electrochemistry and electrocatalysis of reduced glutathione onCNFs–PDDA/PB nanocomposite film modified ITO electrode for biosensors” ,in Colloids and Surfaces B: Biointerfaces,2011, 83, pp. 347–354.
13. F. Ran, X. Zhang, Y. Liu, K. Shen, X. Niu, Y. Tan, L. Kong, L. Kang, C. Xu, S. Chen,” Super long-life supercapacitor electrode materials based on hierarchical porous hollow carbon microcapsules” ,in RSC Advances, 2015, 5, pp.87077–87083.
14. W. Gu, G. Yushin, “Review of nanostructured carbon materials for electrochemical capacitor applications: advantages and limitations of activated carbon, carbide-derived carbon, zeolite-templated carbon, carbon aerogels, carbon nanotubes, onion-like carbon, and grapheme”, in Wiley Interdisciplinary Reviews: Energy and Environment , 2014, 3, pp.424– 473.
15. Y.T. Li, Y.-T. Pi, L.-M. Lu, S.-H. Xu, T.-Z. Ren, “Hierarchical porous active carbon from fallen leaves by synergy of K2CO3 and their supercapacitor performance”, in J Power Sources, 2015, 299, pp.519–528.
16. Y. Zhang, H. Feng, X. Wu, L. Wang, A. Zhang, T. Xia, H. Dong, X. Li, L. Zhang, “Progress of electrochemical capacitor electrode materials: A

review", in Int. J. Hydrogen Energy, 2009, 34,pp. 4889–4899.
17. G. Wang, L. Zhang, J. Zhang, "A review of electrode materials for electrochemical supercapacitors", in Chem. Soc. Rev. , 2012 , 41, pp.797–828.
18. C. Kim, K.S. Yang, W.J. Lee, "The use of carbon nanofiber electrodes prepared by electrospinning for electrochemical supercapacitors", in Electrochem. Solid State Lett., 2004, 7, pp.A397–A399.
19. B.H. Kim, K.S. Yang, H.G. Woo, K. Oshida, "Supercapacitor performance of porous carbon nanofiber composites prepared by electrospinning polymethylhydrosiloxane (PMHS)/polyacrylonitrile (PAN) blend solutions", in Synth. Met., 2011, 161, pp.1211–1216.
20. A.M. More, H. J. Sharma, S.B. Kondawar, S.P. Dongre, "Ag-SnO2/Polyaniline composite nanofibers for low operating temperature hydrogen gas sensor", inJournal Material NanoSci, 2017, 4(1), pp.13-18.
21. D.V. Jamkar, B. J. Lokhande, S. B. Kondawar, "Improved electrochemical performance of free standing electrospungraphene incorporated carbon nanofibers for supercapacitor", in Journal Material NanoSci, 2019, 6(1),pp. 32-37.
22. K. Jiang, B. Sun, M. Yao, N. Wang, W. Hu, S. Komarneni, "In situ hydrothermal preparation of mesoporous Fe_3O_4 film for high performance negative electrodes of supercapacitors", in Microporous and Mesoporous Materials, 2018, 265, pp189–194.
23. O. Pech, S. Maensiri, "Electrochemical performances of electrospun carbon nanofibers, interconnected carbon nanofibers, and carbon-manganese oxide composite nanofibers",in Journal of Alloys and Compounds, 2019, 781,pp. 541-552.

Materials Today: Proceedings 49 (2022) 1827–1832

Contents lists available at ScienceDirect

Materials Today: Proceedings

journal homepage: www.elsevier.com/locate/matpr

Investigation of structural and electrical properties of nickel chloride doped pyrrole aniline copolymer

H.V. Ganvir [a,*], V.Y. Ganvir [a,*], R.S. Gedam [b]

[a] Department of Applied Physics, Yeshwantrao Chavan College of Engineering, Nagpur 441110, India
[b] Department of Physics, Visvesvaraya National Institute of Technology, Nagpur 440010, India

ARTICLE INFO

Article history:
Received 26 May 2021
Accepted 6 August 2021
Available online 23 August 2021

Keywords:
Pyrrole
Aniline
Copolymer
FTIR
SEM

ABSTRACT

Chemical oxidative copolymerization has been employed for the synthesis of pyrrole and aniline copolymer at room temperature, in equal proportion. The prepared copolymer was undoped and then further doped with 10% NiCl2 using immersion method. Structural characterization of self-doped, undoped and doped copolymer was performed using FTIR, WAXD and SEM techniques. Results reveal the modifications in the original copolymer structure accompanied by various shifts in the band positions and appearance of the new bands in IR spectrum due to doping. The X-ray diffractograms reveals presence of modified and shifted peaks indicating the changes due to doping. The scanning electron micrographs of undoped and doped copolymers show globular structure due to doping when compared with that of the parent copolymer. In addition, using two probe methods the dc electrical conductivity of these samples was recorded in the temperature range of 313 K to 673 K, at a field of 27 V/cm. The log σ Versus 1/T plots of the self-doped and doped samples display the transformation of the sample at a given temperature from metallic to semi conducting and vice versa. The I-V plots for the self-doped and doped copolymer has also been plotted at a fixed temperature of 323 K which shows linear behavior of the samples. The conductivity measurements show reduction in conductivity of prepared samples thereby suggesting the presence of bipolarons as charge carrier. The results confirm the effect of doping on the copolymer properties.

Selection and Peer-review under responsibility of the scientific committee of the Global Conference on Recent Advances in Sustainable Materials 2021.

1. Introduction

The quest of novel materials with improved structural, optical, electrical and thermal properties has resulted into a series of investigations. The traditional polymers can be designed and modified with a view to maximize their processibility and enhancing the conductivity. Thus various applications of these polymeric materials like polymeric batteries, display properties, photovoltaic cell, diodes, and electromagnetic shielding properties, dielectric, and magnetic properties have stimulated the researchers to study the properties of various polymers, composites and copolymers [1–3]. In comparison to composites, copolymerization provides the prospect of producing various functional polymers with unique composition, characteristics, and structure. Copolymerization also acts as a means of polymerizing/synthesizing certain monomers that do not individually polymerize [4]. Therefore, two completely separate monomers can be simultaneously polymerized in the same reaction formulation and desired chemical heterogeneity may be imparted. Thus copolymerization is considerably significant to study the effect of complexation on copolymer chain formation and its propagation.

Aniline and Pyrrole are the most exciting conducting polymers as they have fast polymerization capacities, and are environmentally safe and highly conductive. Amid these advantages, the two monomers have been frequently polymerized electrochemically (low yield) and to a little extent chemically as per literature. Hence aniline and pyrrole have been chemically polymerized in the present work so as to study the bulk properties. From literature survey it has been observed that very little work is devoted to study of doping of copolymers of pyrrole and aniline. Hence it was thought very interesting to investigate the doping mechanism and effect of NiCl2 on the structural and electrical properties of the copolymers.

* Corresponding authors.
E-mail addresses: hrwasnik@gmail.com (H.V. Ganvir), vyganvir@gmail.com (V.Y. Ganvir).

https://doi.org/10.1016/j.matpr.2021.08.049
2214-7853/
Selection and Peer-review under responsibility of the scientific committee of the Global Conference on Recent Advances in Sustainable Materials 2021.

Thus in the present work, the copolymer was synthesized and was doped using the NiCl2. Hence it was quite interesting to observe the different changes in structural and electrical properties of undoped and doped copolymers samples and are reported here.

2. Experimental procedure

2.1. Sample preparation

The raw materials Aniline and Pyrrole (SRL chemicals, Mumbai) were distilled before use. Acidic medium was developed using H2SO4 (Qualigen, Mumbai) and anhydrous ferric chloride was employed for initiation of copolymerization. The copolymerization was conducted chemically in the present work by bringing the monomers into equimolar proportions. Aniline and Pyrrole were rigorously mixed for fifteen minutes and 30 ml of sulphuric acid (0.5 M) was poured. The reaction mix was continuously stirred till it became apparent and then estimated volume of anhydrous FeCl3 (0.25 M) was added. The entire reaction mixture was stirred continuously at room temperature for around 1 h. Then the resulting mixture was permitted to polymerize for 24 h. The solution was then filtered, and the precipitate was washed with water and acetone alternatively in order to eliminate impurities. The sample was further dried and weighed to establish a constant weight.

To ensure copolymer formation during above mentioned process, a solubility test was conducted.

Polypyrrole (PPy) and polyaniline (PANI) are fully insoluble in DMF and DMSO; while the synthesized substance is soluble to a good degree in all these solvents [5]. Further the FTIR spectrum of physical mixture of aniline and pyrrole (1:1 proportion by weight) was compared with that of the copolymer. The bands produced in the two situations reside at different sides of the spectral range. Thus it can be claimed that copolymer has been produced.

Further insertion method was employed for doping of the prepared copolymer. For this purpose the sample was immersed in 50% ammonia solution for a period of 4.5 h. After that the sample was thoroughly cleaned with distilled water and acetone alternatively in order to eliminate excess ammonia. Further the sample was dried at 333 K till it was completely dried. Afterwards the sample was immersed in 10% NiCl2 again for a period of 4.5 hrs. The doped copolymer was then washed repeatedly with acetone and distilled water to reduce the surplus of NiCl2. The washed black powder was then dried at 333 K till it was completely dried and was studied further. The designations of the prepared copolymer, undoped copolymer and doped copolymer are tabulated in Table 1.

2.2. Infrared spectroscopy

The self doped, undoped and doped copolymers were then subjected to FTIR analysis. The transmission spectrums were recorded using a Schimadzu IR spectrometer in the wave number range 400–4000 cm^{-1} (FTIR-8101A).

Table 1
Designation of synthesized copolymer samples.

Designation	Sample
A	Self-doped Copolymer
A1	Undoped Copolymer
A2	10% $NiCl_2$ doped

2.3. Wide angle X-ray diffraction

Further the X-ray diffractograms of the self doped, undoped and doped samples were recorded with the help of XRD system PANalytical Xpert Pro. The source of radiation was the copper k alpha1-line from a sealed tube with a copper anode. The specimen sample was fixed on an aluminum holder in the form of a powder. On the revolving diffractometer stage, the holder was set. The sample was then scanned from 5o to 40o over a spectrum of 2θ in the reflection mode.

2.4. Scanning electron microscopy

To examine the morphology of the self-doped, undoped and doped copolymer samples, scanning electron microscopy was used. The amorphous powder was covered with platinum metal using a sputtering technique for this purpose. The scanning was done with the assistance of the JEOL 6380 A scanning electron microscope with different magnifications.

2.5. Measurement of DC electrical conductivity

The two probe method was used to determine the dc electrical conductivity of the prepared samples. Conductivity was evaluated at 323 K with differing voltage. Secondly, the conductivity at a field of 27 V/cm was measured within the temperature range of 313 K to 673 K. With the aid of the KEITHLY 6514 ELECTROMETER & Testronix digital operated dc power supply (0–300 V & 0–500 mA) measuring device, all measurements were carried out. Throughout the measurement, the heating rate was kept steady, i.e. 5oC per minute.

3. Results and discussion

In this work chemical copolymerization has been carried out by using FeCl3 as a catalyst. Further the self doped sample was undoped and then redoped using NiCl2. Hence self doped sample has been considered for comparative study of various physical properties.

For identifying the structure of prepared copolymers FTIR spectroscopy was employed. The respective IR band position of the self doped, undoped and doped samples along with PANI and PPy samples are being tabulated in Table 2. From the table, it is noticed that the charge delocalization peak appearing at 618 cm^{-1} in PANI is retained at 620 cm^{-1} in A sample only and C–H in plane vibration peak appearing in PPy at 610 cm^{-1} is vanished in all the three samples.

However the peak appearing at 780 cm^{-1} due to C–H out of plane bending in pyrrole is retained in A and A2 copolymer samples but vanished in the undoped sample. Moreover the out of plane C–H bending mode peak appearing at 816 cm^{-1} in PANI and at 830 cm^{-1} in PPy is not observed in all the three samples. The C–H out of plane deformation peak of PPy appearing at 910 cm^{-1} is shifted to 930 cm^{-1} in undoped copolymer only. Also the Charge delocalization peak appearing at 1048 cm^{-1} in PPy is retained in undoped sample and is modified in self doped and doped sample. Likewise the peak appearing at 1114 cm^{-1} owing to charge delocalization in PANI is retained only in self doped sample. Also the C-N stretching peaks appearing at 1250 cm^{-1}& 1290 cm^{-1} in PPy and 1302 cm^{-1} & 1385 cm^{-1} in PANI have totally disappeared from the IR spectrum of all the three copolymers. Similarly the ring stretching vibrational peak observed at 1451 cm^{-1} and C–C stretching vibrational peak occurring at 1510 cm^{-1} of PPy and benzenoid peak of PANI occurring at 1493 cm^{-1} have also disappeared from the copolymer spectrum [6–9]. In addition to

Table 2
IR band positions of PANI, Ppy, self-doped, undoped and doped copolymer samples.

PANI (cm^{-1})	Ppy (cm^{-1})	A (cm^{-1})	A1 (cm^{-1})	A2 (cm^{-1})
––	––	415	––	414
––	––	–	––	585
618	610	620	–––	––
––	780	700, 790	700, 750	770
816	830		––	–––
––	910	955	930	942
––	1048	1040	1049	1056
1114	––	1120	–––	–––
1160	1185	–	–––	–––
––	1250	1210	––	–––
––	1290	––	––	–––
1302	––		––	–––
1385	––		––	–––
––	1451		1400	1400
1493	––	––	––	–––
––	1510	––	––	–––
1599	––	1565	–––	–––
––	––	––	––	–––
1706	––	––	1830	1724
––	––	––	––	–––
––	––	2340	2360	2350
––	2843	–	–––	–––
––	2906	–	––	2855
––	2963		2920	2930
––	3441	3410	––	––

this several new peaks have been observed in the spectrum of self-doped, undoped and doped copolymers.

Thus from the analysis of IR bands of undoped copolymer sample, it appears that the IR spectrum of the copolymers is different from that of the homopolymers namely PANI and PPy. Further the IR spectrum of doped copolymers also shows different band positions from that of the parent copolymer as well as from that of the homopolymers. Now the shifting of the peaks to low wavenumber side may be due to transformation of chains from curly to outstretched; via the action of electrostatic interactions and hydrogen bonds, promoting thereby the degree of conjugation of the copolymer chains [10].

Further the interaction between temporary and permanent charges developed during the doping process leads to polar effects [11–13] due to which shifting or disappearance of peaks occur. A close observation of undoped and doped samples reveals that various new bonds are established between the basic copolymer backbone and the dopant groups thereby offering various new IR bands.

All the samples were subjected to X-ray diffraction analysis in order to determine the structure of the material produced. The individual diffraction peaks of these copolymers have been tabulated in Table 3. Figs. 1 and 2 display the X-ray diffractograms of undoped and doped copolymers respectively.

From table it is clear that PANI exhibits diffraction peaks at 9.5o, 14.7o, 20.4o, and 25.1o [6–9,14–15]. Similarly, PPy exhibits the diffraction peaks at only two positions i.e. at 23.6o & 25.8o [9]. From the close observation of 2θ values for all the copolymers, it is clear that samples A & A1shows common peak at 24o. However a common peak around 35o is observed in all the copolymer samples. Also the peak occurring at 25.1o in PANI and typical amorphous peak of polypyrrole observed at 25.8o, as well as the scattering of PPy chains at the interplanar spacing [9] has disappeared in all the samples.

This implies that these peaks must correspond to some common hetero linkage present in all the copolymers. This common linkage may be viewed as attachment of pyrrole and aniline unit with each other at some characteristic position of the monomers (i.e. C–N or C–H or N–H). From the table it can be seen that, in the as prepared copolymer there are more number of peaks as compared to the homopolymers. Most of these peaks correspond to higher values of 2θ. It can be further added that during copolymerization more pyrrole units have been oxidized as FeCl3 is a good initiator for pyrrole [5]. The undoping process removes the dopant ions but still primary chain remain unaffected hence changes in the diffractograms are seen.

Thus, owing to the copolymerization process structural changes occur and are again further modified/altered due to doping. This is revealed from the peak positions of A, A1 and A2. Hence it is interesting to note that FeCl3 has been used to synthesize the copolymer and NiCl2 is used as dopant. Thus the band positions of sample A are different than sample A2 indicating different association between the hetero units and dopant groups.

Also closer observation of d-values indicates that with increase in the diffraction angle there is a decrease in the d-values. This

Table 3
2θ peak positions and d-values for PANI, Ppy, A, A1 and A2 samples.

PANI	d-values (Å)	Ppy	d-values (Å)	A	d-values (Å)	A1	d–values (Å)	A2	d–values (Å)
9.5	4.6653	23.6	1.9233	9.5	4.6653	6	7.3664	12.3	3.6145
14.7	3.034	25.8	1.7691	14	3.1828	11	4.0354	26	1.7565
20.4	2.2090	––	––	14.8	3.0143	24	1.8931	30.2	1.5307
25.1	1.8151	––	––	18	2.4917	25.7	1.7755	35.4	1.3292
				21.5	2.1009	32.8	1.4214	39	1.2235
				24	1.8931	35	1.3424		
				29.4	1.5685	39.5	1.2105		
				33	1.4137				
				35.7	1.3195				

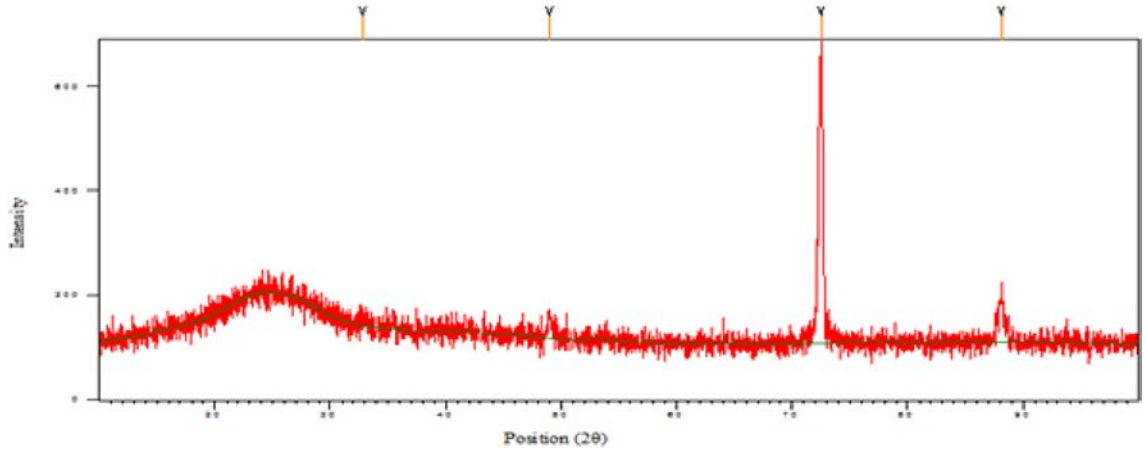

Fig. 1. X-ray diffractograms of undoped copolymer.

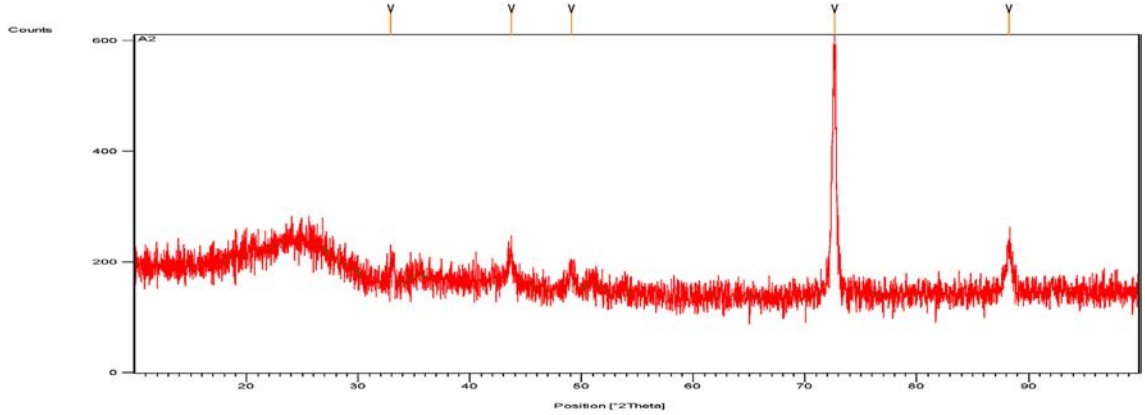

Fig. 2. X-ray diffractograms of NiCl2 doped copolymer.

decrease in the d-values indicates that all these polymeric chains are parallel to each other for homo polymer and constitute a particular plane. It can also be stated that due to hetero association small units may get created due to which the unit cell dimensions of the homopolymers are hindered. Further due to hetero linkages these crystal planes get closer and closer, implying that the copolymer chains are getting closer. The hetero attachment disturbs this parallel pattern and ultimately the geometry of the copolymer thereby making the samples amorphous.

The scanning electron micrographs for the self doped, undoped and doped copolymer samples are shown in Figs. 3, 4 and 5 respectively. From the comparative study of these electron micrographs the morphological changes can be prominently observed. From the SEM images it is clear that the self doped copolymer samples exhibit diffused cauliflower like structure in which small agglomerated spheres are observed throughout [16]. In this sample FeCl3 is getting self doped to small extent and thus small globular structure scattered in the amorphous region is observed. But when the sample is undoped, the globular structures are reduced and material appears to be amorphous matrix [5]. This can be attributed to hindrance in the particular chain alignment due to undoping. Moreover when the same sample is doped by using NiCl2 flake like structure clustered together with some agglomerated spheres were obtained.

The general observation of scanning electron micrograms indicates that the aniline and pyrrole units are getting copolymerized in such a way that uniform spherical structures are produced having size 10–20 μm. It can be further added that the morphology of the copolymer is affected by the feed ratio, synthesis temperature, initiator concentration and dopant concentration. This result is in good agreement with the x-ray diffractograms of the samples [17–21].

Further all the samples were subjected to dc electrical conductivity measurements. For this log I Versus log V plots for self doped and doped samples have been plotted at constant temperature and shown in Fig. 6. Both the curves are almost linear following the Ohm's law. Thus from these graphs it can be observed that as volt-

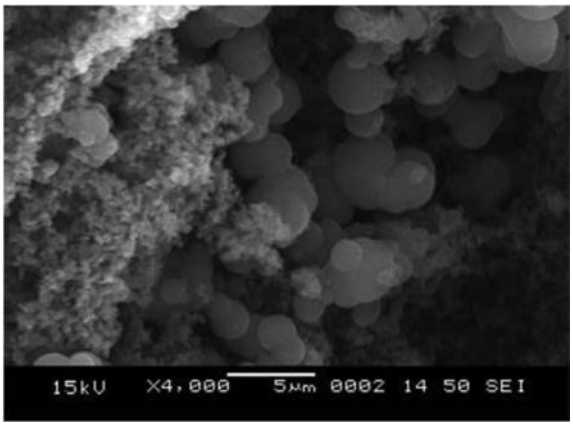

Fig. 3. SEM images sample A.

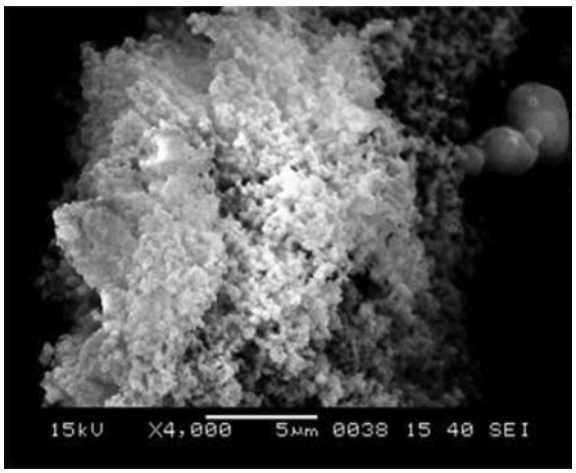

Fig. 4. SEM images sample A1.

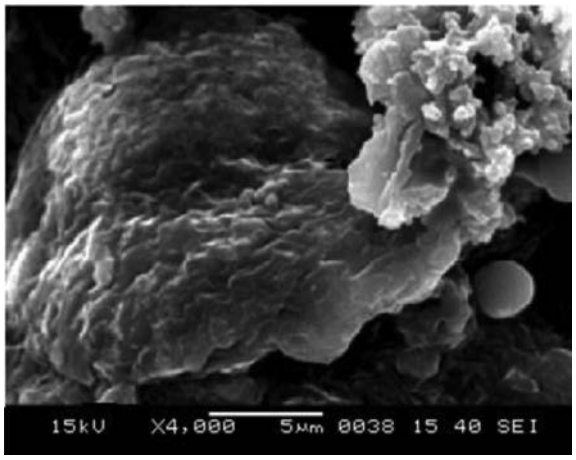

Fig. 5. SEM images sample A2.

age increases the current increases due to the alignment of the charge carriers in the direction of applied field. Polyaniline and polypyrrole exhibits non linear (non– Ohmic) behavior as the charge conduction is only due to free electrons in such type of intrinsic semiconductors.

However in case of copolymers polarons and bipolarons also participate in conduction process along with electrons [22]. Further the development of polarons and bipolars often rises as voltage increases thereby resulting in higher sample currents. The undoped samples purely represent the hetero association of pyrrole and aniline units. The dopant units attached to the primary polymer chain are removed due to undoping and very few charge carriers are left for conduction purpose. Hence the conductivity of undoped copolymers is very less and is recorded only at room temperature.

The electrical conductivity was also measured in the temperature range of 318–673 K at a fixed field of 27 V/cm using two probe method. The log σ Versus 1/T plot for the self doped and doped copolymer are shown in Fig. 7 and in Table 4, the conductivity of all the samples at 318 K is tabulated. From the table it is noticed that all the samples show reduced values of electrical conductivity. The reduction in the conductivity of copolymer can be attributed to steric impact of bulky substituent groups which offer torsional turns to the copolymer backbone. Hence the average delocalization interval of electron and co-planarity of the structure is reduced. Similar observations have been reported by Chen et al. [23], Huang et al. [24] and Wasnik et al. [25] in case of substituted polyanilines and aniline-substituted aniline copolymers. It is thus evident from the conductivity plots that the sample exhibit a transition at a certain temperature from metallic to semi conducting and vice versa above this transition temperature.

From Table 4. It is observed that doping does not increases the conductivity of the sample. In case of sample A, the FeCl3 is incorporated in such a manner that charge carriers are transported along and across the chain. But when same sample is undoped and then redoped the charge carriers are trapped at certain hetero linkages thereby reducing the conductivity. 1/T (K-1).

4. Conclusion

Pyrrole and aniline have been copolymerized chemically using FeCl3 as an initiator at room temperature successfully (self doped sample). The synthesized copolymer was then doped with 10% NiCl2. Further the samples were subjected to FTIR and X-ray diffraction studies which show various shifts in the IR as well as 2θ peak positions of undoped and doped samples thereby confirming the impact of doping on the primary copolymer chain. The Scanning electron micrographs confirms the structural changes in self doped and doped samples. Further conductivity measurement data shows that self doped sample is more conducting than the doped sample.

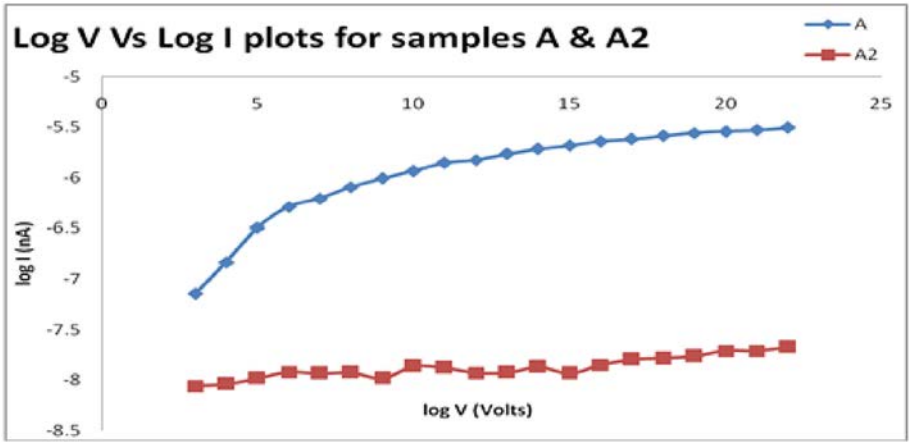

Fig. 6. Log I Versus log V plots for sample A & A2.

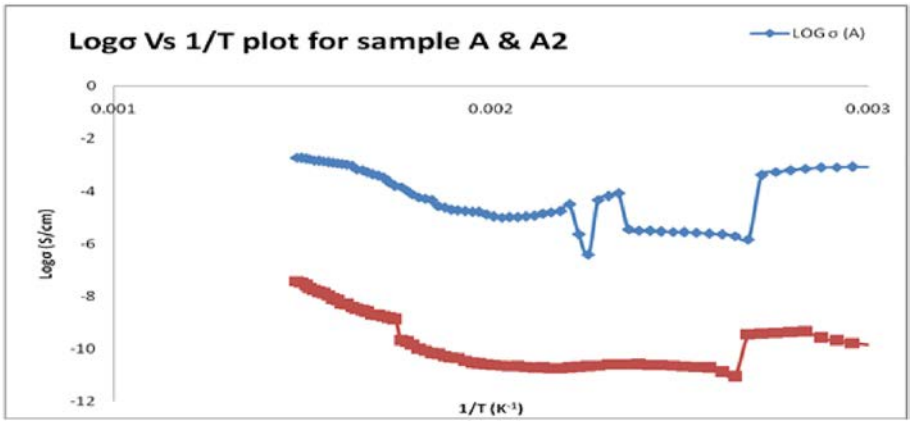

Fig. 7. Log σ Versus 1/T plots for sample A & A2.

Table 4
Values of conductivity σ (S/cm) for all the samples at 318 K.

Sample	Conductivity (S/m)
A	8.94529×10^{-8} S/cm
A1	9.65856×10^{-11} S/cm
A2	1.20218×10^{-10} S/cm

Declaration of Competing Interest

The authors declare that they have no known competing financial interests or personal relationships that could have appeared to influence the work reported in this paper.

References

[1] S. Panero, P. Prosperi, F. Bonino, B. Scrosati, A. Corradini, M. Mastragostino, Characteristics of electrochemically synthesized polymer electrodes in lithium cells—III. Polypyrrole, Electrochim. Acta 32 (1987) 1007–1011, https://doi.org/10.1016/0013-4686(87)90025-9.
[2] T.F. Oterol.C. B., Azcano Optimization of poly-3-methylthiophene to be used in advance polymer batteries, Int. J. Hydrogen Energy 25 (2000) 221–233, https://doi.org/10.1016/S0360-3199(99)00048-8.
[3] S.K. Dhawan, D. Kumara, M.K. Ram, S. Chandra, D.C. Trivedi, Application of conducting polyaniline as sensor material for ammonia, Sens. Actuators, B 40 (2–3) (1997) 99–103, https://doi.org/10.1016/S0925-4005(97)80247-X.
[4] H.L. Wang, A.G. MacDiarmid, Y.Z. Wang, D.D. Gebier, Application of polyaniline (emeraldine base, EB) in polymer light-emitting devices, Synth. Met. 78 (1) (1996) 33–37, https://doi.org/10.1016/0379-6779(95)03569-6.
[5] D.K. Moon, J.Y. Yun, K. Osakada, T. Kambara, T. Yamamoto, Synthesis of random copolymers of pyrrole and aniline by chemical oxidative polymerization, Mol. Cryst. Liq. Cryst. 464 (1) (2010) 177–185, https://doi.org/10.1080/15421400601030878.
[6] W. Chen, X. Li, G. Xue, Z. Wang, W. Zou, Magnetic and conducting particles: preparation of polypyrrole layer on Fe3O4 nanospheres, Appl. Surf. Sci. 218 (1–4) (2003) 16–222, https://doi.org/10.1016/S0169-4332(03)00590-7.
[7] M.E. Nicho, H. Hu, Fourier transform infrared spectroscopy studies of polypyrrole composite coatings, Solar Energy Mater. & Solar Cells 63 (4) (2000) 423–435, https://doi.org/10.1016/S0927-0248(00)00061-1.
[8] Y. Furukawa, S. Tazawa, Y. Fujii, I. Harada, Raman spectra of polypyrrole and its 2,5–^{13}C-substituted and C-dueterated analogues in doped and undoped states, Synth. Met. 24 (4) (1988) 329–341, https://doi.org/10.1016/0379-6779(88)90309-8.
[9] B. Tian, G. Zerbi, Lattice dynamics and vibrational spectra of polypyrrole, J. Chem. Phys. 92 (6) (1990) 3886–3894, https://doi.org/10.1063/1.457794.
[10] R.E. Partch, S.G. Gangoli, E. Matijevic, W. Cai, S. Arajs, Conducting polymer composites I: surface-induced polymerization of pyrrole on Iron(III) and Cerium (IV) Oxide particles, J. Colloid Interface Sci. 144 (1) (1991) 27–35, https://doi.org/10.1016/0021-9797(91)90234-Y.
[11] Y. Wei, R. Hariharan, S.A. Patel, Chemical and electrochemical copolymerization of aniline with alkyl ring-substituted anilines, Macromolecules 23 (3) (1990) 758–764, https://doi.org/10.1021/ma00205a011.
[12] H R Wasnik, D S Kelkar, Study of dc electrical conductivity, magnetic susceptibility and thermal behavior of pyrrole aniline copolymer, Mater. Sci. Eng. 73 (2015) 012026, https://doi.org/10.1088/1757-899X/73/1/012026.
[13] N. Gospodinova, L. Terlemezyan, Conducting polymers prepared by oxidative polymerization: polyaniline, Prog. Polym. Sci. 23 (8) (1998) 1443–1484, https://doi.org/10.1016/S0079-6700(98)00008-2.
[14] C.Y. Yang, P. Smith, A.J. Heeger, Y. Cao, J.E. Osterholm, Electron diffraction studies of the structure of polyaniline-dodecylbenzenesulfonate, Polymer 35 (6) (1994) 1142–1147, https://doi.org/10.1016/0032-3861(94)90004-3.
[15] H.L. Wang, J.E. Fernandez, Conducting polymer blends: Polypyrrole and Poly (vinyl methyl ketone), Macromolecules 25 (1992) 6179–6184, https://doi.org/10.1021/ma00049a014.
[16] N. Li, D. Shan, H. Xue, Electrochemical synthesis and characterization of poly (pyrrole-co-tetrahydrofuran) conducting copolymer, Eur. Polym. J. 43 (6) (2007) 2532–2539, https://doi.org/10.1016/j.eurpolymj.2007.01.048.
[17] H.R. Wasnik, D.S. Kelkar, V.Y. Ganvir, Yield analysis of copolymers: effect of temperature, feed ratio and initiator concentration on the copolymerization, J. Polym. Eng. 35 (2) (2014), https://doi.org/10.1515/polyeng-2014-0027.
[18] E. Unur, L. Toppare, Y. Yagci, F. Yilmaz, synthesis and characterization of thiophene-capped polytetrahedrofuran conducting copolymers, Mater. Chem. Phy. 91 (2–3) (2005) 261–268, https://doi.org/10.1016/j.matchemphys.2004.10.051.
[19] W.L. Wang, Y.H. Lai, synthesis and characterization of a novel 1,4-naphthalene based thiophene copolymers, Thin Solid Films 417 (1–2) (2002) 211–214, https://doi.org/10.1016/S0040-6090(02)00644-2.
[20] X.G. Li, L.X. Wang, M.R. Huang, Y.Q. Lu, M.F. Zhu, A. Menner, J. Springer, synthesis and characterization of pyrrole and anisidine copolymers, Polymer 42 (14) (2001) 6095–6103, https://doi.org/10.1016/S0032-3861(01)00092-1.
[21] Y. Feng, J.N. Hey, The characterization of random propylene-ethylene copolymer, Polymer 39 (25) (1998) 6589–6596, https://doi.org/10.1016/S0032-3861(97)10171-9.
[22] D. Patidar, N. Jain, N.S. Saxena, K. Sharma, T.P. Sharma, Electrical properties of Cds/polyaniline heterojunction, Braz; J. Physics 36 (4) (2006) 1210–2112, https://doi.org/10.1590/S0103-97332006000700016.
[23] S.A. Chen, G.W. Huang, Water soluble self- acid-doped conducting polyaniline: structure and properties, J Am. Chem. Soc. 117 (40) (1995) 10055–10062, https://doi.org/10.1021/ja00145a017.
[24] L.M. Huang, T.C. Wen, A. Gopalan, synthesis and characterization of soluble conducting poly (aniline-co-2, 5-dimethoxyaniline), Mater. Let. 57 (12) (2003) 1765–1774, https://doi.org/10.1016/S0167-577X(02)01066-2.
[25] H.R. Wasnik, D.S. Kelkar, IOP Conf. Ser.: Mater. Sci. Eng. 73 (2015), https://doi.org/10.1088/1757-899X/73/1/012026 012026.

Materials Today: Proceedings 51 (2022) 1201–1205

Contents lists available at ScienceDirect

Materials Today: Proceedings

journal homepage: www.elsevier.com/locate/matpr

Physical and optical study of Nd_2O_3 doped sodium borosilicate glasses

V.Y. Ganvir [a,*], H.V. Ganvir [a], R.S. Gedam [b]

[a] Department of Applied Physics, Yeshwantrao Chavan College of Engineering, Nagpur 441110, India
[b] Department of Physics, Visvesvaraya National Institute of Technology, Nagpur 440010, India

ARTICLE INFO

Article history:
Received 10 April 2021
Received in revised form 7 July 2021
Accepted 8 July 2021
Available online 7 August 2021

Keywords:
Optical properties
Concentration quenching
Borosilicate Glasses
Band gap
Density

ABSTRACT

In this research, Nd_2O_3 doped sodium borosilicate glasses were produced using a standard melt quench technique. Various characterization techniques, such as XRD analysis, FTIR spectroscopy, density analysis, absorption and photoluminescence spectroscopy measurements, were used to investigate the synthesized glassy samples. XRD spectra demonstrated the amorphous existence in the studied glasses. FTIR analysis was used to determine the stretching and bending vibrations of various borate groups. The high molecular weight of Nd_2O_3 and the broader ionic radius of Nd^{3+} ions resulted the rise in molar volume (V_m) and density (ρ) with inclusion of Nd_2O_3. The optical band gap was observed to shrink with increasing Nd^{3+} ion concentrations. The intensity of Nd^{3+} emission spectra improved from 0.5 mol per cent to 1.0 mol per cent with Nd_2O_3 material and the concentration quenching was reported at concentrations higher than 1.0 mol percent. The emission spectra of the synthesised glass shows three notable peaks found at 902 nm ($^4F_{3/2}\rightarrow{}^4I_{9/2}$), 1063 nm ($^4F_{3/2}\rightarrow{}^4I_{11/2}$) and 1334 nm $^4F_{3/2}\rightarrow{}^4I_{13/2}$ of Nd^{3+} ions transitions.

Selection and peer-review under responsibility of the scientific committee of the 1st International Conference on Computations in Materials and Applied Engineering – 2021.

1. Introduction

Recent studies have centered on REO doped glasses owing to their versatile applications like laser, optical amplifiers, sensors, display devices, light emitting diodes etc. [1,2]. In addition, the optical characteristics of REO doped glass materials play a crucial role in the progress of glass lasers and in the fabrication of various types of optical fibers and filter glass elements [3].

A comprehensive investigation on REO-doped glasses is necessary due to their variety of applications in optical storage devices, immobilization of radioactive waste materials, laser technology and optical communications [4,5]. Among different RE, neodymium oxide is mostly investigated and discovered to have a wide range of uses in photonic devices [1,3,4,6,7]. Nd_2O_3 doped glassy materials are continuously fascinating to scientist and researchers due to their extensive applications as laser materials and luminescent solar concentrators [8]. Furthermore, sodium borosilicate glasses are an outstanding host material for high-performance optics because of strong UV transmission and low exposure to defect [9,10].

Neodymium is indeed most finest rare earth elements used in solid-state lasers, with an emission wavelength of 1060 nm and the ability to lase at additional wavelengths such as 1800, 1350, and 880 nm, which is advantageous for broadband laser amplifiers and other photonic applications [9,10].

Due to wide applications and advantages of neodymium doped glasses, it is quite exciting to investigate the influence of Nd_2O_3 doping on sodium borosilicate glasses to examine their potential use as a laser medium. So in present work, we discuss in-depth analysis of various physical and optical characteristics of Nd_2O_3 doped sodium borosilicate glasses.

2. Experimental

The glass formulations employed in the current study '$30Na_2O$: ($70 - x\ Nd_2O_3$) {$1/7\ SiO_2$:$6/7\ B_2O_3$}' was prepared with normal melt quenching process where 'X' ranged from 0 to 2 in the stage of 0.5 mol percentage. High purity preliminary raw materials such as SiO_2, Na_2CO_3, B_2O_3 and Nd_2O_3 (Purity Quality greater than 99.9 per cent of make E-MERCK) were used for sample preparations. These additives were thoroughly blended in acetone for around 1 h in adequate amounts and then this mixture was kept for 3 h in a crucible made of platinum in an electric furnace at 1223–1273 K. Then this hot melt was poured into an aluminium

* Corresponding author.
E-mail address: vganvir291@gmail.com (V.Y. Ganvir).

https://doi.org/10.1016/j.matpr.2021.07.207
2214-7853/
Selection and peer-review under responsibility of the scientific committee of the 1st International Conference on Computations in Materials and Applied Engineering – 2021.

Table 1
Compositions of prepared glass samples.

Sample code	Na_2CO_3	B_2O_3	SiO_2	Nd_2O_3
0 BSNA	30	60	10	0
0.5 BSNAND	30	59.57	9.93	0.5
1.0 BSNAND	30	59.14	9.86	1
1.5 BSNAND	30	58.71	9.79	1.5
2.0 BSNAND	30	58.29	9.71	2

moulding at normal temperature to obtain the desired form of the bulk glass samples. Then immediately, these quenched bulk glasses were shifted to furnace at 590 K for three hours. This facilitates in the dissipation of thermal stress caused by quenching and then holding it for cooling till room temperature. The designation of samples along with their composition variation is listed in Table 1.

X-ray diffractograms of the synthesised glasses were recorded using 'X'pert pro-PANalytical'. FTIR spectrum was reported by a 'Perkin Elmer spectrometer' in the region 450–2000 cm^{-1}. SHIMADZU SMK-401 density measuring instruments (Archimedes principle based) was employed to estimate the density of prepared glasses where toluene is used as dipping solvent.

These prepared glasses were then converted in powder form by crushing which was used for photoluminescence research. The luminescence and excitation spectra of the synthesized glass specimens were performed using a fluorescence spectrometer model 'JASCO-FP-8200'. The optical absorption spectrum was obtained using the JASCO V-670 Spectrometer at room temperature.

3. Results and discussion

Fig. 1 presents the XRD pattern of all synthesized glasses having different concentration of Nd_2O_3. This X-ray spectrum is characterised by broad humps and a lack of prominent peaks associated with any of the sample components. This demonstrates the amorphous nature of the material.

The FTIR spectra of samples of sodium borosilicate glass doped with Nd_2O_3 is shown in Fig. 2. The 460 cm^{-1} band refers to B-O-Si stretching and Si–O–Si and O–Si–O bending. The Si-O-Si stretching vibration is assigned to the 701 cm^{-1} band. [4,11]. The band present about 819 cm^{-1} is associated with the vibration of the B-O bond in the BO_4 unit. The band at 943 cm^{-1} is related to the B-O bond stretching in the di borate functional unit [4,11]. The stretching modes of BO_4^- tetrahedral boron are responsible for the weak band that emerged at 1121 cm^{-1}.

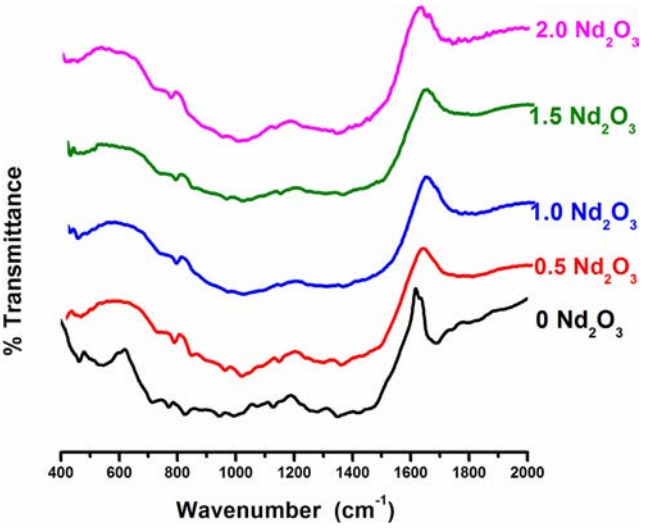

Fig. 2. FTIR spectra of Nd_2O_3 containing sodium borosilicate glasses.

The band at 819 cm^{-1} shifts little bit towards the lower wave number side, while the band at 1121 cm-1 switches slightly to the higher wave number side. This change in the band's location demonstrates the structural changes and formation of BO_4 units [4,11]. Thus from this spectra, the presence of BO_4^- tetrahedra is confirmed by observed bands for Nd_2O_3 doped sodium borosilicate glasses [4,11].

Fig. 3 depicts the variation molar volume (V_m) and density (ρ) for Nd_2O_3 comprising studied glasses. The molar volume (V_m) and density increases with increasing Nd_2O_3 material, as seen in this graph. The relatively high molecular weight of neodymium oxide than other additives (Molecular weight of Nd_2O_3 is 336.48 gm/mol, Na_2CO_3 = 105.9888 g/mol , SiO_2 = 60.08 g/mol, B_2O_3 = 69.63 g/mol) and a larger Nd^{3+} ion radius are accountable for the rise in molar volume and density This large radius of Nd^{3+} ion causes expansion of glassy structures thereby increasing the molar volume. Also Nd^{3+} ions are fitted to the voids connected with the BO_4^- units that open the glassy structure. These findings are

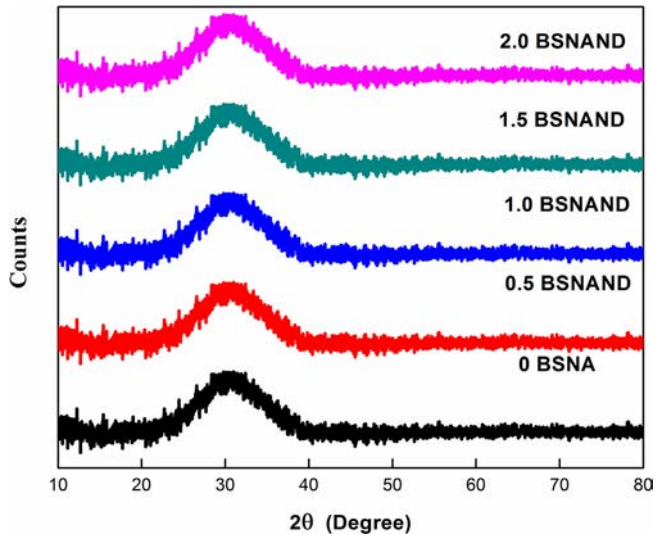

Fig. 1. XRD diffraction spectra of sodium borosilicate glasses doped with Nd_2O_3.

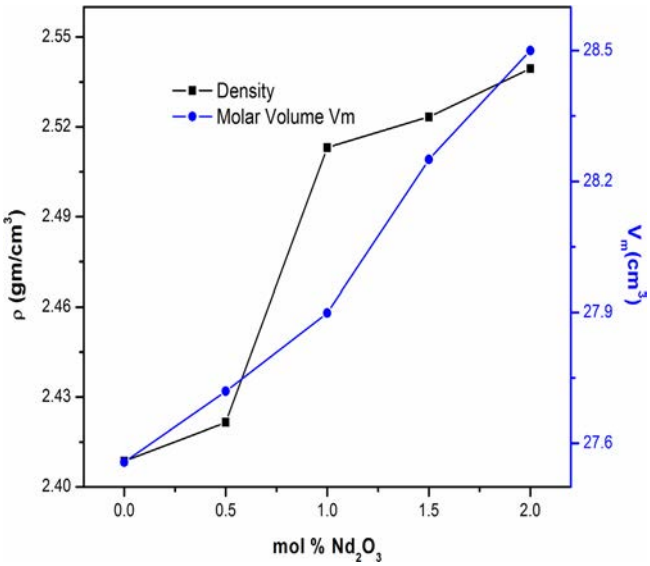

Fig. 3. Density and molar volume as a function of Nd_2O_3 concentration.

reasonably compatible with the published results, where molar volume and glass density increase with REOs [11,12]. In addition to this, different physical parameters like neodymium ions concentration (N), molar volume (V_m), polaron radius (r_p), field strength (F) and inter nuclear distance (r_i) were determined using the density values. These physical parameters were estimated using standard formulae [12-14]. The physical parameters perform a trivial role in clarifying atomic arrangements in the glass network and provide useful knowledge regarding glass structure [11-15].

Tables 2 represent the physical properties acquired for the studied glass system. It is found that with rise in Nd^{3+} ions, polaron radius (r_p) and inter-nuclear distance (r_i) values declines. Reduction in r_i and r_p values indicates an improvement in Nd-O bond power, which increases overall field strength (F) around Nd^{3+} ions. These physical parameter values reinforce the density findings and the compactness of glass construction with the rise of Nd^{3+} ions.

Fig. 4 illustrates the optical absorption spectra of studied glass system carried at room temperature and its assignment of different absorption bands. This spectra indicates that Nd^{3+}-containing glasses display a variety of absorption bands in contrast to base glass. It is also noticed that the absorbance intensity enhances with the addition of Nd_2O_3. The various bands found in the absorption spectra are 1) 350 nm ($^2I_{11/2}$), 2) 356 nm ($^4D_{3/2}$), 3) 430 nm ($^2P_{1/2}$), 4) 474 nm ($^2G_{9/2}$), 5) 511 nm ($^4G_{9/2}$), 6) 524 nm ($^4G_{7/2}$), 7) 583 nm ($^4G_{5/2}$), 8) 625 nm ($^2H_{11/2}$), 9) 680 nm ($^4F_{9/2}$), 10) 746 nm ($^4S_{3/2}$ + $^4F_{5/2}$), 11) 803 nm ($^4F_{5/2}$) and 12) 873 nm ($^4F_{3/2}$) . These bands were identified by contrasting their energy to that of Carnall et al. [16] and those reported in the literature [17-19].

It is obvious from this figure that the absorption edge is not precisely and sharply established for all glasses due to its amorphous existence. The optical edges offers valuable knowledge pertaining to optical band gap and optically induced transitions in glassy materials. The linear part of the plot is extended to in order to evaluate the energy band gap values of all synthesized glasses, as given in table 3 which illustrates that optical energy band gap (E_g^{Opt}) declines as the content of Nd_2O_3 increases. This reduction in the energy band gap (E_g^{Opt}) with the inclusion of Nd_2O_3 could be attributed to structural modifications [20-22] which are apparent from the FTIR findings. Theses structural modifications increases the degree of localizations, resulting in the amount of the donor centres in the glass network [20-22]. The formation of donor centres as a consequence of the inclusion of Nd_2O_3 reduces the optical band gap.

Fig. 5 displays the 0.5 mol% excitation spectra of Nd_2O_3 doped sodium borosilicate glass sample monitoring emission at 1063 nm. The excitation spectra reveals seven prominent peaks owing to quantum transition from lower energy state to excited state. These peaks corresponds to 432 nm ($^4I_{9/2}\rightarrow{}^2P_{1/2}$), 474 nm ($^4I_{9/2}\rightarrow{}^2G_{9/2}$), 513 nm ($^4I_{9/2}\rightarrow{}^4G_{9/2}$), 527 nm ($^4I_{9/2}\rightarrow{}^4G_{7/2}$), 588 nm ($^4I_{9/2}\rightarrow{}^4G_{5/2}$), 682 nm ($^4I_{9/2}\rightarrow{}^4F_{9/2}$) and 744 nm ($^4I_{9/2}\rightarrow{}^4F_{7/2}$). It is found that the peak at 588 nm is more prominent among all which is chosen as an excitation wavelength for measurement of emission spectra.

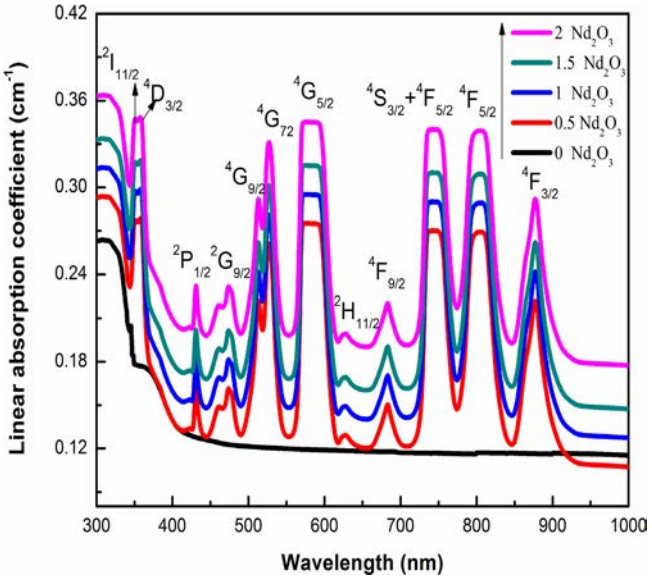

Fig. 4. Absorption spectra of studied glass samples (carried at Room temperature).

Table 3
Optical energy band gap for Nd_2O_3 doped sodium borosilicate glasses.

Mol % Nd_2O_3	Band gap E_g^{Opt}(eV)
0	3.4734
0.5	3.3333
1	3.2208
1.5	3.1714
2	3.1313

Fig. 6 illustrates the emission spectra (excited at 588 nm) of Nd^{3+} containing sodium borosilicate glass samples. This spectrum has three prominent bands at 902 nm ($^4F_{3/2}\rightarrow{}^4I_{9/2}$), 1063 nm ($^4F_{3/2}\rightarrow{}^4I_{11/2}$) and 1334 nm ($^4F_{3/2}\rightarrow{}^4I_{13/2}$) attributable to Nd^{3+} ions transitions. The emission spectrum demonstrates that the emission intensity rises till 1 mol% Nd_2O_3 and emission intensity declines with the further increase in Nd_2O_3. This phenomenon is known as luminescence quenching. The intensity of emission spectra depends on number of active centers. The active centers are Nd^{3+} ions in the present glassy matrix. The density of Nd^{3+} ions rises with the doping of Nd_2O_3 at the expense of B_2O_3 and SiO_2. As a result of which, emission rate rises up to 1 mol% Nd_2O_3. With a rise in the concentration of Nd^{3+} ions, the intermolecular gap decreases and above 1 mol percent of Nd_2O_3, the Nd^{3+} ions are very closed resulting significant interaction between Nd^{3+} ions. Thus, there is an effective transfer of energy among Nd^{3+} ions leads to luminescence quenching as displayed in Fig. 6. These findings are reasonably consistent with previously published results [18-22].

Table 2
Physical properties of the glasses.

Parameters	Unit	0	0.5	1.0	1.5	2.0
P	(g/cm^3)	2.4086	2.4215	2.5131	2.5233	2.5394
V_m	(cm^3)	27.5569	27.7193	27.8989	28.2501	28.5001
(N) ($\times10^{22}$)	($ions/cm^3$)	–	1.0769	2.1919	3.2383	4.2641
r_i	(Å)	–	4.5283	3.5732	3.1373	2.8624
r_p	(Å)	–	1.8246	1.4398	1.2641	1.1533
(F) ($\times10^{17}$)	(cm^{-2})	–	1.8023	2.8945	3.7547	4.5107

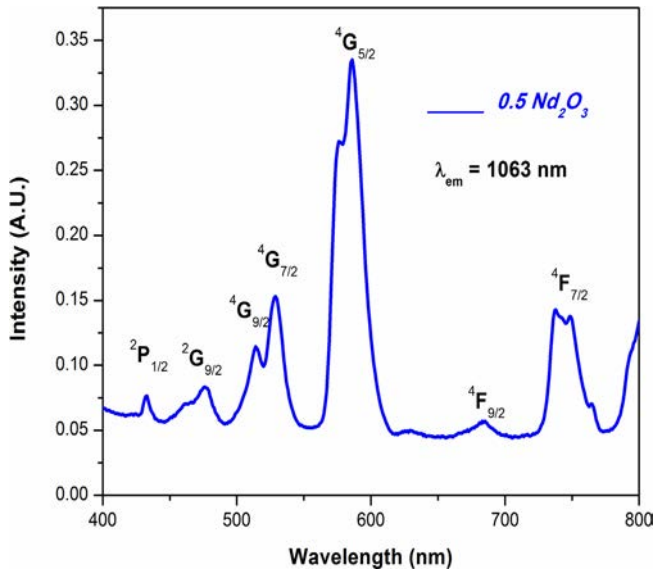

Fig. 5. Excitation spectra of 0.5-BSNAND glass sample (λ_{em} = 1063 nm).

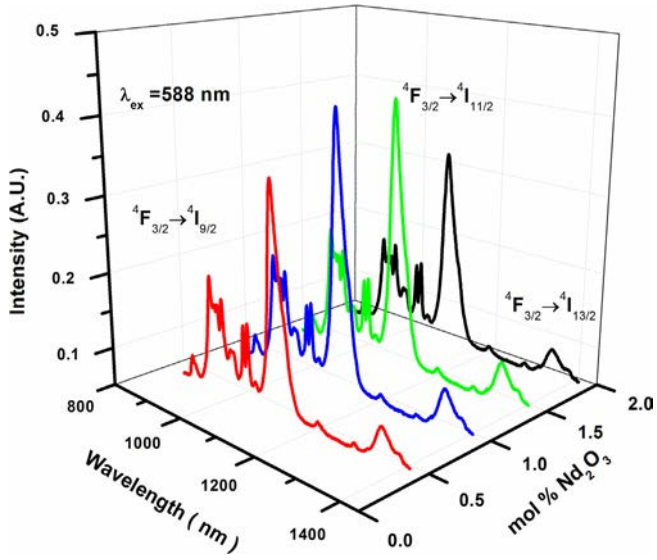

Fig. 6. Emission spectra for Nd_2O_3 containing sodium borosilicate glass samples.

4. Conclusion:

The current study used the melt-quench process to prepare various concentrations of Nd^{3+} doped LBS glasses. XRD, FTIR, absorption and photoluminescence were used to assess their structural and spectroscopic characteristics. All synthesized glasses revealed to be amorphous by XRD study. The FTIR analysis verified the different functional groups. The addition of neodymium oxide increased the density of produced glass samples, which is ascribed to the molecular weight of Nd_2O_3. The estimated values for different physical properties such as neodymium ion concentrations (N), polaron radius (r_p), mean spacing between RE ions (r_i), and field intensity (F) of Nd-O bonds appear to support change in glass density and molar volume. Optical absorption study shows increase in absorbance with the additions of neodymium oxide. The optical energy band gap (E_g^{Opt}) of prepared glass samples found to decrease with the inclusion of neodymium oxide due to structural changes. The emission spectra of Nd_2O_3 comprising sodium borosilicate glasses emits infrared emissions at 902 nm, 1062 nm and 1334 nm attributable to '$^4F_{3/2}\rightarrow{}^4I_{9/2,\ 11/2,\ 13/2'}$ Nd^{3+} ions transitions. The luminescence quenching anomaly is observed above 1 mol percent. This is effectively interpreted by means of neodymium ions content and 'Nd^{3+} - Nd^{3+}' interaction in the glassy matrix. A significantly greater $^4F_{3/2}\rightarrow{}^4I_{11/2}$ transitions intensity indicates the glass can be suitable for 1.06 μm IR laser applications. The excellent correlation between physical and optical properties is observed in studied glass system.

CRediT authorship contribution statement

V.Y. Ganvir: Investigation, Writing – original draft. **H.V. Ganvir:** Conceptualization, Writing - review & editing, Supervision. **R.S. Gedam:** Formal analysis, Data curation.

Declaration of Competing Interest

The authors declare that they have no known competing financial interests or personal relationships that could have appeared to influence the work reported in this paper.

References

[1] Yogesh Kumar Sharma, Priyanka Goyal, Sudha Pal, Umesh Chandra Bind, Optical and physical analysis of Nd3+ doped borosilicate glasses, J. Mater. Sci. Eng. B. 5 (12) (2015), https://doi.org/10.17265/2161-6221/2015.11-12.002.
[2] P.P. Pawar, S.R. Munishwar, R.S. Gedam, Physical and optical properties of Dy3 +/Pr3+ Co-doped lithium borate glasses for W-LED, J. Alloy. Compd. 660 (2016) 347–355, https://doi.org/10.1016/j.jallcom.2015.11.087.
[3] A. Rajiv, M.S. Reddy, J. Uchil, C.N. Reddy, Thermal and optical properties of sodium-phospho - zinc - neodymium oxide glass system, J. Adv. Sci. Res. 5 (2014) 32–39.
[4] D.D. Ramteke, K. Annapurna, V.K. Deshpande, R.S. Gedam, Effect of Nd3+ on spectroscopic properties of lithium borate glasses, J. Rare Earths 32 (12) (2014) 1148–1153, https://doi.org/10.1016/S1002-0721(14)60196-4.
[5] M. Dejneka, B. Samson, Rare-earth-doped fibers for telecommunications applications, MRS Bull. 24 (9) (1999) 39–45, https://doi.org/10.1557/S0883769400053057.
[6] K Gatterer, G Pucker, W Jantscher, H.P Fritzer, S Arafa, Suitability of Nd (III) absorption spectroscopy to probe the structure of glasses from the ternary system Na 2 O ± B 2 O 3 ± SiO 2, 231 (1998) 189–199. https://doi.org/10.1016/S0022-3093(98)00375-5
[7] P. Chimalawong, J. Kaewkhao, C. Kedkaew, P. Limsuwan, Optical and electronic polarizability investigation of Nd3+-doped soda-lime silicate glasses, J. Phys. Chem. Solids 71 (7) (2010) 965–970, https://doi.org/10.1016/j.jpcs.2010.03.044.
[8] J. Li, Y.Z. Mei, C. Gao, F. Ren, A.X. Lu, Variation of luminescence properties of Na2O–CaO–SiO2: Nd3+ glass with crystallinity, J. Non. Cryst. Solids. 357 (2011) 1736–1740, https://doi.org/10.1016/j.jnoncrysol.2010.12.073.
[9] W. Krupke, Induced-emission cross sections in neodymium laser glasses, IEEE Journal of Quantum Electronics, 10 (4) (1974), 450-457, April 1974, doi: 10.1109/JQE.1974.1068162.
[10] M.J. Weber, Science and technology of laser glass, J. Non-Crystall. Solids 123 (1–3) (1990) 208–222, https://doi.org/10.1016/0022-3093(90)90786-L, ISSN 0022–3093.
[11] R. Limbach, A. Winterstein-Beckmann, J. Dellith, D. Möncke, L. Wondraczek, Plasticity, crack initiation and defect resistance in alkali-borosilicate glasses: From normal to anomalous behavior, J. Non. Cryst. Solids. 417-418 (2015) 15–27, https://doi.org/10.1016/j.jnoncrysol.2015.02.019.
[12] V Y Ganvir, R S Gedam, Effect of La $_{2\ O}$ 3 addition on structural and electrical properties of sodium borosilicate glasses, Mater. Res. Express 4 (3) (2017) 035204, https://doi.org/10.1088/2053-1591/aa66e4.
[13] R.S. Gedam, D.D. Ramteke, Influence of CeO2 addition on the electrical and optical properties of lithium borate glasses, J. Phys. Chem. Solids 74 (10) (2013) 1399–1402, https://doi.org/10.1016/j.jpcs.2013.04.022.
[14] V.Y. Ganvir, R.S. Gedam, Influence of Sm $_{2\ O}$ 3 addition on electrical properties of lithium borosilicate glasses, Integr. Ferroelectr. 185 (1) (2017) 102–108, https://doi.org/10.1080/10584587.2017.1370346.
[15] V.Y. Ganvir, H.V. Ganvir, R.S. Gedam, Effect of Dy2O3 on electrical conductivity, dielectric properties and physical properties in lithium borosilicate glasses, Integr. Ferroelectr. 203 (1) (2019) 1–11, https://doi.org/10.1080/10584587.2019.1674947.
[16] W.T. Carnall, P.R. Fields, K. Rajnak, Electronic energy levels in the trivalent lanthanide aquo ions. I. Pr3+, Nd3+, Pm3+, Sm3+, Dy3+, Ho3+, Er3+, and Tm3+, J. Chem. Phys. 49 (10) (1968) 4424–4442, https://doi.org/10.1063/1.1669893.
[17] A.D. Sontakke, K. Biswas, A.K. Mandal, K. Annapurna, Concentration quenched luminescence and energy transfer analysis of Nd3+ ion doped Ba-Al-

metaphosphate laser glasses, Appl. Phys. B 101 (1-2) (2010) 235–244, https://doi.org/10.1007/s00340-010-4010-1.
[18] A.D. Sontakke, K. Annapurna, Spectroscopic properties and concentration effects on luminescence behavior of Nd3+ doped Zinc-Boro-Bismuthate glasses, Mater. Chem. Phys. 137 (2013) 916–921, https://doi.org/10.1016/j.matchemphys.2012.11.002.
[19] S.N. Rasool, L. Rama Moorthy, C.K. Jayasankar, Optical and luminescence properties of Eu3+-doped phosphate based glasses, Mater. Express. 3 (2013) 231–240, https://doi.org/10.1166/mex.2013.1123.
[20] S. Rada, E. Culea, Structural and optical properties in gadolinium–aluminum–lead-germanate quaternary glasses, J. Non. Cryst. Solids. 357 (2011) 1724–1728, https://doi.org/10.1016/j.jnoncrysol.2011.01.017.
[21] T.G.V.M. Rao, A. Rupesh Kumar, K. Neeraja, N. Veeraiah, M. Rami Reddy, Optical and structural investigation of Dy3+-Nd3+ co-doped in magnesium lead borosilicate glasses, Spectrochim. Acta - Part A Mol. Biomol. Spectrosc. 118 (2014) 744–751, https://doi.org/10.1016/j.saa.2013.09.061.
[22] R.S. Gedam, D.D. Ramteke, Synthesis and Characterization of Lithium Borate Glasses Containing La2O3, Trans. Indian Inst. Met. 65 (1) (2012) 31–35, https://doi.org/10.1007/s12666-011-0107-4.

Feature Selection Techniques for Bioinformatics Data Analysis

Dipti Theng ; K. K. Bhoyar All Authors

Abstract:
The emergence of microarray datasets sparked a new branch of bioinformatics research. An important problem in microarray research is the selection of true biomarkers (a most relevant feature subset) for disease identification/classification using gene expression data. This problem has received the most interest in the context of cancer research to date. In this work we have experimented with various machine learning techniques for true biomarker selection for cancer classification. This research work carried on two bioinformatics datasets with application of six feature selection algorithms. Major contribution of the work is to identify these top performing efficient feature selection algorithms through an exhaustive survey and then implementing ensemble learning technique using these algorithms. A novel contribution of this research work is to implement feature weighting as an ensemble operator and compare efficiency of feature set selection using this approach with the others. The experimental results revealed that the proposed feature weighting as an ensemble operator can choose feature sets efficiently.

Published in: 2022 International Conference on Green Energy, Computing and Sustainable Technology (GECOST)

Date of Conference: 26-28 October 2022
INSPEC Accession Number: 22514733
Date Added to IEEE *Xplore*: 12 January 2023
DOI: 10.1109/GECOST55694.2022.10010541
▸ ISBN Information:
Publisher: IEEE

Deepfake Video Detection using Neural Networks

Publisher: IEEE Cite This PDF

Mayur Jiwtode ; Aman Asati ; Shailesh Kamble ; Lalit Damahe All Authors

Abstract:
Over the past few years, free mobile application tools on Artificial Intelligence and deep learning have made it easy to create reliable face exchanges in a video called "DeepFake" (DF) video that leaves a little hint of traces to check if its fake. Creating a computerized edited video has been demonstrated for quite a long time by actually taking advantage of enhanced visual effects. Recently, Artificial Intelligence has led to a rise in fake content and the ability to access free tools to create it. These purported AI-engineered media are normally called DeepFake(DF). Making a DF with a computerized AI tool is a simple job. However, with regards to identifying this DF, it's a major challenging dispute. Preparing the calculations and training the model to distinguish DF is difficult. The challenge to train an algorithm model to spot the DeepFake (DF) is not simple. We have tried recognizing DF with the use of CNN and RNN. The framework utilizes a CNN for feature extraction at the frame level. The model uses features extracted from the frame level to train the RNN, which then learns to classify videos according to their temporal inconsistencies. Anticipated results, when compared with a large number of hoax videos, were gathered from standard datasets. Using a simple architecture, we will show you how this errand can make your framework accurate.

Published in: 2022 IEEE International Conference on Blockchain and Distributed Systems Security (ICBDS)

Date of Conference: 16-18 September 2022

INSPEC Accession Number: 22238569

Date Added to IEEE *Xplore*: 09 November 2022

DOI: 10.1109/ICBDS53701.2022.9935984

More Like This

Video Anomaly Detection using Pre-Trained Deep Convolutional Neural Nets and Context Mining
2020 IEEE/ACS 17th International Conference on Computer Systems and Applications (AICCSA)
Published: 2020

A Moving Object Detection Method Based on Graph Neural Network
2023 4th International Conference on Computer Vision, Image and Deep Learning (CVIDL)
Published: 2023

Show More

NATIONAL ELECTRICAL

Data Engineering for Smart Systems pp 109–121 | Cite as

Detection of Abnormal Activity at College Entrance Through Video Surveillance

Lalit Damahe, Saurabh Diwe, Shailesh Kamble, Sandeep Kakde & Praful Barekar

Conference paper | First Online: 14 November 2021

Part of the Lecture Notes in Networks and Systems book series (LNNS,volume 238)

A Review on Various Types of Clinical Thermometers with Respect to Technological Advancements, Pros and Cons, and Accuracy as Crucial Diagnostic Devices

ECS Transactions, 107 (1) 16223-16232 (2022)
10.1149/10701.16223ecst ©The Electrochemical Society

A Review On Various Types Of Clinical Thermometers With Respect To Technological Advancements, Pros And Cons And Accuracy As Crucial Diagnostic Devices

Avanti Dhepe[a], Dr. Yogita Shrivas[b], Sujata Shamkuwar[c], Ranjit Sidram Ambad[d], Nandkishor Bankar[e] and Lalit B. Damahe[f]

[a]Undergraduate studentBAMS, Datta Meghe Ayurvedic Medical College Hospital& Research Center
[b]Professor , Department of Kaumarbhritya, Datta Meghe Ayurvedic Medical College Hospital& Research Center, Nagpur
[c]Assistant professor, Dept of Streeroga –PrasutiTantra, GAC, Jabalpur
[d]Associate Professor Dept. of Biochemistry Datta Meghe Medical College, Shalinitai Meghe Hospital and Research center, Nagpur
[e]Associate Professor Dept. of Microbiology Jawaharlal Nehru Medical College, Datta Meghe Institute of Medical Sciences Sawangi (Meghe), Wardha
[f]Computer Science and EngineeringAssistant Professor, Yeshwantrao Chavan College of Engineering, Nagpur

Clinical thermometers are considered to bethe most important diagnostic devices in diagnosis of any febrile disorders. The last two decades, have witnessed major changes in the clinical thermometrytechnology after the introduction of various types of modified thermometer for convenient diagnosis. Mercury thermometer stands up as the gold standard method for assessment of body temperature, but they are gradually getting replaced with newer devices that not only offer faster readings but inconvenience to the patients is also minimalized. This review focuses on accuracy, pros and cons of gold standard mercury-in-glass thermometer and also various technologically advanced thermometers like electronicdigitalthermometer, tympanic thermometer, non-contact infrared thermometer, liquid crystal skin thermometer, pacifier thermometer and smart thermometer. Various studies suggest that differentfactors can cause variation in the accuracy provided by such devices, like physical barriers, and calibration including the manner in which they are used.The review does not conclude that a particular clinical thermometer has better accuracy and reliabilitythanthe other. Rather, there were contradictory findings for all of the clinical thermometers evaluated.

Keywords: Diagnostic devices, mercury thermometer, electronicdigitalthermometer, tympanic thermometer, contactless infrared thermometer, liquid crystal skin thermometer, pacifier thermometer, smart thermometer.

Introduction

Body temperature is the vital parameter and is an indication to express the health condition or pathological state. Normal body temperature is around 37°C.There may be minor fluctuations during the day and nighttime. A fever or pyrexia is a temporary increase in body temperature, often occurs in response to infection, inflammation and trauma. Fever is the most common medical sign. Many diseases start manifesting with raised body temperature, thus determining a febrile state. Although, no single threshold for diagnosing fever is accepted, a value above the interval between 37.7°C and 38.3°C is generally said to be a febrile response.

Fever may be caused by infectious conditions that may be viral or bacterial.Fever can also be due to non-infectious reasons like inflammatory conditions, malignancies, autoimmune disorders and adverse drug events.Sometimes, it may have idiopathic origin, too. Body temperature is an important clinical parameter for diagnosis, monitoring and management, hence clinical thermometers are important screening tools in assessment of body temperature. If the thermometerfailsto measure accurate body temperature, abnormal body temperature may get missed. Therefore, the accurate assessment of temperature is the necessity for the early identification and management of febrile disorders.

Aims

To gain an understanding of various types of thermometers

Objective

1. To develop understanding regarding the accuracyofvarious thermometers,
2. To know about technological advancement of thermometers as diagnostic devices
3. To review pros &cons and reliability of various types of thermometers

Material and methods

References of mercury thermometer, digital electronic thermometer, tympanic thermometer, contactless infrared thermometer, liquid crystal skin thermometer, pacifier thermometer and smart thermometer were collected, compiled, analyzed and discussed in depth from authentic sources and research articles.

Discussion

During initial years of 1800s, the thermometer used to be foot-long size which posed a significant difficulty in its use (Pearce, 2002). By 1852, a bulb as a reservoir for the mercury was added and the column was narrowed down which made the thermometer more advanced (Pearce, 2002).
Allbutt (1836–1925) brought down the size of the mercury thermometer to about six inches, andinitiated the clinical practice of routine temperature assessment with the help of thermometer.[1]

The selection of anatomical location for measuring body temperature matters a lot as there are significant variations between core temperature of the body and the surface temperature.Also, a person's body temperature varies during the day and depends on activity being performed by him or her .[2]

Use ofinfraredthermometer over skin of superficial temporal artery is not that reliable for measuring core body temperature, especially in febrile conditions and patients in operation theatre.[3]

The most accurate way is to take temperature readings from the core of the body, such as the temperature of the coronary arteries.This is, however, impossible to achieve without resorting to intrusive surgical operations.[4]

Considering the above facts, a review of various clinical thermometers includingmercuryglass thermometer,digitalelectronic thermometer, tympanic thermometer, contactless infrared thermometer, liquid crystal skin thermometer, pacifier thermometer and smart thermometer is discussed as follows.

Mercury-in-glass Thermometer

French astronomer and priest, Ismael Boulliauwas is the first to invent mercury in glass thermometer in 1659. It was two centuries later in 1866 that Sir Thomas Allbut made the short clinical thermometer, the earlier version of the thermometer that we use today.[5]

Mercuryglass thermometers have been used extensively in the past both institutionally as well as in research. Mercuryglass thermometers consists of sealed glass tube calibrated in degrees Centigrade and/or degrees Fahrenheit, with a mercury-filled reservoir at one end. Mercuryhas a due to its high coefficient of expansion mercury move in the thermometers easily. Also, boiling point of mercury make it suitable for measuring higher temperatures. Hence mercury is used in thermometers .The mercury in the reservoir expands with increase in temperature, climbing higher up the glass tube and contracts and recedes as the temperature falls.[6] Mercury-in-glass thermometers generally have one of three different tips: Slim (oral or axillary) tip, the short-rounded tip (also known as stubby), and the pear-shaped (rectal) tip. Mercury-in-glass thermometers are available for oral (sublingual), axillary as well as forrectal route use.

Mercury-in-glass thermometer is considered as the gold standard method for temperature measurement especially for rectal temperature measurement.[7]Various studies suggests that mercury thermometers should be banned, as there is significant public health risk due to breakage of the thermometer which causes spillage of the mercury dispersed into tiny droplets. These droplets are difficult to see and may get easily trapped emitting a toxic vapor which is inhaled or absorbed through the skin.[8]

Electronic Digital Thermometer

This is the most commonly used item amongst the equipments that measure temperatureand sideline the traditional liquid-based thermometers.Thermistor at its tip measures the peak temperature of the nearbytissue and transform it into a digitally displayedreading .[9]Electronic digital thermometry can be done by oral (sublingual), axillary and rectal routes.

The convenience of getting an instant reading in any temperature scale Celsius orFahrenheit make it more advantageous over the rest of the thermometers.Further

advantage claims in digital thermometers are easy reading, less time for measuring temperature, use of changeable and disposal probes to prevent cross infection and durability.[8]But one of their disadvantages is the measurement of the temperature very closely and momentarily, that may show quite dramatic fluctuations. So, sometimes taking an accurate readingis difficult. Also most of the electronic digital thermometers necessitate the sensor to read the temperature at the equilibrium, so that accurate temperature reading can be achieved in a shorter duration of time in comparison to the conventional glass thermometer.

Though it is thought to be a less time-consuming device, the digital thermometer is used in general more for a diagnostic purpose.But data suggests that it may play a possible role as a vector to transmit nosocomial infections.Outbreak of Enterobactor cloacae in the NICUdue to disinfected thermometers made anews in the past. Hence it was suggested that replacement with disposable probe could prevent this problem, but it is not cost effective and expensive.[9]

New technologies are being used nowadays for improving the diagnosis through diagnostic devices. A digital thermometer have been developed in the form of a wearable patch which detectsincrease in body temperature as much as 180 minutes prior than the standard monitoring. This Bluetooth enabled patch is capable of measuring temperature every 10 minutes rather than four hours which is the usual care practice. It sends readings to compatible mobile devices.[10]

The accuracy of digital thermometer could be more acceptable as compared to the mercury-in-glass thermometer.Studies suggest that rectal digital thermometer are more accurate than axillary digital thermomter.[9]

Evidence suggests that the size of the temperature sensor and the speed of the sensor response leading to greater sensitivity of local, acute vasomotor activity are major problems with new oral thermometers. Potential solutions are to increasethe sensor size and reduce the response speed.[11]

Tympanic Thermometer

The initial reference of theuse of tympanicthermometerwasdocumented in the year 1986, but they were not popularly used till early1990s (Betta et al, 1997). The function of tympanic thermometers is based on acknowledging the tympanic membrane temperature in the ear and converting it into reading.[12]

Structually tympanic thermometers are small devices and can be hold in hand. It contains one probe that is to be entered into the patient'sauditory canal to reach thetympanicmembrane.Tympanic membrane isthinbut has good blood perfusion. There is a sensor at the tip of the probe that is enabled to record the infrared radiation (IRR) emitted by the thin tympanic membrane due to its warmth and change this into a digital temperature reading.The probe can be covered by a disposable cover, which can bereplacedbefore use in every patient and proves to be helpful cross-infection in patients . Some researchers have suggested that tympanic thermometers represent real body temperature more accurately as the position of tympanic membrane is in the close

vicinity of the temperature regulating centresituatedin the hypothalamus and bothhave common arterial supply.[12]

The speed and the convenience are the benefits of using tympanic thermometer for temperature readings. To obtain accurate reading mercury thermometer needs to be in patientcontactfor 6-11 minutes, whereas tympanic thermometers require only few seconds to get a reading.[12]

Different studies conducted for checking the accuracy of tympanic thermometers suggest that tympanic thermometersingeneral,candisplay temperatures in the range of 1.02°C below and 0.91°C above the temperatures noted by other devices like mercury thermometers placed in oral cavity and arm pit or invasive thermometry such asesophagealand in the pulmonary arteryordigital probe thermometers placed in oral, axillary and rectal sites. Hence some authors disapprove the use of tympanic thermometers for recording body temperature.But there are contradictory findings about accuracy of tympanic thermometer as many researchers have concluded that though tympanic thermometers can record body temperatureaccuratelythere is no statistically significant difference among the various temperature recording devices.[12]

Though, tympanic membrane thermometers show enough sensitivity and specificity, the study concluded that recording 'core' body temperature using them in children is not reliable.[13]Angle between the tympanic membrane and external auditory canal is important for assessment of temperature by tympanic thermometers. If the membrane is perpendicular to the detector, more IR radiation (more heat) will typically be detected than if the membrane is at an acute angle to the detector. Age also affects the angle between the membrane and the external auditory canal. Usually, this open angle is not attained until about 7–9 years of age. Therefore the data suggests that using tympanic thermometer is difficult in childen.[11]

Evidence suggests that problems with the tympanic thermometers are because of the range of normal anatomical variability. The combination of an Otto scope with the tympanic thermometers is advised and discussed as a potential solution to view the external auditory canal so that there is no obstruction and inspection of the tympanic membrane to ensure that it is healthy.[11]

Non- contact infrared thermometer

The NCIT is a contactless device operated by battery and records body temperature or ambient temperature. There is an inbuilt infrared laser pointer which recordtemperatureboth in Celsius as well as Fahrenheit. NCIT comes as an instrument that calibrates very fastin15 secondsautomaticallywhen it is switched on. The NCIT capture the thermal radiation that comefrom a point, concentrate it on a sensor and convert it to an electronic signal. After digitally processing this signal, temperature value is presented to the reader.[14]

The NCIT is a contactless,fast and portable temperature measuring instrument; it measures temperature from frontal bone and temporal artery from a distance of less than 5 cm.During COVID-19 pandemic it has proved to be of a great help for mass screening without the need of sterilization, thus avoiding cross infection.

In febrile patients, non-contact infrared thermometer has less Clinical efficiency than axillary digital thermometer as well as mercury glass thermometer.[15]Though, this may be untrue in many clinical settings.Feveris defined as a rectal temperature of 38°C or higher. One study that measuredfeverusing a mercury-in-glass thermometer found that NCITs had high sensitivity and specificity for detecting fever.[15]

Liquid crystal thermometer

Responding to the changes in temperature cholesteric liquid crystals change their molecular structure.Temperature measurement using liquid crystals utilizes the same property. Liquid crystals in a plastic strip change their color on different temperatures. With the help of this change The temperature can be measured within 15 seconds of placing on the forehead.[16]The LCT comes in two variants: first one measures direct skin temperature (range26—38 °C); the other is designed to display a temperature 1.9 ° C more than the temperature of skin and is assumed to estimate the core temperature(range 29-41 °C) of body .A hypo-allergenic adhesive backing allows the attachment of the thermometer to a smooth skin surface**.**[17]

LCT could be a safe and easy way to monitor temperature, irrespective of the need for sterilization and hence have low risk of cross infection.[18]Thismonitoring method may be useful for detecting early temperature rise in malignant hyperthermia cases.[18] Several in-vitro investigations demonstrate that, under laboratory settings, LCT temperature displays are like some well-known commercial thermocouple system.Because of the phenomena of hysteresis, which may get affected due to multiple conditions, evaluating the accuracy of the LCT on patients is more challenging.LCTs are sensible to detect temperature that can be comparedto that of a mercury in glass thermometer, hence they are potentially useful in the identification of hyperthermia and can become good indicators of core temperature during surgical procedures.[18]According to one study, liquid crystal thermometers are ineffective for determining core temperature during surgical procedures because, in most preoperative situations, forehead temperature is 1-4°C lower than core temperature, but in this study, the patient's skin-surface temperature exceeded core temperature.[19]

Pacifier Thermometer

The Pacifier Thermometer is a soother with an early-warning system that is primarily used to check the temperature of children. A temperature detecting mechanism is included with a pacifier that may be inserted into the mouth. The sensors are capable of processing and transmitting input temperature information and displaying it on a screen.[20] Pacifier thermometer fast measures temperature and causes no discomfort in pediatric patients, and is easy to use. But the main disadvantages are expensiveness and all models of thermometer nipples are not allowed to disinfect.

Data from various studies comparing rectal thermometer and pacifier thermometer shows that that pacifier thermometry is a welcome method of temperature reading in young children.[21]

Smart thermometer

A medical device called smart thermometer can convey its readings,collection, storage and analysis. These thermometers send readings to the application on the users' phone and users can seethehistory of previous temperatures thus enabling them to record symptoms.[22] Information can also show a consolidated temperature chart. This shows hot spots with exceptional level of high temperatures and can be used to identify outbreaks of disease.[23]The mass usage of these smart thermometers can help inrapid and efficient surveillance at the everyhousehold.

Fever measures taken with smart thermometers and mobile devices are geolocated and measure a clinical indication in real time. Furthermore, thermometer findings along with demographic info and symptomaticdata provided by individual users can help in understanding specific characteristics of any connected pandemic or enhance traditional epidemiological field work.

In a study looking at geo-located measures from smart thermometers for monitoring Influenza-like disease, it was observed that thermometer readings were closely associated with national ILI activity and activity patterns across regions and age groups. {ILI }.[24]

Clinical signs and symptoms of febrile episodes, the time duration of fevers, incidence rate of biphasic fevers, and the frequency of potential transmission of influenza or COVID-19 like febrile epidemic or pandemic situations can be monitored in real time anywhere and for all age groups with the help of smart thermometers. The thermometer's mobile app's capacity to track users through numerous profiles aids in the acquisition of data that would otherwise be difficult or impossible to get using traditional means.Thermometer-based data can be helpful in providing many opportunities for future. A personalized public health intervention (viz. vaccination reminders) can be built up using broadcasting time and location-specific alerts. Currently the thermometer's app can give inputs regarding clinical symptoms (e.g., cough, diarrhea), diagnosis and medication timing reminders.[24]These features make these devices special and prove their utility.

Conclusion

Clinical thermometers are important screening and diagnostic tools for assessment of body temperature in healthy as well as ill people. The inaccurate temperature measurements may cause serious consequences like improper diagnosis, wastage of resources, and no optimal patient and population health results. For this reason technological improvements in lesser time duration, ease of use and safety should be achieved with no loss of accuracy and reliability. Factors like cost-effectiveness and infection control have are the needs while using such medical diagnostic devices.

References

1. Black JA, An Integrative Review Focusing on Accuracy and Reliability of Clinical Thermometers, Walden UniversityProQuest Dissertations Publishing, 2016. 10110908.
2. Pecoraro V, Petri, D, Costantino G, Squizzato A, Moja L, Virgili G, Lucenteforte E, The diagnostic accuracy of digital, infrared and mercury-in-glass thermometers in measuring body temperature: a systematic review and network meta-analysis. *Intern Emerg Med*,2020.
3. Mangat J, Standley T, Prevost A, Vasconcelos J, White P, A comparison of technologies used for estimation of body temperature, *Physiol. Meas*.2010, 31,1105–1118
4. Chung W, Chen C, Evaluation of Performance and Uncertainty of Infrared Tympanic Thermometers, Sensors2010, 10, 3073-
5. Blumenthal I, Should we ban the mercury thermometer? Discussion paper, *Journal of the Royal Society of Medicine*,85:553-555
6. Mercury Thermometers, United States Environmental Protection Agency, Available from: https://www.epa.gov/mercury/mercury-thermometers .
7. Mercury Thermometers, United States Environmental Protection Agency, Available from: https://www.epa.gov/mercury/mercury-thermometers .
8. Shanks NJ, Lambourne A, Morton C, Sanford J, Comparison of accuracy of digital and standard mercury thermometers*, British medical journal*, 1983, 287:1263
9. Kitsommart R, Accuracy and Precision of Digital Thermometer in Neonatal Temperature Measurement,*Siriraj Med J* 2005, 57:128-131
10. Abassi J, Wearable Digital Thermometer Improves Fever Detection,*JAMA*. 2017;318(6):510
11. Latman NS, Clinical Thermometry: Possible Causes and Potential Solutions to Electronic, Digital Thermometer Inaccuracies, Biomedical Instrumentation & Technology2002; 37:190–196
12. Gallimore D, Reviewing effectiveness of tympanic thermometer, Nursing times 2004, 100(32):32
13. Gasim G, Musa I, Abdien M, Adam I, Accuracy of tympanic temperature measurement using an infrared tympanic membrane thermometer, *BMC Res Notes*. 2013; 6: 194
14. Khan S, Saultry B, Adams S, Kouzani AZ, Decker K, Digby R, Bucknall T, Comparative accuracy testing of non-contact infrared thermometers and temporal artery thermometers in an adult hospital setting, *American Journal Of Infection Control* 2021,49:597-602
15. Teran CG, Torrez-Llanos J, Teran-Miranda TE, Balderrama C, Shah NS, Villarroel P. Clinical accuracy of a non-contact infrared skin thermometer in paediatric practice. *Child Care Health Dev*. 2011
16. Rahman N, Kasem FB, Islam MR, Islam MR, Sultana R, Matin A, Comparison Between Mercury and Liquid Crystal Forehead Thermometers for Measurment of Body Temperature, J ShaheedSuhrawardy Med Coll, 2012;4(2) :60-61
17. MacKenzie R, Asbury J, Clinical evaluation of liquid crystal skin thermometers, *British Journal of Anaesthesia* 1994; 72:246-249
18. Lees DE, Schuette W, Bul l JM, Whang-Peng J, AtkinsonER, Macnamara TE. An evaluation of liquid-crystal thermometry as a screening device for intraoperative hyperthermia. *Anesthesia and Analgesia* 1978; 57:669

19. Lou MM, Sesselar DI, Failure of Intraoperative Liquid-Crystal Temperature Monitoring, *Anesthesia & Analgesia* 1996, 82(5):1102-1104
20. Digital Pacifier Thermometer, Google Patents, Availablefrom:https://patents.google.com/patent/US5211479A/en
21. Press S, The Pacifier ThermometerComparison of SupralingualWith Rectal Temperatures in Infants and Young Children, Arch PediatrAdolesc Med. 1997;151(6):551-554; Braun C, Accuracy of pacifier thermometers in young children, *PediatrNurs*2006; 32(5):413-8
22. Ackley SF, Pilewski S, Petrovic VS, Worden L, Murray E, Assessing the utility of a smart thermometer and mobile application as a surveillance tool for influenza and influenza-like illness, *Health Informatics Journal* 2020, Vol. 26(3) 2148 – 2158
23. Donald G. McNeil Jr., "Can Smart Thermometers Track the Spread of the Coronavirus?"
24. Miller A, Singh I, Koehler E, Polgreen P, A Smartphone-Driven Thermometer Application for Real-time Population- and Individual-Level Influenza Surveillance, CID 2018,67:388-397
25. Periasami V, Naaraayan S, Vishvanathan S, Diagnostic accuracy of digital thermometer compared to mercury in glass thermometer for measuring temperature in children, *Int J ContempPediatr*. 2017 Jul;4(4):1476-1479
26. S. Arya et al. , Journal of the Electrochemical Society, 10, 023002(2021). DOI: https://doi.org/10.1149/2162-8777/abe095
27. S. Arya et al. Journal of The Electrochemical Society,168 027505(2021). DOI: https://doi.org/10.1149/1945-7111/abdee8
28. S.K.Oruganti t et al, *IEEE Access*, 8, 187965(2020), doi: 10.1109/ACCESS.2020.3030658
29. S.K. Oruganti et al, *Sci Rep* 10, 925 (2020). https://doi.org/10.1038/s41598-020-57554-1
30. Song et al, 13, 1826(2019), doi: 10.1049/iet-map.2018.5286
31. J. Malik et al., Applied Physics Letters, 112, 234102 (2018); https://doi.org/10.1063/1.5029307
32. F. Bien et al, IEEE Sensors Journal,15, 2062(2015). 10.1109/JSEN.2014.2363195
33. F. Bien et al. IEEE Wireless Power Transfer Conference (WPTC), 247(2014)
34. S.K. Oruganti et al., IET Electronics Letters, 50, 886(2014).
35. N. Nguyen, et al., *IEEE Transactions on Vehicular Technology*, vol. **63**, 3651(2014). https://doi.org/10.1109/TVT.2014.2304453
36. Thi Thu Ngoc Nguyen,et al., *IET Power Electronics,* 8, 458(2015). https://doi.org/10.1049/iet-pel.2013.0657
37. J. Malik, *IEEE International Symposium on Radio-Frequency Integration Technology (RFIT)*, 1(2019), 10.1109/RFIT.2019.8929138
38. S. K. Oruganti and Ajit Khosla 2020 ECS Trans. 98 55 https://doi.org/10.1149/09813.0055ecst
39. Paul, D., Oruganti, *Sustainable Solutions and Society*, *1*(1) (2020)https://spast.org/ojspath/article/view/4
40. F. Bien, *URSI Asia-Pacific Radio Science Conference (URSI AP-RASC)*, 318(2016), doi: 10.1109/URSIAP-RASC.2016.7601321.
41. Bien, F. , et. al, Signal and Power transmission system US000010636565B2; US2018/0226187A1 08/2018, US Patent.

42. Bien, F.,., et. al, Wireless Power transmission and communication system, US000010797399B2; US2019/0214734A1, US patent
43. Bien, F.,et al." Fine pulse generator and method for generating fine pulse" US 20140361822 A1, Dec 11, 2014. US Patent.
44. Bien, F., et. al,Signal and power transmission system, US 10,636,565B2, 2020. US Patent
45. Bien, F., et. al, Door lock charging system and door lock apparatus US20190006875A1. US Patent
46. Sheng-Joue Young, et al, ACS Applied Electronic Materials. 2, 3522(2020). https://doi.org/10.1021/acsaelm.0c00556
47. D. Chung *et al*.,IEEE *SENSORS,*1893(2011). doi: 10.1109/ICSENS.2011.6127372.
48. Chu, Yen-Lin, ECS Journal of Solid State Science and Technology 10, 127001 (2021). https://doi.org/10.1149/2162-8777/ac3e43
49. Jalandra, Rekha, Nishu Dalal, Amit K. Yadav, Damini Verma, Minakshi Sharma, Rajeev Singh, Ajit Khosla, Anil Kumar, and Pratima R. Solanki, *Applied Microbiology and Biotechnology* 105, 7651(2021) https://doi.org/10.1007/s00253-021-11582-7
50. A. Khosla et al., Scientific reports 8, 1 (2018): https://doi.org/10.1038/s41598-018-30846-3
51. Li, et al., Proc. SPIE 7929, Microfluidics, BioMEMS, and Medical Microsystems IX, 79290G (2011); https://doi.org/10.1117/12.873197
52. Ahmed, *Polymer* (2021): 123926. https://doi.org/10.1016/j.polymer.2021.123926
53. Y. Takishima, *ECS Journal of Solid State Science and Technology* 10,037002 (2021). https://doi.org/10.1149/2162-8777/abea5f
54. H. Furukawa et al. *ECS Journal of Solid State Science and Technology* 9, 061024(2020). https://doi.org/10.1149/2162-8777/aba913
55. A. Singh, A. Sharma, A. Ahmed, A. K. Sundramoorthy, H. Furukawa, S. Arya, and A. Khosla, Biosensors 11, 336(2021). https://doi.org/10.3390/bios11090336
56. T.K. Saha et al. *Microsyst Technol* (2018). https://doi.org/10.1007/s00542-018-4260-0
57. Khosla, Ajit, and Bonnie L. Gray. " ECS Transactions 45.3 (2012): 477. https://doi.org/10.1149/1.3700913

A Review of *Nidra* (Sleep) and *Nidranash* (Insomnia) According to *Samhita*

ECS Transactions, 107 (1) 16297-16302 (2022)
10.1149/10701.16297ecst ©The Electrochemical Society

A Review- Nidra (Sleep) and Nidranash (Insomnia)According to Samhita

Santosh Suryakant Pusadkar[1],Deepika Ruturaj Patil[2],Prashant Chandrakant Sarade[3]Dr. Anil Akulwar[4]Dr. Yashwant Lamture[5]Rupa A. Fadnavis[6]

[1]Assistant Professor, Department of Rasashastra, DattaMeghe Ayurved College Hospital & Research Centre, Nagpur

[2]Assistant Professor, Vasantdada Patil Ayurved College Sangli

[3]Assistant Professor, SST'S Ayurved College, Sangamner

[4] Professor and HOD Dept. of Surgery Datta Meghe Medical college, Nagpur

[5] Professor Dept. of Surgery Jawaharlal Nehru Medical College Datta Meghe Institute of Medical Sciences Sawangi (Meghe) Wardha

[6]Computer Science and EngineeringAssistant Professor, Yeshwantrao Chavan College of Engineering, Nagpur

[*]Corresponding author-

Dr. Santosh Suryakant Pusadkar
Department ofRasashastra, Datta Meghe Ayurved Medical College Hospital and Research Centre, Wanadongri, Nagpur, Maharashtra
pusadkarsantosh@gmail.com

Abstract: In the modern era, high percentage of people remains in a state of stress and frustration due to changing lifestyle, which predisposes the individual towards psychological and psychosomatic disorders.Insomnia is spreading silently all over the world. Each and every one is running endlessly after success and money. People today sleep 20% less than the required sleep.In India, more than 5% of the population and 30% of professionals are suffering from primary insomnia. Symptoms of primary insomnia and "Nidranash" are almost same hence we correlate it.

Keywords: *Nidra, Nidranash, Sleep,Insomnia*

Introduction:

Ayurveda is an ancient science of life which deals with both preventive and curative measures.

Aim of ayurveda is –

P`ayaaojanaMcaasyasvasqasyasvaasqarxaNamaatursyaivakarp`SamanaMca | | ca. sau 30À26

Ayurveda has defined concept of ‘swastha’ in a nice way.

samadaoYa:samaaignaScasamaQaatumalaikyaa:

p`sannaa%maoMid`yamanaasvasqaM[%yaiBaQayatoca. sau 15À4

It means the equilibrium state of the doshas , the unaltered state of agni the active principle of metabolism as well as the saptadhatus including the regular and natural excretory functions and in addition a pleasant feeling by the soul (Atma) , senses

of mind. That is balance state of body, sense organ and mind is defined as swastha meaning healthy.

Every one who wants to live long and healthy life is expected to follow the rules of conducts which are given as Dincharyaupakrama in Ayurved.

According to Ayurveda, Nidranasha is caused by aggravation of Vata and Pitta, exhaustion of mind, loss of tissues and injury to the body. Lakshanas of Nidranasha are Shirogaurav (Heaviness of Head), Angamarda (Bodyache), Jrumbha (yawning) and Alasya (Lazziness).

Primary Insomnia is described as the difficulty getting to sleep or staying a sleep over a time period of at least 1 month or experience of non-refreshing sleep (U.S. Nation Institutes of Health)

Review

Review of *Nidra*

Derivation of the word NIDRA:-

The term Nidra feminine gender. It is derived from the root ‘DRA’ with suffix ‘NI’and the root ‘DRA’ means undesired ‘GATU’to lead, it is a state which is hated, therefore, it is termed as ‘NIDRA’.

The word Nidranash is composed of two words, Nidra and Nash. The definition nidra is as follows,

Nidra is state of life where, gnanedriyas and karmendriyas are not doing their functions.

Nidra is the stage of mind and intellects are at rest.

Nidra can be defined as the state where predominance of kapha and tamas is seen.

ShabdastomaMahanidhi explains Nasha as palayan (escaping), adarshana (invisible), anupalabde (unavailable).

Nasha in other words being lost, elimination, disappearance, destruction.

Based on the above description, the term Nidranash can be brodly defined as the loss of sleep or the derangement in the quantity and quality of sleep.

HISTORICAL REVIEW OF NIDRANASH

PRE VEDIC PERIOD

In pre Vedic period (2500 BC) no literature is available.

VEDIC PERIOD

In Vedic period (2500 BC -500 BC) in Atharvaveda Shounakeeyashakha, the reference is available as Nidrajanan as Karma, while explaining the Moulvikasidhanta in Dravyaguna.

SAMHITA KALA (1000BC-100BC)

The books written were Charaksamhita, Sushrutasamhita, Bhelasamhita, and Haritasamhita. All of these are having the descriptions of nidranashaCharak&Sushruta have not explained this separately. But Bhela&Harita have mentioned special chapters on NIDRA.

SANGRAHA KALA (500 BC – 800 BC)

In Bhavaprakashanidranash has been explained in some contest. In Yogratnakar the reference available Nidranash as lakshana in some diease and chikitsa of Nidranash.

In sangrahakalaAshtangSangraha, AshtangHridaya and Madhavnidana were written, nidana and chikitsa of Nidranash in AshtangHridaya and Ashtangsangraha are available. In Madhavnidana the Nidranash is mentioned as lakshana in some disease.

In Ayurvedic formulary of India the reference available is indication of Swarnamakshikbhasma and til tail in treating Nidranash.

AYURVEDIC REVIEW OF NIDRANASHA

The ancient acharyas of Ayurveda considered Nidra – among the three upastambhas for the maintenance of the living organism. While discussing about Nidra and Nidranash in the context of Astauninditiyaadhyaya, Acharya Charaka has stated that happiness and sorrow,

growth and wasting, strength and weakness, virility and importance, the knowledge and ignorance as well as existence of life and its cessation depend on the sleep. Nidra is pushtida&nidranash is karshana of the body. Untimely and excessive sleep and vigil take away both happiness and longevity, like night of destruction.

Charaka has included the Aswapna in 80 nanatmajvatavikaras. Acharya Sushruta included this under Garbha Vyakarana Shariram, might be because of Nidra plays a role of nuitrition and development of the body. He also explained the VaikarikiNidra in the same chapter, which can be correlated to sleep disorders.

Acharya sharangdhara, concerted the Nidranash in vatajnanatmajvikara, ALPA nidra in pittajnanatmajvikara and atinidra under kaphajnanatmajvikara.

Conclusion

By observing regarding Nidra and Nidranasha, it can be concluded that all acharyas considerd the importance of Nidra, hence Nidranasha are explained along with the physiology of nidra only. Nidranasha or salpanidra is seen in many diseases as lakshana and it may be upadrava or arista lakshana also.

Bibliography

1. Charaka Samhita- Ayurveddipika: Chakrapanidatta, ChaukhambaPrakashan, Varanasi.2000.
2. Charaka Samhita- SavimarshaVidyotini Part I and II :Rajeshwardatta Shastri, ChaukhambaPrakashan, Varanasi, 1998.
3. Sushruta Samhita – Ayurved TattawaSandipika Hindi Vyakhya : Dr. AmbikaduttaSharstri, ChaukhambaPrakashan, Varanasi, 2001.
4. Ashtanga Hridya- Commentaries by Arundatta and Hemadri : Annotated by Vd. Anny MoreshwarKunte, ChaukhambaPrakashan, Varanasi, 1997
5. Aasan,Pranayaam,Mudra,Bandha- Swami SatyaanandSaraswati,BiharYogVidyalaya,Munger(Bihar) 16th edition-2014.
6. Ashtanga Sangraha- Acharya Vagbhata, Shrimad AatreyaPrakashan Pune.
7. Madhava Nidanam : Acharya Madhavkar, Chaukhamba Sanskrit Series, Varanasi.
8. Sharangadhara Samhita- Dipika Commentary :Aadhamalla, ChukhambaPrakashan, Varanasi.
9. S. Arya et al. , Journal of the Electrochemical Society, 10, 023002(2021). DOI: https://doi.org/10.1149/2162-8777/abe095
10. S. Arya et al. Journal of The Electrochemical Society,168, 027505(2021). DOI: https://doi.org/10.1149/1945-7111/abdee8

11. S.K.Oruganti t et al, IEEE Access, 8, 187965(2020), doi: 10.1109/ACCESS.2020.3030658
12. S.K. Oruganti et al, Sci Rep 10, 925 (2020). https://doi.org/10.1038/s41598-020-57554-1
13. Song et al, 13, 1826(2019), doi: 10.1049/iet-map.2018.5286
14. J. Malik et al., Applied Physics Letters, 112, 234102 (2018); https://doi.org/10.1063/1.5029307
15. F. Bien et al, IEEE Sensors Journal,15, 2062(2015). 10.1109/JSEN.2014.2363195
16. F. Bien et al. IEEE Wireless Power Transfer Conference (WPTC), 247(2014)
17. S.K. Oruganti et al., IET Electronics Letters, 50, 886(2014).
18. N. Nguyen, et al., IEEE Transactions on Vehicular Technology, vol. 63, 3651(2014). https://doi.org/10.1109/TVT.2014.2304453
19. Thi Thu Ngoc Nguyen,et al., IET Power Electronics, 8, 458(2015). https://doi.org/10.1049/iet-pel.2013.0657
20. J. Malik, IEEE International Symposium on Radio-Frequency Integration Technology (RFIT), 1(2019), 10.1109/RFIT.2019.8929138
21. S. K. Oruganti and Ajit Khosla ECS Trans. 98 55(2020) https://doi.org/10.1149/09813.0055ecst
22. D. Paul, et al, Sustainable Solutions and Society, 1(1) (2020)https://spast.org/ojspath/article/view/4
23. F. Bien, URSI Asia-Pacific Radio Science Conference (URSI AP-RASC), 318(2016),
24. doi: 10.1109/URSIAP-RASC.2016.7601321.
25. Bien, F. , et. al, Signal and Power transmission system US000010636565B2; US2018/0226187A1 08/2018, US Patent.
26. Bien, F.,., et. al, Wireless Power transmission and communication system, US000010797399B2; US2019/0214734A1, US patent
27. Bien, F.,et al.” Fine pulse generator and method for generating fine pulse” US 20140361822 A1, Dec 11, 2014. US Patent.
28. Bien, F., et. al, Signal and power transmission system, US 10,636,565B2, 2020. US Patent
29. Bien, F., et. al, Door lock charging system and door lock apparatus US20190006875A1. US Patent
30. Sheng-Joue Young, et al, ACS Applied Electronic Materials. 2, 3522(2020). https://doi.org/10.1021/acsaelm.0c00556
31. D. Chung et al.,IEEE SENSORS,1893(2011). doi: 10.1109/ICSENS.2011.6127372.
32. Chu, Yen-Lin, ECS Journal of Solid State Science and Technology 10, 127001 (2021). https://doi.org/10.1149/2162-8777/ac3e43
33. Jalandra, Rekha, Nishu Dalal, Amit K. Yadav, Damini Verma, Minakshi Sharma, Rajeev Singh, Ajit Khosla, Anil Kumar, and Pratima R. Solanki, Applied Microbiology and Biotechnology 105, 7651(2021) https://doi.org/10.1007/s00253-021-11582-7
34. A. Khosla et al., Scientific reports 8, 1 (2018): https://doi.org/10.1038/s41598-018-30846-3
35. A. Li, et al., Proc. SPIE 7929, Microfluidics, BioMEMS, and Medical Microsystems IX, 79290G (2011); https://doi.org/10.1117/12.873197
36. A. Ahmed, Polymer (2021): 123926. https://doi.org/10.1016/j.polymer.2021.123926
37. Y. Takishima, ECS Journal of Solid State Science and Technology 10,037002 (2021). https://doi.org/10.1149/2162-8777/abea5f
38. H. Furukawa et al. ECS Journal of Solid State Science and Technology 9, 061024(2020). https://doi.org/10.1149/2162-8777/aba913

39. A. Singh, A. Sharma, A. Ahmed, A. K. Sundramoorthy, H. Furukawa, S. Arya, and A. Khosla, Biosensors 11, 336(2021). https://doi.org/10.3390/bios11090336
40. T.K. Saha et al. Microsyst Technol (2018). https://doi.org/10.1007/s00542-018-4260-0
41. Khosla, Ajit, and Bonnie L. Gray. " ECS Transactions 45.3 (2012): 477. https://doi.org/10.1149/1.3700913
42. Ujwal Shreenag Meda, Libin Lal, Sushantha, Paridhi Garg; Solid Electrolyte Interphase (SEI), a boon or a bane for lithium batteries: A review on the recent advances; Journal of Energy Storage; , , Article No. 103564, 2021, https://doi.org/10.1016/j.est.2021.103564
43. U. S. Meda, et al. E3S Web of Conferences; 287, 4010, (2021) https://doi.org/10.1051/e3sconf/202128704010
44. S N Adithya, K C Sachin, Radhakrishna, Ujwal S. Meda; IOP Conference Series: Earth and Environmental Science; 822, 012005, (2021) https://doi:10.1088/1755-1315/822/1/012005
45. Manjunatha C., Ujwal S. Meda, S Lakshmikant, S Ashoka, BW Shivraj, M. Selvaraj, G Satheesh Babu; Surfaces and Interfaces; 25, 101161, (2021). https://doi.org/10.1016/j.surfin.2021.101161

Back

Chapter 3

Contamination Monitoring System Using IOT and GIS

Kavita R. Singh, Ravi Wasalwar, Ajit Dharmik, Deepshikha Tiwari

Book Editor(s):R. Arokia Priya, Anupama V Patil, Manisha Bhende, Anuradha Thakare, Sanjeev Wagh

First published: 24 August 2022
https://doi.org/10.1002/9781119842286.ch3

Summary

Contamination or pollution is one of the biggest challenges when environmental issues are considered. However, air pollution is one among all the key issues of our times and has become a primary issue, acknowledged by the international community. Owing to air pollution, medical problems have been emerging at a quicker rate, particularly in urban areas of the rising nations where industrial development and increasing vehicles lead to advent of a ton of gaseous contaminations. Therefore, pollution monitoring becomes a very important area of research to analyze the polluted and non-polluted area of a region based on which further decision can be taken by the authorities. In this context, we propose an analysis of particular areas that are more contaminated or polluted in Nagpur City, Maharashtra, India by calibrating the air quality index as an IOT-based air contamination monitoring framework and plotting the data using Geographical Information System. Additionally, the data analysis is done with the help of Tableau, and different parameters like air quality index, and temperature are provided to the end user through the Android application.

References

Tudose , D. Ş. , Pătraşcu , N. , Voinescu , A. , Tataroiu , R. , Ţăpuş , N. , Mobile Sensors in Air Pollution Measurement , in: *IEEE Positioning Navigation and Communication* (*WPNC)* , pp. 166 – 170 , 7 Apr 2011 .

Vjnattha , P. , Arvind , R. , Sangeetkumar , B. , Pollution monitoring system using wireless sensor network in Visakhapatnam . *IJETT* , **4** , 591 – 595 , April 2013 .

RESEARCH ARTICLE | MARCH 21 2022

Overview on spatial analysis framework to examine land use and flooded zone

Sabiha M.Zamir ; Roshni S. Khedgaonkar; Mr. Ajit Dharmik

+ Author & Article Information
AIP Conf. Proc. 2424, 050001 (2022)
https://doi.org/10.1063/5.0077923

Natural disasters can adversely influence the life of living beings. Flood has global evidence that causes massive destruction of land use areas. This literature review has all the related papers which use various algorithms such as GIS-based frameworks, multi-criteria, Analytical Hierarchical Process, Hydraulic methods, Synthetic Aperture Radar data with GIS data, logistic regression, cellular automata, Markov Chain models, 1D and 2D models of flood hydraulics, Naïve Bayes and so on to get the blend for examine the land use and evaluate the damages and destructions after flood hazard. Different authors have implemented different techniques in their specific areas. We also proposed our algorithm to calculate the flood hazard losses, the Governments, Disaster Management, Insurance companies can take benefits out of it

Topics
Theoretical computer science, Natural disasters, Optical computing, Hydraulics, Public and occupational health and safety, Review, Markov processes

RESEARCH ARTICLE | MARCH 21 2022

Malnutrition detection in infants using machine learning approach

Rakhi Wajgi ; Dipak Wajgi

+ Author & Article Information
AIP Conf. Proc. 2424, 040006 (2022)
https://doi.org/10.1063/5.0076876

Balanced nutrition is the main source of energy. It is necessary for healthy life of people. Healthy nutrients enable cells to perform their regular activities at pace. Deficiency of proper nutrition while birth causes various complications in further life. These complications include wasting, stunting, edema, mental illness, low immune system, ridged or spoon-shaped nails, brittle, dry hair, and underweight etc. Malnutrition is a condition that occurs when a person consumes a diet that is deficient in one or more major nutrients, or has too many of them. Marasmus, kwashiorkor and intermediate states of marasmus-kwashiorkor are included in the term Protein-Energy Malnutrition (PEM) disorders. PEM is the cause of underweight (low weight for age), stunting (low height for age), and wasting (low weight for height). In India, stunting affects 48% of infants under five years age, wasting affects 20%, and underweight affects 43%. Most children suffering from undernutrition in mild to moderate forms are unnoticed in India, which affects their growth at early ages. Detecting malnutrition at early stage reduces further healthcare cost and improve health outcome. To alleviate the problem of malnutrition, this paper describes a decision tree model for classification of infants being between the ages of 0 and 59 months as normal, acute malnourished or severely malnourished for three categories: Stunting, Wasting and Underweight. In decision tree model, Gini index is adopted as an impurity measure. The accuracy obtained using decision tree for stunting is 82.22%, for wasting 72.23 % and underweight 78.35% using Gini index.

Topics
Machine learning, Decision theory, Proteins, Immune system, Health care

RESEARCH ARTICLE | MARCH 21 2022

A coding platform: For all programming labs and practical examination

Roshan Bhanuse ; Uttkarsh Bawankar; Durgesh M. Sharma; Mayuresh Patle; Vedashree Narsapurkar; Shubham Sawate

+ Author & Article Information
AIP Conf. Proc. 2424, 060001 (2022)
https://doi.org/10.1063/5.0076793

Manual code assessment in this modern age is not a feasible way of evaluating student competencies. Relying of random and limited test cases can result in inconsistent conclusions. Neither is it viable nor possible to judge rationally using naive procedures. The online coding platforms existing today are too general for this purpose, so this system is developed distinctively for this purpose. In this system, all the evaluation processes are automated. Thus, creating a trouble- free platform for teachers and a judicious assessment for students.

Topics

Students, **Educational assessment**, **Teaching**

Enhancing Customer 360 With Better Service Management using Salesforce CRM

Publisher: IEEE

Nilesh Sambhe ; Ganesh Yenurkar ; Shivkumar Karale ; Laxmikant Umate ; Ganesh Khekare All Authors

Abstract: In this age of global e-market, most of our transaction, buying or selling or both have become online through various ecommerce websites and mobile application. The most ... **View more**

Abstract:
In this age of global e-market, most of our transaction, buying or selling or both have become online through various ecommerce websites and mobile application. The most important phase during these transactions is proper and effective communication between the parties involved in these transactions. To bridge the gap between the parties involved in these transactions comes "Sales force Service Cloud." The service cloud makes things easier and manageable for the customer and the service provider. In this project, we have used various features of the Salesforce cloud to effectively provide customer service. These features include Omni-Channel, Case Management, Knowledge Base, Process and Routine Automation, Service Analytics, Self-Service Communities, Einstein Bots, etc. Agents no longer need to use multiple resources to manage a case. All the information for case management is available on one platform. Similarly, for customers, knowledge articles, public communities, and platform independent complaint registration and case generation make it easier for them to solve their problems.

Published in: 2022 International Conference on Emerging Trends in Engineering and Medical Sciences (ICETEMS)

Date of Conference: 18-19 November 2022

INSPEC Accession Number: 22932601

Date Added to IEEE *Xplore*: 11 April 2023

DOI: 10.1109/ICETEMS56252.2022.10093576

▸ **ISBN Information:**

Publisher: IEEE

Conference Location: Nagpur, India

Contents

Retinal Damage Detection Using Conv2D Net

Roshni.S. Khedgaonkar ; Anagha Nagrare ; Amogh Pande ; Aniket Funde ; Brajesh Rathi ; Ashutosh Bagde **All Authors**

Abstract: In today's world, eye damage has become common among people with issues like glaucoma, CNV, and other retinal diseases. The retinal image is the basic factor for ophthalm... **View more**

Abstract:
In today's world, eye damage has become common among people with issues like glaucoma, CNV, and other retinal diseases. The retinal image is the basic factor for ophthalmologists to diagnose the different damages in the eye. Traditional eye check-ups are done using an ophthalmoscope or retinoscope. These are the traditional methods wherein the diagnosis is based on the observation of the doctor. To capture a high-resolution cross-section of the retina of patients, the Retinal optical coherence Tomography (OCT) imaging technique was used. OCT images are effective in the display and diagnosis of many retinal conditions. Artificial intelligence (AI) has made a major impact in the domain of medical surgery. In this paper, we have used data consisting of OCT images to identify abnormalities occurring in them compared to a healthy normal eye. We have used Deep learning methods to make effective use of OCT images in processing data and training the model to interpret the type of damage illustrated in it and make decisions based on it. We have proposed to implement a Sequential Model in Keras to detect which retinal damage is present in the OCT image and classify them into four classes- CNV, DME, DRUSEN & NORMAL based on its validation accuracy. To improve the accuracy, we have modified the sets of convolutions with a varied number of layers. We have further tried to increase the validation accuracy by the use of the Sequential model, ResNet50 model, and ResNet50V2 model. Out of all the models that have been used, the Resnet50 model proved to give the highest validation accuracy of97%. The given project would be helpful to Ophthalmologists to give fast, reliable, and efficient diagnoses of the eye with would aid them to begin the treatment of that damage at an early stage.

Published in: 2022 International Conference on Emerging Trends in Engineering and Medical Sciences (ICETEMS)

Date of Conference: 18-19 November 2022

INSPEC Accession Number: 22932652

Date Added to IEEE *Xplore*: 11 April 2023

DOI: 10.1109/ICETEMS56252.2022.10093422

ISBN Information:

Publisher: IEEE

Conference Location: Nagpur, India

Blockchain Based Solution for Secured Transmission of Examination Paper

Smita Kapse ; Mrudula Umalkar ; Atharva Gajbe ; Kaushik Vrudhula ; Ritik Gour ; Shital Telrandhe All Authors

Abstract: In a traditional examination management system, a request for setting question papers and the actual question papers from the Controller of Examination (COE) to various t... **View more**

Abstract:
In a traditional examination management system, a request for setting question papers and the actual question papers from the Controller of Examination (COE) to various teachers and vice-versa, is done physically. Further, the work of sending the finalized paper from the COE to various superintendents of examination is also done physically. In this system, the need for a safe and secure method of setting up and circulating the examination paper is high. The work of sending the finalized paper from COE to various superintendents of examination is done physically, which raises a lot of security concerns. The Blockchain-based system will eliminate the need for physical circulation of the paper, which in turn will reduce extra costs and time required for the paper. The proposed system fulfills all the above criteria with many different technologies working together as one system to provide the desired functionality. The proposed system uses a combination of Blockchain and Interplanetary File System (IPFS) to achieve decentralization and secure peer-to-peer communication between teacher and superintendent.

Published in: 2022 IEEE 2nd International Symposium on Sustainable Energy, Signal Processing and Cyber Security (iSSSC)

Date of Conference: 15-17 December 2022

INSPEC Accession Number: 22723703

Date Added to IEEE *Xplore*: 28 February 2023

DOI: 10.1109/iSSSC56467.2022.10051340

▸ **ISBN Information:**

Publisher: IEEE

Conference Location: Gunupur, Odisha, India

Contents

- **Source:** Grenze International Journal of Engineering & Technology (GIJET) . Jun2022, Vol. 8 Issue 2, p12-16. 5p.
- **Author(s):** Singh, Kavita R.; Lal, Grace; Ninave, Anushree; Wahekar, Vinaya; Deshpande, Devang

- **Abstract:** Algorithms are finite pieces of statements or instructions that are used together to solve a problem. Data and the process applied on the data constitute the scope of our application. Algorithms and data structures along with methods to store and process that data are an integral part of computer science. It is necessary today that students and instructors have a clearer and better understanding of how the common algorithms function and how data behaves. We have created an application that allows its users to perform both of these crucial tasks in a platform-independent fashion. Data visualization means presenting data in a graphical or pictorial form clearly and effectively. There are few standalone-agnostic data visualization and algorithm simulation applications. However, they implement very few Data Structures and Algorithms, not covering different types of algorithms. We have implemented algorithms from different areas in computer science such as Machine Learning, Data Structures, and Algorithms, Data Visualizations, etc. There are various platforms for each domain however very few platforms provide the facility to implement on a single platform. Our web or desktop application would possibly include algorithms of major domains for Educational purposes.

Grenze International Journal of Engineering and Technology, June Issue

Creating a Voice based Email for Blind

Roshni Khedgaokar[1], Anushree Bhure[2] , Janhavi Nagmote[3] ,Sakshi Thakre[4] and Bhushan Surjuse[5]
[1-5]Computer Technology Department, Yeshwantrao Chavan College of Engineering, Nagpur, India
Email: { rskhedgaonkar@ycce.edu, anushreebhure23@gmail.com , janhavinagmote36@gmail.com, thakresakshi26@gmail.com , bhushansurjuse04@gmail.com }

***Abstract*—Many visually impaired people face problems in their life while using apps of the phone for contacting people through calls or emails due to which it is very difficult for them to survive at any workplace and become jobless. So, we are building a voice-based email application for visually challenged people to complete their day-to-day activities quickly and efficiently. It will be fully based on voice command; it will just prompt the blind people for doing different activities then the blind user just has to say a command prompted by the application. Here we are using Google Text to Speech for converting text written in an email to voice and Speech to text library for analyzing and converting it into a body of the email. The use of the keyboard is removed, and the user just must interact with it through voice for doing their work. All the actions will solely depend on voice input given by the user. The main objective of building these applications is to make visually impaired people independent and work efficiently at their work to send, read emails without taking the help of a second person. There will be 4 features in this application: Send Email, Check Inbox, Download an Attachment of a mail, search a mail for which the user gets prompted and he must choose one option at a time. We are adding 2 more features of downloading an attachment from a specified sender and searching mail related to a specified user.**

***Index Terms*— Speech to Text(STT), Text to Speech(TTS),Interactive Voice Response(IVR).**

I. INTRODUCTION

Globally, at least 2.2 billion people have vision impairment near or distance. Vision impairment poses an enormous global financial burden with the annual global costs of productivity losses associated with vision impairment from uncorrected myopia and Presbyopia alone is estimated to be US$ 244 billion and US$ 25.4 billion.[1] This is a major problem nowadays and we must look for it and use an alternative to tackle this problem to avoid unwanted loss. To solve this problem, we came up with a solution to create a voicebased email system. A voice-based email application is a way of sending and receiving emails through voice commands. It is specially designed for blind people so that they can contact other people through emails. Here the blind user just must choose an option by giving voice input to the application and depending on the input by the blind user the application will perform its work. By this, some things of blind people will get easy like it will be easy for them to interact with other people through emails. Also contacting people through the mail over voice input will save a lot of time and energy.

II. LITERATURE SURVEY

On studying various similar research papers and models regarding the voice-based email application, the commonly used technologies which are used in those systems are:

Grenze ID: 01.GIJET.8.2.508_2

Screen Readers: Screen readers[2] are the software programs that act as the interface between the computer and operating system and then with application and user. It allows the user to read the data from the screen using a speech synthesizer. The thing is one needs to point the pointer and the application will read.
Braille Keyboards : These are braille typewriters which are like a normal keyboard that is the standard keyboard that is connected to the computer, and accepts its input.
IVR: An Interactive Voice response [3]is a business phone system that interacts which the user. It listens to the user analyses the user's voice and then replies in the form of voice.
Speech to text conversion: The voice of the user is taken as input by the server and then get converted to the text.
Text to speech conversion: The text is taken as input by the server and then get converted into speech.
A survey conducted showed that there were more than 250 million visually challenged people around the globe who were unaware about of how to use Internet or E-mail.
The only way by which a visually impaired person can send an E-mail was, they must dictate the entire content of the mail to a third person (not visually challenged) and then the third person will compose the mail and send on the behalf of the visually impaired person. But this was not a correct way to deal with this problem. It was very less likely that every time a visually challenged person can find someone for help. So, for the betterment of society and giving an equal status to such especially abled people many of them came up with this idea which provided the user with ability to send mails using voice commands.
Internet has become one of the basic amenities for day-to-day living. Every human being is widely accessing the knowledge and information through internet. However, blind people face difficulties in accessing these text materials, also in using any service provided through internet. The advancement in computer based accessible systems has opened many avenues for the visually impaired across the globe in a wide way[1]
In 2014, a web-based application was developed stands as the inclusive practice that can be used by all kind of people afterwards it was used for visually challenged people. The proposed system allows blind people to use Email system easily. As the input to the system does not use keyboard or mouse, users can easily give input by speaking the message.[2]
The advancement in computer based accessible systems has opened many avenues for the visually impaired across a wide majority of the globe. Audio feedback based virtual environment like, the screen readers have helped Blind people to access internet applications immensely. However, a large section of visually impaired people in different countries, the Indian sub-continent could not benefit much from such systems.[3]
A similar idea was proposed in 2016 In this system mainly three types of technologies were used namely: STT (Speech-to-text), TTS (text-to-speech), IVR (Interactive voice response). [4]
An adaptive email access for blind was developed in 2017 which was based on IVR-Interactive Voice Response While using this system the computer will be prompting the user to perform specific operations. [5]
In 2019, an idea was proposed that focused on providing the basic functionalities like composing, reading, sending, and receiving emails along with voice-based interaction. [5]
IVR describes the interaction between the user and the system in the way of responding using keyboard for the respective voice message [6]
Interactive voice response (IVR) is an advanced technology which allows a computer to interact with humans using keyboard. IVR allows user to interact with an email host system via a system keyboard, after that user can easily service their own enquiries by listening to the IVR dialogue. [7]. IVR systems generally respond with pre-recorded or dynamically generated audio voice to further assist users on how to proceed [8]. The main goal of this architecture is to provide visually challenged people got know more about the type of conditions they must survive. The prevailing email systems don't give any means of feedback or Talkback service[9]
The most common mail services that we tend to use in our day-to-day life cannot be used by visually challenged people. This is because of they do not offer any facility in order that the person in front will listen the content of the screen. As they cannot visualize what is already present on screen they cannot build out where to click to perform the required operations[10]
Limitations of the existing system are as followed:
1. Screen readers always require someone to point the cursor and then only the visually impaired person could listen to the text, and it cannot spell various technical and biological words.
2. Every person could not know the braille language and here again, one could be required to connect the keyboard to the computer.
3. If the system requires a fingerprint one can easily acquire that through various malpractices. These disadvantages are tried to remove in this application.

III. METHODOLOGY

Block diagram:

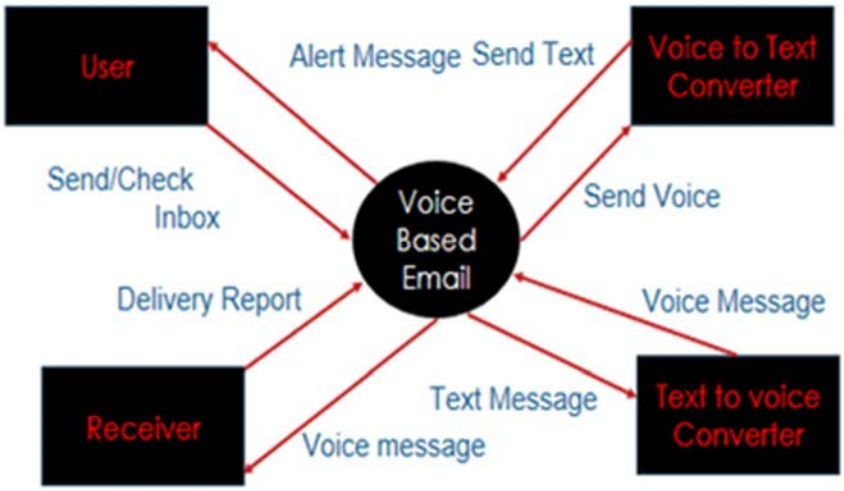

Fig 1.1: Block diagram of Voice-Based Email

In the block diagram of the proposed approach as shown in fig 1.1, we can see that users can check their inboxes, read emails, send emails, and receive alert messages from the proposed approach. Voice recognition (SR) is a multidisciplinary subject of linguistics[7] that develops approaches and technology that allow computers to recognize and translate speech into text. "Automated Voice Recognition" (ASR), "computer speech recognition," or simply "Speech to Text" are all terms used to describe it (STT). It brings together knowledge and research from the domains of linguistics, computing, and electrical engineering. Some SR systems employ[6] "Training" (also known as "Enrollment"), in which a single speaker reads text or isolated vocabulary into the proposed method. The proposed method examines a person's unique voice and uses it to fine-tune the popularity of that person's speech, resulting in improved accuracy. Users can utilize the suggested approach to give voice commands, and the Voice to Text Converter will translate those commands into text, i.e., the mail will be delivered to the chosen recipient after the user provides voice inputs. The proposed approach will teach the user in the form of voice commands to ask for completing various operations. For example, the user can check their mailbox, read their emails, send emails, and receive alert messages. Voice recognition (SR) is a multidisciplinary subject of linguistics that develops approaches and technology that allow computers to recognize and translate speech into text. "Automated Voice Recognition" (ASR)[4], "computer speech recognition," or simply "Speech to Text" are all terms used to describe it (STT). It brings together knowledge and research from the domains of linguistics, computing, and electrical engineering. Some SR systems employ "Training" (also known as "Enrollment"), in which a single speaker reads text or isolated vocabulary into the proposed method. The proposed method examines a person's unique voice and uses it to fine-tune the popularity of that person's speech, resulting in improved accuracy. Users can send voice commands through the proposed approach and then Voice to text converter will convert those commands into text i.e., the mail will be sent to the specified recipient after taking voice inputs from a user. Text to voice converter will instruct the user in the form of voice commands to ask for performing different actions.

The proposed technique gets started after encountering Start, and it examines whether the user is a new or existing one, as shown in fig 1.2. If the user is new, he must register for the proposed approach; otherwise, if the user is already registered, he must log in with credentials to the proposed approach. If a user enters the wrong login credentials, then he is prompted by the message Invalid login/ Password else Login is successful. After the user is logged in, the proposed approach gives a count of seen and unseen emails in the inbox. Also, it reads out the message of recent emails. (here Text-to-Speech is used). Users can also compose an email to send it to a valid recipient. The user must select the compose mail option to do so. If the user selects the compose a mail option, the proposed technique listens to the user's voice commands. Speech to Text is the technology used in this case. Other features added are Download an attachment and Search mail. As a result, the proposed method generates output based on the user's input. Finally, the user has the option to Logout from the voice-based email system.

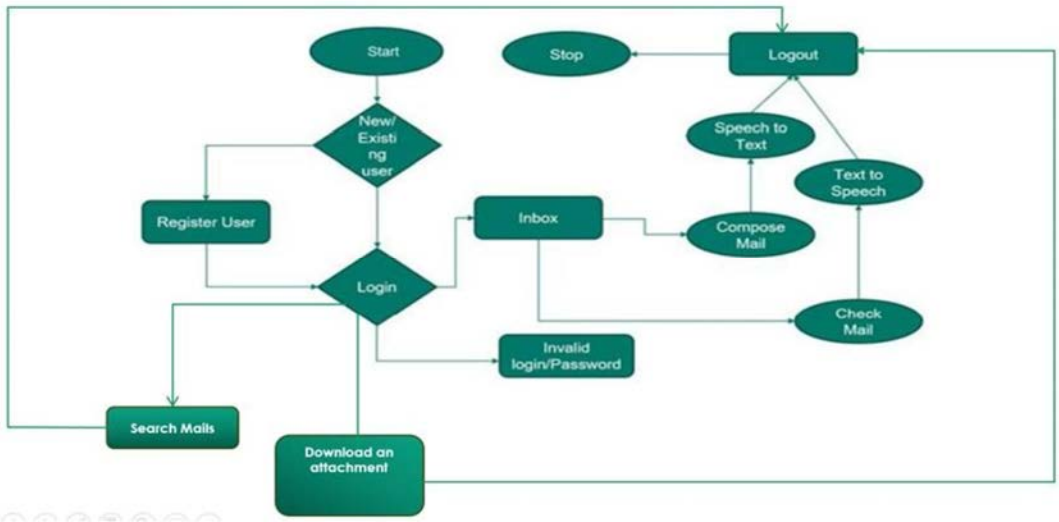

Fig 1.2: Flowchart for Voice-Based Email for blind

The proposed approach developed by us includes the following modules as follows:

Self-sign-up/sign-in: As shown in fig 1.3, This e-mail system has a feature of speech to text(STT)as well as text to speech(TTS) which makes the proposed approach easy to handle. Users can log in without taking the help of any other person. Users can give voice input of their email address and password as well for signing up into the proposed approach. The user's credentials will already be kept at the backend by the developer.

Compose a mail: Following the selection of the required category, the user can create an email by giving voice input for the recipient's email address and the email's subject text. As a result of which email can be composed. Send a message: The constructed email can be sent to the appropriate recipient, and the user will be notified once the message has been sent. For sending the email, the user must give voice input of the receiver's email address.

Read inbox: The proposed approach, on the other hand, will read emails received in the inbox section after asking the user whether they should be read or not. In addition, the proposed approach displays the total number of viewed and unseen emails in the user's mailbox. The voice engine(proposed approach) will continue to ask the user what action they want to take to support the activity. When the user has finished with the module, he can return to the main page by following the commands/instructions.

Download Attachment: In this feature an attachment is downloaded which is sent by the sender to the respective recipient. The attachment can be of any type of pdf, image, word file, etc. It will be saved in a particular path that we have specified in our code. So, the attachment will be saved in a particular folder. This helps us to download files present in the mail number provided. It also reads out the mail content.

Search Email: In this feature, we get to know how many emails for the mail number associated with a username are present. Mail related to username will be given in the form of ids.

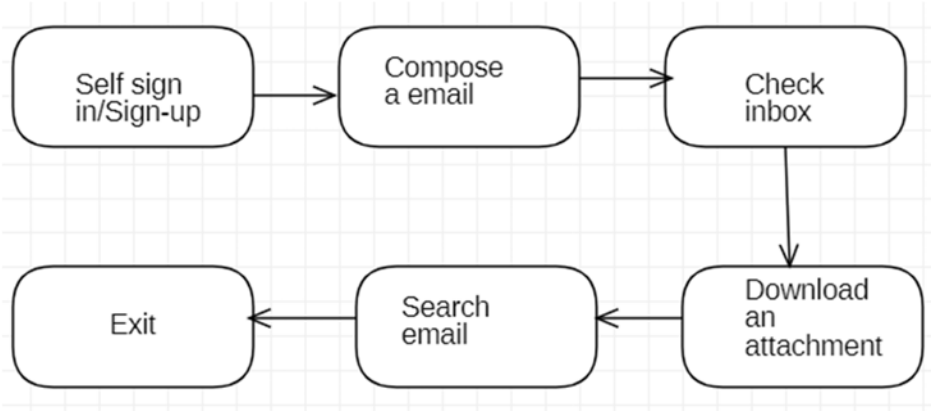

Fig 1.3: Flow diagram for modules

ALGORITHM: The proposed approach uses an algorithm that converts passwords or other credentials into hash functions and stores them in the database using various Hashing Algorithms (MD5, SHA)[5], resulting in stronger security than traditional systems. MD5 stands for the message-digest algorithm. SHA stands for secure hashing algorithm. Figure 1.3 depicts the procedure of utilizing the hashing algorithm:

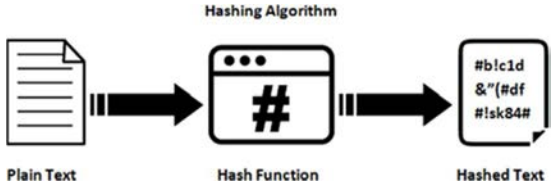

Fig 1.3: Hashing Algorithm

The user will give voice input which will be in the form of a wave and that voice input will be converted into text by the system. The waveform is shown in fig 1.4 as below.

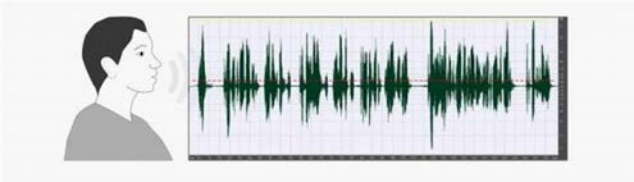

Fig 1.4: Waveform of a human voice

IV. Experimental Results

The proposed system will make it easier for visually impaired people to use various email services. Here one doesn't need to learn the keyboard key's location and various shortcuts to run the email application as keyboard need is eliminated. As here everything must be performed only just by using voice commands the application will do the required action internally on its own. Aside from that user may be able to feed information as of messages, email through voice inputs itself.

V. Conclusion and Future Scope

Speech recognition (Speech to Text) is used in this proposed approach, and anything we say is transformed into text. Similarly, when the user receives a message, the suggested method converts the text to a voice, allowing the user to comprehend the message. One of the primary advantages is that users do not need to utilize a keyboard. All actions will be based on click events. This proposed strategy will assist blind persons in overcoming the challenges they previously had in accessing emails. We've stopped using keyboard shortcuts in conjunction with screen readers, which can help with the cognitive strain of knowing shortcuts. This study presents the structural architecture of a Voicemail system that a blind person may use to access emails more easily. The study uses a computer to assist blind people in sending and receiving voice-based email messages in their native language. As a result, visually challenged people will find the proposed method simple to utilize. Future Scope includes:

1. Users will receive voice-based notifications.
2. Users can search any email by saying it.
3. Users can delete unwanted emails.

References

[1] G.Shoba1, G.Anusha2 , V.Jeevitha3 , R.Shanmathi4. An interactive mail for the visually impaired. International Journal of Advanced Research in Computer and Communication Engineering. Vol. 3, Issue 1, January 2014.

[2] PranjalIngle ,HarshadaKanade , Arti Lanke(2016). Voicebased e-mail system for Blinds International Journal of Research Studies in Computer Science and Engineering (IJRSCSE) Volume 3, Issue 1, 2016.

[3] V.Priyadharshini,C.Nandhini,R.Nivathi, 1 R.Nivetha, 2 R.Madhumitha 1 UG students, 2 Assistant Professor(2017). Smart Assistance System for the Visually Impaired. International Journal of Scientific & Engineering Research Volume 8, Issue 5, May2017 120 ISSN 2229-5518.

[4] Belinda, M.J. &Nandhagopal, Rupavathy& Mahalakshmi, N.R.. (2018). A voice based text mail system for visually impaired. International Journal of Engineering and Technology(UAE). 7. 132-136. 10.14419/ijet.v7i1.7.10633.

[5] Prof. Priya U. Thakare, Kote Shubham, Pawale Ankit, Rajguru Ajinkya, Shelke Om (2017). Smart Assistance System for the Visually Impaired. International Journal of Scientific and Research Publications, Volume 7, Issue 12, December 2017 378 ISSN 2250- 3153.
[6] Bishal Kalita and Santosh Kumar Mahto, "Voice Based Email for Blind People". International Journal of Engineering Science and Computing (IJESC) - Volume 9, Issue 10, October2019, pp. 23789-23799.
[7] Latha L, Babu B, Sowndharya S(2019). Voice Based Email with Security for Visually Challenged. International Journal of Engineering and Advanced Technology (IJEAT) ISSN: 2249 – 8958, Volume-8, Issue-6S3, September 2019.
[8] V. Priyadharshini, C. Nandhini, R. Nivathi, R. Nivetha, R. Madhumitha (2017). An Adaptive Email access for blind people. International Journal of Scientific & Engineering Research Volume 8, Issue 5, May-2017 120 ISSN 2229-5518.
[9] M.J. carmel Mary Belinda, Rupavathy Nandhagopal, N.R. Mahalakshmi. A Voice based text mail system for visually impaired. International Journal of Engineering and Technology 7(1):132-136. DOI: 10,14419/ijet. v7i1.7.10633.
[10] Poonam Pate, Zeeshan Tamboli, Harsh Panchal, Diksha Jain "Voice Based E-mail Application for Blind/Visually Impaired People" IJARIIE, 2017, Vol-3, Issue3, ISSN (O)-2395-4396. www.ijariie.com.

Visualization Of Furniture Model Using Augmented Reality

Publisher: IEEE

Gendlal M Vaidya ; Yugant Loya ; Pranav Dudhe ; Rohan Sawarkar ; Sankalp Chanekar **All Authors**

Abstract:AR furniture aims at providing a platform to visualize a furniture model using augmented reality (AR) so that it will be easy to choose the furniture according to color c... **View more**

Abstract:
AR furniture aims at providing a platform to visualize a furniture model using augmented reality (AR) so that it will be easy to choose the furniture according to color combinations and combinations of furniture. This application provides a real representation of furniture as a 3D model interpreting in a real world. This Application let user choose the choice of furniture from a range of furniture and let them place 3D object of the same furniture on empty area so that they can look at the way it will feel at that area. You can view multiple objects at the same time. It will help in decorating empty room. By looking at multiple object user will be able to choose object that he/she desires. The project is developed on Unity Software and Visual Studio

Published in: 2022 Fifth International Conference on Computational Intelligence and Communication Technologies (CCICT)

Date of Conference: 08-09 July 2022

Date Added to IEEE *Xplore*: 12 October 2022

ISBN Information:

INSPEC Accession Number: 22136765

DOI: 10.1109/CCiCT56684.2022.00092

Publisher: IEEE

Conference Location: Sonepat, India

Contents

Smart Intelligent Computing and Applications, Volume 2 pp 339–347

Deep Neural Network for Generation and Detection of an Image

Roshni S. Khedgaonkar, Kavita Singh, Pravinkumar M. Sonsare & Sabiha Zamir

Conference paper | First Online: 22 May 2022

292 Accesses

Part of the Smart Innovation, Systems and Technologies book series (SIST,volume 283)

Abstract

Deep learning is a boon for the industry in today's era. Deep learning comes up with powerful algorithms like generative adversarial network (GAN) and convolutional neural network (CNN) for synthetic image generation and to detect different objects from an image. In this paper, both GAN and CNN were demonstrated in a consecutive manner so the objective of generation and detection will be figured out in a single implementation. In essence, the GAN will induce synthetic images from the real image dataset, and the output of GAN will dispense as an input to CNN for detection purposes. The experimentation has performed on celebrity face dataset. This model will be implemented for security, health diagnosis, E-commerce, etc.

Keywords

Generative adversarial network (GAN)

Convolutional neural network (CNN) **CovNet first section**

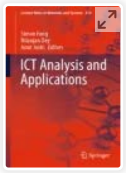

ICT Analysis and Applications pp 47–55

Efficient Strategies to Manage Road Traffic Using Big Data Analytics

Yogesh Golhar & Manali Kshirsagar

Conference paper | First Online: 07 January 2022

Part of the Lecture Notes in Networks and Systems book series (LNNS,volume 314)

Abstract

The on-road traffic increases due to the exponential growth of the number of vehicles on the road. That leads to undesirable road conditions and makes urban population life uncomfortable. It includes traffic congestion, traffic jams, and long queues at traffic signals and toll booths. Many people violate road traffic rules and regulations rules every day. Manual human effort and supervision are not enough to resolve these issues. Still, many road traffic managements follow the traditional approach, which results increase in road accidents that makes humans seriously injured and even loss of life. To address these issues, we have proposed four strategies as (1) congestion status on square, (2) efficient toll tax collection, (3) fine collection on road for the people who violate road traffic rules and (4) shortest pathfinder for drivers. This research work mainly focuses on the various strategies and their implementation with the help of the MapReduce framework. We have combined video surveillance, big data analytics algorithm and implemented efficient road traffic management system.

Keywords

Big data **Congestion degree** **HDFS** **Hadoop** **Video surveillance**

Segregation and User Interactive Visualization of Covid-19 Tweets Using Text Mining Techniques

Chaudhary, G.; Kshirsagar, M..

International Conference on Machine Learning and Big Data Analytics, ICMLBDA 2021 ; 256:268-279, 2022.
Article in English | Scopus | ID: covidwho-1473934

ABSTRACT
One of the worst calamities the world is facing since early 2020 is corona virus or Covid-19 disease which has turned into a pandemic claiming millions of lives across the globe. Twitter sources huge number of tweets related to this disease from users globally. This research focuses on mining Covid-19 tweets using machine learning techniques. The tweets are first pre-processed and converted to a form suitable for applying clustering algorithms. Principal Components Analysis is used to separate most significant components. Similar tweets are categorized using Hierarchical agglomerative clustering. The segregated tweets are visualized on novel and interactive cluster plots, members of which can be identified on user interface interactively by user for easy interpretation. The implementation is done using R programming. Clusters of similar tweets can be used to analyze the response of people to the pandemic across countries, compare and adopt best practices across countries to address the pandemic based on people views, combat spread of rumors and other such applications. © 2022, The Author(s), under exclusive license to Springer Nature Switzerland AG.

RESEARCH ARTICLE | OCTOBER 31 2022

Design of band gap reference circuit in 45nm for low voltage applications

Ujwala Ghodeswar ; G. G. Sarate; Pravin Dakhole

+ Author & Article Information
AIP Conf. Proc. 2494, 060001 (2022)
https://doi.org/10.1063/5.0107007

In this paper band gap reference circuit is proposed operating at 1 V supply voltage. This circuit is operated from −50°C to 80°C with temperature coefficient of 150ppm/0C. This circuit gives 0.96 V output voltages. Aspect ratio is adjusted to achieve the desired voltage. Proposed circuit reduces number of transistors as compared to the conventional method. Conventional and modified Band gap reference is implemented in 45nm and the results are compared. Proposed circuit is implemented in LTSPICE software with level 54, 45nm technology model file.

Topics

Transistors

RESEARCH ARTICLE | OCTOBER 31 2022

CMOS implementation for low power analog multiplier

Pravin Dakhole ; Ankita Tijare; Ujawala Ghodeswar

+ Author & Article Information
AIP Conf. Proc. 2494, 070012 (2022)
https://doi.org/10.1063/5.0108145

A novel CMOS four quadrant Analog multiplier in voltage mode configuration is designed and simulation. The results are analyzed using CMOS 180nm technology. The input voltage is applied to bulk terminal MOS to make it operate in exponential manner. The proposed multiplier architecture uses this exponential circuit and provides high performance characteristics for the Multiplier circuit. The results aresimulated on 180 nm technology. The 3dB measured bandwidth is 200.33MHz, power consumption achieved is 598nW. The designed multiplier architecture is feasible for many applications because of low voltage, low power high bandwidth and simple structure.

Topics
Analog circuits, Energy use and applications

Design and analysis of wireless sensor network for intelligent transportation and industry automation

Author(s): Prabhakar D. Dorge [1] ; Prasanna M. Palsodkar [2] ; Divya Dandekar [3]

View affiliations

Affiliations: 1: Department of Electronics and Telecommunication Enginnering, Yeshwantrao Chavan College of Engineering, India
2: Department of Electronics Engineering, Yeshwantrao Chavan College of Engineering, India
3: Department of Electronics Engineering, Hochschule Breman University, USA

Source: Intelligent Network Design Driven by Big Data Analytics, IoT, AI and Cloud Computing,2022

Publication date September 2022

- « Previous Chapter
- Table of contents
- Next Chapter »

Abstract

This work is based on the wireless sensor networks (WSN), which contain an insufficient number of device nodes, regularly similarly stated nodes or sensors, and sensor knots that are associated with all other wireless communications. There are numerous assumptions or overall possessions of WSNs, and a lot more applications of WSNs around the creation are presented, making it unbearable to protect all their application areas. Applications of WSNs span ecological and animal monitoring, factory and manufacturing monitoring, farming monitoring and mechanization, healthiness monitoring, and many other areas. One of the most characteristics of WSNs is that they are strongly coupled with their application. In this chapter, WI-MAX without wormhole attack is explained, and the related results are explained with their outputs The NS2 evaluation system is applied to production out of all imitations.

Chapter Contents:

Book DOI: 10.1049/PBPC054E
Chapter DOI: 10.1049/PBPC054E_ch11
ISBN: 9781839535338
e-ISBN: 9781839535345

Preview this chapter:

Related content

No related content was found for this content

Quality Assessment Method for Image Inpainting

Shweta Dhondse ; Milind Mushrif All Authors

Abstract:A comprehensive study of types of quality assessment methods used for inpainted images is presented in this paper. Both quantitative and qualitative measures are studied ... **View more**

Metadata

Abstract:
A comprehensive study of types of quality assessment methods used for inpainted images is presented in this paper. Both quantitative and qualitative measures are studied in detail. The process of inpainting can be compared to blind convolution problem. Therefore, a quality assessment metric with no reference is discussed for assessing the inpainted image quality quantitatively. The objective assessment of inpainted image is done by Degree of Noticeability and Average Squared Visual Salience score. It is observed that the objective score does not always match with the human perception and hence subjective analysis is proposed on the basis of observer score.

Published in: 2022 International Conference on Emerging Trends in Engineering and Medical Sciences (ICETEMS)

Date of Conference: 18-19 November 2022

INSPEC Accession Number: 22932643

Date Added to IEEE *Xplore*: 11 April 2023

DOI: 10.1109/ICETEMS56252.2022.10093282

ISBN Information:

Publisher: IEEE

Conference Location: Nagpur, India

Contents

I. Introduction

Image quality assessment is referred as the problem of evaluating the perceptual image quality level. Several methods are proposed in [1], [2], [3], [4], [5], [7], [8] to predict the image quality. The goal of quality assessment of inpainted image is to evaluate that the restored image is visually pleasing. The method of inpainting can be thought of as a specialised picture restoration challenge that cannot be applied to all images. Because of this specific nature of the problem of inpainting the Image Inpainting quality assessment (IIQA) methods cannot be directly applied. In case of object removal and reconstruction which include large areas, the reconstructed region may be completely different than

the original one because of ill construction of structures or amount of occlusion. The goal of the Image Inpainting Quality Assessment (IIQA) measure is to assess whether the inpainted regions are visually pleasing with respect to spatial coherence of the existing parts of the image.

References

References is not available for this document.

Authors

Figures

References

Keywords

Metrics

More Like This

A New TwIST: Two-Step Iterative Shrinkage/Thresholding Algorithms for Image Restoration
IEEE Transactions on Image Processing
Published: 2007

Loss Functions for Image Restoration With Neural Networks
IEEE Transactions on Computational Imaging
Published: 2017

Show More

References

References is not available for this document.

Design of Universal Set of CMOS Gates using Multiple Valued Logic

Publisher: IEEE

Yashika Gaidhani ; Ashutosh Bagade ; Monica Kalbande ; Archana Kishorrao Vaidya All Authors

Abstract: The design and implementation of digital circuits are performed in the binary logic switching algebra. The binary logic switching algebra is used to design and build digi... **View more**

Metadata

Abstract:

The design and implementation of digital circuits are performed in the binary logic switching algebra. The binary logic switching algebra is used to design and build digital circuits. We are developing a generic collection of gates for use in the synthesis and simplification of digital MV Logic circuits. Using digital circuits with multiple-valued logic, we can reduce the number of connections. MVL digital circuits can be designed by expanding the representation domain from the binary level (N=2) switching algebra to N > 2 levels. The implementation of an MVL digital circuit uses universal sets of MVL CMOS gates. The design and implementation of a universal set of CMOS gates are the topics of this work. In this paper we are dealing with the design and implementation of a universal set of CMOS gates, which includes extended AND operators: eANDI, eAND2,eAND3, Maximum operator and Successor operators for designing of any MVL digital circuits. Implemented circuits gives the proper functionality of the MVL combinational and sequential circuit design. In this MVL digital circuit uses voltage mode for operation having different range of voltages.

Published in: 2022 International Conference on Emerging Trends in Engineering and Medical Sciences (ICETEMS)

Date of Conference: 18-19 November 2022

INSPEC Accession Number: 22932644

Date Added to IEEE *Xplore*: 11 April 2023

DOI: 10.1109/ICETEMS56252.2022.10093527

ISBN Information:

Publisher: IEEE

Conference Location: Nagpur, India

Contents

I. Introduction

The two level logic (binary logic) switching algebra, where D is the domain of numerical representation, is typically used to implement digital circuits. The value of the digital representation domain must be increased to N levels in order to design Multiple Valued Logic circuits. D={0,1, 2 N- 1}. Many-valued or multi-valued logic are additional namesfor multiple valued logic (MVL). The universal gate design setis used to implement the sequential and combinational operators that operate in the B domain. As we embed several systems on a single integrated circuit (IC), or System on a Chip (SoC), the delay time as well as the complexity and length of the interconnections rise. To deal with the interconnection issues Multiple Valued logic is suitable optionas it reduces the number of interconnections [1].There are two technologies we can use for build MVL ICs, these are voltage mode and current mode. In the voltage mode, there are N number of logic levels. For defining logic levels different voltages as threshold are used in CMOS gates that is PMOS and NMOS transistors [3] and [4]. Supplementary Symmetrical Logic Circuit(SUSLOC) technology said that the MVL implementation needs less power consumption, improves the response time of MVL circuits compared with the binary logic and reduces the number of interconnection length [5]. Very few ICs are built in voltage mode proposals.

References

References is not available for this document.

Authors

Figures

References

Keywords

Metrics

More Like This

Majority logic gate synthesis approaches for post-CMOS logic circuits: A review
IEEE International Conference on Electro/Information Technology
Published: 2014

A novel current-mode design scheme for multi-valued logic gates
2002 23rd International Conference on Microelectronics. Proceedings (Cat. No.02TH8595)
Published: 2002

Show More

References

References is not available for this document.

A Survey on Floating Point Arithmetic Units for Non-Linear Application

Publisher: IEEE

Kuldeep G Pande ; Pradeep T Karule All Authors

Abstract: This paper contributes to the comprehensive study of floating point arithmetic. It lists many researchers' contributions to improving the general functionality of floatin... **View more**

Metadata

Abstract:
This paper contributes to the comprehensive study of floating point arithmetic. It lists many researchers' contributions to improving the general functionality of floating point arithmetic units through the development of numerous new and updated algorithms in a variety of engineering and technological applications. An extensive analysis and presentation of a collection of over 20 research articles and more than 10 survey papers pertaining to various algorithms for various arithmetic units was done to assist future researchers in making meaningful contributions to the field of VLSI. The survey articles considered for this literature are classified into different categories based on performance, accuracy, and area for some specific applications. Because of significant amount of research work has been focused on reducing power consumption during execution, the paper's comparative study focuses primarily on Performance, takes the parameters into account, and compares them to existing Algorithms. According to the paper that was part of our study, the main goal was to develop various arithmetic units that would keep the overall performance of the floating point arithmetic units balanced over their lifetime while decreasing the area, increasing performance, and requiring less energy for different operations performed by a single arithmetic unit. The work also contributes to the discussion of the difficulties in designing an architecture and algorithm for floating point arithmetic units taking into account the interdependency of different performance criteria. Designing effective floating point architecture is a challenge nowadays because changing floating point architectures is such a challenging subject for researchers.

Published in: 2022 International Conference on Emerging Trends in Engineering and Medical Sciences (ICETEMS)

Date of Conference: 18-19 November 2022

INSPEC Accession Number: 22932665

Date Added to IEEE *Xplore*: 11 April 2023

DOI: 10.1109/ICETEMS56252.2022.10093408

ISBN Information:

Publisher: IEEE

Conference Location: Nagpur, India

References

References is not available for this document.

Contents

In the past, fixed-point arithmetic has been used by the majority of DSP applications to reduce power consumption, latency, and chip size. In fixed-point arithmetic, there are a number of major overflow, underflow, scaling, and other issues. To prevent The idea of floating point arithmetic is highly helpful for overflow, underflow, and to offer automated scaling. Compared to fixed point numbers, floating point numbers are more accurate and have higher resolution. As seen in figures 1 and 2, the structure for 64-bit and 32-bit IEEE 754 floating-point numbers is essentially separated into three blocks: the sign field, exponent field, and mantissa field. The sign field uses the "1" bit, which is available in both 32-bit and 64-bit versions. In 32 bit and 64 bit Signals, the exponent field uses 8 bits while the mantissa field uses 23 bits and 52 bits, respectively. While the operation that must be performed on the sign bit and exponent bit is rather simple, the operation on the mantissa, one of the enormous fields, is more difficult [1]. Addition and subtraction are two of the processes that are required by nearly all DSP processors, microprocessors, and other FIR filters. The primary drawback of FP operations in comparison to fixed-point operations is their slowness. As a result, in order to accelerate FP arithmetic, many operations must be combined into a single FP unit. This will thus decrease power, space, and time lag [1] [3].

References

References is not available for this document.

Computationally Optimized Approximate Computing for Signal Processing Applications

Publisher: IEEE

Prasanna Palsodkar ; Prachi Palsodkar ; Pravin Dakhole ; Roshan Umate ; Ajay Gurjar ; Aniket Gokhale All Authors

Abstract: Computational optimization through approximation approach proves to be an effective way for Digital Signal Processing (DSP) at anemometric scales. Here approximation meth... **View more**

Metadata

Abstract:
Computational optimization through approximation approach proves to be an effective way for Digital Signal Processing (DSP) at anemometric scales. Here approximation methodology is discussed to design arithmetic blocks of DSP. Implementation on Xilinx ISE 13.2 on Spartan 6 is done for approximate arithmetic block analysis like adder and multiplier which are capable to do area, power and delay optimization if some error is tolerable. Approximate Computational Complexity (ACC) method based 4:2 compressor is designed for image compression gives area, delay and power reduction as 18%, 7% and 49% respectively. Area and power optimized 8 * 8 image compression obtained at the cost of 20% increase in error rate which is tolerable with reference to adequate PSNR.

Published in: 2022 International Conference on Emerging Trends in Engineering and Medical Sciences (ICETEMS)

Date of Conference: 18-19 November 2022

Date Added to IEEE *Xplore*: 11 April 2023

ISBN Information:

INSPEC Accession Number: 22932651

DOI: 10.1109/ICETEMS56252.2022.10093398

Publisher: IEEE

Conference Location: Nagpur, India

Contents

I. Introduction

Due to the diminishing benefits from semiconductor technology scaling on one hand and to keep the explosive growth in data on other hand introduces a new method of computing i.e. Approximation and Stochastic. optimization of speed is permissible at some permitted rate of approximation. Approximation is determined by considerations of energy efficiency. Stochastic computing is a random selection methodology provides a paradigm to improve fault tolerance with the reduction in area

References

References is not available for this document.

Authors

Figures

References

Keywords

Metrics

References

References is not available for this document.

Machine Learningcloud-Based Approach to Identify and Classify Disease

Brijendra Gupta ; Vilas D. Alagdeve ; Pydimarri Padmaja ; T. Coumaressin ; V. Naresh Kumar Reddy ; R. Ganesh Kumar All Authors

Abstract: The term "Internet of Things" (IoT) describes the process of creating and modeling web-related physical objects across computing systems. IoT-based healthcare application... **View more**

Metadata

Abstract:

The term "Internet of Things" (IoT) describes the process of creating and modeling web-related physical objects across computing systems. IoT-based healthcare applications have offered multiple real-time products and benefits in recent years. For millions of people, these programmers provide hospitalization can get regular medical records and healthy lives. The introduction of IoT devices in the health sector has several technological developments. This study uses the IoT to construct a disease diagnostic system. Wearable sensors in this system initially monitor the patient's sympathy impulses. The impulses are then sent by a network environment to a server. In addition, a new hybrid approach to evaluation decision-making was presented as part of this research. This technique starts with the development of a set of features of the patient's pulses. Based on a learning approach qualifications are neglected. A fuzzy neural model was used as a diagnostic tool. A specific diagnosis of a particular ailment, such as the diagnosis of a patient's normal and abnormal pulse or the assessment of insulin issues, would be modeled to assess this technology.

Published in: 2022 IEEE 2nd Mysore Sub Section International Conference (MysuruCon)

Date of Conference: 16-17 October 2022

Date Added to IEEE *Xplore*: 13 December 2022

ISBN Information:

INSPEC Accession Number: 22443633

DOI: 10.1109/MysuruCon55714.2022.9972738

Publisher: IEEE

Conference Location: Mysuru, India

Contents

I. Introduction

IoT represents the practical and functional connection between different parts of the Internet of Things. IoT deals with the problem that more powerful mobile phones, servers, and laptops are preferable to less powerful network components [1]-[2]. Watches, mobile phones, and electronic gadgets are examples of such small gadgets. Ingeniously designed by computers, real-world sensors and results have been integrated into common human objects such as refrigerators [3]. Electronics could now create a smart grid ecosystem are more efficient than a black gadget. These IoT devices have the cognitive and decision-making abilities to function independently of human management [4]. The concept that gadgets might accomplish everything change, like multiplexing. An object can process data from a person or source and send them to the result [5].

Sign In to Continue Reading

References

References is not available for this document.

Authors

Figures

References

Keywords

Metrics

Back to Results

More Like This

Non-Invasive Assessment Model of Liver Disease Severity by Serum Markers Using Cloud Computing and Internet of Things
IEEE Access
Published: 2018

Health Disease Prediction Using Machine Learning and Internet of Things
2023 4th International Conference on Intelligent Engineering and Management (ICIEM)
Published: 2023

Show More

References

References is not available for this document.

Sensor Cloudlet Interconnecting System for water Reservoirs Security

Prachi Palsodkar ; Rishabh Shrivastav ; Anvesh Ayangar ; Sayali Atkare ; Suraj Yadav ; Prasanna Palsodkar All Authors

Abstract:DAM management systems in India are executed manually and not having any emergency control, unexpected and overcast management. Manual DAM maintenance is one of the chall... **View more**

▸ **Metadata**

Abstract:
DAM management systems in India are executed manually and not having any emergency control, unexpected and overcast management. Manual DAM maintenance is one of the challenging tasks due to large geological area and depth. This paper has proposed an design strategy using ESP826 node MCU based auto regulation operation cloudlet design with distinct sensors such as Ultrasonic sensors, temperature and humidity sensor, rainfall sensor and servomotors to detect water pressure, water level, and water flow and warning system. An AI and Block chain (BC) based secure system with sensor cloudlet is effective future technologies to avoid any disaster with added security to DAM infrastructure. IoT systems challenges like heterogeneity, poor interoperability, supply limits, confidentiality and safety loopholes can be overcome with BC and IOT collaboration, improves privacy and security with more reliable solution.

Published in: 2022 IEEE 10th Region 10 Humanitarian Technology Conference (R10-HTC)

Date of Conference: 16-18 September 2022

Date Added to IEEE *Xplore*: 03 November 2022

▸ **ISBN Information:**

▸ **ISSN Information:**

INSPEC Accession Number: 22237790

DOI: 10.1109/R10-HTC54060.2022.9929471

Publisher: IEEE

Conference Location: Hyderabad, India

Contents

I. Introduction

India has total 5264 manmade water reservoirs, out of which 2069 are in Maharashtra state. Manual maintenance of these reservoirs is quite difficult and inefficient. Dam over water level can be disastrous. Challenges of Dam failure are poor maintenance, earthquakes, extreme rainfall, design error, inadequate capacity, instability caused by changes in water level. Dam maintenance team does checking in pre-monsoon and post monsoon for gate opening system, head regulators earth bunds and spillway [1]. These all maintenance arrangement is manual and need a smart sensor system for emergency to give an indication of a rise in water level, an increase in rainfall, gate status along with automatic control and alert.

References

References is not available for this document.

Authors

Figures

References

Keywords

Metrics

Back to Results

More Like This

Artificial Intelligence and Internet of Things for Robotic Disaster Response
2020 International Conference on Advanced Robotics and Intelligent Systems (ARIS)
Published: 2020

Prominent Rule Control-based Internet of Things: Poultry Farm Management System
2022 International Conference on Power, Energy, Control and Transmission Systems (ICPECTS)
Published: 2022

Show More

References

References is not available for this document.

Machine Learningcloud-Based Approach to Identify and Classify Disease

Brijendra Gupta ; Vilas D. Alagdeve ; Pydimarri Padmaja ; T. Coumaressin ; V. Naresh Kumar Reddy ; R. Ganesh Kumar All Authors

Abstract: The term "Internet of Things" (IoT) describes the process of creating and modeling web-related physical objects across computing systems. IoT-based healthcare application... **View more**

Metadata

Abstract:
The term "Internet of Things" (IoT) describes the process of creating and modeling web-related physical objects across computing systems. IoT-based healthcare applications have offered multiple real-time products and benefits in recent years. For millions of people, these programmers provide hospitalization can get regular medical records and healthy lives. The introduction of IoT devices in the health sector has several technological developments. This study uses the IoT to construct a disease diagnostic system. Wearable sensors in this system initially monitor the patient's sympathy impulses. The impulses are then sent by a network environment to a server. In addition, a new hybrid approach to evaluation decision-making was presented as part of this research. This technique starts with the development of a set of features of the patient's pulses. Based on a learning approach qualifications are neglected. A fuzzy neural model was used as a diagnostic tool. A specific diagnosis of a particular ailment, such as the diagnosis of a patient's normal and abnormal pulse or the assessment of insulin issues, would be modeled to assess this technology.

Published in: 2022 IEEE 2nd Mysore Sub Section International Conference (MysuruCon)

Date of Conference: 16-17 October 2022

INSPEC Accession Number: 22443633

Date Added to IEEE *Xplore*: 13 December 2022

DOI: 10.1109/MysuruCon55714.2022.9972738

ISBN Information:

Publisher: IEEE

Conference Location: Mysuru, India

Contents

IoT represents the practical and functional connection between different parts of the Internet of Things. IoT deals with the problem that more powerful mobile phones, servers, and laptops are preferable to less powerful network components [1]-[2]. Watches, mobile phones, and electronic gadgets are examples of such small gadgets. Ingeniously designed by computers, real-world sensors and results have been integrated into common human objects such as vehicles [3]. Electronics could now create a smart grid ecosystem are more efficient than a black gadget. These IoT devices have the cognitive and decision-making abilities to function independently of human management [4]. The concept that gadgets might accomplish everything change, like multiplexing. An object can process data from a person or source and send them to the result [5].

References

References is not available for this document.

Authors

Figures

References

Keywords

Metrics

Back to Results

More Like This

Non-Invasive Assessment Model of Liver Disease Severity by Serum Markers Using Cloud Computing and Internet of Things
IEEE Access
Published: 2018

Health Disease Prediction Using Machine Learning and Internet of Things
2023 4th International Conference on Intelligent Engineering and Management (ICIEM)
Published: 2023

Show More

References

References is not available for this document.

Greeniot: A Smart IoT Gateway for Connected Farming

Publisher: IEEE

Ujwala Ghodeswar ; Trakshay Balagotra ; Aditya Borale ; Ketan Pawar ; Tejas Parate ; Sanika Mahajan All Authors

Abstract: This paper elaborates the use of Cloud computing and IoT for farmers. This brings the farm-land to the farmer's doorstep. Greeniot is a comprehensive Internet of Things s... **View more**

Metadata

Abstract:

This paper elaborates the use of Cloud computing and IoT for farmers. This brings the farm-land to the farmer's doorstep. Greeniot is a comprehensive Internet of Things solution to help farmers for execution of agricultural operations in smarter and efficient ways. The high-precision sensors are used to provide proper data for assessing soil quality, detect diseases in plants, predict ambient conditions, sunlight, humidity, moisture, and pH required for production and data driven farming for better crop production and smart use of farming resources. The devices are mapped to the local server and the data is sent to the server. The server can retain the data for some time and then transfers it to the cloud-based platform, which then provides predictive analytics for specific plant and crop models. Using this technique farmers can get all the analytics, insights, and personalized recommendations in layman's language on a mobile app.

Published in: 2022 IEEE 7th International conference for Convergence in Technology (I2CT)

Date of Conference: 07-09 April 2022

Date Added to IEEE *Xplore*: 18 July 2022

ISBN Information:

INSPEC Accession Number: 21883033

DOI: 10.1109/I2CT54291.2022.9824907

Publisher: IEEE

Conference Location: Mumbai, India

I. Introduction

In today's world, the population is rapidly growing, it is predicted to reach 9.8 billion by 2050, hence one of the world's problem is to generate more yield by 2050, cultivate more and more crops as per the need of the increasing population in the world. Along with this day by day, the requirement of additional farmable land, and water is increasing. Solution to these difficulties faced by today's farmers is the need of a device or Equipment which can speed up production and reduce loss of time and crops which gets wasted and damaged due to weather conditions which can be solved by an IoT Device. This device will be helping farmers to control and monitor crops. In this paper Smart IoT solution for farmers is proposed that brings the farms-land to the farmer doorstep.

Authors

Figures

References

Keywords

Metrics

Back to Results

More Like This

Artificial Intelligence and Internet of Things for Sustainable Farming and Smart Agriculture
IEEE Access
Published: 2023

Internet of Things in Agriculture: A Decision Support System for Precision Farming
2019 IEEE Intl Conf on Dependable, Autonomic and Secure Computing, Intl Conf on Pervasive Intelligence and Computing, Intl Conf on Cloud and Big Data Computing, Intl Conf on Cyber Science and Technology Congress (DASC/PiCom/CBDCom/CyberSciTech)
Published: 2019

Show More

References

References is not available for this document.

Identification of Fraudulent Credit Card transactions using Machine Learning Algorithms

Publisher: IEEE

P. A. Jadhav ; Urvashi Lalwani ; Ayush Gour ; Mohammad Shayan ; Shubham Motwani **All Authors**

Abstract: Ever since the existence of e commerce payments systems came into being, people have found new ways to access someone's credentials illegally. This is a major issue in cu... **View more**

Metadata

Abstract:

Ever since the existence of e commerce payments systems came into being, people have found new ways to access someone's credentials illegally. This is a major issue in current era as more and more transactions are being done online. Every year fraud cost generated in the economy is more than $4 trillion internationally. This is not surprising, as the return on investment for fraud detection and preventior$ 100 million. Financial institutions such as commercial and investment banks operations are increasingly being targeted and require some method to handle and support the progress of credit card fraud detection. To avoid fraud and to secure transactions systems they require some advanced technology that support the use of artificial intelligence (AI) and machine learning (ML) approaches to stay one step ahead of criminals. Being a classification type problem, we propose a ML model incorporating XGBoost algorithm along with SMOTE analysis. Our aim is to minimize the number of fraudulent transactions being predicted as legitimate transactions as the gravity of these type of errors outweighs that of the other in a real world scenario.

Published in: 2022 IEEE 7th International conference for Convergence in Technology (I2CT)

Date of Conference: 07-09 April 2022

INSPEC Accession Number: 21882896

Date Added to IEEE *Xplore*: 18 July 2022

DOI: 10.1109/I2CT54291.2022.9824165

ISBN Information:

Publisher: IEEE

Conference Location: Mumbai, India

Contents

I. Introduction

Credit card fraud is one of the forms of identity theft where individuals make purchases or obtain money using a credit card that has been assigned to someone else. This can occur in multiple methods either by physical theft of credit card, account PIN, or by opening new credit card accounts in someone's name without any permission. Once in, the thieves then make illegal transactions leaving the card holder and the company with the bill.

Authors

Figures

References

Keywords

Metrics

Back to Results | Next >

References

References is not available for this document.

More Like This

Features of Low and Highly Susceptible Individuals in Retail Investment Fraud: A Machine Learning – Based Analysis
2023 International Conference in Advances in Power, Signal, and Information Technology (APSIT)
Published: 2023

Performance Evaluation of Machine Learning Methods for Credit Card Fraud Detection Using SMOTE and AdaBoost
IEEE Access
Published: 2021

Show More

References

References is not available for this document.

Yocto Based Home Automation using Open BMC Platform and RestAPI

Publisher: IEEE

Prachi Palsodkar ; Mohit Wankhede ; Chaitanya Borkute ; Atharva Chaudhari ; Bhavesh Waghwani ; Prasanna Palsodkar All Authors

Abstract: Automation in electronics growing and requires mass manufacture in an automated fashion with enhanced efficiency. Yocto based project gets built the tool named Bit bake. ... **View more**

Metadata

Abstract:
Automation in electronics growing and requires mass manufacture in an automated fashion with enhanced efficiency. Yocto based project gets built the tool named Bit bake. It works on multi-threading and scheduling, which aids in parallel testing of numerous boards in unit attempt. This paper expresses the innards of Yocto based system design for efficient automation using Open BMC. Open BMC supports open source Linux collaboration with a goal of producing baseboard management controllers to work across heterogeneous systems.

Published in: 2022 IEEE Delhi Section Conference (DELCON)

Date of Conference: 11-13 February 2022

INSPEC Accession Number: 21759707

Date Added to IEEE *Xplore*: 20 April 2022

DOI: 10.1109/DELCON54057.2022.9753045

ISBN Information:

Publisher: IEEE

Conference Location: New Delhi, India

Contents

Yocto is an open embedded (OE) project progress, which needs a tool for development of Linux images [1]. It is a partnership project which provides template, tools and technique to set up customized Linux based embedded product [2]. Yocto project provides reduced memory footprint at kernel and at package level. It provides a flexibility to do addition as per application need. Bit Bake (command-line interface) and hob (GUI based interface) are two possible procedures to customize Linux packages in Yocto project to build optimum sized image with selected features [3]. Some Commonly known Yocto projects are Poky (It includes the Open Embedded-Core layer along with Bit Bake and metadata to help users get started on creating their own Linux distributions), Bit Bake is a build engine that allows the running of shell and Python scripts in parallel effectively. Layers in Yocto are collections of methods, generally clustered around a central theme, e.g. web development, Python or Java support, or secure repository for application data. Board support packages, or BSPs, contain information about certain devices, consisting of any hardware present (or missing) from the device, drivers, and information about the device kernel. There are several BSP-s available for Poky, with the option of developers to make their own custom BSP with the Yocto-BSP tool [4]

References

References is not available for this document.

Authors

Figures

References

Keywords

Metrics

Back to Results

References

References is not available for this document.

Congestion Avoidance Mechanism in Adhoc On-Demand Distance Vector Routing Protocol for Mobile AdHoc Networks

Publisher: IEEE

Abstract: The Mobile AdHoc Network (MANET) is a wireless network of mobile nodes with limited energy and bandwidth that operates in a dynamic environment. It is based on decentrali... **View more**

Metadata

Abstract:
The Mobile AdHoc Network (MANET) is a wireless network of mobile nodes with limited energy and bandwidth that operates in a dynamic environment. It is based on decentralized management. Because of the limited amount of resources available, maintaining long-term contact with a large number of activities in a dense network is difficult. It is possible to communicate effectively in a light network without a congestion control strategy by using Adhoc On-Demand Distance Vector (AODV). Congestion, on the other hand, occurs in dense networks because of the high volume of traffic and the need to send packets in a continuous stream. Increased energy consumption and a shortened network lifespan are both consequences of congestion. With higher QoS in high-density networks, this research proposes a Congestion Avoidance Mechanism (CAMA) for AODV to reduce congestion. In order to reduce energy consumption and end-to-end delay while simultaneously improving packet delivery ratio and throughput, the suggested architecture makes use of the cross-layer idea. The suggested CAMA's performance assessments are superior to those of the Congestion Control AODV (CCAODV) and the AODV.

Published in: 2022 International Conference on Electronics and Renewable Systems (ICEARS)

Date of Conference: 16-18 March 2022

INSPEC Accession Number: 21688308

Date Added to IEEE *Xplore*: 13 April 2022

DOI: 10.1109/ICEARS53579.2022.9752198

ISBN Information:

Publisher: IEEE

Conference Location: Tuticorin, India

Contents

I. Introduction

A MANET is a self-configuring and self-healing wireless ad hoc network made up of several mobile nodes without any central management. It is possible for each mobile node to establish communication with other nodes in the transmission range, or to assist other nodes in their communication. Packet collision, packet retransmission, packet losses, and many other problems are brought on by mobile nodes' dual nature in congested networks [1], [2]. For low-density networks, ADOV delivers higher service quality, but its performance degrades as the number of services in the network grows. MANET nodes' limited bandwidth and energy must be efficiently utilised to both extend the life of the network and improve communication between nodes.. A mobile node's limited bandwidth can't manage a slew of packets coming from a variety of sources and intended for a variety of purposes. This excessive transmission of packets uses the limited energy of the mobile nodes and hence shortens the network's lifespan. As a result of congestion, routing protocols' packet delivery capacity and latency suffer. Congestion in MANETs is a major concern for researchers, who are looking for ways to improve congestion control mechanisms in existing routing protocols. Overheads or excessive energy usage are required to reduce congestion in [1]-[3] and [5]-[10], respectively. Current routing protocols can't use congestion control because of limitations imposed by MANET. Cross-layer strategy to reducing energy consumption and congestion control mechanism to improve network performance for stable and dependable route are some of the contributions made by this work. We employ a cross-layer (CL) strategy to make efficient use of finite energy while also reducing communication delays from end to end. The CL method violates the TCP/IP model's layering requirements by sharing information between layers that are not contiguous. This non-adjacent information sharing contributes to the long-term viability of the network. Analysing traffic flow at each node is necessary for congestion management mechanisms, so that packet drops can be avoided. Control packets can be used as a counter in order to record and manage packets in a fashion that is useful in analysing traffic flow. AdHoc network performance improves as a result of the CL congestion control method. When multiple nodes are involved in a multihop communication, it can lead to connection breakages, higher energy usage, and longer delays. If a weak node joins in communication, the route discovery procedure is restarted since the weak node may abandon communication owing to depleted energy. Delays and congestion are caused by these issues, which are energy-intensive.

Authors

Figures

References

Keywords

Metrics

References

References is not available for this document.

Back to Results | Next >

References

References is not available for this document.

Paper_ID: ICCIES_164

Review of Control Methods for Power Converters in DG system and Microgrids.

Bharat Sudame[1,a)], Sumant Kadwane[2,b)], Laxmikant Padamwar[3,c)]

[1,2]Yeshwantrao Chavan College of Engineering, Nagpur, [3]MSETCL, Mumbai.

[a)]bharat_sudame@rediffmail.com,[b)]sgkadwane@gmail.com,[c)]laxmikant.padamwar@gmail.com

Abstract. In recent years, various advanced control methods have been successfully proposed as an alternative to traditional cascade linear controllers for power converters in distributed electrical systems and microgrids. The main transport of this research is to discuss advanced controllers to improve the dynamic performance and visibility of dynamic electronic power converters in these applications. This article introduces the main roles and functions of voltage source converters in distributed generation systems and microgrids. Although such power electronics systems are non-linear in nature but the design of the controller can be done in a linearized way. Next, the most popular advanced control methods will be reviewed. In this context, key principles and implementation principles, benefits and advantages of data-based advanced control methods are present. This article concludes with a discussion of good research directions in the field of advanced controls for power electronic converters.

Keywords. Advanced Control, Distributed Generation (DG), Voltage Source Converters (VSC), Microgrids

Paper_ID: ICCIES_107

Solar Based Garbage Cleaning and Surveillance Ship for Lake

Gaurav C. Gondhalekar[1,a)], Pranay S. Shete[2,b)], Vaibhav R. Doifode[3,c)], Dr. Pradip B. Jain[4,d)]

[1]Assistant Professor, Electrical Engg. Dept., YCCE,Nagpur, [2]Assistant Professor, Electrical Engg. Dept., YCCE, Nagpur,[3]Assistant Professor, Electrical Engg. Dept., YCCE Nagpur, [4]Prof. and Hod, DMIMS, Wardha.

[a)]gg.ycce@gmail.com, [b)]pranay.shete85@gmail.com, [c)]vaibhawdoifode85@gmail.com,
[d)] unicorn.gaurav@gmail.com

Abstract. Water pollution has been a topic of concern in recent years both in India and worldwide. The floating objects on the water surface many times get clogged in the drainage system and cause choking of the system which results in other harmful effects. Also, such floating objects are consumed by the animals residing in the waters as food items and become the cause of their death. Another concern is the security of the water bodies. To deal with this problem we are proposing this Garbage Cleaning System (Ship). This system works on solar energy so it is non-polluting. The ship is so constructed that it has two metal frames with a mechanical arm on one of the frames and the solar panel on the other. Two dc motors are used for navigation of the ship and two motors are for the movement of the arm and the bucket. As the ship is designed for the operations in water wireless communication system ZigBee is used to communicate with the ship for reliable operation. When the operator identifies any garbage in the water, then according to his/her commands from the laptop, the ship goes to the desired place, picks up the garbage and comes back. For security and surveillance purpose it has a camera mounted on it which records audio-video footage which can be seen when the ship docks back home. This device is a prototype that can prove to be useful in cleaning lakes, rivers, ponds, etc. and if implemented wisely can prove to be a great aid for security and surveillance.

Keywords. Design of ship, Construction of ship, Control Circuit, Navigation.

Paper_ID: ICCIES_138

Automatic Home Renewable Energy Management and Distribution System

Ankita Suresh Satdeve[1,a)], Ravindra M. Moharil[2,b)]

[1,2]Department of Electrical Engineering, Yeshwantrao Chavan College of Engineering, Nagpur

[a)]ankisatdeve78@gmail.com, [b)]rmm_ycce_ep@yahoo.com

Abstract. The energy generated from Renewable Energy Sources (RES) are eco-friendly, sustainable, reduces global warming and greenhouse effect. Reduction in the capital cost of solar photovoltaic panels and wind generator helps to enhance the utilization of Renewable energy sources. Indian government has an ambitious plan to install 100 GW of solar PV system out of which 40 GW is through roof top solar system. The Roof Top Solar Photovoltaic (RTSPV) policy declared by Maharashtra State Government in 2015, major industry sector preferred to install RTSPV. Indian homes are also now preferring to shift from conventional power from the grid to RTSPV connected to the grid. Along with the usage of renewable energy the smart grid technology is preferred by these homes over traditional grid. Smart grid uses Advanced metering infrastructure and Demand side management techniques to balance the load and generation. The objective of this paper is to utilize maximum amount of renewable energy from the RTSPV and minimize the electricity bill. To reduce the dependency on grid further, Energy Storage System (ESS) is used. The strategy used in this paper is maximize the usage of Renewable energy sources with a proper usage of Home Energy Management System architecture. This renewable or green energy is used to fulfill the demand of Home load and also it reduced (nearly negligible) the cost of the electricity bill of prosumer (producer +customer). When the energy generation is more than the demand of the home load, the storage is checked. If there is a scope for storage then it is stored first and then remaining will be penetrate into the grid. If the load demand is not fulfilled through RTSPV and ESS then the electricity is imported from the grid. The amount of selling energy to main grid and energy consumed from main grid is calculated by Net metering and gives electricity bill. The Real time pricing (day-ahead price signal) tariff is used for this system in which cost of energy changes hourly basis. A proper strategy for Power Scheduling at low price time slot and high price time slot reduced the energy cost according to day-ahead price signal is also mentioned. Further the roof top space is better utilized by using double sided solar panels. Here the analysis of the same is provided. If there is increase in energy generation, the cost of energy will decrease, hence doubled area of solar panel gives more benefits from the system with less investment. By increasing the capacity of the Energy storage system, the losses of energy reduced. The High Peak-to-Average ratio lowered the cost of energy, therefore energy cost as well as Peak-to-Average ratio have maintained accordingly.

Keywords. Energy management and distribution, Smart grid, Main controller, Smart meter, Electric storage system, Power scheduling.

Paper_ID: ICCIES_156

Analysis Of Electrical Energy Conservation For Hotel

Mr.P.B.Joshi [1,a)], Dr.S.R.Vaishnav [2,b)]

[1]Department of Electrical Enginnering YCCE,Nagpur,India, [3]Department of Electrical Enginnering JDCOEM,Nagpur,India

[a)]joshiprasad1985@gmail.com [b)]vaishnavsatish@gmail.com

Abstract. Energy is very important constraints in all sectors for any country's economy. The economic development of any country is closely linked with consumption of energy. The availability of conventional sources of energy are in limited forms. These sources are important for electricity generation. Energy demand has increased as its consumption increased so proper energy conservation methodology to be adopted. Energy Conservation avoids wasteful use of energy. A study of energy audit and conservation is carried out in many sectors like industrial, Academic and commercial. Commercial sector is one of the major energy consuming sectors. The main focus is on identification of energy conservation in commercial sector. In this paper, Nagpur five star hotel energy audit was done. Estimation of monthly energy consumption is studied through analysis of electric bills. Energy conservation areas are identified. It will help to implement the energy efficient project for improving energy efficiency of hotel. Also, the electrical energy audit and safety audit was carried out to find the harmonics in voltage and current. Readings were taken under the power quality analyzer condition.

Keywords. Energy Audit, Energy Conservation, Electrical safety audit, power quality analyzer.

Paper_ID: ICCIES_167

Design and analysis of Z source multilevel Inverter for speed control of Induction motor.

Akshay Kadu[1,a)], Bhushan Bagde[2,b)]

[1,2]Yeshwantrao Chavan College of Engineering Nagpur

[a)]akshaykadu001@gmail.com, [b)]by.bagde@rediffmail.com

Abstract. This work deals with design and analysis of Z source based multilevel inverter for Induction motor application. Z source inverter have unique feature to boost the output voltage and also conventional two level voltage source inverter have certain drawback which is overcome by multilevel inverter therefore utilizing all these advantages of Z source and Multilevel Inverter technology this paper introduces a new electrical drive system for speed control of Induction motor. This Z source topology reduces two conversion stages to single stage having low complexity thereby reducing the overall cost and size of an electrical drive. Z source multilevel Inverter is controlled by pulse width modulation technique. Simulation is carried out using MATLAB/SIMULINK software. It was found that the designed electrical drive circuit have offer less total harmonic distortion with Phase disposition pulse width modulation (PDPWM) after compared to other Pulse width modulation techniques.

Keywords. Z source, Multilevel Inverter, Pulse width modulation.

Paper_ID: ICCIES_152

Reliability Analysis of Quadratic Converter Based Solar PV System

Aniket P. Munshi[1,a)], Sumant G. Kadwane [2,b)], Nitesh Y. Funde[3,c)]

[1,2]Electrical Engineering Department, Yeshwantrao Chavan College of Engineering, Nagpur, M.S., India

[3]Skywing Technologies, Pune, M.S., India

[a)]aniketmunshi@gmail.com, [b)]sgkadwane@gmail.com, [c)]nitesh_funde@gmail.com

Abstract. A Photo Voltaic (PV) based generation system is nowadays widely used and requires most reliable and cost effective inverter configuration. In case of PV based systems, a buck boost converter which is commonly used is essential for maximum power point tracking (MPPT) and load matching. This paper investigates the reliability of conventional boost converter and impedance source based inverters for PV based systems. Also, more reliable inverter configuration with a Quadratic impedance source based converter topology is evaluated for improved reliability. The overall reliability of a PV based generation system is presented with buck – boost converter and quadratic impedance source inverter. The simulations are carried out in MATLAB and the results show that the proposed Quadratic converter based inverter is emerging out to have more reliable configurations. Further, experimental results of quadratic converter based inverter are also presented.

Keywords. Grid connected inverter, Quadratic converter, Reliability, Solar PV.

Paper_ID: ICCIES_153

REVIEW ON CONSERVATION ENERGY IN POWER PLANT

Nisha Shrirao[1,a)], Tomesh Sahu[2,b)], Shital Telrandhe[3,c)]

[1]Yeshwantrao Chavan College of Engineering,Nagpur, [2]Canara bank ,Mumbai,
[3]Jawaharlal Nehru Medical Sciences,DMIMS,Sawangi,Wardha.

[a)]sahu.nisha11@yahoo.in, [b)]ATOMU111@gmail.com, [c)]shital.telrandhe88@gmail.com

Abstract. As one of the foremost important power sources in modern society, electricity takes up a large proportion of modern energy consumption. Among all those methods of power generation, fossil-fuel thermal power generation is one among the earliest ways of large¬scale electricity production. Its popularity within the modern society comes from its stability and controllability. Given the wide applications of electricity round the world, improving the efficiency of thermal power plants would be an efficient thanks to reduce the entire energy consumption and protect the environment. The paper discusses the efficiency of energy transition and its determinant during each stage of power generations along side proposals to improve the efficiency of thermal power generation.

Keywords. BOILER, ID FAN, FD FAN.

Paper_ID: ICCIES_163

Scope And Opportunities Of Energy Conservation And Monitoring In Rolling Mills

Pranay S. Shete[1,a)], Prasad B. Joshi[2,b)], Kshitij Tikle[3,c)], Roshan Umate[4,d)]

[1,2]Assistant Professor YCCE, Nagpur, [3]M-Tech Scholar CoE, Pune, [4]Research Consultant JNMC-DMIMS, Wardha

[a)]pranay.shete85@gmail.com, [b)]joshiprasad1985@gmail.com , [c)]kshtikle10@gmail.com, [d)]roshanumate111@gmail.com

Abstract. Efficient control, monitoring and energy conservation plays important role in the assessment of annual investment on electricity consumption in every industry. In central India there are few industries who invest approx. one third from their profit on electricity bills on every month. Out of several loads the one which is considered as most energy intensive load is process where to reduce the thickness of the cold rolling coils as per requirement. Here the power requirement is fulfilled by a distribution transformer which is used to drive the mill motors, entry tension reel, dispatch tension reel and auxiliaries. The data available in an industry can be used to reduce the power consumption and ultimately which may lead to lessen the electricity bill of an industry. To reduce the thickness of the sheet is limited and in order to reduce the power consumption, the constraints such as grade of coil, number of passes and mill reduction capacity has to be taken into consideration. The data such as weight of the coil, number of existing passes, the starting thickness and ending thickness is available in industry and can be used to calculate length of coil and further using the length average speed and total time can be calculated using simple mathematics. In order to monitor and control the several physical quantities such as flow, pressures, temperatures, liquid levels and their detection, several transducers are used in an industry. Proper selection of these devices and the knowledge associated with them are necessary for their implementation and figure out the faults associated with it. Thus, the overall measuring processes are improved and cost of future expansion is reduced by proper knowledge and ratings of the transducers.

Keywords. Consumption Pattern, calculation, exiting energy consumption pattern, scope and opportunity for energy saving, process flow.

Paper_ID: ICCIES_108

Rural Electrification Using Maintenance Free Hybrid Generation

Prof. Vaibhaw R. Doifode[1,a)], Prof. Pranay S. Shete[2,b)], Prof. Gaurav C. Gondhalekar [3,c)], Prof. Avishkar V. Wanjari[4,d)]

[1-3]Department of Electrical Engineering Yeshwantrao Chavan College of Engineering Nagpur, India ,

[4]Department of Electrical Engineering Govindrao Wanjari College of Engineering Nagpur, India

[a)]vaibhawdoifode85@gmail.com,[b)]pranay.shete85@gmail.com ,[c)]gg.ycce@gmail.com,[d)]avishkarwanjari@gmail.com

Abstract. Electrical power plays a vital role in our lives. We need electricity for industry, agriculture, transport, communication etc. The fundamental relationship between energy and economics is more people with more income, means a rise in production and hence more consumption of energy. Electric power demand is increasing day by day in all sectors along with population. Population and income growth are the most powerful driving forces behind electrical power demand globally. To deal with the situation power engineers continuously focuses on the increase in the utilization of the new and renewable energy. Till date only wind generator and the solar PV are the two energy sources which gives promising results and the mobility to utilize the energy generated through them. Due to technical limitations, the size of the wind generator or solar PV is more than that of the generating electric power. After so many years of research researchers said that the power utilization which generated through solar PV and wind turbine can be easily possible for less load rating.

Keywords. Wind generator, Solar PV, Charge Controller, Boost Converter, Battery, Protection Circuitary.

Paper_ID: ICCIES_129

Solar Water Pumping System For Automatic Irrigation Based On GSM Module

Ameya Potdar[1, a)], Anvesh Wadaskar[2,b)], Ashish Shriwas[3, c)], Vaishnavi Deshmukh[4, d)], Medhavi Patil[5, e)], Rohan Khonde[6, f)]

Yeshwantrao chavan college of engineering wanadongri hingna road Nagpur[1,2,3,4,5,6]

[a)]ameypotdar99@gmail.com, [b)]wadaskaranvesh@gmail.com, [c)]ashushriwas10@gmail.com, [d)]vaishnavigajanandeshmukh@gmail.com, [e)]medhavipatil2000@gmail.com, [f)]Khonderohan@gmail.com

Abstract. Today, we live in 21st century where automation is playing a major role in human race. Automation ensures higher production rates, improved safety and shorter workweeks for labours. Many farmers today can't afford to use automation and control machines owing to their high cost. Many villages in India have to use fuel based irrigation system due to a shortage of electricity. Fuels cause global warming and pollution in environment. In this paper our aim is to propose an automatic irrigation system which is cost effective and farmers can use it in an agricultural field. As the system is automated, the pump turns ON/OFF only when the moisture content of soil is below critical level which is regulated by a soil moisture sensor. The objectives of this paper are to control the automatic irrigation system with the help of a GSM module. The farmer at his own discretion can send a message to ON/OFF the pump without going to the field. PIC microcontroller, LCD display, sensors have been used as prime components. Farmer can control the system in automatic or manual mode also substantially reduce the electricity and water cost. We would discuss the design and implementation of the automated irrigation system. Finally, a prototype is designed and implemented and the experimental results are presented.

Keywords. Solar Energy based Automated Water Pumping System, GSM module based Automated Water Pumping System, Intelligent Microcontroller based Circuit Board, Design and Implementation of the Automated Solar Water Pumping System.

Paper_ID: ICCIES_147

Microbial Fuel Cell: Development in Design and Material

Xma Pote[1,a)], Swapnali Kurhade[2,b)], Shital Telrandhe[3,c)]

[1]YESHWANTRAO CHAVAN COLLEGE OF ENGINEERING., [2]Sardar Patel Institute of Technology,Mumbai., [3]DMIMS,Sawangi,Wardha.

[a)] potexma@gmail.com[b)]swapnali.kurhade@spit.ac.in [c)] shital.telrandhe88@gmail.com

Abstract. Energy is the fundamental need of every living organism to carry out various processes internally (metabolic process) and externally. For years together sources like Coal, Diesel, Petrol have been used to generate electrical energy. But, in the perspective of power generation need, focus on renewable energy sources have to be enhanced so as to suffice the future generation energy demand. During recent years, Microbial Fuel Cell technology seems to be the most emerging technology in the renewable field. It includes biological production of electricity in the presence of bacteria, substrates and some chemical solution. This paper fully focuses on different designs of fuel chamber and use of different combinations of materials such as Bacteria, substrate material, Microbes to enhance the generation of electricity by using this technology.

Keywords. Energy, Bacteria, Substrate, Microbes.

RESEARCH ARTICLE | OCTOBER 31 2022

Analysis of temperature effect, incidence angle, fill factor, air mass and pollution factor of solar power generation with rooftop system by monocrystalline solar panel

Shital. S. Kewte ; Shashikant. G. Kewte

+ Author & Article Information

AIP Conf. Proc. 2494, 040002 (2022)
https://doi.org/10.1063/5.0106560

Solar power generation is most clean form of generation among all type of generation. Hence is gaining the first choice of the electricity generating authority all over the world. Still, it is under research and development stage. Solar cell has very low efficiency and due to above facts, these efficiency decreases which ultimately effects the power generation. Mono crystalline solar panels are made up of pure crystal silicon in which there are more mobility for electrons to move hence the efficiency of such panels are more as compared to poly crystalline panels. Moreover, the dimensions area for these panels is near about same. In this paper effect of pollution and incidence angle of solar panels along with temperature and fill factor on roof top systems by using mono crystalline panels are discussed. The panel has significantly reduction in cost since the year 2021. While calculating the power generation of solar roof top power plant, there are some points are to be considered. a) Total energy required or utilizes by load, b) Power Backup required for how many numbers of hours, c) Future expansion of load in coming few years. According to that technical analysis are done. While installing solar roof top system these points are also consider, p) Incident Angle, q) Pollution level of the area in last 5 to 10 year and other point like future expansion of load in coming next 20-year, Available space for roof top, Total shadow free area, Type of roof available at premise, longitude and latitude location of premises, Total sunny days available in that location, Air density and air pollution, Optimum temperature of location.

Topics

Power plants, **Solar energy**, **Solar panels**, **Atmospheric thermodynamics**, **Atmospheric dynamics**, **Air pollution**

RESEARCH ARTICLE | OCTOBER 31 2022

UPFC for enhancing power flow of an AC transmission system using d-q control scheme

Rohan S. Khonde ✉; Priya P. Gaikwad; Saurabh Pingade; Sandeep R. Gaigowal; Ashutosh Bagde

+ Author & Article Information
AIP Conf. Proc. 2494, 070003 (2022)
https://doi.org/10.1063/5.0111160

This paper presents power flow control in electric power systems with the use of a unified power flow controller (UPFC). Voltage regulation, series compensation and phase shifting can be control independently with UPFC which is the most adaptable FACTS controller. It offers both the advantages of STATCOM and SSSC by connecting two VSC's with common dc link. In this paper, the active and reactive power controlled simultaneously without and with UPFC model. This paper also demonstrates control scheme based on p-q transformation. The active and reactive power flow control in the line with the help of network studies are presented in MATLAB Simulink.

Topics
MATLAB, **Electric power**, **Flow control**

RESEARCH ARTICLE | OCTOBER 31 2022

GSM based intelligent solar water pumping system using buck boost converter

Sandeep R. Gaigowal ✉; Rohan S. Khonde; Sandeep Bhongade

+ Author & Article Information
AIP Conf. Proc. 2494, 070005 (2022)
https://doi.org/10.1063/5.0110522

The solar PV based water pumping system is increasing its popularity day by day. Conventional energy sources such as coal, gas, oil is limited reserve. Solar energy is the best substitute to it. Solar water pumping system can be easily installed at the places where electricity is not reached. It can be used for water pumping in dense forest areas where electricity is not present. The advanced solar water pumping system is proposed in this paper. It will realize maximum utilization of solar energy with the help of Buck Boost Converter. A DC-DC converter is positioned between solar PV system and inverter circuit. BLDC motor is operated with the help of hall sensors and rotor position. System study simulation is performed in MALAB Simulink software. Simulation is demonstrated with different value of solar irradiation. A closed loop system is also demonstrated such that inverter fed BLDC motor input voltage remains unchanged. GSM operated water pump system hardware prototype is also developed in this work. Water pump operator can easily control motor turn On/OFF by sending message through GSM.

Topics
Electronic circuits, DC/DC converter, Buck-boost converter, Photovoltaics, Solar energy, Sensors, DC motors

RESEARCH ARTICLE | MARCH 21 2022

Solar radiation forecasting using random forest

Anuradha Munshi ; R. M. Moharil

+ Author & Article Information
AIP Conf. Proc. 2424, 050003 (2022)
https://doi.org/10.1063/5.0076827

Power generation from renewable energy sources is key to a clean energy future and solar energy is world's fastest growing energy sector. Solar energy is renewable, CO2-free and with low operational cost. There are several advantages of using solar energy; however, it does have a few drawbacks such as hefty initial cost, high-priced storage, weather dependency, sizable space requirement, etc. As such, it is critical to predict solar radiation (SR) in an accurate and efficient way to install solar plants in optimal locations. Factors like global horizontal irradiance (GHI), temperature, humidity, cloud cover, wind speed, etc. make SR highly intermittent and variable. Accurate forecasting of SR is vital to finalize installed capacity of the proposed power plant but is extremely challenging due to unpredictability of sunlight. Even the world's best organizations such as the International Energy Agency (IEA) finds it difficult to accurately predict SR. In this work, we analyze global and diffuse SR data gathered from India Meteorological Department (IMD) Pune. This data is first analyzed for features, dominant features are identified, and several machine learning algorithms are employed. Random forest method provides the best results on this data based on several quantitative measures.

Topics
Power plants, Renewable energy, Solar energy, Atmospheric radiation, Machine learning

Development of Data Logger for COVID Vaccine Temperature Monitoring System

Publisher: IEEE

Ketan L. Kasar ; Vijaya S. Rajguru ; Sarala P. Adhau **All Authors**

Abstract: The Data Logger (DL) is a unique tool created to carry out the typical duty of gathering data in a specific area. This common task can include measuring humidity, tempera... **View more**

Metadata

Abstract:
The Data Logger (DL) is a unique tool created to carry out the typical duty of gathering data in a specific area. This common task can include measuring humidity, temperature, pressure or any other physical quantities. Due to the current pandemic situation, its use in temperature monitoring of Covid vaccine will be crucial. According to World Health Organization (WHO) guidelines, COVID vaccine can be stored and transported at -80 °C, -20°C and +2-8°C and shelf life is reduced as vaccine is transferred from one storage temperature to another. So cost effective, efficient and standalone Data Logger (DL) is the need of the hour. The Data logger is proposed to be developed with the use of ESP8266 Node MCU microcontroller. It takes power from a 5V Battery. DS18B20 sensor will be used for temperature sensing. Here we will use Wi-Fi module of ESP8266 Node MCU to send the temperature data from sensor to the Google Sheet over the internet. This real time data will be stored in the format of time and month/date/year. Data logged in Google Sheet will be displayed to the user with the help of graphical user interface (GUI) which is developed using PYTHON scripting language. GUI will allow user to interact with Data Logger through visual graphs. The Data Logger components are mounted on a double layered PCB.

Published in: 2022 IEEE Conference on Interdisciplinary Approaches in Technology and Management for Social Innovation (IATMSI)

Date of Conference: 21-23 December 2022

Date Added to IEEE *Xplore*: 15 May 2023

ISBN Information:

INSPEC Accession Number: 23159800

DOI: 10.1109/IATMSI56455.2022.10119279

Publisher: IEEE

Conference Location: Gwalior, India

Contents

Introduction

Under controlled environmental conditions, including temperature, humidity, pressure, speed, and others, various product categories must be managed. Due to its enormous and unpredictable impacts, temperature is one of these characteristics that is most crucial. Accurate temperature monitoring is becoming crucial in many modern sectors or organizations that concentrate their work primarily on medicines. In these kinds of enterprises, keeping the temperature within the prescribed ranges prevents product loss. Accurate temperature monitoring is necessary for pharmaceutical product processing and storage, including COVID vaccines. COVID vaccine can be stored and transported at -80 °C, -20°C and +2-8°C. There will be a drop in quality if the temperature of these vaccines goes above the limitations that have been set. Reduced vaccine effectiveness in these applications due to inadequate storage temperature settings and temperature changes has a negative impact on safety and cost. Vaccines that are improperly stored lose their effectiveness, endangering patients. Pharmaceutical products are especially susceptible to this typeof scenario since even a slight fluctuation in temperature over brief periods of time can have an adverse effect on the product or render it hazardous. To preserve patient health and life, pharmaceutical items [1] must be kept at the proper temperature. Accurate temperature monitoring is necessary for the processing and storage of medicinal goods, such as vaccines [1]–[3]. Continuous data for a fairly long period oftime is not easy to obtain and it requires development of techniques and technologies for logging the data. The rapid developments in the field of electronics have brought advances in the field of sensors, microcontrollers and data storages. At present there are different types of temperature sensors, both analog and digital. In addition, improvement of the ability of microcontrollers,large capacities of flash memory IC components and on board Wi-Fi based modules give the possibility of merging these basic components into a portable efficient data logger.

Authors

Figures

References

Keywords

Metrics

GIS based Asset Management in Electrical Distribution Utilities

Foolchand Ahirwar ; Ravindra Moharil All Authors

Abstract: Geographical Information System (GIS) is the system through which all the information can be gathered about the distribution system. Reformation information can be gather... **View more**

Metadata

Abstract:
Geographical Information System (GIS) is the system through which all the information can be gathered about the distribution system. Reformation information can be gathered from remote place about distribution network using geo coordinates. Asset management and consumer indexing are the main functionality of the distribution utilities. Currently distribution system faced challenges about the revenue collection, monitoring and controlling the distribution due to limited access during CORONA-19 pandemic. IT based infrastructure of all electrical equipment's and other assets through GIS helps to organize the workflow with less human resource requirement. This paper represents the effective implementation of GIS in the distribution utility for developing the strategical road map for fixing the accountability and achieve the analytical targets. It can be inferred that implementation of GIS in distribution system plays a vital role in planning, improvement in billing, revenue collection, proper asset management. GIS also helps in curtailing power loss by restructuring the distribution network in optimal manner.

Published in: 2022 International Conference on Emerging Trends in Engineering and Medical Sciences (ICETEMS)

Date of Conference: 18-19 November 2022

INSPEC Accession Number: 22932625

Date Added to IEEE *Xplore*: 11 April 2023

DOI: 10.1109/ICETEMS56252.2022.10093288

ISBN Information:

Publisher: IEEE

Conference Location: Nagpur, India

Contents

I. Introduction

Now a days, after Electricity Act 2003 implementation from 2003 onwards, electric power is provided to the consumers mainly by the utilities known as Distribution company (DISCOM). DISCOM is responsible to supply the power to the consumers within their predefined territory in a safe and efficient manner. In most of the DISCOMs, proper mechanism is not available to locate all the assets and consumers under the Supply Division in the proper manner. For proper asset management it is necessary to define and tagged all the assets. Adopting the technique of Geographical Information System (GIS) in the respective Supply Division is the easier methodology to access and analyze the total asset and consumer database to supply the power to the particular distributor division.

Authors
Figures
References
Keywords
Metrics

Power Flow Control through Transmission Line using DSSC

Publisher: IEEE

Sandeep R. Gaigowal ; Sandeep Bhongade ; Ashish Bhagat ; Muzahid Sheikh **All Authors**

Abstract: Static Synchronous Series Compensator (SSSC) is a series lumped FACTS device enabling active power flow control through the transmission line. Highly rated power electron... **View more**

Metadata

Abstract:
Static Synchronous Series Compensator (SSSC) is a series lumped FACTS device enabling active power flow control through the transmission line. Highly rated power electronics converter and coupling transformer circuits makes SSSC installation very limited due to its high cost. Instead, Low cost Distributed Static Series Compensator (DSSC) is reliable option for series compensation. It is one of the Distributed FACTS device which injects voltage in series with the line at 90° angle to line current which is similar to SSSC. It emulates inductive and capacitive reactance and changes effective line reactance for active power flow control in the line. In this paper DSSC is presented. A particle swarm optimization (PSO) method is used to obtain the best location of DSSC placement as well it is applied to find number of DSSC's to achieve active power flow control in optimum way. MATLAB simulation results are presented to demonstrate active power flow control in the line with the help of DSSC devices

Published in: 2022 International Conference on Emerging Trends in Engineering and Medical Sciences (ICETEMS)

Date of Conference: 18-19 November 2022

Date Added to IEEE *Xplore*: 11 April 2023

ISBN Information:

INSPEC Accession Number: 22932671

DOI: 10.1109/ICETEMS56252.2022.10093270

Publisher: IEEE

Conference Location: Nagpur, India

Contents

I. Introduction

India is amongst the highest energy consuming countries and nearabout electricity demand is doubled since 2000. To fulfil electricity demand, power generation is increased in a large extent. The major generated power is from thermal power plants and hydro power plants. Now a day a keen attention is paid on the power generation from renewable sources. All these generated power adds more and more power into existing grid. As a result existing transmission systems are working overloaded or some of the cases; it is near to its thermal limit. This problem can be solved by erecting new transmission lines. Land acquisition problem, environmental issues and high initial investment are the problems in commissioning of new lines. One solution to avoid overloading is to alter line reactance so that power flow can be diverted from overloaded line to underloaded line. Hence it is an urgent need to make transmission system intelligent and controllable. Flexible AC Transmission system (FACTS) finds a solution to control power flow through line by altering line reactance, bus voltage and power angle. Conventionally thyristor controlled inductor and capacitor can be used for power flow control. TCSC, TSSC, SVC are some of the examples. Power Electronics technology enables to use high rating power electronics switches for high rating voltage source inverter. New generation FACTS devices use high power inverters to control power flow. STATCOM, SSSC, UPFC and IPFC are VSC based FACTS devices [1] [2]. But lumped FACTS devices makes system costly and any problem in devices will collapse the whole system. Deepak Divan gives an idea of distributed FACTS. He proposed distributed static series compensator (DSSC). Number of DSSC's are deployed to alter line reactance to control power flow. Deepak Divan and Harjeet Johal proposed distributed series impedances and distributed series reactors as distributed FACTS devices [3] [4]. It provides change in impedance or voltage. It can be implemented with the help of single turn transformer (STT). Number of small rated DSI devices (-10kVA) are connected along the transmission line and provides significant power flow control. In distributed static reactor (DSR), magnetizing reactance of STT tuned to the desired value by air gap setting can be inserted in series with the line [3]. Its power rating is low and it can be provided on the existing line. It does not require any communication links. If current through line exceeds a predetermined value (it can be line thermal rating), DSR devices switched in and injects inductive reactance. As a result effective reactance increases and line current of overloaded line is diverted to other path of less reactance which is underloaded.

Authors
Figures
References
Keywords
Metrics

More Like This

Flexible AC Transmission Systems (FACTS)
2013 International Conference on New Concepts in Smart Cities: Fostering Public and Private Alliances (SmartMILE)
Published: 2013

Power transfer capability enhancement with multitype FACTS controllers using particle swarm optimization
TENCON 2010 - 2010 IEEE Region 10 Conference
Published: 2010

Show More

Solar and Grid Power Integration for Water Pump Application

Publisher: IEEE

Atul Lilhare ; Sumant G Kadwane **All Authors**

Abstract: Water pumping system plays an very important role in irrigation sector However its mostly depend on conventional electricity supply or diesel generator. Dependency on suc... **View more**

Metadata

Abstract:
Water pumping system plays an very important role in irrigation sector However its mostly depend on conventional electricity supply or diesel generator. Dependency on such supply create a burden on non renewable sources. Hence in order to reduce its burden on such energy an effort has been taken in this article. This article consist of solar water pump, which is not only fed by grid but also its supported by non renewable energy i.e. solar photovoltaic. Results in reduction of burden on conventional energy. Proposed system consist of single phase induction motor, DC Boost converter, Inverter and PV array. The system is simulated with MATLAB/SIMULINK software and its results show good response.

Published in: 2022 International Conference on Emerging Trends in Engineering and Medical Sciences (ICETEMS)

Date of Conference: 18-19 November 2022

INSPEC Accession Number: 22932621

Date Added to IEEE *Xplore*: 11 April 2023

DOI: 10.1109/ICETEMS56252.2022.10093631

ISBN Information:

Publisher: IEEE

Conference Location: Nagpur, India

Contents

high diesel costs. Photovoltaic (PV) technology, which converts solar energy into electrical energy to power a DC or AC motor grounded water pump, is the foundation of solar water pumping. Solar water pumping is intended to be more cost-effective than electricity or diesel-powered systems for irrigation and water inventory in pastoral, urban, and rural areas [1].One similar, trustworthy option that is utilised in a variety of ways by the world's ever-evolving technologies is solar power. By compelling a grid-tied system rather than a standalone system to provide just to the load, the power can be exercised and used directly to the load, pushed to the grid if it is available in fat. In terms of stability difficulties, the independent system has an edge over the grid-tied method, making irrigation more practical. As a result, steps are done to provide an achievable result for irrigation at remote locations [2].

Authors

Figures

References

Keywords

Metrics

2022 IEEE 2nd International Symposium on Sustainable Energy, Signal Processing and Cyber Security (iSSSC) | 978-1-6654-9056-6/22/$31.00 ©2022 IEEE | DOI: 10.1109/iSSSC56467.2022.10051280

Impact Analysis of PV Penetration on Voltage Dynamics of Radial Distribution System using Backward Forward Sweep Load Flow Algorithm

Nivedita Padole
Electrical Engineering Department
Yeshwantrao Chavan College of Engineering
Nagpur, India
niveditapande1@gmail.com

Dr. R. M. Moharil
Electrical Engineering Department
Yeshwantrao Chavan College of Engineering
Nagpur, India
rmm_ycce_ep@yahoo.com

***Abstract*— Solar Photovoltaic (SPV) power penetration in the distribution grid is considered as a viable alternative for fossil fuel power plants in the current deregulated power system. SPV power penetration helps to reduce the distribution losses, improves voltage profile of distributor, reduces load on the substation etc. However, increased SPV penetration has concerns about protection, reverse power flow, voltage rise etc. In this paper load flow analysis is done with and without SPV for voltage variation and power loss calculations with forward/backward sweep method for radial distribution network. Various case studies are considered for the comparative analysis. The results revealed that radial distributor performance is better with distributed SPV over concentrated SPV penetration for voltage profile and low power loss parameters.**

Keywords— Backward and Forward Sweep (BFS), Centralized SPV, Distributed SPV, Radial Distribution Network (RDN), Renewable Energy System (RES).

I. INTRODUCTION

Renewable Energy System (RES) integration in the low voltage distribution network has the ability to feed peak energy demands, reduce energy losses in distribution feeders, and offer voltage support. The exponential development of RES installations, on the other hand, may have adverse implications for the existing distribution network, posing various power quality, stability, and protection difficulties. Considering the adverse implications of RES installations, it is of vital importance to understand the technical impacts of high penetration levels of SPV systems on the operating performance of these networks [1]. The potential power quality impacts on LV distribution networks with high penetration levels of solar PV are analyzed by considering IEEE test feeder systems [2].

The spectacular expansion in integrated SPV capacity has resulted in recent developments in distribution networks, where the SPV power from most distributed SPVs is first expended by local loads, with the spare power supplied to the grid [3]-[4]. This integration of SPV leads to massive changes in distribution networks, such as changes in power flow characteristics, increases in load forecast uncertainty, effects on supply of voltage and power loss [5], and even changes in network structure and control mechanism. As a result, power flow analysis is essential for voltage profile assessment of LV distribution networks [6] with significant PV penetration.

According to a thorough literature evaluation, the Backward-Forward Sweep (BFS) load flow algorithm is the appropriate control for the Radial Distribution Network (RDN) load flow analysis [7]. However, a large number of research publications [8] – [12] have reported on the application of the BFS method to several RDN. SPV expansion on the LV grid has alarmed distribution network operators, who are concerned about the negative impact of high PV penetration levels. The behavior of the standard LV grid is being influenced by issues such as abrupt voltage rise and reverse power flow [13] – [16].

This paper discusses the impact analysis of SPV penetration on the voltage profile of the single phase 6 Bus RDN by applying the BFS load flow algorithm. The voltage profile has been analyzed by considering the system with and without PV penetration. The system performance has been investigated in terms of voltage variation and power loss with distributed and centralized PV installations cases. A comparative analysis has been done to identify the appropriate PV installation location for RDN.

In this paper, section II describes the BFS algorithm applied to 6 Bus RDN with and without PV integration. The voltage dynamics at different PV capacities with distributed and centralized installation cases have been illustrated in section III. Conclusions have been drawn in section IV.

II. LOAD FLOW ANALYSIS OF DISTRIBUTION SYSTEM

One of the most significant tools for analyzing power systems at both the design and operation stages is load flow. Although many academicians have developed load flow algorithms for transmission systems, such as the Newton Raphson technique, the rapid decoupling approach, and the Gauss Seidel method etc. When analyzing the load flow in distribution systems, different approaches or algorithms have been preferred. This is due to the distribution system's characteristics of being poorly conditioned, having a high R/X ratio, and having a higher penetration of unpredictably distributed energy resources (DER).

A load flow analysis is required for various planning and operational issues. Before tackling issues like network reconfiguration, loss reduction, load balancing, or service restoration, load flow studies are required. The load flow studies play a significant part in achieving correct voltage

978-1-6654-9056-6/22/$31.00 @2022 IEEE

management in a distribution system. This is basically necessary as distribution companies commit to provide the power with a narrow voltage margin of ± 10 % or less in the competitive market. To maintain this voltage range customer as well as Distribution Company takes efforts by managing volt var optimization. Programs created especially for distribution systems are more effective and straightforward than those created for high voltage systems. Load flow studies in distribution networks are required for studying balanced as well as unbalanced systems. The algorithm suggested for the radial distribution systems has been presented in the following subsection.

A single phase 6 bus radial distribution network has been examined to investigate and analyze the consequences of renewable energy penetration, particularly significant PV integration in the distribution network. The load flow study of a 6-bus radial distribution network without PV penetration and with PV penetration was carried out using a distribution system-specific methodology. In radial networks, the forward and backward substitution method is extensively utilized because it provides good convergence while eliminating tedious matrix calculations.

Majority of radial distribution load flow methods are based on the BFS methodology of network tree representation.

A. 6-Bus Radial Distribution without PV Penetration

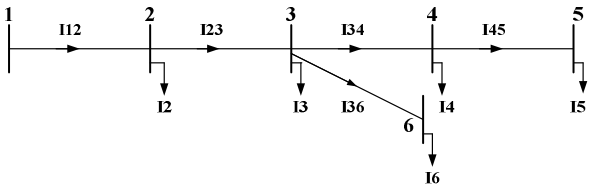

Fig. 1.: 6-Bus Single Phase Radial Distribution Network without PV Penetration.

Fig. 1 depicts the 6 bus single phase radial distribution network used by the course teacher for teaching learning process [17]. System consists of 5 electrical consumers supplied by an 11 kV feeder line. Table I represents the line data and Table II shows the bus data of 6 Bus system.

TABLE I. LINE DATA

Branch	Input Bus	Output Bus	R (Ohm)	X (Ohm)
1	1	2	0.279	0.015
2	2	3	0.444	0.439
3	3	4	0.864	0.751
4	4	5	0.864	0.751
5	3	6	1.374	0.774

TABLE II. BUS DATA

Bus No.	Active Power (KW)	Reactive Power (kVAr)
1	0	0
2	0	0
3	1572	174
4	1936	312
5	189	63
6	1336	112

The steps involved in Forward/Backward Sweep load flow is as given below:
Step 1. Set up node voltage and import network parameters.
Step 2. For each node, compute the injected load current.
Step 3. In the backward sweep, determine the current for every branch from end to root node.
Step 4. In the forward sweep, determine the voltage for every node using the voltage source.
Step 5. Check the voltage difference's convergence condition in two subsequent iterations; if the condition is satisfied, go to step 6; otherwise, go to step 2.
Step 6. Output results.

B. 6 Bus Radial Distribution system with PV Penetration

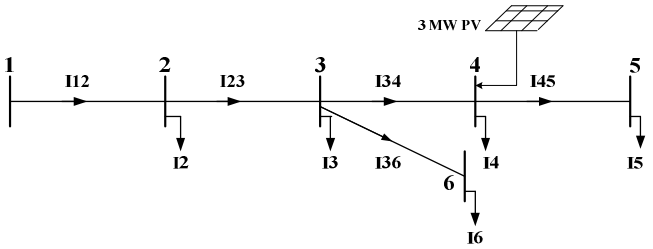

Fig. 2: 6-Bus Single Phase Radial Distribution Network with PV penetration.

TABLE III. BUS DATA

Bus No.	Active Power (kW)	Reactive Power (kVAr)
1	0	0
2	0	0
3	1572	174
4	-1064	312
5	189	63
6	1336	112

Fig. 2 represents the 6-bus system with an SPV source connected to the system. Distribution line data remains the same as represented in Table 1, nevertheless the bus data gets modified as represented in Table III. Table III is similar to Table II with only difference in active power at the bus where SPV is connected to the system. Fig. 3 depicts the flow chart for calculations of voltage using BFS load flow for an 11 kV feeder with six electrical users. The feeder's overall load is 5 MW. When PV output power is more than the load requirement, the excess power might be sent back to the substation through reverse power flow, causing problems with protection coordination and voltage rise. Considering this aspect, the SPV penetration is not allowed to exceed the total load demand of the distributor.

According to Table IV, a 3 MW PV system with a 60% penetration is installed at a single location to investigate the impact of centralized SPV system installation.

The root node voltage is set at 11 kV in this analysis. Fig. 4 (a) and (b) shows the feeder voltage profiles and power loss respectively for without PV and when the centralized SPV system is connected at Bus 2, Bus 3, Bus 4, and Bus 5, respectively.

TABLE IV. LOCATION OF THE 3 MW PV SYSTEM

Location of the 3 MW PV system				
Connecting Bus	2	3	4	5

Flow Chart:

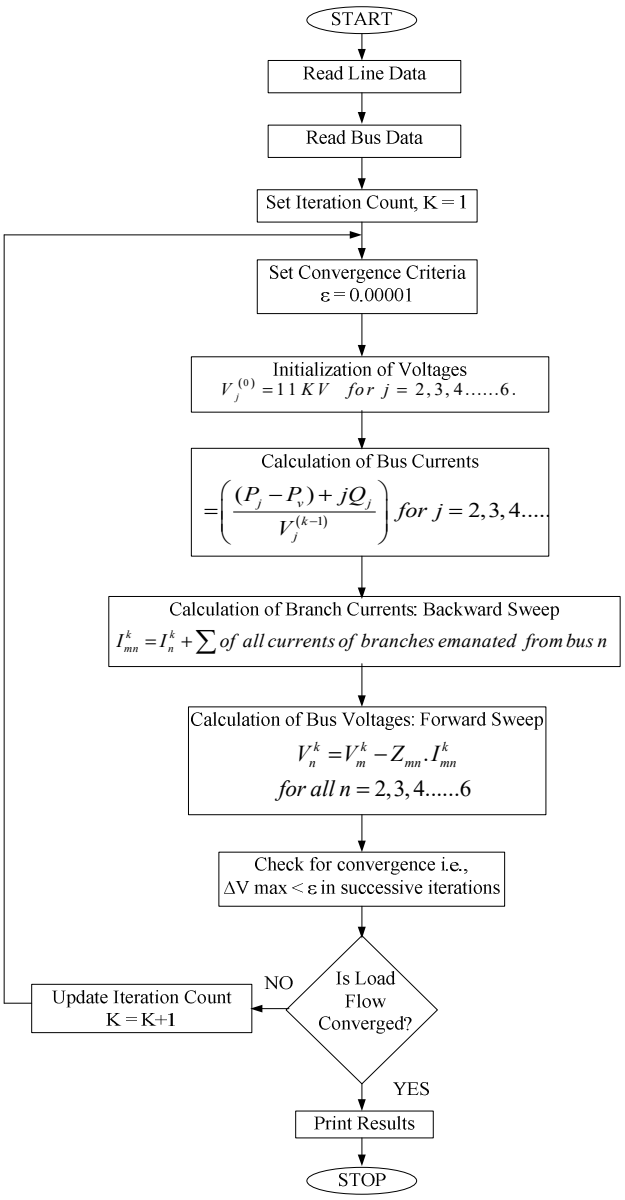

Fig. 3. Flow chart of Backward Forward Sweep Algorithm with PV system

After connecting the SPV system, the feeder voltage increases throughout, as seen in Fig. 4 (a). When the SPV system is connected at bus 2 and bus 3, the voltage of the connected bus continues to drop throughout the feeder, but when it is connected at bus 4 and bus 5, the voltage of the associated bus rises, with the maximum value at bus 5. The power flow direction is reversed because the available PV power exceeds the local load requirement. The local load on bus 5 is just 189 KW, and the PV integration on bus 5 is 3000 KW.

However, when the SPV system is connected at bus 4, the power losses (49.76 KW and 36.13 kVAr) are lower than when the SPV system is connected at the other PV locations, as shown in Fig. 4. (b).

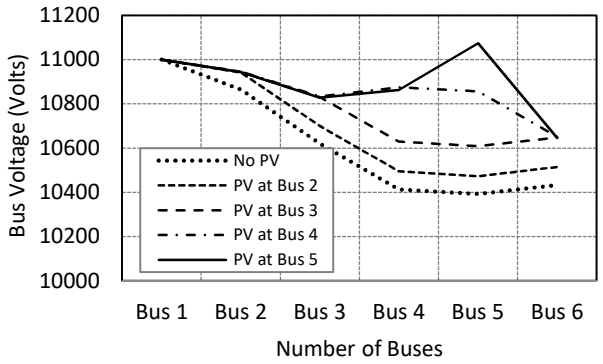

Fig.4 (a) Feeder Voltage profiles at different PV locations (3 MW)

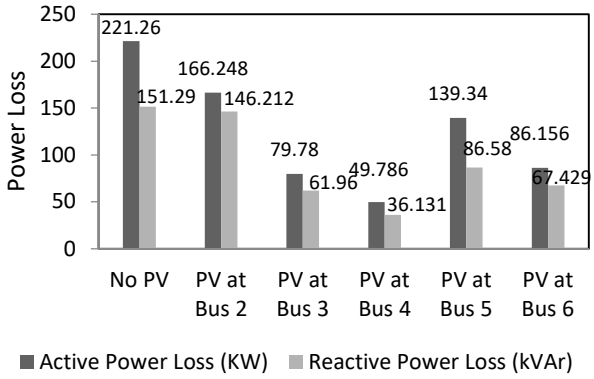

Fig.4 (b) Power losses under different PV locations

III. Result and Discussion

A. *Voltage profile at different capacities of the distributed PV system*

TABLE V. DIFFERENT PV CAPACITIES

Different capacities of the distributed PV system					
PV capacity (MW)	1	2	3	4	5

Fig. 5 illustrates the feeder voltage profiles for centralized SPV installed with capacities mentioned in Table V at various buses of distributed feeder. The results show that when the size of the SPV capacity rises, compared to SPV systems installed at the feeder's beginning, those attached at the feeder's end improve voltage and increase line voltage more effectively, as demonstrated in Fig. 5 (a), (b), (c), and (d), respectively, at a given capacity. When the PV system's capacity surpasses 4 MW, the voltage peak arises at bus 2, 3, 4, and 5, as shown in Fig. 5. The voltage is higher than at the feeder's root bus when the PV capacity at buses 4 and 5 reaches 5 MW. If the voltage rise exceeds the permitted range, that is 11 kV ± 10%, it can have serious repercussions. The moment a 5 MW PV installation is integrated to bus 5, the voltage rise is the biggest related to when the PV is installed at bus 2 or bus 3.

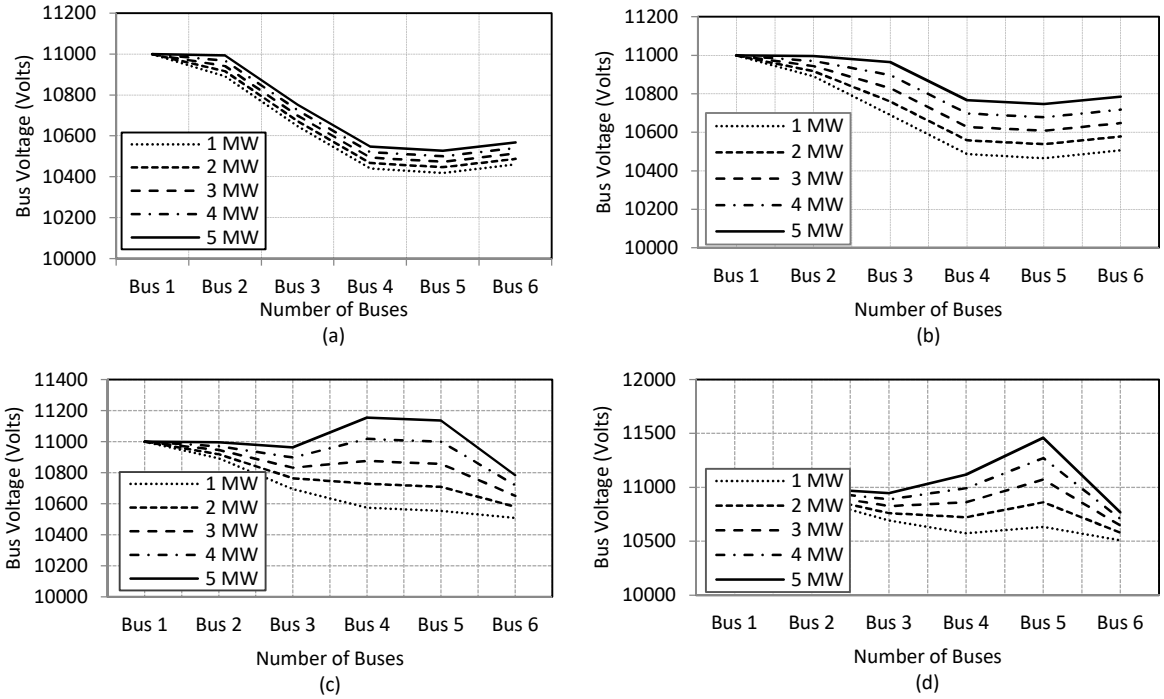

Fig. 5 (a) Feeder Voltage profiles at different PV capacities at Bus 2. (b) Feeder Voltage profiles at different PV capacities at Bus 3. (c) Feeder Voltage profiles at different PV capacities at Bus 4. (d) Feeder Voltage profiles at different PV capacities at Bus 5.

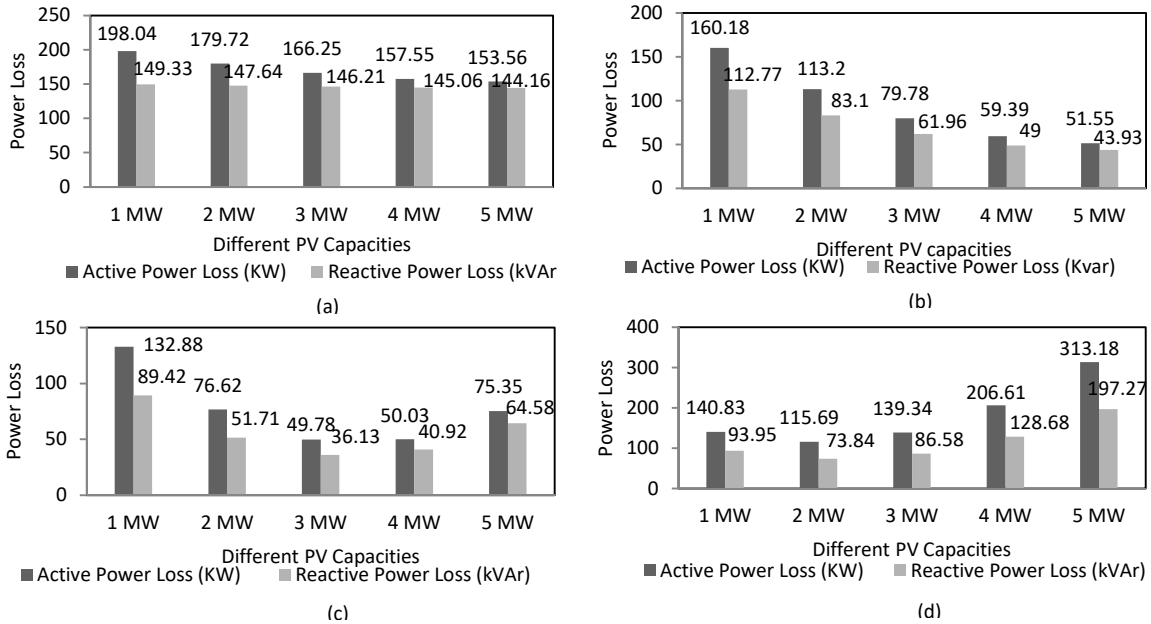

Fig. 6. Power Loss at different buses for - (a) Centralized PV connected at Bus 2. (b) Centralized PV connected at Bus 3. (c) Centralized PV connected at Bus 4. (d) Centralized PV connected at Bus 5.

Fig. 6 depicts power loss of various PV capacities on various buses. When different PV capacities are connected at the feeder's beginning, such as bus 2, active and reactive power losses are larger, as shown in Fig. 6. (a). However, when 3 MW PV is put at bus 4 as illustrated in Fig. 6, the lowest power loss (49.78 KW and 36.13 kVAr) is seen (c). Because of the reverse power flow at bus 5, power losses increase as PV capacities increase. As a result, a 3 MW PV system will be best installed at bus 4, which has a superior feeder voltage profile and the lowest power loss. As bus 6 is connected to bus 3, the effect of different PV

capacities at bus 6 will be similar to that of bus 3. Hence only bus 3 is considered along with bus 2, bus 4 and bus 5 for various PV installations.

Now, the analysis has been carried out by integrating SPVs to multiple buses rather than a single bus that is distributed SPV in place of centralized SPV as shown in Table VII. The overall PV capacity is 3 MW (3 * 1 MW), there are three PV systems on the feeder, each with a 1 MW capacity. As shown in Table VII, three PV systems are connected to various buses. Similarly, 5 MW overall PV capacity is also considered for the impact analysis. The capacity of one PV system is 1 MW, the capacity of the other two PV systems is 2 MW, and there are three PV systems on the feeder. As shown in Table VII, three PV systems are connected to various buses.

Under 3 MW, in case 1, the PV systems are connected from Bus 1 to Bus 3 at the start of the feeder. The feeder has a uniform distribution of PV systems in case 2 and is positioned downstream of the feeder from bus 4, 5 and 6 in case 3. The PV capabilities in all three situations are 3 MW, with a slight voltage rise in case 1 and a substantially better voltage profile in case 3 than in cases 2 and 1. It can be observed that case 3 provides a superior voltage profile and lower power losses when a 3 MW PV system is deployed on multiple feeder buses, namely Buses 4, 5, and 6.

In case 4, the PV systems are connected from Bus 1 to Bus 3 at the starting of the feeder. In case 5, PV systems are evenly dispersed along the feeder, whereas in case 6, PV systems are positioned downstream of the feeder on buses 4, 5, and 6. In all three situations, the PV capacities are 5 MW; the voltage rise is minor in case 4, but in case 6, the voltages of several buses are much greater than the root bus, as seen in Table VII. This could result in an overvoltage problem. As a result of the PV systems being scattered along the feeder, case 5 does not experience a voltage rise.

Looking into centralized installation cases, case 8 has a better voltage profile than case 7 and has lower losses than case 7 and case 9. Case 11 is better in terms of enhanced voltage profile than case 10 and has lower losses than case 10 and case 12, as shown in Table VII. As the voltage surpasses the permitted voltage variation limit in case 12, a voltage rise issue occurs.

If a 3 MW centralized PV system is examined from Table VII, the voltage profile for the centralized installation scheme has a wider variation range between 10. 39 kV and 11.7 kV than the voltage profile for the distributed installation scheme, which has a range between 10.49 kV and 10.94 kV. Hence, it can be inferred that the distributed installation is preferable over the centralized installation of a single big system for optimizing the voltage profile without exceeding the permitted voltage variation limit.

It is also inferred from Table VII that case 13 and case 14 provides the best feeder voltage profile than all the other cases, when 5 MW is distributed at the buses 4, 5, 6 and 3, 4, 5 respectively. However, the voltage at bus 6 in case 13 is 11.10 kV which is on borderline as per recommended voltage variation limit. Hence, case 14 will be more preferable than case 13, despite the fact that power loss is slightly greater than case 13.

To avoid the negative impacts of high PV penetration, the PV power at the connected bus should not be exceeded than the local load demand on that connected bus in case of distributed PV installation cases. Therefore, depending upon the local load on the respective buses, it is essential to know about how much PV capacity is needed to improve the voltage profile of the RDN without causing the negative consequences. Hence, the new term is proposed here, which will reveal the required PV capacity to be connected at the respective buses according to their local load. The term "Required PV Capacity" is expressed below,

$$\text{Required PV Capacity} = \frac{\text{Local load on the bus}}{\text{Total load on the feeder}} \times 100 \quad (1)$$

TABLE VI. PREDICTED PV CAPACITY

Buses	Total Load on the Feeder	Local Load on the Bus (KW)	Required PV capacity at the Bus (%)
2	5000 KW	0	0
3		1572	31.44
4		1936	38.72
5		189	3.78
6		1336	26.72

At Bus 4,

$$\text{Required PV Capacity}_{at\ bus\ 4} = \frac{1936\ KW}{5000\ KW} \times 100 = 38.72\ \% \quad (2)$$

As per eq. (1), the predictable PV penetration at bus 5 is around 4 % and presently 60 % is penetrated at bus 5 in case of centralized installation. Therefore, SPV penetration exceeds the load demand at bus 5. As a result, this may cause reverse power flow and voltage rise. Highest PV integration is required (38.72 %) at bus 4 because of the higher load demand which is 1936 KW.

Hence, for this 6-bus single phase RDN considered here, the recommended % PV penetration, depending upon the local load connected, should vary from 20 % to 60 %. The PV penetration level exceeding 60 % under distributed as well as centralized PV installation may cause negative impacts on the system performance.

CONCLUSION

In this paper centralized SPV and distributed SPV systems are analyzed with BFS load flow. Various cases have been considered to observe the impacts of SPV at various locations with varying SPV capacities. The voltage rise on the feeder is caused by the reverse power flow instigated by the surplus SPV power. Without SPVs, the voltage drops from the start to the end of the feeder. When connecting SPV systems, the node voltages at the SPV node increase and sometimes even surpass the voltage of the substation with the peak value. It can also be inferred that the multiple SPV systems under distributed installation cases connected at the downstream nodes (3, 4 and 5) or (4, 5 and 6) of the feeder provide a better voltage profile and less power loss than the centralized SPV systems. Among distributed PV installation cases, case 14 is providing the best result in terms of power loss and voltage profile. Hence, decentralized SPV systems are recommended. Further, the voltage profile can be studied by considering an unbalanced radial distribution network with a higher number of buses to analyze the actual system performance. Also, by applying modern optimization techniques the optimal location of the DG's can be investigated.

REFERENCES

[1] D. Chathurangi, U. Jayatunga, M. Rathnayake, S. Perera, "Potential power quality impacts on LV distribution networks with high penetration levels of solar PV", *IEEE Int. Conf. on Harmonics and Quality of Power (ICHQP), Ljubljana, Slovenia*, pp. 1-6, May 2018.

[2] M. Emmanuel, R. Rayudu and D. Burmester, "Impact of large-scale integration of distributed photovoltaic with the distribution network," *2016 IEEE International Conference on Power System Technology (POWERCON)*, pp. 1-6, 2016. doi: 10.1109/POWERCON.2016.7753858.

[3] Nivedita Padole, Ravindra Moharil, and Anuradha Munshi, "Performance Investigation Based on Vital Factors of Agricultural Feeder Supported by Solar Photovoltaic Power Plant", *Energies,* 15, no. 1: 75, pp.1-18, 2021.

[4] Bishwajit Dey, Saurav Raj, Sheila Mahapatra, Fausto Pedro García Márquez, "Optimal scheduling of distributed energy resources in microgrid systems based on electricity market pricing strategies by a novel hybrid optimization technique", *International Journal of Electrical Power & Energy Systems,* Vol. 134, Iss. 1, pp. 1-17 , 2022. https://doi.org/10.1016/j.ijepes.2021.107419.

[5] M. C. Vargas, M. A. Mendes and O. E. Batista, "Impacts of High PV Penetration on Voltage Profile of Distribution Feeders Under Brazilian Electricity Regulation", *13th IEEE International Conference on Industry Applications (INDUSCON)*, pp. 38-44, 2018. doi: 10.1109/INDUSCON.2018.8627070.

[6] K. Balamurugan, Dipti Srinivasan, "Review of Power Flow Studies on Distribution Network with Distributed Generation", *IEEE Power Electronics Drives and Energy Systems (PEDS), Singapore*, pp. 411-417, 2011.

[7] U. Eminoglu And M. H. Hocaoglu, "Distribution Systems Forward/Backward Sweep-based Power Flow Algorithms: A Review and Comparison Study", *Electric Power Components and Systems, Taylor and Francis*, Vol.37, Iss.1, pp. 91-110, Dec 2008.

[8] Mamdouh Abdel-Akher, "Voltage stability analysis of unbalanced distribution systems using backward/forward sweep load-flow analysis method with secant predictor", *IET Generation, Transmission & Distribution*, Vol. 7, Iss. 3, pp. 309–317, 2013.

[9] S.Sunisith1, K.Meena," Backward/Forward Sweep Based Distribution Load Flow Method", *International Electrical Engineering Journal (IEEJ)*, Vol. 5, Iss. 9, pp. 1539-1544, 2014.

[10] Saad Ouali and Abdeljabbar Cherkaoui," An Improved Backward/Forward Sweep Power Flow Method Based on a New Network Information Organization for Radial Distribution Systems", *Hindawi Journal of Electrical and Computer Engineering*, Vol. 2020, pp. 1-11, 2020.

[11] Bryan B. Navarro, Datu Amil Hussien O. Asakil , Maricar M. Navarro, "Medium Voltage to Low Voltage Power Flow Solution Using Modified Backward/Forward Sweep Algorithm", *41st Annual Conference of the IEEE Industrial Electronics Society (IECON),Yokohama,* pp. 1115-1120, 2015.

[12] Guzmán Díaz, Javier Gómez-Aleixandre, "Direct Backward/Forward Sweep Algorithm for Solving Load Power Flows in AC Droop-Regulated Microgrids", *IEEE Transactions On Smart Grid*, Vol. 7, Iss. 5, pp.1-10, Sept. 2015.

[13] P. Chen *et al*., "Analysis of Voltage Profile Problems Due to the Penetration of Distributed Generation in Low-Voltage Secondary Distribution Networks," in *IEEE Transactions on Power Delivery*, vol. 27, no. 4, pp. 2020-2028, Oct. 2012, doi: 10.1109/TPWRD.2012.2209684.

[14] A. K. Saonerkar and B. Y. Bagde, "Optimized DG placement in radial distribution system with reconfiguration and capacitor placement using genetic algorithm," *IEEE International Conference on Advanced Communications, Control and Computing Technologies*, pp. 1077-1083, 2014. doi: 10.1109/ICACCCT.2014.7019263.

[15] A. P. Kenneth, K. Folly, "Voltage Rise Issue with High Penetration of Grid Connected PV", *IFAC Proceedings Volumes*, *47*(3), 4959–4966, 2014. https://doi.org/10.3182/20140824-6-za-1003.01989

[16] B. B. Pokhrel, A. Shrestha, S. Phuyal, S. K. Jha, "Voltage profile improvement of distribution system via integration of Distributed Generation Resources", *Journal of Renewable Energy, Electrical, and Computer Engineering*, Vol. 1, Iss. 1, pp. 33-41 2021. https://doi.org/10.29103/jreece.v1i1.3519.

[17] https://drive.google.com/file/d/1tZXJ1VseiY29BF9UVSeffOItS7aaZSVk/view

TABLE VII. COMPARATIVE ANALYSIS OF CENTRALIZED AND DISTRIBUTED INSTALLATION CASES

Total PV Capacity	**Voltage and Total Power Loss**	**Cases**	**Connected Bus**	**Distributed PV Installations**						**Cases**	**Connected Bus**	**Centralized PV Installations**					
			Buses	**1**	**2**	**3**	**4**	**5**	**6**		**Buses**	**1**	**2**	**3**	**4**	**5**	**6**
3 (MW)	kV	1	1 (1 MW) 2 (1 MW) 3 (1 MW)	11.00	10.91	10.71	10.51	10.49	10.53	7	1 (1 MW) 1 (1 MW) 1 (1 MW)	11.00	10.86	10.62	10.41	10.39	10.43
	KW			142.24								221.26					
	kV	2	1 (1 MW) 3 (1 MW) 5 (1 MW)	11.00	10.91	10.76	10.64	10.70	10.58	8	3 (1 MW) 3 (1 MW) 3 (1 MW)	11.00	10.94	10.83	10.63	10.61	10.64
	KW			94.41								79.78					
	kV	3	4 (1 MW) 5 (1 MW) 6 (1 MW)	11.00	10.94	10.83	10.79	10.85	10.78	9	5 (1 MW) 5 (1 MW) 5 (1 MW)	11.00	10.94	10.82	10.86	11.07	10.64
	KW			38.21								139.34					
5 (MW)	kV	4	1 (1 MW) 2 (2 MW) 3 (2 MW)	11.00	10.91	10.71	10.51	10.49	10.53	10	1 (1 MW) 1 (2 MW) 1 (2 MW)	11.00	10.86	10.62	10.41	10.39	10.43
	KW			92.33								221.26					
	kV	5	1 (1 MW) 3 (2 MW) 5 (2 MW)	11.00	10.91	10.76	10.64	10.70	10.58	11	3 (1 MW) 3 (2 MW) 3 (2 MW)	11.00	10.99	10.96	10.76	10.74	10.78
	KW			62.15								51.55					
	kV	6	4 (2 MW) 5 (1 MW) 6 (2 MW)	11.00	10.94	10.83	10.79	10.85	10.78	12	5 (2 MW) 5 (1 MW) 5 (2 MW)	11.00	10.99	10.94	11.11	11.45	10.76
	KW			19.79								313.28					
				Distributed PV Installations (New Cases)													
5 (MW)	kV	13	4 (2 MW) 5 (0.5MW) 6 (2.5MW)	11.00	10.99	10.96	10.97	10.99	11.10								
	KW			15.47													
	kV	14	3 (2.5MW) 4 (2 MW) 5 (0.5MW)	11.00	10.99	10.96	10.97	10.99	10.79								
	KW			19.26													

A Safety Assessment Model for Automotive Embedded Systems Networks

Publisher: IEEE

Gaurav Gondhalekar ; B. Ashreeth ; Gopala Rao Thellaputta ; D Venkataramireddy ; M. Sumithra ; Nagarjuna Karyemsetty **All Authors**

Abstract:A significant shift towards autonomous and connected cars is currently expected in the automotive sector. This creates new risks in terms of privacy and the complexity of... **View more**

Metadata

Abstract:
A significant shift towards autonomous and connected cars is currently expected in the automotive sector. This creates new risks in terms of privacy and the complexity of electrical and electronic systems. Although safety risk management is still in its infancy, it is encouraging that the auto industry has well-known and regulated safety risk management practices. They propose a showed improved risk assessment framework and show its validity with an actual use-case to make it easier to derive safety procedures & safety solutions for automotive integrated devices. The adequacy of functional safety to existing methods and accessibility for non-safety professionals are some of the important aspects. Risk analysis is an essential element of the methodology used to assess properties and capacity risks. The level of hazard and the level of effect are estimated in the next stage of the risk management process. This step uses several existing guidelines and requirements to make amendments as necessary. To create high-level security objectives, a level of security has finally been determined. This architecture should be well adapted to the requirements of the automobile industry due to its excellent convergence with current principles and specifications.

Published in: 2022 IEEE 2nd Mysore Sub Section International Conference (MysuruCon)

Date of Conference: 16-17 October 2022

Date Added to IEEE *Xplore*: 13 December 2022

ISBN Information:

INSPEC Accession Number: 22443965

DOI: 10.1109/MysuruCon55714.2022.9972628

Publisher: IEEE

Conference Location: Mysuru, India

Contents

I. INTRODUCTION

Cars were typically thought of as solitary, static, and closed systems, but increasingly a paradigm shift toward connected and autonomous vehicles to started & cars are becoming more individualized and connected to the Internet of Things (IoT).By 2022, 85 percent of all vehicles would be connected to the Internet, according to a market survey [1]–[3]. Future cars would present new security and protection hazards as the use of technologies and the complexity of electrical and electrical components both continue to grow. In the automotive sector, safety is considered a non-negotiable critical component [4]. An operational safety requirement for road cars, ISO 26262, which would be based on the more general safety requirements [5], would be an example of a methodology and process that has been created and regulated to attain an acceptable level of protection during the implementation of safety-critical components. However, although security issues against a transport can endanger the security of drivers, passengers, and other road users [6], safety has lately received attention in the automotive sector, and security issues have scarcely been properly handled. Researchers have already shown that it is possible to commit acts of violence that greatly jeopardize security. Therefore, to increase the caliber and protection of cars, safety concerns and dangers should be carefully handled.

Agricultural Information System Model to Improve Crop Yield Through IoT

Publisher: IEEE

Vaibhaw Rameshrao Doifode ; Subhashree Darshana ; Selina Mishra ; Sheik Faritha Begum ; Y Md.Riyazuddin ; G. Naga Rama Devi **All Authors**

Abstract: The application of Agricultural Information Technology (AIT) in all facets of agriculture has made it the most efficient method and set of instruments for increasing agri... **View more**

Metadata

Abstract:
The application of Agricultural Information Technology (AIT) in all facets of agriculture has made it the most efficient method and set of instruments for increasing agricultural production and fully using farming methods. The use of Agriculture Information Management technology, a crucial sub-technology of AIT, has a direct impact on the level of agricultural informationalization and the effectiveness of agricultural production decisions. The requirements specification and architectural style of the Intelligent Agriculture MIS were thoroughly addressed in this section based on promoting the idea of agricultural information management and analyzing the characteristics of Agricultural data. Eventually, this paper provides an integration illustration of the framework in agricultural output.

Published in: 2022 IEEE 2nd Mysore Sub Section International Conference (MysuruCon)

Date of Conference: 16-17 October 2022

Date Added to IEEE *Xplore*: 13 December 2022

ISBN Information:

INSPEC Accession Number: 22443716

DOI: 10.1109/MysuruCon55714.2022.9972553

Publisher: IEEE

Conference Location: Mysuru, India

Contents

Since that time, the idea of "Digital Earth" has caused considerable worry and has emerged as one of the newest research hotspots in the area of international science and technology. It has significantly sped up the process of digitization in several sectors [1]. One of the most significant components of the "Digital Earth" is "Digital Agriculture," which is the extension of the "Information Superhighway," "Digital Earth," and "Knowledge Economy" into the agricultural sector. Changes in cultivation practices, production, and administration as well as changes in agricultural research, innovation, and training have been brought about by it [2]–[4]. Electronic agricultural production, also known as information processing agriculture or intelligent agriculture, is the use of many high-new-tech types of crops, including the quick acquirement of farmland knowledge, the cultivation and managerial staff of grassland, the use of agro-chemicals, the prevention of contamination, and the modernization of transportation engineering hardware [5]. Information systems, a key component of the software-specific application and the foundation for wise agricultural production decisions are a key component of digital agribusiness.

Authors

Figures

References

Keywords

Metrics

Grenze International Journal of Engineering and Technology, June Issue

IoT based Monitoring of Lathe Machine Motor in Metal Industry

Akshay D Kadu [1], Punit Fulzele[2], Vaibhav V Jiraphe [3], Harshwardhan Mandhare [4] and Kaustubh Dani [5]
[1, 3-5] Yeshwantrao Chavan College of Engineering Nagpur, Dept. of Electrical Engineering, Nagpur, India
Email: akshaykadu001@gmail.com, vaibhav190620@gmail.com, harshwardhanmandhare04@gmail.com, kaustubhdani95@gmail.com
[2]Jawaharlal Nehru Medical College, Datta Meghe Institute of Medical Sciences, Wardha, India
Email: punit001@gmail.com

***Abstract*—Optimized use of electrical energy is prime objective of various metalworking Industry. The problem definition for this work is considered from the industry located in Hingna MIDC, Nagpur, Maharashtra, India. It is conveyed that during operational hours most of the operator working on lathe machine keeps the motor of lathe machine in running condition even when they are not performing any metal job on the machine. Leads to wastage of electrical energy and increased electricity bill. As per the guidelines issued by bureau of energy efficiency industry should conserve the electrical energy in every energy conversion process. This research work deals with IoT based monitoring of lathe machine operator so as to cut down the idle running of the lathe machine which benefits in conservation of electrical energy and reduced electricity bill. This work is also extended to monitor the various parameters of electric motor. System design consists of low budget sensors and microcontroller. A open source Thing Speak IoT based cloud service is used for data analytics and data storage purpose. Experimental results reveal the effectiveness of implemented prototype.**

***Index Terms*— Internet of Things, Energy Conservation, Induction Motor.**

I. INTRODUCTION

Induction motors is commonly used in various Industries to achieve certain objective. This motor has several advantages such as robust, low cost, easy to operate and highly reliable. [1- 3] generally rotating machine required more attention and maintenance as compared to static electrical machine. Regular maintenance is carried out in industries of various auxiliaries installed. Predictive maintenance and preventive maintenance is regularly carried out in industries so as to reduce the down time of manufacturing process. Predictive maintenance is carried out by analysing the performance of machine. To judge the performance of machine data of certain set of motor parameter is required e.g. motor voltage, current, motor speed in rpm, temperature of winding, rotor eccentricity and motor assembly vibration. These values then compared with standard values if there is any deviation found in value accordingly maintenance of that machine is initiated. [4-5] conventionally predictive maintenance data is monitored by on site methods using analog or digital measuring instruments [6] now a days with the evolution of technology any data can be monitor remotely with the help of Internet of things [7].

Work is carried out in different dimensions regarding induction motor maintenance [8] discuss wireless sensor

Grenze ID: 01.GIJET.8.2.539

network used in industries its design, working, architecture, development and hardware implementation.
To monitor and control the induction motor connected in agricultural system is presented in [9] In this work implementation of IOT technology to monitor, to control and diagnose the condition of Induction motors by recording key operation indicators is carried out. Now day's smart meters are also installed to observe various electrical and mechanical parameters of the induction motor [10] deals with smart way of monitoring induction machine data by LoRa technique. But this technology suffers from disadvantage of very high installation cost. IoT based Health examination of Induction motor is proposed in [11] using GSM based technology, which is used to monitor health of electrical motor by measuring the parameters such as winding temperature, assembly vibration and current. It can be measured through the sensors, like accelerometer, current sensor and thermocouple. Submersible motor temperature and vibration data monitoring techniques detailed literature survey is carried out in [12] and various algorithms for problem diagnosis is presented. A low-cost design for real time monitoring of induction motor for predictive maintenance is presented in [13] it is based on Industrial IoT [IIOT] In this module only motor vibrations and temperature is monitored. After this comprehensive literature survey carried out work presented in this paper is unique and innovative. This works also tell us about the operator efficiency which can be utilized for analysis purpose.
Objective of this work is to find out idle time, no load time and load time of motor. Acquire motors current, speed and temperature information for the motor condition monitoring. Detect any faulty condition or abnormality of motor. Design and testing of prototype using an ATMEGA 328 PU microcontroller module. To apply Internet of Things (IoT) system for condition monitoring in electric motor.
This paper presents wireless monitoring of data using sensors and IoT technology. It is used to find out the working abnormality and maintenance of the machine. This paper is planned in following manner section I discuss the introduction and prior art related to methods of data acquisition of motor parameters. Section II deals with proposed technique of motor parameter acquisition and monitoring of workers efficiency Section III presents prototype design and experimental results. Section IV discussed conclusion and future scope of the work.

II. Wireless Motor Parameter Estimation

The most used machine in any section of the society including industries is Induction machine, so IM are "Workhorse of Industries". Induction motor is used to perform various tasks in industries such as lathes, mills, routers and grinders. Machine operator handles these machines to perform above mention task. Due to carelessness of machine operator Industry have to bear losses. Any small fault occurred in a motor will led to complete motor failure if not addressed in time so condition monitoring of IM is desirable to avoid downtime of any industry. This project deals with improvement in production efficiency and condition monitoring of Industrial motors

A. System Design

System as shown in the fig.1 which consists of motor assembly which is fed by three phase power supply using starter and contactor.

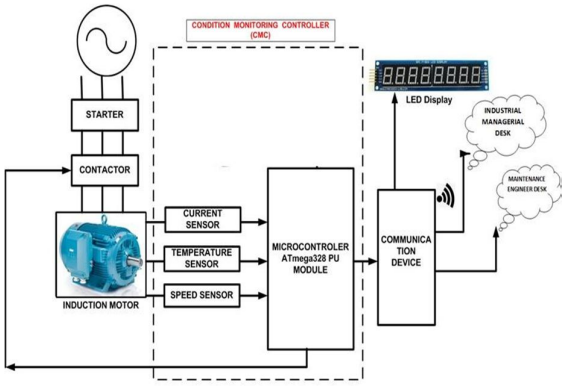

Fig.1 Block diagram of IoT based monitoring of motor

Basically, to fetch various parameters of motor in this work various sensor are used such as to get the value of current a series connected current sensor is used to obtain the data of temperature of winding temperature sensor

and to get the rotation –per minute data speed sensor is used. This data is fed to microcontroller circuit analog pins. Microcontroller process that data to digital output pins. Communication device is connected to the digital pins of microcontroller which is used to transfer this data to cloud. After that this data is used by Industrial managerial desk or maintenance engineer.

B. Methodology

To achieve the above-mentioned objective following methodology is discussed in which first step is inspect the site and type of motor is used in this work induction motor is used but this method can be implemented for any other electric motor. Selection of parameters to be required from motor end and accordingly selection of sensors is carried out there are various sensor available in market sensor should be selected on the basis of cost, accuracy and its compatibility with the microcontroller generally sensor is fed by DC power supply for that DC supply source is required. After this step location identification on motor assembly placement of sensor generally, voltage sensors are placed inside motor assembly near to the winding which must temperature resistant.

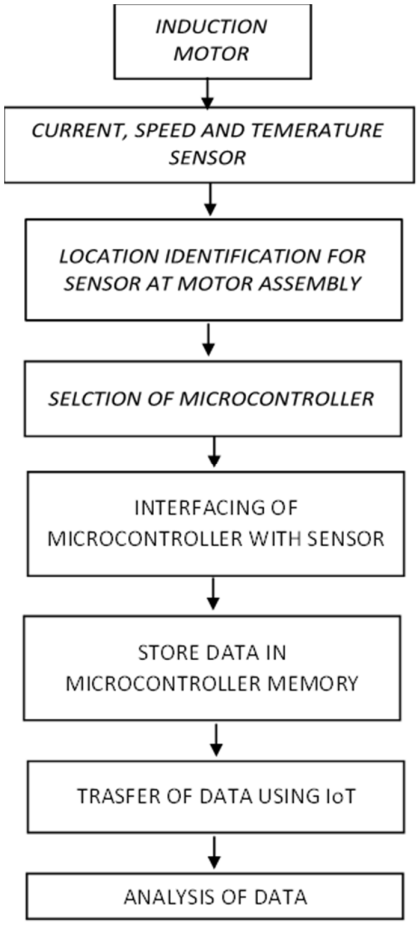

Fig.2 Flow chart of methodology

Microcontroller selection depends on number of input output pins required then interfacing of microcontroller with sensor and programming of microcontroller finally data get transferto the cloud with the help of Internet of thing technology.

III. HARDWARE IMPLEMENTATION

The proposed monitoring system discusses various scope and application at industrial level. It also describes the future possibilities along with the use of various technologies.

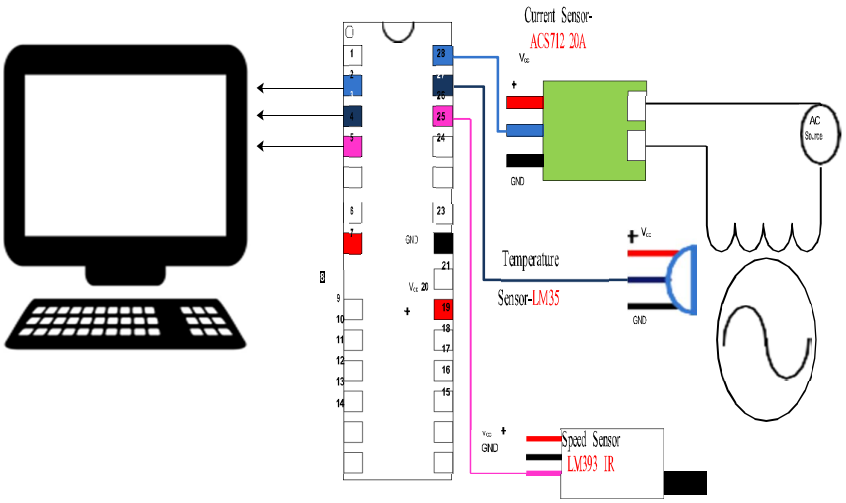

Fig.3 Flow chart of methodology

Fig 3 shows the pin diagram for the connection of Current sensor is connected to the pin no 38, temperature sensor is connected to pin no 37 and speed sensor connected to pin no 36 of the microcontroller. which are the analog input pins of the microcontroller.

Current Sensor: ACS712 20A

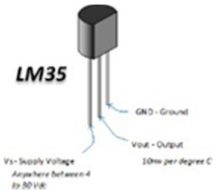

Temperature Sensor LM35

Speed Sensor LM393

Wifi Module ESP8266

While that of wifi module ESP8266 is connected to the digital output pins of the microcontroller.

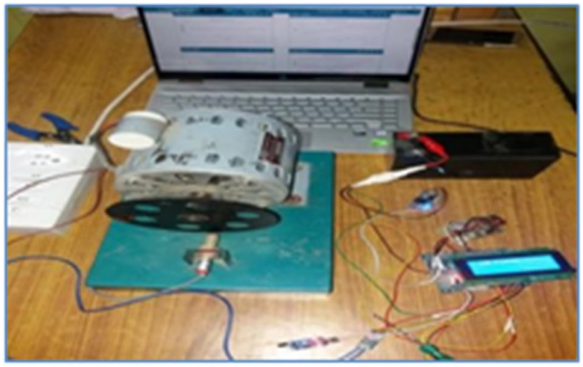

Fig no.4 shows the hardware implementation circuit

Fig no.4 shows the hardware implementation circuit in lab where all the sensors are assembled near the motor to measure the voltage, current, speed and temperature of the motor.

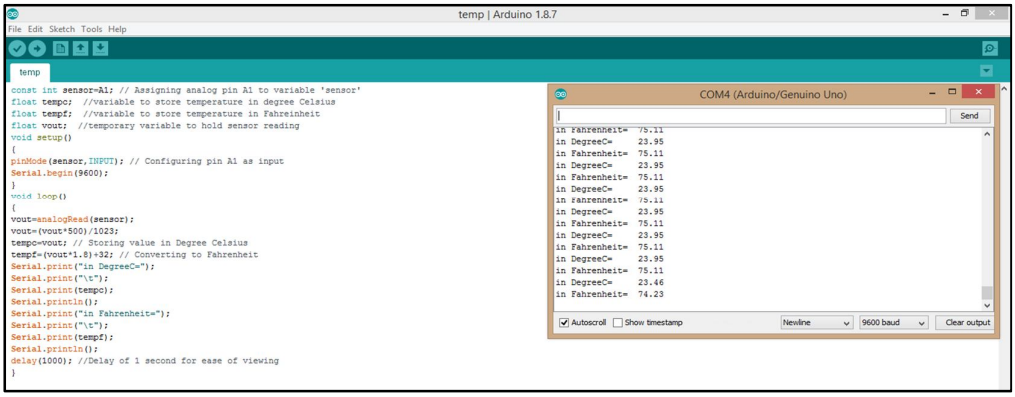

Fig.5 IDE software temperature sensor output display

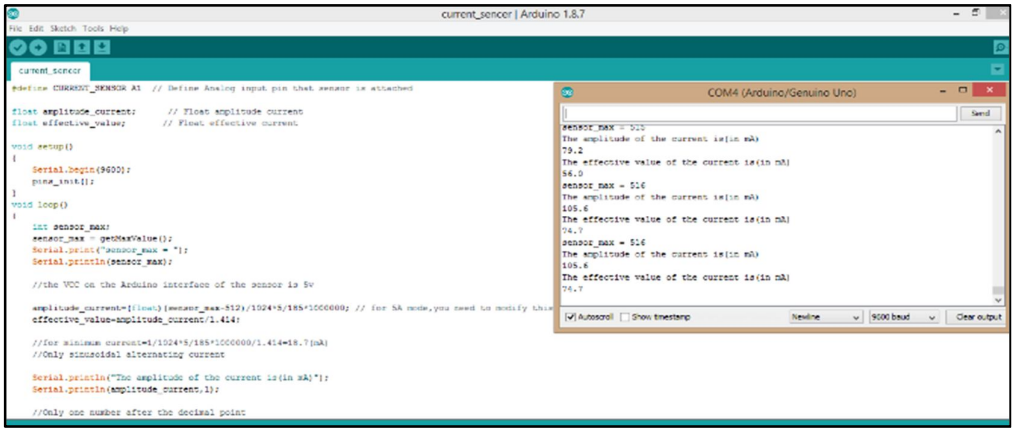

Fig.6 IDE software current sensor output display

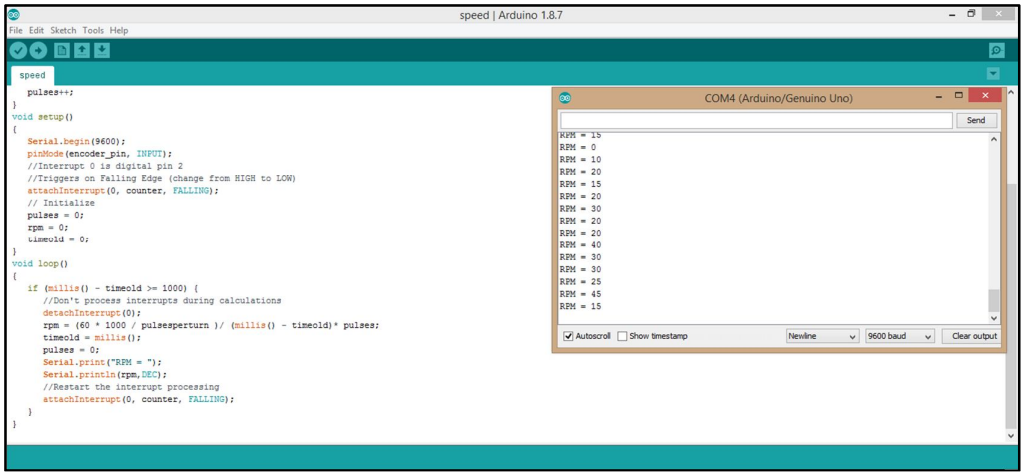

Fig.7 IDE software speed sensor output display

Fig. no. 5 to Fig. No. 7 shows the output results of temperature, current and speed sensor on IDE platform. Then this data is fed to wifi module which is send to thins speak cloud.

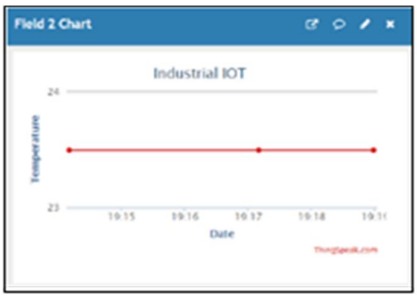

Fig.8 Thing Speak platform temperature sensor output display

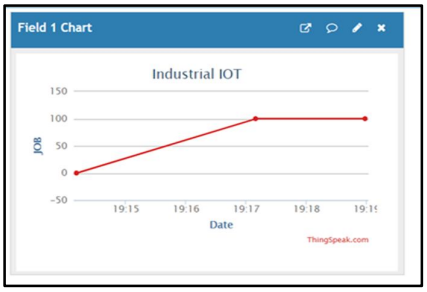

Fig.9 Thing Speak platform JOB timing (Load) output display

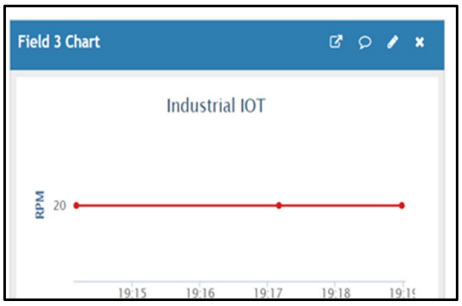

Fig.10 Thing Speak platform speed in RPM display

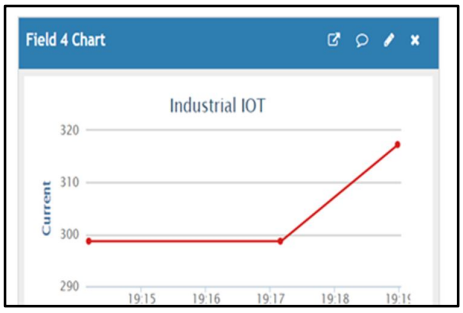

Fig.11 Thing Speak platform current in RPM display

Fig 8 to 11 shows the result of thing speak platform whichshows the output in graph forms which is easy for data analysis purpose.

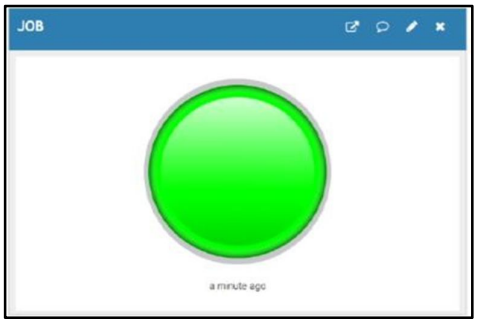

Fig.12 Thing Speak platform load is placed on motor Indication

An additional feature is also provided with this is if a load is placed on motor, then it will show green indication to the user as shown in fig. 10.

IV. CONCLUSIONS

The authors can conclude on the topic discussed and proposed. Future enhancement can also be briefed here. This work presents the concept of condition monitoring of motor using sensor technology. Current sensor, temperature sensor and speed sensor successfully interface with ATMEGA 328 PU module. The monitoring of the motor system presents the measurement of different parameters namely temperature, speed and current consumption stored in controller memory. The various accuracies presented in this thesis are subject to the number and type of input parameters selected. The presented results can be further verified by taking different set of parameters of motor

A real-time system can be developed based on this study wherein the motor data can be acquired and fed into intelligent system simultaneously. The intelligent system would evaluate the condition of the motor and issue appropriate command accordingly. The proposed approach has been verified only with the single motor set the

approach may be applied to motors of other design parameters and the result can be analysed . The proposed work can be extended for considering the presence of a combination of two faults occurring simultaneously.

REFERENCES

[1] S.B.Bodkhe, N.M. deshkar, “Basic Electrical Engineering” Published by Professional Publishing House Pvt.Ltd. 2nd edition 2008.

[2] P.S.Bimbhra, “Electrical Machinery “Published by Khanna Publishers, new delhi,7th edition 2014.

[3] Ashfaq Husain, “Electrical Machines”, published by Dhanpat Rai &Co.(P)Ltd. Delhi ,2nd edition 2015.

[4] Al-Senaidi, S.; Alolah, A.I.; Alkanhal, M.A. Magnetization-Dependent Core-Loss Model in a Three-Phase Self-Excited Induction Generator. Energies 2018, 11, 3228.

[5] K. Ágoston “Fault Detection of the Electrical Motors Based on Vibration Analysis” 8th International Conference Interdisciplinarity in Engineering, 2014.

[6] Subrata Karmakar, Surajit Chattopadhyay, Madhuchhanda Mitra, Samarjit Sengupta, “Induction Motor and Faults”, Springer, 2nd edition 2015.

[7] D.Shyamala ,J.Laxmi Prasanna, A. Ajitha, D.Swathi, “IoT platform for condition monitoring of Industrial motor “, International conference on Internet of Things,2017, pp 236-241

[8] Vehbi C. Gungor and Gerhard P. Hancke, “Industrial Wireless Sensor Networks: Challenges, Design Principles, and Technical Approaches”, IEEE Transactions on Industrial Electronics, vol. 56, no. 10, october 2009, pp 4258-4265

[9] Sandeep Kolhe, Pawan C Tapre, “Condition Monitoring & Control of Induction Motors by using IoT Platform for Agriculture System”.

[10] A. Cano-Ortega and F. Sánchez-Sutil, “Monitoring of the Efficiency and Conditions of Induction Motor Operations by Smart Meter Prototype Based on a LoRa Wireless Network”, MDPI electronics journal Electronics 2019, 8, 1040 pp.1-24

[11] Jakkrit Kunthong, Tirasak Sapaklom, Mongkol Konghirun, “IoT based traction motor drive condition monitoring in electric vehicle”, IEEE PEDS 2017, pp. 1184-1188.

[12] D. Ganga, V. Ramachandran "IoT-Based Vibration Analytics of Electrical Machines" IEEE Internet of Things Journal, 5(6), 2018

[13] L. Magadán, F.J. Suárez , J.C Granda, D.F. García, “Low-cost real-time monitoring of electric motors for the Industry 4.0”, International Conference on Industry 4.0 and Smart Manufacturing (ISM 2019).

2022 Third International Conference on Intelligent Computing Instrumentation and Control Technologies (ICICICT) | 978-1-6654-1005-2/22/$31.00 ©2022 IEEE | DOI: 10.1109/ICICICT54557.2022.9917958

Effects of Electric Vehicles Charging on the distribution system

Ameya K. Saonerkar
Dept. of Electrical Engineering
Yeshwantrao Chavan College of Engineering
Nagpur, India
ameya.coventry@gmail.com

Akshay D. Kadu
Dept. of Electrical Engineering
Yeshwantrao Chavan College of Engineering
Nagpur, India
akshaykadu001@gmail.com

Nivedita S. Padole
Dept. of Electrical Engineering
Yeshwantrao Chavan College of Engineering
Nagpur, India
niveditapande1@gmail.com

Osman M. Mohamed
Dept. of Electrical Design
g2energy
Milton Keynes, United Kingdom
osmmoh@hotmail.com

Walid N. Alnabulsi
Dept. of Research & Development
SHIFAMED LLC
California, United States
walidalnabulsi94@gmail.com

Purva P. Khot
Dept. of Mathematics and Humanities
Yeshwantrao Chavan College of Engineering
Nagpur, India
purvakhot5511@gmail.com

B. Y. Bagde
Dept. of Electrical Engineering
Yeshwantrao Chavan College of Engineering
Nagpur, India
by.bagde@rediffmail.com

Punit Fulzele
Dept. of Research and Development
Jawaharlal Nehru Medical College, Datta Meghe Institute of Medical Sciences
Wardha, India
punitr007@gmail.com

***Abstract*—This paper presents effects of charging electric vehicles (EV) on distribution system. Precisely, effects on bus voltage profile and power losses, due to charging on radial distribution system (RDS) to ring main distribution system (RMDS) and advance RMDS networks with the assistance of Distributed Generation (DG) as well as capacitor banks. Framework assimilate DG which replicates current inceptions due to solar photo voltaic (PV), wind, biogas and other upcoming renewable power sources along with traditional power factor correction measures like capacitor banks in the first place, so that system is pragmatic in design to replicate the real distribution system. The work will be conducted on steady state system and implemented on IEEE 33-Bus test system using the MATLAB programming environment on manifold case studies.**

Keywords—Voltage profile, Power loss, radial distribution system (RDS), ring main distribution system (RMDS), plug-in hybrid electric vehicles (PHEV), electric vehicle (EV), Battery Electric Vehicle (BEV), Distributed Generation (DG).

I. INTRODUCTION

With the rise of acceptance to electric vehicles, due to their performance benefits, higher motor efficiency at low speed, ability to get charged from renewable or conventional sources, recently developed fast chargers, conductive and inductive chargers, copious production of electricity at keenly priced tariffs, pruning in development cost of renewable energy installations, pioneering of Giga factories for battery manufacturing, minuscule count of spare parts, higher redundancy due to multiple motors, lower center of gravity, preponderance robust components, nominal maintenance, soaring fuel prices of petroleum, climate change environmental concerns and different nations pledge to become carbon neutral by 2050 or 2070, it is obvious to see surge in popularity of electric vehicles. Electric Vehicles (EV) load patterns are given in [1].

Even today many of the power distribution systems (DS) globally operate under radial mode configuration [2] due to their simplicity and uniform power flow direction, although inceptions from DG's, capacitor banks have even affected it. [3] delineate the superiority of switching from radial to ring main distribution system for the case studies in [2] commencing with just reconfiguration with available resources effects in loss reduction, voltage profile improvement, redundancy in supply. For a distribution system, the prima facie is to dispatch uninterrupted consumer power under permissible individual parameter limits for intangible nature of load.

Aware governmental bodies along with enterprises, and investors are persuading modern power networks, to acclimate to the change. Especially when new blend of loads, such as charging of electric vehicles, IPM-SynRM, PMDC, BLDC motors, robotic stepper motors, for modern industries have come to the fore. Few new innovations make living more valuable and elegant. They do, however, prove detrimental to the conventional structure of power systems. [4]

The size of distributed generation (DG) facilities can vary between just few kilowatts up to megawatts technology could be renewable or non-renewable. DG units are stimulated by the availability of renewable energy resources such as micro wind, mini and micro hydro, solar photovoltaic (SPV), micro turbine, fuel cell. Because most of the units are modular, they are governed by the topographical conditions that prevail, DG has a competitive improvement in terms of versatility. Its construction time is trivial. [5] Performance analysis of SPV system in distribution network for PV contribution and grid dependency is propound in [6].

One of the most unrivalled parameter for adoption and acceptance of Electric era is charger. About 6000 EV chargers are installed in Shenzhen, China while total EV in the city has exceeded 80,000 in 2017 [7]. Charging time is now competing with time required to get the vehicle filled with petroleum

978-1-6654-1005-2/22/$31.00 ©2022 IEEE

products, although there is no direct competition still if we manage the charging time during our daily schedules, things could become practical, yet no one can deny the luxury to get the car charged in a while at least for daily commute. EV and PHEV conductive and inductive chargers range vary from few kW up to 200 kW [8]-[10]. Automated charger for scaling adoption of electric vehicles is proposed in [11] near future technology is still unpredictable and behold.

Using a small-scale laboratory distribution system, researchers discovered the repercussions of electric vehicle charging [12], however these does not quantify the impact on real scale transmission or practical distribution system dispatching few MWs and MVAr's. Q-learning technique based on the Artificial Neural Network (ANN) and recurrent neural networks (RNN) was proposed for the PHEV load forecasting in [13], visible scope for the newer study is in pure EV charging loads for practical distribution system, since these are intended for quick charging, which will garner significant market share as current budget consumers are mostly complaining about charging range anxiety and looking forward as a primary vehicle to a cleaner future. This study will be conducted on considering 96 kW charger to be used for charging on the case studies in [2]-[3].

II. Problem Formulation

A. Power Flow Solution

A power flow study, also known as a load flow study, is a steady-state solution in a power system. They are utilised for the planning, control of an existing system with future extension and economic scheduling. It guesstimates active and reactive power flow at each line, phase angle and magnitude of voltages at each bus and. It computes for a specific set of power system condition non dynamic. The system buses are classified into three types, namely first slack bus for which magnitude and phase angle of voltage is specified. This bus compensates between scheduled loads and generated power that is caused by network losses. Second load buses having only load, it may or may not contain capacitor banks. Final is regulated buses which have generator or DG buses. Iterative techniques such as Gauss-Seidel, Newton-Raphson (NR), and Fast Decoupled is often used to quantify power flow. In this paper, Newton-Rapson is preferred for quantization.

The flow path of active and reactive power to be distributed to customers is enhanced via network reconfiguration. It is crucial to evaluate the optimal ring main network framework that addresses the minimal power loss whilst striving to meet all of the system's restrictions.

B. Network Reconfiguration

The flow path of active and reactive power to be distributed to customers is enhanced via network reconfiguration. It is crucial to evaluate the optimal ring main network framework that addresses the minimal power loss whilst striving to meet all of the system's restrictions.

The disparities in power loss after reconfiguring from RDS to RMDS are evaluated in this work by total power loss reduction, ΔP_{Loss}^{R} in the system.

$$\Delta P_{Loss}^{R} = \sum_{i=1}^{n} P_{T,Loss}(i,i+1) - \sum_{i=1}^{n} P'_{T,Loss}(i,i+1) \quad (1)$$

Before reconfiguration, power loss in any of the transmission line sections linked to buses *i* & *i+1* can be quantified by

$$P_{Loss}(i,i+1) = R_{(i,i+1)} \frac{((P_i)^2 + (Q_i)^2)}{|V_i|^2} \quad (2)$$

Likewise, after reconfiguration, the power loss of individual transmission line linked between buses *i* & *i+1* can be assessed by

$$P'_{Loss}(i,i+1) = R_{(i,i+1)} \frac{((P'_i)^2 + (Q'_i)^2)}{|V'_i|^2} \quad (3)$$

Where, $\sum_{i=1}^{n} P_{T,Loss}(i,i+1)$ is before reconfiguration total power loss, $\sum_{i=1}^{n} P'_{T,Loss}(i,i+1)$ is after reconfiguration total power loss, $P_i, P'_i, Q_i, Q'_i, V_i, V'_i$, are bus *i* active reactive powers, prior to and following reconfiguration and voltages at bus *i* before and after reconfiguration respectively.

C. Distributed Generation

When a Distributed Generation/s is/are deployed at a haphazard point in the network, the power loss is assessed by

$$P_{DG,Loss} = R_{(i,i+1)} \frac{((P_i)^2 + (Q_i)^2)}{V_i^2} + \frac{R_{i,i+1}}{V_i^2}(P_G^2 + Q_G^2 - 2P_iP_G - 2Q_iQ_G)\left(\frac{G}{L}\right) \quad (4)$$

$$\Delta P_{Loss}^{DG} = \frac{R_{i,i+1}}{V_i^2}(P_G^2 + Q_G^2 - 2P_iP_G - 2Q_iQ_G)\left(\frac{G}{L}\right) \quad (5)$$

Where, P_G, Q_G are active reactive power injected by DG's, G is the length in kilometers betwixt the source and the DG site and L is the length of transmission line, betwixt source and bus *i* in kilometers.

D. PHEV and EV Chargers

Many countries have their own charging standards. The conductive and inductive chargers ratings vary from manufacturer to manufacturer also. Conductive charging can be AC or DC. Inductive is always AC. In AC Electric Vehicle Supply Equipment (EVSE), the alternating current power is transferred to the EV's onboard charger, which converts it to direct current (DC). A DC EVSE extrinsically converts electricity and supplies direct current to the battery, bypassing the onboard charger. In TABLE I., P is Power.

TABLE I. The Indian Standard EVSE Power Ratings [11]

Type	*Power level (kW)*	*Current type*	*Compatible EV segments*
Nominal power charger	P ≤ 7	AC & DC	E-2Ws, e-3Ws, e-cars, other LCVs (up to 1 ton)
	7 < P ≤ 22	AC & DC	
High power charger	22 < P ≤ 50	DC	E-cars, LCVs and MCVs (1-6 tons)
	50 < P ≤ 200	DC	

TABLE II. The Indian Standard Battery Specifications for Differenet EV Segments [11]

Vehicle Segment	*Battery Capacity (kWh)*	*Battery Voltage (V)*
E-2W (Scooter)	1.2 - 3.3	48 - 72
E-3W (passenger/ goods)	3.6 - 8	48 - 60

978-1-6654-1005-2/22/$31.00 ©2022 IEEE

Vehicle Segment	*Battery Capacity (kWh)*	*Battery Voltage (V)*
E-cars (1st Generation)	21	72
E-cars (2nd Generation)	30 - 80	350 - 500

TABLE III. THE PHEV CHARGERS IN [9]

Power type	*Charger type*	*Input voltage (V)*	*Maximum Power (kW)*
AC	Level 1	120	1.44
AC	Level 2	208-240	11.5
AC	Level 3	208-240	96
DC	Level 3	208-600	240

For AC level 3 EV charger, from [9] the active power is 96 kW i.e., 0.096 MW. Power factor of chargers vary from 0.97-0.95. Assuming power factor to be 0.95 as industry standard. Apparent power is given as,

$$Apparent\ power\ (kVA) = \frac{Active\ power\ (kW)}{power\ factor} \quad (6)$$

EV charger Reactive power can be evaluated as,

$$Reactive\ Power = \sqrt{Apparent\ power^2 - Active\ power^2} \quad (7)$$

III. NEWTON-RAPSON POWER FLOW SOLUTION

Newton-Rapson has quadratic convergence and thus outperforms the Gauss-Seidel method mathematically. It is less likely to succumb to deviations when confronted with ill-conditioned problems. The iterations required to find a solution is impartial of network size, yet every iteration necessitates more functional evaluations. The power flow equation is formulated in polar form.

The complex power at bus *i* is,

$$P_i = \sum_{j=1}^{n} |V_i||V_j||Y_{ij}|cos(\theta_{ij} - \delta_i + \delta_j) \quad (8)$$

$$Q_i = -\sum_{j=1}^{n} |V_i||V_j||Y_{ij}|sin(\theta_{ij} - \delta_i + \delta_j) \quad (9)$$

The Jacobian matrix asserts the linearized association between perturbation in voltage angle $\Delta\delta$ and voltage magnitude $\Delta|V|$ with perturbation in real and reactive power ΔP_i and ΔQ_i.

$$\begin{bmatrix}\Delta P \\ \Delta Q\end{bmatrix} = \begin{bmatrix}J_1 & J_2 \\ J_3 & J_4\end{bmatrix}\begin{bmatrix}\Delta\delta \\ \Delta|V|\end{bmatrix} \quad (10)$$

The diagonal and off-diagonal elements of J_1 are

$$\frac{\partial P_i}{\partial \delta_i} = \sum_{j\neq i} |V_i||V_j||Y_{ij}|sin(\theta_{ij} - \delta_i + \delta_j) \quad (11)$$

$$\frac{\partial P_i}{\partial \delta_j} = -|V_i||V_j||Y_{ij}|sin(\theta_{ij} - \delta_i + \delta_j) \quad j \neq i \quad (12)$$

The diagonal and off-diagonal elements of J_2 are

$$\frac{\partial P_i}{\partial |V_i|} = 2|V_i||Y_{ii}|cos\theta_{ii} + \sum_{j\neq i} |V_j||Y_{ij}|cos(\theta_{ij} - \delta_i + \delta_j) \quad (13)$$

$$\frac{\partial P_i}{\partial |V_j|} = |V_i||Y_{ij}|cos(\theta_{ij} - \delta_i + \delta_j) \quad j \neq i \quad (14)$$

The diagonal and off-diagonal elements of J_3 are

$$\frac{\partial Q_i}{\partial |\delta_i|} = \sum_{j\neq i} |V_i||V_j||Y_{ij}|cos(\theta_{ij} - \delta_i + \delta_j) \quad (15)$$

$$\frac{\partial Q_i}{\partial |\delta_j|} = -|V_i||V_j||Y_{ij}|cos(\theta_{ij} - \delta_i + \delta_j) \quad j \neq i \quad (16)$$

The diagonal and off-diagonal elements of J_4 are

$$\frac{\partial Q_i}{\partial |V_i|} = -2|V_i||Y_{ii}|sin\theta_{ii} - \sum_{j\neq i} |V_j||Y_{ij}|sin(\theta_{ij} - \delta_i + \delta_j) \quad (17)$$

$$\frac{\partial Q_i}{\partial |V_j|} = -|V_i||Y_{ij}|sin(\theta_{ij} - \delta_i + \delta_j) \quad j \neq i \quad (18)$$

The terms $\Delta P_i^{(k)}$ and $\Delta Q_i^{(k)}$ are the power residuals, which are the deviation between both the scheduled and predicted values, given by

$$\Delta P_i^{(k)} = P_i^{sch} - P_i^{(k)} \quad (19)$$

$$\Delta Q_i^{(k)} = Q_i^{sch} - Q_i^{(k)} \quad (20)$$

The new estimates for bus voltages are

$$\delta_i^{(k+1)} = \delta_i^{(k)} + \Delta\delta_i^{(k)} \quad (21)$$

$$|V_i^{(k+1)}| = |V_i^{(k)}| + \Delta|V_i^{(k)}| \quad (22)$$

IV. COMPUTATION PROCEDURE

Newton-Rapson has quadratic convergence and thus outperforms the Gauss-Seidel method mathematically. It is less likely to succumb to deviations when confronted with ill-conditioned problems. Although the number of iterations expected to reach a solution is impartial of network dimension, each iteration necessitates more workable assessments. The Newton-Raphson method is used to solve power flow problems as follows:

1) Voltage magnitudes and phase angles are taken equal to the slack bus values, or 1.0 and 0.0, for load buses where P_i^{sch} and Q_i^{sch} are given, voltage magnitudes and phase angles are set equal to the slack bus values, or 1.0 and 0.0. When $|V_i|$ and P_i^{sch} are stipulated for voltage-regulated buses, phase angles are arranged to a slack bus angle, or 0.
2) $P_i^{(k)}$ and $Q_i^{(k)}$ are calculated from (8) and (9) for load buses and $\Delta P_i^{(k)}$ and $\Delta Q_i^{(k)}$ are calculated from (19) and (20)
3) $P_i^{(k)}$ and $\Delta P_i^{(k)}$ are calculated from (8) and (19) for voltage-controlled buses
4) The Jacobian matrix is calculated from (11)-(18)
5) The linear simulatineous equation (10) can be solved directly using optimally organised Gaussian elimination and triangular factorisation
6) The updated voltage magnitudes and phase angles are computed from (21) and (22)
7) The procedure is iterated til the $\Delta P_i^{(k)} and\ \Delta Q_i^{(k)}$ are less than the accuracy specified,

$$|\Delta P_i^{(k)}| \leq \epsilon$$
$$|\Delta Q_i^{(k)}| \leq \epsilon \quad (23)$$

V. CASE STUDY

The framework for entire case studies is an IEEE 33 bus radial distribution system, as brandished in Fig. 1. [1] provides the line data and load data. In the view of advantage described in [2] Radial Distribution System (RDS) is modified into Ring Main Distribution System (RMDS).

The total real and reactive load for the original RDS system is 3.715 MW and 2.300 MVAr, respectively. Lines are normally closed which range from 1 to 32, while tie-switch lines are normally open range from 33 to 37. Sectionalizing switches or transmission line 1-9 have current carrying capacities of 400 A, whilst rest of the lines, including tie-switches, have current carrying capacities of 200 A. Permitted voltage constraints for voltage levels of 12.66 kV at each bus are 1.05 and 0.95 per unit, respectively. Case A is original RDS, IEEE-33 bus distribution system. Case studies I from [2] along with 96 kW EV chargers case studies J and K are ring main networks. The following four cases are assessed as shown in table IV and V. In a perspicuous way both tables describe individual case study of network structure (RDS/RMDS), values and locations for DG, capacitors. EV chargers units, bus location with size is add-ons in table V. In table IV all case studies are either reconfigured to reduce the power loss and improve bus voltage profile without installing any new equipment as in Case A.

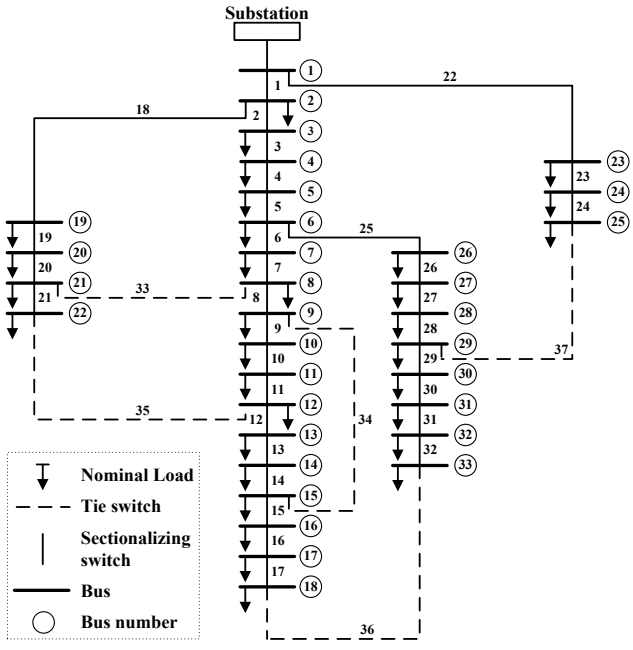

Fig. 1. Test system for Case A, RDS

In Case A, the system performance exceeds the lower voltage limit of 0.95 per unit by 0.037 per unit. The total power loss is 203 KW. Lower voltages contribute in additional current to be drawn from the substation, resulting in an increase in power loss. Outcomes of which are procreated and assimilated in table VI. In Case I, all 37 lines are reconfigured to deliver power in RMDS mode, such that exorbitant loss-making lines are eliminated and could be used only during contingencies. To take into account modern era renewable sources, DGs and capacitor banks are installed at few buses as shown in Fig. 2, table IV.

Case J, K are tantamount as Case I, with the revamp with genesis of "EV chargers" (AC level 3 from table III). Buses with EV charger will take on additional individual charging load of 0.096 MW and 0.031551 MVAr respectively.

TABLE IV. THE NON CHARGER LOAD CASE STUDIES OF DISTRIBUTION SYSTEM

Case	Parameters	Unit	Bus/Line No.	Individual Rating (MW/MVAr)
A	Lines open, no Reconfigure	5	All tie lines	-
	DG units	0	-	0
	Capacitor	0	-	0
I	Lines open, Reconfigure	5	7, 9, 15, 27, 34	-
	DG units	5	14, 16, 22, 30, 33	0.2, 0.25, 0.25, 0.5, 0.2
	Capacitor	5	15, 18, 24, 29, 30	0.3, 0.3, 0.2, 0.3, 0.5

TABLE V. THE CHARGER LOAD CASE STUDIES OF DISTRIBUTION SYSTEM

Case	Parameters	Unit	Bus/Line No.	Individual Rating (MW/MVAr)
J	Lines open, Reconfigure	5	7, 9, 15, 27, 34	-
	DG units	5	14, 16, 22, 30, 33	0.2, 0.25, 0.25, 0.5, 0.2
	Capacitor	5	15, 18, 24, 29, 30	0.3, 0.3, 0.2, 0.3, 0.5
	Chargers	3	18, 22, 33	0.096 MW, 0.031551 MVAr (each)
K	Lines open, Reconfigure	5	7, 9, 15, 27, 34	-
	DG units	5	14, 16, 22, 30, 33	0.2, 0.25, 0.25, 0.5, 0.2
	Capacitor	5	15, 18, 24, 29, 30	0.3, 0.3, 0.2, 0.3, 0.5
	Chargers	10	4, 5, 7, 9, 10, 11, 13, 17, 26, 27	0.096 MW, 0.031551 MVAr (each)

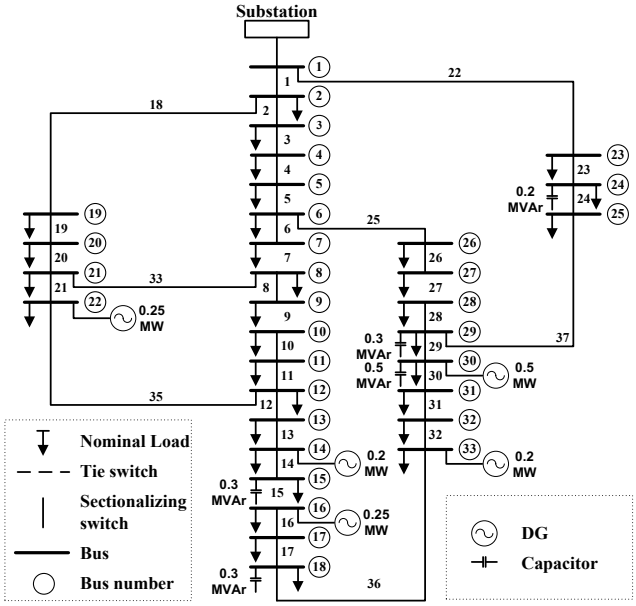

Fig. 2. Test system for Case I, RMDS proposed system of [2]

Case J, and K inspects on effects of 3 and 10 chargers respectively as per the details shown in Fig. 3, 4 and table V. EV Charger locations for Case J, is selected such that, they are installed at (bus located at extreme end) worst part of the

978-1-6654-1005-2/22/$31.00 ©2022 IEEE

network. This is due to the consideration that, bus voltage profile is generally lowest at these buses.

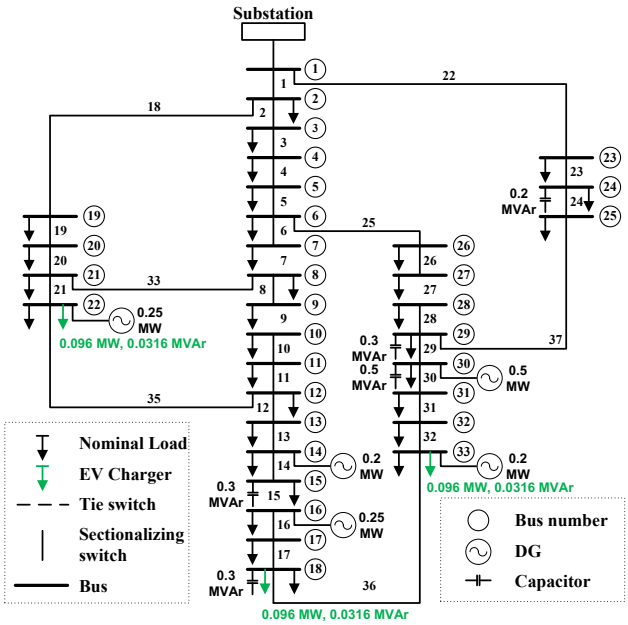

Fig. 3. Test system for Case J, RMDS with three units of AC level 3 charger load

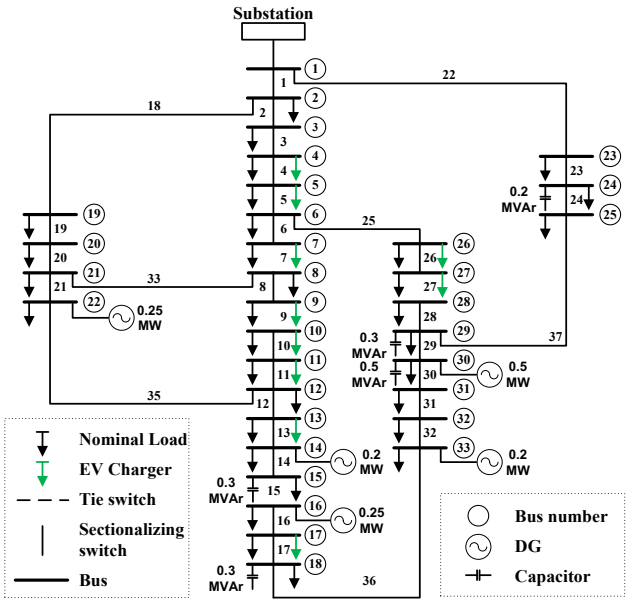

Fig. 4. Test system for Case K, RMDS with ten units of level 3 charger load

EV Charger locations for Case K are purely kept at random locations due to their sheer amount 10 chargers at peak load on power system.

Outcomes by NR are shown in table VI, which delineate the case study comparison with the outputs of [2] and [3]. Main system parameters are evaluated such as total system power loss in (kW), minimum bus voltage in per unit and identification of that bus and percentage loss reduction compared to the base case A.

For RMDS case study I, power loss has improved from 203 kW (case A) to 28 kW (Case I), which is 86.206% improvement, NR's method demonstrates its efficacy compared to paper [3], which has nearly identical replications in overall power loss. i.e., 202.612 to 31 kW and percentage loss reduction of 84.699% from Case A. The voltage profile in [3] and NR are indistinguishable.

The active load on the Case A system is 3.715 MW, while the reactive load is 2.3 MVAr. In EV charging case studies, real and reactive load increased to 4.003 MW, 2.396 MVAr for Case J. In Case K, the real and reactive loads rise to 4.675 MW and 2.620 MVAr, respectively. Loading effects on different bus can be visualized by Fig. 5, 6.

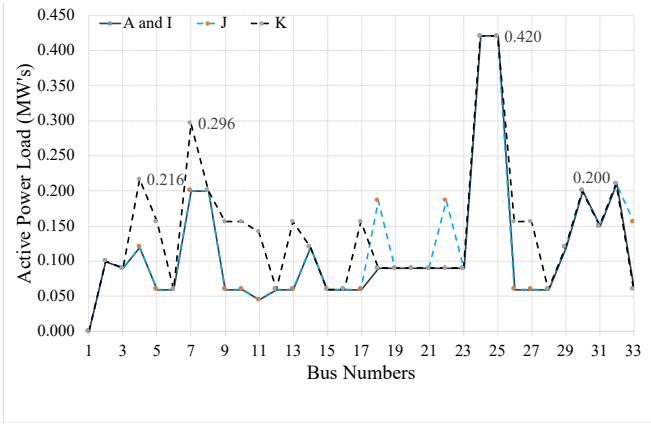

Fig. 5. Active Power Load increase from base to peak load case

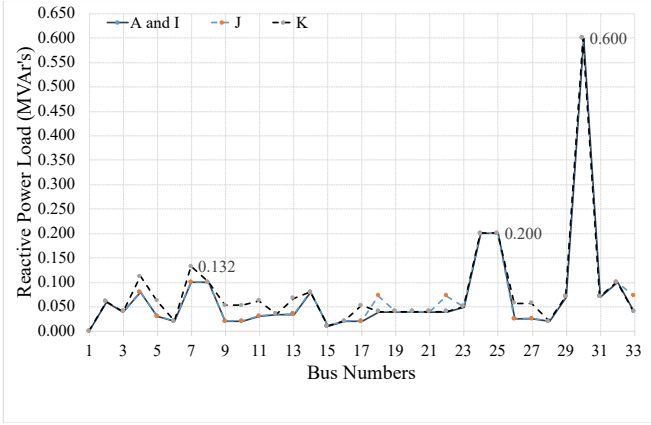

Fig. 6. Reactive Power Load increase from base to peak load case

TABLE VI. THE OUTCOMES OF THE 33 BUS-RADIAL AND RING MAIN DISTRIBUTION SYSTEM

Case	*Assessment of Diverse Case Studies*			
	Methodology	*By GA [2]*	*By GA [3]*	*By N-R*
A	Power Loss (kW)	202.612	202.612	203
	Min. Voltage (p.u.)	0.913	0.913	0.913
	Min. Voltage bus	-	-	18
I	Power Loss (kW)	-	31	28
	Min. Voltage (p.u.)	-	0.980	0.980
	Min. Voltage buses	-	-	31, 32
	% Loss reduction	-	84.699	86.206
J	Power Loss (kW)	-	-	42
	Min. Voltage (p.u.)	-	-	0.972
	Min. Voltage bus	-	-	32
	% Loss reduction	-	-	79.310

978-1-6654-1005-2/22/$31.00 ©2022 IEEE

Case	*Assessment of Diverse Case Studies*			
	Methodology	***By GA [2]***	***By GA [3]***	***By N-R***
K	Power Loss (kW)	-	-	63
	Min. Voltage (p.u.)	-	-	0.974
	Min. Voltage bus	-	-	10, 11, 13, 31, 32
	% Loss reduction	-	-	68.965

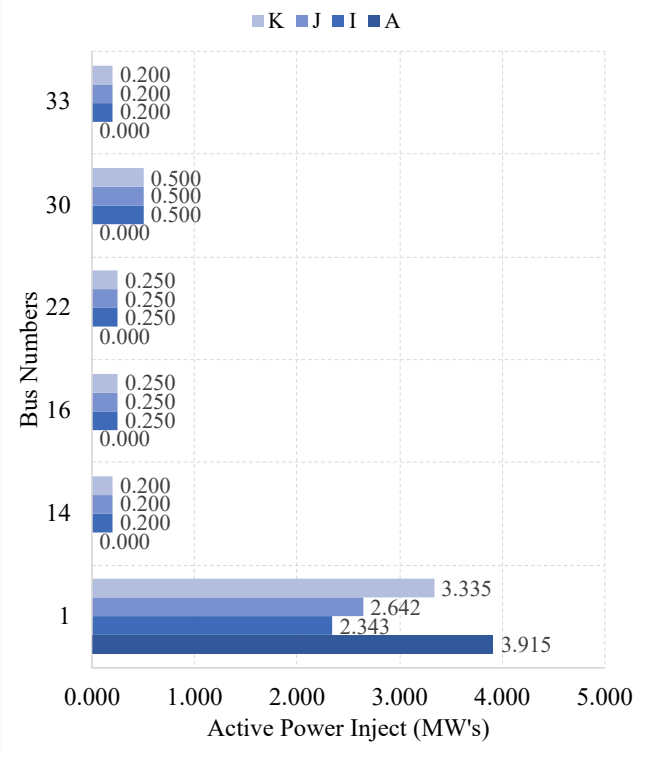

Fig. 7. Outcomes of Active power supplied by Substation and DGs at individual bus.

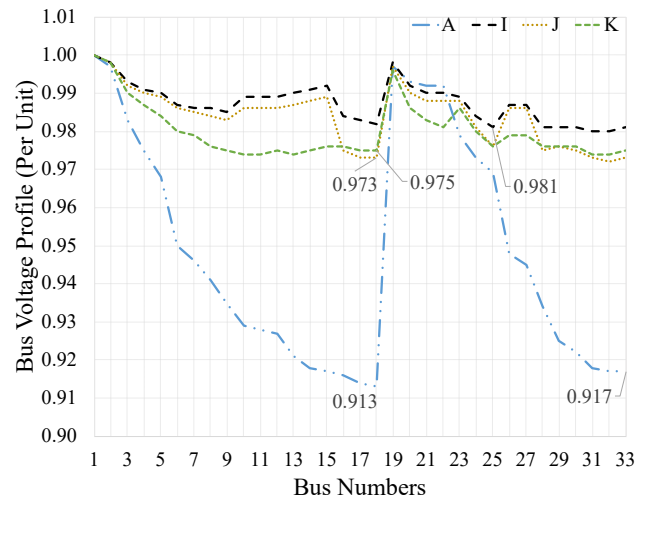

Fig. 8. Outcomes of Bus voltage profiles

For case studies J, K, comprehensive RMDS system designed in [3] is put to test with the EV charger load. Power loss compared from, K to A is still 68.965% better. Voltage profile falls from 0.98 to 0.974 which is superior to acceptable limit of 0.95 per unit, although the system is under test to almost the worst-case scenario in Case K. For 3 EV charger cases in J power loss reduction is 79.31% respectively and lowest bus voltage profile for both at 0.972 per unit, which is outstanding as system is ready to take on EV chargers up to 10 even during peak load hours. Outcomes of bus voltage profile in A, I, J, K are depicted in Fig. 8 which clearly portray the best among all is I at 0.98 per unit and weakest is A at 0.931 per unit. It's clearly visible that, I profile is definitely improved from A due to presence of local reactive power supply through capacitor banks, and it has its effects on EV charger case studies too.

Outcomes of active power supplied by substation and DG for cases K, J, I, A as shown in Fig. 7. Results portray that substation load (at bus 1) is higher in A and it drops down in I, J, K albeit J, K has higher active loads by 7.75% and 25.84%. Similar is the effect with reactive power demands.

Case K imply system can handle even higher load, so no need for additional transformer capacity and new lines along with new protection equipment's, which could have been a case if DG's and capacitor banks would have been absent.

VI. Conclusion

The hard-headed studies on framework divulges that, even with "ten number of AC level 3 chargers", system performance for Case K is paramount in terms of all parameters to that of original IEEE 33-bus power system. Research purveys strong corroboration that, DGs and capacitor banks have indispensable advantage to system performance and designers should contribute towards find buses on practical distribution system and bolster more consumers to install their own renewable system and invigorate to a greener tomorrow. It's essential that governing agencies must provide the data for such studies. Some may argue that adding renewables have adverse effect but, we must not forget, "nothing is perfect", its essential to keep bold steps to become "carbon neutral" within stipulated time, and renewable DGs are our best hope. Previous grid failures may be tacked with more advance machine learning and deep learning algorithms. As the studies suggest, more and more renewable energy used to make power, the narrower the CO_2 emissions of BEVs [14]. Charging with renewables is the current way forward.

Outcomes covers basic RDS to RMDS and advance RMDS networks with DGs and capacitor banks. Also EV Chargers of 96 KW capacity are generally suitable to be installed at voltage levels of 11 KV or higher, which makes this study more relevant to practicality of the system conditions. Loading effects are generally absurd on different buses due to EV charging meaning that random few will be loaded to limits and few buses may remain unloaded. Hence, this study implicates more practical purport rather than just assuming power system load uniformly increased on each bus by 20-40%. Albeit, we assumed all EV chargers are fully loaded with peak load of power system, which is extreme scenario. Selecting EV chargers of different sizes making them active, inactive as per real time and its effect is future scope. Smart grids with such predicting and controlling capabilities can be envisage.

References

[1] Y. Amara-Ouali, Y. Goude, P. Massart, J.-M. Poggi, and H. Yan, "A review of Electric Vehicle Load Open Data and models," *Energies*, vol. 14, no. 8, p. 2233, 2021, Apr. 2021.

[2] A. K. Saonerkar, B. Y. Bagde, "Optimized DG Placement in Radial Distribution System with Reconfiguration and Capacitor Placement

Using Genetic Algorithm," in *Proc. ICACCT, IEEE Conf.*, Ramanathpuram, India, pp. 1077-1082, May 2014.

[3] A. K. Saonerkar, S. Tiwari, A. S. Pande, P. G. Sharma, B. Y. Bagde, "Optimized Distribution Loss Evaluation in Ring main Distribution System with DG Placement, Reconfiguration and Capacitor Placement Using GA," in *Proc. ICICT, IEEE Conf.*, Coimbatore, India, Aug. 2016.

[4] C. Wang, R. Dunn, Q. Yang, B. Lian, W. Yuan, and J. Li, "The active and reactive power dispatch for charging station location impact factors analysis," *Energy Procedia*, vol. 103, pp. 237–243, Apr. 2016.

[5] A. K. Barnwal, L. K. Yadav, and M. K. Verma, "A multi-objective approach for voltage stability enhancement and loss reduction under PQV and P buses through reconfiguration and Distributed Generation Allocation," *IEEE Access*, vol. 10, pp. 16609–16623, 2022.

[6] N. Padole, R. Moharil, A. Munshi, "Performance Investigation Based on Vital Factors of Agricultural Feeder Supported by Solar Photovoltaic Power Plant," *Energies*, vol. 15, no. 1, pp. 1-18, Dec. 2021.

[7] Y. Lu, Y. Li, D. Xie, E. Wei, X. Bao, H. Chen, X. Zhong, "The Application of Improved Random Forest Algorithm on the Prediction of Electric Vehicle Charging Load," *Energies*, vol. 11, no. 11, pp. 1-16, Nov. 2018. https://doi.org/10.3390/en11113207

[8] G. Li, X. Zang, "Modeling of Plug-in Hybrid Electric Vehicle Charging Demand in Probabilistic Power Flow Calculations," *IEEE Trans. Smart Grid*, vol. 3, no. 1, pp. 492-499, March. 2012.

[9] M. Rostami, A. Fard, and T. Niknam, "Expected Cost Minimization of Smart Grids With Plug-In Hybrid Electric Vehicles Using Optimal Distribution Feeder Reconfiguration," *IEEE Trans. Industrial Informatics*, vol. 11, no. 2, pp. 388-397, Apr. 2015.

[10] *Handbook of Electric Vehicle Charging Infrastructure Implementation*, 1st ed., NITI Aayog, MoP, DST, BEE, WRI India, Delhi, New Delhi, India, 2021, pp. 1-92.

[11] S. Faddel, T. Youssef, A. T. Elsayed, and O. A. Mohammed, "An automated charger for large-scale adoption of electric vehicles," *IEEE Transactions on Transportation Electrification*, vol. 4, no. 4, pp. 971–984, 2018.

[12] S. Faddel, A. Elsayed, T. Youssef, O. Mohammed, "Experimental Verification of the Effect of Uncoordinated Charging of Electric Vehicles on Power Grids," in *Proc. ISGT, IEEE Conf.*, Washington, DC, USA, Feb. 2019.

[13] M. Dabbaghjamanesh, A. Moeini, A. Kavousi-Fard, "Reinforcement Learning-Based Load Forecasting of Electric Vehicle Charging Station Using Q-Learning Technique," *IEEE Trans. Industrial Informatics*, vol. 17, no. 6, pp. 4229–4237, Jun. 2021.

[14] R. Kawamoto, H. Mochizuki, Y. Moriguchi, T. Nakano, M. Motohashi, Y. Sakai, and A. Inaba, "Estimation of CO2 emissions of Internal Combustion Engine Vehicle and battery electric vehicle using LCA," *Sustainability*, vol. 11, no. 9, pp. 2690–2705, 2019.

[15] Å. L. Sørensen, K. B. Lindberg, I. Sartori, and I. Andresen, "Residential Electric Vehicle Charging datasets from apartment buildings," *Data in Brief*, vol. 36, p. 107105, Apr. 2021.

[16] D. Gielen, F. Boshell, D. Saygin, M. D. Bazilian, N. Wagner, and R. Gorini, "The role of renewable energy in the global energy transformation," *Energy Strategy Reviews*, vol. 24, pp. 38–50, Jan. 2019.

[17] X. Wu, Z. Tian, and J. Guo, "A review of the theoretical research and practical progress of carbon neutrality," *Sustainable Operations and Computers*, vol. 3, pp. 54–66, Oct. 2021.

[18] L. A.-W. Ellingsen, B. Singh, and A. H. Strømman, "The size and range effect: Lifecycle greenhouse gas emissions of electric vehicles," *Environmental Research Letters*, vol. 11, no. 5, p. 054010, 2016.

[19]

A Robust Performance Analysis of a Solar PV-battery based Islanded Microgrid Inverter output Voltage Control using Dual-loop PID Controller

Publisher: IEEE

Maneesh Kumar ; Sachidananda Sen ; Sanjay Kumar **All Authors**

Abstract: This paper proposes a performance indices-based voltage control of an isolated microgrid (MG) system. For this purpose, the system performance parameters such as integral... **View more**

Metadata

Abstract:

This paper proposes a performance indices-based voltage control of an isolated microgrid (MG) system. For this purpose, the system performance parameters such as integral absolute error (IAE), integral square error (ISE), integral time absolute error (ITAE), and integral time square error (ITSE) are obtained. The output voltage of a voltage source inverter (VSI) connected to a solar photo-voltaic (SPV) and battery energy storage system (BESS) based isolated MG is controlled using a dual-loop strategy, and the error profiles are observed. The control signals are generated through the pulse width modulation (PWM) technique. The SPV unit extracts maximum power infeed by using the maximum power point tracking (MPPT) algorithm. The BESS is also provided with PID based charge controller. The uncertainties in the solar irradiance pattern are considered by using a series of random variations at various time instants in the solar insolation data. The overall inverter output voltage control is done using a dual-loop PID-based controller. For this purpose, a closed-loop 'dq' controller is realized by taking the reference signal from the peak value of the 3- phase AC output voltage of the inverter. Various above mentioned performance indices are obtained for the different test cases, and a comparison between the proposed scheme and the model reference adaptive control (MRAC) based scheme is made. Results show the performance of a dual-loop PID controller is more promising as compared to the model reference-based approach.

Published in: 2022 IEEE IAS Global Conference on Emerging Technologies (GlobConET)

Date of Conference: 20-22 May 2022

Date Added to IEEE *Xplore*: 09 September 2022

ISBN Information:

INSPEC Accession Number: 22028707

DOI: 10.1109/GlobConET53749.2022.9872377

Publisher: IEEE

Conference Location: Arad, Romania

Contents

I. Introduction

Microgrids (MGs) are crucial establishments that allow the penetration of renewable energy into the system for supplying the connected loads reliably. These grids also have their own control capabilities. Broadly MGs can be operated in two modes; the grid-connected mode and the islanded mode. Out of the two types of grids, the isolated MG is more sensitive towards the voltage and frequency variations and requires a more precise operation all the time. Hence, from the viewpoint of voltage and frequency control, the isolated MGs require more robust techniques, as the system itself is of highly dynamic nature with generation arbitrage and load variation models. For this purpose, the model reference adaptive control (MRAC) based approach in conjunction with a few heuristic technique has to be realized. However, these methodologies requires a more complicated centralized control mechanism for optimizing the plant model [1], [2]. A modified MRAC control approach is presented in [3], [4] for the voltage control in an isolated MG. Here, the tracking performance of the proposed control scheme has been observed under different load scenarios. In [5], a modified MIT rule-based MRAC approach is proposed for the converter voltage control of an SPV-storage-based isolated MG under the intermittent energy infeed from the renewables. However, the proposed approach lacks to find a robust control under higher system dynamics. [6] proposed a d-q control strategy for an ac microgrid using two loops for active and reactive power control in the MG system. [7] provided an elaborated architecture with design and analysis of an islanded MG system having the penetration of solar photo-voltaic using a local decentralized controller that is applied across the developing nations. [8] proposed an improved an improved strategy to control the power for a hybrid MG bidirectional voltage source converter without using PLL. This approach reduces the delay and improves the transient behaviour of the system. A fuzzy logic-based power control approach for solar PV inverter without PLL is proposed in [9]. In [10], aggregating a robust control technique, viz., sliding mode control (SMC) in the outer loop resulting in SMC-PID based controller, is proposed. Implementing fractional order PID method in [11], [12], etc., can also improve the overall performance of conventional dual-loop PID at the expense of increased computational burden. However, the implementation of these control strategies needs a wide scope of implementation in an isolated MG system. Stringent control requirements calls for accurate MG modeling and robust controller design especially during the islanded operating mode [13], [14].

Maximum Power Point Tracker (MPPT) for Photovoltaic Power Systems-A Systematic Literature Review
2018 European Control Conference (ECC)
Published: 2018

Show More

MPC Based Energy Management System for Grid-Connected Smart Buildings with EVs

Publisher: IEEE

Sachidananda Sen ; Maneesh Kumar All Authors

Abstract: With rapidly rising urban population, the concepts of smart cities are evolving to accommodate its dwellers. As a person most of the time remains within a building (resid... **View more**

Metadata

Abstract:
With rapidly rising urban population, the concepts of smart cities are evolving to accommodate its dwellers. As a person most of the time remains within a building (residential or work), it becomes utmost important to convert these into energy efficient smart buildings. It uses renewable energy resources (RESs), viz., solar PV and wind turbines, diesel generator, electric vehicles (EVs), and connected to low voltage distribution grid. It has lighting, heating and cooling, as well as motoring loads. This combination of multiple sources and loads results into building integrated microgrids (BIMG) having a system of systems (SoSs) architecture. This article presents a model predictive control (MPC) based energy management of BIMG under grid-connected operation. It involve forecasting information of both generation and load profiles, power tariffs throughout the day, storage unit capacity and EVs coordination. Various test case scenarios and actual operating conditions of RESs were considered to determine the effectiveness of the proposed MPC method.

Published in: 2022 IEEE IAS Global Conference on Emerging Technologies (GlobConET)

Date of Conference: 20-22 May 2022

Date Added to IEEE *Xplore*: 09 September 2022

ISBN Information:

INSPEC Accession Number: 22028775

DOI: 10.1109/GlobConET53749.2022.9872436

Publisher: IEEE

Conference Location: Arad, Romania

Contents

Smart cities are being realized to bridge the gap between the current amenities in a conventional city to the ones required to sustainably accommodate increasing urbanization. Various features like smart transportation, smart living, smart grid, smart waste management, etc. To improve the living standards of its population, the vision of smart cities aims for continuous Readings areas using latest technology [1]. Now, peoples spend most of their time indoor be it in a residential building, offices, commercial buildings, etc. A city has all these buildings as the most essential component. Hence, smart buildings plays a very crucial role to realize a smart city [2].

Study and Analysis of Solar Photo Voltaic Modules with Real Time Experimentation on Solar Simulator/Solar Emulator

Publisher: IEEE

S.P. Adhau ; R. M. Moharil ; V. S. Rajguru ; Mrunmayee Gujar Pradhan **All Authors**

Abstract: The solar cell technology is now well developed and attempts are made to increase its efficiency for delivering maximum power. But because of fundamental limitations of v... **View more**

Metadata

Abstract:

The solar cell technology is now well developed and attempts are made to increase its efficiency for delivering maximum power. But because of fundamental limitations of various cell parameters, efficiency is restricted and losses are taking place in it. In this paper, environmental conditions and other parameters influencing the solar photo voltaic module output voltage and efficiency are studied. To find the finest output current and power with respect to voltage, characteristics are plotted for different cell temperature and solar irradiation values for the solar PV model, which includes the effect of the series resistance. Here the parallel resistance, which is too high, can be eliminated for simplification. Simulation performance of effect of solar irradiation and PV cell temperature has been carried out. Also the issues of series/parallel connection of solar PV module are discussed. Study is carried out on a solar simulator designed and built in the laboratory and results are validated/compared with solar emulator (Texas Instruments C2000)

Published in: 2022 International Conference on Electrical, Computer and Energy Technologies (ICECET)

Date of Conference: 20-22 July 2022

Date Added to IEEE *Xplore*: 09 September 2022

ISBN Information:

INSPEC Accession Number: 22028457

DOI: 10.1109/ICECET55527.2022.9872753

Publisher: IEEE

Conference Location: Prague, Czech Republic

Contents

The use of nonpolluting renewable energy resources to regulate greenhouse gases is getting motivation from the government of India. The National solar mission, which is part of the National Action Plan on Climate Change has been set up to indorse the progress and utilization of solar energy for power production and other purposes with the eventual thinking of making solar energy inexpensive with fossil-based energy choices. The Solar Photo-Voltaic (SPV) schemes for power production had been arranged in the many parts in the nation for electrification where the grid connection is either not possible or not price effective as also some times in combination with gasoline based generating plants in remote areas and communication transmitters at far places. With descending tendency in the price of solar energy and indebtedness Sign in necessity for Reading of solar power, solar power plants have now been installed. A substantial share of the bulky potential of solar energy in the nation could be established by encouraging grid associated SPV power systems of changing magnitudes as per the requirement and affordability together with confirming acceptable return on asset. Solar simulators are used in study of solar PV characteristics under changing environmental conditions. The key benefit of the simulator/emulator is its capability to simulate various kinds and dimensions of solar arrays beneath changing irradiance and temperature via actual loadings [1]. Modelling, recreation and investigation of SPV system is an important stage former to implement SPV system at any site, which benefits to comprehend the performance and features in real climatic situations of the site [2]

2022 2nd International Conference on Intelligent Technologies (CONIT)
Karnataka, India. June 24-26, 2022

DSTATCOM under Unbalanced and Distorted Load Conditions: A Comparison of Different Formulations

Nivedita Padole
Department of Eectrical Engineering
Yeshwantrao Chavan College of Engineering
Nagpur, India
niveditapande1@gmail.com

Vivek Jawade
Department of Eectrical Engineering
Yeshwantrao Chavan College of Engineering
Nagpur, India
jawade.vivek@gmail.com

Nilesh Kuike
Department of Eectrical Engineering
Yeshwantrao Chavan College of Engineering
Nagpur, India
kuikenilesh@gmail.com

Punit Fulzele
Research and Development,
Jawaharlal Nehru Medical College,
Datta Meghe Institute of Medical Sciences
Wardha, India
punitr007@gmail.com

2022 International Conference on Intelligent Technologies (CONIT) | 978-1-6654-8407-7/22/$31.00 ©2022 IEEE | DOI: 10.1109/CONIT55038.2022.9848399

***Abstract*— The behavior of several control algorithms used to create reference currents for the Distribution Static Compensator (DSTATCOM) in a 3-ph, 4-wire system is investigated in this work. A three level Neutral Point Clamped (NPC) inverter topology is considered for DSTATCOM operation in order to attain load compensation. For unbalanced and non-linear load conditions, the Instantaneous active and reactive power (PQ) theory, Synchronous Reference Frame (SRF) theory, Averaged Global Control (AGC) theory, and Instantaneous Symmetrical Component (ISC) theory are graphically and analytically studied. The major goal of these control schemes under balanced source and various load situations is to create completely balanced and ripple-free source currents. On the basis of compensation parameters and performance metrics, a comparative assessment of the aforementioned algorithms is carried out. Under unbalanced and distorted load conditions, a comprehensive simulation was done utilizing the MATLAB environment to validate the proficiency of the ISC theory in comparison to the other schemes.**

Keywords*— DSTATCOM, balanced source, NPC, Unbalanced & distorted load.

I. INTRODUCTION

DSTATCOM, a shunt connected special power device, can boost the effectiveness of a distribution network [1]. It is the best suitable solution for the mitigation of power quality issues now a day. The key component of DSTATCOM is the Voltage Source Inverter (VSI) [2]-[3]. Multilevel converter topologies [4], [5] have recently demonstrated the capacity to tackle the issues associated with two-level topologies. Multilevel inverter topology are gaining significant importance in shunt applications because to their efficient characteristics. The three-level NPC inverter [6] is gaining popularity among the many multilevel topologies because to its resilience.

The shunt compensator's performance is influenced not only by the dc link or interface inductor, but also by the control approach employed. A variety of control algorithms are proposed in the literature [7]. Some of these algorithms are named as - Instantaneous PQ theory, SRF theory, AGC theory and ISC theory. All of the preceding algorithms have well-established basic approaches for operating under unbalanced and distorted load situations. Unbalanced and distorted sources are not considered in this paper, for which the above-mentioned algorithms are unable to work; as a consequence, a synchronous detection method (SDM) [8]-[9] has been established to work under such circumstances. According to the simulation results, AGCT and ISC theory are able to operate effectively to increase system performance over the other algorithms while dealing with load unbalance and distortions.

This paper examines the four algorithms stated above in depth, taking into account several key considerations discussed in the following sections. The theoretical benefits as well as a comparison of various methods under unbalanced and distorted load conditions are presented. A comprehensive simulation is also performed to showcase the effectiveness of the various methods.

II. SYSTEM CONFIGURATION

Figure 1 depicts a three-phase, four-wire system with a three-level NPC-based DSTATCOM structure [10]-[11]. The interface reactor, $R_f + jX_f$, connects the compensator in shunt at the Point of Common Coupling (PCC). The source and loads are connected at PCC, along with the compensator. The load causes unbalance in the stiff system under consideration, as well as non-linearity, due to the three-phase unregulated rectifier drawing 1.83 A. The hysteresis current regulated Pulse Width Modulation (PWM) approach is employed to generate the switching pulses required for the 3-level NPC inverter [12].

By introducing a dead band (δ) between the hysteresis bands, this control aids in achieving the desired three levels (V_{dc}, 0,$-V_{dc}$) (h). Table 1 lists the parameters [13] that are required to mimic the system.

III. REFERENCE CURRENT CONTROL ALGORITHMS

To increase system performance, a control technique was used to extract reference compensator currents and is solely accountable for DSTATCOM's control. Various control strategies, such as PQ, SRF, AGC, and ISC theories, are briefly reviewed in the following section.

Operation of Circuit Breaker with Authentication

Bharat Sudame, *Department of Electrical Engineering, YCCE*, Nagpur India, bharat_sudame@rediffmail.com

Roshan Umate, *Department of Research, DMIMS, Sawangi(M)*, Wardha, roshanumate111@gmail.com

Harshwardhan Mandhare, *Department of Electrical Engineering YCCE* Nagpur, India. harshwardhanmandhare04@gmail.com

Saloni Bhoyar, *Department of Electrical Engineering YCCE* Nagpur, India, salonibhy@gmail.com

Viplav Bisen, *Department of Electrical Engineering YCCE* Nagpur, India, viplavbisen7@gmail.com

Mrunali Dukare, *Department of Electrical Engineering YCCE* Nagpur, India, mrunalighanshyam@gmail.com

Sanket Mate, Depatment of Electrical Engineering,YCCE Nagpur, India, smate869@gmail.com

Vaishnavi Bambal, Department of Electrical Engineering, YCCE Nagpur, India vaishnavibambal15@gmail.com

Vaibhav Jiraphe, Department of Electrical Engineering, YCCE Nagpur, India vaibhav190620@gmail.com

2022 Second International Conference on Power, Control and Computing Technologies (ICPC2T) | 978-1-6654-5858-0/22/$31.00 ©2022 IEEE | DOI: 10.1109/ICPC2T53885.2022.9777043

***Abstract*—As the world is becoming technosavy, heading towards invention of advance electronic devices so is the safety factor of technicians becoming an important trouble of worry. The life of operators is in danger as they work on these electrical appliances. They work by changing off the circuit breakers but sometimes someone can unknowingly on the circuit breaker while they are working and this could result in massive accidents sometimes it can even result in fatal accidents. To avoid such accidents there must be system for ensuring security of technicians. Also, if sometimes the current of a particular electronic device exceeds its rated current, the device may get damaged. To resolve all these difficulties, we derived up with a solution of Circuit Breaker that is authenticated i.e., password based and a current sensor which produces an alarming sound as the current of particular device exceeds its rated value. When the Circuit Breaker is authenticated, it also has high security that no one can operate it without knowing the password.**

Index Terms- Arduino UNO, 4x4 Matrix Keypad, Relay, LCD Display, Battery.

I. INTRODUCTION

Along with the continuous upgrading of altered electronic devices, Operators, Workers, Engineers, Contractors, etc which work in the industry needs to encouraged that they are working in a Safe Environment. Their Safety is a major area of importance since technicians are always at risk during their work around circuits even if the circuit is switched off. That is because many a times technicians can be still on job on circuit breakers while someone has accidentally switched on the circuit [1].

Due to above reason Communication and co-ordination between the staff around circuit is very important since majority of the accidents happen due to miscommunications between the maintenance staff and electric substation staff. Such faults not only kill one but can also kill many and can affect the working environment of Industry. It is difficult for people to work in such High-Risk areas. The main aim of our project is to reduce the chances of such fatal accidents that happened due to human error. These kinds of accidents take place due to large distance between main supply station and maintenance area [2]. To prevent this password control system will be used to stop sudden power supply that will ensure that until the password from both end (main supply station and maintenance area) is same till then power supply will not start. This will prevent death of technician due to electric shock. Thus, the entire charge of the maintenance line is on a single person or say Group of Authority who is leading that particular job. He takes the charge of operating the Circuit Breaker, As a result the chances of Faulty Operation, Imposters or Human error in operation are eliminated and thus the maintenance of the line can be done in safer way [3].

II. EXISTING SYSTEM

The existing technology for power regulation and protection contain various features. The current tech used electronic circuit is connected to circuit breaker along with an electrical power circuit, communication device and monitoring devices. The electronic circuit is used to determine electric supply to send to electric circuit with feedback provided by circuit breaker and other connected devices. If power is supplied to circuit then circuit can be operated by other connected devices, charge the account and activates circuit if monitoring devices detects any fault.

To make better communication in commercial and residential areas, a system associated with intelligent circuit breaker is now used to communicate, monitor and control devices. It also uses information relating to current state and

978-1-6654-5858-0/22/$31.00 ©2022 IEEE

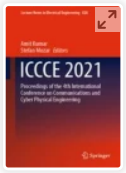

ICCCE 2021 pp 915–922

Spontaneous Detection of Potholes and Humps

Swati K. Mohod, Anjula Wararkar, Swaranjali Bokade, Rupali Lende, Rahul Lichade, Yash Mahure & Sagar Fartode

Conference paper | First Online: 16 May 2022

Part of the Lecture Notes in Electrical Engineering book series (LNEE,volume 828)

Abstract

Roads are the major means of transportation and it supports the nation's economy only if they are well maintained. It is necessary to identify holes and potholes so the accidents can be avoided and the damage caused to the vehicle is less. It also contributes in saving fuel. Here is a simple and effective solution regarding the problem of accidents by detection of potholes and humps and help drivers. Detection of potholes will be done by image processing technique and humps would be detected by ultrasonic sensor. Raspberry Pi is the controlling device. Wi-Fi will be used to acquire geographical position of potholes and will be send to the authority to take appropriate measures.

Keywords

Raspberry Pi **Wi-Fi** **Ultrasonic sensor** **GPS receiver** **GSM SIM900** **Camera**

References

1. Patil KD, Patil SR, Kale VV, Thorat SS (2018) Automatic detection and notification of potholes and humps on roads. Int J Adv Res Sci Eng 07(03). ISSN: 2319-8354

2. Sahu RM, Kher M, Hasan N, Panchal L. Automatic detection of potholes and humps on roads to aid driver. IJARIIE 3(2). ISSN(0)-2395-4396

3. Djamaluddin D, Achmad A, Parung R (2017) Prototype of vehicles potholes detection based blob detection method. J Theoret Appl Inf Technol 95(11). ISSN: 1992-8645, E-ISSN: 1817-3195

4. Gayathri S, Mamatha RG, Manasa B, Patil M, Sanjana BM (2019) Automatic pothole detection system. Int J Eng Res Technol (IJERT) 7(10). In: NCRACES—2019 conference proceedings, 2278-0181

Author information

Authors and Affiliations

Yeshwantrao Chavan College of Engineering, Nagpur, India
Swati K. Mohod, Anjula Wararkar, Swaranjali Bokade, Rupali Lende, Rahul Lichade, Yash Mahure & Sagar Fartode

Editor information

Editors and Affiliations

BioAxis DNA Research Centre (P) Ltd., Hyderabad, India
Dr. Amit Kumar

Dynexsys, Sydney, NSW, Australia
Dr. Stefan Mozar

Rights and permissions

Copyright information

About this paper

Cite this paper

Mohod, S.K. *et al.* (2022). Spontaneous Detection of Potholes and Humps. In: Kumar, A., Mozar, S. (eds) ICCCE 2021. Lecture Notes in Electrical Engineering, vol 828. Springer, Singapore. https://doi.org/10.1007/978-981-16-7985-8_97

.RIS .ENW .BIB

DOI	Published	Publisher Name
https://doi.org/10.1007/978-981-16-7985-8_97	16 May 2022	Springer, Singapore

Print ISBN	Online ISBN	eBook Packages
978-981-16-7984-1	978-981-16-7985-8	Engineering Engineering (R0)

Development of Fuzzy Controller Using 8-Bit Microcontroller for Switch Mode DC Servo Motor Control

Jyoti M. Kumbhare, IEEE member
Electrical Engineering Department
Yeshwantrao Chavan College of Engineering
Nagpur, India
jkumbhare04@gmail.com

Sumant G. Kadwane, SMIEEE
Electrical Engineering Department
Yeshwantrao Chavan College of Engineering
Nagpur, India
sgkadwane@gmail.com

Manoj Patil
Research Consultant
Jawaharlal Nehru Medical College,
Datta Meghe Institute of Medical Sciences, Sawangi (M), Wardha
India
mpatil98dent@gmail.com

***Abstract*— This paper describes the challenges and solutions for low cost control of DC-DC converter with robust fuzzy logic based controller for robotic/servo applications. Robotic applications need design of compact and versatile controllers for its manipulator. Control of the DC servomotors as actuators for robotic arm is done recently by DC-DC converters with PWM control methods as a single processor multi-motor system. Design approaches for PWM controller is often investigated because of its nonlinear nature due to inherent switching in DC-DC converters. Robust controller for this system can be designed using fuzzy logic which is difficult to implement on low cost digital processors. The proposed approach makes it possible to design the fuzzy controller with low cost microcontroller for PWM based control of DC servomotor.**

Keywords—fuzzy logic, robotic, switch mode dc servo motor, microcontroller, speed control.

I. INTRODUCTION

PD controller is often used for the control of DC servomotors in most of the commercial applications like robotic arm manipulator. Many control strategies like variable structure control and sliding mode control for DC motor have already been suggested in literature [1]. because of the convenience of production of PWM and benefits of digital processors over analog counterparts, servomotors can be controlled via DC-DC converters as single processor multi-motor system that is often needed in robotic applications. However, DC-DC converters are nonlinear system due to nonlinear components and inherent switching [2] [25]. for that reason, traditional design strategies frequently fail to give satisfactory results in these instances in which intrinsic nonlinear time changing characteristics of continuous conduction mode power converters impose problems in obtaining correct mathematical model required for design.

Fuzzy logic has immerged as a powerful approach to cope up the nonlinearity and uncertainty over past decade [3]. Fuzzy based controller for DC-DC converters have proved to be superior over conventional PD control techniques [4-6], [8]. The implementation of fuzzy controller through digital signal processors (DSP) is provided through application notes by way of some leading manufactures [7]. With the use of nonlinear state-space model, power electronic converters analysis, modelling and simulation is described in [10-11], [13] have made significant enhancements in traditional design strategies and simulations. Implementation of PI like fuzzy controller for DC-DC converter is provided these days in [14-16], [20-21] using digital signal processor. The foremost obstacle about this work is the increased cost of the overall system due to the use of DSP processors. stability analysis [22] is another matter of challenge for implementing fuzzy controller. Researchers have been investigating the application of fuzzy logic principles to control the switching-mode power converters, however, the logic and arithmetic calculations of the fuzzy logic algorithm can be tough to apply on several microcontrollers [9], [22-23]. Alternatively, higher cost of DSPs and associated hardware limit their utility. Low cost microcontrollers frequently include a means of control and communication functions in hardware, but computational power and resolution of processor are limited in general. thus, in this paper, a few demanding situations of imposing fairly complex fuzzy logic based algorithm on microcontroller were addressed. A small experimental prototype for real time DC servomotor speed control with the aid of fuzzy sliding mode controller using low cost 89C51RD2 microcontroller is investigated for improving the dynamic response. This control scheme ensures accurate response in terms of rejection of load variations, input voltage changes and even parameter uncertainties having low cost implementation as its constraint. The paper is prepared as follows. section II confers the system overview wherein the overall proposed scheme is discussed. section III covers the implementation of PID controller with microcontroller. section IV covers the implementation of PD like fuzzy controller with it challenges and solutions with five membership functions and nine membership functions. section V covers the hardware configuration and test setup specifications. subsequent section discusses the experimental responses and analysis with the proposed scheme. Conclusions are summarized in section VII.

II. SYSTEM OVERVIEW

The speed control scheme is shown in Fig. 1. Here we have eliminated the capacitor across the load of buck converter. The reason is for eliminating this capacitor in parallel with load is that DC servomotor itself is an inductive load that has a characteristic of low-pass filtering the armature voltage. Additionally, this extra capacitor which is in parallel with load will increase the system order by means of, which in addition complicates the plant's dynamics and the following controller layout and system analysis. an additional inductor in series with the armature coil could similarly assist to alleviate speed variations because of

2022 IEEE Delhi Section Conference (DELCON) | 978-1-6654-5883-2/22/$31.00 ©2022 IEEE | DOI: 10.1109/DELCON54057.2022.9752923

2022 International Conference for Advancement in Technology (ICONAT)
Goa, India. Jan 21-22, 2022

Remote Sensing Application for Analysis of Forest Change Detection

Swati Mohod,
Dept. of Electrical Engg.
Yeshwantrao Chavan College of Engg,
Nagpur, India,
swatimohod6882@gmail.com

Rajesh D. Thakare
Dept. of Electronics Engg.
Yeshwantrao Chavan College of Engineering,
Nagpur, India,
rdt2909@gmail.com

Dinesh B. Bhoyar,
Dept. of Electronics and Tele. Engg.
Yeshwantrao Chavan College of Engg,
Nagpur, India,
dinesh.bhoyar23@gmail.com

Sachin S Khade
Dept. of Electronics and Tele. Engg.
Yeshwantrao Chavan College of Engg,
Nagpur, India,
sac_mob@rediffmail.com

Punit Fulzele
Datta Meghe Institute of Medical Sciences,
Wardha, India,
Punit007@gmail.com

2022 International Conference for Advancement in Technology (ICONAT) | 978-1-6654-2577-3/22/$31.00 ©2022 IEEE | DOI: 10.1109/ICONAT53423.2022.9725898

Abstract: **Forest cover is generally defined as the relative in percent or square kilometers/square miles of land area which is occupied by forests. And the coverage of global forest cover is most essential for soil health, climate, water cycle and air quality. The condition can be improved by reforestation and afforestation to some extent but cannot be restored to full range. Once the natural forests are converted to various lands uses it's impossible to restore these ecological services. The terms "deforestation" and "forest area net change" are different as deforestation is defined as the forest losses while forest net change may possess some expansion and degradation of forests in a given period. The rate of deforestation has increased the loss of forests and due to this environmental misbalance is occurring. So if this continued then various parameters of environment like climate, quality of soil etc. can be degraded and may not be cured. Therefore, the following research is geared towards analyzing the parts of deforestation using remote sensing technology of a particular Yavatmal district of Maharashtra state, India. The satellite images used for this analysis of forest change detection are of planet scope having 3 m resolution. The target of this research is to detect the forest cover change using remote sensing and GIS. For the identification of forest covers various techniques like segmentation and classification are used. The best classification is by Normalized Difference Vegetation Index (NDVI) which identifies the health of vegetation along with the changes in the different parameters. After using NDVI some values generated will detect the areas of forest changes with the amount of change. And with the help of this research it is observed that out of total forest area i.e. 76740.32 hectares, the negative forest change is reduced to 29.44% due to degradation of forests maybe due to fires, deforestation, leaf shedding etc.**

Keywords: Remote sensing, forest change, image enhancement, image segmentation, image classification, K means, Normalized difference vegetation

I. INTRODUCTION

Remote sensing is a method which acquires information of an object on land without having physical contact with that object. It is mainly used to acquire the information about Earth and its various parameters [1] Remote sensing plays a vital role for forest ecology. The most important part for this study is monitoring the land parameters, vegetation, and land cover changes with various properties of forests [2]. The multispectral remote sensing is used to obtain the information of these parameters of environment. Here, the information is acquired and features are extracted depending on certain things, areas of vegetation, agriculture and water bodies' [3]. Remote sensing along with GIS will manage the information and provide various tools for forest analysis and statistics [4].

Deforestation is the loss of forests.The reason for this degradation may be due to loss in mining, road construction etc. If we consider deforestation rate in India, it stands at the 10^{th} position worldwide as per 2009 survey [5]. Likewise, the world estimates 13.7 million hectares (i.e. $34x10^6$ acres) of deforestation per year. From this we get to know how deforestation has become a serious topic of discussion throughout the world. Depending on the statistics of forest report 2019 the cover of forest is 712,249 sq.km.

Digital satellite image processing of satellite images provides a numerous operations for doing the image analysis efficiently with the help of different algorithms and different math's index [6].Generally, features of these are based on reflectance parameters while the indices help in highlighting the areas of interest. But for this study we have considered vegetation indices in which NDVI is the most common index [7]. Thus, remote sensing with satellite image processing has numerous applications in fields like astronomy; cloud computing and various research and development. And python along with various packages will play an essential role in this processing.

II. LITERATURE REVIEW

Remote sensing is a great technique having number of applications in forest ecology. It monitors and manages many parameters of species and habitat, different characteristics of land and forest with changes and mitigation of people. It is the most important and essential technique which helps in forest ecology with several other applications like monitoring land cover changes, their species, fragmentation of habitat and numerous other properties of forest[6].

Remote sensing uses multispectral images which are most efficient in obtaining the information of an environment. It will acquire the images in the form of information and extract essential features based on various aspects like vegetation objects, land covers, water, agriculture etc. it has numerous applications in forest classification, snow mapping, land cover classification, water classification etc. [7]

The excessive use of forest in the form of technological and industrial growth leads to major factors responsible in

Fuel Cell Based DC-AC Single Phase QZSI for Low Voltage Grid Utility

Publisher: IEEE

Shilpa B. Sarode ; Sumant G. Kadwane ; Ritesh. K. Keshri ; Aniket Pathade All Authors

Abstract:1ϕ qZSI inverter is most popular for renewable energy sources like PV and fuel cell due to its unique shoot through large boost voltage capability. A fuel cell is a clean... **View more**

Metadata

Abstract:
1ϕ qZSI inverter is most popular for renewable energy sources like PV and fuel cell due to its unique shoot through large boost voltage capability. A fuel cell is a clean and efficient source of electricity. Fuel cell needs fuel for continuous production of electricity but it can give good performance irrespective of seasonal changes, unlike PV cell. In this paper, proton exchange membrane fuel cell (PEMFC) based 1ϕ qZSI is interfaced to a low voltage grid. PEMFC is operated with low temperature and has lower emission of carbon dioxide. This paper focuses on the performance of PEMFC based 1ϕ qZSI on low voltage grid utility in the presence of 100Hz ripple. As in single-phase circuit, 100Hz ripple is more dominant; it causes more energy loss and shortens the lifetime of renewable source like a fuel cell. Hence, this article will also discuss how much percentage of 100Hz ripple present in qZS inductor current and capacitor voltage using proper calculation. The simulation results are found using MATLAB/SIMULINK

Published in: 2022 International Conference for Advancement in Technology (ICONAT)

Date of Conference: 21-22 January 2022

INSPEC Accession Number: 21660933

Date Added to IEEE *Xplore*: 10 March 2022

DOI: 10.1109/ICONAT53423.2022.9725822

ISBN Information:

Publisher: IEEE

Conference Location: Goa, India

Contents

I. Introduction

In today's era the non-conventional energy sources becomes more popular due to limited availability of fossil fuel and pollution free environment. The difference between PV and fuel cell is that PV is uncontrollable source where its output power is controlled by solar irradiance and not by the plant operation. The fuel cell is controllable source that can produce power when needed as long as the fuel is supplied. Similarly the comparison between the battery and fuel cell shows that comparative to battery, fuel cell supply uninterrupted energy as long as hydrogen fuel and oxidants are provided. Due to this property and its broad size range, fuel cell is popular to use for many application such as transportation/automation [1], motor drive application[2], grid connected residential application[3]–[4], standalone power system[5],and micro grid [6] in spite of its expensiveness[7]. The PEMFC is popular in small scale power generation due to its minimum operating temperature and minimum discharge of greenhouse gases. The power is generated at low voltage (230V RMS, 50Hz) which can be mostly used for single phase grid application [8]. Most of the fuel cell interfaced to grid application through two stage inverter topology. In this topology separate dc to dc booster are required which not only increases the size of the system but also increases its cost. Hence to overcome this issue the focus is given on single stage inverter topology [9].

Authors
Figures
References
Keywords
Metrics

More Like This

Modeling of proton exchange membrane fuel cell for simulation of hybrid systems with renewable energy sources
2014 18th International Symposium on Electrical Apparatus and Technologies (SIELA)
Published: 2014

Fuzzy Logic Control-Based Interleaved Boost Converter for Proton Exchange Membrane Fuel Cell System Applications
2022 International Conference on Electrical Engineering, Computer and Information Technology (ICEECIT)
Published: 2022

Show More

EV Vehicle Mileage Booster Using SolarTechnology

Publisher: IEEE

Dhiraj Thote ; Harsha Tembhekar ; Nitin Chakole ; Manthan Nawathe ; Pratyush Pimpalkar ; Punit Fulzele All Authors

Abstract: Currently due to limited sources of fuel the world is moving to Electric Vehicle (EV) technology, as we can see that the number of use of EV Vehicles is increasing day by... **View more**

Metadata

Abstract:

Currently due to limited sources of fuel the world is moving to Electric Vehicle (EV) technology, as we can see that the number of use of EV Vehicles is increasing day by day. Still the EV Vehicle is not going upto the mark because of its mileage. The mileage is the [illegible] to overcome this issue we have tried to propose a system that will increase the mileage to some extent. In this work we have introduce the technology to boost the EV mileage which will be increased by using another renewable source of energy i.e. solar power. Due to use of solar power there is no fuel emission which is ecofriendly to nature.

Published in: 2022 IEEE International Women in Engineering (WIE) Conference on Electrical and Computer Engineering (WIECON-ECE)

Date of Conference: 30-31 December 2022

INSPEC Accession Number: 23320463

Date Added to IEEE *Xplore*: 19 June 2023

DOI: 10.1109/WIECON-ECE57977.2022.10151407

ISBN Information:

Publisher: IEEE

Conference Location: Naya Raipur, India

Contents

Due to huge demand and limited sourcesavailability of petrol and diesel it is now becomeessential to switch to a less cost effectiverenewable source for driving a vehicles Now a day the alternative which is available is electricvehicles, but it has not got that popularity becauseof its less mileage. To overcome this issue we haveproposed a system which tackles this situation. Wehave made a system to increase the mileage whichwill also be cost effective and nature friendly.

References

References is not available for this d

Authors

Figures

References

Keywords

Metrics

More Like This

Control scheme for electrical drive of solar powered vehicles
2008 Annual IEEE India Conference
Published: 2008

A very high efficiency controller for an axial flux permanent magnet wheel drive in a solar powered vehicle
1998 International Conference on Power Electronic Drives and Energy Systems for Industrial Growth, 1998. Proceedings.
Published: 1998

Show More

References

References is not available for this d

Machine Monitoring for Industry using Computer Vision

Sujata S. Chiwande ; Piyush Meshram ; Abhishek Charde ; Shreya Bhave ; Sushma Nagdeote **All Authors**

Abstract: There are numerous approaches from which computer vision has been investigated. It moves beyond simply recording raw data to incorporate methods and concepts for computer... **View more**

Metadata

Abstract:

It moves beyond simply recording raw data to incorporate methods and concepts for computer graphics, pattern detection, digital image processing, and machine learning. This paper gives an outline of current technological advancements and theoretical ideas that describe how computer vision, mainly relates to image processing, and how it has evolved through time. It uses a technique for large-scale data analysis and a variety of application domains. The various research papers on computer vision and different techniques on object detection are reviewed in this paper. This paper gives the application of computer vision for factory and machine monitoring which will help to detect the object is moving or stable using YOLO algorithm. We also give a succinct summary of the most recent data regarding the effectiveness of the strategies.

Published in: 2022 IEEE Conference on Interdisciplinary Approaches in Technology and Management for Social Innovation (IATMSI)

Date of Conference: 21-23 December 2022

INSPEC Accession Number: 23123230

Date Added to IEEE *Xplore*: 15 May 2023

DOI: 10.1109/IATMSI56455.2022.10119424

ISBN Information:

Publisher: IEEE

Conference Location: Gwalior, India

Contents

I. Introduction

Have you ever questioned how we can comprehend what we see? Whether we are aware of it or not our brain uses the necessary knowledge to understand what is happening and saves it as information when we see some activity going around. Imagine our complete lack of response when we gaze at anything into obscurity. We have always been curious about the mechanism through which our brain decodes the visuals we view. It appears relatively simple to give machines a human brain and impulses. We frequently have a tendency to ignore the limitations of computers in comparison to our biological capacities. Even with just human intelligence, the complexity of visual perception is eternally variable and constantly changing. Our brain has the capacity to recognize the item, process the information, and make a decision, accomplishing a difficult task in a fraction of a second. The goal is to make it possible for computers to perform similar tasks. As a result, it is a research area that combines machine learning with artificial intelligence, involving the learning of algorithms and specific techniques to interpret what the computer perceives.

Back to Results | Next >

References

References is not available for this d

References

References is not available for this d

References

References is not available for this d

IET Digital Library

Intelligent Network Design Driven by Big Data Analytics, IoT, AI and Cloud Computing

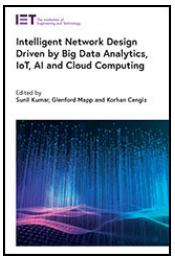

Editors: Sunil Kumar [1] ; Glenford Mapp [2] ; Korhan Cengiz [3]
View affiliations
Affiliations: 1: Amity University, India
2: Middlesex University, UK
3: Trakya University, Turkey
Publication Year: 2022

Description

As enterprise access networks evolve with a larger number of mobile users, a wide range of devices and new cloud-based applications, managing user performance on an end-to-end basis has become rather challenging. Recent advances in big data network analytics combined with AI and cloud computing are being leveraged to tackle this growing problem. AI is becoming further integrated with software that manage networks, storage, and can compute.

This edited book focuses on how new network analytics, IoTs and Cloud Computing platforms are being used to ingest, analyse and correlate a myriad of big data across the entire network stack in order to increase quality of service and quality of experience (QoS/QoE) and to improve network performance. From big data and AI analytical techniques for handling the huge amount of data generated by IoT devices, the authors cover cloud storage optimization, the design of next generation access protocols and internet architecture, fault tolerance and reliability in intelligent networks, and discuss a range of emerging applications.

This book will be useful to researchers, scientists, engineers, professionals, advanced students and faculty members in ICTs, data science, networking, AI, machine learning and sensing. It will also be of interest to professionals in data science, AI, cloud and IoT start-up companies, as well as developers and designers.

Book DOI: 10.1049/PBPC054E
Chapter DOI: 10.1049/PBPC054E
ISBN: 9781839535338
e-ISBN: 9781839535345
Page count: 427
Format: PDF

Related content

No related content was found for this content

As enterprise access networks evolve with more mobile users, diverse devices and cloud-based applications, managing user performance on an end-to-end basis has become next to impossible. Recent advances in big data network analytics, combined with AI and cloud computing are being leveraged to tackle this growing problem. The book focuses on how new network analytics platforms are being used to ingest, analyze and correlate a myriad of infrastructure data across the entire network stack with the goal of finding and fixing the quality of service network performance problems.

This book presents new upcoming technologies in the field of networking and telecommunication. It addresses major new technological developments and reflects on industry needs, current research trends and future directions. The authors focus on the development of AI-powered mechanisms for future wireless networking applications and architectures which will lead to more performant, resilient and valuable ecosystems and automated services. The book is a primary readership and is a "must-read" for researchers, academicians, engineers and scientists involved in the design and development of protocols and AI applications for wireless communication devices and wireless networking technologies.

All chapters presented here are the product of extensive field research involving applications and techniques related to data analysis in general, and to big data, AI, IoT and network technologies in particular.

- **2 Role of automation, Big Data, AI, ML IBN, and cloud computing in intelligent networks**

p. 13 –33 (21)

There are more smart devices in our world today than individuals. A growing number of people are linked to the Internet 24 hours a day, in some form or another. A growing number of people own three, four, or more smart devices and rely on them. Smartphones, fitness and health trackers, e-readers, and tablets are just a few examples. It is forecast that on average there will be 3.4 smart devices or connections for every person on earth. The Internet of Things (IoT) is relevant to many industries. IoT systems contribute to the environmental controls, retail, transportation, healthcare, and agriculture industries among many others. According to Statista, the number of IoT devices that are in use across all relevant industries is forecast to grow to more than 8 billion by 2030. As for consumers, important growth areas are the Internet and digital media devices, which include smartphones. This area is also predicted to grow to more than 8 billion by 2030. Other applications with more than 1 million connected devices are connected and autonomous vehicles, IT infrastructure, asset management, and electric utility smart grid.

All of this is made possible through intelligent networks. The planet is rapidly becoming covered in networks that allow digital devices to communicate and interconnect. Consider the network mesh as a digital skin that surrounds the earth. Mobile devices, electronic sensors, electronic measuring equipment, medical gadgets, and gauges can all link with this digital skin. They keep track of, communicate with, analyze, and, in some situations, automatically adjust to the data collected and transmitted.

- **3 An intelligent verification management approach for efficient VLSI computing system**

p. 35 –60 (26)

Any masterpiece is conjoined with all works of engineering, which includes the field of computer science or an electrical and electronics or mixture of both computer and electronics. Today, this gives the industry to understand research, evolve and develop into newer technology unfolding many scriptures behind the engineering works. In the similar manner, this chapter unfolds the prominent works involved in the verification of the designs involved in VLSI domain. Considering machine learning (ML), neural networks and artificial intelligence (AI) concepts and applying these to a wide range of verification approaches are quite interesting. The specific kinds of Register Transfer

Level (RTL) design require rigorous verification which is targeted over any type of Field Programmable Gate Array (FPGA) or application-specific integrated circuits (ASICs). The verification process should be closed with testing all possible scenarios that too with intelligent verification methods. This chapter in the following pages brings the unique way of verification procedure involved in the RTL development methodologies using hardware description languages. With the help of system Verilog language, the developed reusable testbench is used for verification. The injected inputs to the testbench are randomized with constraints, such that the design should produce accurate output. To unify the verification language, there is a dedicated methodology commonly known as Universal Verification Methodology (UVM); by this, the chapter is extended to experience the readers also through the coverage-based formal verification. For continuous functional verification, an intelligent regression model is also developed with the help of ML and scripting. With this repeated injection of various test cases is possible in order to verify the functionality. Thus, with the adoption of the presented verification environment and distinctive approach, one can affirm that the design is ready to be deployed over the targeted semiconductor chips. As the verification is an unignorable procedure, this can be used to classify the algorithms developed in ML for data clustering, data encoding and its accurate analysis. More importantly, this chapter allows us to understand an intelligent verification model for testing the design with regression run with the corresponding set-up and the pass/failure analysis steps. This structure may result in a significant reduction of the simulation time for a VLSI verification engineer.

- **4 Evaluation of machine learning algorithms on academic big dataset by using feature selection techniques**

p. 61 –91 (31)

Identifying the most accurate methods for forecasting students' academic achievement is the focus of this research. Globally, all educational institutions are concerned about student attrition. The goal of all educational institutions is to increase the student's retention and graduation rates and this is only possible if at-risk students are identified early. Due to inherent classifier constraints and the incorporation of fewer student features, most commonly used prediction models are inefficient and incur. Different data mining algorithms like classification, clustering, regression, and association rule mining are used to uncover hidden patterns and relevant information in student performance big datasets in academics. Naïve Bayes, random forest, decision tree, multilayer perceptron (MLP), decision table (DT), JRip, and logistic regression (LR) are some of the data mining techniques that can be applied. A student's academic performance big dataset comprises many features, none of which are relevant or play a significant role in the mining process. So, features with a variance close to 0 are removed from the student's academic performance big dataset because they have no impact on the mining process. To determine the influence of various attributes on the class level, various feature selection (FS) techniques such as the correlation attribute evaluator (CAE), information gain attribute evaluator (IGAE), and gain ratio attribute evaluator (GRAE) are utilized. In this study, authors have investigated the performance of various data mining algorithms on the big dataset, as well as the effectiveness of various FS techniques. In conclusion, each classification algorithm that is built with some FS methods improves the performance of the classification algorithms in their overall predictive performance.

- **5 Accurate management and progression of Big Data Analysis**

p. 93 –114 (22)

Statistical investigations are concerned with circumstances including arranging, information assortment, association of data, and scrutiny of compiled data, conversion, and exposure in a clear and chosen procedure. To do so, research techniques can be distinguished in two different ways: conclusion overviews and statistical surveying. In

assessments of public sentiment, the primary objective is to assemble data about deciding subjects dependent on close-to-home meetings. Statistical surveying is directed through the market investigation of a specific item. Descriptive statistics are responsible for collection, association, depiction of information, estimation, and translation of coefficients, whereas inductive or inferential statistics, also known as the proportion of vulnerability or techniques that rely on likelihood hypothesis, are responsible for investigation and understanding of information related to an edge of vulnerability. In statistics, we look at how to use tables and charts. The tables organise and classify the data, while the graphics convey the information in a clear and easy manner, aiding in goal attainment.

- **6 Cram on data recovery and backup cloud computing techniques**

p. 115 –134 (20)

The present digital world technology is evolving at a rapid pace. To store, manage and protect the digital information, it is necessary to back up and recover the data with utmost efficiency. As a solution, cloud computing that offers customers a wide range of services can be used. Storage-as-a-Service (SaaS) is one of the cloud platform's services, in which a large volume of digital data is maintained in the cloud database. Enterprise's most sensitive data are stored in the cloud, ensuring that it is secure and accessible at all times and from all locations. At times, information may become unavailable due to natural disasters such as windstorms, rainfall, earthquakes, or any technical fault and accidental deletion. To ensure data security and availability under such circumstances, it is vital to have a good understanding of the data backup and recovery strategies. This chapter examines a variety of cloud computing backup and recovery techniques.

- **7 An adaptive software-defined networking (SDN) for load balancing in cloud computing**

p. 135 –157 (23)

The Internet of Things can be perceived as a collection of millions of devices that are connected among each other and with the internet as a connectivity backbone to acquire and share real-time data for providing intelligent services. The tremendous rise in the number of devices requires an adequate network infrastructure to remotely deal with data orchestration. To overcome this issue, a new approach of infrastructure sharing over the cloud among service providers has transpired, with the goal of lowering excessive infrastructure deployment costs. The software-defined networking (SDN) is a networking architecture that enables network operators and users to monitor and manage the network devices remotely and more flexibly by using software that runs on external servers. As SDN and cloud integration improves reliability, scalability, and manageability, this chapter combines cloud infrastructure with SDN. Although SDN-based cloud networks have numerous advantages as mentioned above, there still exist certain challenges that draw the attention of researchers like energy efficiency, security, load balancing, and so on. The work carried out in this chapter is an attempt to address one of the challenging tasks, namely the load balancing, by developing a new multiple-controller load-balancing strategy. The proposed strategy effectively balances the load even if one or more super controllers fail. Furthermore, results are simulated and compared under different operational environments, both with and without the Modified Bully algorithm. The comparison results ensure that the introduced technique exhibits better performance with metrics such as packet loss, packet transmission ratio, and throughput.

- **8 Emerging security challenges in cloud computing: an insight**

p. 159 –183 (25)

Cloud computing has been evolved as a new computing prototype with the aim of providing reliability, quality of service and cost-effective with no location barrier. More massive databases and applications are relocated to an immense centralized data center known as the cloud. Cloud computing has enormous benefits of no need to purchase physical space from a separate vendor instead of using the cloud, but these benefits have security threats. The resource virtualization, the data and the machine are physically absent in the cloud; the storage of data in the cloud causes security issues. An unauthorized person can penetrate through the cloud security and can cause data manipulation, data loss or theft might take place. This chapter has described cloud computing and various security issues and challenges that are present in different cloud models and cloud environment. It also gives an idea of different threat management techniques available to encounter security issues and challenges. The RSA algorithm implementation has been described in detail, and the Advance Encryption Standard policy, along with its implementation, has also been discussed. For better clarification, several reviews are conducted on the existing models.

- **9 Factors responsible and phases of speaker recognition system**

p. 185 –211 (27)

The method of identifying a speaker based on his or her speech is known as automatic speaker recognition. Speaker/voice recognition is a biometric sensory device that recognizes people by their voices. Most speaker recognition systems nowadays are focused on spectral information, which means they use spectral information derived from speech signal segments of 10-30 ms in length. However, if the received speech signal contains some noise, the cepstral-based system's output suffers. The primary goal of the study is to see the various factors responsible for improved performance of the speaker recognition systems by modeling prosodic features, and phases of speaker recognition system. Furthermore, in the presence of background noise, the analysis focused on a text-independent speaker recognition system.

- **10 IoT-based water quality assessment using fuzzy logic controller**

p. 213 –233 (21)

Water is an essential resource that we use in our daily life. The standard of the water quality must be observed in real time to make sure that we obtain a secured and clean supply of water to our residential areas. A water quality-monitoring and decision-making system (WQMDMS) is implemented for this purpose based on Internet of Things (IoT) and fuzzy logic to decide the usage of water (drinking or tap water) in a common water tank system. The physical and chemical properties of data are obtained through continuous monitoring of sensors. The work describes in detail the design of a fuzzy logic controller (FLC) for a water quality measurement system, to determine the quality of water by decision-making, and accordingly, the usage of water is decided. The WQMDM system measures the physico-chemical characteristics of water like pH, turbidity, and temperature by the use of corresponding analog and digital sensors. The values of the parameters obtained are used to detect the presence of water contaminants and accordingly, the quality of water is determined. The measurements from the sensor are handled and processed by ESP32, and these refined values follow the rules determined by the fuzzy inference system (FIS). The output highlights the water quality that is categorized as very poor, poor, average, and good. The usage of the water will be determined by the results obtained using the FLC and as per the percentage of water quality, the water is decided as drinking water or tap water.

- **11 Design and analysis of wireless sensor network for intelligent transportation and industry automation**

p. 235 –255 (21)

This work is based on the wireless sensor networks (WSN), which contain an insufficient number of device nodes, regularly similarly stated nodes or sensors, and sensor knots that are associated with all other wireless communications. There are numerous assumptions or overall possessions of WSNs, and a lot more applications of WSNs around the creation are presented, making it unbearable to protect all their application areas. Applications of WSNs span ecological and animal monitoring, factory and manufacturing monitoring, farming monitoring and mechanization, healthiness monitoring, and many other areas. One of the most characteristics of WSNs is that they are strongly coupled with their application. In this chapter, WI-MAX without wormhole attack is explained, and the related results are explained with their outputs The NS2 evaluation system is applied to production out of all imitations.

- **12 A review of edge computing in healthcare Internet of things: theories, practices and challenges**

p. 257 –278 (22)

The pandemic has forced industries to move immediately their critical workload to the cloud in order to ensure continuous functioning. As cloud computing expansions pace and organisations strive for methods to increase their network, agility and storage, edge computing has shown to be the best alternative. The healthcare business has a long history of collaborating with cutting-edge information technology, and the Internet of Things (IoT) is no exception. Researchers are still looking for substantial methods to collect, view, process, and analyse data that can signify a quantitative revolution in healthcare as devices become more convenient, and smaller data becomes larger. To provide real-time analytics, healthcare organisations frequently deploy cloud technology as the storage layer between system and insight. Edge computing, also known as fog computing, allows computers to perform important analyses without having to go through the time-consuming cloud storage process. For this form of processing, speed is key, and it may be crucial in constructing a healthcare IoT that is useful for patient interaction, inpatient treatment, population health management and remote monitoring. We present a thorough overview to highlight the most recent trends in fog computing activities related to the IoT in healthcare. Other perspectives on the edge computing domain are also offered, such as styles of application support, techniques and resources. Finally, necessity of edge computing in the era of Covid-19 pandemic is addressed.

- **13 Image Processing for medical images on the basis of intelligence and biocomputing**

p. 279 –302 (24)

Intelligence in medical imaging explores how intelligent computing can create a large amount of changes to existing technology in the field of medical image processing. The book presents various algorithms, techniques, and models for integrating medical image processing with artificial intelligence (AI) and biocomputing. Bioinformatics solutions lead to an effective method for processing the image data for the purpose of retrieving the information of interest and collecting various data sources for extracting the knowledge. Moreover, image processing methods and techniques help scientists and physicians in the medical field with diagnosis and therapies. It describes evolutionary optimization techniques, support vector machines (SVMs), fuzzy logic, a Bayesian probabilistic framework, a reinforcement learning-based multistage image segmentation algorithm, and a machine learning (ML) approach. It discusses how these techniques are used for image classification, image formation, image visualization, image analysis, image management, and image enhancement. The term "medical image processing" illustrates the provision of digital image processing, particularly for medicine. Medical imaging intends to identify internal structures hidden in the human body. It helps to find abnormalities in the body. Digital images can be

processed effectively, also evaluated, and utilized in many circumstances concurrently with help of suitable communication protocols.

- **14 IoT-based architecture for smart health-care systems**

p. 303 –327 (25)

Internet of Things (IoT) provides a pathway for connecting physical entities with digital entities using devices and communication technologies. The rapid growth of IoT in recent days has made a significant influence in many fields. Healthcare is one of those fields which will be hugely benefited by IoT. IoT can resolve many challenges faced by patients and doctors in healthcare. Smart health-care applications allow the doctor to monitor the patient's health state without human intervention. Sensors collect and send the data from the patient. Recorded data are stored in a database that enables medical experts to analyze those data. Any abnormal change in the status of the patient can be notified to the doctor. This chapter aims to study different research works made on IoT-based health-care systems that are implemented using basic development boards. Various hardware parameters of health-care systems and sensors used for those parameters are explored. A basic Arduino-based health-care application is proposed using sensors and global system for mobile communication (GSM) module.

- **15 IoT-based heart disease prediction system**

p. 329 –355 (27)

In India, almost 80% of patients who die from heart disease do not receive adequate care. This is a challenging task for doctors because they often seem unable to make an accurate diagnosis. This condition is extremely expensive to treat. The proposed solution uses data mining technologies to simplify the decision support system in order to increase the cost-effectiveness of therapy. To oversee their patients' care, most hospitals use a hospital management system. Unfortunately, many of these tools do not employ large amounts of clinical data to derive useful information. Because these systems generate a considerable amount of data in many embodiments, the data is rarely accessed and remains unusable. As a result, making sensible selections requires a lot of effort during this procedure. The process of diagnosing a disease currently entails identifying the disease's numerous symptoms and characteristics. This research employs a number of data mining approaches to assist with medical diagnostics.

- **16 DIAIF: Detection of Interest Flooding using Artificial Intelligence-based Framework in NDN android**

p. 357 –370 (14)

In today's world, information-centric networking (ICN) is a brand-new next-generation network for distributing multimedia content. ICN focuses on sharing content across the network rather than obtaining content from a single fixed server [1]. In-network caching aids in the dissemination of content from the network, and the ICN also includes a number of intrusive security mechanisms. Despite the ICN network's many security measures, several attacks, especially interest flooding attacks (IFA), continue to wreak havoc on the network's distribution capability. In order to address security threats, the literature includes a number of mitigating procedures. However, legitimate users' requests are misclassified as an attack in an emergency circumstance, affecting the network's QoS [2]. In this chapter, Detection of Interest Flooding Attack using Artificial Intelligence Framework (DIAIF) is proposed in ICN. DIAIF seeks to lighten the load on ICN routers by removing the source of the attack without interfering with legitimate user requests. DIAIF depends on router feedback to assign a beneficial value (BV) to each piece of content and to block dangerous users based on the BV. The ICN testbed

was designed to assess the proposed DIAIF's performance in terms of QoS during severe flood scenarios, responding with malicious content without interfering with genuine user requests, and identifying the source of attack in a communication scenario.

- **17 Intelligent and cost-effective mechanism for monitoring road quality using machine learning**

p. 371 –396 (26)

Nowadays, one of the most significant components of road infrastructure is monitoring road surface conditions, which leads to better driving conditions and reduces the chance of a road accident. Traditional road condition monitoring systems are incapable of gathering real-time information concerning road conditions. In previous generations, road surface condition monitoring was done for fixed roadways and vehicles travelling at a constant pace. Several systems have presented a method for exploiting the sensors installed in automobiles. However, this method will not assist in forecasting the precise placement of potholes, speed bumps, or staggered roads.

As a result, smartphone-based road condition evaluation and navigation are becoming increasingly popular. We propose exploring several machine learning techniques to accurately assess road conditions using accelerometer, gyroscope, and Global Positioning System (GPS) data collected from cellphones. We also recorded footage of the roadways in order to reduce noise in the data. This two-pronged approach to data collection will aid in the exact positioning of potholes, speed bumps, and staggered roads. This method of data collection will aid in the classification of road conditions into numerous features such as roads with smooth surfaces, potholes, speed bumps and staggered highways using machine learning algorithms. machine learning algorithms are used to create characteristics such as smooth roads, potholes, speed breakers, and staggered highways. The user will receive this information via the map, which will classify the various road conditions. Accelerometers and gyroscope sensors will analyze multiple features from all three axes of the sensors in order to produce a more precise location of designated routes. To classify the road conditions, we investigate the performance utilizing support vector machine (SVM), random forest, neural network and deep neural network. As a result, our findings demonstrate that models trained using a dual data gathering strategy will produce more accurate outcomes. Data classification will be substantially more accurate when neural networks, are used. The methods described here can be used on a broader scale to monitor roads for problems that pose a safety concern to commuters and to give maintenance data to appropriate authorities.

- **18 Conclusion**

p. 397 –399 (3)

This book presented applications, technologies, challenges, and implementation design models of intelligent networks design by Big Data, Internet of Things, artificial intelligence (AI), and cloud computing approaches in different sectors. Research into real-time fault tolerance, security, and data analytics by addressing significant data volume and velocity measurement are essential in intelligent networks, for example, where different analytical models and AI and machine learning algorithms improve end-to-end performance, efficiency, and quality of service (QoS) [1-10].

The availability of Big Data, AI, cloud computing, low-cost commodity hardware, and new information management and analytic software has produced a unique moment in the history of intelligent networks [11-21]. The convergence of these trends means that we have the capabilities required to analyze unique data sets quickly and cost-effectively. They represent a genuine leap forward and a clear opportunity to realize enormous efficiency, productivity, revenue, and profitability.

This book also discussed issues and challenges that can be addressed and overcome in the future using the new upcoming technologies. The age of intelligent networks is here, and these are truly revolutionary times if business and technology professionals continue to work together and deliver on the promise.

Thank you for taking the time to read this book, and we hope you enjoyed reading it as much as we did write it.

- **Back Matter**

p. (1)

Comparative Analysis of Normal Washroom Vs. IoT-Based WPS Washroom

Prachi Gawande ; Yogesh Kale ; Prachi Dabhade All Authors

Abstract: In this 21 st -century water and electricity waste is the major problem in commercial/common washrooms this wastage is more as there is maximum use and the handling of st... **View more**

▸ **Metadata**

Abstract:

In this 21 st -century water and electricity waste is the major problem in commercial/common washrooms this wastage is more as there is maximum use and the handling of style is different for different people. If any user kept water taps, toilet flush, light switch, or exhaust fan switch ON then it will waste water as well as electricity. It can be overcome by using IoT-based water power savers. IoT is the next generation technology, it has interconnected the physical and digital world. In this IoT-based WPS presence of a human being is detected, and according to that it will activate the microwave sensor and the electromagnetic valve, light, and exhaust fan will get ON. Lights, fans, washbasin tap, and toilet flush won't operate in the absence of a human in the washroom.

Published in: 2022 International Conference on Emerging Trends in Engineering and Medical Sciences (ICETEMS)

Date of Conference: 18-19 November 2022

INSPEC Accession Number: 22932632

Date Added to IEEE *Xplore*: 11 April 2023

DOI: 10.1109/ICETEMS56252.2022.10093610

▸ **ISBN Information:**

Publisher: IEEE

Conference Location: Nagpur, India

I. Introduction

In commercial washrooms the water and electricity consumption is far worse it's around 10-151trs/person. It's a study by the WHO regional office of south-East Asia. Our society pebbledash outrageous water usage for both purposes local as well as commercial and it is a major concern, it not also distresses the sustainability of nature. Water used by people for toilet flushing is 30 ltrs, for other work nearly 100ltrs [1]. It is useful but the wastage is more than usage. Low maintenance of commercial toilets is also one of the problems of wastage. A leaking toilet for example can waste nearly 400 liters of water per day. Dripping taps are even worse and one of the least resolved causes of water wastage in both commercial and domestic locations with as per the use of water, toilet flush uses more in commercial washrooms, they are ON for 24×7, which causes electricity wastage. Water is very important and there is amajor need to save water wastage. For water and electricity waste reduction, we must use technology and intelligence, i.e., IoT-based washrooms. In IoT-based washrooms, water supply and unnecessary use of electricity are controlled [2]. It is done with the WPS (water power saver) and sensors. Applying a 12 V power supply as the user enters the washroom, a microwave sensor for human detection will activate and it will ON the electromagnetic valve, exhaust fan& Lights [3].

References

References is not available for this d

Authors

Figures

References

Keywords

Metrics

Back to Results

References

References is not available for this d

References

References is not available for this d

Quality Assessment Method for Image Inpainting

Shweta Dhondse ; Milind Mushrif All Authors

Abstract: A comprehensive study of types of quality assessment methods used for inpainted images is presented in this paper. Both quantitative and qualitative measures are studied ... **View more**

Abstract:
A comprehensive study of types of quality assessment methods used for inpainted images is presented in this paper. Both quantitative and qualitative measures are studied in detail. The process of inpainting can be compared to blind convolution problem. Therefore, a quality assessment metric with no reference is discussed for assessing the inpainted image quality quantitatively. The objective assessment of inpainted image is done by Degree of Noticeability and Average Squared Visual Salience score. It is observed that the objective score does not always match with the human perception and hence subjective analysis is proposed on the basis of observer score.

Published in: 2022 International Conference on Emerging Trends in Engineering and Medical Sciences (ICETEMS)

Date of Conference: 18-19 November 2022

INSPEC Accession Number: 22932643

Date Added to IEEE *Xplore*: 11 April 2023

DOI: 10.1109/ICETEMS56252.2022.10093282

▸ **ISBN Information:**

Publisher: IEEE

Conference Location: Nagpur, India

Contents

Image quality assessment is referred as the problem of evaluating the perceptual image quality level. Several methods are proposed in [1], [2], [3], [4], [5], [7], [8] to predict the image quality. The goal of quality assessment of inpainted image is to evaluate that the restored image is visually pleasing. The method of inpainting can be thought of as a specialised picture restoration challenge that cannot be applied to all images. Because of this specific nature of the problem of inpainting the Image Inpainting quality assessment (IIQA) methods cannot be directly applied. In case of object removal and reconstruction which include large areas, the reconstructed region may be completely different than the original one because of ill construction of structures or amount of occlusion. The goal of the Image Inpainting Quality Assessment (IIQA) measure is to assess whether the inpainted regions are visually pleasing with respect to spatial coherence of the existing parts of the image.

Authors
Figures
References
Keywords
Metrics

Back to Results | Next >

References

References is not available for this d

References

References is not available for this d

Change Detection of Vegetation by Satellite Image Analysis

Nita Nimbarte ; Prathamesh Sayam ; Sanjay Balamwar All Authors

Abstract: Image analysis has been said to be an efficient approach for research in a broad variety of subjects as well as application agriculture. Its importance will be that it se... **View more**

▸ **Metadata**

Abstract:

[redacted]iety of subjects as well as application agriculture. Its importance will be that it serves as a crucial venture across many countries economies. The age of remote sensing has arrived as a critical function in research of the earth for the detection of vegetation. Plant life estimation is vital for everyone and all farmers and agricultural organizations strive to classify plant life profitably because faroff sensing images are used as input for agricultural applications. Identifying vegetative places using remotely sensed images is critical and monetary making plans via means of authorities and non-public agencies. The technique for these paintings is the choice of satellite TV for photographs, the detection of plant life, and the usage of a suitable category method. Although it can capture the land surface features in a vast territory quickly and simultaneously, surveying is indeed the key source for information extraction. It identifies the changes from images taken at different times in the same area using ERDAS software. This work consists of supervised category strategies like the minimal distance category and most probability category. This work affords a precise example of how those category strategies may be used to pick out plant life through the usage of photograph processing.

Published in: 2022 International Conference on Emerging Trends in Engineering and Medical Sciences (ICETEMS)

Date of Conference: 18-19 November 2022

INSPEC Accession Number: 22932676

Date Added to IEEE *Xplore*: 11 April 2023

DOI: 10.1109/ICETEMS56252.2022.10093368

▸ **ISBN Information:**

Publisher: IEEE

Conference Location: Nagpur, India

Contents

I. Introduction

In recent decades, many developing regions have seen a growth in urbanization. Where agriculture on the globe meets limitations and obstacles in agricultural production via the building of guidelines which involve technology, regulations, and institutions, a crucial consideration is given to obstructions to productive production. In most regions, vegetation output is seen as one of the most essential aspects of environmental protection and increasing requirements through sustainable agriculture, forestry, and land use to start producing more food and resources to meet growth demands. Additionally, agriculture is regarded as among the most important natural resources in the dry parts of the world It is regarded as one of the key sources of livelihood in many nations, resulting in severe environmental situations and features in the dry lands and semi-arid regions. Agriculture is seen as a fundamental pillar of all regions' economic and social growth. Agriculture has begun to play a vital part in environmental conservation, biodiversity protection, and preserving an environmental balance that aids in ensuring sustainable resource use and preservation for future generations during the last three decades. Accuracy farming is an important agricultural systematic methodology that can alleviate agricultural challenges and problems while also contributing to increased output by applying correct information about agricultural resources. Accuracy farming uses a variety of technologies. Remote sensing, Geographical Information Systems (GIS), the Global Positioning System (GPS), yield and vegetation change detection and monitoring, crop growth models, and variable rate application are among them. Remote sensing must monitor particular phenomena and analyse land coverings using precise methods, as well as track crop conditions and changes. The proportion of vegetation is calculated using the spectral reflectance of various plant coverings from satellite data and vegetation indices such as the Normalized Difference Vegetation Index (NDVI) [1–2]. The percentage of plant cover is utilized as a criterion to estimate the vegetation cover, which was assessed by digitizing and visiting locations, with satellite photos also being used for large regions the monthly removal of vegetation, which relates to the state of degrading in dry lands and semi-arid regions geographically. Generally, the major goal of this research is to use satellite image data in an infrared band for the detection of vegetation cover and analysis between Pauni, Bhandara, and certain Nagpur regions from October 2019 to March 2022. The vegetation cover of green vegetation in the research region refers to forests that are concerned about environmental sustainability.

Authors
Figures
References
Keywords
Metrics

References

References is not available for this d

< Previous | Back to Results | Next >

More Like This

Agriculture change detection model using remote sensing images and GIS: Study area Vellore
2012 International Conference on Radar, Communication and Computing (ICRCC)
Published: 2012

Feature extraction algorithm for estimation of agriculture acreage from remote sensing images
2016 World Conference on Futuristic Trends in Research and Innovation for Social Welfare (Startup Conclave)
Published: 2016

References

References is not available for this d

Show More

References

References is not available for this d

Rectangular Patch Antenna with EC Slot and Stubs for emerging wireless Applications

Ketki Kotpalliwar ; Sachin S Khade ; Chitra V. Bawankar ; P.L. Zade ; Diksha Ninawe All Authors

Abstract: The proposed antenna is designed for Wi-Fi, Wi- Max, 5G and WLAN applications. The antenna operated over the bandwidth starting from 4.16 GHz to 5.46 GHz. The dimension o... **View more**

Abstract:

The proposed antenna is designed for Wi-Fi, Wi- Max, 5G and WLAN applications. The antenna operated over the bandwidth starting from 4.16 GHz to 5.46 GHz. The dimension of the antenna is 15 mm x23 mm x1.6 mm. There are two stubs that are identical with produced capacitive effect and also used for impedance matching. The insertion of E and C slots resulted in shifting of band to desired range. The Gain of proposed antenna ranges from 1.884 dB to 2.358 dB in all the bands with maximum efficiency of 90.5%. The proposed antenna is suitable for n77 and n79 5G application bands, 4.9 GHz WLAN band, 5, 5.15 and 5.45 GHz Wi-Fi and Wi-Max bands.

Published in: 2022 International Conference on Emerging Trends in Engineering and Medical Sciences (ICETEMS)

Date of Conference: 18-19 November 2022

INSPEC Accession Number: 22932668

Date Added to IEEE *Xplore*: 11 April 2023

DOI: 10.1109/ICETEMS56252.2022.10093388

▸ **ISBN Information:**

Publisher: IEEE

Conference Location: Nagpur, India

I. Introduction

Designing a wideband Microstrip patch antenna with small dimensions and a partial ground is a major challenge [1]. The design of a patch antenna with two identical stubs [2] and a feed line with a discrete port, placed at the center on the edge of feed line with partial ground. By incorporating some changes the desired results and performance improvement is achieved [3].

References

References is not available for this d

Authors

Figures

References

Citations

Keywords

Metrics

Back to Results

References

References is not available for this d

References

References is not available for this d

4 Bit and 8 Bit Convolution Using Vedic Multiplier

Rahul Kamdi ; Prasheel Thakre ; Aniket Pathade ; Sandeep Kumar Tiwari ; Kamlesh Kalbande All Authors

Abstract: One of the fundamental processes in digital signal processing is convolution. The mathematical process of mixing two signals to create a third signal is called convolutio... **View more**

Abstract:
One of the fundamental processes in digital signal processing is convolution. The mathematical process of mixing two signals to create a third signal is called convolution. Utilizing a Vedic multiplier, Urdhava Triyagbhyam Sutra or UT sutra, based on one of the sixteen Vedic mathematics sutras, linear and circular convolution processing is accelerated. The Urdhava Triyagbhyam multiplier compared to other traditional multipliers offers faster results. Multiplier having pipelining architecture is also used to compute the convolution (circular and linear) of two sequences because it speeds up the multiplication process. Xilinx ISE Design suite 14.7 software is used to carry out the simulation and synthesis using VHDL. The area and delay for 4 bit and 8 bit circular and linear convolution is computed.

Published in: 2022 International Conference on Emerging Trends in Engineering and Medical Sciences (ICETEMS)

Date of Conference: 18-19 November 2022

INSPEC Accession Number: 22932616

Date Added to IEEE *Xplore*: 11 April 2023

DOI: 10.1109/ICETEMS56252.2022.10093621

▸ **ISBN Information:**

Publisher: IEEE

Conference Location: Nagpur, India

I. Introduction

The idea is first introduced in the Vedas and is known as Vedic Mathematics. It has various methods/sutras for quickly and easily resolving mathematical problems. It is made up of 16 Sutras and 13 Sub-Sutras [1–2] and may be used to solve issues in geometry, calculus, algebra, and other sections. Application of Vedic mathematics sutras, especially in the area of VLSI design, can result in advancement of current technology. In the recent past, signal processing has been crucial to VLSI design. Power, area, and latency are crucial factors to take into account while designing VLSI. Digital signal processing always involves the time-consuming task of multiplying, which lowers the DSP chip's quality.

Authors
Figures
References
Keywords
Metrics

Back to Results | Next >

References

References is not available for this d

References

References is not available for this d

Empirical Analysis of Predictive Models For Insurance Claim Classification

Ankit Harale ; Yogita Dubey ; Vikas Gupta ; Abhijeet Motghare ; Megha Chakole ; Aniket Pathade All Authors

Abstract: In this paper, a framework is proposed to assist in predicting the health insurance claim. Several theories have demonstrated that health insurance claim prediction may b... **View more**

Abstract:
In this paper, a framework is proposed to assist in predicting the health insurance claim. Several theories have demonstrated that health insurance claim prediction may be used to estimate the expenses using machine learning algorithms, which a company must incorporate in the early financial budget. Six machine learning models are suggested and analyzed to create the ideal model that will properly forecast claims and lower the cost to the organization.

Published in: 2022 International Conference on Emerging Trends in Engineering and Medical Sciences (ICETEMS)

Date of Conference: 18-19 November 2022

INSPEC Accession Number: 22932646

Date Added to IEEE *Xplore*: 11 April 2023

DOI: 10.1109/ICETEMS56252.2022.10093335

▸ **ISBN Information:**

Publisher: IEEE

Conference Location: Nagpur, India

Contents

In this study, model for predicting whether an insurance claim will be filed or not is proposed by applying various machine learning techniques to the data. Some of the features including age, sex, body mass index, steps, children, smokers, regions, and costs. These features must be trained and tested in order to create the model and determine the evaluation parameter [1].

References

References is not available for this d

Authors

Figures

References

Keywords

Metrics

Back to Results

References

References is not available for this d

References

References is not available for this d

Framework for Alzheimer Diseases Classification using Machine Learning Algorithms

Pushkar Wankhede ; Nandini Sakhare ; Yogita Dubey ; Manu Varghese ; Shrutika Gawande ; Manoj Patil All Authors

Abstract: At Least 50 million people in the world are assumed to have Alzheimer Disease (AD). Hence early diagnosis as well as early dose of memantine is required to inhibit furthe... **View more**

Abstract:

At least 50 million people in the world are assumed to have Alzheimer Disease (AD). Hence early diagnosis as well as early dose of memantine is required to inhibit further increase of this disease. In this paper a framework is proposed for classification of Alzheimer using five different Machine Learning models. Dataset is taken from Kaggle website after that Data preprocessing takes place. Five different models viz. Logistic Regression, Support Vector Machine, Random Forest, Decision Tree and Gradient Boosting Classifier are compared using various evaluation metrics such as Accuracy, Precision, Recall, Log loss and AUC-ROC.

Published in: 2022 International Conference on Emerging Trends in Engineering and Medical Sciences (ICETEMS)

Date of Conference: 18-19 November 2022

INSPEC Accession Number: 22932663

Date Added to IEEE *Xplore*: 11 April 2023

DOI: 10.1109/ICETEMS56252.2022.10093641

▸ **ISBN Information:**

Publisher: IEEE

Conference Location: Nagpur, India

I. Introduction

Alzheimer Disease (AD) is one of the most dangerous diseases in the world. It starts slowly and progressively the condition of the patient becomes worse. Looking at the survey within the healthcare domain, machine learning is widely used for addressing the analysis of Alzheimer's diseases. The structural MRI is utilized for the detection of this disorder. [1] [2] [3]. It is observed that in the last few decades, considerable works about mind feature research had been accomplished with the aid of the use of fMRI. The preliminary priority of those pieces turned into the neurophysiological foundation of the fMRI signal. [4]. The bare brain images are too enormous and loud to be presently operated on for diagnosis. To facilitate the morphological evaluation, MR mind illustration is partitioned into a pair of anatomical parts, i.e., regions of interest (ROIs), via clustering voxels through the distortion of marked atlas and then the restricted dimensions are computed as credentials for image class. Nowadays, in-depth studying strategies have won a remarkable prominence specially to extract informative characteristics for computer vision and clinical report analysis. There is likewise an expanding measure of longitudinal information gathered at the subsequent time focuses which frequently give helpful data about the neurotic movement of the infection [5]. The minimental state examinations (MMSE) and Clinical Dementia Rating (CDR) are the most usually involved strategies in the clinical Alzheimer's brain science conclusion. With the instantaneous advancement of neuroimaging innovation, neuroimaging finding turns into the most instinctive and the most solid technique for the determination of Alzheimer's illness. Among the neuroimaging techniques, magnetic resonance imaging (MRI) is normally utilized for the finding of AD. [6].

References

References is not available for this d

Authors
Figures
References
Keywords
Metrics

Back to Results | Next >

More Like This

Analyzing Suicide and Contributing Factors in Thailand Using Classification by Logistic Regression, Decision Tree and Support Vector Machine
2023 IEEE 3rd International Conference on Electronic Communications, Internet of Things and Big Data (ICEIB)
Published: 2023

Liver Disease Prediction Using Support Vector Machine and Logistic Regression Model with Combination of PCA and SMOTE
2022 1st International Conference on Technology Innovation and Its Applications (ICTIIA)
Published: 2022

Show More

References

References is not available for this d

References

References is not available for this d

Classification of Lung CT Scan Images using Machine Learning

Nivedita A. Pande ; Ritik Pusadekar ; Kajal Mitra All Authors

Abstract: Timely discovery of COVID-19 may safeguard numerous diseased people. Several such lung diseases can turn to be life threatening. Early detection of these diseases can hel... **View more**

Abstract:

such lung diseases can turn to be life threatening. Early detection of these diseases can help in treating them at an early stage before it becomes threatening. In this paper, the proposed 3D CNN model helps in classifying the CT scans as normal and abnormal, which can then be used to treat the patients after recognizing the diseases. Chest X-ray is fewer commanding in the initial phases of the sickness, while a CT scan of the chest is advantageous even formerly symptoms seem, and CT scan accurately identify the anomalous features which are recognized in images. Besides this, using the two forms of images will raise the database. This will enhance the classification accuracy. In this paper the model used is a 3D CNN model; using this model the predictions are done. The dataset used is acquired from NKP Salve Medical Institute, Nagpur. This acquired dataset is used for prediction while an open source database is used for training the CNN model. After training the model the prediction were successfully completed, with these proposed 3D CNN model total accuracy of 87.86% is achieved. This accuracy can further be increased by using larger dataset.

Published in: 2022 International Conference on Futuristic Technologies (INCOFT)

Date of Conference: 25-27 November 2022

INSPEC Accession Number: 22932966

Date Added to IEEE *Xplore*: 13 April 2023

DOI: 10.1109/INCOFT55651.2022.10094435

▸ **ISBN Information:**

Publisher: IEEE

Conference Location: Belgaum, India

Contents

I. Introduction

Lung cancer is a life threatening disease to any human. Lung cancer is the leading cause of cancer deaths worldwide. Lungs are the organs in chest that inhale the oxygen and release carbon dioxide when we breathe out. Smoking people will have the maximum threat of lung cancer. Lung cancer also has been seen in people who have not ever smoked. So, if we somehow manage to detect the cancer module early, it can be successfully treated and cured. So a cancer detection model will be used to detect the module with CT scan [1].

Authors

Figures

References

Keywords

Metrics

< Previous | Back to Results | Next >

References

References is not available for this d

References

References is not available for this d

References

References is not available for this d

Best Suitable Routing Protocol for Mobile Ad Hoc Networks

Publisher: IEEE

Abstract:A Mobile Ad Hoc Network is one kind of wireless communication networks. MANET is an unplanned network having number of versatile nodes. This node interacts with each othe... **View more**

Abstract:
A Mobile Ad Hoc Network is one kind of wireless communication networks. MANET is an unplanned network having number of versatile nodes. This node interacts with each other without any fixed infrastructure. In MANET nodes are versatile, each node act as a router and send data from source to destination. Due to dynamic topology of the MANET, it undergoes under several attacks. There are various ways to secure MANET but still several attacks are there which will slow down the performance of the network. Hence a strong cryptography technique is required to secure communication in the MANET. Network is generated using NS2 platform. AODV, DSDV, OLSR routing protocols are compared with respect to evaluating parameters like PDR, throughput. AODV is suitable for MANET. As a successful data transmission increases the throughput increase.

Published in: 2022 International Conference on Smart Generation Computing, Communication and Networking (SMART GENCON)

Date of Conference: 23-25 December 2022

Date Added to IEEE *Xplore*: 06 April 2023

ISBN Information:

INSPEC Accession Number: 22928741

DOI: 10.1109/SMARTGENCON56628.2022.10084259

Publisher: IEEE

Conference Location: Bangalore, India

Contents

I. Introduction

Ad hoc networks have tremendous demand in wireless communication. Basically it is developed for applications where huge infrastructure management is not possible. MANET is a self-organizing, distributed network. In this network multi hop routing takes place.

Sign in to Continue Reading

References

References is not available for this d

Authors

Figures

References

Keywords

Metrics

< Previous | Back to Results | Next >

References

References is not available for this d

References

References is not available for this d

Smart Bus Fleet Management System Using IoT

Sandip Desai ; Ronak Suthar ; Vikaskumar Yadav ; Vaishnavi Ankar ; Vikas Gupta **All Authors**

Abstract: Resource and time management is very crucial in everyday living. To avoid economic loss, non-renewable resources, such as fuel, must be managed effectively. This problem ... **View more**

Metadata

Abstract:

ic loss, non-renewable resources, such as fuel, must be managed effectively. This problem must be addressed with a proper solution. A bus is a common method of transportation in everyday life that provides a low-cost way to go from point A to point B. But there are also some problems related to this, like often valuable time of passengers getting wasted waiting for their bus without knowing the bus's predicted arrival time and position, as well as also if we look at the management side, managing the fleet is itself a tedious task. Every bus fleet organization must assure the safety of its passengers, and a reliable and secure transportation service is required. The proposed system provides real-time data of a variety of vehicle features, including location, route, speed, passenger list, and driver compliance, schedule and more. In this system, we use the Raspberry Pi 3b+ to connect GPS, RFID, and PIR technologies to a Firebase server Cloud over WiFi. The vehicle's current geographic coordinates are determined using a Neo 6M GPS module. PIR sensor module is used to get a count of passengers in the vehicle. An RFID card Module is used to track passengers for fare calculation and with perspective of the safety and security of passengers. All the data from the used module is sent over the real-time database which we have used at firebase and the data can be accessed by the passengers, fleet manager, and the driver by using a website. A website is used to show all the data to the passengers and also to the fleet manager who is managing the bus and the drivers.

Published in: 2022 Fourth International Conference on Emerging Research in Electronics, Computer Science and Technology (ICERECT)

Date of Conference: 26-27 December 2022

INSPEC Accession Number: 22810483

Date Added to IEEE *Xplore*: 15 March 2023

DOI: 10.1109/ICERECT56837.2022.10059646

▸ ISBN Information:

Publisher: IEEE

Conference Location: Mandya, India

References

References is not available for this d

Contents

Travelling from one location to another location using public vehicle is arduous task itself. As passengers are often unaware of the bus arrival and departure timings. It is common for passenger to board the incorrect buses and disembark at the incorrect stop. The suggested system is a cost effective comprehensive bus monitoring system that tracks the bus location, the number of on board passengers, adherence to route, schedule and other bus-related data. Passengers can spend more time doing other things instead of waiting for a delayed bus. Thanks to the bus real-time tracking and notification system, which ensures each passenger, how long they have to wait for bus so that they can utilize that time properly.

Back to Results | Next >

More Like This

The Development of an Internet of Things Mobile Application for Tracking an Electric Bus in a Campus
2019 Joint International Conference on Digital Arts, Media and Technology with ECTI Northern Section Conference on Electrical, Electronics, Computer and Telecommunications Engineering (ECTI DAMT-NCON)
Published: 2019

Internet of Things-based Vehicle Tracking and Monitoring System
2021 15th International Conference on Open Source Systems and Technologies (ICOSST)
Published: 2021

Show More

References

References is not available for this d

References

References is not available for this d

Solar Powered Garden Monitoring System

Vaishali. B Niranjane ; Ashish Bhagat ; Krushil. M. Punwatkar ; Pornima Niranjane All Authors

Abstract: India is the rapid developing country with huge economic system in the world. Agriculture is main source of income of two third population of India. In today's world of d... **View more**

Metadata

Abstract:

Agriculture is main source of income of two third population of India. In today's world of digitization a person is accompanying with automation which makes the work easy and very simple. In this hectic schedule people forgot many small things such as watering the little plants in their garden on the regular basis as per necessity of plants for good and healthy growth. The main idea of our research is to adapt latest technology to provide adequate amount of water for house garden, agricultural form, municipal garden etc. In our research we developed a system that can be used instead of old watering systems of garden. In the present situation people look for automation for their daily work which makes their life more convenient. IoT is advanced technology that focuses on people comfort. In our research we combine the IoT technology with the solar power. Solar power is economical and suitable for remote areas which are not connected to energy grids. The proposed system is focuses on developing automated garden monitoring system with solar power. This system is integrated using soil sensor, moisture sensor, humidity sensor .All the data collected by the sensor are monitor and track by system using IoT technology. The module is equipped with solar power using power battery backup. Our system is the best union of IOT, solar power system and an Android mobile app. As a result, the effectiveness, monitoring, and preservation of the garden plants can all be considerably improved by this approach. Based on resource-efficient energy use, users will also be able to manage their plants' health and growth with the least amount of human intervention.

Published in: 2022 Seventh International Conference on Parallel, Distributed and Grid Computing (PDGC)

Date of Conference: 25-27 November 2022

INSPEC Accession Number: 22723960

Date Added to IEEE *Xplore*: 01 March 2023

DOI: 10.1109/PDGC56933.2022.10053212

▸ ISBN Information:

▸ ISSN Information:

Publisher: IEEE

Conference Location: Solan, Himachal Pradesh, India

References

References is not available for this d

Contents

I. INTRODUCTION

Nowadays water crisis and energy crisis are huge issues faced by people in the world. So conservation of energy and water is today's need. To keep offices, school, institutes, government offices and houses fresh and energetic, garden systems are developed. Garden system also improves the beautifulness of the place. The lush green place keeps people happy also. Garden also reduces the pollution level and it also increases the oxygen in environment. In today's world the people need everything automated. Now A day's number of IoT applications for agriculture have been devolved .these applications are divided into categories depending on their goals, such as monitoring, tracking and traceability and production. [13] The aim of our research is to make solar based module to irrigate the garden automatically.[1] It is very helpful to the people who are busy in doing every day task and their garden being watered automatically at low cost. People won't be worried about overwatering or under watering their gardens .As well as they will not worry about wastage of water, expense of electricity uses.[2] For implementing automatic garden monitoring system using solar power, Raspberry Pi is used. Solar panel is used to give power supply to Raspberry Pi. Raspberry Pi receives the information from soil moisture sensor, Humidity, temperature and LDR sensor. [3] The data received from various sensors are processed by Raspberry Pi. This data is displayed on user interface using blink Application. If system is on Auto mode then automatically it will operate. If system is in manual mode then user have to control the system. [4]So we can operate our garden remotely.

Authors

Figures

References

Keywords

Metrics

Back to Results | Next >

More Like This

Smart Agriculture Using Internet of Things with Raspberry Pi
2020 10th IEEE International Conference on Control System, Computing and Engineering (ICCSCE)
Published: 2020

An Overview of Internet of Things (IoT) and Data Analytics in Agriculture: Benefits and Challenges
IEEE Internet of Things Journal
Published: 2018

Show More

References

References is not available for this d

References

References is not available for this d

Smart System with IoT for Water Quality Monitoring

Nivedita Pande ; Aakib Sayyad All Authors

Abstract: Nowadays Internet of Things (IoT) has found its applications in diverse fields for research and analysis of data across geographies. Because of the massive growth in glob... **View more**

Abstract:

[redacted]earch and analysis of data across geographies. Because of the massive growth in global industry, rural to urban gist and the maximum consumption of natural resources like sea, land etc., the quality of water obtainable to human beings has worsened prominently. The continuous increase in usage of chemicals and fertilizers in farming as well as industries has badly affected the water quality worldwide. Water is a essential necessity for human existence and hence there should be a mechanism to test the superiority of water that is available from the sources such as rivers, water bodies, Lake Etc. for domestic use. The accessibility of good quality water is extremely important in avoiding outbursts of water-borne diseases as well as cultivating the quality of life. The diseases are caused by low water quality [12]. Water quality monitoring and IoT can improve the existing measurement

Published in: 2022 International Conference on Augmented Intelligence and Sustainable Systems (ICAISS)

Date of Conference: 24-26 November 2022

INSPEC Accession Number: 22540318

Date Added to IEEE *Xplore*: 16 January 2023

DOI: 10.1109/ICAISS55157.2022.10011108

▸ **ISBN Information:**

Publisher: IEEE

Conference Location: Trichy, India

Contents

I. Introduction

Fresh water is a most important natural resource available on earth - it is in fact, life. It is important to all the living beings as life cannot survive and flourish without water. Currently, drinking water faces a new world problem. The water quality is significantly worsening because of growing population, urban shifting, contamination of water because of industrial use, usage of fertilizers and chemicals in farming, excess salt removal from sea water etc[14], [15].

Authors

Figures

References

Keywords

Metrics

References

References is not available for this d

< Previous | Back to Results | Next >

References

References is not available for this d

References

References is not available for this d

Machine Learning based Object Detection with Theft Alert System

Swati Nitnaware ; Ashutosh Bagde All Authors

Abstract: Object detection and tracking is popular area in computer vision. Because of its vast applications in different fields such as surveillance, tracking modules used for sec... **View more**

Metadata

Abstract:

applications in different fields such as surveillance, tracking modules used for security and many other applications. This has allowed researchers to come up with a number of enhanced and focused methods. In the presented method live input video is used where objects are detected and it can be computer-generated for real-time through additional hardware added. An enhanced and well-organized algorithm for object detection and for security is presented. It is used to identify the objects in real time this also ensures accuracy of the system. By adding some more features in it, this system is found quietuseful for keeping a record of valuablebelongings or devices. Open CV isis used here. Thisis helpful to write complex programs using C/C++ and create a Python wrapper for it. Which can be used as modules of Python.

Published in: 2022 6th International Conference on Electronics, Communication and Aerospace Technology

Date of Conference: 01-03 December 2022

INSPEC Accession Number: 22539076

Date Added to IEEE *Xplore*: 16 January 2023

DOI: 10.1109/ICECA55336.2022.10009061

ISBN Information:

Publisher: IEEE

Conference Location: Coimbatore, India

Contents

I. Introduction

Humans canidentify and locate things that make an image. With least effort, the visual system in humans can accomplish complicated tasks like identification of an object and detection of obstaclesvery fact andvery correctly. We can now quickly program computers to recognize and classify items that make an image with great accuracy. This is possible as large data, faster GPUs, and better algorithms are available. We have worked ondetection and localization of objects in an image, loss function for object detection and localization, and also the “You only look once” approach for object detection (YOLO).

References

References is not available for this d

Authors

Figures

References

Keywords

Metrics

Back to Results | Next >

References

References is not available for this d

References

References is not available for this d

Design and Analysis of Low Power Full Adder using Reversible Logic

Sujata S. Chiwande ; P.K. Dakhole All Authors

Abstract: The reversible Logic system will be effective in low power dissipation. For the optimization of power in VLSI design, number of researchers is using reversible logic regu... **View more**

Abstract:
The reversible Logic system will be effective in low power dissipation. For the optimization of power in VLSI design, number of researchers is using reversible logic regularly. In the VLSI design, the use of reversible logic has many advantages because of its high speed, and low power dissipation. This paper provides the design and comparative analysis of reversible full adder using Peres gate with conventional full adder circuits. During comparison it is found that 44% improvement in total thermal power dissipation over the conventional adder circuit. These reversible logic circuits are verified and simulated using Verilog coding, Intel Quartus Prime 20.1

Published in: 2022 6th International Conference on Electronics, Communication and Aerospace Technology

Date of Conference: 01-03 December 2022

INSPEC Accession Number: 22539043

Date Added to IEEE *Xplore*: 16 January 2023

DOI: 10.1109/ICECA55336.2022.10009431

ISBN Information:

Publisher: IEEE

Conference Location: Coimbatore, India

Contents

In reversible logic each input pattern generate different output pattern. It is denoted as N*N since it has N number of inputs and N numbers of outputs. Thus, the following can be used to signify a N x N reversible gate: and . Where I and 0 denote the i/p and o/p to the circuit. To implement a reversible circuit a basic gates are required that produces an exclusive o/p bits for each given i/p bits pattern, and vice-versa. In reversible logic we can predict the input bit from output by considering the ideal output bit and other output. The Reversible logic is used to decrease power loss and guard against information loss. Applications of reversible logic are in various fields such as low power VLSI design, optical, quantum computing, nanotechnology, QCA and continue Reading computing technologies. Decreasing power is an enchanted word that has gained significance with the increase of deep sub-micron and nanotechnologies. There are numerous Low Power design methods such as GDI, Adiabatic logic are available in literature. The Reversible Logic Design fascinates more interest due to low power and high seed application. In this logic reduction in energy dissipation is achieved without destroying the information bits. In many research papers combination of three gates FG (Feynman Gate), TG (Toffoli Gate) and FRG (Fredkin gates) is used to create a unique reversible full and half adder. Limitations in the reversible Logic circuits are the feedback and fan out is not possible. In reversible logic gates, performance parameters like the Gate count and garbage output we have to focus.

Sign In or Purchase

References

References is not available for this d

Authors

Figures

References

Keywords

Metrics

Back to Results | Next >

References

References is not available for this d

References

References is not available for this d

Comparison of Cryptographic Techniques: Classical, Quantum and Neural

Minal Ghute ; Yogesh Suryawanshi All Authors

Abstract: Now days, the necessity of highly secured and reliable network is tremendously increased in the wireless communication network. There are various routing attacks occurs i... **View more**

Abstract:

Now days, the necessity of highly secured and reliable network is tremendously increased in the wireless communication network. There are various routing attacks occurs in wireless communication network there for secure routing is one of the most challenging research area in a mobile ad-hoc network-MANETs. Several methods are available for providing safety of the MANET, still various attacks are there which reduces network performance. Hence a strong cryptography technique is required to secure communication in MANET. An efficient cryptographic method is required, which will not only generate and maintain key also distribute it safely to the nodes which are not malicious. The method proposed here detects the nodes which are malicious and keeps them away from communication in the network so that packet delivery rate is increased by reducing delay in the network. The reliable communication in MANET is achieved by applying strong cryptography methods. In this paper comparison of classical, quantum and neural cryptography are given.

Published in: 2022 6th International Conference on Electronics, Communication and Aerospace Technology

Date of Conference: 01-03 December 2022

INSPEC Accession Number: 22539248

Date Added to IEEE *Xplore*: 16 January 2023

DOI: 10.1109/ICECA55336.2022.10009164

▸ **ISBN Information:**

Publisher: IEEE

Conference Location: Coimbatore, India

Contents

I. Introduction

MANETs has a dynamic topology i.e. nodes enter and leave the network randomly, due to which it often undergoes attacks. To prevent the attacks on the network the essential cryptographic techniques play vital role. In MANETs due to unavailability of central administrator nodes have to communicate and coordinate with each other for the successful data transmission from source node to destination node. When nodes become spiteful it does not takes part in the communication. Malicious node does not send information to other nodes in the network. Cryptography is the method in which the original data which is called plain text is encrypted by using a particular key. The modified data is called cipher text which is not possible for the malicious node to decrypt it without licensed key.

Authors

Figures

References

Keywords

Metrics

Back to Results | Next >

References

References is not available for this d

References

References is not available for this d

References

References is not available for this d

IoT Based Pet Day-Care Robot

Minal Ghute ; Shreyas Deshpande ; Abhishek Sondavle ; Swaraj Bhalerao ; Mayur Deshmukh **All Authors**

Abstract: People love their pets and they have emotional attachment with them. People play with pets, spend time with their pets and treat them as their family member or as a best ... **View more**

Metadata

Abstract:

with pets, spend time with their pets and treat them as their family member or as a best friend. However a problem occurs to look after the pets whenever nobody is present in the house, so to overcome these problems Pet Day Care Robot is the exact solution. This robot is an IoT based robot. It means that the owner will successfully and easily look after his/her pet by operating the robot with his/her smart phone. This robot is capable of working on IoT and cloud platform where, both of these principles are capable to connect the robot with mobile phone so that it can be operated with the help of Wi-Fi connectivity from any corner of the world. This robot is designed with the help of Raspberry Pi 4 and Arduino Uno which are interfaced with each other. Arduino provide motion to the robot using L298N motor driver and center shaft gear motor whereas raspberry pi is capable of monitoring, observing and mapping the position and appearance of pet with help of pi camera module which is interfaced with arduino.

Published in: 2022 6th International Conference on Electronics, Communication and Aerospace Technology

Date of Conference: 01-03 December 2022

INSPEC Accession Number: 22539109

Date Added to IEEE *Xplore*: 16 January 2023

DOI: 10.1109/ICECA55336.2022.10009244

ISBN Information:

Publisher: IEEE

Conference Location: Coimbatore, India

Contents

When owners are not able to feed their pets according to their food cycle, they will have to keep feeder section of the robot full before going to work, as to take care of pets food cycle. For the protection of the main module and to give a solid frame to the robot steel mesh is used. Another small case robot module is also needed for some other modules and camera. A lot of features can be installed in the pet feeder. Most of the working feeders founded are still working manually. IoT has given an idea of designing of pet feeders which is operated manually even some alarm systems have manual settings to be done by the user, hence to make the process easier and more efficient IoT concepts can be used as it is the internet dominated world, we can use it for more efficient and smart process of the feeder.

References

References is not available for this d

Back to Results

References

References is not available for this d

References

References is not available for this d

Improvement of QoS Parameters using FAN Shaped Clustering Method

Minal Patil ; Manish Chawhan All Authors

Abstract: Clustering in MANET provides greater efficiency in terms of energy and mobility of the node. It has better stability and scalability of the nodes in the network, as energ... **View more**

Abstract:

Clustering in MANET provides greater efficiency in terms of energy and mobility of the node. It has better stability and scalability of the nodes in the network, as energy and mobility of node is the key parameter for the nodes in the network. Cluster Head (CH) selection and Cluster maintenance are the two perspectives for clustering in MANET. CH is the vital node in the network to collect the data from the member nodes. CH requires more energy when compared to other nodes in the cluster. It calculates the distance of the nodes and energy of the node in the cluster by the ration of energy and distance based on sector design. If energy of the cluster head is less than threshold value, the reclustering occurs and again a CH is elected. There are different geometries of the clustering, and Fan shaped clustering approach is proposed in this paper. This clustering scheme result is expected in terms of Quality of Service (QOS) parameters. QOS parameters have been evaluated with fan shaped clustering and without fan shaped clustering. QOS parameters such as throughput, packet delivery ratio, path loss etc. are validated on the NS2 Simulation Platform. It extends the network life in terms of energy throughput, delay and Packet Delivery Ratio.

Published in: 2022 6th International Conference on Electronics, Communication and Aerospace Technology

Date of Conference: 01-03 December 2022

INSPEC Accession Number: 22539061

Date Added to IEEE *Xplore*: 16 January 2023

DOI: 10.1109/ICECA55336.2022.10009497

ISBN Information:

Publisher: IEEE

Conference Location: Coimbatore, India

Contents

I. Introduction

Clustering is a group of similar nodes. One of the extensively used methods for energy conservation is clustering, in which mobile nodes are arranged into clusters. A Cluster Head (CH) and additional nodes referred to as members typically make up each cluster. CH is the vital member in the cluster. CH basically works as a leader in the cluster. CH has the highest energy than the other nodes in the cluster. Therefore, it should be chosen carefully to enhance network performance. Each member gathers data and transmits it to its CH, which then gathers all the data into a single packet and transmits it to the sink. The clustering strategy can significantly reduce network stress, allowing nodes to use less energy and live longer. Particularly in MANET, network in cluster has some merits, such as energy efficiency and scalability.

Authors

Figures

References

Keywords

Metrics

Back to Results

References

References is not available for this d

References

References is not available for this d

References

References is not available for this d

A Review paper on Milli-Meter Wave Communications

Abhishek A. Madankar ; Atish Khobragade All Authors

Abstract: From the literature review analysis, it is evident that NYUSIM, METIS, FRFT and Machine learning techniques are better for channel modelling than other techniques. Moreov... **View more**

Abstract:
for channel modelling than other techniques. Moreover, these techniques showcase the most optimum performance for one of more parameters, and thus they must be used in combination for an effective channel modelling system.Milli-meter wave communication systems usually work towards improving the throughput of the system. Channel modelling plays a vital role in achieving this task. Modelling channels requires a lot of complex mathematical analysis, and this analysis changes with changes in traffic patterns, number of communicating nodes, actual channel type and many other real-time parameters. Due to these changes, a static channel model is usually insufficient for real- time use cases. Our problem statement is to integrate machine learning into channel modelling, so that the prepared channel model incorporates most of the real-time changes in network parameters.

Published in: 2022 6th International Conference on Electronics, Communication and Aerospace Technology

Date of Conference: 01-03 December 2022

INSPEC Accession Number: 22539065

Date Added to IEEE *Xplore*: 16 January 2023

DOI: 10.1109/ICECA55336.2022.10009475

▸ **ISBN Information:**

Publisher: IEEE

Conference Location: Coimbatore, India

Contents

I. Introduction

Due to the exponential growth in data-consumption patterns of users, there has been a massive demand for high-bit rate networks. We've shifted from speeds of 2.4 kbps in 1980s to 10 Gbps in 2020. Figure 1 showcases the exponential growth in data speeds over the years. In order to tackle such high rates of communication, network designers have shifted from high frequency (HF) antennas to very high frequency (VHF) and finally to extremely high frequency (EHF) antennas. Figure 1:

Data speed growth over the years [20]

Authors

Figures

References

Keywords

Metrics

Back to Results

References

References is not available for this d

References

References is not available for this d

References

References is not available for this d

Design of Advanced Encryption Standard Algorithm

Megha Chakole ; S. S. Dorle All Authors

Abstract: With the AES algorithm is used in almost all the digital communication for transmitting the data. Many of the researchers have designed the AES algorithm for ensuring mor... **View more**

Metadata

Abstract:

With the AES algorithm is used in almost all the digital communication for transmitting the data. Many of the researchers have designed the AES algorithm for ensuring more secured communication between the end users. In this research work an approach is made to design the AES algorithm in hardware by using the VHDL language by using 128 bits. The use of encryption and decryption process will be faster for any of the application as compared to the other 128 bits algorithm. The design also shows the significant improvement in the parameters like time period, faster output, etc

Published in: 2022 6th International Conference On Computing, Communication, Control And Automation (ICCUBEA

Date of Conference: 26-27 August 2022

INSPEC Accession Number: 22540184

Date Added to IEEE *Xplore*: 16 January 2023

DOI: 10.1109/ICCUBEA54992.2022.10011065

ISBN Information:

Publisher: IEEE

ISSN Information:

Conference Location: Pune, India

Contents

end user. Cryptography is the technique used to authenticate the secure transmission of data within the channel. It also deals with the protected way of data transfer between the source and destination. With the help of cryptography technique, the destination user can only see the actual contents of the data sent by the source user. In cryptography, the text is jumbled and additional content is added, which is known only to the source user and destination user. In cryptography, text data is encrypted at the source end and the encrypted data is transmitted through the channel. Later, at the destination end, the data is decrypted and original text data is recovered. In short, cryptography is a mechanism to transmit data in the specific format recognised by the allowed users. There are various ways to carry out the encryption and decryption process.

Authors

Figures

References

Keywords

Metrics

References

References is not available for this d

References

References is not available for this d

References

References is not available for this d

Image Processing based Vehicle Number Plate Recognition

K.P. Kamble ; Kalyani Chaudhary ; Rachana Admane ; Samiksha Wagde ; Ritika Shekar All Authors

Abstract: The growing prosperity of India's urban areas has made car ownership a necessity. This has led to an unexpected civil society problem: traffic control and vehicle identif... **View more**

▸ **Metadata**

Abstract:

This has led to an unexpected civil society problem: traffic control and vehicle identification. Due to the increased number of cars on the roads today, parking lots are congested. Vehicle license plate recognition systems (VNPR) play a key role in addressing these issues, from parking permits to city traffic monitoring to car theft tracking. The development of this system makes it easier to keep records and use them when needed. The objective of this research is to design an automatic identification system for identification of number from vehicle number plate which is based on embedded platform. A number of VNPR systems based on various methods are now available. This process basically consists of phases: localization and character recognition. The haar cascade classifier is used for license plate recognition. Segmentation of images is done by using image segmentation process. To identify characters, optical character recognition is used. The performance of VNRR system is tested against a data set –JPEG image. This system can be used for different type of applications like toll booths.

Published in: 2022 Sixth International Conference on I-SMAC (IoT in Social, Mobile, Analytics and Cloud) (I-SMAC)

Date of Conference: 10-12 November 2022

INSPEC Accession Number: 22445870

Date Added to IEEE *Xplore*: 22 December 2022

DOI: 10.1109/I-SMAC55078.2022.9987261

▸ **ISBN Information:**

Publisher: IEEE

▸ **ISSN Information:**

Conference Location: Dharan, Nepal

Contents

I. Introduction

Vehicle license plate recognition (VNPR) is a part of life and is expected to be integrated into proposed transportation technologies. Self-driving car concepts offer many opportunities to transform the basic transportation system. VNPR technology is a part of intelligent transportation systems and it is a part of human intervention. It's not just cameras on roadsides and parking lot fences. The rapid urbanization of countries is a major advancement in the modern world. People prefer to stay away from the countryside and live mainly in cities. Local governments are often unaware of the current and potential mobility needs of residents and visitors as traffic increases in these areas. VNPR is being used more and more to study the free flow of traffic and promote intelligent transportation. The VNPR (Vehicle Number Plate Recognition) system is based on image processing technology. It is one of the systems necessary for license plate recognition. The development of this system makes it easier to keep records and use them when needed. The objective of this research is to design an effective automated vehicle identification system based on vehicle license plates.

Authors

Figures

References

Keywords

Metrics

References

References is not available for this d

< Previous | Back to Results | Next >

References

References is not available for this d

References

References is not available for this d

Knowledge Based Classifier and Pattern Recognition Technique for Satellite Image Analysis

Publisher: IEEE

Abstract: Pattern Recognition is quickly becoming a popular topic of image processing. It is a branch of remote sensing, and it can be useful where it is difficult to visit and ana... **View more**

Abstract:

Pattern Recognition is quickly becoming a popular topic of image processing. It is a branch of remote sensing, and it can be useful where it is difficult to visit and analyze geographical locations such as forestry or islands, and it can also be difficult to visit areas affected by natural disasters. To do this, a system to distinguish areas such as buildings, greenery, cultivated land, land, water, and so on must be devised. Previously, research on these themes had been conducted, but it was confined to one or two remote sensor items. This work introduces a method for identifying items such as buildings, greenery, water, and land. Because the knowledge basis for this recognition is based on analysis, it is also unbound to specific types of locations. This method is useful for determining the area under civilization as well as the percentage area of a given pattern. The Image classification technique uses supervised and unsupervised classification methods. The supervised classification uses a maximum likelihood classifier. The unsupervised classification uses the ISO Cluster classifier to classify images. ArcGIS PRO and ERDAS IMAGINE software are used for algorithm analysis.

Published in: 2022 IEEE 3rd Global Conference for Advancement in Technology (GCAT)

Date of Conference: 07-09 October 2022

INSPEC Accession Number: 22443388

Date Added to IEEE *Xplore*: 12 December 2022

DOI: 10.1109/GCAT55367.2022.9972053

▸ **ISBN Information:**

Publisher: IEEE

Conference Location: Bangalore, India

Contents

I. Introduction

Pattern recognition is used to seek out the maximum probable parameters from the query image. This is one of the interesting techniques used for the analysis of GIS images. As the texture of remotely sensed images are varying, a new and superior sets of rules or algorithms and strategies are advanced for automatic evaluation. In this process first, the high resolution satellite image is segmented due to which the pixels of the same category are grouped together which simplifies the class selection and after that classification is done.

Authors

Figures

References

Keywords

Metrics

Back to Results | Next >

References

References is not available for this d

References

References is not available for this d

References

References is not available for this d

Zone Based Selective Neighbours to Mitigate Flooding & Reliable Routing for WSN

Poonam T. Agarkar ; Manish D. Chawhan ; Kishor D. Kulat ; Pratik R. Hajare **All Authors**

Abstract: Growing demand in wireless Mobile Adhoc Networks due to their immense potential and effectiveness in varied applications had motivated researchers to control and optimize... **View more**

Metadata

Abstract:

Growing demand in wireless Mobile Adhoc Networks due to their immense potential and effectiveness in varied applications had motivated researchers to control and optimize various parameters for efficient routing in mobile environment. The rapidly changing environment of the network due to mobility of nodes results in unpredictable topology and thus introduces primary challenge to design better and an efficient routing protocol. The network in such case lacks fixed infrastructure and common head centric design. MANET routing schemes use flooding to propagate packets in the network resulting retransmissions, collisions, and congestions which significantly degrade the performance of the network. Using GPS, knowing the geographical position of the sensor nodes, the protocol performance can be improved while reducing the number of retransmissions. The proposed work is a future extension of efficient flooding based on selective neighbours where the surrounding region limiting the transmission range is divided into eight quadrants or zones with the source at the centre called zone based selective neighbours (ZBSN). Flooding based on selective four neighbours suffers from few selection of hoping or forwarding nodes when the node density is low and does not meet the selection criteria around the source or forwarder node and may miss the chance of approaching the destination or requires large number of hops. This neighbour selection scheme uses the modified approach of the Adhoc on Demand Distance Vector (AODV) protocol to reduce the flooding of Route request (RREQ) packets, control the network overall traffic, improves link stability and the residual energy reducing the overheads by 24%.

Published in: 2022 International Conference on Connected Systems & Intelligence (CSI)

Date of Conference: 31 August 2022 - 02 September 2022 **INSPEC Accession Number:** 22213255

Date Added to IEEE *Xplore*: 01 November 2022 **DOI:** 10.1109/CSI54720.2022.9924006

▸ **ISBN Information:**

Publisher: IEEE

Conference Location: Trivandrum, India

▸ **Funding Agency:**

References

References is not available for this d

Contents

Authors

Figures

References

Keywords

Metrics

Back to Results

References

References is not available for this d

References

References is not available for this d

Brain Tumor Classification Using Deep Learning Framework

Yogita Dubey ; Neeraj Thosar ; Kajal Mitra ; Mahek Narlawar ; Dewang Bhalerao All Authors

Abstract: Brain tumor is the mass or abnormal growth of a cells in the brain. Various types of brain tumors exist. The ability of a radiologist to diagnose a brain tumor early is m... **View more**

Abstract:

radiologist to diagnose a brain tumor early is mostly dependent on his or her experience. As a result, it is vulnerable to human error. It is critical to build an effective diagnostics tool for tumor detection and classification to acquire exact diagnostics and prevent surgery and subjectivity, Although surgery is the most common treatment for brain tumors, tumors that cannot be surgically removed may be treated with radiation or chemotherapy to limit their growth. One of the most popular techniques used to diagnose brain tumors is magnetic resonance imaging (MRI), which produces detailed images of the brain. In this paper, a technique is proposed for classification of brain tumor as glioma, meningioma and pituitary tumor using the framework of convolutional neural network. CNN architecture RESNET with a skip connection is used in this framework. T1 weighted (Axial View) real MR images from hospital and simulated images from Kaggle dataset are used for experimentation.

Published in: 2022 IEEE 10th Region 10 Humanitarian Technology Conference (R10-HTC)

Date of Conference: 16-18 September 2022

Date Added to IEEE *Xplore*: 03 November 2022

ISBN Information:

ISSN Information:

INSPEC Accession Number: 22237781

DOI: 10.1109/R10-HTC54060.2022.9929922

Publisher: IEEE

Conference Location: Hyderabad, India

Contents

I. Introduction

Brain tumors are lumps that form as a result of aberrant brain cell proliferation and the loss of the brain's regulatory mechanisms. Brain tumor detection and classification is very important to suggest the appropriate treatment option at early stage.

Sign In to Continue Reading

References

References is not available for this d

Authors

Figures

References

Keywords

Metrics

< Previous | Back to Results | Next >

More Like This

BAT Algorithm With fuzzy C-Ordered Means (BAFCOM) Clustering Segmentation and Enhanced Capsule Networks (ECN) for Brain Cancer MRI Images Classification

IEEE Access

Published: 2020

Investigation of Brain Tumor Recognition and Classification using Deep Learning in Medical Image Processing

2022 International Conference on Augmented Intelligence and Sustainable Systems (ICAISS)

Published: 2022

Show More

References

References is not available for this d

References

References is not available for this d

Design of Multi-band MIMO Antenna for 5G Wireless Applications

Publisher: IEEE

Sachin Khade ; Shruti Meshram ; Asha Mandhalkar ; Isha Shival All Authors

Abstract: This research shows a multi-band multiple-input multiple-output (MIMO) antenna with four radiating elements. The CST programme is used to design and simulate antennas. PE... **View more**

Metadata

Abstract:

This research shows a multi-band multiple-input multiple-output (MIMO) antenna with four radiating elements. The CST programme is used to design and simulate antennas. PEC is used for the ground and patch, while FR4 (lossy) is used for the substrate, which measures 130 mm x 74 mm x 1.6 mm. L-Slot can be incorporated into a rectangular microstrip antenna measuring 21 mm x 18 mm x 0.035 mm to provide the required bands. 3.28-3.72 GHz, 4.33-5.25 GHz, and 5.81-6.00 GHz are among the frequencies covered. At operational frequencies of 3.416 GHz, 5.04 GHz, and 5.896 GHz, the reflection coefficients of four antennas are -21.815 dB, -32.345 dB, and -14.114 dB, respectively. Wi-Fi, Wi-MAX, WLAN, and 5G are all applications that use this frequency. The VSWR, impedance, reflection coefficient, mutual coupling, radiation pattern, gain, directivity, surface current of an antenna are all measured. The geometry of the provided antenna, as well as related factors such as S-parameters, radiation pattern plots, gain, directivity values, are shown and explored in detail in this paper.

Published in: 2022 Third International Conference on Intelligent Computing Instrumentation and Control Technologies (ICICICT)

Date of Conference: 11-12 August 2022

Date Added to IEEE *Xplore*: 18 October 2022

ISBN Information:

INSPEC Accession Number: 22189945

DOI: 10.1109/ICICICT54557.2022.9917598

Publisher: IEEE

Conference Location: Kannur, India

Contents

I. INTRODUCTION

A dual band MIMO antenna for 5G communication is proposed in this paper. The intended antenna consists of four antennae. The study of the 5G smartphone antenna has a lot of potential in terms of meeting the requirements of modern 5G wireless communication systems [1]. For dual-band frequency response, we employed L-slot. After developing a single antenna with dual frequency response, convert it to a Multiple Input Output antenna (MIMO).[2]. An inverted L-shaped monopole is used to show a monopole eight output (MIMO) antenna system. The multi-antenna system is based on a low-cost 0.8 mm thick FR4 substrate with dimensions of 136 68 mm2, resonating at 3.5 GHz with a 6db measured bandwidth of 450 MHz, higher-than-15-db inter element isolation, and gain of 4 dbi.[3]

Authors

Figures

References

Citations

Keywords

Metrics

Back to Results | Next >

References

References is not available for this d

References

References is not available for this d

References

References is not available for this d

Design of KVM Switch using USB Technology

Abhishek A. Madankar ; Rashmi Kapare ; Sagar Jadhav ; Minal S. Patil ; Shital Telrandhe ; Neha Chaudhary All Authors

Abstract: A KVM switch (KVM is the abbreviation for keyboard, video (monitor and mouse) allows a user to control several computers from a single device. It is generally known that ... **View more**

Abstract:

A KVM switch (KVM is the abbreviation for keyboard, video (monitor and mouse) allows a user to control several computers from a single device. It is generally known that the normal switches cannot be connected with laptops and computers, as the KVM switches are originally made for connecting with laptops and computers. It is difficult to connect one or more devices with laptops and computers with the help of the KVM switches. Recent advancement in KVM switch technology is the integration of Universal Serial Bus (USB) items. USB gives PCs true plug-and-play capabilities. USB-ready PCs can be connected to any external de vice without including an inside card or setting up the gear manually. When you plug in a USB-viable gadget, it is recognized by the USB PC. The proposed scaled-down system will plan a USB Hub KVM Switch. This USB innovation permits the KVM change to introduce the console and mouse's supported presence to every appended PC. This gives an extraordinary advantage – every appended PC, PC, Macs, and Suns, can be booted up all the while. It can also be used as a captive to control USB PCs in numerous stage setups. This permits clients to merge control of both inheritance and USB-empowered PCs in a single design.

Published in: 2022 3rd International Conference on Electronics and Sustainable Communication Systems (ICESC)

Date of Conference: 17-19 August 2022

INSPEC Accession Number: 22068275

Date Added to IEEE *Xplore*: 19 September 2022

DOI: 10.1109/ICESC54411.2022.9885324

▸ **ISBN Information:**

Publisher: IEEE

Conference Location: Coimbatore, India

Contents

I. INTRODUCTION

As the mouse and other I/O anchorages became common in trading, the keyboard videotape switch was used to demonstrate control centers and screen trading bias. With the expanding utilization of Microsoft Windows, the mouse and other I/O anchorages became widespread in trading. In 1995, Remigius Shatas, co-creator of Cybex, broadened the concept to include Keyboard, Video, and Mouse. Subsequently, Universal Periodical Machine began to transform into the new business standard format PC peripherals a couple of times. Given the creating need to switch peripherals regardless of the control center, mouse, and screen, a couple of associations are as of now selling "KVMP" switch contraptions [1], [2]. In the proposed system performance analysis of different open-source virtual machine monitures like OpenVZ, XenCom and KVM using [3]. Audio signal transceiver module is implemented in FPGA; it is used for increasing the bandwidth of system and it also guarantee precision of the serial transmission [4]. For improving the efficiency of system centralized control unit is used to manage the communication between many set of KVM [5]. A KVM switch reduces the need for numerous consoles, screens, and mice to control multiple PCs using the equipment. Figure 1 illustrates just how a KVM switch enables a client to control the choice (PC 2) using their console and mouse and view the video led from the chosen PC via a screen, as though the two PCs were directly connected. Choose PC 1 at the switch and you will see and control PC 1, and after that select second PC 2.

Sign In to Continue Reading

Authors

Figures

References

Keywords

Metrics

Back to Results

References

References is not available for this d

References

References is not available for this d

References

References is not available for this d

Accident Prevention and Detection System using IoT Integrated in an Electric Pole

Minal S. Patil ; Harshal Dharmik ; Nikita Borate ; Ritikesh Gokhe ; Abhishek A. Madankar ; Roshan Umate All Authors

Abstract: In today's world, the technology has skyrocketed and has an impact on almost everyone's life, so much that an average person starts a day after checking their phone, so w... **View more**

▸ **Metadata**

Abstract:

In today's world, the technology has skyrocketed and has an impact on almost everyone's life, so much that an average person starts a day after checking their phone, so why not use the same technology to save lives and prevent accidents? In hilly terrains and ghats, many vehicle accidents occur on ghats and as there is no one to monitor the situation and alert the officials, those victims often die. Also, the most common reason of these accidents is that the drivers are not aware of vehicle approaching towards them in those ghats. So, this problem can be overcome by using proposed system. In the proposed system when a vehicle comes from opposite direction and it may lead to accident so it providing the accident prevention before it's occurring. An indicator lights up if it detects a moving vehicle coming from the other side of the road. And if the accident happens then in this, AI technology is used to detect accidents and send an email with the location of accident to nearest Police Station/Hospitals. This will save so much time of the emergency services arrival that it can even save the victim's life. And also, as stated in the scope of environment, Thermal cameras are used to determine the fatality of accident and count the number of victims to get accurate help.

Published in: 2022 3rd International Conference on Electronics and Sustainable Communication Systems (ICESC)

Date of Conference: 17-19 August 2022

Date Added to IEEE *Xplore*: 19 September 2022

▸ **ISBN Information:**

INSPEC Accession Number: 22068262

DOI: 10.1109/ICESC54411.2022.9885559

Publisher: IEEE

Conference Location: Coimbatore, India

Contents

I. INTRODUCTION

As the work life of an average person is increasing every day, there is nothing more irritating than a traffic jam, and to see that most traffic jams occur due to some type of accident / vehicle management problems on traffic signals. But we live in an era of advanced technology and we have come up with a way to avoid accidents in most of the places including mountain areas. Every Year many people die or gets heavily injured just because they're unaware of the vehicles approaching from other turns towards them, so to prevent this from of accident the proposed system is designed by these accidents can be reduced. If the accidents happen then in this, AI technology is used to detect accidents and send an email with the location of accident to nearest Police Station/Hospitals in very less time hence increasing the chances of saving victims life. This system can heavily impact on the statistics of accidents that occurs in mountain areas. The ongoing research work for detecting and preventing accidents is going on and many studies have used various technologies or methods for achieving the same, such as Sensors data from various sensors is processed to determine the presence of vehicles. Sending SOS [4] Incase the accident occurs it needs to send a signal to nearest emergency services, but using sensors has its disadvantages such as Cannot determine whether the data collected by sensor is actually valid or not, it can be anything from an insect to some other fluctuation in sensor's data. Data [5] Vast amount of data is required for training the model and the methods to decrease the chances of an accident. IOT [6] by using IoT the model gets a huge accessibility for sending and receiving data. The aim of proposed system is simply to reduce the accidents occurring in the mountainous terrains by implementing a smart pole that can determine whether a vehicle is approaching from the other side or not, and if it is it should alert the driver on other side of road [1], [2]. Hence it should be able to prevent accidents, and in case an accident does happen, it should be able to detect the accidents and collect significant data of accident and send a SOS to nearest authorities. For implementing the proposed system a dataset (Made by us) of toy cars for both purposes, accident detection as well for detecting running vehicles is used [3], [6]-[15]. The proposed system can be significantly improved by using IR / Thermal scanning cameras, by training the model with real world images of vehicles and accidents and it can also create a separate network of poles only to communicate between themselves and remove the need of internet

Sign In to Continue Reading

Authors

Figures

References

Keywords

Metrics

Back to Results

References

References is not available for this d

Published: 2022

References

Show More

References is not available for this d

References

References is not available for this d

Wireless Floating WQ(Water Quality) Monitoring System

Amoli Belsare ; Labhesh Bokde ; Himanshu Wadyalkar ; Piyush Kokate All Authors

Abstract: The wireless sensors for environmental parameters monitoring are getting very popular due to their low power working capacity. Continuous real-time water quality (WQ) mon... **View more**

Metadata

Abstract:

...lar due to their low power working capacity. Continuous real-time water quality (WQ) monitoring is critical for the environmental engineer due to non-accessorily at many sampling locations. Therefore, a system needs to be designed that will practically work 24X7 using real-time sensors data and a Graphical User Interface (GUI) system. At the same time, such systems demand a continuous power supply source to send the data from node to base station.This paper presents a unique design of a floating low-cost wireless WQ monitoring system that can be deployed in water bodies. The calibrated pH, turbidity, temperature, water level sensors were interfaced to the PIC microcontroller with a GPS module. The system was communicating from 100-500 m using-WIR-1186 modules. The nodes were solar-powered and floating above the water body for 24X7 with a duel power supply.The obtained results using low-cost sensors demonstrate the system's feasibility in deployment and long-term use over larger water bodies like ponds, lakes, rivers etc. The floating designs will be a reliable and cost-effective solution for pollution monitoring agencies to monitor water quality.

Published in: 2022 3rd International Conference for Emerging Technology (INCET)

Date of Conference: 27-29 May 2022

INSPEC Accession Number: 21865659

Date Added to IEEE *Xplore*: 15 July 2022

DOI: 10.1109/INCET54531.2022.9824080

ISBN Information:

Publisher: IEEE

Conference Location: Belgaum, India

Contents

I. Introduction

The Water is a key parameter of current environmental research as it is very essential for agriculture, industries & human beings. The water quality (WQ) includes physicochemical and biological parameters for monitoring surface water bodies [1], [2]. The pollutants in the water bodies can spread at a longer distance, inflowing rivers, waterways, etc. However, in stagnant water bodies, the pollutants normally saturate near a smaller area or centre. Therefore, monitoring the water bodies due to their dynamic nature is crucial for researchers.

Authors

Figures

References

Citations

Keywords

Metrics

Back to Results

References

References is not available for this d

References

References is not available for this d

References

References is not available for this d

International Conference on Advances in Electrical and Computer Technologies

ICAECT 2021: **Advances in Electrical and Computer Technologies** pp 703–714

Analysis of Daubechies 2 Wavelet in WPM System for Adhoc Network

M. B. Chakole & S. S. Dorle

Conference paper | First Online: 26 June 2022

Part of the Lecture Notes in Electrical Engineering book series (LNEE,volume 881)

Abstract

Wavelet packet modulation (WPM) has been proven as one of the multi-carrier modulation (MCM) techniques with improved features and improved characteristics. To make the WPM system more efficient, different techniques were used. In this research work, WPM system is designed by using db2 wavelet on three different modulation schemes BPSK, QPSK and 16-PSK. Further, each modulation scheme was tested under three different channel conditions, i.e. AWGN, Rayleigh and Rician. After successfully experimentation, it has been concluded that the WPM system with QPSK modulation under AWGN channel condition using Daubechies (db2) wavelet gives a better performance for adhoc network parameters like BER, throughput and energy consumption.

Keywords

Wavelet packet modulation (WPM) **Multi-carrier modulation (MCM)**

Daubechies 2 (db2) **Quadrature phase shift keying (QPSK)**

Binary phase shift keying (BPSK) **16-phase shift keying (16-PSK)**

Additive white Gaussian noise (AWGN)

References

1. Chakole MB, Dorle SS (2020) Design of WPM system using QPSK modulation for different wavelets. Int J Innov Technol Explor Eng (IJITEE) 9(3). ISSN: 2278-3075

2. Van Bouwel C, Potemans J, Schepers S, Nauwelaers B, Van de Capelle A (2000) Wavelet packet based multicarrier modulation. In: IEEE Benelux chapter on vehicular technology and communications. Symposium on communications and vehicular technology. SCVT-2000. Proceedings (Cat. No. 00EX465), pp 131–138. https://doi.org/10.1109/SCVT.2000.923351

3. Nawaz T, Baig S (2011) Wavelet OFDM—a solution for reliable communication in a frequency selective Rayleigh fading channel. In: IEEE IBCAST, pp 413–417

4. Chakole M, Dorle S (2017) Evaluation of WPM-BPSK based peer-to-peer network using wavelets for different channels. In: The 8th IEEE international conference on computing communication and networking technology. IIT Delhi, India

5. Lindgren A, Schelén O (2002) Infrastructured ad hoc networks. In: Proceedings of the 2002 international conference on parallel processing workshops (international workshop on ad hoc networking)

6. Meshram SL, Dorge PD (2017) Design and performance analysis of mobile ad hoc network with reactive routing protocols. In: IEEE international conference on communication and signal processing, ICCSP, pp 443–447

7. Ghaith A, Hatoum R (2013) Performance analysis of the wavelet-OFDM new scheme in AWGN channel. In: ICCIT-2013 wireless communication and signal processing. IEEE, pp 225–229

8. Arianandа DD, Lakshmanan MK, Nikookar H (2011) A wavelet packet transceiver for spectral analysis and dynamic spectrum access. IEEE

9. Li N, Gao Y, Du C, Hao X (2012) Optimizing performance of WIMAX system based on WPM. In: The 7th international conference on computer science & education (ICCSE 2012), Melbourne, pp 372–375

10. Bajpai A, Lakshmanan MK, Nikookar H (2011) Channel equalization in wavelet packet modulation by minimization of peak distortion. In: IEEE 22nd international symposium on personal, indoor and mobile radio communications, pp 152–156

11. Effendi MR, Mengko TLR, Gunawan AH, Munir A (2019) Performance evaluation of wavelet packet modulation for wireless digital communications. In: International symposium on networks, computers and communications (ISNCC), pp 1–4. https://doi.org/10.1109/ISNCC.2019.8909167

Author information

Authors and Affiliations

Department of Electronics and Telecommunication Engineering, Yeshwantrao Chavan College of Engineering, Nagpur, India
M. B. Chakole

Department of Electronics Engineering, G H Raisoni College of Engineering, Nagpur, India
S. S. Dorle

Corresponding author

Correspondence to M. B. Chakole .

Editor information

Editors and Affiliations

Department of Electrical and Electronics Engineering, SVS College of Engineering, Coimbatore, India
Thangaprakash Sengodan

Department of Electronics and Communication Engineering, Kuwait College of Science and Technology, Safat, Kuwait
M. Murugappan

Department of Computer and Information Sciences, Covenant University, Ota, Nigeria
Sanjay Misra

Rights and permissions

Copyright information

About this paper

Cite this paper

Chakole, M.B., Dorle, S.S. (2022). Analysis of Daubechies 2 Wavelet in WPM System for Adhoc Network. In: Sengodan, T., Murugappan, M., Misra, S. (eds) Advances in Electrical and Computer Technologies. ICAECT 2021. Lecture Notes in Electrical Engineering, vol 881. Springer, Singapore. https://doi.org/10.1007/978-981-19-1111-8_53

RIS ENW BIB

DOI	Published	Publisher Name
	26 June 2022	Springer, Singapore

https://doi.org/10.1007/978-981-19-1111-8_53

Print ISBN	Online ISBN	eBook Packages
978-981-19-1110-1	978-981-19-1111-8	Computer Science Computer Science (R0)

Automatic Feature Abstraction from High Resolution Satellite Data for Urban Land Cover and Land Use

Publisher: IEEE

Pooja Pandey ; Yogita Dubey ; Sanjay Vasantrao Balamwar **All Authors**

Abstract: Urbanization is a beginning trend of the once two centuries, shaping numerous confines of the ultramodern world. To guide this miracle and support growth of metropolises ... **View more**

Abstract:
Urbanization is a beginning trend of the once two centuries, shaping numerous confines of the ultramodern world. To guide this miracle and support growth of metropolises that are competitive and sustainably give demanded services, there's a need for information on the extent and nature of civic land cover. Still, measuring urbanization is grueling, especially in developing countries, which frequently warrant the coffers and structure demanded to produce dependable data. With the increased vacuity of ever tasted data, new styles are available to collude civic land. Yet, being bracket products vary in their description of "civic" and generally characterize urbanization in a specific point (or points) in time. Arising pall grounded computational platforms now allow one to collude land cover and land use (LC/LU) across space and time without being constrained to specific bracket products. We perform a Automatic point abstraction image bracket procedure in Google Earth Engine (GEE), using two sources of reference data (executive data and hand-labeled exemplifications). By fusing intimately available optic and radar data as input to the classifier, we achieve accurate charts of constructed-up LC/LU in the fiefdom. In moment's period of big data, an fluently deployable system for accurate bracket of constructed-up LC/LU has expansive operations across a wide range of disciplines and is essential for assembling the foundation for a sustainable mortal.

Published in: 2022 8th International Conference on Advanced Computing and Communication Systems (ICACCS)

Date of Conference: 25-26 March 2022

INSPEC Accession Number: 22481232

Date Added to IEEE *Xplore*: 07 June 2022

DOI: 10.1109/ICACCS54159.2022.9785032

Publisher: IEEE

▸ **ISBN Information:**

▸ **ISSN Information:**

Conference Location: Coimbatore, India

References

References is not available for this d

Contents

Automatic Point abstraction has plant its operations in colorful areas like LULC mapping, change discovery, civic planning, disaster operation also numerous other socio-profitable conditioning. Remote seeing and Civilian's ways play a major part in similar operations. Still, operation areas of remote seeing have been vastly increased with vacuity of sub-metre resolution data from high-resolution drone image by flying over certain place it can capture the image depending upon the quality of the image we provide. HRS imagery facilitates to identify colorful civic affiliated features, similar as, road, tree, structure and all the other area that are present on the earth that also includes the one which ismanmade [1] [2]. Since, homemade birth of structures using satellite imagery is time consuming and expensive affair, hence, automated styles for birth been on a rise as a time and will be cost effective result with minimum stoner involvement [3] [4].

Back to Results

References

References is not available for this d

References

References is not available for this d

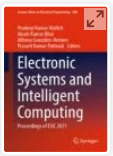

Electronic Systems and Intelligent Computing, pp 277–288

Detection of Stress with Deep Learning and Health Parameters Monitoring Using Raspberry Pi

Sujata S. Chiwande, Ashutosh Bagade, Sakshi Deshmukh & Sushma Nagdeote

Conference paper | First Online: 03 June 2022

369 Accesses | **1** Citations

Part of the Lecture Notes in Electrical Engineering book series (LNEE,volume 860)

Abstract

Now in day-to-day life, every individual faces some sort of stress due to workload, school, or form their lifestyle. Stress is an unwanted portion of life that is seen in people. As stress can have some positive effects, but it has adverse effects on your health if it is for a long time. Therefore, it is crucial to detect a person's stress, as it can lead one to depression. It is observed that stress leads to worse health situations. It is also found that stress can affect health by increasing heart rate, decrease in oxygen level of the body, and increase in weight. It can lead to obesity. Regular change in BMI also indicates that a person is stressed. Stress is threatening mankind's well-being. Due to stress, body releases a hormone that speeds up your heart rate and breathing. In the detection of stress, facial expressions have a pivotal spot. The proposed system will detect stress based on three stress-related facial expressions sad, angry, and fear. The proposed work in this paper is to make individuals aware of their physical condition. The aim of this paper is to detect stress by using deep learning concepts and health parameters monitoring such as heart rate, oxygen level, and BMI using Raspberry pi. And the measured results of the different persons with the proposed system and the existing system are given in the table.

Keywords

Deep learning **Facial expression** **Heart rate** **Oxygen level** **BMI**

References

1. Raichur N, Lonakadi N, Mural P (2017) Detection of stress using image processing and machine learning techniques. IJET 9(3)

2. Lia J, Zhanga D, Zhanga J, Zhanga J, Lia T, Xiaa Y, Yana Q, Xuna L (2017) Facial expression recognition with faster R-CNN. In: International congress of information and communication technology (ICICT 2017). Proc Comput Sci 107:135–140

3. Tarnowski P, Kołodziej M, Majkowski A, Rak RJ (2017) Emotion recognition using facial expressions. Proc Comput Sci 108(2017):1175–1184

4. Patil A, Mangalekar R, Kupawdekar N, Chavan V, Patil S, Yadav A (2020) Stress detection in IT professionals by image processing and machine learning. Int J Res Eng Sci Manage 3(1)

5. Yashaswini1 DK, Bhat SS, Sahana YS, Shama Adiga MS, Dhanya SG (2019) Stress detection using deep learning and IoT. Int J Res Eng Sci Manage 2(8)

6. Venkataraman D, Parameswaran NS (2018) Extraction of facial features for depression detection among students. Int J Pure Appl Math 118(7):455–463

7. Begum S, Ahmed MU, Funk P, Xiong N, von Schele B, Minor M (2006) Using calibration and fuzzification of cases for improved diagnosis and treatment of stress. In: 8th European conference on case-based reasoning workshop proceedings, pp 113–122, September 2006

8. Saxena S, Palaniswamy S, Tripathi S (2016) Real-time emotion recognition from facial images using Raspberry Pi II. In: 3rd International conference on signal processing and integrated networks (SPIN), 978-1-4673-9197-9/16/$31.00©2016 IEEE

9. Saransh, Muthamil Selvan T. Human facial expression recognition using tensor flow and open CV. School of Information Technology and Engineering, VIT University, Vellore. https://doi.org/10.13140/RG.2.2.19218.89288

10. Mahmood A, Hussain S, Iqbal K, Elkilani WS (2019) Research "Recognition of facial expressions under varying conditions using dual-feature fusion" Hindawi. Math Prob Eng 2019, article ID 9185481

11. Zhang H, Feng L, Li N, Jin Z, Cao L (2020) Video-based stress detection through deep learning. Sensors 20:5552. https://doi.org/10.3390/s20195552

12. Jaymon N, Nagdeote S, Yadav A, Rodrigues R (2021) Real time emotion detection using deep learning. In: 2021 International conference on advances in electrical, computing, communication and sustainable technologies (ICAECT), pp 1–7. https://doi.org/10.1109/ICAECT49130.2021.9392584

13. Keote ML, Karule PT (2016) Design and implementation of energy efficient Adiabatic ECRL and basic gates. In: International conference on soft computing techniques and implementations, ICSCTI 2015, pp 87–91, 7489543

Author information

Authors and Affiliations

Yeshwantrao Chavan College of Engineering, Nagpur, Maharashtra, India
Sujata S. Chiwande & Sakshi Deshmukh

Datta Meghe Institute of Medical Sciences, Sawangi, Wardha, Maharashtra, India
Ashutosh Bagade

Fr. Conceicao Rodrigues College of Engineering, Mumbai, Maharashtra, India
Sushma Nagdeote

Editor information

Editors and Affiliations

School of Computer Engineering, Kalinga Institute of Industrial Technology(KIIT) Deemed to be University, Bhubaneswar, Odisha, India
Dr. Pradeep Kumar Mallick

KIET Group of Institutions, Delhi-NCR, Ghaziabad, India
Dr. Akash Kumar Bhoi

Research on Agent based, Social and Interdisiciplinary Applications (GRASIA), Complutense University of Madrid, Madrid, Spain
Dr. Alfonso González-Briones

School of Computer Engineering, Kalinga Institute of Industrial Technology(KIIT) Deemed to be University, Bhubaneswar, Odisha, India
Dr. Prasant Kumar Pattnaik

Rights and permissions

Copyright information

About this paper

Cite this paper

Chiwande, S.S., Bagade, A., Deshmukh, S., Nagdeote, S. (2022). Detection of Stress with Deep Learning and Health Parameters Monitoring Using Raspberry Pi. In: Mallick, P.K., Bhoi, A.K., González-Briones, A., Pattnaik, P.K. (eds) Electronic Systems and Intelligent Computing. Lecture

Notes in Electrical Engineering, vol 860. Springer, Singapore. https://doi.org/10.1007/978-981-16-9488-2_25

.RIS .ENW .BIB

DOI	Published	Publisher Name
https://doi.org/10.1007/978-981-16-9488-2_25	03 June 2022	Springer, Singapore

Print ISBN	Online ISBN	eBook Packages
978-981-16-9487-5	978-981-16-9488-2	Engineering Engineering (R0)

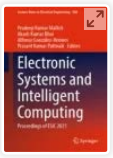

Electronic Systems and Intelligent Computing, pp 289–301

Energy-Efficient Automated Guided Vehicle for Warehouse Management System

Minal Keote, Tanmay Choudhari, Tanmay Alone & Ashar Ahmad

Conference paper | First Online: 03 June 2022

372 Accesses | **1** Citations

Part of the Lecture Notes in Electrical Engineering book series (LNEE,volume 860)

Abstract

The automation business has grown at a breakneck pace, breathing new life into an otherwise dormant industry. The use of robots has lowered human workload and freed up the workforce from boring, non-creative professions, allowing them to focus on more gratifying tasks. This project's purpose is to develop a bot that will be employed in storage and retrieval systems. Instead of carrying the individual components in the shelf, the robot's goal is to translate long shelves in storage buildings to new locations. A lead screw mechanism will be used to lift the shelf in its principal function. The key issues were evenly dispersing the load distribution over the chassis to achieve maximum stability and restricting the robot to shelf weight ratio to an optimal level. Design and analysis of the bot were carried out using FUSION 360 software. The second objective of this project is to develop a GUI for placing order and logistics management. It is done on VISUAL STUDIO 2019 software.

Keywords

Automation industry **OpenCV** **FUSION 360** **Visual studio 2019** **Lead screw mechanism** **Data matrix** **PID (proportional integral derivative)** **BFS algorithm**

References

1. Pakdaman M, Sanaatiyan MM (2019) Design and implementation of line follower robot. In: 2009 IEEE Second international conference on computer and electrical engineering, 28–30 December 2009

2. Yoshitake H, Kamoshida R, Nagashima Y (2019) New automated guided vechicle system using real-time holonic scheduling for warehouse picking. IEEE Robot Autom Lett 4(2)

3. Zhang H, Zhang C, Yang W, Chen C-Y (2015) Localisation and navigation using QR code for mobile robot in indoor environment. In: 2015 IEEE International conference on robotics and biomimetics (ROBIO), 6–9 December 2015

4. Marot J, Bourennane S (2017) Raspberry Pi for image processing education. In: IEEE European signal processing conference (EUSIPCO), 28 August–2 September 2017, Kos, Greece

5. Marengoni M, Stringhini D (2011) High level computer vision using OpenCV. In: IEEE Tutorials of the Brazilian symposium on computer graphics and image processing (SIBGRAPI Tutorials), 28–30 August 2011, Alagoas, Brazil

6. Guizzo E (2008) Kiva systems: three engineers, hundreds of robots, one warehouse. IEEE Spectr 45(7)

7. Vimal Kumar N, Selva Kumar C (2018) Development of collision free path planning algorithm for warehouse mobile robot. In: International conference on robotics and smart manufacturing (RoSMa2018), Madurai, India

8. Masram BY, Dhokale A, Shirsat P, Keote M (2018) Smart (dual) mode operating cooling system. In: 2018 First international conference on secure cyber computing and communication (ICSCCC), 978-1-5386-6373-8/18/$31.00©2018 IEEE

9. Thakre AK, Chiwande SS, Chafale SD (2014) Design of low power multiplier using reversible logic gate. In: 2014 International conference on green computing communication and electrical engineering (ICGCCEE)

Author information

Authors and Affiliations

Yeshwantrao Chavan College of Engineering, Nagpur, Maharashtra, India
Minal Keote, Tanmay Choudhari, Tanmay Alone & Ashar Ahmad

Editor information

Editors and Affiliations

School of Computer Engineering, Kalinga Institute of Industrial Technology(KIIT) Deemed to be University, Bhubaneswar, Odisha, India
Dr. Pradeep Kumar Mallick

KIET Group of Institutions, Delhi-NCR, Ghaziabad, India
Dr. Akash Kumar Bhoi

Research on Agent based, Social and Interdisiciplinary Applications (GRASIA), Complutense University of Madrid, Madrid, Spain
Dr. Alfonso González-Briones

School of Computer Engineering, Kalinga Institute of Industrial Technology(KIIT) Deemed to be University, Bhubaneswar, Odisha, India
Dr. Prasant Kumar Pattnaik

Rights and permissions

Copyright information

About this paper

Cite this paper

Keote, M., Choudhari, T., Alone, T., Ahmad, A. (2022). Energy-Efficient Automated Guided Vehicle for Warehouse Management System. In: Mallick, P.K., Bhoi, A.K., González-Briones, A., Pattnaik, P.K. (eds) Electronic Systems and Intelligent Computing. Lecture Notes in Electrical Engineering, vol 860. Springer, Singapore. https://doi.org/10.1007/978-981-16-9488-2_26

.RIS .ENW .BIB

DOI	Published	Publisher Name
https://doi.org/10.1007/978-981-16-9488-2_26	03 June 2022	Springer, Singapore
Print ISBN	Online ISBN	eBook Packages
978-981-16-9487-5	978-981-16-9488-2	Engineering, Engineering (R0)

Identification and prevention of Gray hole attack using IDS mechanism in MANET

Publisher: IEEE

Manish Devendra Chawhan ; Kruttika Karmarkar ; Gargi Almelkar ; Disha Borkar ; Kishor. D. Kulat ; Bhumika Neole All Authors

Abstract: Since the mid-1990s, the growth of laptops and Wi-Fi networks has led to a great increase in the use of MANET (Mobile ad hoc network) in wireless communication. MANET is ... **View more**

Abstract:

Since the mid-1990s, the growth of laptops and Wi-Fi networks has led to a great increase in the use of MANET (Mobile ad hoc network) in wireless communication. MANET is a group of mobile devices for example mobile phones, computers, laptops, radios, sensors, etc., that communicate with each other wirelessly without any support from existing internet infrastructure or any other kind of fixed stations. As MANET is an infrastructure-less network it is prone to various attacks, which can lead to loss of information during communication, security breaches or other unauthentic malpractices. Various types of attacks to which MANET can be vulnerable are denial of service (DOS) and packet dropping attacks such as Gray hole, Blackhole, Wormhole, etc. In this research, we are particularly focusing on the detection and prevention of Gray hole attack. Gray hole node drops selective data packets, while participating in the routing process like other nodes, and advertises itself as a genuine node. The Intrusion Detection System (IDS) technique is used for identification and aversion of the Gray hole attack. Use of AODV routing protocol is made in the network. The network is incorporated and simulation parameters such as PDR (Packet Delivery Ratio), Energy Consumption, End-to-end delay, and Throughput are analyzed using simulation software.

Published in: 2022 10th International Conference on Emerging Trends in Engineering and Technology - Signal and Information Processing (ICETET-SIP-22)

Date of Conference: 29-30 April 2022

Date Added to IEEE *Xplore*: 15 June 2022

ISBN Information:

INSPEC Accession Number: 21843009

DOI: 10.1109/ICETET-SIP-2254415.2022.9791594

Publisher: IEEE

Conference Location: Nagpur, India

▸ ISSN Information:

References

References is not available for this d

Contents

The communication technologies have advanced significantly over the years, as a result, wireless technologies have emerged and became the most rapid and easy way to communicate. MANET is one of such wireless technology which grew in mid 1990s. It is a decentralized type of wireless network, that does not need any pre-existing infrastructure, such as routers, hubs, switch, cables in wired networks or access points in wireless networks [1]. Dynamic topology, autonomous behavior, energy constraint operation and less human intervention are some of the key features of MANET. In wireless network, security plays an important role. Achieving, safeguarding the aspects of security such as confidentiality, authentication, integrity, availability, access control, and no repudiation in a network is important. As MANET does not require any infrastructure, there is no centralized control over the communication, hence it becomes more challenging to secure such kind of network against various attacks, such as Gray hole, Blackhole, Wormhole attack, denial of service attacks, etc. It is easier to implement such type of attacks in AODV protocol. AODV is designed to be self-starting in an environment of mobile nodes, withstanding variations in behavior of network such as mobility of node, link failures and packet losses [2].

Back to Results

More Like This

Mitigating the effects of Black hole attacks on AODV routing protocol in mobile ad hoc networks
2015 International Conference on Pervasive Computing (ICPC)
Published: 2015

Secure routing protocols for mobile ad hoc networks
2016 International Conference on Information Technology for Organizations Development (IT4OD)
Published: 2016

Show More

References

References is not available for this d

References

References is not available for this d

Advanced IoT based parcel locking system

Dhiraj K Thote ; Punit Fulzele ; Swarali N Bokade **All Authors**

Abstract: Security is one of the prominent concerns with everything being digitized around us these days. One relating application of Iot based devices as result of this digitizati... **View more**

Metadata

Abstract:

Security is one of the prominent concerns with everything being digitized around us these days. One relating application of Iot based devices as result of this digitization for security of parcels is parcel locking system. In today's scenario when majority population steps out for work it becomes a problem for customers as well as delivery personnel to receive and deliver parcel on time to the right person. In case of important deliveries like passports or legal documents the customer needs to ensure safety, even if they aren't physically present to collect it. This advanced locking system discussed in this paper is effectively designed for user convenience by operating this lock by oneself through our customized website; this feature makes it unique as the entire control is in users hand without involvement of external person. This locking system reduces multiple challenges faced by logistics and increases security of parcels at the same time.

Published in: 2022 10th International Conference on Emerging Trends in Engineering and Technology - Signal and Information Processing (ICETET-SIP-22)

Date of Conference: 29-30 April 2022

Date Added to IEEE *Xplore*: 15 June 2022

ISBN Information:

ISSN Information:

INSPEC Accession Number: 21842933

DOI: 10.1109/ICETET-SIP-2254415.2022.9791760

Publisher: IEEE

Conference Location: Nagpur, India

Contents

References

References is not available for this d

I. Introduction

Due to the pandemic and also otherwise, the popularity of platforms for online shopping and deliveries has resulted in a large increase in parcel deliveries. As it significantly grew in the state of lockdown as majority of shopping by the customers was done online and products were delivered to them at various locations there was a need for provision. Not only that but also earlier when product weren't ordered using e-commerce on such a large scale, commercial products are popularly known to be shipped out from centralized locations of manufacturing or storage and have to be known to be procured in accordance with the market demand at various locations.

Sign in to Continue Reading

Authors

Figures

References

Citations

Keywords

Metrics

Back to Results

More Like This

Logistics management data security transmission system based on Internet of things technology
2021 International Conference on Intelligent Transportation, Big Data & Smart City (ICITBS)
Published: 2021

Enhanced Logistics Security Techniques Using IoT and 5G
2020 International Conference on Wireless Communications Signal Processing and Networking (WiSPNET)
Published: 2020

Show More

References

References is not available for this d

References

References is not available for this d

Performance Improvement of AODV Under Worm Hole Attack

Publisher: IEEE

Manish Devendra Chawhan ; Vedant Narayan Shrikhande ; Miss.Shivani Madelwar ; Miss.Sharvari Umredkar ; Kishor. D. Kulat ; Mrs.Bhumika Ne… All Authors

Abstract: All across the world, majority of humans rely upon wireless ADHOC network. So, it turns into the maximum priority to lessen the vulnerability of wireless network. Wireles... **View more**

Abstract:

…turns into the maximum priority to lessen the vulnerability of wireless network. Wireless networks are exposed to many distinct varieties of attacks out of which wormhole attack is most dangerous. Unlike many different attacks on ad hoc routing, wormhole attack could be very effective and cannot be avoided with cryptographic approach due to the fact intruders do now no longer modify the packet data, it replays the packets. An intentionally positioned wormhole can cause a significant breakdown in communication. An analysis was performed in this study that removed wormhole attacks from MANET using changes to the AODV routing protocol. We have used Smart Packet Detection and Prevention Technique (SPDPT) to remove Wormhole. We have examined simulation parameters such as packet delivery ratio, end-to-end delay, energy consumption, and throughput.

Published in: 2022 10th International Conference on Emerging Trends in Engineering and Technology - Signal and Information Processing (ICETET-SIP-22)

Date of Conference: 29-30 April 2022

INSPEC Accession Number: 21842937

Date Added to IEEE *Xplore*: 15 June 2022

DOI: 10.1109/ICETET-SIP-2254415.2022.9791568

ISBN Information:

Publisher: IEEE

ISSN Information:

Conference Location: Nagpur, India

Contents

I. Introduction

Mobile Ad-hoc Networks also are referred to as self-sustaining and decentralized wireless systems. MANET has capabilities like loss of significant monitoring, open medium, management, no clean protection mechanism, converting its topology dynamically, and cooperative algorithms due to those capabilities MANET can also additionally be afflicted by safety attacks. Manet are greater at risk of attacks because of Wireless links. To get admission to the continued conversation, Wireless links make it less difficult for the attacker to move withinside the network. To take part withinside the network, Mobile nodes ought to gift withinside a variety of wireless links. As there may be growing threats of attacks at the Mobile Networks, there are exceptional kinds of attacks and their consequences at the Manet to offer stable conversation and transmission. Communication is primarily based totally on a mutual belief among the nodes due to this MANET is greater open to those sorts of attacks, there may be no authorization facility, no significant factor for network management, vigorously converting topology, and confined resources.

Authors

Figures

References

Keywords

Metrics

< Previous | Back to Results

References

References is not available for this d

References

References is not available for this d

References

References is not available for this d

Flower Image Classification Using Convolutional Neural Network

Publisher: IEEE

Abstract: In the field of pharmaceutical industry, botany and agricultural there is a need of algorithm which will classify the flowers by processing its image. In this context, we... **View more**

▸ **Metadata**

Abstract:

In the field of pharmaceutical industry, botany and agricultural there is a need of algorithm which will classify the flowers by processing its image. In this context, we propose a flower classification approach based on convolutional neural network. We have applied transfer learning approach for classification of flowers. We have used VGG19 convolution neural network architecture for extraction of features. As we wanted to classify flowers in 17 different classes so we have used 17 neurons in final dense layer of VGG19 convolution neural network architecture with the use of softmax activation function. Results show that we have classified flowers with the validation accuracy of 91.1 % and training accuracy of 100%.

Published in: 2022 First International Conference on Electrical, Electronics, Information and Communication Technologies (ICEEICT)

Date of Conference: 16-18 February 2022

Date Added to IEEE *Xplore*: 10 May 2022

▸ **ISBN Information:**

INSPEC Accession Number: 21859492

DOI: 10.1109/ICEEICT53079.2022.9768635

Publisher: IEEE

Conference Location: Trichy, India

I. Introduction

About 369000 different species of flowers plants exists in the world [1]. For flower species classification the traditional feature like color, shape and texture of the flowers are used. But it is complicated and difficult to choose this feature properly. At different times and different environments features of flowers are different but the shape and color of the various flower species are same, which leads a big problem in identification. In past few years, research carried out on flowers identification includes: In [2] the authors suggested a method to place a black color cloth at the back side of the flower. But this method is not feasible and convenient. In [3] used multilevel thresholding to classify foreground and background.

References

References is not available for this d

Authors

Figures

References

Citations

Keywords

Metrics

< Previous | Back to Results | Next >

References

References is not available for this d

References

References is not available for this d

Evaluation of Bit Error Rate (BER) for OWDM System

Megha Chakole ; Mukul Didolkar ; Rutwik Uttarwar ; S.S. Dorle ; Soumitra Joshi All Authors

Abstract: In modern age due to requirement of high bandwidth and increased data transfer rates. A digital multicarrier communication system is known as Orthogonal Wavelet Division ... **View more**

Metadata

Abstract:

es. A digital multicarrier communication system is known as Orthogonal Wavelet Division Multiplexing System (OWDM). This paper proposed the implementation of the OWDM System with BPSK Modulation Scheme to evaluate Bit Error Rate for BPSK-OWDM System in presence of additive White Gaussian noise (AWGN) to achieve high performance both in bandwidth and data transfer rate. A comparison was made between the OFDM-BPSK System with OWDM-BPSK under similar conditions because of this comparison achieved improved BER as compared to OFDM-BPSK System.

Published in: 2022 First International Conference on Electrical, Electronics, Information and Communication Technologies (ICEEICT)

Date of Conference: 16-18 February 2022

Date Added to IEEE *Xplore*: 10 May 2022

ISBN Information:

INSPEC Accession Number: 21859487

DOI: 10.1109/ICEEICT53079.2022.9768526

Publisher: IEEE

Conference Location: Trichy, India

I. Introduction

In recent years, wireless digital communication has Become a necessity for communication, in mobile communication high speed and high data rate needs to be achieved and so has been the need to develop efficient modulation technique has emerged. Due to addition of AWGN the performances of the system decreases [1]. OWDM system is different from OFDM which works on the principal of frequency division multiplexing. AWGN is used to simulate background noise of the channel. This OFDM system is also used in latest technology like 4G OFDM which uses Fast Fourier Transform (FFT) and Inverse Fast Fourier Transform (IFFT) [2]–[3]. OFDM also has limitations like higher phase noise. To overcome this limitation, new system developed known as Orthogonal Wavelet Division Multiplexing (OWDM) System which works on the principal of Wavelet Division Multiplexing where the wavelet decomposition and reconstruction is a main tool for detailed analysis. The OWDM system is a Multicarrier system in which the information Bits are superimposed on n subcarriers also it follows the orthogonality (orthogonal orientation is seen between the side lobes of sub carriers) this system has better Bit Error Rate performance. Since Bit Error Rate is defined as the rate at which error occurs per transmitted bit. Here the Bit Error Rate performance is evaluated in the presence of AWGN fading channel with the equalization process (which takes place at the receiver section). A comparison is made between the BPSK OWDM and OFDM system, both of which are multicarrier systems, and the Bit Error Rate Performance is evaluated. Ideally for good communication system Bit Error Rate is expected to be as low as possible with respect to different SNR values. SNR is the ratio of signal power to noise power whose unit is decibels, to obtain SNR, author subtracted the noise quantity from desired signal. Here ratio is considered, which stands for energy per bit to noise power spectral density which is a normalized SNR ratio. It is very useful while comparing the Bit Error Rate performances of different Digital Communication Systems. The value in the ratio is referred as the signal energy associated with every individual transmitting bit and No in the ratio stands for noise spectral density. We know that the limit of reliable information transmission rate of any communication channel depends upon the bandwidth and Signal to Noise Ratio (SNR), so this principle could be used to establish bound on that can achieve reliable communication. [4]–[5].

Authors
Figures
References
Keywords
Metrics

Back to Results | Next >

References

References is not available for this d

More Like This

Performance evaluation of phase shift keying modulation technique using BCH code, Cyclic code and Hamming code through AWGN channel model in communication system
The 3rd International Conference on Information Sciences and Interaction Sciences
Published: 2010

Investigation of double way-quadrature phase shift key (DW-QPSK) for digital communication consumer applications
2016 13th IEEE Annual Consumer Communications & Networking Conference (CCNC)
Published: 2016

Show More

References

References is not available for this d

References

References is not available for this d

LoRa Communication based Wireless Sensor Monitoring system

K.P. Kamble All Authors

Abstract: The Internet of Things [IoT] technology is recently used to autonomously collect and send data via a wireless channel. However, as the name implies, the primary requireme... **View more**

Abstract:

The Internet of Things [IoT] technology is recently used to autonomously collect and send data via a wireless channel. However, as the name implies, the primary requirement is Internet access, which is the main limitation for low-network locations. To send data from Sender to Receiver, the system employs LoRa Modules, mostly Ra-02, depending on the location. The sender can process the sensor data and send it over the personal network by utilizing LoRa (Long Range) Modules and the ESP8266. Solar panels can also be used for even reduced power usage. The data obtained will then be updated by the Real-Time Database on the Web Server through the Internet via Wi-Fi or GSM/GPRS Modem. Stored data may be accessed via a Web Application (Dynamic Website) on a mobile device. On both the transmitter and receiver sides, a low power OLED display is linked to provide real-time status. Due to the lack of power source on the transmitter side, we will power up utilizing a solar panel, charge controller, and battery. The solar panel will be 4V and the charge controller will be TP4056. The battery rating of 2200mAh is determined by the amount of power consumed.

Published in: 2022 International Conference on Sustainable Computing and Data Communication Systems (ICSCDS)

Date of Conference: 07-09 April 2022

Date Added to IEEE *Xplore*: 27 April 2022

ISBN Information:

INSPEC Accession Number: 21725390

DOI: 10.1109/ICSCDS53736.2022.9760796

Publisher: IEEE

Conference Location: Erode, India

Contents

I. Introduction

The internet's growth is entirely dependent on itself, therefore its non-availability is a constraint. To overcome this shortcoming, the idea of developing a wireless sensor network that does not require internet access or networks such as GSM (Global System for Mobile Communications), CDMA, LTE, and so on. This wireless sensor network design is made up of nodes and a gateway, and it attempts to effortlessly transfer any sensor data across a wide range without any internet connectivity.

Authors

Figures

References

Citations

Keywords

Metrics

< Previous | Back to Results | Next >

References

References is not available for this d

References

References is not available for this d

References

References is not available for this d

Process Improvement of Finishing Machine by Real Time Monitoring using IoT

Publisher: IEEE

Yogita Dubey ; Rasika Patil ; Sanika Sutaone ; Sumant Kundu ; Akshata Mhaski **All Authors**

Abstract: At present many small-scale fabric industries finishing machines are not automated, Human intervention is required for analysis and highlighting the technical parameters ... **View more**

Abstract:

Human intervention is required for analysis and highlighting the technical parameters deviations. In fabric industry parameter analysis like temperature, water level, humidity and pressure has to be done and usually it's done manually. This led to high workload on engineers and operators for parameters logging and communication to engineering department and also its time consuming for maintenance team members to get different types of analysis, e.g., down time %, Repeated breakdown % etc, which may lead to poor analysis process for defectives in fabric. So, to overcome this problem in fabric industry, process improvement can be done by real-time monitoring of finishing machines using IOT. This paper presents the technique to make the finishing process of fabric industry automated i.e. to do real time monitoring of finishing process, using IoT technology. By automation of the finishing process there will be good analysis of poor fabric, and this will also prevent fabric wastage. This process saves human power, as the output is directly received through WhatsApp or Email in form of graphs which prevent manual analysis of parameter. Since the finishing process is automated the cost is controlled by reduction in rejection of fabric and it also increases productivity of machines and human resource. This leads to smart working practices by eliminating paper works and time-consuming methods.

Published in: 2022 IEEE Delhi Section Conference (DELCON)

Date of Conference: 11-13 February 2022

Date Added to IEEE *Xplore*: 20 April 2022

ISBN Information:

INSPEC Accession Number: 21776975

DOI: 10.1109/DELCON54057.2022.9753051

Publisher: IEEE

Conference Location: New Delhi, India

References

References is not available for this d

Contents

I. Introduction

IoT applications provide new paradigms to improve productivity and optimize expenses in fabric manufacturing industries. Till date human intervention is required for analysis and highlighting the technical parameters deviations. Manual monitoring of machine parameters can lead to human errors which can further result in major defects or accidents [1]. In fabric manufacturing industries this can lead to defects in the fabric material. At present many small-scale fabric industries finishing machines are not automated, Human intervention is required for analysis and highlighting the technical parameters deviations. In fabric industry parameter analysis like temperature, water level, Humidity and pressure has to be done and usually it's done manually. This led to high work load on engineers and operators for parameters logging and continuous reading in Continued Sign in to Continue Reading ering department and also its time consuming for maintenance team members to get different types of analysis, e.g., down time %, Repeated breakdown % etc, which may lead to poor analysis process for defectives in fabric. So, to overcome this problem in fabric industry process improvement can be done by real-time monitoring of finishing machines using IOT. The aim of this paper is to use IoT to obtain real time data for monitoring and control of fabric manufacturing process. Internet Of Things helps to capture data and provide simple and hidden insights to decision making authorities. Overall equipment effectiveness can be achieved by real time monitoring physical parameters of production process. Sustainability of the plant can also be enhanced significantly.

Back to Results

More Like This

An Analysis of Fabric Defect Detection Techniques for Textile Industry Quality Control
2023 World Conference on Communication & Computing (WCONF)
Published: 2023

Internet of Things applied to monitoring fermentation process of Cocoa at the Piura's mountain range
2017 CHILEAN Conference on Electrical, Electronics Engineering, Information and Communication Technologies (CHILECON)
Published: 2017

Show More

References

References is not available for this d

References

References is not available for this d

Vaishali Niranjane ; Utkarsha Shelke ; Saili Shirke ; Srushti Dafe All Authors

Abstract: The Objective of this research is to Design and build a IoT Base Digital Production Counting system. It decreases the likelihood of counting errors and improve counting a... **View more**

Metadata

Abstract:

The Objective of this research is to Design and build a IoT Base Digital Production Counting system. It decreases the likelihood of counting errors and improve counting accuracy, which is used in big enterprises since it outperforms human techniques. Production manufacturing and counting can be a time-consuming process that includes quality control, large-scale analysis, and quantity measurement. The classification especially supports the quantity factor, or production rate which is accomplished by human resource present in industry with having either a max or min rate of production but keeping the exact count throughout the manufacturing process is still impossible. The quantity outcome is an important factor in steadfast the industry's economic growth and financial health. As IoT is quickly growing as the next phase of the Internet's development, it's becoming more necessary than ever to understand the several prospective domains for IoT operations. Since the previous few decades, technology has played an increasingly important role in our daily lives. As IOT is developed, industries can increase productivity and data collection efficiency. In order to improve production demographics this project aims to count the multiple products which are counted by IR sensor using IR interruption concept and Microcontroller is used here to keep track of a huge number of items and display on a LCD display as well as upload the data on web via Node MCU (IOT Module)

Published in: 2022 International Conference on Electronics and Renewable Systems (ICEARS)

Date of Conference: 16-18 March 2022

Date Added to IEEE *Xplore*: 13 April 2022

ISBN Information:

INSPEC Accession Number: 21688414

DOI: 10.1109/ICEARS53579.2022.9752399

Publisher: IEEE

Conference Location: Tuticorin, India

References

References is not available for this d

Contents

I. Introduction

The main aim of this research is to expose the IoT Base Digital Production Counting system. This is the main subject of this research. It reduces labour costs and saves time in industries. As internet is widely used in a variety of industries, including transportation, healthcare, agriculture, and manufacturing. The evolution of the IoT has become indispensable in our daily lives. IoT network refers to collections of interconnected devices without interruptions of human involvement. [1] It permits machine-to-machine and machine-to-human communication, and it is widely employed in industrial process. Manufacturing companies may boost production and data collecting efficiency by implementing IoT technologies. IoT also provides the manufacturing business with numerous benefits and conveniences. So with the application of IoT technologies, industries are able to increase productivity. Using IoT and IR sensors with a microcontroller and a node MCU to count products in industries [12It is now possible to acquire huge amounts of data for counting products in industry because of the extension of IoT devices such as sensors, security systems, trackers. The Internet of Things is quickly becoming one of the most essential technologies for improving the efficiency of industrial processes.

Back to Results

More Like This

A Study of Green Development Mode and Total Factor Productivity of the Food Industry Based on the Industrial Internet of Things
IEEE Communications Magazine
Published: 2018

The Research on Monitoring of Discrete Manufacturing Process Based on Internet of Things
2013 IEEE International Conference on Green Computing and Communications and IEEE Internet of Things and IEEE Cyber, Physical and Social Computing
Published: 2013

Show More

References

References is not available for this d

References

References is not available for this d

Design of Substrate Integrated Waveguide Technology Supported Dual Band MIMO Antenna

Publisher: IEEE

Sujata S. Chiwande ; Piyush Meshram ; Abhishek Charde ; Shreya Bhave All Authors

Abstract: This paper introduces an outline of a Dual Band MIMO antenna for applications based on Substrate Integrated Waveguide technology (SIW). SIW has acquired a valuable and va... **View more**

Metadata

Abstract:

This paper introduces an outline of a Dual Band MIMO antenna for applications based on Substrate Integrated Waveguide technology (SIW). SIW has acquired a valuable and various kinds of researches, extending from microwave to optical bands due to their outstanding properties such as low costs, low losses, small footprints followed by incorporating with other types of PCBs. SIW structures can be used to prevail the above-mentioned advantages readily compared to various kinds of technologies such as co-planar waveguides, conventional waveguides, micro-strip transmission lines and so on. The indispensable cavity mode is designed on Substrate integrated waveguide to resonate at 2.4 GHz. Moreover, the 2 nd and 3 rd mode are altered and combined carefully by placing a via inside the cavity to allow the coverage of wideband in 5 GHz WLAN band.

Published in: 2022 International Conference on Electronics and Renewable Systems (ICEARS)

Date of Conference: 16-18 March 2022

INSPEC Accession Number: 21688344

Date Added to IEEE *Xplore*: 13 April 2022

DOI: 10.1109/ICEARS53579.2022.9751845

ISBN Information:

Publisher: IEEE

Conference Location: Tuticorin, India

Contents

I. Introduction

Substrate Integrated Waveguide technology shows a prominent approach for performance and combination of wireless systems, microwave and millimetre wave components. Substrate Integrated Waveguide technology allows active element, passive structures, and antennas to be incorporated into one substrate, eliminating transitions and lowering losses. SIW technology unites the advantages of classical micro-strip circuits (low weight, easy fabrication, low cost, compact size) and metallic waveguides. It appears that Substrate Integrated Waveguide technology is designed to become the standard for the implementation of cost-effective millimetre wave systems in the near future. Radiation, conductor losses, and dielectric losses are the three mechanisms that generate losses in Substrate Integrated Waveguide.[1] The metal used (usually copper), the height of the Substrate Integrated Waveguide, and the roughness of the metal all affect conductor losses. These losses are difficult to regulate since they are dependent on the quality of the substrate's copper lamination. In contrast to micro-strip lines, one of the most significant restrictions of Substrate Integrated Waveguide structures is the single-mode bandwidth (which is limited to one octave) and breadth (which depends on the cut off frequency and the dielectric substrate).[2][3]

References

References is not available for this d

Authors

Figures

References

Keywords

Metrics

Back to Results | Next >

References

References is not available for this d

References

References is not available for this d

Design and Fabrication of Portable Insulation Box for Medical Applications

Minal Keote ; Janvi Patki ; Amisha Jain ; Rashmi Keote All Authors

Abstract: As per the research, the number of diabetic patients in India is very high which makes it the second most diabetes affected country in the world. The insulin pen is large... **View more**

Abstract:

As per the research, the number of diabetic patients in India is very high which makes it the second most diabetes affected country in the world. The insulin pen is largely used to limit the effect of this disease. The insulin should be stored at low temperature and for this purpose a portable insulin box which provides low temperature using solar power has been proposed. The temperature of the insulin box can be monitored by the temperature sensor which is placed on the box.

Published in: 2022 International Conference on Electronics and Renewable Systems (ICEARS)

Date of Conference: 16-18 March 2022

Date Added to IEEE *Xplore*: 13 April 2022

▸ **ISBN Information:**

INSPEC Accession Number: 21688331

DOI: 10.1109/ICEARS53579.2022.9751941

Publisher: IEEE

Conference Location: Tuticorin, India

Contents

This box can be carried along everywhere and hence called portable insulin box. The system provides a solution to control and monitor the temperature of the insulin box. The temperature of the insulin box should be low which is based on the storage temperature of insulin pen. The temperature module which is placed in front of insulin box allows to set the required temperature. The most important component of this project is the Peltier module. The peltier module is used to cool down the temperature of the Insulin box. Through this module, one heat sink sends the cool air inside the box and another heat sink pushes the hot air outside the insulin box. It works on the principal of solar panel which convert light energy into electric energy.

Authors

Figures

References

Keywords

Metrics

Back to Results

References

References is not available for this d

References

References is not available for this d

References

References is not available for this d

IoT Based Access Control System for Vehicles

Tejas Mankar ; Mithilesh Bhorkar ; Aniket Shende ; Minal Ghute **All Authors**

Abstract: In modern society there is a lot of confidentiality inside a firm, which means only an authorized person is allowed inside the premises. To maintain security IoT based Ve... **View more**

▸ **Metadata**

Abstract:

authorized person is allowed inside the premises. To maintain security IoT based Vehicles Access Control System is useful. While creating it the main purpose is security and handling of the data which is done by an online portal. The data of person is stored inside a cloud server and if the data scanned by the RFID is matched to the data stored within the system the doors will get open and the vehicle is allowed inside the premises. While using RFID card uniqueness of each card is ensured so that it handles only one identity. Initially stored RFID unique number inside the Arduino is cross checked for entering inside the premises. Proteus software is used for designing of circuits.

Published in: 2022 Second International Conference on Artificial Intelligence and Smart Energy (ICAIS)

Date of Conference: 23-25 February 2022

INSPEC Accession Number: 21681104

Date Added to IEEE *Xplore*: 30 March 2022

DOI: 10.1109/ICAIS53314.2022.9742983

▸ **ISBN Information:**

Publisher: IEEE

Conference Location: Coimbatore, India

Contents

I. Introduction

In case of vehicles parking in parking lot it is very much essential to ensure that only authorized vehicles are allowed in the reserved parking place, which can be ensured using the card based access control system [1] –[3]. The traditional access control systems which is card-based have various drawback to avoid it new access control system is proposed.

Authors

Figures

References

Keywords

Metrics

Back to Results | Next >

References

References is not available for this d

References

References is not available for this d

Modern E-Trolley For Goods Purchase With Inventory Management Using Android Application

Dhiraj Thote ; Punit Fulzele ; Rajas Nimishe ; Manjeet Thakur ; Shantanu Khasale ; Parth Chinchalkar All Authors

Abstract: The traditional way of shopping will always be in trend, one problem which is always faced by customers is waiting in long queues. Because of this, customers waste a lot ... **View more**

Abstract:

The traditional way of shopping will always be in trend, one problem which is always faced by customers is waiting in long queues. Because of this, customers waste a lot of time which leads to adding some innovation to the existing system. This proposed model will improve the existing shopping system. In this E-trolley, a connection between Arduino and android application through Bluetooth has been established. Arduino is connected with a barcode scanner and using it the user will scan the barcode of the product and the application will show the details of the scanned product. Further, this data will be shared in the database and after that user will be able to make payment through any online payment mode. The stock data which is present in the database will be updated after successful payment. The main aim of the proposed solution is to reduce the long queues and make the whole process hassle-free for the customers which will lead to more profitability in the store.

Published in: 2022 Second International Conference on Artificial Intelligence and Smart Energy (ICAIS)

Date of Conference: 23-25 February 2022

Date Added to IEEE *Xplore*: 30 March 2022

ISBN Information:

INSPEC Accession Number: 21684620

DOI: 10.1109/ICAIS53314.2022.9742900

Publisher: IEEE

Conference Location: Coimbatore, India

Contents

I. Introduction

As known that most of the cities consist of supermarkets and malls, in these markets, there are cash counters where the customer needs to go for paying the bill of products they have added to their trolley. In recent times shopping at these markets has become a hectic job, and there are several people at these shopping markets specially in holidays, festival and when there are special discount days and because of this there is a huge rush at the billing counters. Therefore, customers need to wait in a long queue. Because of this situation, a lot of customer's time is wasted and the supermarkets or malls may face huge losses.

References

References is not available for this d

Authors

Figures

References

Citations

Keywords

Metrics

Back to Results

References

References is not available for this d

References

References is not available for this d

IoT based Face Mask Detection System

Minal Suresh Patil ; Shital Telrandhe ; Ajay Mawaskar ; Rupesh Gharde ; Abhishek A. Madankar ; Manthan Sawarkar All Authors

Abstract: The COVID-19 virus was first reported in December 2019 in China. Since then, it has created havoc on global level by causing health and financial crisis. The novel corona... **View more**

Metadata

Abstract:

The COVID-19 virus was first reported in December 2019 in China. Since then, it has created havoc on global level by causing health and financial crisis. The novel corona virus is continuously evolving into new variants of virus and still spreading in every part of the world. The virus is spread mostly by the droplets transferring from the infected person to an uninfected person. The only direct method of preventing such transfer of droplets can be done by washing of hands, avoiding contact with nostrils, eyes and mouth. Only complete vaccination of citizens can help in containment of virus till then use of face mask and social distancing has been made mandatory by authorities. This project proposes a contactless face mask detection model based on machine learning and image processing technology. It will follow the protocols of social distancing. This project will be helpful in accurately identifying whether a person is wearing a mask properly or not. This model can be easily installed in the entrance of ATMs, malls, educational institutions, offices and in the entrance of public offices. Being a contact less model it will effectively reduce the need of having a manual way of detection and will reduce the spreading of disease to further people. It is highly effective and cheap model as all the tools required for this project are free of cost and easily available online. Proposed model can be easily used on low end computers like Raspberry Pi. The model will encourage people to continuously wear mask in correct manner.

Published in: 2022 Second International Conference on Artificial Intelligence and Smart Energy (ICAIS)

Date of Conference: 23-25 February 2022

Date Added to IEEE *Xplore*: 30 March 2022

ISBN Information:

INSPEC Accession Number: 21681157

DOI: 10.1109/ICAIS53314.2022.9741835

Publisher: IEEE

Conference Location: Coimbatore, India

References

References is not available for this d

Contents

I. Introduction

The Corona virus or the COVID-19 virus is a member of SARS virus family which was originated from WUHAN, CHINA and was first reported in December 2019 [1]. This disease causes infections in respiratory tract and can range from mild to lethal. It is a contagious disease. The virus has evolved into multiple variants [2]. A fatality caused by this disease in old people is high. Furthermore, it can permanently damage lungs as per the reports. Also, it has after effects like fatigue, eye disease like mucormycosis, loss of appetite, body pain, chest pain and muscle pain in cured patients [3–4]. With an incubation period of around 15days the disease can show a symptom after a fortnight which makes it's difficult to diagnose [5]. Hence the authorities have advised people to be quarantined if came into contact with affected person. Its uncontrollable spread has turned out to be a pandemic and is still continuously spreading until now everywhere in world, causing a direct severe health crisis and an indirect financial crisis by long term lockdowns all around the world [6 –8]. Every government & health organization has made eradication of COVID-19 virus as their top priority. So to control the pandemic from spreading preventing it at first is very important as prevention is better than cure [9]. Vaccination all over world has begun yet with an average efficacy over 60% it cannot guarantee one will become immune to this disease after injecting anti-bodies through vaccines [10]. Hence containing it with all possible methods is very important. The disease spread through droplets spread by an infected person because of coughing or sneezing hence it's mandatory for both infected and uninfected person to wear mask [11–12]. The droplets usually, enter the body through nose, mouth and eyes. Multiple guidelines have been issued by WHO (World Health Organization) for prevention of COVID-19 which includes regularly wearing face mask, regularly checking body temperature, sanitization with alcohol based, sanitizer, avoiding crowds and public gatherings, maintaining distance with other individuals if possible. Thus, monitoring individuals that are wearing the mask or not is more significant. Hence the main aim of project is to create a contactless monitoring system that would be beneficial in reducing the spread of this infectious disease and will encourage people to use face masks properly & it can make any public or working space a safer environment [13 –15].

Sign In to Continue Reading

Authors

Figures

References

Keywords

Metrics

< Previous | Back to Results | Next >

Internet of Things for Diagnosis of Alzheimer's Disease: A Multimodal Machine Learning Approach Based on Eye Movement Features
IEEE Internet of Things Journal
Published: 2023

Internet of Things and Synergic Deep Learning Based Biomedical Tongue Color Image Analysis for Disease Diagnosis and Classification
IEEE Access
Published: 2021

Show More

References

References is not available for this d

References

References is not available for this d

Design & implementation of fine ADC block in 8-b folding and interpolation

Rahul P. Kamdi ; Sandeep Kumar Tiwari ; Aniket Pathade **All Authors**

Abstract: Analog design like ADCs, DACs, and PLLs are the crucial analog circuits. Achieving the low supply voltage in data converters design is the challenge task. At the same tim... **View more**

Metadata

Abstract:

Analog design like ADCs, DACs, and PLLs are the crucial analog circuits. Achieving the low supply voltage in data converters design is the challenge task. At the same time achieving the desired conversion rate, resolution, sampling frequency and power dissipation are becoming crucial.Now a day the demand of designing low voltage, high speed, low power consumption, less area and low-cost ADCs is increasing. To fulfill these requirements in designing of ADCs are crucial for many innovative design applications. In this work, folding and interpolation ADC architecture using trans-resistance amplifier followed by current steering folding amplifier is designed and implemented in UMC CMOS 180nm technology. This ADC provides moderated resolution.In several applications Moderated resolution ADCs with low voltage, high speed and low power are in use. Also, the demand of low voltage ADCs is increasing in the field of embedded application. This motivates us to design the folding and interpolating ADC architecture. Furthermore, synchronizing the coarse and fine converters bits is challenging task in folding and interpolation ADCs. Hence, the main aim of my work is to design low voltage folding and interpolation ADC which operates at the input frequency of85 MHz using the less silicon chip area.

Published in: 2022 Second International Conference on Artificial Intelligence and Smart Energy (ICAIS)

Date of Conference: 23-25 February 2022

Date Added to IEEE *Xplore*: 30 March 2022

ISBN Information:

INSPEC Accession Number: 21684532

DOI: 10.1109/ICAIS53314.2022.9743073

Publisher: IEEE

Conference Location: Coimbatore, India

Contents

I. Introduction

In the recent years, there are mainly two structures investigated of folding circuit. First one is the conventional folding amplifier and second one is the current steering folding amplifier. In this thesis work current steering folding amplifier is used as an analog pre-processing block. The power consumption and delay of the current steering folding amplifier block is less compared to the conventional folding amplifier block. At the same power consumption, working speed of the current steering folding amplifier circuit is higher than conventional folding amplifier.

Authors

Figures

References

Keywords

Metrics

References

References is not available for this d

Back to Results

References

References is not available for this d

References

References is not available for this d

Hand Gesture Recognition to Facilitate Tasks for the Disabled

Swati Nitnaware ; Ashutosh Bagde All Authors

Abstract: Deaf and dumb people communicate with gestures. Number of applications have been developed using gesture recognition computer vision, machine learning etc. A simple techn... **View more**

Abstract:

Deaf and dumb people communicate with gestures. Number of applications have been developed using gesture recognition computer vision, machine learning etc. A simple technique to recognize gestures is presented in this paper. Here Python libraries such as Opencv, Numpy are used. The technique involves capture of live gestures and recognition of the same using Opencv functions. Parameters such as the area ratio and convexity defects are considered to differentiate between different gestures. The system will also display text message and an audio file will be used for vocalizing the different gestures. A functionality where gestures are recognized for entertainment purpose is presented. This can be of use to blind people for the purpose of entertainment such as playing music, radio or listening to news. Here Multiprocessing library is used. The tasks are assigned to specific gestures.

Published in: 2022 Second International Conference on Artificial Intelligence and Smart Energy (ICAIS)

Date of Conference: 23-25 February 2022

INSPEC Accession Number: 21681187

Date Added to IEEE *Xplore*: 30 March 2022

DOI: 10.1109/ICAIS53314.2022.9743056

▸ **ISBN Information:**

Publisher: IEEE

Conference Location: Coimbatore, India

I. Introduction

Gesture recognition systems are making their way in numerous applications and provide a starting point for the advancement in smart appliances as well as IoT enabled devices. A gesture recognition system is presented here which recognizes some predefined gestures to perform tasks. The tasks defined here are related to opening various pages on the internet. The focus here is on enabling the user to open entertainment related websites with the use of simple gestures. Human Computer Interaction is based on working together of human and computer. Researchers have observed many ways in which user can interact with a computer and be able to design different types of applications. Thus the aim here is to develop a system which identifies different gestures and generates audio output along with text.

Authors

Figures

References

Keywords

Metrics

Back to Results | Next >

References

References is not available for this d

References

References is not available for this d

References

References is not available for this d

A Mobile App for Smart Electricity Usage Monitoring

Anagha Choudhari ; Jyotsna Gawai ; Arpit Lekurwale ; Sejal Ranglani ; Pankhudi Dhongde All Authors

Abstract: Electricity has a very important role in our lives. In the whole world, India has the third highest consumption of electricity and electricity is now available even in re... **View more**

Metadata

Abstract:

Electricity has a very important role in our lives. In the whole world, India has the third highest consumption of electricity and electricity is now available even in remote and rural areas. A vast government organization works behind the billing process of electricity via meters installed. The electricity bill is received at the end of the month but often due to glitches and irresponsible use of electricity, some people may get the shock of their lives after receiving the bill. The traditional system which is currently in place is tedious, the proposed app is cost-effective as well as time saving. The highlights of the project are that this app will give the statistical data of electricity used while simultaneously uploading the meter readings in the app and will also monitor the power consumption, Daily usage will be known to the user and this app would also provide the value of electricity units. User would be able to know the electricity bill till any time of the month and in addition to this, a report in the form of statistics and numbers will be updated daily in a journal. The prime reason behind developing such an app is to create an overall awareness about amount of electricity usage and consumption.

Published in: 2022 Second International Conference on Artificial Intelligence and Smart Energy (ICAIS)

Date of Conference: 23-25 February 2022

Date Added to IEEE *Xplore*: 30 March 2022

ISBN Information:

INSPEC Accession Number: 21684595

DOI: 10.1109/ICAIS53314.2022.9742787

Publisher: IEEE

Conference Location: Coimbatore, India

Contents

I. Introduction

Electricity has become one of the most essential components in the modern world. At this point humans can't imagine their lives without electricity and the appliances that work on it. Even rural areas have electricity facilities these days, as it has become a necessity in our lives. Thus, the government has set up a vast board of organization for the billing and payment purposes. Since India is a very vast and populated country, electricity theft and mistakes in electricity bills have become a common problem. Electricity is already quite expensive these days, especially for middle class families, and thus paying more than its original cost can burn a hole in anyone's pocket. The old and traditional method of electricity billing is quite tedious, and its generally very hard to detect any mistakes in the bills, that's the reason behind introducing the proposed app. This app is created through flutter app, using Dart language, which is capable of monitoring the daily electricity usage and also promises to give an insight about the pattern of electricity usage.

Authors

Figures

References

Citations

Keywords

Metrics

Back to Results | Next >

References

References is not available for this d

References

References is not available for this d

References

References is not available for this d

Sustainable Water Management using Internet of Things

Vaishali. B Niranjane ; Ashish Bhagat ; Krushil M. Punwatkar ; Kinnari Chaurey ; Pornima Niranjane **All Authors**

Abstract:A water management system with the Internet of things approach is proposed for a framework, where a water network consisting of water pumps and valves at each node is con... **View more**

Abstract:
A water management system with the Internet of things approach is proposed for a framework, where a water network consisting of water pumps and valves at each node is connected to water tanks provided with level sensors which are controlled by an ESP-32 microcontroller which acts as an IoT platform. Output has been observed for different situations based on water availability of tanks. The whole process has been monitored through the blynk app. This research can be used to replace the conventional methods and would be more time-efficient, cost-effective easily monitored, and completely autonomous. This design is useful in many applications of water, sanitation, and industrial projects.

Published in: 2022 4th International Conference on Smart Systems and Inventive Technology (ICSSIT)

Date of Conference: 20-22 January 2022

Date Added to IEEE *Xplore*: 25 February 2022

ISBN Information:

INSPEC Accession Number: 21707398

DOI: 10.1109/ICSSIT53264.2022.9716267

Publisher: IEEE

Conference Location: Tirunelveli, India

Contents

To meet the ever increasing demand of water supply we cannot totally depend on groundwater sources, orthodox and outdated water management systems and uneven rainfalls. Thus there is a need for an effective water management system which can deal with these types of situations effectively and efficiently. To deal with the ever-increasing demand for water, pipelines and tanks have been constructed across the cities, towns, and villages. For a particular framework consisting of water tanks and pipelines when there is sudden shortage of water in one of the tanks due to excessive usage of water. The current way of solving this problem was manually checking the water level and diverting the water from other tanks to these tanks. If these method have not been done in time then people are forced to depend on other water sources such as groundwater and water tankers. But erroneous management of water supply leads to major water crisis [4] [5]. With the help of a proper water management system based on geo-information and IOT, We can try to minimize the problem with an effective and efficient way. [13] The main objective of our research is to provide water to water deficient tanks by transferring water from water available tanks with the help of Internet of Things.[17] To demonstrate this process we have chosen a group of 4 different tanks which is equipped with water level sensors and water pumps and connected to a network with valves connected at each node. These sensors, motors and valves are connected to ESP-32 which acts as a IoT platform for this research, The ESP-32 has an integrated Wi-fi module with the help of this we have connected our project to an IoT cloud to monitor the whole process from anywhere and any period of time. LCD is also connected to the ESP-32 to get alternate real time updates of the process.

References

References is not available for this d

Authors

Figures

References

Keywords

Metrics

< Previous | Back to Results | Next >

References

References is not available for this d

References

References is not available for this d

A comprehensive review of Lung nodule identification using an effective Computer-Aided Diagnosis (CAD) System

Publisher: IEEE

Nivedita A Pande ; Dinesh Bhoyar **All Authors**

Abstract: Lung cancer is a nothing but abnormal swelling of lung tissues and could be a life threatening one. As per statistics, it is responsible for more deaths than any other ty... **View more**

Abstract:

Lung cancer is a nothing but abnormal swelling of lung tissues and could be a life threatening one. As per statistics, it is responsible for more deaths than any other type of cancer. It is important to identify and treat this anomaly from the patient's perspective. For identifying the tumour cells from CT scans, numerous image-processing and soft-computing procedures are used. CT scan images are mostly used in the image processing since these are high quality and clear images with more ppi (pixel per inch). Using this method, small nodes of tissues (nodules) can be found. In primary finding of lung cancer, patient's probabilities of existence are increased. Hence, an effective CAD system for lung tumour detection has been projected. This system comprises three points: initial level processing, segmentation and classification of nodules. The study of lung disorders requires accurate segmentation of lung images which is very important in detecting lung cancer. Lung images contains noise and weak boundaries so, accurate detection of lung nodule is very difficult or challenging task. This paper covers the comprehensive review of methods used for lung nodule detection.

Published in: 2022 4th International Conference on Smart Systems and Inventive Technology (ICSSIT)

Date of Conference: 20-22 January 2022

Date Added to IEEE *Xplore*: 25 February 2022

▸ **ISBN Information:**

INSPEC Accession Number: 21707416

DOI: 10.1109/ICSSIT53264.2022.9716327

Publisher: IEEE

Conference Location: Tirunelveli, India

Contents

I. Introduction

As per World Health Organization (WHO), nearly 10 Million people have died in the year 2020 because of Cancer. The highest amongst these were because of Lung cancer - 1.80 Million or 18%. The Tumours are classified into two categories - non cancerous and cancerous. This infection is named metastasis. Lung cancer can be classified into two forms, one is small cell lung cancer (SCLC) and another is non-small cell lung cancer (NSCLC)[1]. Non-small cell lung cancer is more common than SCLC and it generally raises and spreads very gradually. SCLC is almost related with smoking and grows more speedily and produce large tumours that can spread broadly. Cancer cells frequently start increasing in the bronchi close to the mid of the chest.

Authors

Figures

References

Citations

Keywords

Metrics

References

References is not available for this d

Back to Results

References

References is not available for this d

References

References is not available for this d

Analysis of Greenness in Urban Cities Using Supervised and Unsupervised Classification

Nita Nimbarte, Shraddha Sainis, and Sanjay Balamwar

Abstract Satellite images are widely used in urban planning and growth analysis with different technology being developed. A remotely sensed image is at first pre-processed to remove anomalies from it, thus resulting in a clear and informative image. Image classification is categorized into two techniques, namely supervised and unsupervised techniques. Both the techniques give different outputs and accuracy parameters. This paper describes the analysis of supervised and unsupervised techniques of remotely sensed images for land cover classification and to evaluate greenness in terms of the area over a period of time. Both the methods are used for object detection and classification. The input images were enhanced using the histogram equalization technique and then segmented using supervised and unsupervised classification with the help of ERDAS software. After segmentation or image classification results were analyzed to give the exact measure of greenness in terms of area in hectares or square kilometers calculated over years.

Keywords ERDAS imagine software · Greenness analysis · Histogram equalization · Image processing · Supervised classification · Unsupervised classification

1 Introduction

In the present global situation, maintaining green environment in dense urban area is of utmost importance. Decreasing greenness in urban directly affects the environment quality. Urban green space is known to provide ample benefits to human beings. As many countries all around the world desire to get updated with the latest geographical

N. Nimbarte (✉) · S. Sainis
Yeshwantrao Chavan College of Engineering, Nagpur, India

S. Balamwar
Maharashtra Remote Sensing Applications and Centre, Nagpur, India
e-mail: sanjay.balamwar@mrsac.maharashtra.gov.in

S. Smys et al. (eds.), *Computational Vision and Bio-Inspired Computing*,
Advances in Intelligent Systems and Computing 1420,
https://doi.org/10.1007/978-981-16-9573-5_48

information and activities of their area, this kind of data help the respective authority in the Bureaucracy to plan the development of a particular place geographically [1].

Peijun Du et al. reported the urgency of hybrid approaches of environment analysis of different parameters like vegetation, change detection, land cover, water monitoring, and designed hybrid system for environmental analysis. The effectiveness of this system is confirmed through the case studies [1]. Conghong Huang et. al. described health benefits to urban residents by analyzing the change in green space of megacities from the year 2005 to 2015. The author used 10,823 sights of Landsat images and applies random forest classifier through the google earth engine to map land covers. By increasing urban green spaces directly increased health benefits in megacities [2]. Mugiranez et al. [3] demonstrated a hybrid approach using support vector machines (SVM) and rule-based methods for object-based multi-stage classification. It gives an analysis of actual land cover by using different challenging parameters like low-density areas, roads, informal settlements, and lowland agriculture. The classification accuracy improved by geometric ruleset, greenness density indices, and urban density indices. Researcher [4–7] reported a survey of different enhancement techniques for more suitable outputs for further analysis. The authors described many histogram-based methods for image enhancement. The outcome of these methods may be under contrast or over contrast; every technique has its pros and cons. Jalobenu et al. [8] discussed adaptive Gaussian model automatic algorithm for image enhancement. The algorithm gives good results on high-resolution satellite images. Maximum Likelihood Estimator (MLE) is used to estimate measuring parameters. The author proposed a wavelet-based deconvolution hybrid approach to enhance the outcomes. Patel et al. [9] described that weighted histogram equalization with a recursively separated method. This method preserves scalable brightness due to its recursive nature. The different histogram equalization-based methods were compared through experimental study and error estimation parameters. Šastný and Minarík [10] described different filtering pre-processing methods for object detection. The author reported that speed and accuracy are opposing requirements for edge detection. The object momenta gives good results with a 74% rate of objects recognition. Author [11, 12] reviewed classification methods and presents their own advantages and disadvantages. The research work [13, 14] presented analysis of image classification techniques through different image modalities. Image segmentation techniques [15–18] are used to segment area of interest. Segmentation based image classification algorithms has less computational complexity as compare to pixel level classification method. The classification methods are categories into automatic, manual, and hybrid approaches. Most of the methods are developed using automatic categories. This work presents an analysis of change in the greenness of urban cities for different years. The setup of this paper is stated as: Sect. 2: describes image data used for evaluation and experimentation done through ERDAS software. Section 3: briefly describes the pre-processing method for image enhancement and supervised and unsupervised methods for further classification. Section 4: gives the analysis of classification results. Finally, Sect. 5: ends with the conclusion.

2 Material and Software

In this paper, the sample input images are collected from Google Earth of size 1280 X 784 of Location near Nandanvan Area, Nagpur as shown in Fig. 1. ERDAS IMAGINE software is used [19–21] for geospatial data processing. This software package is used to analyze different imagery, geospatial imaging, and vector data. It is the best software for a vast amount of information extraction and also supports spatial modeling systems.

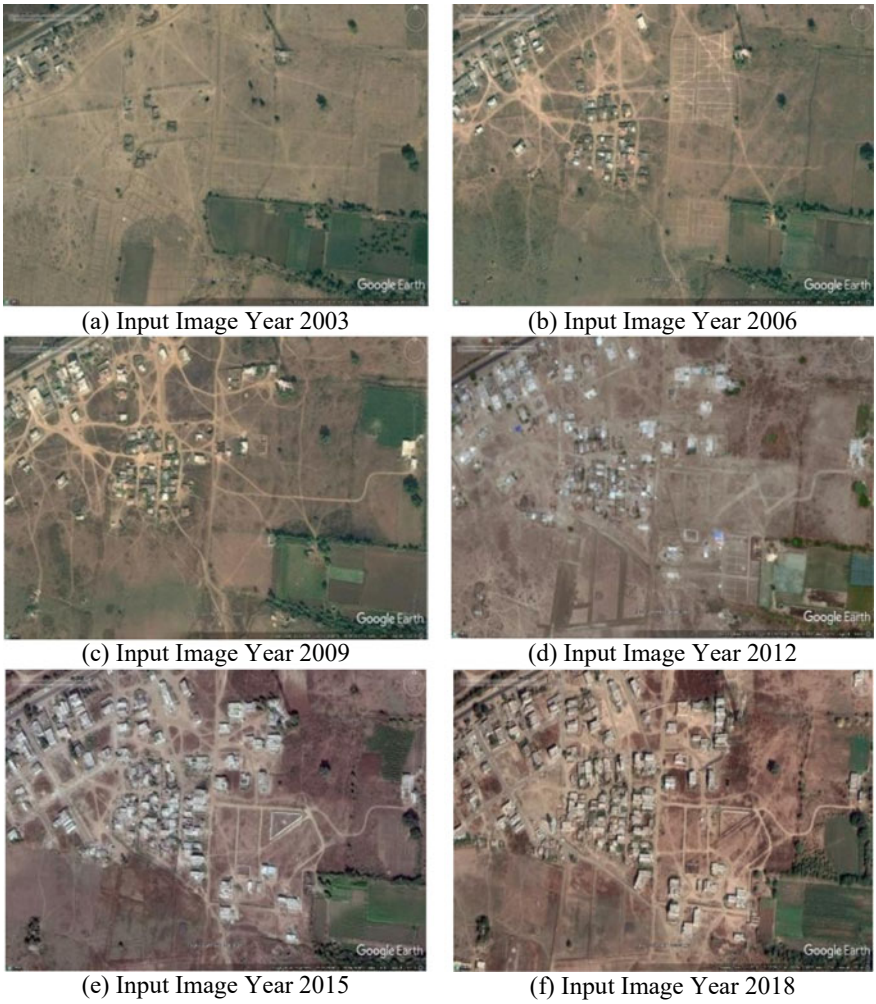

(a) Input Image Year 2003 (b) Input Image Year 2006

(c) Input Image Year 2009 (d) Input Image Year 2012

(e) Input Image Year 2015 (f) Input Image Year 2018

Fig. 1 Source of input images: Maharashtra Remote Sensing and Application Centre, Nagpur

3 Methodology

3.1 Pre-processing

The flow diagram for satellite image classification is shown in Fig. 2. In this work, we used existing available techniques in the ERDAS software for image analysis. We applied Histogram Equalization pre-processing method to enhance the input images [21]. In this method, intensity is uniformly distributed over the range to improve the quality of the input images, see Fig. 3. The quality and visual information is upgraded using enhancement techniques for further processing. Supervised and unsupervised techniques are used for image segmentation and classification.

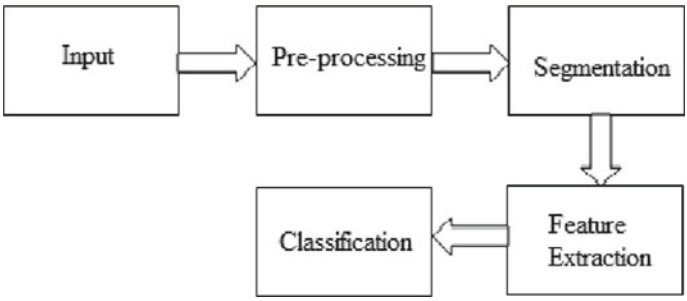

Fig. 2 Basic flow diagram of satellite image analysis system

(a) (b)

Fig. 3 **a** Input image of year 2003, **b** Result of Histogram Equalization on 2003 image

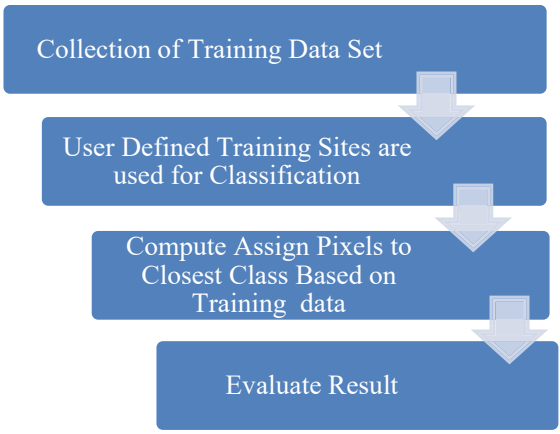

Fig. 4 Algorithm of supervised classification method

3.2 Supervised Classification

Supervised classification is a set of data points from the class of prominence. In the supervised classification process shown in Fig. 4, user needs to define the required training data set for every class. The signature files with respect to each identified classes are then created by using the supervised maximum likelihood method. Every identified class is defined by using probability and is normally distributed in each band. Then, the pixel value of the image is assigned to the class with the highest probability.

3.3 Signature Files in Supervised Classification

Firstly, in the signature files, data is created for different classes, which contains mean and covariance values for each class. Then, every pixel of the image is assigned to a matched class of signatures using the maximum likelihood classifier concept. The noteworthy difference between the unsupervised and supervised methods lies in the creation of the signature files. In supervised classification, the user has command for selecting and digitizing polygons. Then, these polygons are placed in an area of interest, layer which creates the signature files, rather than using a computerized method to define the separate classes. Signature files are used for matching purposes in supervised classification, which consumes more time than unsupervised classification but gives better classification results.

In the ERDAS Imagine software, the supervised classification method includes the following steps: The area of interest is defined as an individual training site with a unique class name as shown in Fig. 5. Signatures are generated using a training site of pixel. By repeating this process user collects several training sites for different classes. Each pixel from the image matches with one of the signatures. So, the system

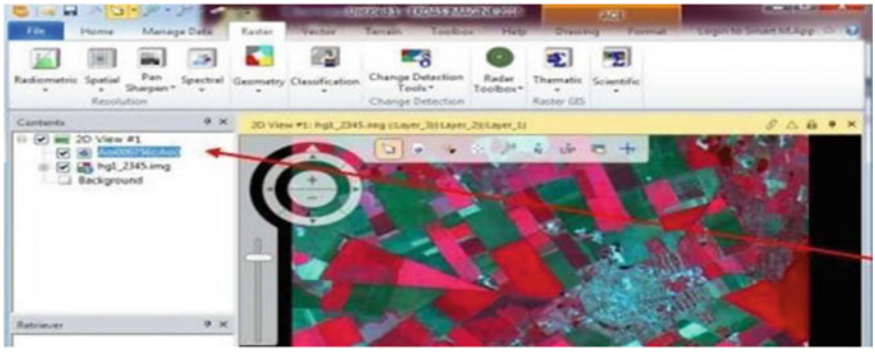

Fig. 5 Choosing area of interest in ERDAS imagine software

will assign matched signature class to that pixel. This signature is used to draw the area of interest as shown in Fig. 6. In all images of Fig. 7, the green color area represents the vegetation.

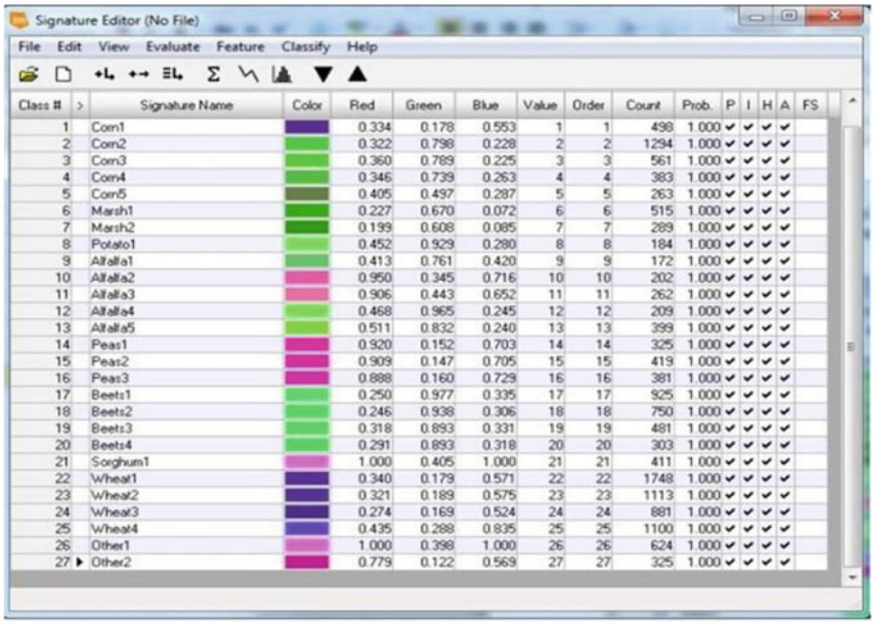

Signature Editor (No File)

File Edit View Evaluate Feature Classify Help

Class #	Signature Name	Color	Red	Green	Blue	Value	Order	Count	Prob.	P	I	H	A	FS
1	Corn1		0.334	0.178	0.553	1	1	498	1.000	✓	✓	✓	✓	
2	Corn2		0.322	0.798	0.228	2	2	1294	1.000	✓	✓	✓	✓	
3	Corn3		0.360	0.789	0.225	3	3	561	1.000	✓	✓	✓	✓	
4	Corn4		0.346	0.739	0.263	4	4	383	1.000	✓	✓	✓	✓	
5	Corn5		0.405	0.497	0.287	5	5	263	1.000	✓	✓	✓	✓	
6	Marsh1		0.227	0.670	0.072	6	6	515	1.000	✓	✓	✓	✓	
7	Marsh2		0.199	0.608	0.085	7	7	289	1.000	✓	✓	✓	✓	
8	Potato1		0.452	0.929	0.280	8	8	184	1.000	✓	✓	✓	✓	
9	Alfalfa1		0.413	0.761	0.420	9	9	172	1.000	✓	✓	✓	✓	
10	Alfalfa2		0.950	0.345	0.716	10	10	202	1.000	✓	✓	✓	✓	
11	Alfalfa3		0.906	0.443	0.652	11	11	262	1.000	✓	✓	✓	✓	
12	Alfalfa4		0.468	0.965	0.245	12	12	209	1.000	✓	✓	✓	✓	
13	Alfalfa5		0.511	0.832	0.240	13	13	399	1.000	✓	✓	✓	✓	
14	Peas1		0.920	0.152	0.703	14	14	325	1.000	✓	✓	✓	✓	
15	Peas2		0.909	0.147	0.705	15	15	419	1.000	✓	✓	✓	✓	
16	Peas3		0.888	0.160	0.729	16	16	381	1.000	✓	✓	✓	✓	
17	Beets1		0.250	0.977	0.335	17	17	925	1.000	✓	✓	✓	✓	
18	Beets2		0.246	0.938	0.306	18	18	750	1.000	✓	✓	✓	✓	
19	Beets3		0.318	0.893	0.331	19	19	481	1.000	✓	✓	✓	✓	
20	Beets4		0.291	0.893	0.318	20	20	303	1.000	✓	✓	✓	✓	
21	Sorghum1		1.000	0.405	1.000	21	21	411	1.000	✓	✓	✓	✓	
22	Wheat1		0.340	0.179	0.571	22	22	1748	1.000	✓	✓	✓	✓	
23	Wheat2		0.321	0.189	0.575	23	23	1113	1.000	✓	✓	✓	✓	
24	Wheat3		0.274	0.169	0.524	24	24	881	1.000	✓	✓	✓	✓	
25	Wheat4		0.435	0.288	0.835	25	25	1100	1.000	✓	✓	✓	✓	
26	Other1		1.000	0.398	1.000	26	26	624	1.000	✓	✓	✓	✓	
27	Other2		0.779	0.122	0.569	27	27	325	1.000	✓	✓	✓	✓	

Fig. 6 Classes creation using signature file

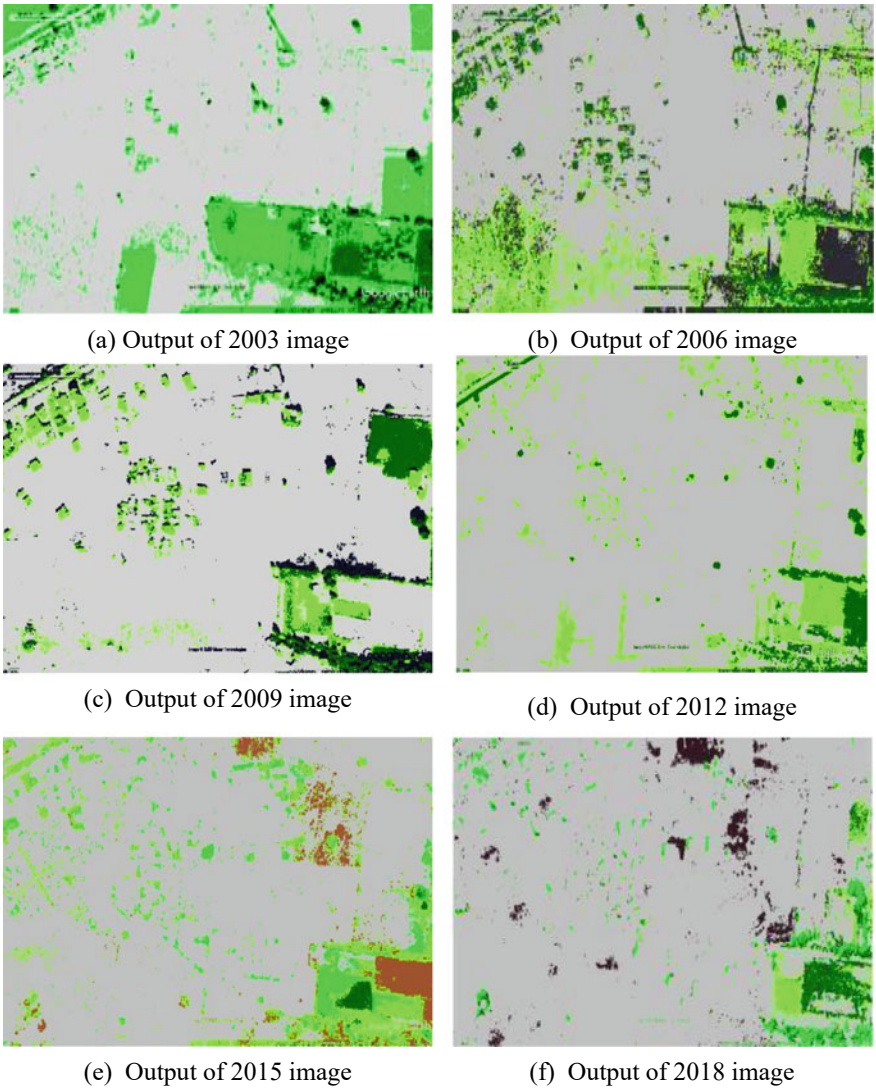

(a) Output of 2003 image (b) Output of 2006 image

(c) Output of 2009 image (d) Output of 2012 image

(e) Output of 2015 image (f) Output of 2018 image

Fig. 7 Results through ERDAS Imagine software of input images of same local area for different years using Supervised Classification method

3.4 Unsupervised Classification

Unsupervised classification is a picture element-centered automated classification method. Figure 8 shows the flow of the algorithm. In this method, the user has to define maximum iterations, the number of classes, and the threshold value to stop

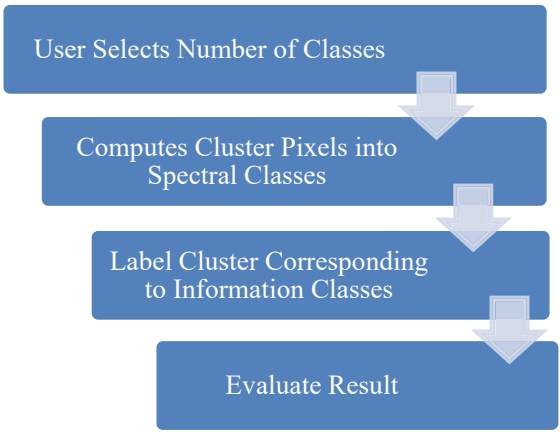

Fig. 8 Algorithm of unsupervised classification

the classification process. After the classification data has to be read, tag and color code the classes consequently.

The Iterative Self-Organizing Data Analysis (ISODATA) clustering technique is used for unsupervised training data set and classification in ERDAS Imagine platform. The statistical data is used to match the pixel values and then matched pixel groups into separate classes. To generate the groups, the whole process went through the number of iterations, until it satisfies the threshold condition. These groups are defined in the signature file which is then used to generate new class values, thus making use of statistics of the data to compute the similarities or differences of the pixel values which are then finally grouped into separate classes. To get the convergence threshold value, this process is performed multiple times. The groups are then specified by a signature file, which is then passed down to create a new raster layer comprising discrete class values. ERDAS Imagine Software uses the ISODATA algorithm for clustering image pixels into spectral clusters using unsupervised classification. Every cluster has included a set of similar spectral characteristic pixels. The ISODATA clustering method begins with randomly creating N cluster means based on mean and standard deviations of the bands in the input file ("N" is a number specified by the user, this is essentially the number of classes the user wants to classify). Every pixel belongs to the "nearest" cluster of the minimum distance criteria. In the iteration process again each pixel is matched with new cluster characteristics and allocated to the matched cluster.

Unsupervised classification is a computer-automated classification method. The spectral classes are formed by numerical information in the data, only the user has to define several classes. In the image, pixels are grouped based on spectral similarity. Figure 9 depicts outputs for unsupervised classifications, where three classes are made which are represented using three different colors. Black color is a region of interest detecting greenness.

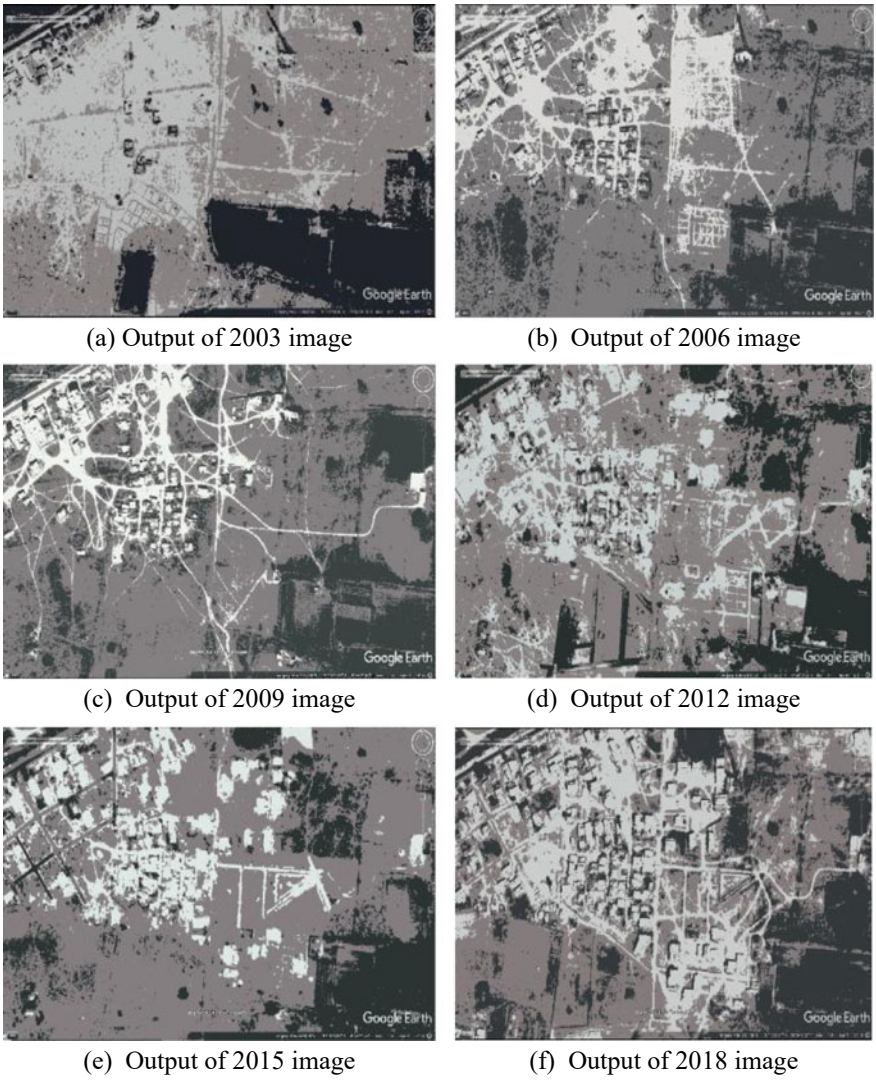

(a) Output of 2003 image (b) Output of 2006 image

(c) Output of 2009 image (d) Output of 2012 image

(e) Output of 2015 image (f) Output of 2018 image

Fig. 9 Results through ERDAS Imagine software of input images of same local area for different years using Unsupervised Classification method

4 Results and Discussion

From the analysis of experimental results of images year 2003 to 2018, the green area is decreasing day by day. The supervised classification gives better results as compared to the unsupervised classification method as demonstrated in Figs.7 and 9. The input images are taken in the gap of three years in the analysis of change in

Table 1 Green area calculation from output images for Supervised Classification and Unsupervised Classification Methods

Sr. No	Year of image	Supervised Classification		Unsupervised Classification	
		No. of Green Pixels	Area in Hectares	No. of Green Pixels	Area in Hectares
1	2003	377,747	*37.7747*	336,144	*33.6144*
2	2006	451,866	45.1866	359,735	35.9735
3	2009	276,523	27.6523	396,342	39.6342
4	2012	224,429	22.4429	337,709	33.7709
5	2015	292,427	29.2427	325,995	32.5995
6	2018	177,438	*17.7438*	433,748	*43.3748*

Table 2 Green area difference between two years for Supervised Classification and Unsupervised Classification Methods

Sr. No	Comparison of years	Difference in Areas for Supervised Classification	Difference in Areas for Unsupervised Classification
1	2003 and 2006	*7.4119*	*2.3591*
2	2006 and 2009	− 17.5343	3.6607
3	2009 and 2012	− 5.2094	− 5.8633
4	2012 and 2015	6.7998	− 1.1714
5	2015 and 2018	*− 11.4989*	*10.7753*

vegetation. Nowadays, this is a concerning topic for the betterment of urban cities. As we analyze input images visually from 2003 to 2018, the green area decreases faster. From the experimental results, for the supervised classification method greenness area is decreasing continuously. The calculation of greenness is the count of green pixels in an image after the segmentation process. As shown in Table 1, in 2003 green area in Hectares is 37.7747, after 15 years it reduced to 17.7438 Hectares. The unsupervised classification method gives false results, due to misclassification of the pixel values, as it is a fully automatic classification method. Table 2 depicts the comparative analysis of change in the green area between two years.

5 Conclusion

This paper presents the comparative analysis of the supervised and unsupervised classification methods. A supervised classifier based on training sites defined by the user gives more accurate results. An unsupervised classifier generates the different classes based on spectral details, not on visual analysis. Spectral information can be changed from time to time, so supervised classification can be used for segmentation

and further calculations of greenness in terms of the area presented. With the developed algorithm using the software, images are being studied and analyzed based on greenness. Proper measures can be suggested to overcome the problems which were stated during the analysis for the betterment of urban cities.

Acknowledgements The research work is carried out in the MRSAC (Maharashtra Remote Sensing Applications & Centre), Nagpur. We are thankful for their kind support for this research work.

References

1. Du, P., Liu, P., Xia, J., Feng, L., Liu, S., Tan, K., Cheng, L.: Remote sensing ımage ınterpretation for urban environment analysis: methods, system and examples. Remote Sens. **6**, 9458–9474 (2014). ISSN 2072–4292. https://doi.org/10.3390/rs6109458
2. Huang, C., Yang, J., Hui, L., Huang, H., Le, Y.: Green spaces as an indicator of urban health: evaluating its changes in 28 mega-cities. Remote Sens. **9**, 1266 (2017). https://doi.org/10.3390/rs9121266
3. Mugiranez, T., Nascetti, A., Ban, Y.: WorldView-2 data for hierarchical object-based urban land cover classification in kigali: integrating rule-based approach with urban density and greenness indices. Remote Sens. **11**, 2128 (2019). https://doi.org/10.3390/rs11182128
4. Hanspal, R.K., Sahoo, K.: A survey of ımage enhancement techniques. Int. J. Sci. Res. (IJSR) ISSN (Online) **6**(5), 2319–7064 (2017)
5. Arora, S., Agarwal, M., Kumar, V., Gupta, D.: Comparative study of image enhancement techniques using histogram equilization on degraded images. Int. J. Eng. Technol. **7**(2.8), 468–471 (2018)
6. Gonzalez, R.C., Woods, R.E.: Digital Image Processing, Third Edition (2009)
7. Bhosale, P., Gokhale, A.: Segmentation of color images based on different segmentation techniques. Int. J. Electron. Comput. Sci. Eng. **2**(2), 640–644 (2013)
8. Jalobeanu, A., Blanc-F´eraud, L., Zerubia, J.: An adaptive Gaussian model for Satellite image deblurring. IEEE Trans. Image Process. **13**(4) (2004). https://doi.org/10.1109/TIP.2003.819969
9. Patel, O., Maravi, Y.P.S., Sharma, S.: A comparative study of histogram equalization based ımage enhancement techniques for brightness preservation and contrast enhancement. Int. J. (SIPIJ) **4**(5), 2013
10. Šastný, J., Minarík, M.: A brief ıntroduction to ımage pre-processing for object recognition. In: International Conference on Soft Computing Applied in Computer and Economic Enviroment, Kunovice (2007)
11. Abburu, S., Golla. S.B.: Satellite ımage classification methods and techniques: a review. Int. J. Comput. Appl. **119**(8), 0975–8887 (2015)
12. Marnur, A.M., Gavade, A.B.: Satellite image classification and feature extraction using various classification techniques: A Survey. Int. J. Adv. Res. Ideas Innov. Technol ISSN **4**(3), 2454–3132 (2018)
13. Ranganathan, G.: A study to find facts behind preprocessing on deep learning algorithms. J. Innov. Image Process. (JIIP) **3**(01), 66–74 (2021)
14. Manoharan, J., Samuel: Study of variants of extreme learning machine (ELM) brands and its performance measure on classification algorithm. J. Soft Comput. Paradigm (JSCP) **3**(02), 83–95 (2021)
15. Manoharan, S., Sathish: Early diagnosis of Lung Cancer with probability of malignancy calculation and automatic segmentation of lung CT scan images. J. Innov. Image Process. (JIIP) **2**(04), 175–186 (2020)

16. Tesfamikael, H.H., Fray, A.., Mengsteab, I., Semere, A., Amanuel, Z.: Simulation of eye tracking control based electric wheelchair construction by ımage segmentation algorithm. J. Innov. Image Process. (JIIP) **3**(01), 21–35 (2021)
17. Nimbarte, N.M., Mushrif, M.M.: Multi-level thresholding algorithm for color ımage segmentation. In: IEEE Conference on Computer Engineering and Applications, at Bali Island, IndonesiaI, CTTA, vol. 2, pp. 231–233 (2010). https://doi.org/10.1109/ICCEA.2010.198
18. Mohane, V., Gode, C.: Object recognition for blind people using portable camera. In: 2016 World Conference on Futuristic Trends in Research and Innovation for Social Welfare (WCFTR'16), 978–1–4673–9214–3/16/ 2016 IEEE
19. ERDAS Customer Education: Introduction to the ERDAS IMAGINE Developer's Toolkit (2009). www.erdas.com
20. Ali, A.: Lab Introduction to ERDAS IMAGINE Software. Project: Ph.D. (Remote Sensing & GIS), May 2017. https://doi.org/10.13140/RG.2.2.13730.43203
21. Sainis, S., Barahate, V., Bandawar, S., Tarak, S., Nimbarte N., Balamwar, S.: Enhancement techniques for analysis of satellite ımages through ERDAS software. In: Proceedings of the International Conference on Artificial Intelligence and Smart Systems (ICAIS-2021) IEEE Xplore Part Number: CFP21OAB-ART; ISBN: 978–1–7281–9537–7

Combating Fake News with Computational Intelligence Techniques pp 327–343

Framework for Fake News Classification Using Vectorization and Machine Learning

Yogita Dubey, Pushkar Wankhede, Amey Borkar, Tanvi Borkar & Prachi Palsodkar

Chapter | First Online: 16 December 2021

855 Accesses | 1 Citations

Part of the Studies in Computational Intelligence book series (SCI,volume 1001)

Abstract

Fake news are widely offered in digital media to raise the visitors hit and in an offbeat, it acts on users emotions. The foremost ordinary example of such fake news throughout this pandemic, are the various remedies to cure covid. As a result of which individuals are unable to acknowledge any kind of genuine news. People try and attempt numerous things which will never help in curing this contagious disease. Moreover, it might lead to some other major health issues. In this paper, a framework is provided for the classification of news as fake vs real. Text data is pre-processed using Natural Language Processing (NLP) by performing tokenization, text cleaning and vectorization. N-gram and TF-IDF vectorization is used. Seven Machine Learning (ML) algorithms are then applied for classification. Two different datasets Kaggle and ISOT is used for experimentation and evaluated on the same scale using different evaluation metrics to demonstrate the efficacy of the proposed framework.

Keywords

Fake news **Classification** **Natural Language Processing** **Machine learning** **Model evaluation**

References

1. Allcott, H., & Gentzkow, M. (2017, May). Social Media and fake news in the 2016 election. *Journal of Economic Perspectives*, *31*(2), 211–236.

2. Soll, J. (2016, Dec). The long and brutal history of fake news. *POLITICO Magazine*, *18*

3. Gabielkov, M., Ramchandran, A., Chaintreau, A., & Legout, A. (2016). Social Clicks: What and Who Gets Read on Twitter? In *International conference on measurement and modelling of computer science* (pp. 179–192)

4. Fiske, S. T., & Taylor, S. E. (2013). Social cognition: From brains to culture (2nd ed.). CA: SAGE.

5. Lim, C. (2017). Checking how facts- checkers check. 16 May 2017

6. Shao, C. (2018). Anatomy of online misinformation network. *PLOS ONE*, *13*(4), 196087

7. Klyuev, V. (2018). Fake news filtering: Semantic approaches.

8. Horne, B. D., & Adali, S. (2017). This just in: Fake news packs a lot in title, uses simpler, repetitive content in text body, more similar to satire than real news. In *International AAAI conference on web and social media* Vol. 8.

9. Castelo, S., Almeida, T., Elghafari, A., Santos, A., Pham, K., Nakamura, E., & Freire, J. (2019). A topic-agnostic approach for identifying fake news pages. *World Wide Web Conference, 2019*, 975–980.

10. Qazvinian, V., Rosengren, E., Radev, D. R., & Mei, Q. (2011). Rumor has it: Identifying misinformation in microblogs. *Conference on Empirical Methods in Natural Language Processing, EMNLP, 2011*, 1589–1599.

11. Pérez-Rosas, V., Kleinberg, B., Lefevre, A., & Mihalcea, R. (2017). Automatic detection of fake news. In *International Conference on Computational Linguistics* (pp. 3391–3401). Santa Fe, New Mexico, USA.

12. Yang, Y., Zheng, L., Zhang, J., Cui, Q., Li, Z., & Yu, P. S. (2018). TI-CNN: Convolutional neural networks for fake news detection.

13. Sivasangari, V., Anand, P. V., & Santhya, R. (2018). A modern approach to identify the fake news using machine learning. *International Journal* of *Pure* and *Applied*

Mathematics, *118*(20).

14. Ahmed, S., Hinkelmann, K., & Corradini, F. (2019). Combining machine learning with knowledge engineering to detect fake news in social networks—A survey. In *Proceedings of the AAAI 2019 spring symposium* Vol. 12.

15. Ruchansky, N., Seo, S., & Liu, Y. (2017). CSI: A hybrid deep model for fake news detection. *ACM on Conference on Information and Knowledge Management, CIKM, 2017*, 797–806. https://doi.org/10.1145/3132847.3132877

16. Okoro, E. M., Abara, B. A., Umagba, A. O., Ajonye, A. A., & Isa, Z. S. (2018). A hybrid approach to fake news detection on social media. The Nigerian *Journal* of *Technology*, *37*(2).

17. Kaggle, (2018). Fake news. San Francisco, CA, USA: Kaggle. https://www.kaggle.com/c/fake-news

18. ISOT, Fake News. University of Victoria, Engineering, Canada. https://www.uvic.ca/engineering/ece/isot/datasets/fake-news/index.php

19. Bird, S., Klein, E., & Loper, E. (2009) Natural language processing with Python—Analyzing text with the natural language toolkit.

20. Patil, S. M., & Malik, A. K. (2019). Correlation based real-time data analysis of graduate students behaviour. In K. Santosh, R. Hegadi (eds.), *Recent trends in image processing and pattern recognition*. *RTIP2R 2018*. Communications in Computer and Information Science Vol. 1037. Springer.

21. Shetty, B. (2018). Natural language processing (NLP) for machine learning. at towardsdatascience, Medium.

22. Ultimate guide to deal with Text Data (using Python) – for Data Scientists and Engineers by Shubham Jain, February 27, 2018

23. Ranjan, A. (July 2018) Fake news detection using machine learning. Department Of Computer Science & Engineering Delhi Technological University.

24. Mitchell, T. M. (2006). *7e Discipline of machine learning*. Carnegie Mellon University.

25. Chao-Ying Joanne Peng, Kuk Lida Lee, Gary M. Ingersoll, "An Introduction to Logistic Regression", Indiana University-Bloomington, September 2002

26. Crammer, K., Dekel, O., Shalev-Shwartz, S., & Singer, Y. (2006, March). Passive-Aggressive Algorithms. School of Computer Science & Engineering, The Hebrew University, Jerusalem 91904, Israe.

27. Patel, H. H., Prajapati, P. (2018, Oct). Study and analysis of decision tree based classification algorithms. Dept. of Information Technology, CSPIT, Charotar University of Science and Technology, Changa, Gujarat, India.

28. Breiman, L. (2001, Jan). Random forests. Statistics Department University of California Berkeley, CA 94720.

29. Natekin, A., Knoll, A. (2013). Gradient boosting machines. Department of Informatics, Technical University Munich, Garching, Munich, Germany.

30. Kaviani, P. (2017, Nov). Mrs. Sunita Dhotre, Short survey on naive bayes algorithm. *International Journal of Advance Engineering and Research, Department of Computer Engineering*, Bharati Vidyapeeth University, College of Engineering, Pune.

31. Thandar, M., & Usanavasin S. (2015). Measuring opinion credibility in Twitter. In H. Unger, P. Meesad, S. Boonkrong (eds.), *Recent Advances in Information and Communication Technology 2015*. Advances in Intelligent Systems and Computing Vol. 361. Springer.

Author information

Authors and Affiliations

Yeshwantrao Chavan College of Engineering, Nagpur, India
Yogita Dubey, Pushkar Wankhede, Amey Borkar, Tanvi Borkar & Prachi Palsodkar

Editor information

Editors and Affiliations

Hassan II University, Casablanca, Morocco
Prof. Mohamed Lahby

United International University, Dhaka, Bangladesh
Al-Sakib Khan Pathan

Sultan Moulay Slimane University, Khouribga, Morocco
Prof. Yassine Maleh

Taibah University, Madinah, Saudi Arabia
Prof. Wael Mohamed Shaher Yafooz

Rights and permissions

Copyright information

About this chapter

Cite this chapter

Dubey, Y., Wankhede, P., Borkar, A., Borkar, T., Palsodkar, P. (2022). Framework for Fake News Classification Using Vectorization and Machine Learning. In: Lahby, M., Pathan, AS.K., Maleh, Y., Yafooz, W.M.S. (eds) Combating Fake News with Computational Intelligence Techniques. Studies in

Computational Intelligence, vol 1001. Springer, Cham. https://doi.org/10.1007/978-3-030-90087-8_16

.RIS .ENW .BIB

DOI	Published	Publisher Name
https://doi.org/10.1007/978-3-030-90087-8_16	16 December 2021	Springer, Cham

Print ISBN	Online ISBN	eBook Packages
978-3-030-90086-1	978-3-030-90087-8	Intelligent Technologies and Robotics Intelligent Technologies and Robotics (R0)

Analysis of Greenness in Urban Cities Using Supervised and Unsupervised Classification

Nita Nimbarte, Shraddha Sainis, and Sanjay Balamwar

Abstract Satellite images are widely used in urban planning and growth analysis with different technology being developed. A remotely sensed image is at first pre-processed to remove anomalies from it, thus resulting in a clear and informative image. Image classification is categorized into two techniques, namely supervised and unsupervised techniques. Both the techniques give different outputs and accuracy parameters. This paper describes the analysis of supervised and unsupervised techniques of remotely sensed images for land cover classification and to evaluate greenness in terms of the area over a period of time. Both the methods are used for object detection and classification. The input images were enhanced using the histogram equalization technique and then segmented using supervised and unsupervised classification with the help of ERDAS software. After segmentation or image classification results were analyzed to give the exact measure of greenness in terms of area in hectares or square kilometers calculated over years.

Keywords ERDAS imagine software · Greenness analysis · Histogram equalization · Image processing · Supervised classification · Unsupervised classification

1 Introduction

In the present global situation, maintaining green environment in dense urban area is of utmost importance. Decreasing greenness in urban directly affects the environment quality. Urban green space is known to provide ample benefits to human beings. As many countries all around the world desire to get updated with the latest geographical

N. Nimbarte (✉) · S. Sainis
Yeshwantrao Chavan College of Engineering, Nagpur, India

S. Balamwar
Maharashtra Remote Sensing Applications and Centre, Nagpur, India
e-mail: sanjay.balamwar@mrsac.maharashtra.gov.in

S. Smys et al. (eds.), *Computational Vision and Bio-Inspired Computing*,
Advances in Intelligent Systems and Computing 1420,
https://doi.org/10.1007/978-981-16-9573-5_48

information and activities of their area, this kind of data help the respective authority in the Bureaucracy to plan the development of a particular place geographically [1].

Peijun Du et al. reported the urgency of hybrid approaches of environment analysis of different parameters like vegetation, change detection, land cover, water monitoring, and designed hybrid system for environmental analysis. The effectiveness of this system is confirmed through the case studies [1]. Conghong Huang et. al. described health benefits to urban residents by analyzing the change in green space of megacities from the year 2005 to 2015. The author used 10,823 sights of Landsat images and applies random forest classifier through the google earth engine to map land covers. By increasing urban green spaces directly increased health benefits in megacities [2]. Mugiranez et al. [3] demonstrated a hybrid approach using support vector machines (SVM) and rule-based methods for object-based multi-stage classification. It gives an analysis of actual land cover by using different challenging parameters like low-density areas, roads, informal settlements, and lowland agriculture. The classification accuracy improved by geometric ruleset, greenness density indices, and urban density indices. Researcher [4–7] reported a survey of different enhancement techniques for more suitable outputs for further analysis. The authors described many histogram-based methods for image enhancement. The outcome of these methods may be under contrast or over contrast; every technique has its pros and cons. Jalobenu et al. [8] discussed adaptive Gaussian model automatic algorithm for image enhancement. The algorithm gives good results on high-resolution satellite images. Maximum Likelihood Estimator (MLE) is used to estimate measuring parameters. The author proposed a wavelet-based deconvolution hybrid approach to enhance the outcomes. Patel et al. [9] described that weighted histogram equalization with a recursively separated method. This method preserves scalable brightness due to its recursive nature. The different histogram equalization-based methods were compared through experimental study and error estimation parameters. Šastný and Minarík [10] described different filtering pre-processing methods for object detection. The author reported that speed and accuracy are opposing requirements for edge detection. The object momenta gives good results with a 74% rate of objects recognition. Author [11, 12] reviewed classification methods and presents their own advantages and disadvantages. The research work [13, 14] presented analysis of image classification techniques through different image modalities. Image segmentation techniques [15–18] are used to segment area of interest. Segmentation based image classification algorithms has less computational complexity as compare to pixel level classification method. The classification methods are categories into automatic, manual, and hybrid approaches. Most of the methods are developed using automatic categories. This work presents an analysis of change in the greenness of urban cities for different years. The setup of this paper is stated as: Sect. 2: describes image data used for evaluation and experimentation done through ERDAS software. Section 3: briefly describes the pre-processing method for image enhancement and supervised and unsupervised methods for further classification. Section 4: gives the analysis of classification results. Finally, Sect. 5: ends with the conclusion.

2 Material and Software

In this paper, the sample input images are collected from Google Earth of size 1280 X 784 of Location near Nandanvan Area, Nagpur as shown in Fig. 1. ERDAS IMAGINE software is used [19–21] for geospatial data processing. This software package is used to analyze different imagery, geospatial imaging, and vector data. It is the best software for a vast amount of information extraction and also supports spatial modeling systems.

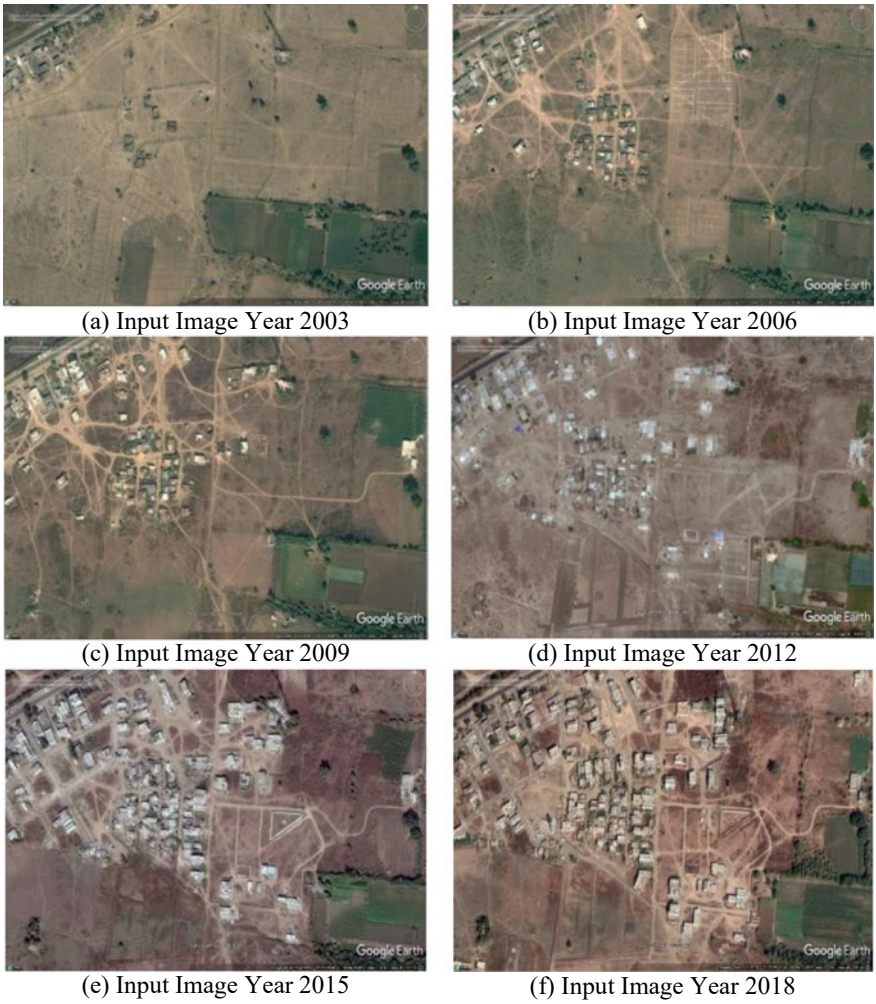

(a) Input Image Year 2003 (b) Input Image Year 2006

(c) Input Image Year 2009 (d) Input Image Year 2012

(e) Input Image Year 2015 (f) Input Image Year 2018

Fig. 1 Source of input images: Maharashtra Remote Sensing and Application Centre, Nagpur

3 Methodology

3.1 Pre-processing

The flow diagram for satellite image classification is shown in Fig. 2. In this work, we used existing available techniques in the ERDAS software for image analysis. We applied Histogram Equalization pre-processing method to enhance the input images [21]. In this method, intensity is uniformly distributed over the range to improve the quality of the input images, see Fig. 3. The quality and visual information is upgraded using enhancement techniques for further processing. Supervised and unsupervised techniques are used for image segmentation and classification.

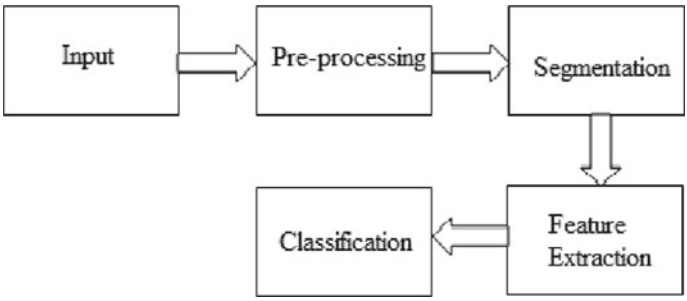

Fig. 2 Basic flow diagram of satellite image analysis system

(a) (b)

Fig. 3 **a** Input image of year 2003, **b** Result of Histogram Equalization on 2003 image

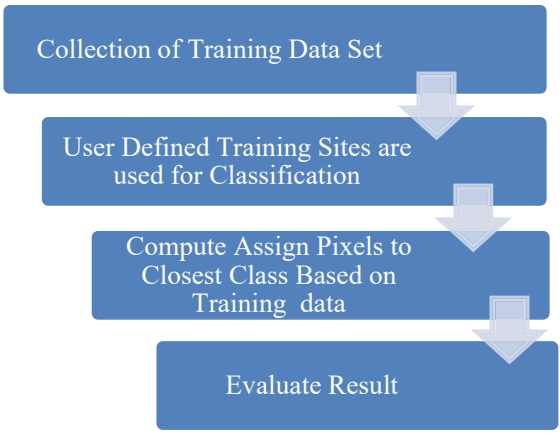

Fig. 4 Algorithm of supervised classification method

3.2 Supervised Classification

Supervised classification is a set of data points from the class of prominence. In the supervised classification process shown in Fig. 4, user needs to define the required training data set for every class. The signature files with respect to each identified classes are then created by using the supervised maximum likelihood method. Every identified class is defined by using probability and is normally distributed in each band. Then, the pixel value of the image is assigned to the class with the highest probability.

3.3 Signature Files in Supervised Classification

Firstly, in the signature files, data is created for different classes, which contains mean and covariance values for each class. Then, every pixel of the image is assigned to a matched class of signatures using the maximum likelihood classifier concept. The noteworthy difference between the unsupervised and supervised methods lies in the creation of the signature files. In supervised classification, the user has command for selecting and digitizing polygons. Then, these polygons are placed in an area of interest, layer which creates the signature files, rather than using a computerized method to define the separate classes. Signature files are used for matching purposes in supervised classification, which consumes more time than unsupervised classification but gives better classification results.

In the ERDAS Imagine software, the supervised classification method includes the following steps: The area of interest is defined as an individual training site with a unique class name as shown in Fig. 5. Signatures are generated using a training site of pixel. By repeating this process user collects several training sites for different classes. Each pixel from the image matches with one of the signatures. So, the system

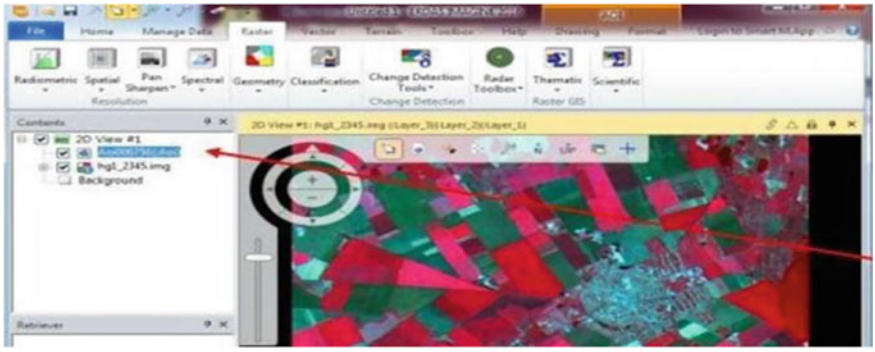

Fig. 5 Choosing area of interest in ERDAS imagine software

will assign matched signature class to that pixel. This signature is used to draw the area of interest as shown in Fig. 6. In all images of Fig. 7, the green color area represents the vegetation.

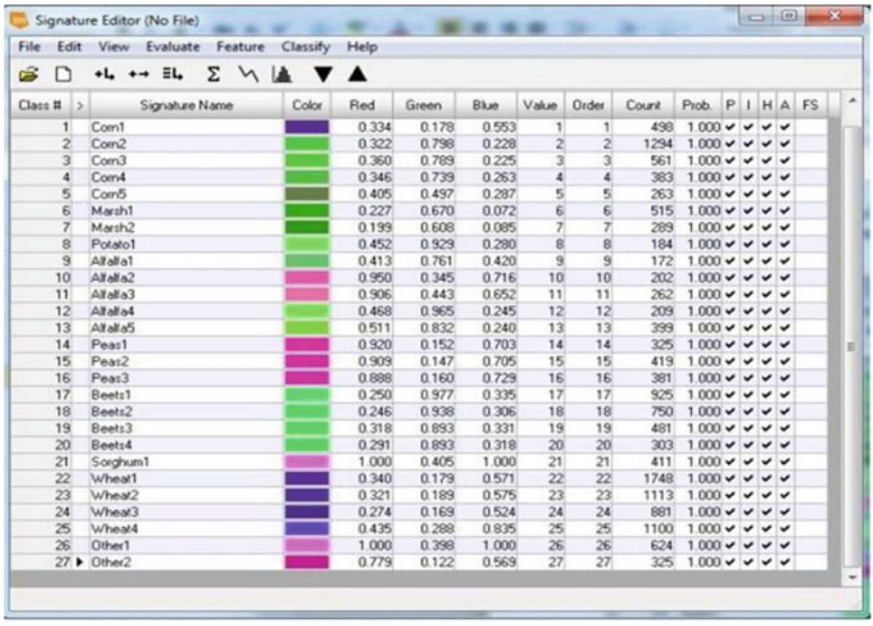

Signature Editor (No File)

File Edit View Evaluate Feature Classify Help

Class #	Signature Name	Color	Red	Green	Blue	Value	Order	Count	Prob.	P	I	H	A	FS
1	Corn1		0.334	0.178	0.553	1	1	498	1.000	✓	✓	✓	✓	
2	Corn2		0.322	0.798	0.228	2	2	1294	1.000	✓	✓	✓	✓	
3	Corn3		0.360	0.789	0.225	3	3	561	1.000	✓	✓	✓	✓	
4	Corn4		0.346	0.739	0.263	4	4	383	1.000	✓	✓	✓	✓	
5	Corn5		0.405	0.497	0.287	5	5	263	1.000	✓	✓	✓	✓	
6	Marsh1		0.227	0.670	0.072	6	6	515	1.000	✓	✓	✓	✓	
7	Marsh2		0.199	0.608	0.085	7	7	289	1.000	✓	✓	✓	✓	
8	Potato1		0.452	0.929	0.280	8	8	184	1.000	✓	✓	✓	✓	
9	Alfalfa1		0.413	0.761	0.420	9	9	172	1.000	✓	✓	✓	✓	
10	Alfalfa2		0.950	0.345	0.716	10	10	202	1.000	✓	✓	✓	✓	
11	Alfalfa3		0.906	0.443	0.652	11	11	262	1.000	✓	✓	✓	✓	
12	Alfalfa4		0.468	0.965	0.245	12	12	209	1.000	✓	✓	✓	✓	
13	Alfalfa5		0.511	0.832	0.240	13	13	399	1.000	✓	✓	✓	✓	
14	Peas1		0.920	0.152	0.703	14	14	325	1.000	✓	✓	✓	✓	
15	Peas2		0.909	0.147	0.705	15	15	419	1.000	✓	✓	✓	✓	
16	Peas3		0.888	0.160	0.729	16	16	381	1.000	✓	✓	✓	✓	
17	Beets1		0.250	0.977	0.335	17	17	925	1.000	✓	✓	✓	✓	
18	Beets2		0.246	0.938	0.306	18	18	750	1.000	✓	✓	✓	✓	
19	Beets3		0.318	0.893	0.331	19	19	481	1.000	✓	✓	✓	✓	
20	Beets4		0.291	0.893	0.318	20	20	303	1.000	✓	✓	✓	✓	
21	Sorghum1		1.000	0.405	1.000	21	21	411	1.000	✓	✓	✓	✓	
22	Wheat1		0.340	0.179	0.571	22	22	1748	1.000	✓	✓	✓	✓	
23	Wheat2		0.321	0.189	0.575	23	23	1113	1.000	✓	✓	✓	✓	
24	Wheat3		0.274	0.169	0.524	24	24	881	1.000	✓	✓	✓	✓	
25	Wheat4		0.435	0.288	0.835	25	25	1100	1.000	✓	✓	✓	✓	
26	Other1		1.000	0.398	1.000	26	26	624	1.000	✓	✓	✓	✓	
27	Other2		0.779	0.122	0.569	27	27	325	1.000	✓	✓	✓	✓	

Fig. 6 Classes creation using signature file

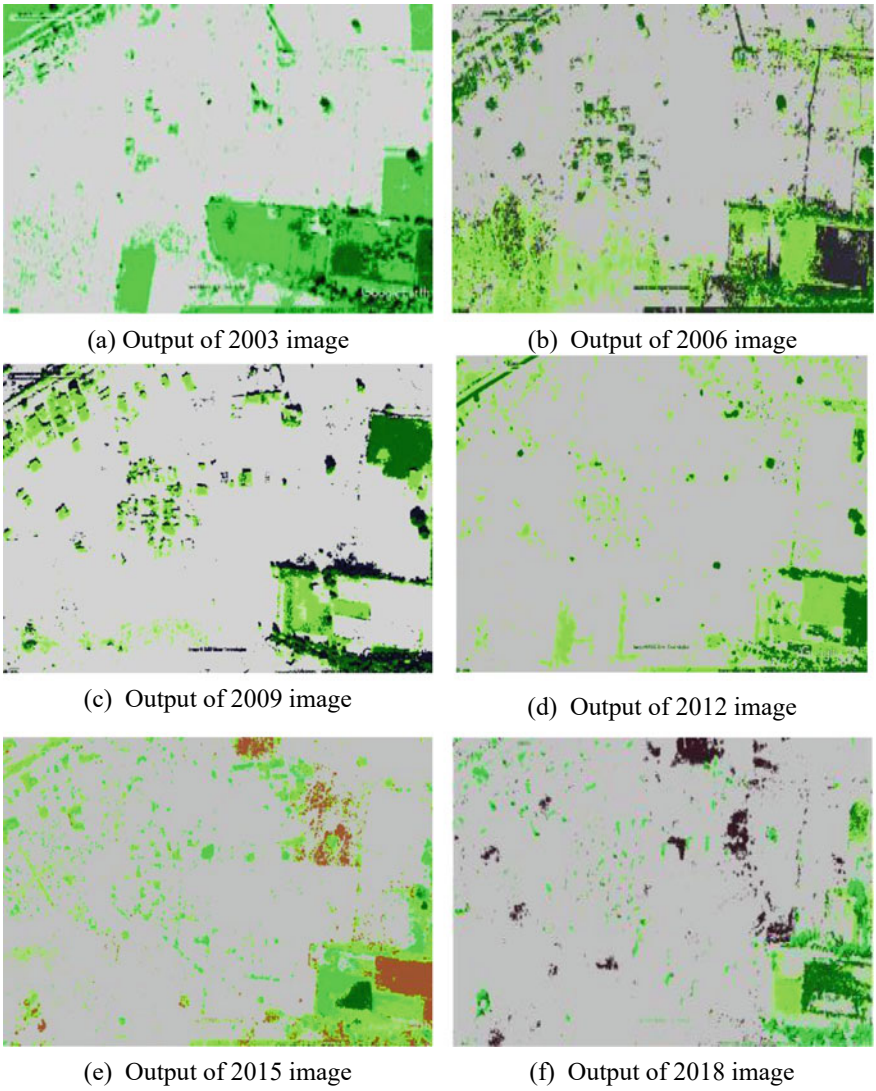

(a) Output of 2003 image (b) Output of 2006 image

(c) Output of 2009 image (d) Output of 2012 image

(e) Output of 2015 image (f) Output of 2018 image

Fig. 7 Results through ERDAS Imagine software of input images of same local area for different years using Supervised Classification method

3.4 Unsupervised Classification

Unsupervised classification is a picture element-centered automated classification method. Figure 8 shows the flow of the algorithm. In this method, the user has to define maximum iterations, the number of classes, and the threshold value to stop

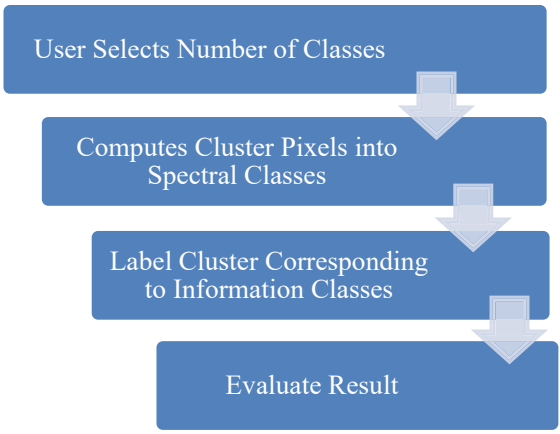

Fig. 8 Algorithm of unsupervised classification

the classification process. After the classification data has to be read, tag and color code the classes consequently.

The Iterative Self-Organizing Data Analysis (ISODATA) clustering technique is used for unsupervised training data set and classification in ERDAS Imagine platform. The statistical data is used to match the pixel values and then matched pixel groups into separate classes. To generate the groups, the whole process went through the number of iterations, until it satisfies the threshold condition. These groups are defined in the signature file which is then used to generate new class values, thus making use of statistics of the data to compute the similarities or differences of the pixel values which are then finally grouped into separate classes. To get the convergence threshold value, this process is performed multiple times. The groups are then specified by a signature file, which is then passed down to create a new raster layer comprising discrete class values. ERDAS Imagine Software uses the ISODATA algorithm for clustering image pixels into spectral clusters using unsupervised classification. Every cluster has included a set of similar spectral characteristic pixels. The ISODATA clustering method begins with randomly creating N cluster means based on mean and standard deviations of the bands in the input file ("N" is a number specified by the user, this is essentially the number of classes the user wants to classify). Every pixel belongs to the "nearest" cluster of the minimum distance criteria. In the iteration process again each pixel is matched with new cluster characteristics and allocated to the matched cluster.

Unsupervised classification is a computer-automated classification method. The spectral classes are formed by numerical information in the data, only the user has to define several classes. In the image, pixels are grouped based on spectral similarity. Figure 9 depicts outputs for unsupervised classifications, where three classes are made which are represented using three different colors. Black color is a region of interest detecting greenness.

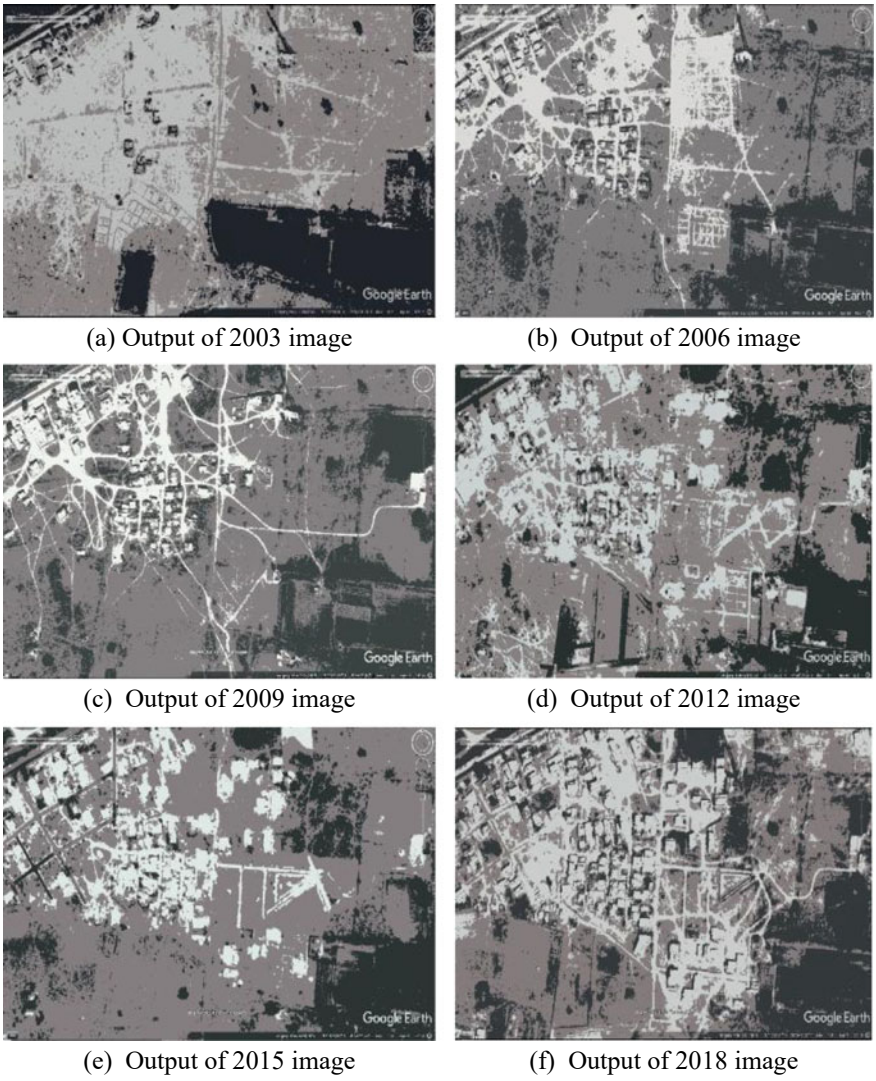

(a) Output of 2003 image (b) Output of 2006 image

(c) Output of 2009 image (d) Output of 2012 image

(e) Output of 2015 image (f) Output of 2018 image

Fig. 9 Results through ERDAS Imagine software of input images of same local area for different years using Unsupervised Classification method

4 Results and Discussion

From the analysis of experimental results of images year 2003 to 2018, the green area is decreasing day by day. The supervised classification gives better results as compared to the unsupervised classification method as demonstrated in Figs.7 and 9. The input images are taken in the gap of three years in the analysis of change in

Table 1 Green area calculation from output images for Supervised Classification and Unsupervised Classification Methods

Sr. No	Year of image	Supervised Classification		Unsupervised Classification	
		No. of Green Pixels	Area in Hectares	No. of Green Pixels	Area in Hectares
1	2003	377,747	*37.7747*	336,144	*33.6144*
2	2006	451,866	45.1866	359,735	35.9735
3	2009	276,523	27.6523	396,342	39.6342
4	2012	224,429	22.4429	337,709	33.7709
5	2015	292,427	29.2427	325,995	32.5995
6	2018	177,438	*17.7438*	433,748	*43.3748*

Table 2 Green area difference between two years for Supervised Classification and Unsupervised Classification Methods

Sr. No	Comparison of years	Difference in Areas for Supervised Classification	Difference in Areas for Unsupervised Classification
1	2003 and 2006	*7.4119*	*2.3591*
2	2006 and 2009	− 17.5343	3.6607
3	2009 and 2012	− 5.2094	− 5.8633
4	2012 and 2015	6.7998	− 1.1714
5	2015 and 2018	*− 11.4989*	*10.7753*

vegetation. Nowadays, this is a concerning topic for the betterment of urban cities. As we analyze input images visually from 2003 to 2018, the green area decreases faster. From the experimental results, for the supervised classification method greenness area is decreasing continuously. The calculation of greenness is the count of green pixels in an image after the segmentation process. As shown in Table 1, in 2003 green area in Hectares is 37.7747, after 15 years it reduced to 17.7438 Hectares. The unsupervised classification method gives false results, due to misclassification of the pixel values, as it is a fully automatic classification method. Table 2 depicts the comparative analysis of change in the green area between two years.

5 Conclusion

This paper presents the comparative analysis of the supervised and unsupervised classification methods. A supervised classifier based on training sites defined by the user gives more accurate results. An unsupervised classifier generates the different classes based on spectral details, not on visual analysis. Spectral information can be changed from time to time, so supervised classification can be used for segmentation

and further calculations of greenness in terms of the area presented. With the developed algorithm using the software, images are being studied and analyzed based on greenness. Proper measures can be suggested to overcome the problems which were stated during the analysis for the betterment of urban cities.

Acknowledgements The research work is carried out in the MRSAC (Maharashtra Remote Sensing Applications & Centre), Nagpur. We are thankful for their kind support for this research work.

References

1. Du, P., Liu, P., Xia, J., Feng, L., Liu, S., Tan, K., Cheng, L.: Remote sensing ımage ınterpretation for urban environment analysis: methods, system and examples. Remote Sens. **6**, 9458–9474 (2014). ISSN 2072–4292. https://doi.org/10.3390/rs6109458
2. Huang, C., Yang, J., Hui, L., Huang, H., Le, Y.: Green spaces as an indicator of urban health: evaluating its changes in 28 mega-cities. Remote Sens. **9**, 1266 (2017). https://doi.org/10.3390/rs9121266
3. Mugiranez, T., Nascetti, A., Ban, Y.: WorldView-2 data for hierarchical object-based urban land cover classification in kigali: integrating rule-based approach with urban density and greenness indices. Remote Sens. **11**, 2128 (2019). https://doi.org/10.3390/rs11182128
4. Hanspal, R.K., Sahoo, K.: A survey of ımage enhancement techniques. Int. J. Sci. Res. (IJSR) ISSN (Online) **6**(5), 2319–7064 (2017)
5. Arora, S., Agarwal, M., Kumar, V., Gupta, D.: Comparative study of image enhancement techniques using histogram equilization on degraded images. Int. J. Eng. Technol. **7**(2.8), 468–471 (2018)
6. Gonzalez, R.C., Woods, R.E.: Digital Image Processing, Third Edition (2009)
7. Bhosale, P., Gokhale, A.: Segmentation of color images based on different segmentation techniques. Int. J. Electron. Comput. Sci. Eng. **2**(2), 640–644 (2013)
8. Jalobeanu, A., Blanc-F´eraud, L., Zerubia, J.: An adaptive Gaussian model for Satellite image deblurring. IEEE Trans. Image Process. **13**(4) (2004). https://doi.org/10.1109/TIP.2003.819969
9. Patel, O., Maravi, Y.P.S., Sharma, S.: A comparative study of histogram equalization based ımage enhancement techniques for brightness preservation and contrast enhancement. Int. J. (SIPIJ) **4**(5), 2013
10. Šastný, J., Minarík, M.: A brief ıntroduction to ımage pre-processing for object recognition. In: International Conference on Soft Computing Applied in Computer and Economic Enviroment, Kunovice (2007)
11. Abburu, S., Golla. S.B.: Satellite ımage classification methods and techniques: a review. Int. J. Comput. Appl. **119**(8), 0975–8887 (2015)
12. Marnur, A.M., Gavade, A.B.: Satellite image classification and feature extraction using various classification techniques: A Survey. Int. J. Adv. Res. Ideas Innov. Technol ISSN **4**(3), 2454–3132 (2018)
13. Ranganathan, G.: A study to find facts behind preprocessing on deep learning algorithms. J. Innov. Image Process. (JIIP) **3**(01), 66–74 (2021)
14. Manoharan, J., Samuel: Study of variants of extreme learning machine (ELM) brands and its performance measure on classification algorithm. J. Soft Comput. Paradigm (JSCP) **3**(02), 83–95 (2021)
15. Manoharan, S., Sathish: Early diagnosis of Lung Cancer with probability of malignancy calculation and automatic segmentation of lung CT scan images. J. Innov. Image Process. (JIIP) **2**(04), 175–186 (2020)

16. Tesfamikael, H.H., Fray, A.., Mengsteab, I., Semere, A., Amanuel, Z.: Simulation of eye tracking control based electric wheelchair construction by ımage segmentation algorithm. J. Innov. Image Process. (JIIP) **3**(01), 21–35 (2021)
17. Nimbarte, N.M., Mushrif, M.M.: Multi-level thresholding algorithm for color ımage segmentation. In: IEEE Conference on Computer Engineering and Applications, at Bali Island, IndonesiaI, CTTA, vol. 2, pp. 231–233 (2010). https://doi.org/10.1109/ICCEA.2010.198
18. Mohane, V., Gode, C.: Object recognition for blind people using portable camera. In: 2016 World Conference on Futuristic Trends in Research and Innovation for Social Welfare (WCFTR'16), 978–1–4673–9214–3/16/ 2016 IEEE
19. ERDAS Customer Education: Introduction to the ERDAS IMAGINE Developer's Toolkit (2009). www.erdas.com
20. Ali, A.: Lab Introduction to ERDAS IMAGINE Software. Project: Ph.D. (Remote Sensing & GIS), May 2017. https://doi.org/10.13140/RG.2.2.13730.43203
21. Sainis, S., Barahate, V., Bandawar, S., Tarak, S., Nimbarte N., Balamwar, S.: Enhancement techniques for analysis of satellite ımages through ERDAS software. In: Proceedings of the International Conference on Artificial Intelligence and Smart Systems (ICAIS-2021) IEEE Xplore Part Number: CFP21OAB-ART; ISBN: 978–1–7281–9537–7

Color Image Segmentation using Fuzzy Histon

Milind M. Mushrif ; Yogita Dubey ; Vikas Gupta All Authors

Abstract: Fuzzy histon, an extension of histon, is a contour plotted on the top of the histograms of the color components such that the pixels with high degree of correlation are v... **View more**

Abstract:
s of the color components such that the pixels with high degree of correlation are visualized as belonging to one singular value. In this paper, we propose a fuzzy histon roughness index based thresholding algorithm for the segmentation of color images. The quantitative evaluation of the proposed approach against the existing thresholding technique and Compression-based Texture Merging (CTM) algorithm proves its effectiveness.

Published in: 2021 IEEE International Women in Engineering (WIE) Conference on Electrical and Computer Engineering (WIECON-ECE)

Date of Conference: 04-05 December 2021

Date Added to IEEE *Xplore*: 19 July 2022

▸ **ISBN Information:**

INSPEC Accession Number: 22046679

DOI: 10.1109/WIECON-ECE54711.2021.9829678

Publisher: IEEE

Conference Location: Dhaka, Bangladesh

Contents

Image segmentation is a critical, yet essential preprocessing step in many applications in which an image is divided into a set of homogeneous regions such that the union of any two adjacent regions is non-homogeneous [1, 2]. The color image segmentation techniques may be viewed as combination of two or more approaches such as those based on statistical, region growing, thresholding, clustering, graph based, visual perception and those based on physical reference models [2, 3, 4]. Histogram based thresholding has been widely used as a tool for the image segmentation [5, 6, 7, 8]. This approach does not need any prior information of the image but, the drawback is that, it does not consider the spatial correlation of pixels with respect to each other. Whereas, in real-world images, there is usually a strong correlation among the pixels in an object [9].

Authors

Figures

References

Keywords

Metrics

Back to Results | Next >

References

References is not available for this d

References

References is not available for this d

References

References is not available for this d

Nagar Yuwak Shikshan Sanstha's
Yeshwantrao Chavan College of Engineering
(An Autonomous Institution Affiliated to Rashtrasant Tukadoji Maharaj Nagpur University)
Hingna Road, Wanadongari, Nagpur-441110
NAAC Accredited with 'A++' Grade
Ph. : 07104- 295083, 295085
Website : www.ycce.edu , Email : principal@ycce.edu

Declaration by the Head of the Institution

I hereby declare that the data, information and support documents attached herewith are genuine and correct to my knowledge.

Dr. U.P. Waghe
Principal
Principal
Yeshwantrao Chavan
College of Engineering
Wanadongri Hingna Road,
NAGPUR-441110

Y. C. COLLEGE OF ENGINEERING AUTONOMOUS INSTITUTION SEAL NAGPUR